
# Towards Novel Luminescent Probes for Monitoring β-Galactosidase Activity

by

**Francesca Jo Yates**

A thesis submitted to

The University of Birmingham

for the degree of

Doctor of Philosophy

School of Chemistry

The University of Birmingham

July 2010

**Acknowledgements**

I would like to thank my supervisor, Dr. Liam Cox, for his continual support and patience throughout my time at the University of Birmingham. I cannot imagine a better supervisor and I am very grateful for the friendship, opportunities, advice and education that he has given me.

I have been a member of the University of Birmingham for eleven years now, and throughout that time I have also had the support and friendship of many staff members and students. I would like to particularly thank Nick May, Peter Ashton, Neil Spencer, Lianne Hill and Graham Burns for their expert technical knowledge and sense of humour. My appreciation and thanks extend to all members of the School of Chemistry.

I am also grateful to the past members of the Cox group: Drs. Simon Simpkins, Julien Beignet, Kevin Jolie, Katia Arico, Iwan Williams, Rui Ramalho, Peter Jervis, Michael Weller, and Yoel Garcia-Diaz, and also to my current fellows Andreas Bergman and Renate Gleixner – thanks for all the fun times. A special mention as well for Sascha Tiede, my first Erasmus student, and ever remembered. Members of the John Snaith, Paul Davies and John Preece groups also have my thanks for their friendship, humour and the occasional loan of reagents.

Thanks also go to my close circle of friends and the members of the HMSA forum for entertainment, support and encouragement. The biggest thanks go to my parents, Sue and Trevor, my brother Fredi, Kate and my baby nephew Felix for being the best family in the world who are always there with a shoulder, a kick or a hug – you are all inspiring and I love you all. Finally, to James who has been my rock and supporter through thick and thin for almost ten years, truly my other half and best friend – thank you for everything.

# Abstract

This thesis describes efforts made towards the synthesis of a biologically stable, luminescent molecular probe, which could be used to investigate *in vivo* the processing of sugars by β-galactosidases. To this end, a lactose-based probe was designed, featuring a Lanthanide held within a chelate and appended to the glucosyl unit, and a proximal naphthyl moiety, attached to the galactose unit, which would function as a sensitiser for luminescence.

A β-galactosidase enzyme from *B. circulans* was chosen to carry out the investigation. A number of novel methyl glucosides, functionalised with a naphthyl moiety at C6 of the sugar, were prepared. These were then used as glycosyl acceptors to make disaccharides (lactose analogues), with the enzyme (functioning in reverse) catalysing the glycosylation. The enzymatic reaction was optimised by varying the amount of enzyme, the reaction pH, the ratio of glycosyl acceptor to donor, the reaction temperature, concentration and solvent mixture. The optimal conditions were found to be a 0.4 M reaction solution at pH 7.0 with 20% acetonitrile, a 7:1 ratio of glycosyl acceptor to donor, 19.6 U of enzyme per mmol of acceptor, and a reaction temperature of 30 $^{o}$C. The resulting disaccharide products exhibited unusual regioselectivity for the β-galactosidase from *B. circulans,* with unexpected β(1→3) and β(1→2) glycosidic linkages being formed.

In an effort to increase the efficiency of the process of identifying suitable substrates for the enzyme, a dynamic combinatorial chemistry approach was also explored. This used disulfide bonds to attach the naphthyl moiety to the methyl glucoside using linkers of different lengths. From this library, the enzyme successfully processed the novel disulfide GlcOMe-S-S-$CH_2$Np as a glycosyl acceptor with *p*-nitrophenyl galactose as the glycosyl donor. This resulted in a novel disaccharide featuring a naphthyl group attached via a disulfide bond to the glucosidic residue.

# TABLE OF CONTENTS

**RESULTS AND DISCUSSION**

## ABBREVIATIONS

Ac : acetyl

$Ac_2O$ : acetic anhydride

AcOH : acetic acid

AIBN : azobisisobutyronitrile

app t : apparent triplet

Bn : benzyl

br : broad

$^t$Bu : tertiary butyl

C : Centigrade

CAN : ceric ammonium nitrate

COSY : correlation spectroscopy

$\delta$ : chemical shift

DCC : dicyclohexylcarbodiimide

DCL : dynamic combinatorial library

dd : doublet of doublets

DEG : diethylene glycol

DIPEA : diisopropylethylamine

DMAP : *N,N*-dimethylaminopyridine

DMF : *N,N*-dimethylformamide

ECD : Electrochemical detection

EG : ethylene glycol

$EI^+$ : electron impact, positive ionisation

eq. : equivalent

$ES^+$ : electrospray, positive ionisation

Et : ethyl

EtOAc : ethyl acetate

Gal : galactose

GH : glycosyl hydrolase (glycosidase)

Glc : glucose

GT : glycosyl transferase

h : hour

HMBC : Heteronuclear Multiple Bond Correlation

HOBT : N-hydroxybenzotriazole

HPLC : high performance liquid chromatography

HRMS : high resolution mass spectrometry

HSQC : Heteronuclear Single Quantum Coherence

Hz : Hertz

ISC : intersystem crossing

IR : infrared

*J* : coupling constant

Lac : lactose

Ln : lanthanide

$\mu$ : micro ($10^{-6}$)

m : medium

m : milli ($10^{-3}$)

m : multiplet

M : molar

Me : methyl

min : minute

mol : mole

m.p. : melting point

MS : mass spectrometry

NBS : *N*-bromosuccinimide

NMR : nuclear magnetic resonance

Np : naphthyl

Nu : nucleophile

*o* : *ortho*

*o*NP : *ortho*-nitrophenyl

OTf : trifluoromethanesulfonate

*p* : *para*

PEG : polyethylene glycol

Ph : phenyl

PMB : *para*-methoxybenzyl

pNP : *para*-nitrophenyl

ppm : parts per million

py : pyridine

q : quadruplet, quartet

quant. : quantitative

rt : room temperature

$R_f$ : retention factor

s : strong

t : triplet

$t_r$ : retention time

TBAF : tetrabutylammonium fluoride

TBDPS : *tert*-butyldiphenylsilyl

TBDMS : *tert*-butyldimethylsilyl

TIPS : tri-*iso*-propylsilyl

TLC : thin layer chromatography

TFA : trifluoroacetic acid

Tf : trifluoromethanesulfonyl

THF : tetrahydrofuran

TMS : trimethylsilyl

TOF : time of fight

Ts : *para*-toluenesulfonic acid

Tr : triphenylmethyl

UV : ultraviolet

w : weak

wrt :with respect to

# 1. Introduction

## 1.1 The Biological Importance of Sugars

Sugars are essential for life, they are ubiquitous in Nature and have roles throughout nearly all biological processes. They are referred to variously as carbohydrates, saccharides, oligosaccharides and starches. Ultimately, the monosaccharide glucose is the source of energy for our cells and without it, life would cease to be.

Carbohydrates are one of the major classes of biological polymers in biology, they can be highly branched and the monosaccharide units can be be connected together using a number of different linkages. Proteins and nuceic acids are almost always linear and contain a single type of linkage; amide bonds for proteins and 3'-5' phospho diester bonds for nuceic acids. The scope for structural complexity in carbohydrates is almost limitless. Whilst carbohydrates can be found without being attached to anything else, the majority of carbohydrates in cells and attached to proteins and lipids, referred to as glycoproteins and glycolipids, and the carbohydrate that is attached to the protein or lipid is often referred to as an oligosaccharide.[1] Glycoproteins are key to a number of biological processes, including but not limited to:

- fertilisation;
- viral replication;
- parasitic infection;
- cell growth;
- cell-cell adhesion;
- degradation of blood clots and
- inflammation.

Glycoproteins and glycolipids are abundant in the outer surface of mammalian cells. And because of this, it has long been thought that oligosaccharides are critical to cell-cell interactions. The best documented roles of oligosaccharides in cell-cell recognition are that of the selectin family of receptor proteins. These mediate adhesion of white blood cells to endothelial cells (L-selectin), the recognition of white blood cells by stimulation of wounded endothelium (E-selectin) and the interactions of platelets or endothelium with white blood cells (P-selectin). In each case the carbohydrate ligands involved in these recognition events are sialylated fucosylated sugar chains like sialyl Lewis$^x$ (sometimes referred to as sialyl Lex, Figure 1.1a)

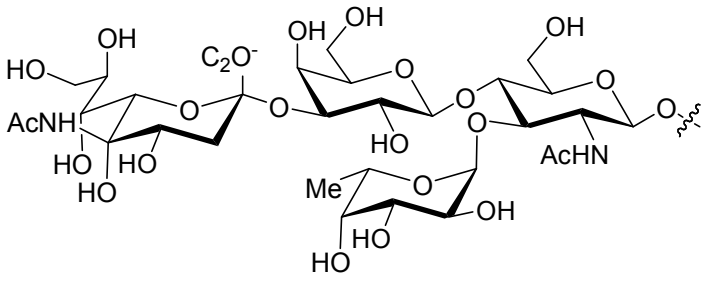


Sialyl Lewis$^x$

**Figure 1.1a: The structure of sialyl Lewis$^x$**

Other biological recognition may depend on the presentation of multiple copies of such oilgosaccharides in a specialised fashion, for example in a sequence on a linear polypeptide chain or in the requisite three-dimensional form. In other words, single-molecule sugar-protein interactions are weak, so it is this oligosaccharide recognition that is a key feature for molecular recognition.[2] Alternatively , specific modifications of oligosaccharides – sulfation for example – might be creating specific binding sites for recognition.[3] Given the complexity of oligosaccharide structure and function it is perhaps obvious that mis-processing of an oligosaccharide structure by enzymes could lead to incorrect or absent cell-cell recognition. Alterations to the cell surface oligosaccharides are associated with various illnesses but the one that always causes the most worry is the malignant change within cells – cancer and consequent tumour metastatis.

Lectins are carbohydrate binding proteins other than enzymes and antibodies and are present in most living organisms. They are involved in numerous biological processes including the adhesion of infectious agents to host cells (viral and bacterial infection), the recruitment of white blood cells to inflammatory sites (the over-recruitment of which are the cause for diseases such as rheumatoid arthritis and lupus, amongst other autoimmune diseases) and cell interactions in malignancy and metastatis. The ubiquitous nature of lectins means that they have great potential for uses in medical science,[4] concanavalin A is amongst the most studied of such Lectins and is used extensively in histochemcial staining.[5]

Given the extensive roles that carbohydrates play within biology it is not surprising that they play important roles in a number of illnesses and diseases, the most obvious of which is diabetes. However, the problem in such illnesses does not always lie with the carbohydrate itself, but more often the countless enzymes present in nature that process carbohydrates and on which a vast number of life processes rely. The subjects of this thesis are the glycosidases, ubiquitous enzymes on which various biological processes depend.

## 1.2 Glycosidases and Glycosyl Transferases

Enzymes are proteins which catalyse most biological reactions. They are therefore extremely important and a great deal of time and effort has been devoted to their study. Some enzymes are also able to catalyse reactions involving both natural and unnatural substances *in vitro* as well as performing their usual task *in vivo*. As biological catalysts they have the following characteristics:

- they operate under mild conditions;
- accelerate the rate of reactions;

- they are highly substrate-specific;
- they demonstrate high chemo-, regio- and stereo-selectivity;
- they are chiral and can show high enantiodifferentiation;
- their stability is highly dependent on the environment in which they are used (causes of instability can be, for example, changes in temperature or pH and also solvent environment);
- they may be subject to regulation in that their catalytic activity may be influenced by the concentration of substrates, products etc.[6]

Amongst the myriad enzymes that exist, there are classes of enzyme which deal solely with the processing of carbohydrates. As discussed in Section 1.1 sugars are incredibly important molecules and many life processes hinge on the proper function of so-called "Carbohydrate-Active Enzymes" (CAZymes) in an organism.

The most comprehensive database of structural information on CAZymes is the CAZy database. The developers of this database have created a dedicated family classification system with which to correlate the structure and mechanism of CAZymes. The CAZy database classifies glycosidases in families based on amino acid sequence and thus the folding similarities of the enzymes in each family. The enzymes are grouped into families which have a similar mode of action and structural features. The families can also be grouped into 'clans' which are groups of families wherein the members have related sequences or structures.[7]

Glycosidases (or 'GH', Glycosyl Hydrolases) are a large group of CAZymes that hydrolyse the glycosidic bond between two or more carbohydrates or between a carbohydrate and a non-carbohydrate moiety *in vivo*.[7] They are ubiquitous in Nature and play an essential role in the biochemical processing of carbohydrates.

Glycosyltransferases (GTs) are CAZymes that catalyse the formation of the glycosidic linkage to form a glycoside. They use 'activated' sugar phosphates as glycosyl donors and catalyse glycosyl group transfer to a nucleophilic group (usually an alcohol) on the acceptor. The product of glycosyl transfer can be an *O*-, *N*-, *S*- or *C*-glycoside which may be part of a monosaccharide glycoside, oligosaccharide or polysaccharide.

In 1982 Whitesides successfully synthesised *N*-acetyllactosamine using the β-1,4-galactosyl transferase (E.C.2.4.1.22). This landmark synthesis was significant because Whitesides included additional enzymes in the reaction mixture to regenerate the co-factors (uridine 5'-diphosphate glucose and uridine 5'-diphosphate galactose) *in situ*.[8] This was a big step forward as the use of GTs had previously been limited by specific and costly co-factors needed in order to perform the desired glycosylation. Figure 1.2a shows the complexity of the cycle needed to use the GT enzyme efficiently. A large number of different enzymes were used, and also a wide variety of substrates were needed for the whole cycle to work.

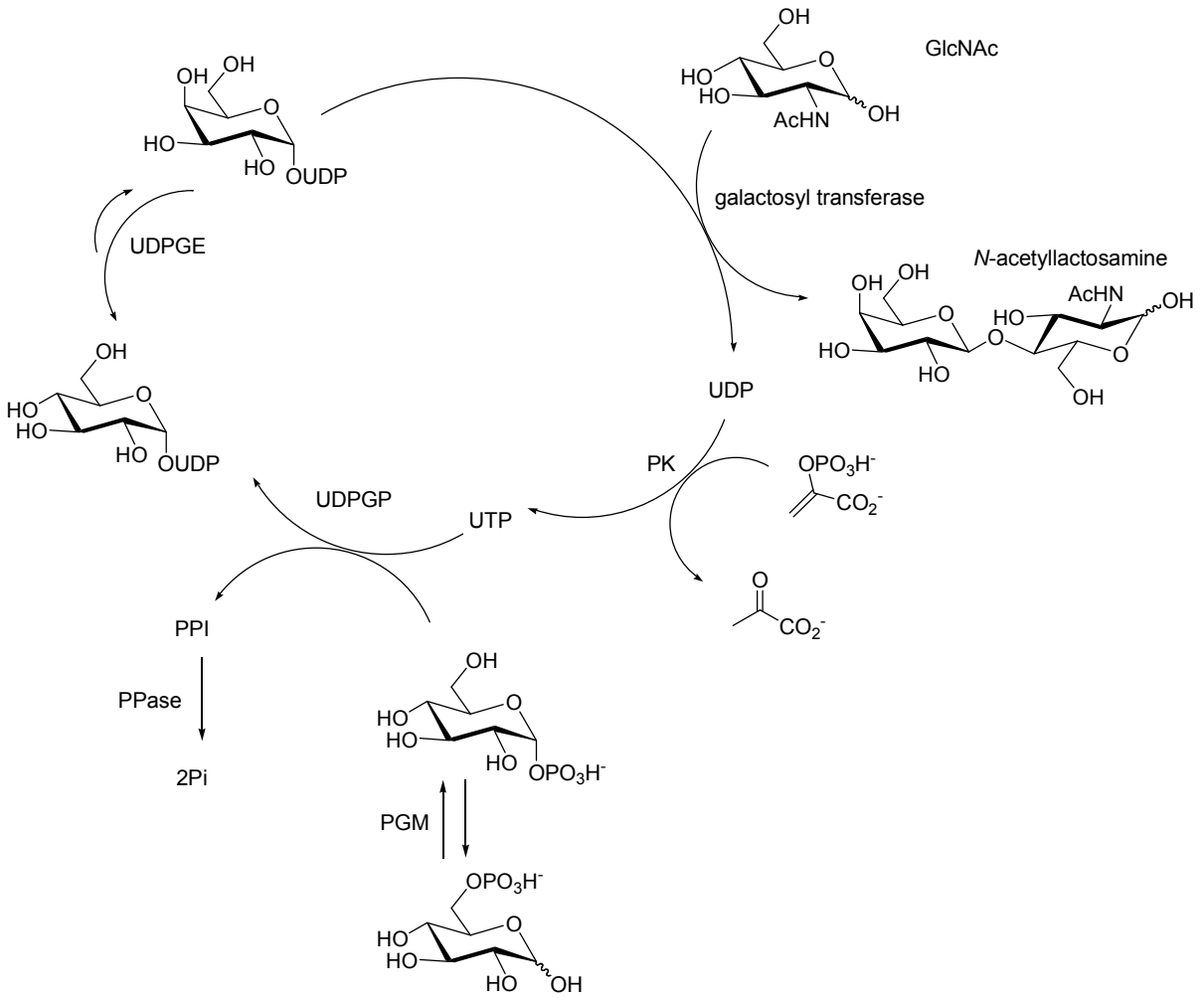


Abbreviations: UDP, uridine 5'-disphosphate; UTP uridine 5'-triphosphate; UDPGE, UDP-galactose 4'-epimerase; UDPGP, UDP-glucose pyrophosphorylasse; PGM, phosphogluco-mutase; PK, pyruvate kinase.

**Figure 1.2a: Whitesides' synthesis of *N*-acetyllactosamine using b-1,4-galactosyl transferases was important as it worked as a system to both perform the transglycosylation and regenerate the co-factors needed for the enzymatic reaction**

In contrast to glycosyl transferases, glycosidases are acknowledged to be much 'easier to handle' and are also significantly cheaper to employ. Although these enzymes have apparently opposite functions, they do share some similarities. Both types of enzymes have been under extensive investigation for oligosaccharide synthesis. It is possible to make glycosidic bonds using a glycosidase by forcing the enzyme to work 'in reverse'. Glycosidases have many potential advantages over glycosyl transferases in these synthetic applications (see Section 1.3.3).

Like many enzymes in the body, a lack, deficiency or surfeit of an enzyme can lead to illness and disease; this is no less the case with GHs and GTs. The study of how these enzymes work in the body is crucial to understanding and working towards treatments and cures for a number of diseases (see Section 1.2.1 for diseases associated with glycosidase deficiency). By designing inhibitors for these enzymes, research groups hope to develop such cures.

### 1.2.1 Glycosidase Inhibition for the Treatment of Illness

Glycosidase inhibitors have two main uses; they are tools through which the understanding of the glycosidase catalysed processes can be understood and they are also excellent candidates for diagnosis and treatement of many illnesses.

Understanding the biological processes mediated by glycosidases can lead to the deveopment of treatments for various illnesses. Most glycosidase inhibitors share two common structural features, i) a basic nitrogen which at physiological pH mimics the positive charge formed during the hydrolysis of the glycosidic bond (see Section 1.2.3.1 for mechanistic details) and ii) an array of hydroxyl groups in a motif which fits selectively into the enzyme active site.[9]

Inhibition of glycosidases (in particular $\alpha$-glycosidases) in the body can have a large effect on the structure of the glycan in question and, because of this, affects the maturation, transport, secretion and function of glycoproteins. This could therefore alter various recognition processes in the organism. This in turn can lead to specialised, directed treatment for various illnesses and diseases whose pathology is bound with the action of glycosidases in the body. For example; Tamiflu is a neuroaminidase inhibitor for the treatment of influenza and the $\alpha$-glucosidase inhibitor 'Glyset' has been used in the treatment of non-insulin-dependant diabetes. The list continues to the treatment of various serious human diseases

such as cancers and various viruses; AIDS, hepatitis B, hepatitis C and Dengue. There has been recent development of five-membered iminocyclitol derivatives for use as antiviral agents and for the treatment of osteoarthritis.[10]

Cancer is one of the most feared illnesses in the present time. Everybody has had contact with the disease, whether directly or indirectly and it significantly alters lives. Glycosidase inhibition is a developing area of cancer treatment. Abnormal cell growth and metastatis can, in some cases, be blocked by use of a glycosidase inhibitor. Tumour and normal cells have different rates of cell growth, so if an inhibitor can be used to block the assembly of a carbohydrate structures relevant to cell growth, it could lead to a therapeutic treatment for cancer by reducing the rate of cell growth (slowing down the pace of cancer growth) or by blocking metastatis.[11]

Investigations into the role and inhibition of glycosidases are therefore crucial to the advancement of medical sciences.

### 1.2.2 β-Galactosidases

The enzyme that we have chosen to study is a β-galactosidase from *Bacillus circulans*. We are interested in studying β-galactosidases as they are responsible for a variety of essential life processes where any hindrance or lack of the enzyme can have very serious health consequences.

Mammalian β-galactosidases have been studied extensively and there are four reasonably well defined biological functions in which they are active. There are two lysosomal or acid enzymes, a neutral β-galactosidase and an intestinal, membrane-bound enzyme. A hereditary deficiency of one lysosomal β-galactosidase results in GM1 gangliosidosis;

hereditary deficiency of the other leads to Krabbe's disease. Both of these acid β-galactosidases are genetically distinct.[12]

#### 1.2.2.1 GM1 Gangliosidosis and Krabbe's Disease

GM1 gangliosidosis is an inherited lysosomal storage disease due to a deficiency of GM1-β-galactosidase. There are various clinical variants which are different in terms of the onset of symptoms, which include neurodegeneration, seizures, enlargement of the liver and spleen, coarsening of facial features, distended abdomen and skeletal problems, joint stiffness and muscle weakness which causes problems with mobility.[13]

Krabbe's Disease is a similarly devastating degenerative neurological disorder. The onset of the disease occurs between three and six months of age and initial symptoms are spasticity, irritability, abnormal posture, partial or complete blindness, hypertonic fits and loss of tendon reflexes. Sadly, death usually occurs before two years of age. The cause is the deficiency of galactocerebrosidase, and the subsequent build up of unmetabolised glycolipids affects the myelin sheath surrounding nerves which causes hypersensitivity to external stimuli (light, touch etc.,) nerve demyelination (which can lead to hyperallodynia, a severe and chronic pain condition caused by abnormal neurological response to touch and movement) and a severe degeneration of motor skills.[14]

Two very serious diseases, both with devastating effects but thankfully quite rare.

#### 1.2.2.2 Lactose intolerance

A more mundane and much more common illness associated with a β-galactosidase deficiency is lactose intolerance.

The mammalian intestinal, membrane-bound β-galactosidase (often referred to as lactase) is responsible for the hydrolysis of lactose into glucose and galactose, both of which can be transported across the cell membrane. All mammals experience a dramatic decrease in intestinal lactase after weaning; humans lose 90-95% of birth lactase levels by early childhood and this continues to decline throughout the course of a lifetime. Malabsorbtion of lactose occurs in three main types, the most common being primary adult hypolactasia. Secondary or acquired hypolactasia can follow any gastrointestinal illness which damages the wall of the gut or increases transit time of stomach contents through the digestive system. The third type of lactose malabsorbtion is congenital alactasia, which is very rare and describes a life-long, complete absence of this β-galactosidase. Up to 15% of persons of northern European descent, up to 80% of those of African and South American descent, and up to 100% of Native Americans and those of Asian origin exhibit a deficiency of this enzyme.[15] Yoghurts with live cultures (sometimes called 'friendly bacteria' and also pre- and pro-biotics) often contain bacterially derived lactase which aids the processing of lactose, at least in the short term, though various yoghurt manufacturers advertise their products as 'cures' for intestinal tract issues. It is claimed that the bacteria in these cultures help to repopulate the gut with flora, thus aiding digestion.

Diagnosis of lactose intolerance can be difficult. Patients typically present with loose stool, cramps, excessive gas and bloating, all of which can also be due to a number of other disorders. Irritable Bowel Syndrome (IBS) is another extremely common but complex intestinal disorder and often presents with very similar symptoms to lactose intolerance. Establishing a positive diagnosis for either condition through dietary restriction is often difficult, and there is considerable overlap between patients with IBS and lactose intolerance. There are two formal diagnostic tests for lactose intolerance. The first is to administer an oral dose of lactose (1-1.5 g/Kg of body weight) and take serial blood samples to monitor blood glucose levels; however 20% of test results are subject to false-negative or false-positive due to the influence of variable gastric emptying and glucose metabolism. A test which measures breath hydrogen after the ingestion of 25 – 50 g of lactose is more sensitive

and specific. It is based on the principle that the breakdown of carbohydrate in the gut is detectable in exhalation gases – specifically hydrogen. A rise of more than 20 ppm in breath hydrogen from the baseline after lactose ingestion suggests lactose intolerance. Whilst this test is deemed to be more accurate, the results can still be affected by varying levels of bacterial flora in the gut as well as smoking.

A particular goal of the dairy industry, and one that has been successful in recent years to the extent that lactose-free milk is now available in supermarkets in the UK, is the 'removal' of lactose from milk. This would obviously allow people with a lactose intolerance to drink milk from cows rather than having to rely on soya or rice milk. In the early 1990s Bakken *et al*.[16] carried out research into the immobilisation of lactases on a solid support for industrial use in hydrolysing the lactose contained in skimmed milk (milk containing less than 0.1 % fat). One such system featured the β-galactosidase from *B. circulans*.

### 1.2.3 Enzyme-Mediated Carbohydrate Synthesis in the Laboratory

The synthesis and modification of carbohydrates by enzymes is one of the most intensely investigated areas of enzyme applications. Glycosylation is extremely important for the structural modification of compounds of biological interest. The addition of a sugar on to a lipophilic substrate will increase its hydrophilicity and it can change pharmacodynamic properties and lead to novel prodrugs. Importantly, using an enzyme to mediate a glycosylation event in the synthesis of biologically active substances is invaluable if traditional synthetic methods, using synthetic catalysts, are inappropriate for the end application in the medicine and food industries.[17]

The complexities of oligosaccharide synthesis by conventional procedures has led to great interest in using naturally occurring enzymes to form glycosidic linkages because of the potential simplicity of the technique. When using enzymes to make oligosaccharides there is

ordinarily no need for a protection/deprotection strategy to ensure that the glycosylation event occurs with the desired regioselectivity – unlike conventional chemical oligosaccharide synthesis. Glycosylation also takes place with complete control of stereochemistry: either α- or β-linked oligosaccharides are produced depending on the specificity of the enzyme chosen for the synthesis. It is this potential for building complex carbohydrates without multi-step protection/deprotection strategies and with control of the stereochemistry at the glycosidic linkage that is one of the most crucial developments in the field of oligosaccharide synthesis.

Glycosyl transferases offer regio- and stereoselective transfer and high glycosylation yields, but they require expensive commercial nucleotide donors, or donors that must be created *in situ* using additional enzymatic techniques. In addition to this, GTs are highly selective with respect to the glycosyl acceptors so the glycosylation event is unlikely to occur on a modified substrate; although there are examples of this through the diligence and enthusiasm of a number of research groups.[18,19]

In this study, the focus is on glycosidases rather then glycosyl transferases. Glycosidases are much easier to work with than glycosyl transferases, and they are also significantly cheaper. They can accept simple sugars (rather than sugar-nucleotides) and are often promiscuous, accepting a wide variety of modified sugars.[20,21] Glycosidases are abundant in Nature, being produced by animals, plants and bacteria; they are robust and easy to handle in the context of a chemistry laboratory, and crucially, they have the ability to function in reverse. Using certain reaction conditions, a glycosidase can be used to carry out transglycosylation reactions.[22,23]

Glycosidases exhibit extremely high stereoselectivity in transglycosylation reactions; for example use, of a retaining β-glycosidase will always result in the formation of a β-linkage, although the regioselectivity of the glycosylation can be more variable. However, thanks to

the active research in this area there is now a wealth of information on many glycosidases investigating the different regioselectivity of enzymes from different sources and how to optimise the regioselectivity using different reaction conditions and substrates. As a consequence, they are a phenomenally useful synthetic tool for any synthetic chemist.[22,24]

The specific examples pertaining to this investigation are discussed in Chapter 3, but I will give some general information about the use of glycosidases in carbohydrate synthesis here.

The use of CAZymes to synthesise oligosaccharides using sugars, and also organic alcohols, dates back into the 1960s and there is now a plethora of literature on the subject. The refinement of these initial forays over time has led to a deep understanding of the conditions required to facilitate glycosyl transfer in good yield. I will focus on the more recent use of these enzymes, primarily by Crout, Vic and Thiem, although there are others who have made significant contributions to the field. First though, an explanation of the mechanism of action and terminology for describing the mode of glycosidase-mediated oligosaccharide synthesis.

#### 1.2.3.1 Mechanism of action of the β-galactosidase from *B. circulans*

As yet the crystal structure of the β-galactosidase from *B. circulans* has not been determined, but there is structural information to be gleaned from comparisons with other enzymes and through experimental deduction (Section 1.3.4). For example, in the CAZy database the glycosidases are grouped into families which have similar structural characteristics. This is often deduced by comparison of the amino acid sequence of enzymes with an unknown structure to the sequence of one which has a known structure. So it is possible to find out structural information about an enzyme you wish to use but that has not been crystallised. This can give the researcher a good idea of structural characteristics and potentially the active site as well.

The active site of a glycosidase has two recognition centres, one for the glycosyl donor and another for the glycosyl acceptor (Figure 1.2.3.1a). The glycosyl donor is the non-reducing end of the sugar, which must be a galactoside for a galactosidase. Since the β-galactosidase from *B. circulans* hydrolyses lactose in Nature, the glycosyl acceptor site would be occupied by glucose. However, extensive studies have shown that many different glycosyl acceptors can be used with the β-galactosidase from *B. circulans* (noted throughout Chapters 1 and 3).

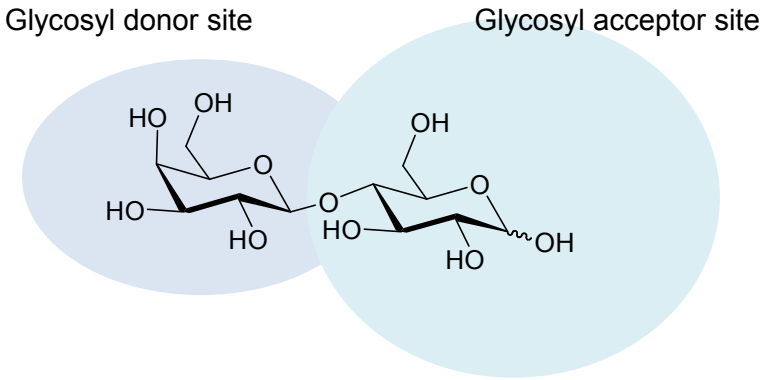


**Figure 1.2.3.1a: Illustration of a glycosidase active site with two areas, one for the glycosyl donor and the other for the glycosyl acceptor.**

The β-galactosidase from *B. circulans* catalyses the hydrolysis of terminal, non-reducing β-D-galactose residues in β-D-galactosides (including lactose) and does so with retention of stereochemistry at the anomeric centre. The general mechanism of action for a retaining glycosidase, also called as an *exo*-glycosidase, was proposed by Koshland in 1953 and still stands more than fifty years later. This mechanism is shown in Figure 1.2.3.1b.[25]

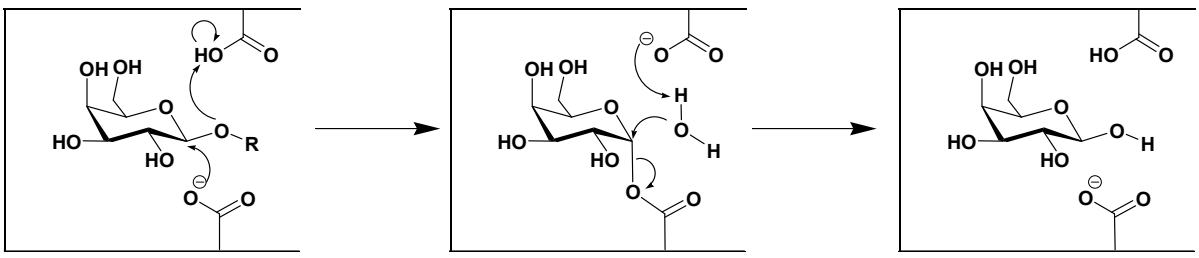


**Figure 1.2.3.1b: The general mechanism for a retaining b-galatosidase, proposed by Koshland in 1953, demonstrates the 'double displacement' action of a retaining glycosidase.**

The mechanism of a retaining glycosidase is believed to function through a 'double displacement' mechanism. In this, a covalent glycosyl enzyme intermediate is formed and hydrolysed *via* oxocarbenium ion-like transition states. The nucleophile and the acid/base catalysts, which will work in concert, have been identified as the carboxylic side chains of glutamic and aspartic acid residues. However, it is difficult to assign these side chains to specific amino acids without access to crystal structures of the enzyme with bound substrates.

#### 1.2.3.2 Transglycosylation and reverse hydrolysis

Most glycosidases used in synthesis are *exo*-glycosidases (retaining). Research using *endo*- (inverting) glycosidases for glycosyl transfer is more limited.[23]

For a glycosidase to be used to form a glycosidic bond between a glycosyl donor and a glycosyl acceptor, the enzyme must be discouraged from performing its natural hydrolysis function.

In terms of mechanism, incubation of a glycosyl donor with an *exo*-glycosidase results in a glycosyl-enzyme intermediate which can then be intercepted either by water (hydrolysis) or by a specific glycosyl acceptor, ROH, which can be an organic alcohol, another glycoside or a different nucleophile altogether (Fig 1.2.3.2a).[23] In the mechanism for a retaining β-glycosidase, the first step is the formation of the glycosyl-enzyme intermediate which occurs with inversion of stereochemistry *via* an $S_N2$ mechanism. In the second step the glycosyl-enzyme intermediate undergoes another $S_N2$ mechanism when it is intercepted by the glycosyl acceptor, again proceeding with inversion of stereochemistry. Overall, the reaction occurs with retention of stereochemistry through this double-displacement mechanism.

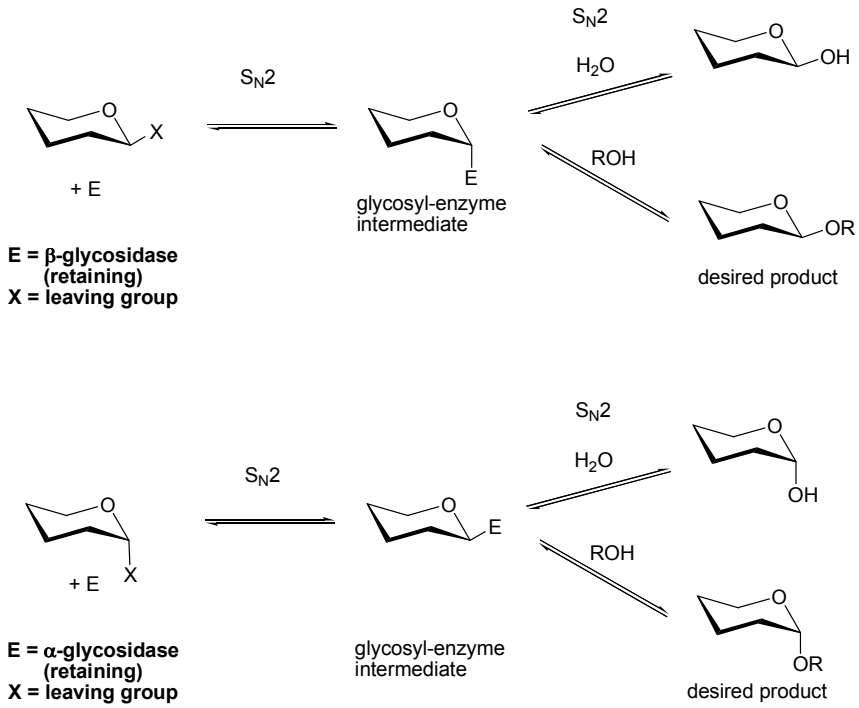


**Figure 1.2.3.2a: The above schematics show the competing hydrolysis and transglycosylation pathways for a retaining b-glycosidase (top) and a-glycosidase (bottom).**

Forcing the enzyme to make a glycosidic bond in preference to hydrolysing the glycosyl donor can be done in two ways, both of which are outlined in Figure 1.2.3.2b.[26]

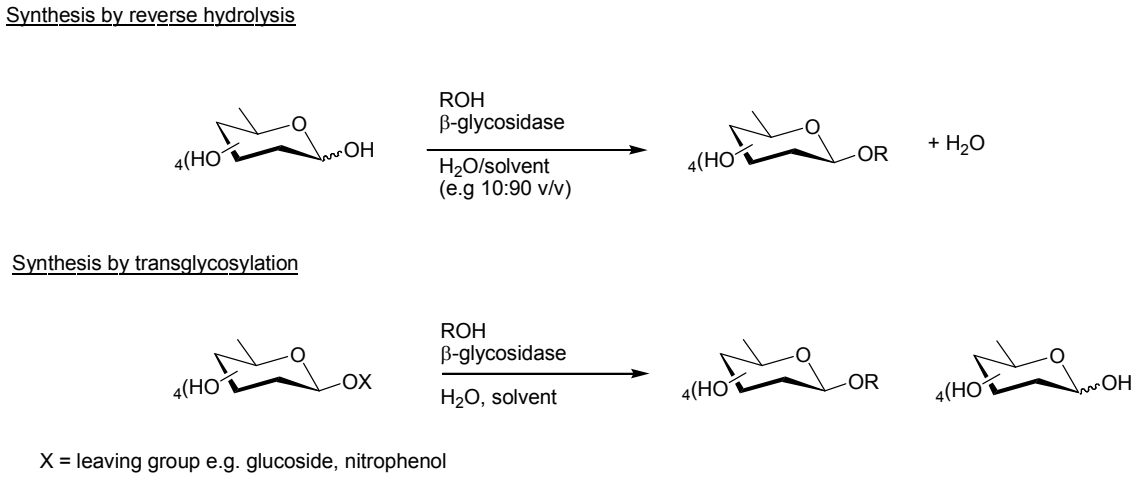


**Figure 1.2.3.2b: Schematic comparing conditions for reverse hydrolysis and transglycosylation. In reverse hydrolysis a low water concentration disfavours hydrolysis, in transglycosylation, a good leaving group is used to move the kinetic equilibrium towards glycosyl transfer.**

**Synthesis by reverse hydrolysis**

In reverse hydrolysis the approach is equilibrium-controlled where the equilibrium is shifted towards synthesis. Reverse hydrolysis is usually brought about by using a high concentration of organic solvent such as *t*-BuOH, which forces the enzyme to use ROH as the acceptor instead of $H_2O$ (see Figure 1.2.3.2b). The organic solvent is more abundant than water, decreasing the local concentration of water around the active site. This alters the equilibrium so that production of the desired glycoside is favoured over hydrolysis.[27] This method of enzymatic synthesis dates back to the 1960s,[28,29] but has been refined over the years.

Vic and Crout first reported the use of almond β-glucosidase to prepare a variety of β-D-glucosides.[30] In this work the approach was that of reverse hydrolysis as hydrolysis was discouraged by using a high concentration (80 to 90% (v:v)) of the organic solvent, *t*-BuOH in this case (Figure 1.2.3.2c). Yields for glucosides **1a**, **1b** and **1c** were 22%, 7% and 17%, respectively, and it was noteworthy that the enzyme remained active and stable at this high concentration of *t*-BuOH.

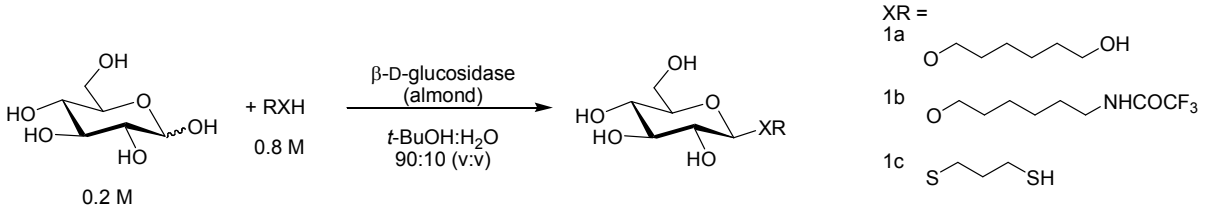


**Figure 1.2.3.2c: The use of almond b-galactosidase to synthesise glucosides using the reverse hydrolysis method.**

Following this, two other approaches were tried in order to increase the yield. The first was to decrease the water concentration, the second to increase the substrate concentration. The water concentration was decreased to 1% by using *t*-butyl methyl ether as the co-solvent. For glucose to be soluble in this solvent mixture it was derivatised as its phenyl boronate derivative (Figure 1.2.3.1d). Whilst glycosides **1a** (yield 7%) and **1c** (yield 10%) were both made successfully using this method, yields were lower than those employing the

conditions in Figure 1.2.3.1c. Since there was such a high level of organic solvent present it suggests that there is a limit to the amount of organic solvent that a given enzyme can tolerate before it is deactivated.

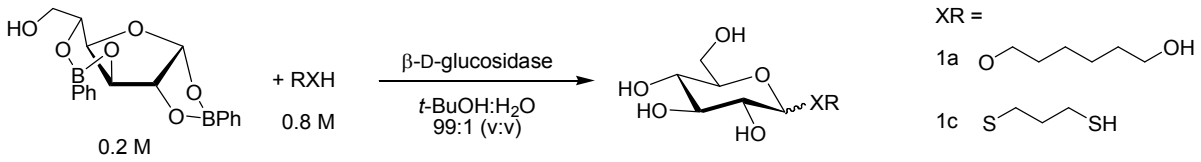


**Figure 1.2.3.1d: An attempt to increase the yield of the reactions with a 1% water concentration required the use of the phenyl-boronate-derivative of glucose.**

To investigate the effect of substrate concentration, the reaction was carried out directly in 1,6-hexane diol with 10% v:v $H_2O$. After five days, glucoside **1a** was obtained in 61% yield. By increasing the amount of water to 20% the reaction was faster but the yield was lower, at 43%. This method is only viable for use with other alcohols that are liquid at <50 $^oC$, do not inhibit the enzyme and can solubilise 10 - 20% (v:v) of water.

**Synthesis by transglycosylation**

The transglycosylation method is a kinetically controlled glycoside synthesis in which the enzyme catalyses the transfer of a glycosyl residue from a glycosyl donor to a glycosyl acceptor. The aim is to increase the yield of the desired product by reducing the extent of competing hydrolysis.[27] Transglycosylation can provide greater versatility as the glycosyl acceptor can be another glycoside, thus leading to oligosaccharide synthesis.

Enzymatic transglycosylation between saccharides was first attempted by Tanaka in the early 1980s using crude enzyme preparations that were commercially available or used for food manufacturing on an industrial scale.[31] This glycosylation method is somewhat different to that employing reverse hydrolysis. In transglycosylation the reaction is not expected to reach equilibrium so a high concentration of the glycosyl acceptor is not required if the

starting glycoside is chosen appropriately.[20] Figure 1.2.3.2e shows this early work on transglycosylation when using β-phenyl glucoside as the glycosyl acceptor.

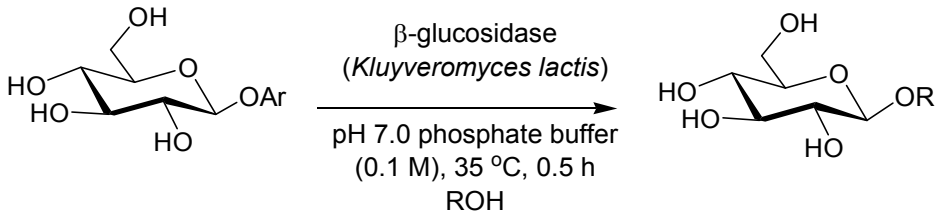


| R | Yield/% | mmol ROH /mL buffer | R | Yield/% | mmol ROH /mL buffer |
|---|---|---|---|---|---|
| $CH_3$- | 67 | 8.0 | $(CH_3)_2C(OH)CH_2CH(CH_3)$- | 9 | 1.5 |
| $CH_3(CH_2)_3$- | 40 | 0.5 | 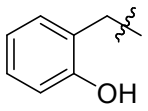 | 27 | 0.26 |
| $(CH_3)_2CH$- | 24 | 1.0 | 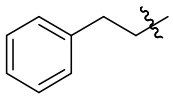 | 22 | *a)* |
| $C_6H_{10}$- | 13 | 0.3 | $CH_3(CH_2)_7$- | 13 | *a)* |
| $HOCH_2CH_2$- | 36 | 1.0 | $(CH_3(CH_2)_3)_2CH$- | 5 | *a)* |
| $(CH_3)_2C(OH)(CH_2)_3$- | 13 | 0.76 | | | |

*1. Two phase (water/nitrobenzene) system used due to hydrophobicity of ROH, carried out at 50 °C*

**Figure 1.2.3.2e: Conditions and substrates used for the investigations into transglycosylation reactions catalysed by the β-glucosidase from *K. lactis***

This study showed that for this particular disaccharide both primary and secondary alcohols can be used for transglucosylation, and that using a primary alcohol will generally result in a higher yield than a secondary alcohol. This is probably on steric grounds as the hydrolysis reaction proceed through an $S_N2$ mechanism which will occur most readily with an unhindered primary alcohol. As with reverse hydrolysis, a higher concentration of alcohol will result in a higher yield, but in each case there is a point where adding more ROH inhibits the enzyme in terms of hydrolysis and transglycosylation.

### 1.2.4 Investigations into the β-galactosidase (*B. circulans)* active site

As already mentioned, there is no precise structural information about the active sites of the β-galactosidase from *B. circulans*; however there is a good deal of work demonstrating the variety of substrates that can be processed by this enzyme. This gives a very useful insight for designing synthetic targets that are likely to be accepted by the enzyme.

In 2001, Usui *et al.* reported on the enzymatic synthesis of sulfated disaccharides using the β-galactosidase from *B. circulans* and *Escherichia coli*. Firstly they looked at the hydrolysis of a functionalised galactoside donor, and found that both enzymes hydrolysed 6-*O*-sulfated sugars but not 3-*O*-sulfated sugars. The enzyme from *B. circulans* was used to catalyse the trans-galactosylation between 4-methylumbelliferyl 6-*O*-sulfo-β-D-galactopyranoside and *N*-acetyl-glucosamine as detailed in the Scheme below (Figure 1.2.4a).

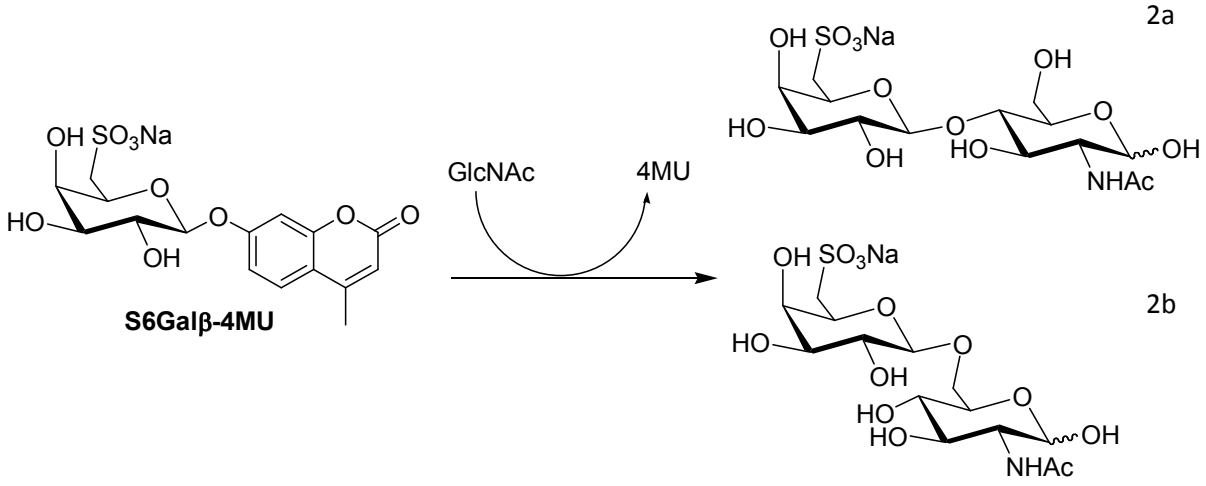


**Figure 1.2.4a: Usui's investigation into the glcosyl transfer of N-acteyl-glucosamine onto 6-*O*-sulfo-β-D-galactospyranoside suggests that the glycosyl donor site of the β-galactosidase from *B. circulans* can tolerate some functionalised galactosyl donors**

The reaction was successful, giving a 49% overall yield of disaccharide product in a ratio of 1:4 of 2a β(1→4):2b β(1→6), linked disaccharides and demonstrated that the enzyme would tolerate the presence of a relatively bulky, negatively charged substituent at C6. This example gives clear evidence that the donor active site is able to tolerate an unnatural sugar

(the natural substrate being lactose). It also gives insight into the glycosyl acceptor active site, which seems capable of handling a large aromatic group, suggesting that a degree of freedom is possible in choosing the glycosyl acceptor.[21]

Work later followed from Thiem and Weingarten who investigated the formation of LacNAc mimetics using novel glycosyl donors and catalysis by the β-galactosidase from *B. circulans* (Figure 1.2.4b).

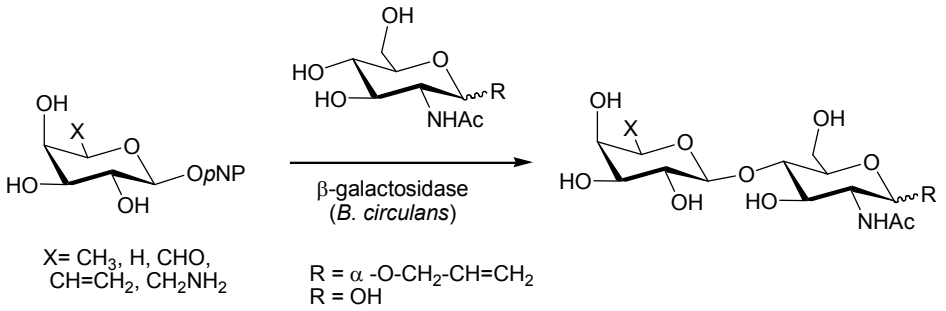


| X | Yield (%) R = O-allyl | Yield (%) R = OH |
|---|---|---|
| $CH_3$ | 76 | 66 |
| H | 13 | traces |
| CHO | 66 | 19 |
| $CH=CH_2$ | 31 | 20 |
| $CH_2NH_2$ | ~10* | - |

* after acetylation

**Figure 1.2.4b: Investigation into LacNAc mimetics featuring a modified C6 substituent on the glycosyl donor**

The R substituent on the GlcNAc acceptor is remote from the donor active site, and the contrast that can be seen in yields seems to indicate that the α-*O*-allyl functionalised acceptor is a slightly better substrate than GlcNAc - the natural substrate. The most significant differences are between the modifications made at C6 of the galactoside donor. Complete removal of the C6 group from the donor significantly reduces the reaction yield, as

does replacing the alcohol with an amine. An amine would likely exist as a positively charged ammonium ion *in vivo*, so a decreased reaction yield would perhaps indicate binding negatively charged residues in the active site, or an unfavourable electrostatic interaction. This may affect the position that the sugar adopts in the active site in such a way that glycosyl transfer is inhibited. However, the enzyme will still process the other three permutations, in high yield for the simple methyl substituent, then lower yields for the aldehyde and olefin derivatives. This, perhaps, indicates that it is a carbon atom at C6 itself which is important for acceptance into the active site, with modification of the substituent on C6 then affecting binding efficacy.[32]

The conclusion from these two examples is that the primary (C6) alcohol group in a galactoside does not seem to be crucial for recognition in the donor site of the β-galactosidase from *B. circulans*. A report by Wong *et al.*[33] seems to confirm this as they used a 6-oxo-D-galactoside (in which the 1° alcohol has been oxidised to an aldehyde) as a glycosyl donor in β-galactosidase (*B. circulans*) catalysed transglycosylation reaction.

The galactoside can be modified quite significantly and the enzyme may still accept it as a donor; however there are not yet any clear rules governing what types and sizes of modification can be tolerated.

## 1.3 Lanthanide Luminescent Probes

The chemistry of the lanthanide series is dominated by the +3 oxidation state and the lanthanide contraction whereby the radii of both lanthanide metal atoms and Ln(III) ions decrease with increasing atomic number. This arises from the *f*-electrons being poorly able to shield the other valence electrons from the nuclear charge. Consequently the effective nuclear charge felt by the valence electrons increases slightly on progressing from left to right along the series which leads to this decrease in atom/ion radii.[34]

The spectroscopic properties of lanthanides are based on f-f- transitions which are weak as they are forbidden by Laporte selection rules. Both ground and excited states have the same $f^n$ electronic configuration so the transitions are parity forbidden so the molar absorptivity of the compound is weak. This means that direct excitation of lanthanide ions is difficult and must be accomplished indirectly *via* an 'antenna' or 'sensitiser' molecule which is ordinarily an organic chromophore.

Ln(III) ions are able to luminesce when excited states are occupied following energy transfer from the sensitiser. The choice of the sensitiser used as an antenna molecule for lanthanide luminescence depends upon the lanthanide ion in use. The chromophore is chosen for a strong UV absorption and a long-lived triplet excited state which is closely matched to (but slightly higher than) that of the lanthanide ion which leads to energy transfer. The energy transfer can occur through-bond or through-space, in the latter case, the orientation to the chromophore to the lanthanide ion can have a large impact on the efficiency of the energy transfer.[35,36] A simple scheme to demonstrate this is shown in Figure 1.4a.

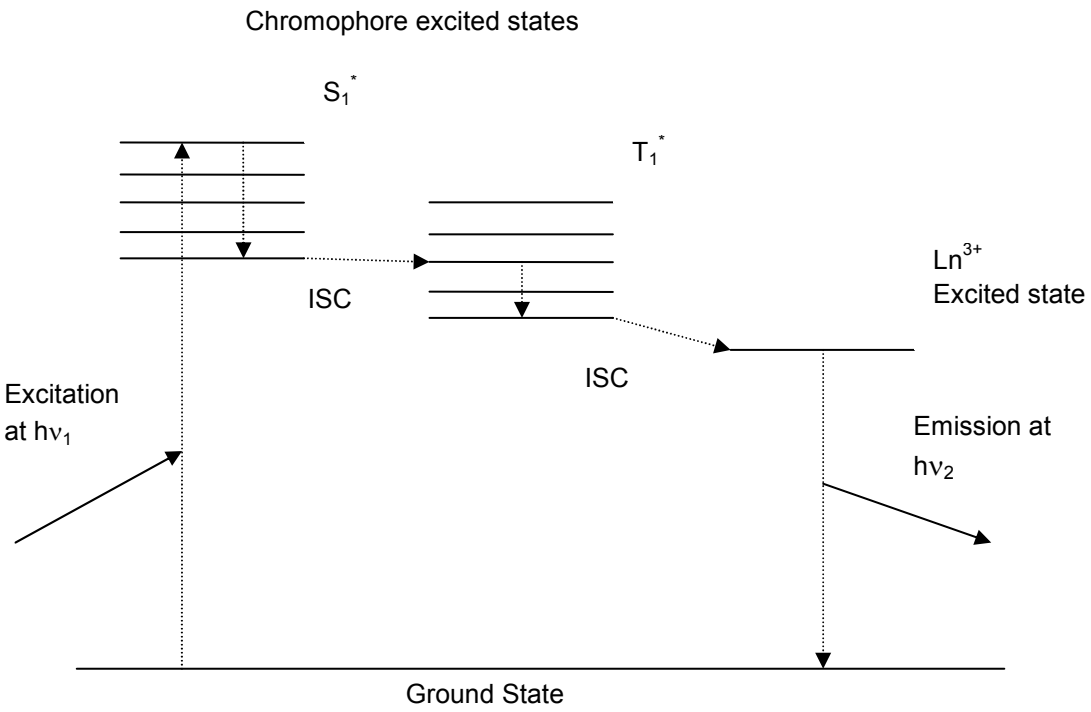


ISC – inter-system crossing

**Figure 1.3a: A simple scheme showing the process of transfer of energy from the excited stae of an organic chromophore to the excited state of a Ln(III) ion, resulting in luminescence**

Absorption of UV light by the antenna chromophore promotes a ligand-based electron from the singlet ground state of the ligand into one of the vibrational levels of the excited singlet state of the ligand. Subsequently, non-radiative Inter system Crossing (ISC) occurs to a vibrational level of the excited triplet state which lies lower in energy than the excited singlet state. After relaxation to the ground vibrational level of the excited triplet state, ISC can again take place to a nearby excited level of the $Ln^{3+}$ ion. Light at a different wavelength is then emitted during relaxation down to the ground state.[37] The consequence of these forbidden transitions is that the decay time (lifetime) on any luminescence caused by the transitions is long, typically in the milli-second range. Europium, terbium, samarium and dysprosium are the only four trivalent lanthanide ions which emit visible light, and of these europium and terbium give the strongest emission and have the longest luminescent lifetimes.

In addition to meeting the energy-level requirements of the lanthanide with respect to the sensitiser, the lanthanide chelate and the sensitiser must be in close proximity in order for

the energy transfer to take place efficiently. For example, quinoline can be used to sensitise both europium and terbium luminescence. Quinoline has a triplet excited state energy of around 22 000 $cm^{-1}$, the $^5D_0$ emissive state of europium(III) is 17 200 $cm^{-1}$, and similarly the $^5D_4$ emissive state of terbium(III) at 20 500 $cm^{-1}$. The energy gap between these states is ideal for such sensitisation processes.[38,39]

There has been enormous interest in the development of lanthanide-based luminescent sensors within the last two decades. A lanthanide-based probe exhibits various properties which offer advantages over organic chromaphores. These factors all lead to a high sensitivity of detection which is of great importance in clinical analysis.

**Light emission**

Lanthanide complexes emit light at long wavelengths, 500 – 700 nm. This light emission occurs in the visible and near IR regions of the electromagnetic spectrum unlike an organic chromophore which will typically fluoresce in the UV region. Thus the measured signal from a lanthanide probe is at a different wavelength to that of an organic chromophore and importantly the background fluorescence found in biological systems (typically 300 – 420 nm).

Lanthanide luminescence occurs *via* excitation of an external organic chromophore requiring UV radiation which results in emission of light from the lanthanide in the visible and near IR region of the spectrum. This difference in wavelength of absorbed and emitted light leads to a large Stoke's shift.[37] Maximising the wavelength split between excitation and the detection of emission wavelengths also reduces scattering and Raman scattering effects.

Lanthanide spectra exhibit sharp emission lines, with each lanthanide exhibiting a characteristic pattern of emission resulting from the different excited state energy levels

populated during the energy transfer process. The emission is observed as multiplets due to several electronic transitions and as sharp bands because of the shielding of the f orbitals.

Lanthanide emission has a long fluorescence lifetime, typically greater than 20 ns. Since the background fluorescence of serum has lifetimes of less than 10 ns this difference in fluorescence lifetime enables interference-free measurements using time-resolved fluorescence.

### 1.3.1 The Design and use of Lanthanide Luminescent Probes for Biological Events

Luminescent lanthanide probes must meet a number of requirements in order to be efficient. They must:

- be water soluble;
- be thermodynamically stable at biological pH and in the presence of biological fluids;
- be kinetically inert;
- have an absorption above 330 nm to minimise destruction of live biological material;
- have efficient sensitisation of the metal luminescence;
- have the Ln(III) ion encapsulated into a rigid, multi-dentate ligand to prevent damping of emitted signal by water;
- have a long excited state lifetime;
- be photostable;
- be non-toxic;
- have the ability to interact specifically with the biological target without interfering with the biological event that it is monitoring;
- be excreted safely and ideally in the span of 12-24 hours.

The lanthanide ion must be encapsulated within an organic chelating agent containing several hard nucleophilic groups which interact with the lanthanide non-covalently. Lanthanide ions can typically accept between eight and nine electron donors, and in the capacity of the sensor as many donor sites as possible must be occupied in order to exclude water molecules which can quench lanthanide luminescence by energy transfer from the lanthanide(III) excited state to the O-H stretching vibrations leading to radiationless transitions. Small ligands, such as water or carboxylic acids, undergo rapid exchange around a lanthanide(III) ion. All f-element complexes with small ligands are very labile, so the ligand sphere cannot exclude water as the small ligands undergo exchange, and so such ligands are not useful for luminescent sensors. There are a variety of multi-dentate ligands suitable for coordinating lanthanide(III) ions. These include polyazacarboxylic acid macrocycles, terpyridines and bipyridines, crown ethers, cryptands and porphyrins. Large multi-dentate macrocycles form the most stable complexes with lanthanide(III) ions, since the chelate effect ensures the formation of a highly thermodynamically stable complex of the lanthanide ion with such a macrocycle.[40]

Large macrocycles such as cyclen (1,4,6,10-tetraazadodecane), have been employed extensively as chelates for lanthanide ions in luminescence signalling studies. The central tetraazadodecane ring can form the basis of the sensor and be functionalised with pendant arms carrying sensitiser chromophores. A typical example of such a sensor is shown in Figure 1.4.1a. The macrocycle is eight-coordinate around the lanthanide(III) ion, blocking most of the coordination sphere and effectively encapsulating the lanthanide ion.

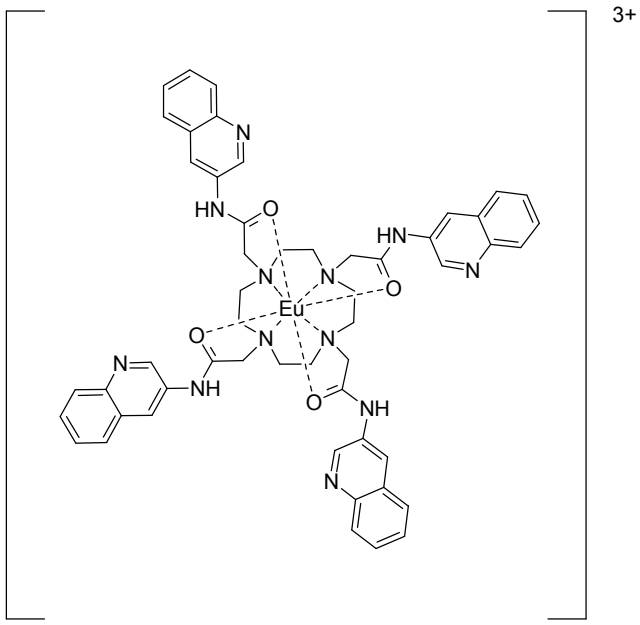


**Eu2**

**Figure 1.3.1a: Europium(III) 1,4,6,10-tetrakis[*N*-(2-methyl-4-quiinolylcarbamoylmethyl)]-1,4,7,10-tetraazacyclododecane**

This particular example by Parker *et. al.*[38] is designed to demonstrate the use of such systems for the signalling of ions and molecules through 'off-on' luminescent sensing. The tetraamide complex **Eu2** (Figure 1.3.2a) detects $H^+$ present in solution by protonation of the quinoline aryl nitrogen moiety. Simply put, the sensor can be 'off' under neutral/basic conditions and 'on' under acidic conditions.

Another widely used chelate for the lanthanide ions is the octa-dentate ligand DTPA-bisamide (diethylene triamine pentaacetic acid, Figure 1.4.1b). The five negatively charged oxygen donor atoms bind strongly to the lanthanide ion in solution. The neutral N bridging atoms and the amide carbonyl groups have been determined to also bind within the lanthanide sphere, leaving the amide NH free for functionalisation. Since the heavily shielded f-orbitals do not interact to any great degree with their environment, complex formation is dominated by electrostatic effects. This ionic type of bonding leads to a lack of directionality in the lanthanide-ligand interactions. The stereochemistry of association is thus determined by the ionic radius of the lanthanide, ligand characteristics and solvation effects.

Since lanthanide complexes are ionic in nature, the kinetics of complexation are normally rapid for simple ligands, and the binding constant of these derivatives with lanthanide(III) ions is high.

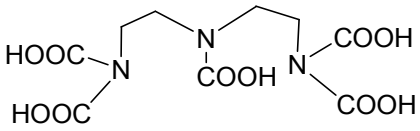


**DTPA**

**Figure 1.3.1b: Diethylene triamine pentaacetic acid**

DTPA formed the framework for a novel heterometallic luminescent lanthanide probe for DNA interacalative recognition developed by Pikramenou *et. al*. (Figure 1.3.1c).[41]

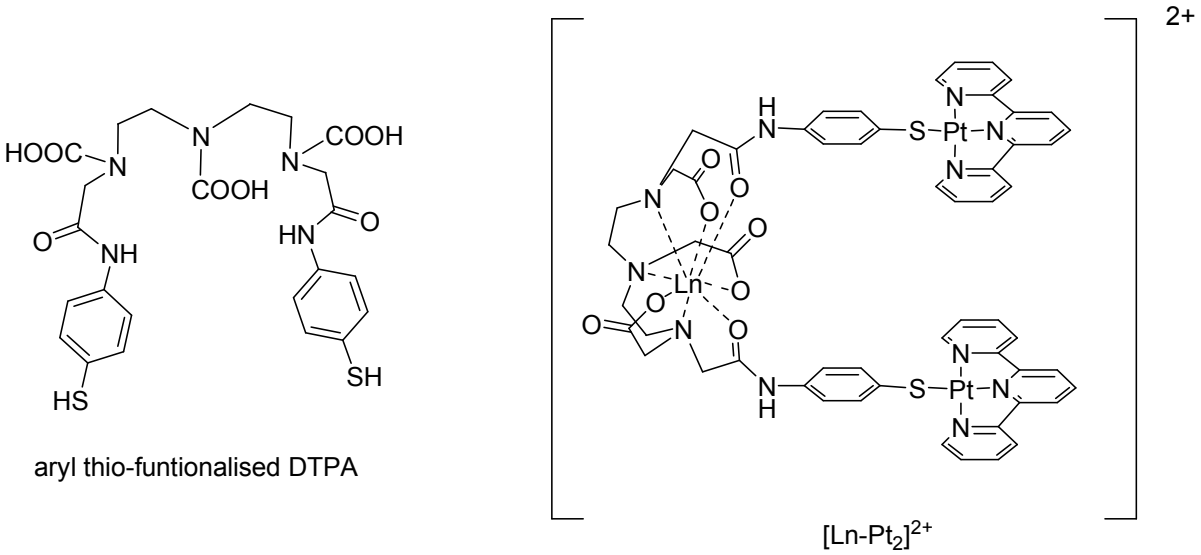


**Figure 1.3.1c: The hairpin-shaped heterometallic lanthanide probe $[Ln\text{-}Pt_2]^{2+}$ for DNA intercalative recognition is based on the DTAP framework**

The thio aryl-functionalised DTPA ligand was designed such that the backbone of DTPA featuring eight hard electron donors would coordinate to a lanthanide (III) ion. The pendant aryl-thiol arms are soft binding sites for other metals, in this case Pt(II) which is bound within a terpyridine ligand. This probe has a 'hairpin' shape allowing the Pt(II) intercalating units to interact with the DNA backbone but leaving the lanthanide luminescent unit remote from that

the DNA backbone. Keeping the signalling unit (the lanthanide chelate) at a distance from the biological recognition event means that the bulky sensor should not inhibit any biological action but is still in a position to report the biological event that it is monitoring.

#### 1.3.1.1 The use of lanthanide luminescent probes for the determination of enzyme activity

Using fluorescent probes to determine enzyme activity has attracted a lot of attention in scientific fields such as *in vivo* imaging and pharmaceutical screening. Luminescent methods to determining the activity of enzyme activity can be classified into four categories:

a. fluorogenic enzyme substrates;
b. substrate bearing a Fluorescence Resonance Energy Transfer (FRET) donor/acceptor system;
c. Immunological assays;
d. specific probes for enzyme substrates or reaction products.

Substrates with a FRET donor/acceptor couple can be used for determining the activity of enzymes including proteases, lipases and esterases. Enzymatic cleavage of each of the substrates leads to disruption of the resonance energy transfer leading to a significant increase of the donor fluorescence, thereby signalling the enzymatic event.[42]

In terms of our project, we are interested in fluorescent probes that are used to monitor the consumption of substrates, in our case this would be a disaccharide. To the best of our knowledge, a luminescent lanthanide probe for monitoring glycosidase activity has not yet been developed.

A number of europium(III) complexes have been reported to respond to phosphate or adenosine triphosphate (ATP) produced during the course of a phosphatase reaction. A europium oxytetracycline complex has been used to determine the concentration of ATP in a

buffered solution. It was postulated that the enhancement in fluorescence occurred because of intermolecular energy transfer in the ternary complexes. Indeed a number of publications relating to europium complexes as luminescent probes for detecting different analytes exemplifies their significant versatility. Conversely, the large versatility points to a lack of selectivity, and due to high sensitivity towards interference in biological conditions it is unlikely that europium probes would be able to be used to quantify the concentration of ATP or another analyte in a complex biological sample. The utility of the probe would then be limited to, for example, pharmaceutical high throughput screening.

In order to investigate the process of a protein kinase with increased specificity, the monitoring of different nucleoside phosphates associated with enzymatic phosphorylation reactions could be the answer. The conversion of ATP to adenosine diphosphate (ADP) is a key step in all kinase-catalysed reactions, in fact a number of molecules are formed from ATP. A europium oxytetracycline complex was used in a direct fluorometric method to monitor the conversion of ATP to its enzymatic reaction product ADP, adenosine-3',5'-cyclic monophosphate (cAMP), and pyrophosphoric acid (PP). It was also used to monitor guanosine phosphate (GTP) conversions. The technique is based on the strong quenching effect of ATP (and GTP) on the luminescence of the europium tetracycline complex. This method offers advantages over existing assays of ATP as it is affordable and straightforward, requires no additional enzymes, requires no fluorescently labelled antibodies and could replace radioactively labelled substrates in such assays.[43]

There is very wide scope for using lanthanide luminescent probes in biological systems. Our intention is to build a lanthanide luminescent probe capable of directly interacting with a β-galactosidase and in so doing giving a direct and measurable response.

## 1.4 Design of a Luminescent Lanthanide Probe for Monitoring β-Galactosidase Activity

Our aim is to develop a biologically stable, luminescent probe in order to investigate the activity and specificity of β-galactosidases *in vivo*. We intend that our work will shed light on the function of glyclosidases in higher mammals – such as humans – so it must be a non-toxic probe which does not inhibit the enzyme and so could potentially be used *in vivo* rather than be restricted to *in vitro* assays.

The probe will feature an intramolecular through-space energy transfer from the antenna molecule to the lanthanide chelate (fig 1.4.a) as described in the examples in Section 1.4.

The mechanism by which the probe works is as follows:

- The disaccharide (lactose) modified with a sensitiser at C6 of the glycosyl donor and a lanthanide chelate at C6 of the glycosyl acceptor should be 'switched on' by intra-molecular energy transfer prior to enzyme processing. The sensor will be emitting a measurable, visible light signal.
- Upon hydrolysis of the modified disaccharide by the enzyme the sensitiser and lanthanide chelate will no longer be in close enough proximity for energy transfer to take place as the two parts of the probe will be separated. The signal will then be 'switched off'

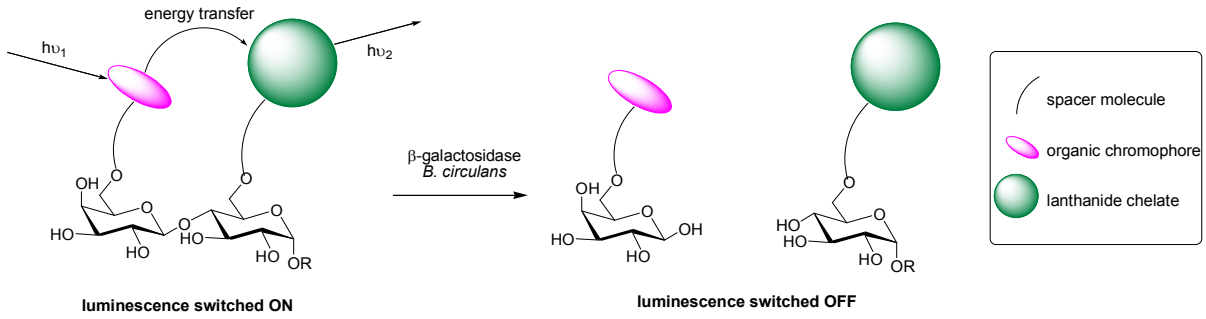


**Figure 1.4a: This schematic shows the idea behind the design of our probe. It will be a 'switch off' system where a decrease in signal intensity from the probe will indicate glycosidase activity**

The decrease in light emission during the assay can be measured and quantified by comparison with the amount of luminesence prior to the addition of the enzyme.

Placing the relatively small, planar antenna on the glycosyl donor, which has to fit into the more specific active site, and using a tether to make it more remote from the sugar we postulate that the enzyme will accept the modified disaccharide. The much larger lanthanide chelate will be attached to the glycosyl acceptor as we know the acceptor active site to be more promiscuous than the donor site in glycosidases. We expect that a tethered lanthanide will allow the modified glycosyl donor to fit into its active site as well. This is discussed in the next Section (2.1) which details the building of the probe and the chemical synthesis of the various components.

# 2. Design and Synthesis of First-Generation Probes for Assessing β-Galactosidase Activity

## 2.1 Initial Design of the Probe

As discussed in the Introduction (Section 1.5) our proposed probe for interrogating β-galactosidase activity is based upon lactose, which is a natural substrate of many β-galactosidases.

In the first instance we need to determine whether the β-galactosidase from *B. circulans* will accept a sugar that has been functionalised with a bulky aromatic sensitiser. We began work on a synthesis to install the sensitiser at C6 of the galactose moiety (glycosyl donor) in lactose; however, however, it quickly became apparent that this would be a long, linear synthesis that could potentially take a long time to complete.

Instead, knowing that the β-galactosidase from *B. circulans* had been successfully employed in the synthesis of oligosaccharides, we thought that a much more elegant solution would be to take advantage of the transglycosylation function of the enzyme and make a disaccharide containing the sensitiser. In this way we would be able to determine if the enzyme could process the modified sugar and use it to make a disaccharide. Owing to the principle of microscopic reversibility, if the enzyme can make a disaccharide containing a modified sugar then it must be able to carry out the reverse reaction and cleave a disaccharide containing that same modification (Figure 2.1a). In this way, we will be able to test whether the enzyme will accept modifications at an earlier stage of the project.

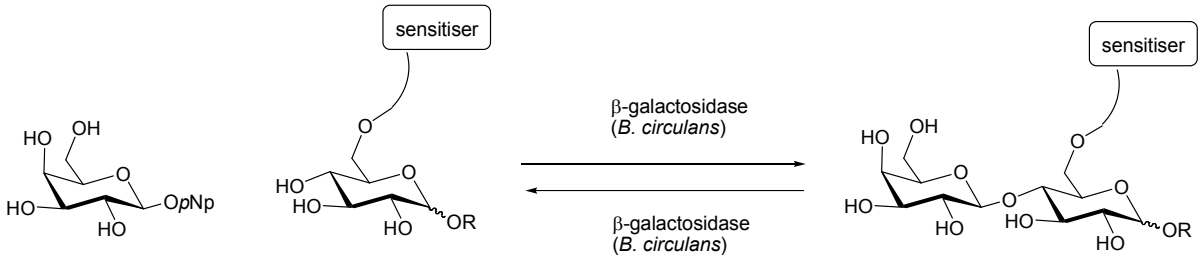


*n.b.*: conditions for the transglycosylation would differ from those for hydrolysis see Chapter for further information.

**Figure 2.1a: This schematic shows the first step of the development of our probe. We will install a chromophore at C6 of the glycosyl acceptor using a number of different linking moieties. We will then use a transglycosylation reaction to discover if the modified sugar is a substrate for the enzyme**

Conformational flexibility, along with changes in the length of the linker, may be needed to allow the modified sugar to fold in such a way that it can enter the active site of the enzyme. We therefore chose to attach the sensitiser, through a range of linkers, to C6-OH of the glycosyl acceptor – glucose – as this is the more flexible part of the sugar and, being the only primary alcohol, most readily derivatised. We were also aware that the acceptor part of the a glycosidase active site is generally more promiscuous than the donor part,[44] so as a first study we would find out if the enzyme will accept the modified glycosyl acceptor and subsequently start work on a modified glycosyl donor. Ultimately though, we would plan to append the smaller sensitiser to the glycosyl donor (as the donor part of the active site is more specific in its substrate choice than the acceptor part) and the bulkier lanthanide complex to the glycosyl acceptor.

The two glycosyl donors we chose to use in these investigations are lactose – the 'natural' substrate for β-galactosidase hydrolysis and *p*-nitrophenyl galactose (GalO*p*NP) which is chemically more reactive than lactose in these circumstances as the cleavage of a glycosidic bond is not always the rate determining step for glycosidase catalysis.[45]

As discussed in the Introduction (Section 1.3.4) the C6 atom itself seems to be important for the recognition of the glycosyl donor in the active site of the β-galactosidase from *B. circulans*, so we must keep the sensitiser quite remote from that carbon atom so that it can be recognised by the enzyme. It is normal practice when attaching sensitising or fluorescent markers to probes for biomolecules to use a 'spacer' or 'linker' to keep the modification somewhat remote from the substrate to which it is attached. This is so that the substrate is able to interact with the biomolecule in its usual fashion (or as close to that as possible). The probe will not be as effective in reporting changes in activity if the biomolecule is unable to process it 'naturally'.

The β-galactosidase from *B. circulans* has a much remarked on preference for forming β(1→4) glycosidic linkages,[46] but will also make β(1→6) linkages.[47-49] By functionalising the glycosyl acceptor at C6 the enzyme will not be able to make β(1→6) linkages as this site will be blocked. We postulated that this may give us a single β(1→4) linked disaccharide, just like lactose, rather than a mixture of regioisomers.

A summary of the proposed development route for making luminescent probes for monitoring β-galactosidase activity is shown in Figure 2.1b.

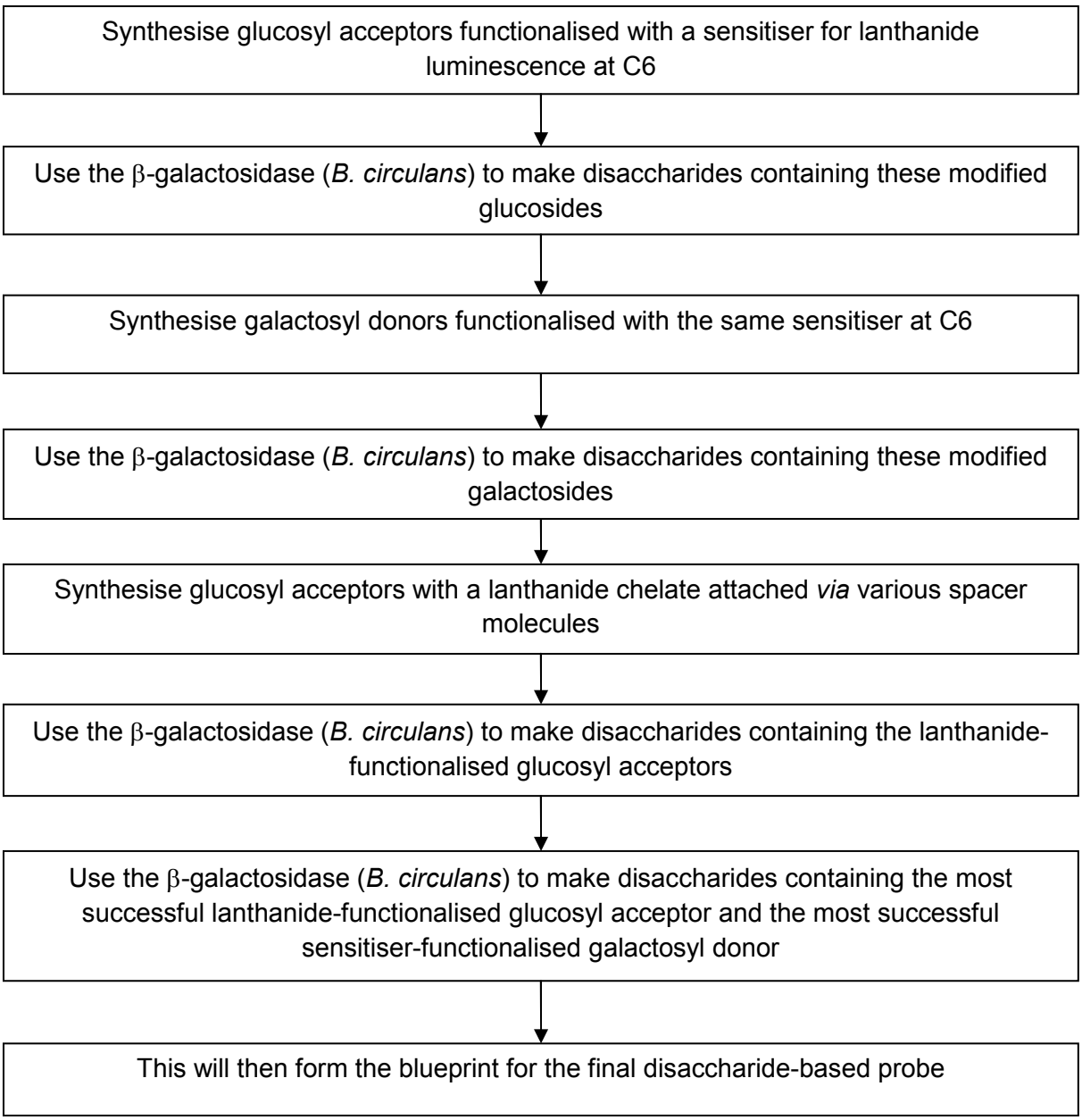


**Figure 2.1b: Summary of the proposed route for the development of a luminescent probe for monitoring β-galactosidase activity**

We first needed to select a sensitiser that would sensitise the lanthanide luminescence, the types and lengths of linker that might be suitable and the method for attaching the linker and sensitiser to the glucoside.

## 2.2 Choice of Sensitiser and Spacer

A number of organic chromophores are capable of sensitising lanthanide luminescence but, mindful that our probe must be able to fit into the active site of the enzyme, we needed to consider the size of the sensitiser carefully. Both quinoline and naphthalene are suitable for sensitising luminescence in europium and terbium complexes. These are the smallest sensitisers suitable for use in our probe. Deciding which of the two to choose will depend upon the ease of synthesis of the chromophore-modified sugar.

We also needed to consider the length of the linker molecule which would be used to attach the sensitiser to the sugar, and the chemical nature of that linker. Amide bonds are used quite frequently as part of the ligands for lanthanides. Whilst the enzyme we are using will not hydrolyse an amide bond, amide linkers may not be suitable to use *in vivo* where other enzymes (*e.g.* proteases) could potentially hydrolyse them. Simple alkyl chains will not be hydrolysed in biological conditions, but may cause solubility issues in an aqueous solution. A commonly used linker in biological probes is one based upon poly-ethylene glycols. Ether chains are not hydrolysed under biological conditions, and various ethylene glycols of different length are readily and cheaply available and they can be functionalised in a number of different ways.

Based on these considerations, we chose to first consider the use of quinaldine-functionalised methyl glucosides and if necessary, examine naphthyl-functionalised methyl glucosides. We selected methyl glucoside (as opposed to glucose) as the glycosyl acceptor as the methyl group positioned at the anomeric carbon would lock the anomeric position facilitating characterisation, and also block any possible glycosylation at that point since we did not expect our enzyme (a β-galactosidase) would be able to process a glucoside.

### 2.2.1 Investigations into Quinaldine-Functionalised Methyl Glucosides

Quinoline has been used extensively as a sensitiser for lanthanide luminescence.[38] 2-Methyl quinoline (quinaldine) has similar photo-physical properties, and has also been used to sensitise lanthanide luminescence and is much cheaper to buy than the quinoline analogues of the compounds we would need.

Sensitisation of $Eu^{3+}$ and $Tb^{3+}$ luminescence by a cyclen-based chelate with a quinaldine antenna was reported by Gunnlaugsson.[38] This quinaldine chromophore has a high extinction co-efficient and its $T_1$ energy is $E$ = 21 980 $cm^{-1}$ (protonated form in glacial enthanol). This $T_1$ energy is close to those of the Eu $^5D_0$ and Tb $^5D_4$ emissive states, hence it is suitable for sensitisation of these two ions.

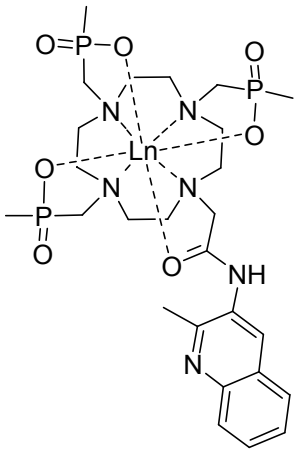


[Eu1] Ln = Eu
[Tb1] Ln = Tb

**Figure 2.2.1a: Cyclen based lanthanide complex with quinoline pendant arm to sensitise lanthanide luminescence**

The complex [Eu1] was investigated as a pH sensor; in alkaline solution the luminescence intensity was said to be 'switched off' as the emission was of low intensity. When the pH of the solution was lowered there was a significant increase in the luminescence intensity, signalling that protonation of the antenna was occurring. Complex [Tb1] also showed a pH dependence similar to that of the [Eu1] complex.

**Design of quinaldine-functionalised methyl glucosides**

Although as already alluded to, amide linkers are not necessarily the best choice for *in vivo* studies, for their potential ease of preparation, we elected for two initial target compounds **3** and **4** (Figure 2.2.1.b), which have different lengths of amide linker chain, and both could be made using 4-aminoquinaldine.

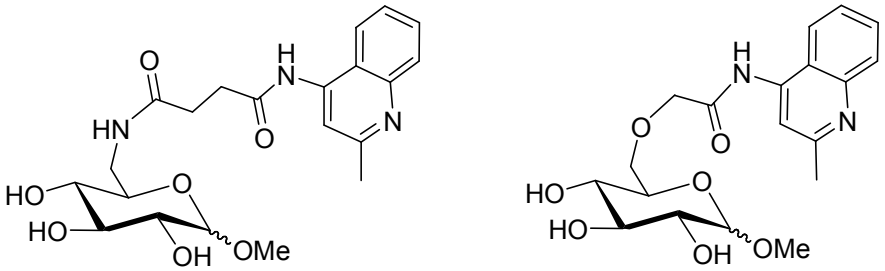


**Figure 2.2.1b: Quinaldine-functionalised methyl glucoside target molecules**

The longer chain would be accessed *via* a succinic anhydride ring opening by 6-(deoxy amino)-methyl glucoside. Quinaldine would then be introduced in a peptide-type coupling reaction between the carboxylic acid and 4-aminoquinaldine. We would take a linear approach to the synthesis, adding the sensitiser in the final step so that it might give us the option to optimise the system by including modified sensors in the final step, should this prove necessary.

The retrosyntheses of the first target compound **3** is shown in Figure 2.2.1c.

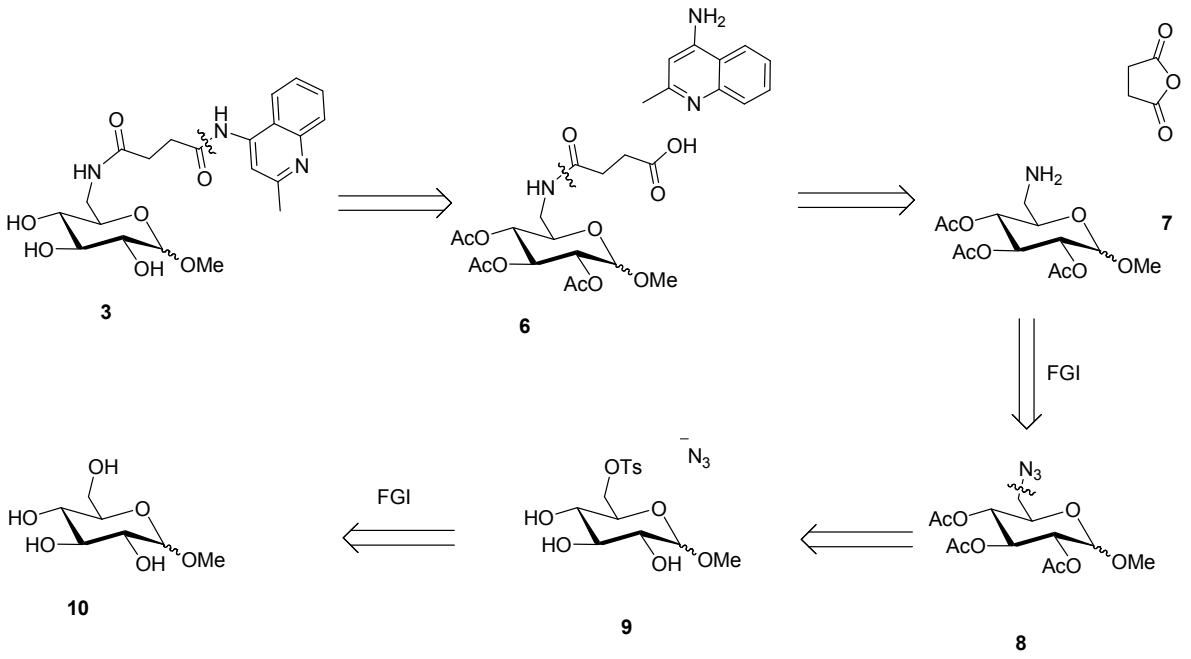


**Figure 2.2.1c: Retrosynthesis for compound 6**

**Attempted synthesis of quinaldine functionalised glucoside 3**

The synthesis of compound **3** began with the synthesis of compound **10** – methyl glucose. This was prepared in quantitative yield from D-glucose by heating a solution of the sugar in MeOH with DOWEX 50W8-400 resin according to a method first published in 1952 by Cadotte *et.al*.[50] In this paper, the use of the method above resulted in the production of $\alpha$-methyl glucoside. In our hands, the method resulted in a mixture of both of the $\alpha$- and $\beta$-anomers in a ratio of 1.0:0.8 respectively. Following this first step, the next steps in our synthesis of **6** are shown in Figure 2.2.1d below.

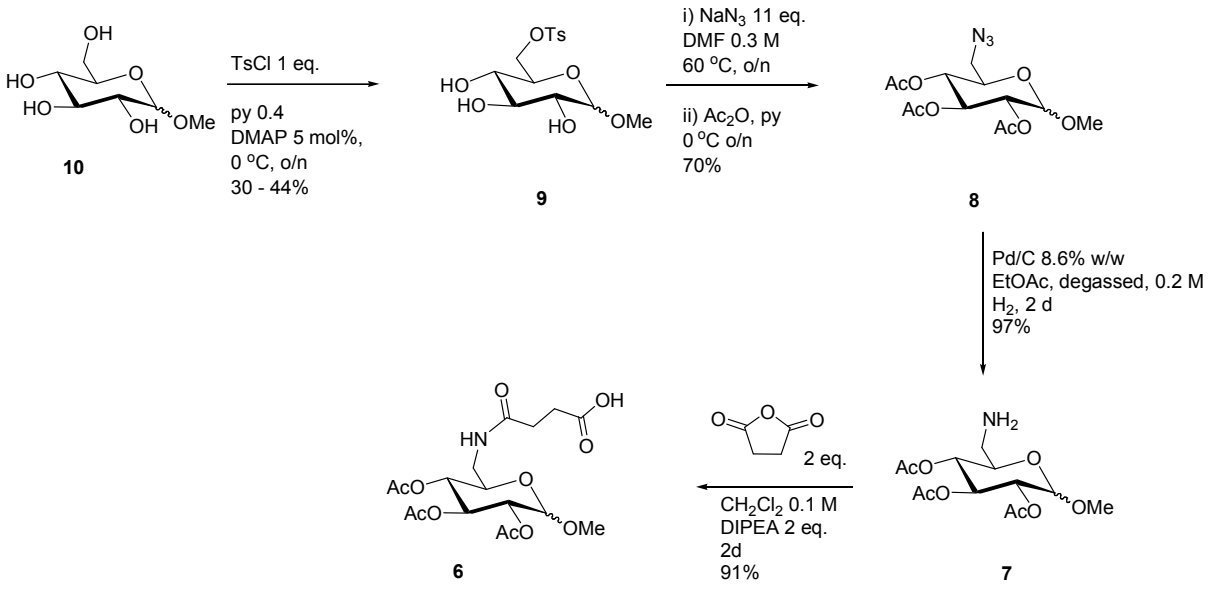


**Figure 2.2.1d: Proposed synthetic route to compound 6**

Methyl 6-*O*-tosyl-D-glucopyranoside **9** was prepared from the methyl glucoside **10** according to a method by Wang[51]. The procedure chosen used a methyl α-D-mannoside rather than a glucoside and reported yields for that compound were 74%. In our hands, yields employing our substrate were much lower, ranging between 30% and 44%. Some of the discrepancy in mass recovery was due to di-tosylated material of which a small amount (~5%) was produced in each reaction. Starting material accounted for the remaining mass balance. We believe that the yields were lower than expected due to the quality of anhydrous pyridine used. Later on in the project when we attempted a similar conversion with TrCl, the use of purchased anhydrous pyridine (as opposed to lab-prepared and stored anhydrous pyridine) improved the yield of that reaction.

Azide **8** was produced following another procedure by Wang[52] by treating tosylate **9** with $NaN_3$ in DMF. Then, in a departure from the published procedure, this was immediately followed by acetylation of the alcohols in the resultant 6-azido sugar under standard conditions[53] to provide the desired acetyl-protected azido glucoside **8** in 70% yield over the two steps. It was necessary to protect the free secondary alcohols as acetates at this stage to facilitate handling and characterisation of the sugars. The hydrogenation[52] reaction to

install the amine at C6 of the sugar proceeded well in 97% yield and without the need for further purification. The final step in this sequence was the succinic anhydride ring-opening to form sugar **6** bearing a pendant carboxylic acid arm, primed for further functionalisation. Following a method by Murphy,[54] the reaction of amine **7** with succinic anhydride proceeded efficiently providing the desired acid in a 91% yield with no need for further purification.

With the synthesis of sugar **6** complete, the next stage was to attach the quinaldine sensitiser to the sugar. We first chose a procedure to form an acid chloride on **6** and then use this to couple with the amine functionality in 4-aminoquinaldine (Figure 2.2.1e).

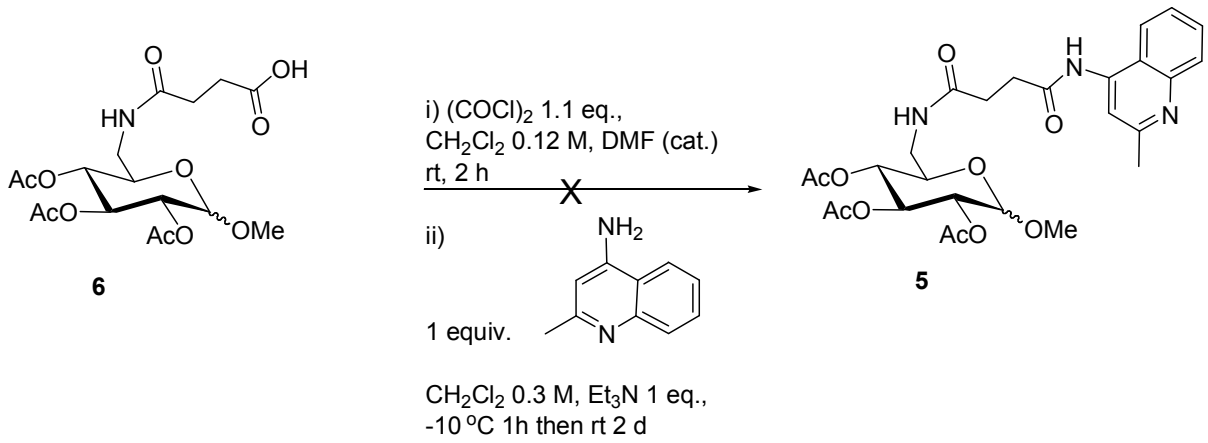


**Figure 2.2.1e: Attempted synthesis of target compound 5 from the succinamic glucoside 6**

Following methods from Domagala[55] and Bernauser,[56] the reaction shown in the scheme above was attempted. Formation of the acid chloride using oxalyl chloride appeared to proceed correctly. Effervescence was observed when adding the substoichiometric amount of DMF and the reaction solution turned green. After two hours, the solvent was removed under reduced pressure and the second stage initiated. The solution of acid chloride in $CH_2Cl_2$ (1 M) was slowly added *via* cannula into a cooled solution of the amine. The reaction was followed by TLC, and a new spot that streaked was observed. We had expected this to indicate the coupling of 4-aminoquinaldine onto the sugar. However after an acid/base work up, and purification of the residue by column chromatography, NMR analysis of the isolated

fractions showed no sign of the desired product. The reaction was repeated, this time leaving the amine coupling step overnight to see if this had an effect on the yield of the desired product. After work up, mass spectrometric analysis of the crude organic residue revealed a peak at *m/z* = 560 corresponding to the desired product, which was confirmed by HRMS. However, none of this was recovered after column chromatography.

After considering the reaction conditions, we concluded that the acidic reaction conditions were affecting the quinaldine moiety. HCl is produced in the formation of the acid chloride and is not removed prior to the addition of 4-aminoquinaldine, and we concluded that protonation of our nucleophile was occurring when 3-aminoquinaldine was added in the second stage (Figure 2.2.1e).[57] We also tried the reaction using $SOCl_2$ instead of oxalyl chloride but still no product formed. Thus we concluded that the reaction was not working and would be unlikely to under these conditions.

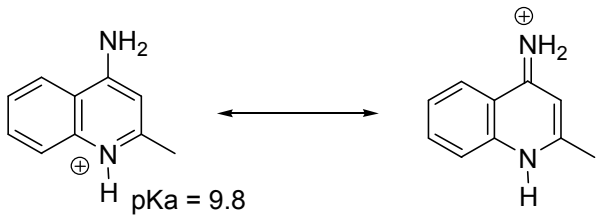


**Figure 2.2.1f: Protonation of 2-methyl-4-aminoquinoline**

We next attempted a DCC coupling between **8** and 4-aminoquinaldine (Figure 2.2.1g). Following a method reported by Stoddart,[58] the DCC coupling was attempted, but proved unsuccessful. It was repeated three times but in each case the reaction none of the desired product was isolated, only dicyclohexylurea (DCU) was obtained.

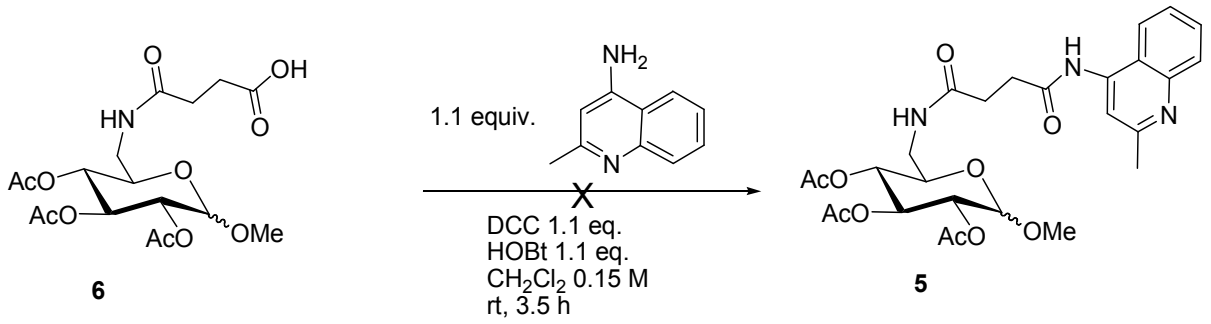


**Figure 2.2.1g: Attempted DCC coupling of 4-aminoquinaldine to succinamic glucoside 6**

An attempt was made to perform the earlier anhydride opening using 4-aminoquinaldine (Figure 2.2.1h) and then perform a DCC coupling onto **7**, but this also proved unsuccessful as the quinalidine was insoluble under the reaction conditions.

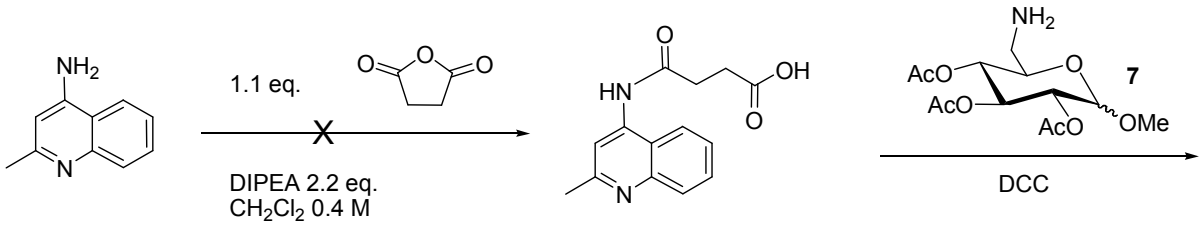


**Figure 2.2.1h: The envisioned alternate route to target compound 3 via a succinic anhydride ring-opening by 4-aminoquinaldine was attempted but unsuccessful**

The formation of compound **3** was proving very difficult, so we chose to leave it and investigate the synthesis of our second target, compound **4**. The retrosynthesis is summarised in Figure 2.2.1i.

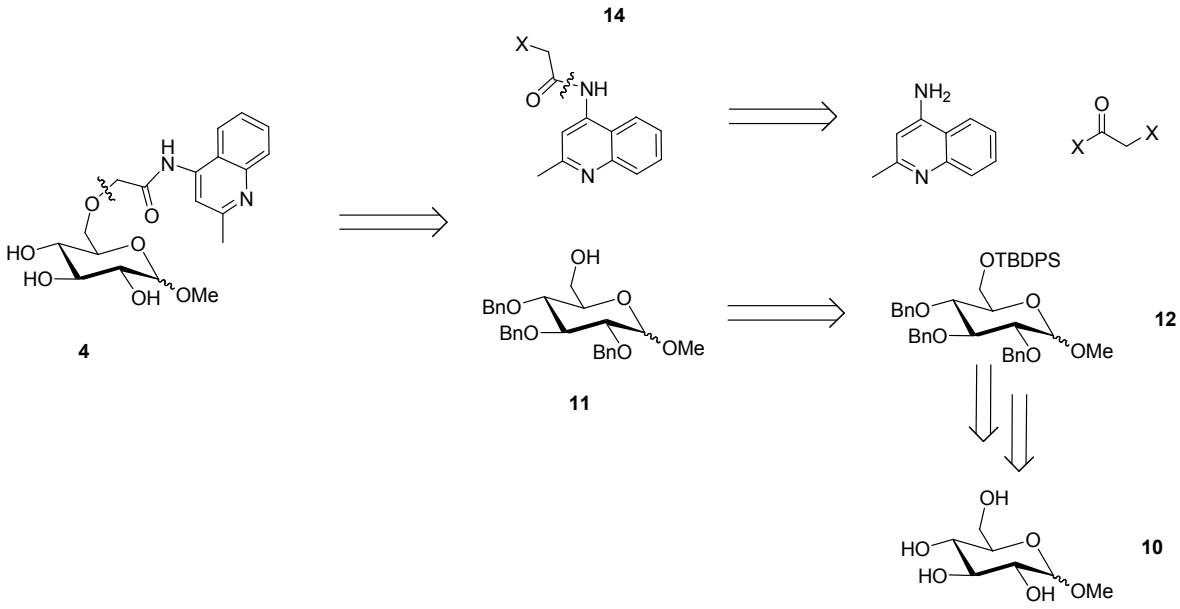


**Figure 2.2.1i: Retrosynthesis of target compound 4**

The first stage in the synthesis of **4** was to acylate 4-amino quinaldine and make the known compound chloro-*N*-(2-methyl-4-quinolyl)-ethanamide (**14a**) and novel bromo-*N*-(2-methyl-4-quinolyl)-ethanamide (**14b**). Both compounds were made following a method by Gunnlaugsson (Figure 2.2.1j).[38] Both reactions resulted in the successful synthesis of the targets although the yields were low. **14a** was produced in only 42% yield (published value 60%) and **14b** in an even lower 20% yield, but this was sufficient for our purposes at the time.

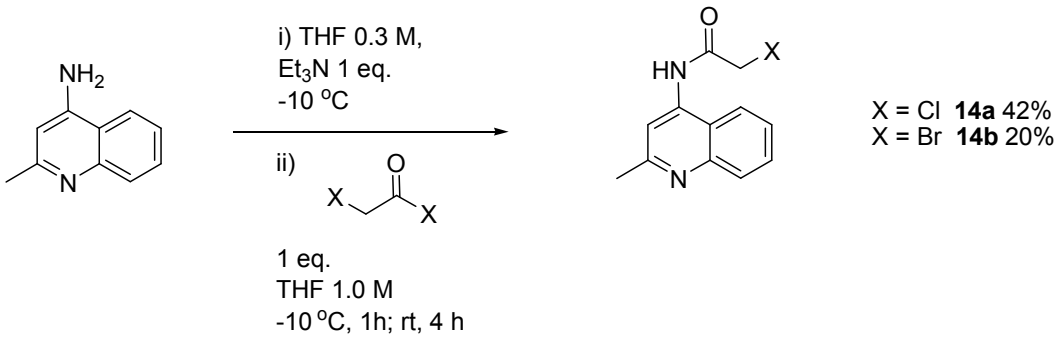


**Figure 2.2.1j: Synthesis of chloro-*N*-(2-methyl-4-quinolyl)ethanamide and bromo-*N*-(2-methyl-4-quinolyl)ethanamide**

An orthogonal protecting group strategy is necessary to produce a methyl glucoside which has a free OH at C6. There are myriad ways of achieving this with the wealth of information available about protecting group strategies, particularly on carbohydrates.

The generally accepted approach to making a glycoside with a free OH at C6 is to first install a bulky protecting group at that position. This alcohol is easily differentiated from the secondary alcohols when using a stoichiometric amount of the sterically demanding group under the requisite conditions. Commonly used groups are TIPS, TBDPS, TBDMS and trityl ethers and tosylates which, due to their steric bulk, all react preferentially at the less sterically hindered C6 position. Then, the remaining secondary alcohols are protected with groups introduced using conditions that will not cleave the bulky group at C6 and that will be stable to conditions required to remove this bulky group at a later stage (Fig 2.2.1k).

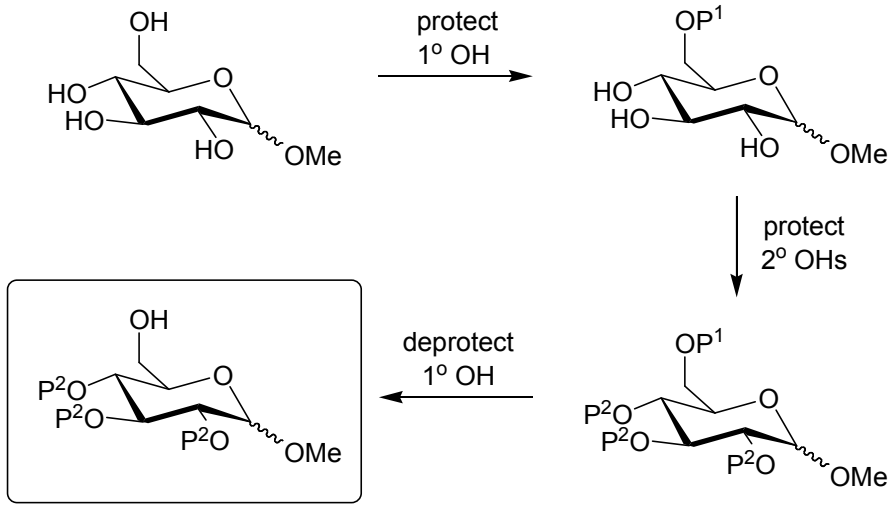


**Figure 2.2.1k: Strategy to reach the selectively deprotected target molecule**

So, in order to install the sensitiser at C6 of the sugar, we used a selective protection/deprotection strategy as shown in Figure 2.2.1k. The 6-hydroxy sugar **11** was made following a procedure by Vasques by selectively protecting C6 of the sugar with TBDPS. Following a method by Vásquez,[59] the TBDPS ether was similarly introduced onto

C6 of our methyl glucoside using imidazole in a concentrated solution of DMF and achieved an 81% yield for the mixture of anomers. TBDPS was chosen as it has more steric bulk than TIPS and TBDMS whilst also being significantly cheaper than TIPS, which is the next largest in terms of bulk. In its first reported use, by Hanessian and Lavallee,[60] TBDPS was noted to silylate primary alcohols in preference to secondary alcohols and was installed by them using imidazole in DMF, a method previously reported by Corey and co-workers[61] with respect to the protection of hydroxyl groups as TBDMS derivatives. Following the same method by Vásquez[59] the secondary alcohols were benzylated using a Williamson ether synthesis in 71% yield. The TBDPS group was then removed using TBAF in THF[62] in a 90% yield (Figure 2.2.1l).

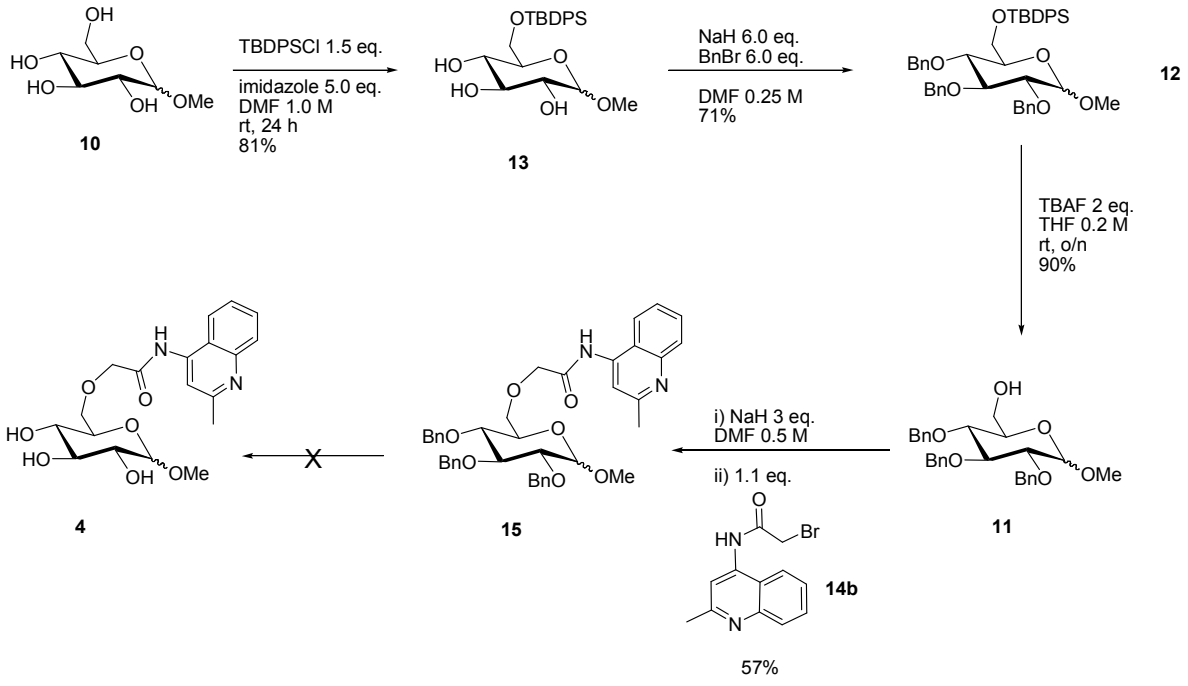


**Figure 2.2.1l: Proposed synthetic strategy to reach quinaldine functionalised glucoside 4**

Using another Williamson ether reaction, **15** was made from **11** using **14b**, and so we had successfully made a methyl glucoside with a quinaldine sensitiser attached. However, our synthesis faltered in the final step as we were unable to remove the benzyl groups. There are a number of ways to do this,[63] we chose to start with hydrogenolysis (Pd/C, $H_2$)[53] which

we attempted first, but which resulted in the recovery of only mono-debenzylated material. We thought that this might be due to the quinaldine poisoning the catalyst we attempted debenzylation using $FeCl_3$;[59] however this did not work either. We then tried the hydrogenolysis using the Degussa-type catalyst $Pd(OH)_2/C$, but this was also unsuccessful and we only recovered starting material from the reaction. Finally we tried Raney Ni[64] but again only recovered starting material

It was very clear at this point that the quinaldine was hampering the syntheses, sometimes in ways that we could rationalise and explain, other times it seemed that it was just a capricious compound to work with. We chose not to waste any more time on installing this sensitiser and instead turned to naphthalene, which is also capable of sensitising lanthanide luminescence. Naphthalene should be inert to acidic and basic conditions compared to quinaldine, and many derivatives are available commercially. Overall we thought that this would have a much better chance of success.

#### 2.2.1.1 Investigations into Naphthalene-Functionalised Methyl Glucosides

Naphthalene is capable of sensitising Ln luminescence but unlike quinoline and quinaldine, it is not a heterocycle. We might expect that synthetic handling of naphthalene would be less problematic than our experience of quinaldine.

Naphthalene typically sensitises luminescence of $Eu^{3+}$. In study by Viswanathan[65] complexes of $Eu^{3+}$ with 1-naphthoic acid and 2,6-naphthalenedicarboxylic acid, the use of these two compounds as ligands was found to sensitise and enhance $Eu^{3+}$ fluorescence in aqueous solutions.

In another report by Quici[66] a detailed study of the luminescence properties of $Eu^{3+}$ and $Tb^{3+}$ complexes it was found that the naphthalene chromophore sensitised the luminescence of the lanthanides and it was confirmed to be through ISC between the excited triplet state of the chromophore and the excited state of the Ln(III) ion. It was also stated in this report that quinoline had a similar effect on the sensitisation of luminescence.

Six new target sugars were originally envisaged, three using amine and amide linker chains based on the amino methyl glucosides we had already synthesised (Figure 2.2.1.1a), and three using ether and ester linker chains (Figure 2.2.1.1b).

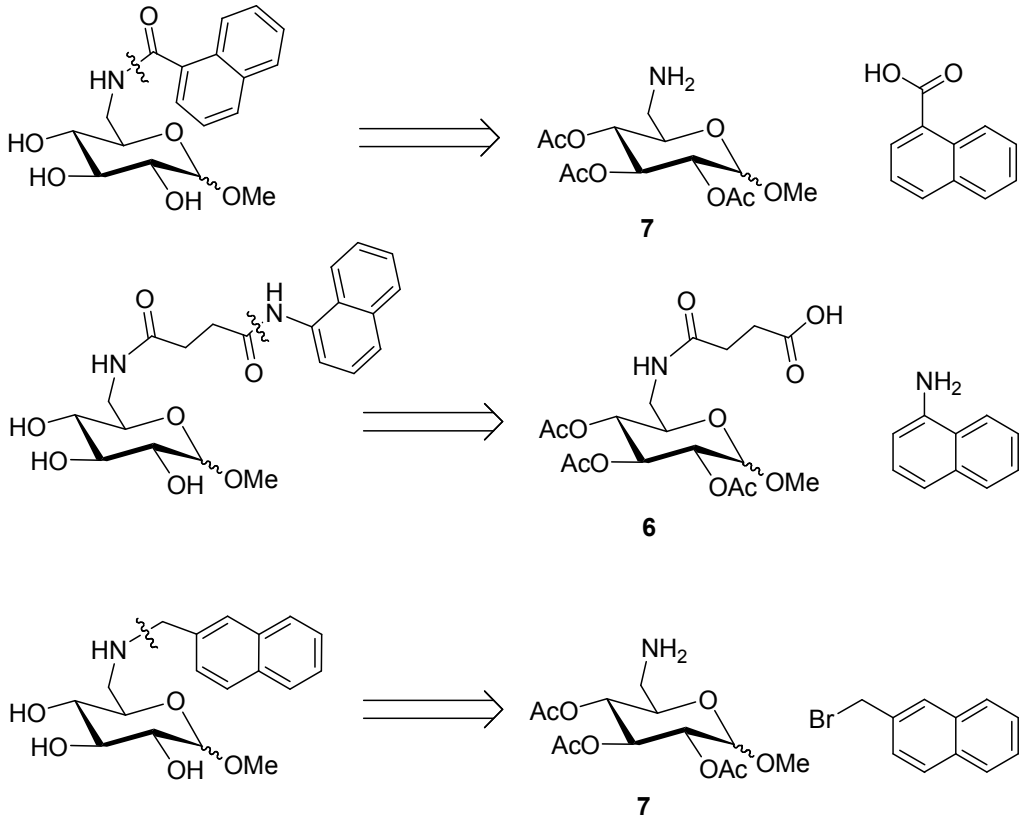


**Figure 2.2.1.1a: Suggested retrosynthesis of amide- and amine-linked naphthyl glucosides**

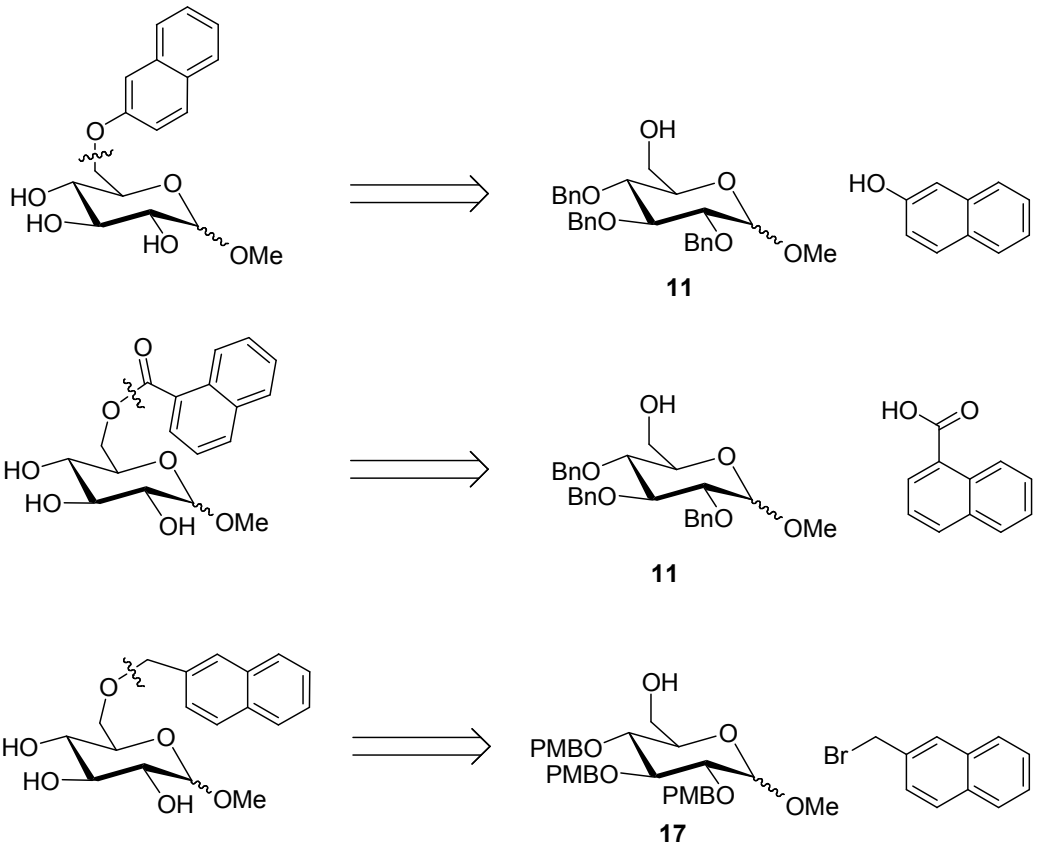


**Figure 2.2.1.1b: Suggested retrosynthesis of ether- and ester-linked naphthyl glucosides**

However, the synthetic pathways to all of these sugars were different. We had spent a great deal of time trying to make quinaldine-functionalised sugars by two different methods, and it had proved very inefficient. We were reluctant to embark upon another synthetic strategy that involved six different sets of reactions to optimise.

We therefore considered the types of linkers that are commonly used in biological probes and those based on poly-ethylene glycols (PEGs) were both abundant and successful. By concentrating solely on making ether linkages we could make our synthesis less complicated and more efficient. After all, the major part of the project was to screen potential substrates using the β-galactosidase from *B. circulans*, and as yet we had no substrates with which to begin the study. The next Section of this work discusses the synthesis of a family of ether-linked naphthalene functionalised glucosides.

## 2.3 Synthesis of a Family of Ether-Linked Naphthalene-Functionalised Glucosides

Having investigated various options for installing a naphthalene moiety at C6 of a methyl glucoside, it was decided that we proceed with a design based upon ether linkages (see Figure 2.3e). These were more analogous to each other, thus more comparable, and they have also been widely used in studies on biological systems as they exhibit good biocompatibility.

Polyethylene glycol (PEG) linkers have been used for many years in biological applications as they are non-toxic, non-biodegradable, non-immunogenic and as such have been widely studied in protein and small molecule modification.[67] They have been used in cell aggregation[68] and also as drug delivery aids due to their enhanced cell permeability and water solubility.[69] PEG has also found frequent employment as a spacer or linker in various sensors and inhibitors. For example, Wong and co-workers investigated the effect of spacer length in the inhibition of E-Selectin using bivalent $sLe^x$ derivatives containing oligoethylene glycols of different lengths (Fig 2.3a).[70]

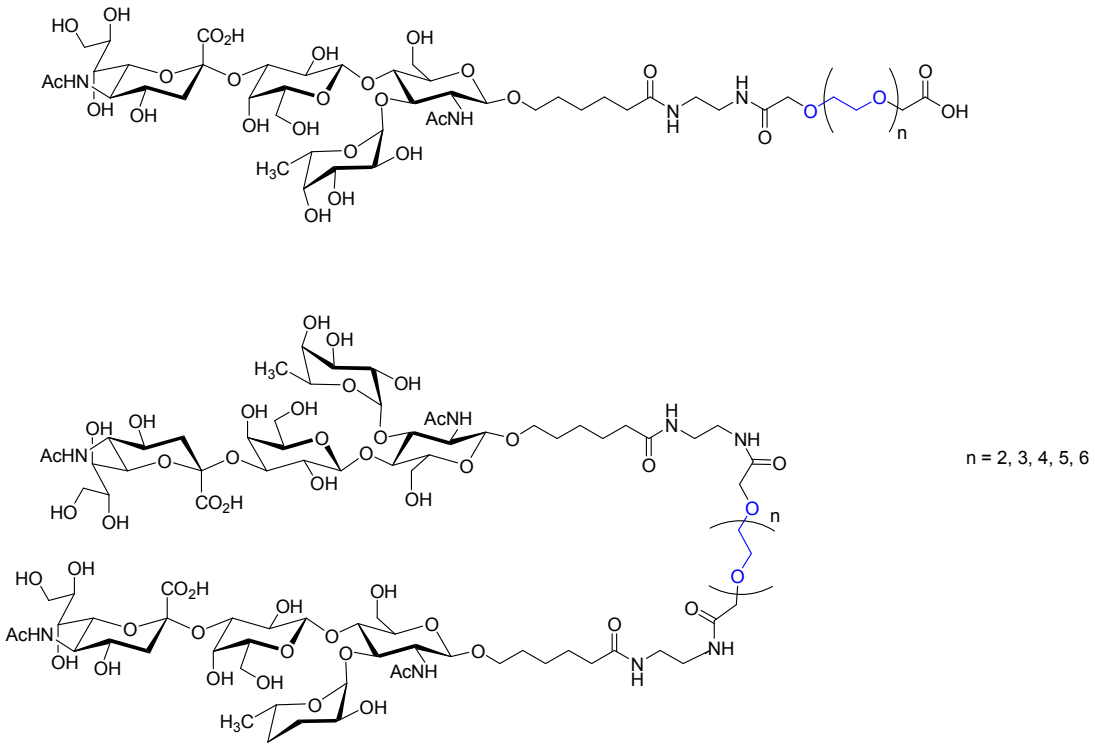


**Figure 2.3a: PEG bridging units used in a E-Selectin inhibitor**

Visintin *et al.* used PEG spacers, including a variable length spacer, in the synthesis of biotin-labelled membrane receptor probes (Fig 2.3b).[71]

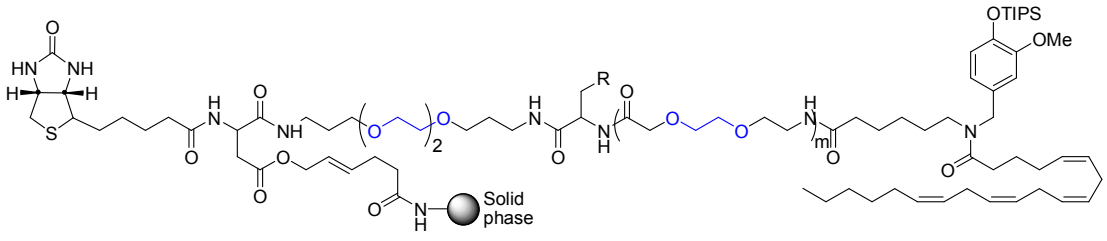


**Figure 2.3b: PEG spacers of varying lengths were used in a membrane receptor probe**

An example from Blais and co-workers describes the attachment of *meso*-tetraphenyl porphyrins to a number of glycosides *via* a diethylene glycol linker (Fig 2.3c).[72] The aim of

this work was to study the photoefficiency of these probes for potential Photodynamic Therapy treatment of retinoblastinomas.

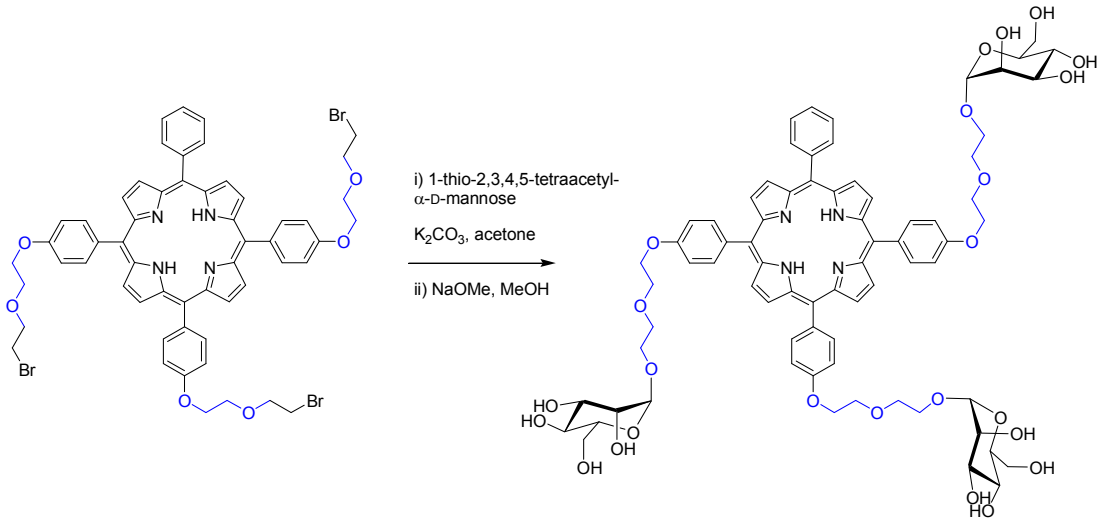


**Figure 2.3c: diethylene glycol spacers were used in this probe for the potential treatment of retinoblastomas**

An example using PEG as a linker attached to a naphthyl group is described in a 2005 paper by Nishimura and co-workers concerning the design and synthesis of novel inhibitors for a human β−1,4-galactosyltransferase.[73] Two inhibitors were synthesised using ethylene glycol spacers (Fig 2.3d), with one inhibitor carrying amide and ester bonds to attach the sugar and naphthyl moiety to the chain (16a, 16b), and the other having simple ether linkages (16c). This report is of particular interest to us as it involves a glycosyl transferase which performs the opposite function to glycosidases in the body, though with a similar mechanism of action. The inhibitors have similar features to our planned probes, though our intention is not to inhibit the β-galactosidase.

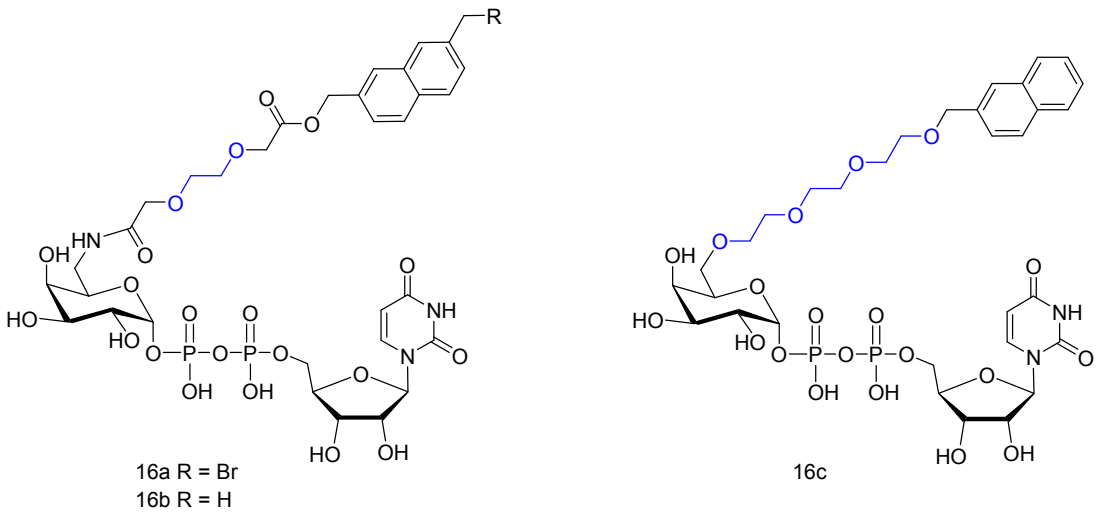


**Figure 2.3d: Use of a PEG spacer in an inhibitor for human β-1,4-galactosyltransferase**

Our design would use the simplest PEGs, ethylene- and diethylene glycols, as linkers between methyl glucoside and the naphthyl sensitiser, and to install these tether molecules using a Williamson etherification. This new synthetic route also meant that a convergent strategy could be used in the synthesis, making the operation more efficient than our previous ideas as each probe would be made from common precursors, the *p*-methoxybenzyl protected sugar **17**. As shown in Figure 2.3e, the simplest probe would be made by installation of the naphthyl group at C6 of the methyl glucoside by a Williamson ether reaction between the sugar and 2-bromomethylnaphthalene. This is a common procedure as the naphthyl group can be used as an orthogonal alcohol protecting group to PMB ethers, which can then be selectively removed. Using hydrogenolysis to remove the PMB groups would actually preferentially remove the naphthyl group. Using CAN removes the PMB ethers, leaving the naphthyl group intact.[74]

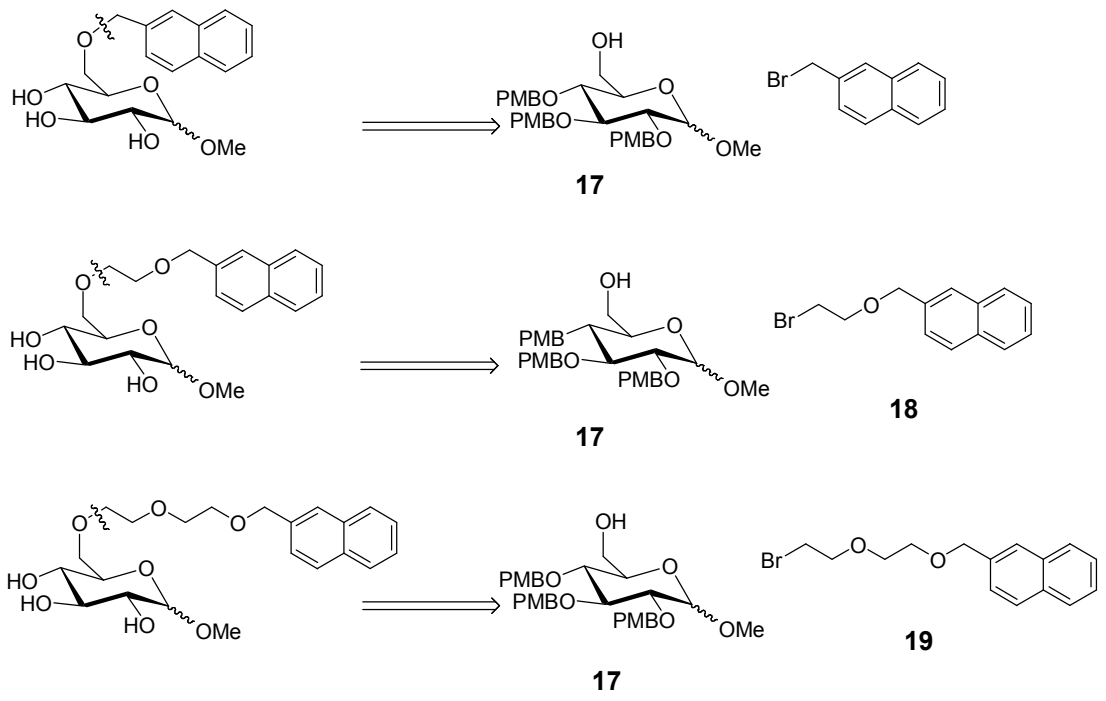


**Figure 2.3e: Retrosynthesis of our three target methyl glucosides featuring ether linkages of different lengths**

The other two glucoside-based probes featuring the longer EG and DEG linkers would be made using the components shown in Figure 2.3e (synthesis of these naphthyl linkers is described later). In keeping with the synthesis of the simplest probe we would functionalise our EG and DEG naphthyl tethers as bromides and use a Williamson etherification to attach these to an appropriate methyl glucoside. There is a potential side reaction when using the longer tether molecules which is due to E2 elimination, as shown in Figure 2.3f.

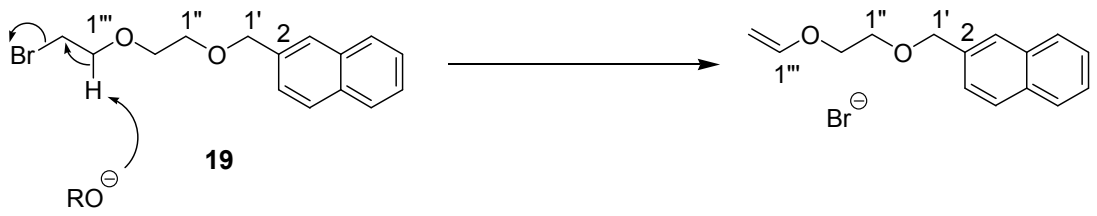


**Figure 2.3.f: Potential elimination side reaction when using the two naphthyl linkers 18 and 19**

Examining work from Nishimura and co-workers (Figure 2.3g),[73] who had installed a PEG naphthyl tether onto C6 of UDP galactose from a chloride-functionalised tether molecule we

had confidence that this side reaction could be minimised. We proceeded with the reaction, knowing that optimising the reaction conditions with the help of literature precedent would hopefully minimise this potential side reaction.

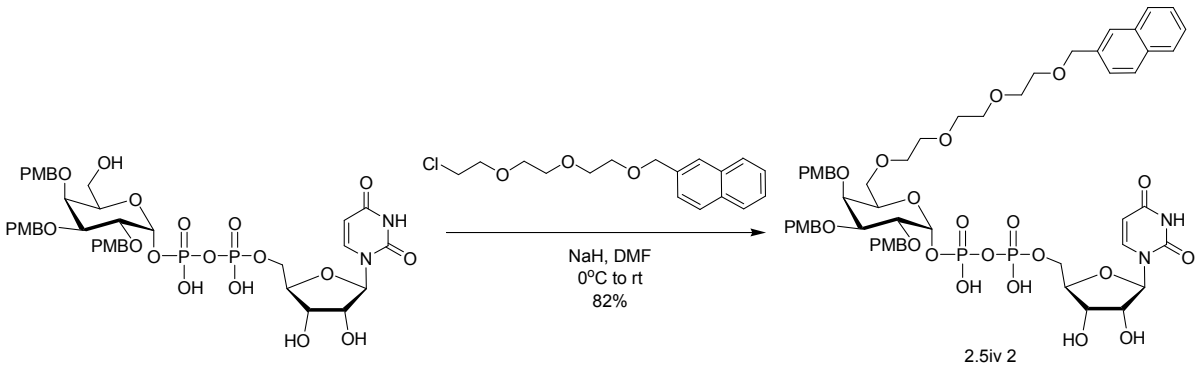


**Figure 2.3g: Synthetic method for the attachment of a halo polyethylene glycol naphthyl group on C6 of a galactoside**

## 2.3.1 Synthesis of Methyl-(2,3,4-*O*-*p*-methoxylbenzyl)-D-Glucopyranoside

### 2.3.1.1 Use of the trityl group to protect C6 of methyl glucoside

At this point we could have gone back to our earlier work on TBDPS protected methyl glucose (Section 2.2.1), but we decided to try a selective trityl protection instead. TrCl is significantly cheaper than the TBDPSCl used to make the compounds in Figure 2.2.1l and does not require handling under an inert atmosphere. Trityl ethers are commonly used as bulky protecting groups in carbohydrate synthesis displaying the expected preference for primary alcohols.[75, 76] The preference of trityl ethers for C6 of $\alpha$-methyl glucosides was first noted in 1926 by Helferich in a report published in *Annalen*.[77] This protecting group also works well as an orthogonal protecting group to PMB ethers despite the acidic conditions that are used to remove the trityl group. Generally a strong acid, such as HBr in acetic acid is

required to deprotect benzylic ethers, but trityl ethers are known to be labile to dilute acetic acid.[78] Thus, the PMB ethers should survive the mildly acidic conditions required for removal of the trityl group.

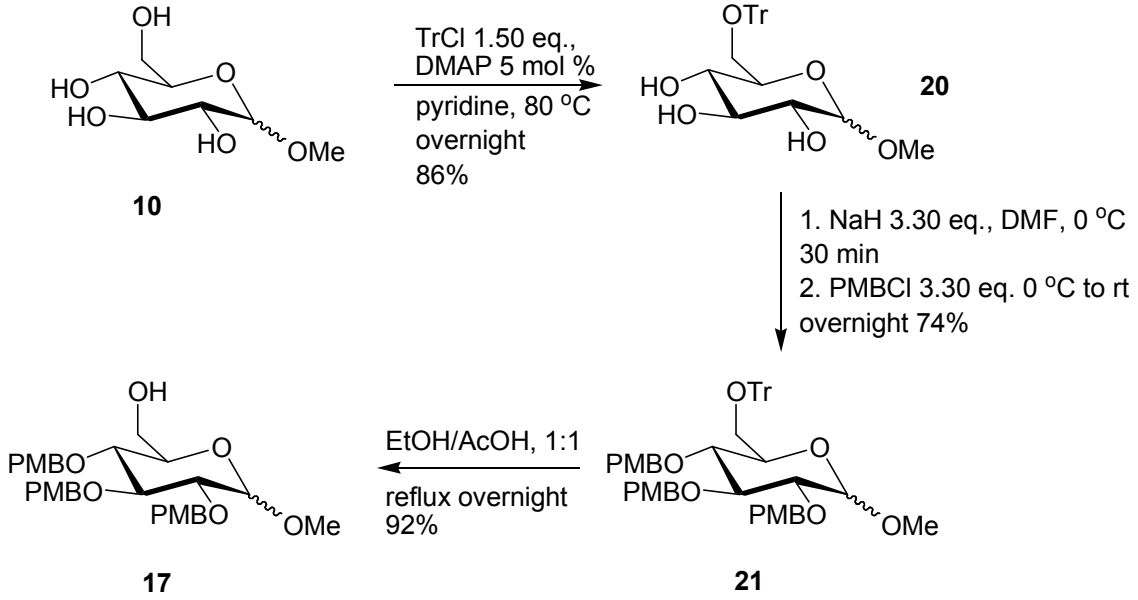


**Figure 2.3.1.1a: Trityl ether approach to a selectively C6 deprotected PMB ether 17**

The reaction scheme shown in Figure 2.3.1.1a was based upon similar work on $\alpha$-methyl mannoside by Fairbanks and coworkers[79] which details the entire process of a selective protection/deprotection strategy to access a free OH at C6 of the sugar.

Trityl protection of **10** using a classical method as detailed in Fairbanks' paper proceeded reasonably well in yields ranged between 63% and 86% which was comparable to the 75% yield for this reaction on an $\alpha$-methyl mannoside. The trityl-protected methyl glucoside was isolated as a mixture of two anomers (1.0:0.8 mixture of $\alpha$:$\beta$ anomers) which were inseparable by column chromatography at this stage. Initial attempts at the installation of the PMB ethers as described in Section 2.3.1 afforded compound **21** in a range of yields from 39% – 58%, which were unsatisfactory. At this point we invested in a bottle of 'extra-dry' DMF, the use of which raised yields to a maximum of 74%. Even though separation was

possible by careful column chromatography **21** was isolated as a mixture of anomers, except for characterisation purposes. Compound **21** was therefore carried through to the de-tritylation as a mixture of anomers as it turned out to be more practical to separate the anomers after the trityl group had been removed.

The Tr group was removed by heating the trityl ether **21** overnight in a 1:1 mixture of AcOH and EtOH. After the reaction was complete (very obvious by TLC stained with ammonium molybdate dip, as the characteristic yellow colour of the Tr group had been removed from the intense blue/violet of the PMB protected sugar). Work up furnished the desired alcohols **17a** and **17b** as a mixture of anomers in a very satisfying 92% yield. This was followed by a very careful column to separate the two anomers for characterisation and use in subsequent experiments.

**Summary**

With an effective and reliable route to our target compounds **17** in hand, work progressed on to installing the naphthyl group at C6 of the methyl glucoside. The next stage was to synthesise the naphthyl linker compounds and then attach them to 6-hydroxy sugar **17** in a Williamson ether process.

### 2.3.1.2 Synthesis of naphthyl tethers using ethylene- and diethylene glycol

As discussed at the beginning of Section 2.3 we planned to make a small family of naphthyl-functionalised methyl glucosides, which were related by using ether linkages of different lengths as the linkers (Figure 2.3.1.2a)

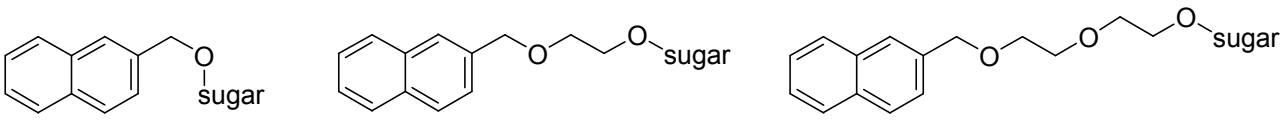


**Figure 2.3.1.2a: Naphthyl linker target compounds**

Ordinarily the purpose of the tether in fluorescent probes is to separate the chromophore from the point of recognition, such that it does not interfere with the molecular recognition event. So, too short a tether may inhibit the action of the enzyme, rendering the probe ineffectual, but in our case, the tether should not be too long as that may make the chromophore too remote to sensitise lanthanide luminescence (see Sections 1.4 and 1.5). For our initial studies we chose to investigate three different tether lengths of a similar type in order to determine if the enzyme was capable of processing the labelled methyl glucosides.

Enzymes function in an aqueous environment. Substrates, whether natural or not, must be water-soluble to a good degree in order for the enzyme to work upon them. The methyl glucoside probes we have designed have three free OH groups which will aid water solubility, but they also have a naphthyl group which is hydrophobic. By using an ether chain for the tether, rather than a simple alkyl chain, we should enhance the water-solubility of the probe so that it can be used under biological or near-biological conditions for the enzyme experiments.

**Synthesis of naphthyl tethers**

The shortest naphthyl tether used in the project is the commercially available 2-bromomethylnaphthalene (2BMN) and this same compound also forms the basis of our route to the other two naphthyl tethers. Whilst it is commercially available it is also rather expensive and somewhat prone to decomposition when exposed to light, heat and air. It was felt that synthesis of 2BMN from the much less costly 2-methylnaphthalene in a radical

bromination with NBS would be prudent. There is ample literature for this reaction, the overwhelming majority of which use $CCl_4$ as the solvent, which is expensive and highly carcinogenic. We decided to go ahead with the radical bromination using a method described by Burke[80] (Figure 2.3.1.2b), which is a rare example of the use of $CH_2Cl_2$ as the solvent, whereby the desired target is obtained in 78% yield.

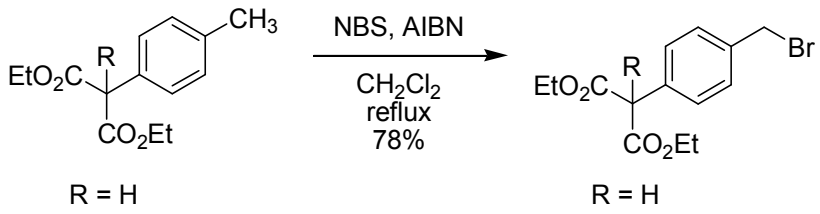


**Figure 2.3.1.2b: This bromination of an aryl methyl group defies convention as it is carried out in $CH_2Cl_2$ rather than $CCl_4$**

The work up described by Burke was to cool the reaction and remove the volatiles by rotary evaporation prior to purification by column chromatography. However, we referred to another paper[81] on the radical bromination of 2-methyl naphthalene (using $CCl_4$ rather than $CH_2Cl_2$) which gave more efficient work up and purification process. By cooling the reaction mixture to 0 $^oC$, the succinimide crystallised out, was filtered off and a basic work up performed prior to removal of solvent under reduced pressure. The residue was then recrystallised from EtOH to furnish 2BMN in 90% yield.

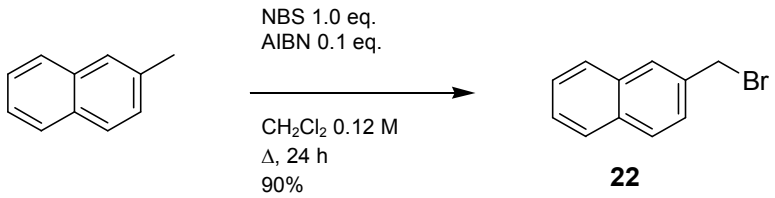


**Figure 2.3.1.2c: Synthesis of 2-bromomethyl naphthalene**

With access to pure and relatively inexpensive 2BMN (**22**), it was now possible to work on the synthesis of the remaining 2 naphthyl tethers. The retrosynthesis for our targets is shown in Figure 2.3.1.2d.

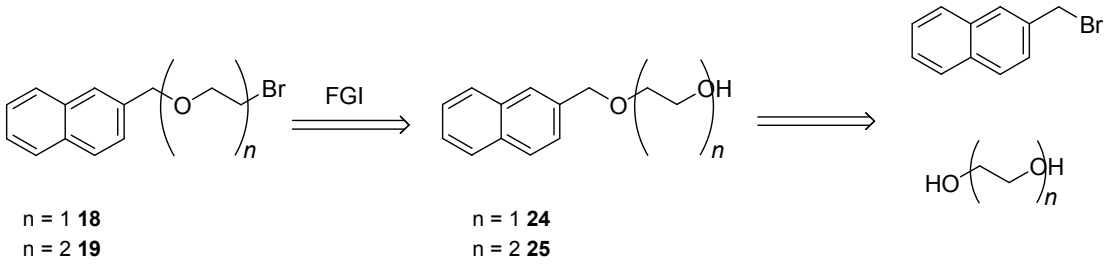


**Figure 2.3.1.2d: Retrosynthetic analysis of the ethylene glycol-based naphthyl linkers**

In the forward synthesis (Figure 2.3.1.2e), a silver(I)-mediated alkylation would be used to install ethylene- and di-ethylene glycol onto 2BMN. This could have been done *via* yet another Williamson etherification, but may well have led to di-functionalised glycol even when using stoichiometric amounts of base and bromide. A paper by Sauvé[82] deals with highly selective silver(I) oxide-mediated monoprotection of symmetrical diols, which is exactly what we wanted to do. In this paper, yields for selective mono protection of ethylene glycol with benzyl bromide were 70%. Yields in our hands varied according to substrate but were generally satisfactory, even up to 96% when using diethylene glycol. Bromination of the remaining alcohol was achieved in a typical fashion using $PPh_3$ and $CBr_4$[83] and normally proceeded in near quantitative yield.

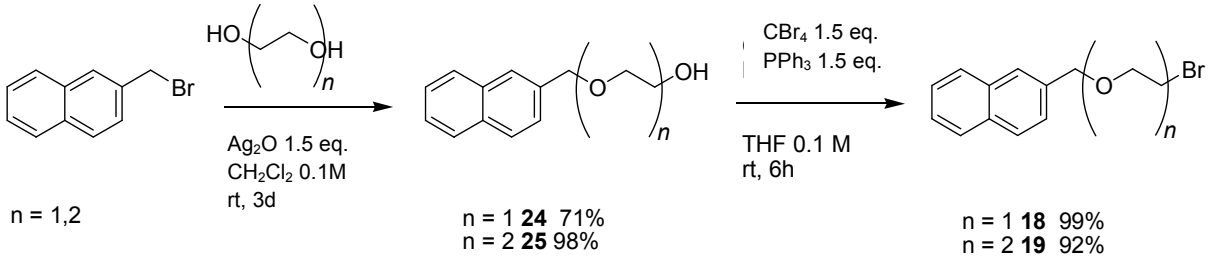


**Figure 2.3.1.2e: Successful synthesis of the target naphthyl-linker bromides**

### 2.3.1.3 Synthesis of naphthyl-labelled methyl glucosides

As discussed at the beginning of this Section, the naphthyl linkers would be attached to the methyl glucosides **18** using a Williamson etherification (Figure 2.3.1.3a).

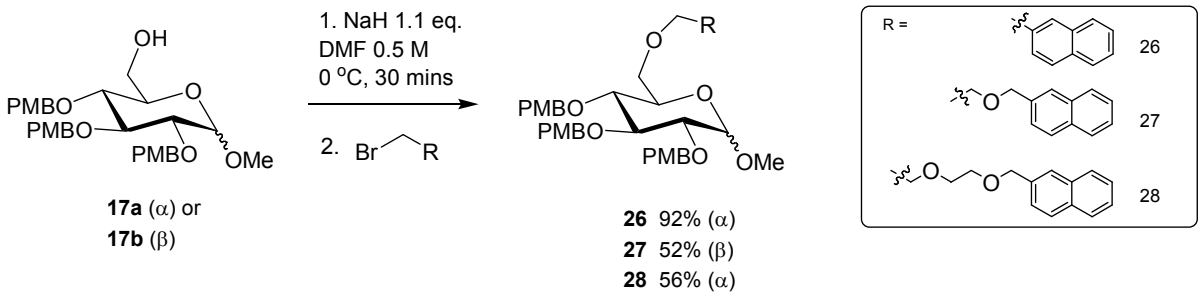


**17a** (α) or
**17b** (β)

**26** 92% (α)
**27** 52% (β)
**28** 56% (α)

**Figure 2.3.1.3a: Attachment of the naphthyl linkers onto the selectively deprotected methyl glucosides**

In order to optimise yield and avoid side-reactions, the bromide was added 30 minutes after the addition of NaH to the solution of the sugar, this is to achieve maximum formation of the alkoxide and minimise reaction of hydride with the bromide when it is added later on.

There is a significant disparity in the yields when attaching 2-bromomethylnaphthalene to the sugar compared to the longer naphthyl linkers. The attachment of the ethylene- and diethylene glycol naphthyl linkers to glucosides **17a** (α) and **17b** (β) gave yields of just over 50%, compared to 92% for the simple 2-bromomethyl naphthalene. This can be rationalised due to the difference in reactivity of the benzylic $CH_2$ on 2-bromomethylnaphthalene compared to the Br-$CH_2$ through which the longer naphthyl linkers react. In 2-bromomethylnaphthalene, the halide is subject to the benzylic effect[84] as the halide is adjacent to a π-bond and thus has increased reactivity towards $S_N2$ substitution. In the case of the longer linkers, the $CH_2$ through which the reaction proceeds is not adjacent to a π-bond and is in fact more susceptible towards elimination by the alkoxide anion which leads to the lower yield of target material.

For ease of characterisation and storage, we chose to remove the PMB groups and re-protect the secondary alcohols as acetates. Removal of the PMB groups was done oxidatively using CAN as this does not remove the naphthyl group.[74] Acetylation of the crude, deprotected sugar was carried out according to our general method (Exptl. Section Method A) using pyridine and acetic anhydride and stirring overnight. Final purification was carried out by column chromatography and yields over these two steps were quite good, ranging from 51-64% (Figure 2.3.1.3b).

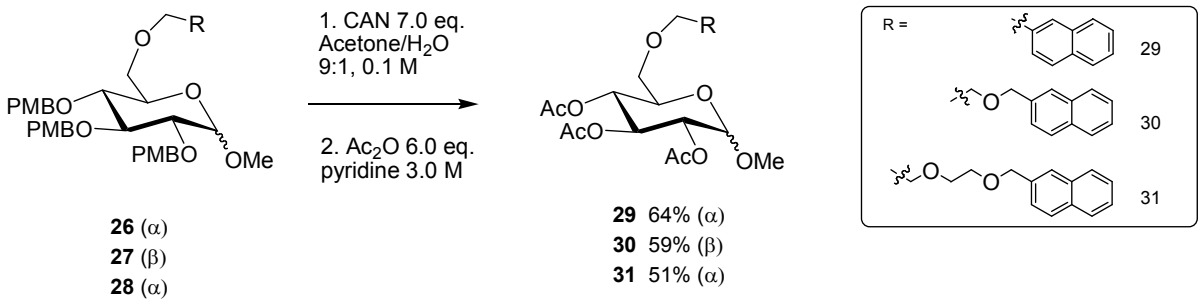


**26** (α)
**27** (β)
**28** (α)

**29** 64% (α)
**30** 59% (β)
**31** 51% (α)

**Figure 2.3.1.3b: Acetylation of the target naphthyl-functionalised methyl glucosides prior to characterisation.**

Full characterisation was carried out and assignment using 2D NMR spectroscopy confirmed the structures, supported by mass spectrometry and elemental analysis. COSY and HSQC were used to assign the resonances in the $^{1}$H- and $^{13}$C-NMR spectra. The protons on the glucose ring were assigned using COSY starting from the anomeric proton – a 1H doublet. COSY also allowed us to single out the resonance due to the benzylic $CH_2$ *AB* system and from that facilitated assignment of the protons in the ethyl chains in compounds **29** and **30.** Subsequent examination of HSQC spectra then allowed us to assign the $^{13}$C- NMR spectra.

Having fully characterised the three sugars protected as acetates, these protecting groups must be removed before embarking on the enzyme studies, which was achieved as shown in Figure 2.3.1.3c (Exptl Section Method B). Yields were high, as expected, and the sugars

needed no further purification after work up. Characterisation of the three compounds was carried out, NMR data was recorded in $d_4$-methanol but a full assignment was not possible due to the close proximity of the sugar C-H peaks in the spectra. The complete assignment of the acetates described above had previously confirmed the location of the naphthyl group on C6 of the methyl glucosides and so such detailed characterisation was deemed unnecessary for the deprotected sugars.

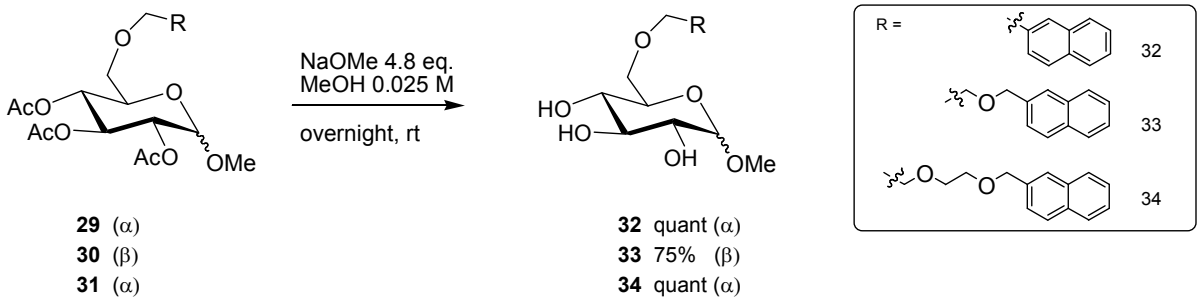


**29** (α)
**30** (β)
**31** (α)

**32** quant (α)
**33** 75% (β)
**34** quant (α)

**Figure 2.3.1.3c: The final stage – deacetylation of our naphthyl-functionalised methyl glucosides in preparation for the enzyme experiments.**

## 2.4 Summary

We have investigated a number of approaches to installing a chromophore at C6 of methyl glucose and decided that the most appropriate linking moiety to use was an ether linkage as they have proven biocompatibility. They were also the most efficient to make synthetically, compared to the initial work on amides *etc.*, as the reaction sets to our target molecules (**32, 33, 34**) followed the same synthetic procedures.

The optimal way to attach a naphthalene chromophore onto the sugar *via* an ether linkage was to bring together the sugar and the naphthyl-functionalised linkers as the final step. To make the naphthyl-functionalised linker, we used a silver (I) mediated coupling reaction between 2-bromo methyl naphthalene and ethylene- or diethylene glycol, which proved an effective method to prepare the longer naphthyl linkers. The resultant alcohols were then

converted to bromides and attached to the selectively protected methyl glucoside **17** using the Williamson etherification. Characterisation of the acetyl protected sugars confirmed their structures and they were then de-acetylated in preparation for the enzyme experiments, which is the focus of the next chapter

# 3. Investigation into Transglycosylation using Novel Naphthyl-Functionalised Methyl Glucosides with the β-Galactosidase from *B. circulans*

Whilst our focus is on a probe for β-galactosidase activity (hydrolysis), in order to investigate suitable labelled substrates for the enzyme more rapidly we decided to take advantage of the glycosyl transfer activity common to glycosidases. A substrate that can be made by a glycosidase will also be a substrate for the enzyme when it is working in its normal sense. So, if we can make naphthyl-functionalised disaccharides using the enzyme they will also be substrates for hydrolysis.

We chose to probe the *B. circulans* enzyme with the three naphthyl-labelled methyl glucosides (**32**, **33** and **34**) discussed in Chapter 2 (Figure 3a) and use either GalO*p*NP [§] or lactose as the glycosyl donor. The glycosidase active site should behave the same way towards acceptable substrates whether operating as a glycosyl hydrolase or as a catalyst for transglycosylation. So, by using the enzyme to make a disaccharide containing our labelled methyl glucoside we can probe which, if any, of these molecules is the best candidate for the final probe.

[§] Synthesis of known compound GalO*p*NP is described in the Experimental Section compounds 54 - 57

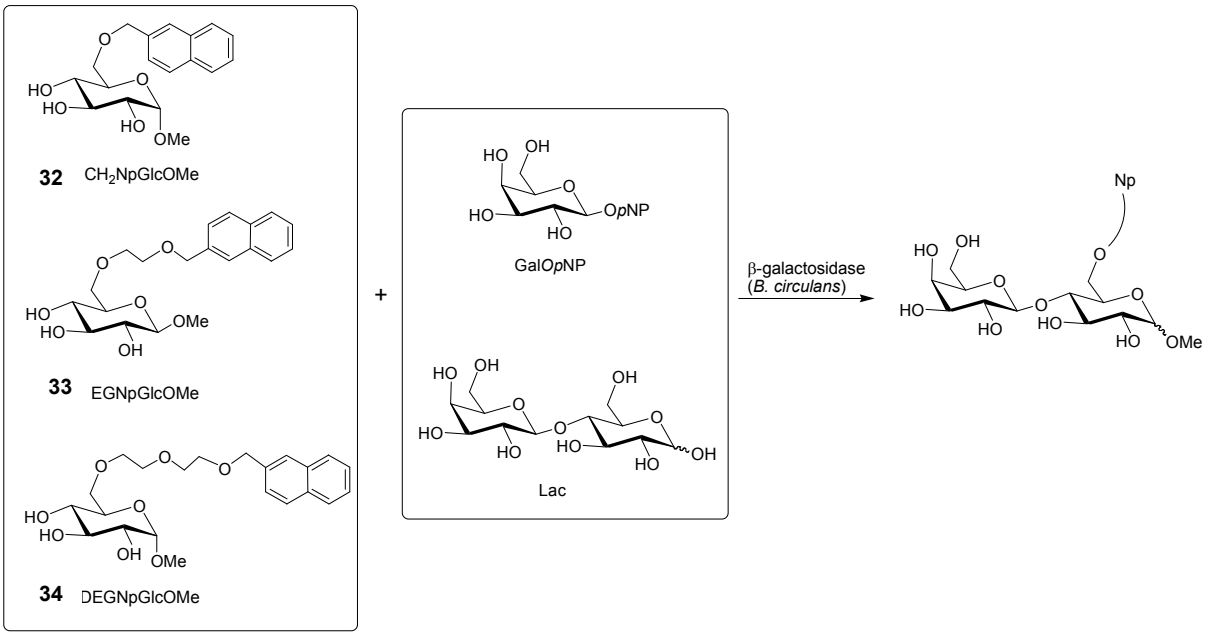


**Figure 3a: General scheme showing the basis of our enzyme experiments; the novel glucosides will each be used in a transglycosylation reaction with the enzyme to test if it will accept them as substrates**

To develop a suitable method for this β-galactosidase-catalysed transglycosylation reaction, we scoured the literature on transgalactosylations carried out using the enzyme from *B. circulans*. We found a wide variety of literature about the enzyme but we were most interested in those papers describing the use of the enzyme in the synthesis of glycosides as the first step on the way to our probe would be to use the enzyme to make disaccharides containing our naphthyl-functionalised sugars.

## 3.1 Glycoside Synthesis Using the β-Galactosidase from *B. circulans*

The enzyme-catalysed approach to the synthesis of glycosides provides a very elegant and efficient route to complex biomolecules for further study and biological evaluation as potential disease therapies. It is a potentially cost-effective procedure, simple to perform and also

very attractive for industrial scale preparation as a lot of the enzymes under investigation are important in the food industry so can be produced on large scale. Crucial for use in industry is the immobilisation of the enzymes on a solid support, which stabilises the enzyme, allowing the catalyst to be reused thereby streamlining the industrial process.[16,85]

There are numerous examples of the use of glycosidases to make oligosaccharides, some of which are discussed in Section 1.3.3.1. Here I will concentrate on the use of the *B. circulans* enzyme to make glycosides. Using the examples in the literature and following a few key rules that seem to apply throughout the sphere of β-galactosidase-catalysed carbohydrate synthesis furnished us with a technique for working with our novel substrates and the β-galactosidase from *B. circulans*.

The decision to use the β–galactosidase from *B. circulans* was heavily influenced by the volume of research that has been carried out on this enzyme. It has been investigated extensively for its regioselectivity during trans-glycosylation. Our probe is based upon lactose which is a β(1→4) linked disaccharide. The *B. circulans* enzyme displays good β(1→4) regioselectivity when used to synthesise oligosaccharides using a galactosyl donor and a glucosyl acceptor, but the effect can be enhanced by using particular acceptors and reaction conditions (Section 3.2). This enzyme is also widely reported to be able to accept a variety of substrates, particularly in the glycosyl acceptor area of the active site, which we hoped would work to our advantage as our substrates are sugars functionalised with bulky naphthyl groups (see Section 2.1).

The scope of this research does not extend to the synthesis of long-chain oligosaccharides or the development of glycosidase inhibitors for medical purposes. We are simply taking advantage of the reverse hydrolysis facility of the β-galactosidase from *B. circulans* in order to begin development of a future probe for galactosidase activity.

As discussed in Chapter 2, our probe will feature a disaccharide which is functionalised at C6 of both of the monosaccharide units. This is a hitherto unexplored area of labelling and monitoring to use with glycosidases. To our knowledge, the ability of the β-galactosidase from *B. circulans* to accept sugars modified at C6 with a large organic group has not been investigated. Our work on this for the development of our luminescent probe is discussed in this section.

Crout *et al.* first used the β-galactosidase from *B. circulans* to synthesise the core trisaccharide of ovarian cyst fluid mucosin, β-D-Gal-(1→4)-β-D-GlcNAc-(1→6)-D-GalNAc (Figure 3.1.a).[49]

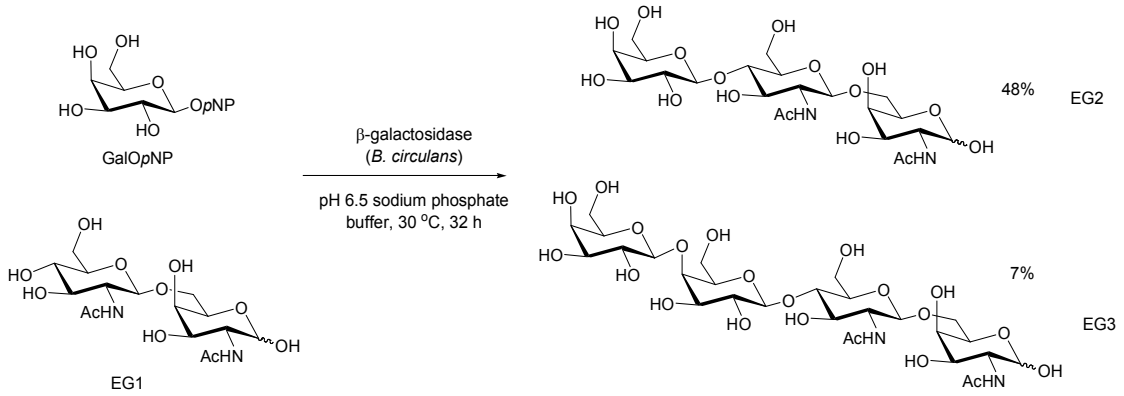


**Figure 3.1a: Synthesis of β-D-Gal-(1→4)-β-d-GlcNAc-(1→6)-D-GalNAc using the β-galactosidase from *B. circulans***

Disaccharide **EG1** was made using the β-*N*-acetyhexosaminidase from *Aspergillus oryzae*. **EG1** was then used to make the target trisaccharide **EG2**, which contains a β(1→4) link, using the β-galactosidase from *B. circulans* in 48% yield. A side product from this reaction was tetrasaccharide **EG3**, which had an added galactose moiety attached via a β(1→4) link. The 'remarkable' selectivity of the enzyme is commented on with respect to the formation this tetrasaccharide. The galactose moiety which has been added onto **EG1** to form **EG2** has a sterically unencumbered 6-OH group. However, the β-galactosidase from *B. circulans* asserts specificity to cause a glycosyl transfer to the 4-OH group of the galactose moiety. The 4-OH group is thought to be one of the least reactive positions in glycosyl acceptors.

The procedure was then assessed for generality by carrying out a transfer between GalO*p*NP and lactose to yield β-D-Gal-(1→4)-β-D-Gal-(1→4)-D-Glc in 52% yield. The conditions for this reaction were a 6:1 ratio of acceptor to donor, in pH 5.0 NaOAc buffer at 30 °C for 3.5 h.

Thiem *et al.* carried out a comprehensive investigation of the conditions needed to promote β(1→4) transglycosylations shown in Figure 3.1b.[86] His intention was to synthesise galactose-containing disaccharides using the β-galactosidase from *B. circulans*. In this case, the glycosyl donor is Gal*Op*NP and the glycosyl acceptors are GlcNAcαOAll, GlcNAcβOAll, GalαOAll, GalβOAll and GalβSPh. The group looked at the effect of the donor-acceptor ratio, buffer pH, reaction time and temperature. The optimised conditions were found to be 1:7.5 donor/acceptor mixture incubated in a 1:1 mixture of sodium phosphate buffer/MeCN. 0.7 – 1.0 U of the enzyme were required with heating at 30 °C for 72 h. The reaction was stopped by heating for 10 minutes at 90 °C which denatures the enzyme.

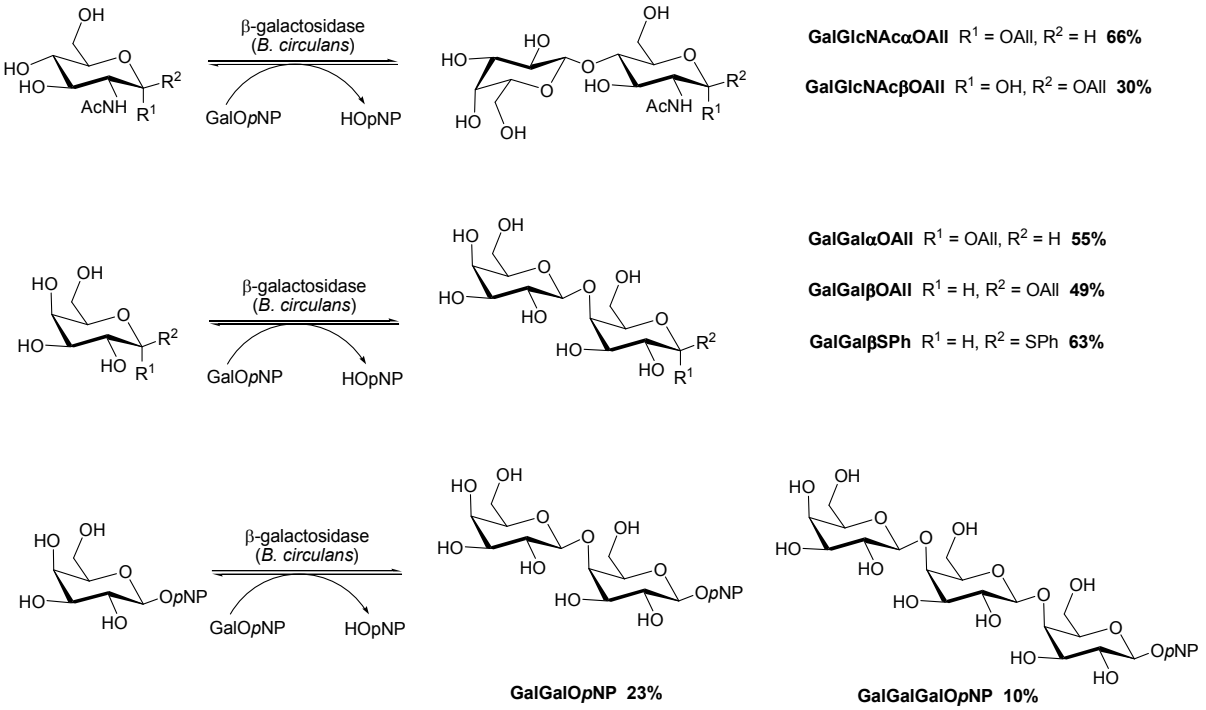


**Figure 3.1b: Thiem's work on optimised conditions for β(1→4) transglycosylations**

The β(1→4) linked disaccharides were produced regioselectively in yields ranging from 30 – 60%. These are high yields when one considers that a 'chemical' synthesis of such compounds would take a number of steps in order to gain the β(1→4) glycosidic linkage. It would also take much longer than 72 hours to do the entire synthesis due to the extensive protection-deprotection strategy involved.

A point to note is that the enzyme catalyses the reaction between our intended glycosyl donor GalO*p*NP, to form di- and tri-saccharides (final scheme in Figure 3.1b). This must be borne in mind for our synthesis as a competing reaction.

Later work by Thiem involved the regioselective synthesis of galactosylated tri- and tetra-saccharides using the β-galactosidase from *B. circulans* (Figure 3.1c).[47] This report contains a method for the transglycosylation between methyl-α-D-glucose and GalO*p*NP or lactose. This is more analogous to our planned reaction than the previous paper as the glycosyl acceptor is methyl glucose.

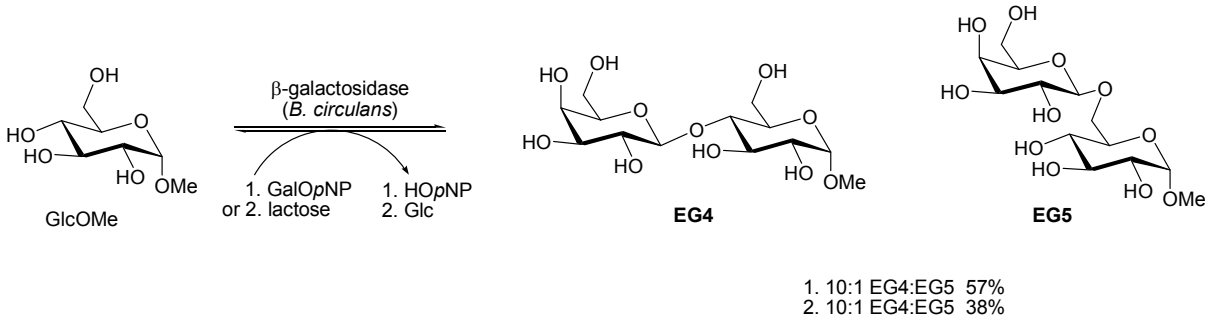


**Figure 3.1c: Synthesis of β(1→4) and β(1→6) disaccharides using the β-galactosidase from *B. circulans***

The procedure for these reactions used a ratio of 10:1 glycosyl acceptor to glycosyl donor, pH 5.0, 50 mM NaOAc buffer and 1.2U/mmol acceptor of the enzyme. The reaction mixture was incubated at 55 $^{o}$C for 2 hours and then the reaction terminated by heating at 90 $^{o}$C for 10 minutes. The yield of disaccharides starting from GalO*p*NP as the glycosyl donor was 57% and from lactose was 38% with a 10:1 ratio of β(1→4) : β(1→6) glycosidic linkages.

In this case, the glycosidic linkages produced were β(1→4) and β(1→6), though the former was the major product from the reaction. This result is in contrast with the previous work where only β(1→4) glycosidic bonds were made. Since our glycosyl acceptor has a naphthyl group attached at C-6 we might expect a β(1→4) linked disaccharide from our synthesis due to the proven regioselectivity of the enzyme. However, the possibility of β(1→2) and β(1→3) linkages cannot be ruled out as the bulky naphthyl substituent on our novel glucoside acceptors may change the way in which the acceptor sits in the active site of the enzyme. We began development of our own procedure for β-galactosidase-catalysed transglycosylation based upon these three reports.

## 3.2 Simple Trans-Glycosylation Experiments

Before starting our investigations into how the enzyme will treat our novel naphthyl-functionalised sugars it was important to gain experience of handling the enzyme. β-Galactosidases are used quite routinely by a number of research groups in oligosaccharide synthesis (as explained in Sections 1.3.3.1 and 3.1) so there is a good amount of experimental literature to start from. Our intention was also to use the enzyme in reverse, to *synthesise* a disaccharide thus proving that the enzyme will accept the modified monosaccharides, giving us evidence to suggest that the enzyme would accept a disaccharide probe with the same structural modifications.

Our initial aims were:

- To determine the activity of the enzyme we had been supplied with;
- To use the enzyme in some simple trans-glycosylation experiments with commonly used substrates (methyl glucose, *p*-nitrophenyl galactose, lactose);
- To determine the best conditions for transgalactosylation reactions involving our napththyl-functionalised methyl glucopyranosides.

### 3.2.1 Determining the Activity of the Enzyme

The 'activity' of the enzyme must be determined before starting the enzyme experiments. One unit of activity for a β-galactosidase is defined as "the amount of enzyme needed to release 1 μmol $min^{-1}$ of *p*-nitrophenol from *p*-nitrophenyl galactose".[86]

Determining the activity of the enzyme was done according to the method outlined by Thiem[86] by adding an aqueous solution of the β-galactosidase from *B. circulans* to a solution of synthesised *p*-nitrophenol β-D-galactose (GalO*p*NP) in 2.0 M sodium acetate buffer at pH 6.0 (see Experimental Section 5.3). When incubated 37 °C, the enzyme hydrolyses the glycosidic bond, thus releasing free *p*-nitrophenyl into solution (Figure 3.2.1a).

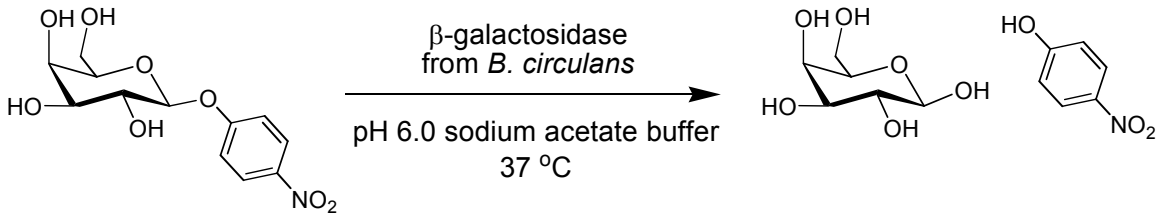


**Figure 3.1.1a: Hydrolysis of GalO*p*NP using the β-galactosidase from *B. circulans***

The solution of GalO*p*NP and enzyme was incubated for 15 minutes at 37 °C and 10 μL aliquots were taken at 1, 2, 4, 6, 8, 10 and 15 minutes to monitor the progress of the reaction. Each aliquot was diluted with 1 mL of 0.1 M NaOH solution, ensuring that enzyme was denatured immediately, stopping the hydrolysis reaction and enabling us to investigate the UV-vis spectrum of the released free *p*-nitrophenol. Since the $\lambda_{max}$ of free *p*-nitrophenol and that of GalO*p*NP are the same (302 nm), it is impossible to tell whether there is any free *p*-nitrophenol in solution until base is added, which deprotonates the phenol and shifts the $\lambda_{max}$ to 400 nm (Figure 3.2.1b). In practice, 15 minutes was an unnecessarily long time for running the experiment, as all of the GalO*p*NP was hydrolysed in one minute, so the figure below shows results up to 6 minutes only.

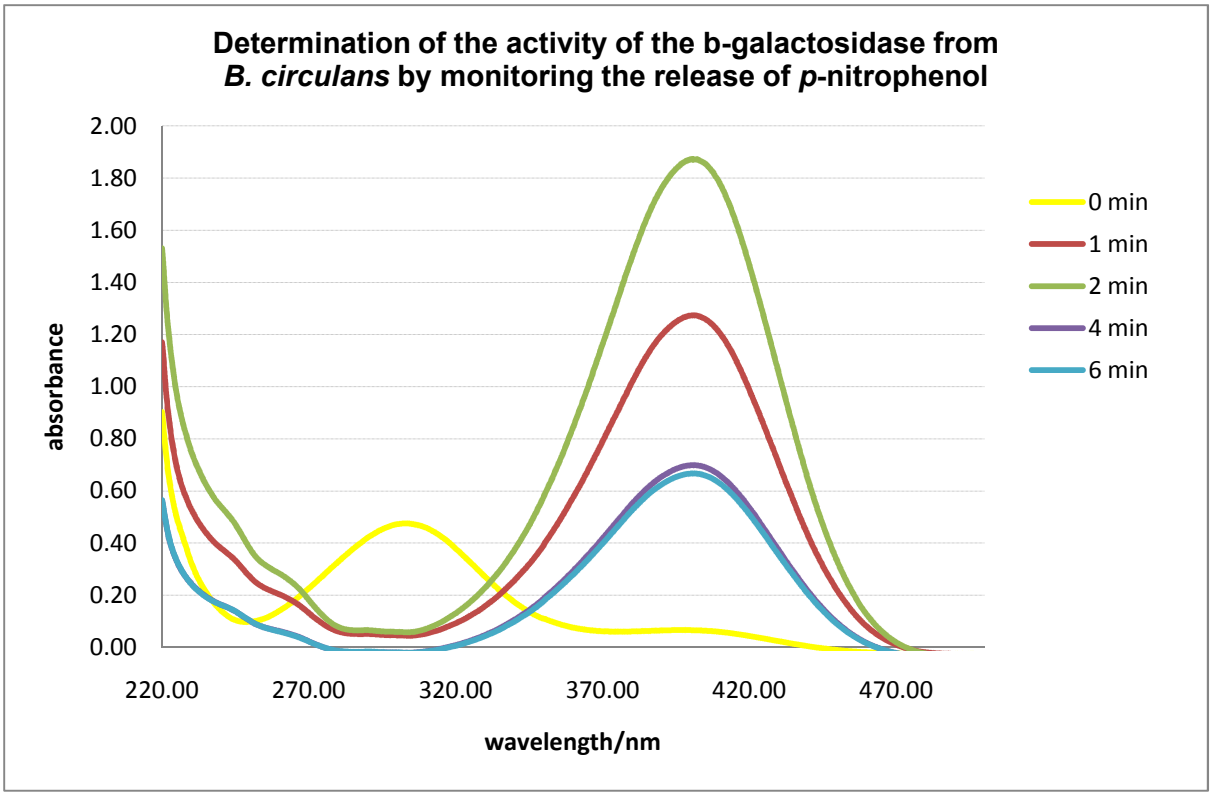


**Figure 3.2.1b: UV plot showing the hydrolysis of GalO*p*NP over time**

From the above graph it can be seen that at 0 minutes, prior to adding the enzyme, all of the UV signal is due to the yellow GalO*p*NP at 302 nm. Once the enzyme is added all of the GalO*p*NP is hydrolysed within one minute, as shown by the green line which has no absorbance at 302 nm but plenty at 400 nm – corresponding to the *p*-nitrophenolate ion hydrolysis product.

At this early stage of the proceedings the task of taking accurate 10 μL aliquots from the small reaction volume in use was rather difficult with the 200 μL pipettor we used at the time, hence the large difference in absorbance seen in Figure 3.2.1b. However, it is still clear that no GalO*p*NP was present in any aliquot taken after one minute. Since all of the GalO*p*NP in the reaction was hydrolysed within one minute, it was only necessary to determine how many moles were put into the reaction in the first place (rather than using the Beer-Lambert Law).

One unit of activity for our enzyme is thus defined as 3 mg as this is the amount of enzyme needed to hydrolyse 1 μmol of GalO*p*NP in 1 minute.

### 3.2.2 Making Disaccharides Using α-Methyl Glucose, *p*-Nitrophenol-β-D-Galactose and Lactose

The next stage would be to familiarise ourselves with the methods for the enzyme-catalysed transglycosylations. We elected to try two different procedures published by Thiem and Crout and compare the results. From this information we would then begin developing our own method. In the experiments, the glycosyl acceptor would be α-methyl glucose, and the glycosyl donors to be evaluated were to be *p*NP-galactose and lactose (Figure 3.2.2a).

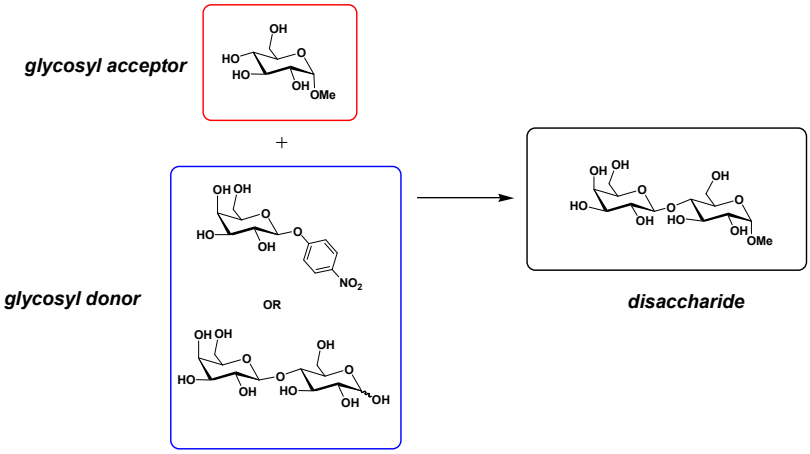


**Figure 3.2.2.1b: Schematic for the initial enzyme experiments**

The conditions of the two methods chosen for investigation are shown in Table 3.2.2b below.

| | Crout | Thiem |
|---|---|---|
| Acceptor/Donor ratio | 10:1 | 6:1 |
| Buffer | 50mM NaOAc pH 5.0 | |
| Reaction conc wrt acceptor | 1.7 M | 0.2 M |
| U β-galactosidase | 1.2 | 30 |
| Temp/$^{o}$C | 55 | 30 |
| Reaction time/h | 2 | 3.5 |

**Table 3.2.2b: Table showing the differences in the two methods that we would test in the trial transglycosylation reactions**

### 3.2.2.1 Testing Thiem's method

The first test reaction carried out was according to Thiem's method (see Exp Section 5.3 ENZ 1).[47] Upon addition of the enzyme to the stirring solution of GlcOMe and GalO*p*NP in pH 5.0 buffer at 55 $^{o}$C, the solution turned bright yellow, signalling hydrolysis of GalO*p*NP.

HPLC analysis of aliquots removed from the reaction mixture at regular intervals showed the appearance of new peaks from the aliquot taken at 5 minutes (see Table 3.2.2.1a) and accompanying graph Figure 3.2.2.1b). $\alpha$-GlcOMe has a retention time of 1.6 minutes, GalO*p*NP of 6.2 minutes.

| | Rel. Area % | | | |
|---|---|---|---|---|
| Reaction time/min | $t_r$ = 1.6 ($\alpha$-GlcOMe) | $t_r$ = 6.2 (GalO*p*NP) | $t_r$ = 7.0 prod. 1 | $t_r$ = 12.2 prod. 2 |
| 0 | 92.59 | 7.41 | 0.00 | 0.00 |
| 5 | 75.40 | 3.10 | 1.95 | 19.55 |
| 10 | 79.84 | 1.67 | 3.13 | 15.36 |
| 20 | 82.83 | 0.92 | 5.02 | 11.23 |
| 40 | 84.77 | 0.77 | 5.60 | 8.86 |
| 80 | 82.91 | 0.94 | 6.39 | 9.76 |
| 120 | 85.61 | 0.92 | 6.02 | 7.46 |

**Table 3.2.2.1a: ENZ 1 tabulated HPLC data**

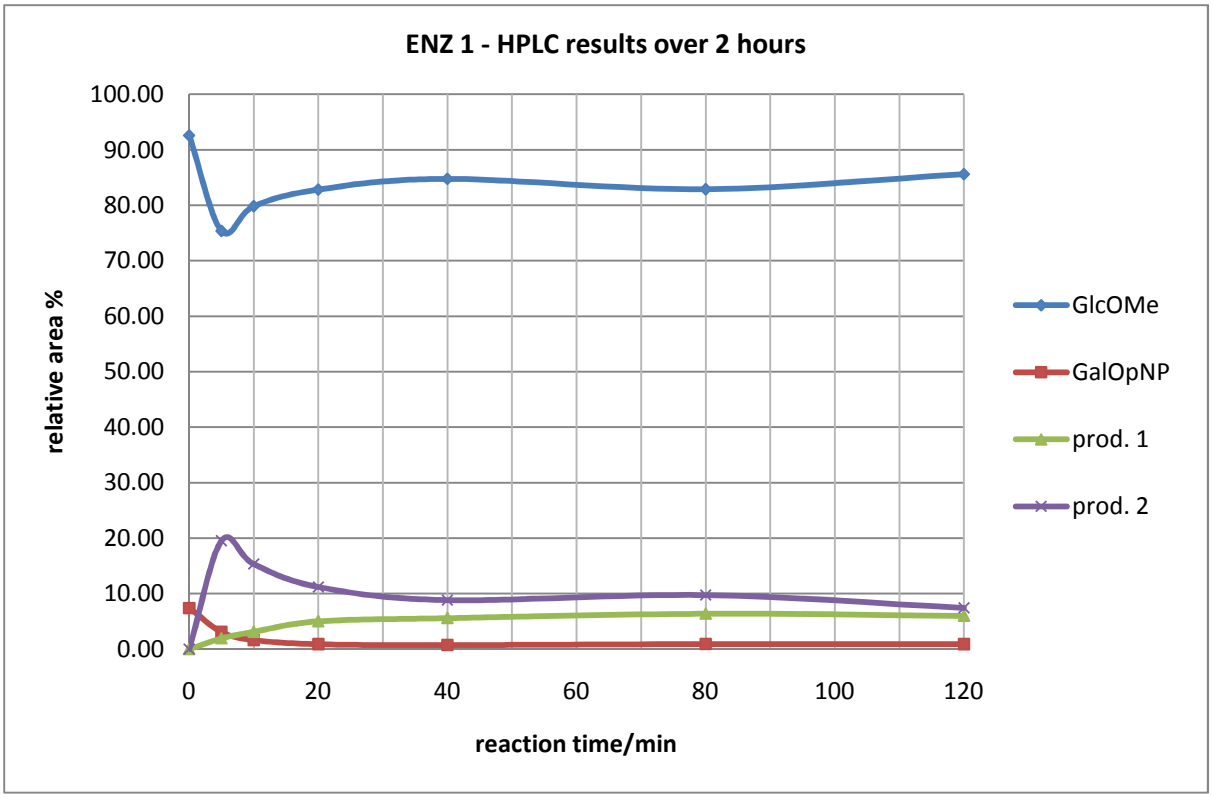


**Figure 3.2.2.1b: ENZ1 – graph showing the changes in the relative area % ofpeaks found by HPLC over 2 hours**

The graph above shows that the peak at $t_r$ = 6.2 minutes corresponding to GalO*p*NP diminishes quickly, within 20 minutes of the enzyme being added. The peak at $t_r$ = 1.6 minutes initially dropped within the first 5 minutes and then began to increase again. A plateau of the peak is seen from 20 minutes onwards. Meanwhile, two new peaks appeared at $t_r$ 7.00 and 12.2 = minutes. The former seemed to plateau at 20 minutes, while that at 12.2 minutes showed a sharp increase between $t_r$ = 0 and 5 minutes and then decreased in intensity.

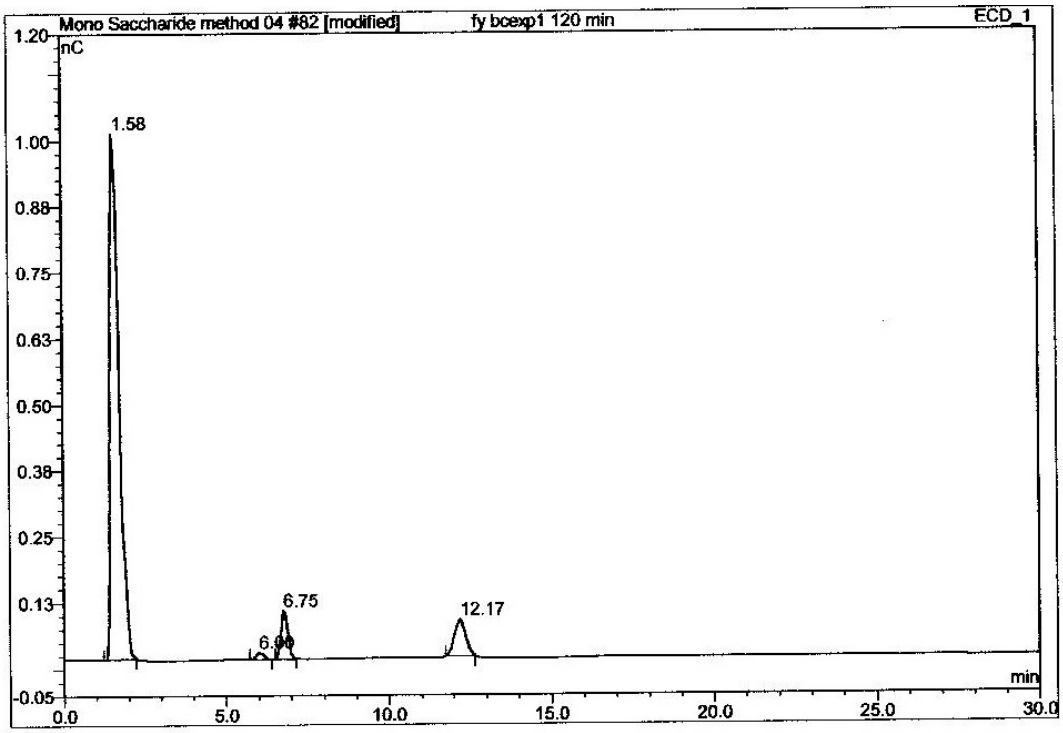


| No. | Ret.Time min | Peak Name | Height nC | Area nC*min | Rel.Area % | Amount | Type |
|---|---|---|---|---|---|---|---|
| 1 | 1.58 | n.a. | 0.995 | 0.318 | 85.61 | n.a. | BMB* |
| 2 | 6.00 | n.a. | 0.012 | 0.003 | 0.92 | n.a. | BMB* |
| 3 | 6.75 | n.a. | 0.090 | 0.022 | 6.02 | n.a. | BMB* |
| 4 | 12.17 | n.a. | 0.069 | 0.028 | 7.46 | n.a. | BMB* |
| Total: | | | 1.166 | 0.371 | 100.00 | 0.000 | |

**Figure 3.2.2.1c: ENZ 1 HPLC trace; reaction time = 2 hours**

Analytical HPLC separation of the final reaction mixture at 2 hours was carried out to isolate the peaks and determine what each one contained. Due to problems with the solvent pump which we experienced using the ECD-HPLC, the retention time of the peaks were often not consistent between experiments although they were consistent within experiments. Because of this, it was better to look at the order in which the compounds eluted during HPLC rather than compare retention times between different experiments. Comparison of Figures 3.2.2.1c and 3.2.2.1d shows the difference in retention times between one day and the next.

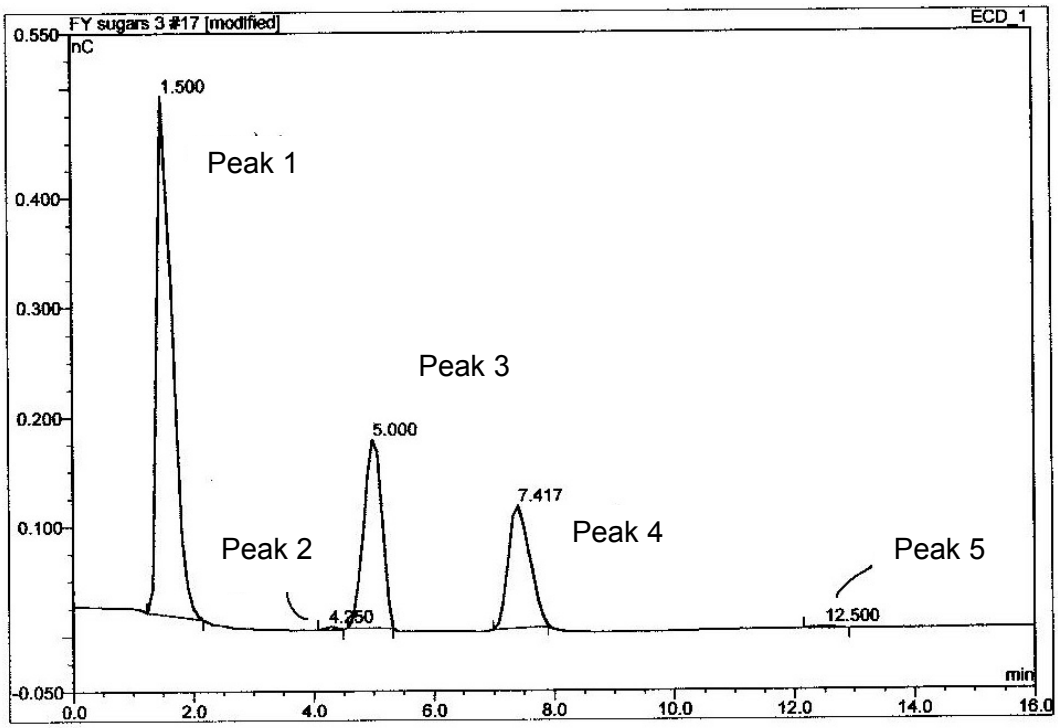


| No. | Ret.Time min | Peak Name | Height nC | Area nC*min | Rel.Area % | Amount | Type |
|---|---|---|---|---|---|---|---|
| 1 | 1.50 | n.a. | 0.473 | 0.142 | 56.90 | n.a. | BMB* |
| 2 | 4.25 | n.a. | 0.002 | 0.001 | 0.21 | n.a. | BMB* |
| 3 | 5.00 | n.a. | 0.171 | 0.061 | 24.21 | n.a. | BMB* |
| 4 | 7.42 | n.a. | 0.111 | 0.046 | 18.49 | n.a. | BMB* |
| 5 | 12.50 | n.a. | 0.001 | 0.000 | 0.19 | n.a. | BMB* |
| Total: | | | 0.759 | 0.250 | 100.00 | 0.000 | |

**Figure 3.2.2.1d: ENZ 1 HPLC trace prior to analytical separation**

The samples obtained from the analytical separation and collection of the peaks found in the HPLC trace (Figure 3.2.2.1d) were submitted for analysis by mass spectrometry. The results are shown in Table 3.2.2.1e below.

| $t_r$/min | Comment on HPLC appearance | m/z found | Compound |
|---|---|---|---|
| 1.5 | Expansion of HPLC shows two peaks overlapping | 217 $[M + 23]^+$ | GlcOMe |
| | | 379 $[M + 23]^+$ | Gal-GlcOMe disaccharide |
| 4.3 | | 324$[M + 23]^+$ | GalO*p*NP (unhydrolysed) |
| 5.0 | | 203 $[M + 23]^+$ | Gal (hydrolysed GalO*p*NP) |
| 7.4 (prod. 1) | | 365 $[M + 23]^+$ | Gal-Gal disaccharide |
| 12.5 (prod. 2) | | 486 $[M + 23]^+$ | Gal-GalO*p*NP disaccharide |

**Table 3.2.2.1e: Assignment of peaks collected from HPLC separation**

The peak at $t_r$ = 2.0 minutes (corresponding to the peak at $t_r$ = 1.6 minutes in the experiment) was found to be two peaks overlapping when that area of the spectrum was expanded. This first peak is due initially to the starting material GlcOMe and, as the reaction progressed, our target disaccharide Gal-GlcOMe appears at the same retention time. We also observed the formation of two more disaccharides, Gal-Gal and Gal-GalO*p*NP. These results were excellent encouragement as it showed that we had successfully used the enzyme to synthesise three different disaccharides.

### 3.2.2.2 Testing Crout's method

The second test reaction was carried out according to the method by Crout (see Exp Section 5.3 ENZ 2).[49] A solution of GlcOMe and GalO*p*NP in pH 5.0 buffer were stirred at 30 $^oC$ with the enzyme and aliquots were taken at regular intervals throughout the course of the reaction. In contrast to the previous experiment the bright yellow colour due to the enzymatic hydrolysis of GalO*p*NP evolved quite slowly over the course of 10 minutes.

HPLC analysis of aliquots removed from the reaction mixture at regular intervals showed the appearance of only one new peak at $t_r$ = 4.6 minutes (see Table 3.2.2.2a and Figure 3.2.2.2b). From the previous experiment, we expected the Gal-GlcOMe target to appear at $t_r$ = 1.6 minutes.

| | Rel. Area % | | |
|---|---|---|---|
| Reaction time/min | $t_r$ = 1.6 (GlcOMe) | $t_r$ = 4.6 (prod. 3) | $t_r$ = 5.4 (GalO*p*NP) |
| 0 | 64.31 | 0.00 | 35.69 |
| 2 | 66.92 | 0.20 | 32.87 |
| 4 | 69.25 | 0.28 | 30.47 |
| 6 | 71.73 | 0.69 | 27.58 |
| 8 | 76.53 | 1.01 | 22.46 |
| 10 | 80.78 | 1.52 | 17.71 |
| 15 | 63.13 | 5.63 | 31.24 |
| 20 | 84.00 | 4.70 | 11.29 |
| 30 | 84.46 | 8.41 | 7.13 |
| 45 | 82.61 | 14.00 | 3.39 |
| 60 | 79.48 | 18.94 | 1.58 |
| 90 | 72.48 | 26.83 | 0.69 |
| 120 | 65.93 | 33.35 | 0.72 |
| 180 | 62.15 | 31.13 | 0.71 |
| 240 | 58.40 | 41.02 | 0.58 |

**Table 3.2.2.2a: ENZ 2 tablulated HPLC data**

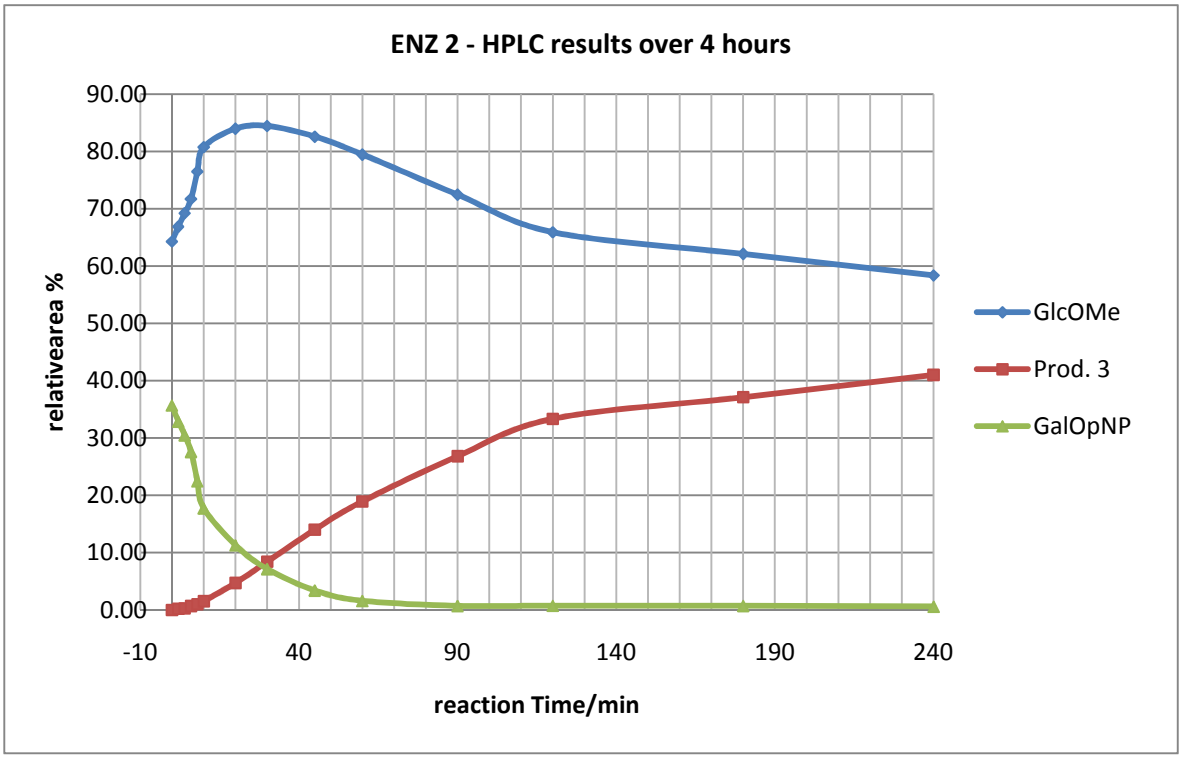


**Figure 3.2.2.2b: ENZ 2 – graph showing the changes in the relative area % of peaks found by HPLC over 2 hours.** (N.B. An anomalous result at 15 minutes due to a sampling error has been removed)

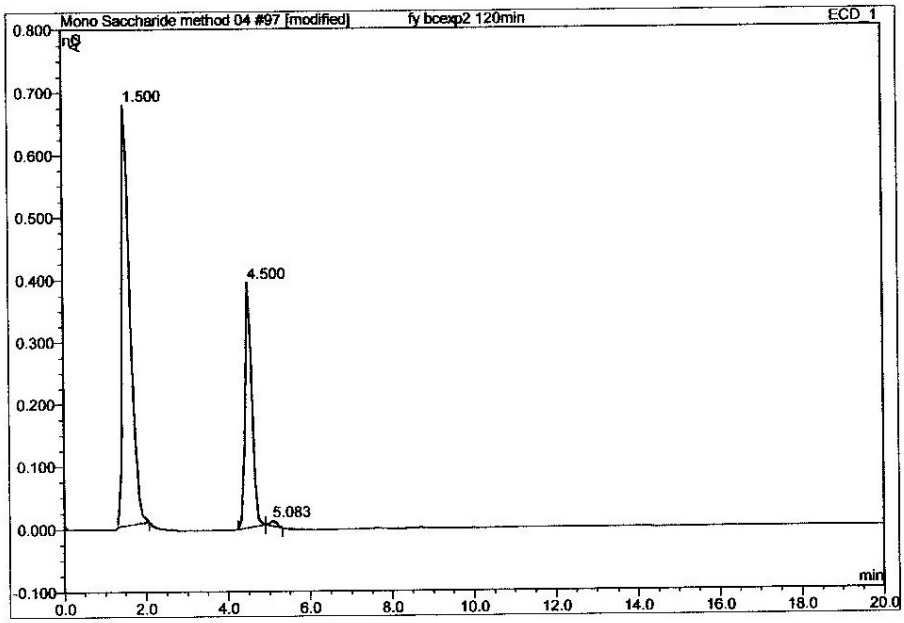


| No. | Ret.Time min | Peak Name | Height nC | Area nC*min | Rel.Area % | Amount | Type |
|---|---|---|---|---|---|---|---|
| 1 | 1.50 | n.a. | 0.676 | 0.155 | 65.93 | n.a. | BMB* |
| 2 | 4.50 | n.a. | 0.394 | 0.078 | 33.35 | n.a. | BMb* |
| 3 | 5.08 | n.a. | 0.008 | 0.002 | 0.72 | n.a. | bMB* |
| Total: | | | 1.077 | 0.235 | 100.00 | 0.000 | |

**Figure 3.2.2.2c: ENZ 2 HPLC trace, reaction time = 2 hours**

Since only one new peak was evolved (see Figure 3.2.2.2c), we analysed the reaction mixture by mass spectrometry without isolating the peaks. A major peak at 379.0 m/z was found, corresponding to the desired Gal-GlcOMe disaccharide.

An HPLC trace of the co-injection of samples from ENZ 1 and ENZ 2 is shown in Figure 3.2.2.2d. This was done to be able to compare peaks in both experiments as the solvent pump problems had meant that the different compounds eluted at different times in each experiment.

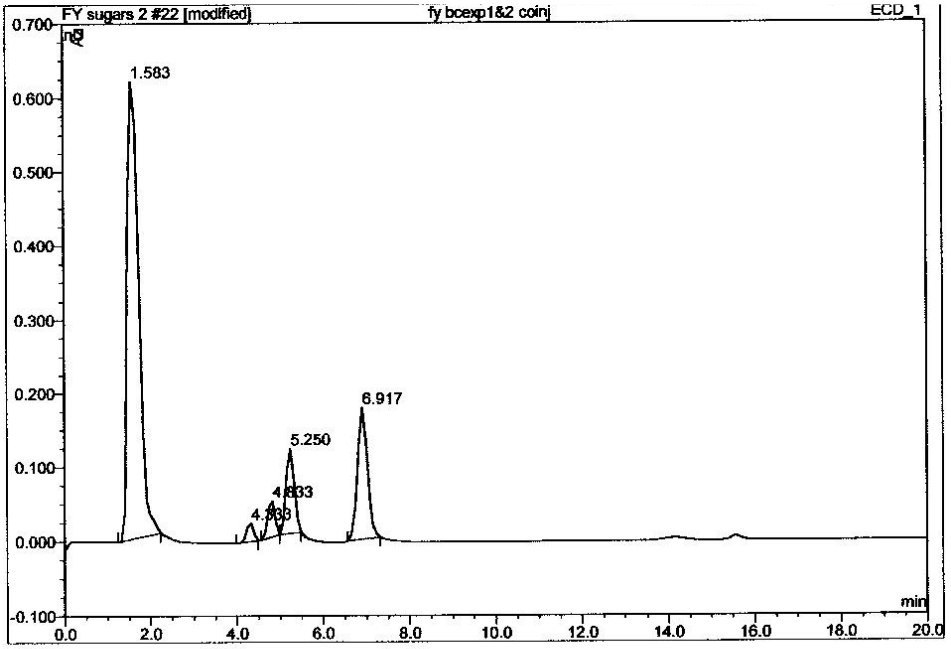


| No. | Ret.Time min | Peak Name | Height nC | Area nC*min | Rel.Area % | Amount | Type |
|---|---|---|---|---|---|---|---|
| 1 | 1.58 | n.a. | 0.619 | 0.190 | 68.80 | n.a. | BMB* |
| 2 | 4.33 | n.a. | 0.024 | 0.005 | 1.70 | n.a. | BMB* |
| 3 | 4.83 | n.a. | 0.047 | 0.010 | 3.45 | n.a. | BMb* |
| 4 | 5.25 | n.a. | 0.114 | 0.025 | 9.05 | n.a. | bMB* |
| 5 | 6.92 | n.a. | 0.178 | 0.047 | 17.00 | n.a. | BMB* |
| Total: | | | 0.981 | 0.276 | 100.00 | 0.000 | |

**Figure 3.2.2.2d: ENZ1 and ENZ 2 co-injection**

The HPLC spectrum shown above has five peaks due to the combined components of BCEXP1 and BCEXP2. When compared with the HPLC trace from BCEXP1 and 2 (Figures 3.2.2.1c and 3.2.2.2c) the difference in retention time of the peaks is modest but obvious.

| Peaks in BCEXP1 | Peaks in BCEXP2 | Proposed peak in combined HPLC | Assignment |
|---|---|---|---|
| $t_r$ = 2.0 | $t_r$ = 1.6 | $t_r$ = 1.6 | GlcOMe + GalGlcOMe |
| $t_r$ = 4.8 | $t_r$ = 4.6 | $t_r$ = 4.33 | Gal |
| $t_r$ = 5.5 | $t_r$ = 5.4 | $t_r$ = 4.8 | GalO*p*NP |
| $t_r$ = 7.8 | | $t_r$ = 5.3 | Gal-Gal disaccharide |
| $t_r$ = 11.8 | | $t_r$ = 6.9 | Gal-GalO*p*NP disaccharide |

**Figure 3.2.2.2e: ENZ 1 and ENZ 2 peak correlation from the co-injection**

Figure 3.2.2.2e shows the correlation between the peaks in the co-injection and the HPLC spectra from the two experiments. In this co-injection the Gal-Gal and Gal-GalO*p*NP peaks which appeared at $t_r$ =7.8 and 11.8 respectively were moved to $t_r$ =5.3 and 6.9 – a very stark contrast.

In summary, we had successfully made a Gal-GlcOMe disaccharide in both experiments. By following Thiem's method we also generated Gal-Gal and Gal-GalO*p*NP disaccharides. However, the differences in retention times due to HPLC problems between the experiments made them difficult to compare and evaluate.

We decided to begin our optimisation studies using Thiem's method as it was faster than the Crout experiment and had produced more types of disaccharides.

### 3.2.2.3 Investigating the effect of temperature on the reaction using Thiem's method

We next compared the effect of carrying out the reaction using Thiem's method at 55 and 30 $^{o}$C. This is important to investigate as Thiem performs his tranglycosylations at 55 $^{o}$C and Crout at 30 $^{o}$C. The β-galactosidase from *B. circulans* is not a thermophilic enzyme, so one would assume that its activity would be best at the more typical biological temperatures

around 37 °C. We chose to investigate the effect of using a lower temperature (used by Crout) with Thiem's method to see if it had any impact on the efficacy of the enzyme.

In this comparison, we chose to take aliquots at more regular intervals so that the hydrolysis of GalO*p*NP could be monitored by UV-vis spectroscopy and the evolution of new peaks in the HPLC could be monitored more closely.

The two experiments were carried out according the method ENZ1 (Section 5.3); **ENZ 3a** at 55 °C and **ENZ 3b** at 30 °C. Since the previous experiment at 55 °C appeared to have ceased at around 20 minutes (no further changes in HLPC), this repeat (**ENZ 3a**) was run for 30 minutes. The 30 °C experiment (**ENZ 3b**) was run for 60 minutes as we did not know how long the reaction would take.

The hydrolysis of GalO*p*NP was monitored by UV-vis spectroscopy in 0.1 M NaOH solution (Figures 3.2.2.3a and Figure 3.2.2.3b). The significant outcome of these results is that GalOpNP was hydrolysed within 8 minutes when the reaction was run at 30 °C and 30 minutes when the reaction was run at 55 °C. This can be rationalised as the enzyme is not thermophilic (as previously stated), so we might expect it to perform hydrolysis optimally at a lower temperature. Running the reaction at 55 °C appears to slow the rate of hydrolysis of GalO*p*NP by the enzyme. This could be because the enzyme is less active at the higher temperature or even that some of the enzyme added was denatured.

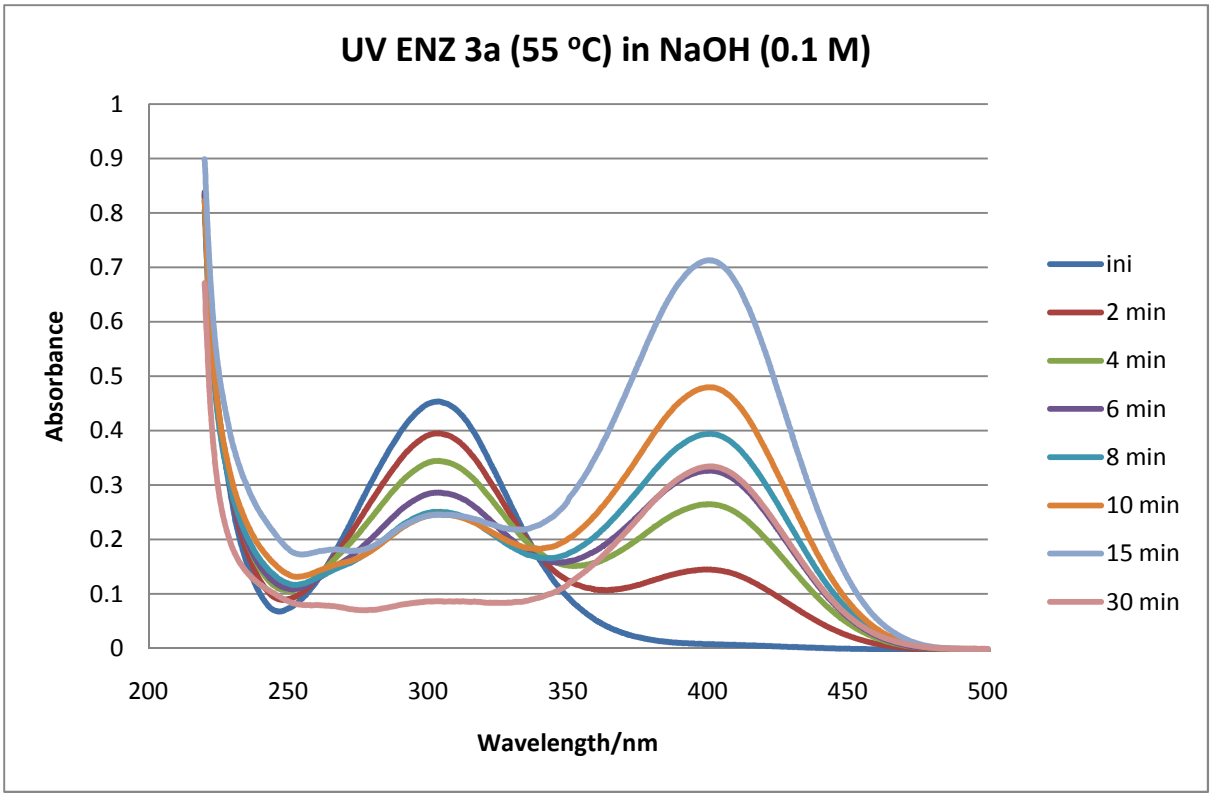


**Figure 3.2.2.3a: Hydrolysis of GalO*p*NP at 55 °C**

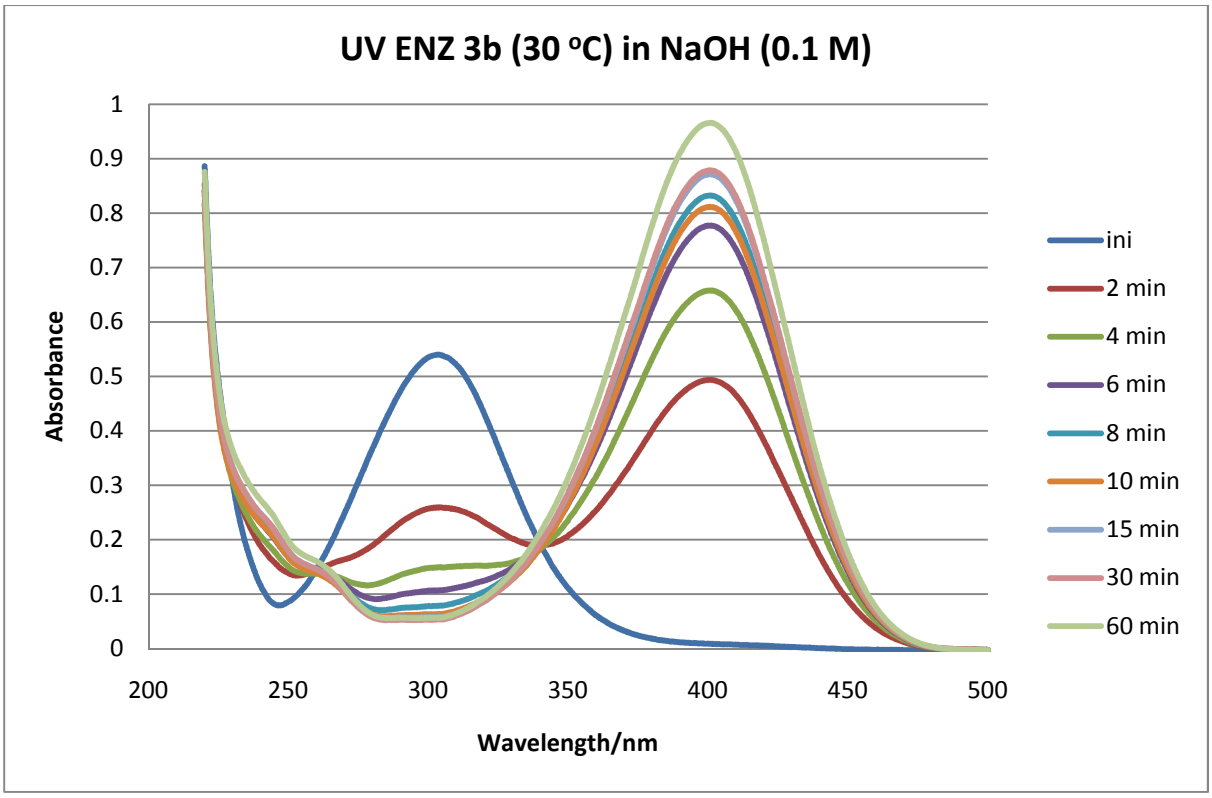


**Figure 3.2.2.3a: Hydrolysis of GalO*p*NP at 30 °C**

The HPLC results are tabulated below (**ENZ 3a** Table 3.2.2.3c and **ENZ 3b** Table 3.2.2.3d).

| | Rel. Area % | | | | | |
|---|---|---|---|---|---|---|
| Reaction time/min | $t_r$ ~ 1.6 (GlcOMe) | $t_r$ = 4.7 (prod.4) | $t_r$ = 5.3 (GalO*p*NP) | $t_r$ = 7.8 (prod. 5) | $t_r$ = 15.7 (negl.) | $t_r$ = 18.7 (prod. 6) |
| 0 | 43.88 | 0.00 | 56.12 | 0.00 | 0.00 | 0.00 |
| 2 | 33.80 | 0.00 | 34.51 | 31.68 | 0.39 | 0.45 |
| 4 | 35.96 | 0.00 | 30.92 | 31.46 | 0.78 | 0.89 |
| 6 | 37.73 | 0.00 | 28.39 | 31.95 | 0.79 | 1.14 |
| 8 | 39.89 | 0.00 | 26.07 | 31.70 | 0.94 | 1.47 |
| 10 | 41.76 | 0.00 | 24.27 | 31.57 | 0.91 | 1.50 |
| 15 | 36.99 | 0.31 | 26.29 | 32.98 | 1.02 | 2.42 |
| 30 | 45.50 | 0.29 | 20.54 | 31.32 | 0.68 | 1.67 |

**Table 3.2.2.3c: Tabulated HPLC results ENZ 3a**

| | Rel. Area % | | | | | |
|---|---|---|---|---|---|---|
| Reaction time/min | $t_r$ ~ 1.6 (GlcOMe) | $t_r$ = 4.7 (prod.4) | $t_r$ = 5.3 (GalO*p*NP) | $t_r$ = 7.8 (prod. 5) | $t_r$ = 15.7 (negl.) | $t_r$ = 18.7 (prod. 6) |
| 0 | 42.85 | 0.00 | 57.15 | 0.00 | 0.00 | 0.00 |
| 2 | 39.92 | 0.26 | 27.69 | 29.88 | 0.98 | 1.27 |
| 4 | 47.62 | 0.68 | 23.96 | 26.58 | 0.00 | 1.15 |
| 6 | 50.93 | 1.13 | 23.18 | 23.81 | 0.00 | 0.95 |
| 8 | 51.97 | 2.08 | 24.54 | 20.69 | 0.00 | 0.73 |
| 10 | 54.72 | 2.07 | 24.04 | 18.48 | 0.00 | 0.69 |
| 15 | 55.30 | 2.78 | 25.24 | 16.21 | 0.00 | 0.46 |
| 30 | 54.52 | 3.03 | 27.10 | 14.94 | 0.00 | 0.41 |
| 60 | 53.33 | 3.48 | 28.56 | 14.25 | 0.00 | 0.37 |

**Table 3.2.2.3c: Tabulated HPLC results ENZ 3b**

Five peaks were separated and collected by HPLC and the samples submitted for analysis by mass spectrometry (Table 3.2.2.3e). The peak at tr = 15.7 minutes was not collected for analysis as it was in such a negligible amount in both experiments.

| tr/min | | m/z found | Compound |
|---|---|---|---|
| 1.6 | | 217 [M + 23]$^+$ | GlcOMe |
| | | 379 [M + 23]$^+$ | Gal-GlcOMe disaccharide |
| 4.7 | Prod. 4 | 324[M + 23]$^+$ | Gal (hydrolysed GalO*p*NP) |
| 5.3 | | 203 [M + 23]$^+$ | GalO*p*NP |
| 7.8 | Prod. 5 | 365 [M + 23]$^+$ | Gal-Gal disaccharide |
| 18.7 | Prod. 6 | 486 [M + 23]$^+$ | Gal-GalO*p*NP disaccharide |

**Table 3.2.2.3e: Combined ENZ3a and 3b mass spectrometry results**

Again we had successfully made three different disaccharides using Thiem's method. At this point we had not investigated the regioselectivity of the disaccharide formation. As per our initial aims, we first wanted to be able to make the disaccharides reliably. The regioselectivity of the transglycosylation reaction would be investigated with the naphthyl-functionalised sugars.

### 3.2.2.4 Control experiments

Before progressing onto the experiments using our naphthyl-functionalised methyl glucosides we decided to carry out a number of control experiments to check the functionality of the enzyme (Figure 3.2.2.3f). Specifically we wanted to answer the following questions:

1. Will the enzyme hydrolyse $\alpha$-methyl glucose?
2. Will the enzyme transfer the *p*NP group onto Gal?
3. Will the enzyme transfer GalO*p*NP onto GalO*p*NP in the absence of other acceptors?
4. Will the enzyme use lactose as the glycosyl donor, and if so is lactose a better glycosyl donor than GalO*p*NP?

Each of these four control experiments were carried out using method ENZ 1

**Control Experiment 1 – will the enzyme hydrolyse α-methyl glucose?**

The enzyme we are using is a β-galactosidase, so it should not hydrolyse the glycosyl acceptor since it is an α-glucoside. However, we still wanted to be certain that hydrolysis of the acceptor was not going on.

Since we had detected free sugar in our previous experiments we wanted to know whether this was glucose (*i.e.* hydrolysed acceptor), galactose (*i.e.* hydrolysed donor) or both. By testing if the enzyme would hydrolyse GlcOMe we would be able to determine if any free glucose could have been present in our previous enzyme reactions.

The reaction was carried out using method ENZ 1 but in this case without any *p*-nitrophenol galactose as the glycosyl donor (Figure 3.2.2.4a). The reaction was monitored by HPLC and the results are shown in Figure 3.2.2.4b.

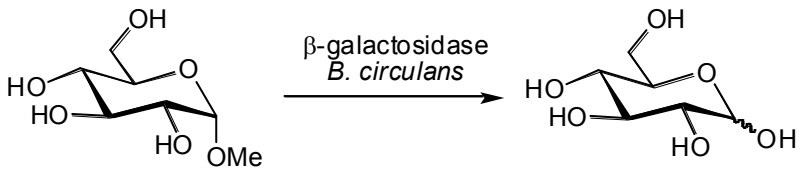


**Figure 3.2.2.4a: Control experiment 1 scheme**

| Reaction time/min | Rel. Area % $t_r$ = 1.6 (GlcOMe) | $t_r$ = 6.5 (Glc) | $t_r$ = 10.9 |
|---|---|---|---|
| 0 | 96.37 | 3.63 | 0.00 |
| 2 | 65.53 | 9.69 | 26.78 |
| 5 | 64.21 | 21.74 | 14.05 |
| 15 | 64.85 | 33.39 | 1.76 |
| 30 | 63.69 | 36.31 | 0.00 |
| 60 | 63.47 | 36.53 | 0.00 |

**Figure 3.2.2.4b: Tabulated HPLC results for control experiment 1**

Mass spectrometric analysis of the samples taken at 5 minutes and 30 minutes revealed peaks corresponding to α-methyl glucose and free glucose as well as two disaccharides Glc-Glc and Glc-GlcOMe (Figure 3.2.2.4c).

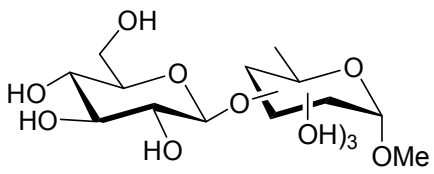


Glc-GlcOMe

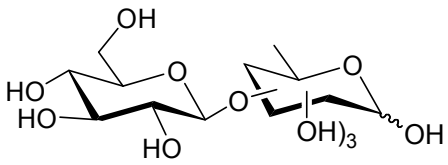


Glc-Glc

**Figure 3.2.2.4c: Products from control experiment 1**

This result is very surprising as we would not expect the β-galactosidase from *B. circulans* to be able to use glucose as a glycosyl donor, much less be able to hydrolyse α-methyl glucose. There was a small amount of free glucose present in the initial reaction sample, but the amount of free glucose then increased over the course of the reaction, giving credence to the hydrolysis of GlcOMe, but we have not found any precedent for this in the literature. Perhaps the most likely answer to this result is that the enzyme has not been purified by us, we are using it directly from the manufacturer, as is done in the literature procedures we have followed. It is much more plausible for the hydrolysis of the methyl glucoside in this

control experiment to be due to small amounts of other types of glycosidases which may be present in the sample of enzyme that we have to work with.

**Control Experiment 2: Will the enzyme transfer the *p*NP group onto Gal?**

This control reaction was carried out using method ENZ 1, substituting D-galactose as the glycosyl donor and *p*-nitrophenol as the glycosyl acceptor (Figure 3.2.2.4d). The reaction was run for 1 hour, aliquots were taken at regular intervals and analysed by HPLC over the course of the reaction.

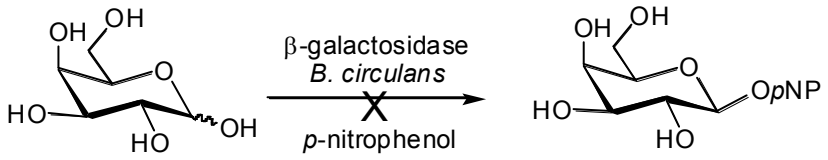


**Figure 3.2.2.4d: Scheme for control experiment 2**

No *p*-nitrophenol galactose was made during the reaction, only Gal-Gal disaccharides were seen in the HPLC and mass spectrometric analysis.

**Control Experiment 3: Will the enzyme transfer GalO*p*NP onto GalO*p*NP in the absence of acceptors?**

In experiments ENZ 1, ENZ 3a and ENZ 3b, Gal-GalOpNP disaccharides were made. We checked whether these would be made if no other sugars were available as glycosyl acceptors (Figure 3.2.2.4e).

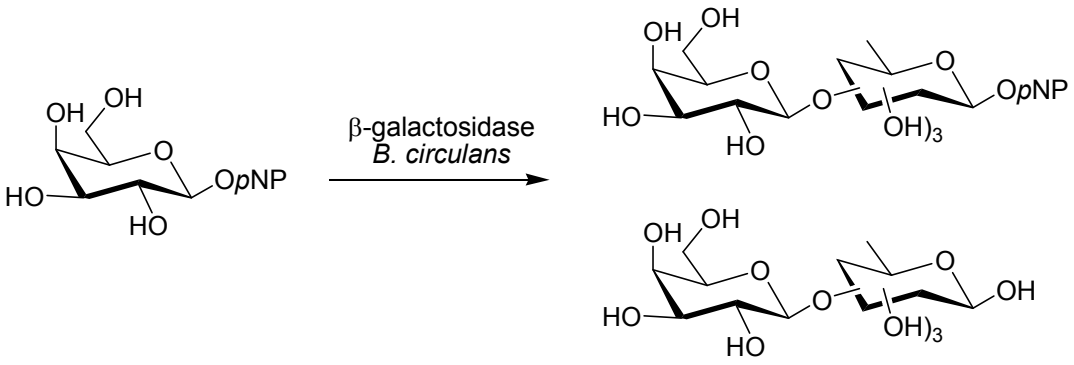


**Figure 3.2.2.4e: Scheme for control experiment 3**

| Reaction time/min | Rel. Area % | | | | |
|---|---|---|---|---|---|
| | $t_r$ =4.7 | $t_r$ = 5.3 | $t_r$ = 5.9 | $t_r$ = 8.0 – 9.0 | $t_r$= 17.0 – 20.0 |
| 0 | 0.00 | 0.00 | 100.0 | 0.00 | 0.00 |
| 2 | 0.00 | 0.00 | 51.78 | 48.22 | 0.00 |
| 5 | 0.00 | 0.00 | 50.07 | 49.93 | 0.00 |
| 10 | 0.26 | 0.13 | 44.90 | 54.72 | 0.00 |
| 15 | 0.26 | 0.25 | 40.32 | 55.36 | 3.81 |
| 30 | 0.59 | 0.83 | 38.84 | 54.96 | 4.79 |
| 60 | 0.70 | 1.66 | 37.22 | 55.46 | 4.97 |

**Table 3.2.2.4f: Tabulated HPLC results for control experiment 3**

The HPLC results shown in Table 3.2.2.4f show the evolution of a number of peaks. Analysis by mass spectrometry showed only three peaks corresponding to three sugars, GalO*p*NP, Gal-Gal and Gal-GalO*p*NP as shown in Figure 3.2.2.4e. The number of compounds found in the HPLC exceeds this, suggesting a number of different glycosidic linkages between the two sugars of the disaccharides.

**Control Experiment 4: Will the enzyme use lactose as the glycosyl donor, and if so is lactose a better glycosyl donor than GalOpNP?**

Lactose is often used as the glycosyl donor in transgalactosylation reactions as it is the enzyme's natural substrate. We evaluated the use of lactose as the glycosyl donor to see if it had a comparable performance to GalO*p*NP (Figure 3.2.2.4g).

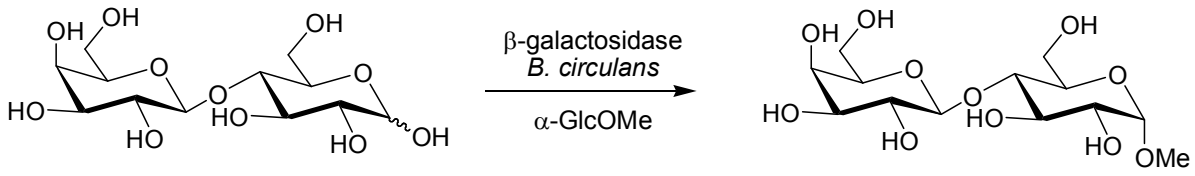


**Figure 3.2.2.4g: Scheme for control experiment 4**

The reaction was monitored by HPLC and only three peaks were found (Table 3.2.2.4h), unlike ENZ 1,ENZ 3a and ENZ 3b, where the same method was used and more than three peaks were detected (Tables 3.2.2.3c and 3.2.2.3e).

| Reaction time/min | $t_r$ = 1.6 (GlcOMe) | $t_r$ = 5.5 (Glc) | $t_r$ = 8.1 (Lac) |
|---|---|---|---|
| 0 | 39.35 | 1.20 | 59.45 |
| 2 | 36.49 | 9.09 | 54.42 |
| 5 | 35.01 | 17.16 | 47.84 |
| 10 | 35.29 | 25.07 | 39.64 |
| 15 | 38.27 | 31.30 | 30.43 |
| 30 | 37.33 | 44.34 | 17.57 |
| 60 | 45.17 | 52.40 | 1.96 |
| 120 | 47.13 | 51.78 | 1.06 |

**Table 3.2.2.4h: Tabulated HPLC results from control experiment 4**

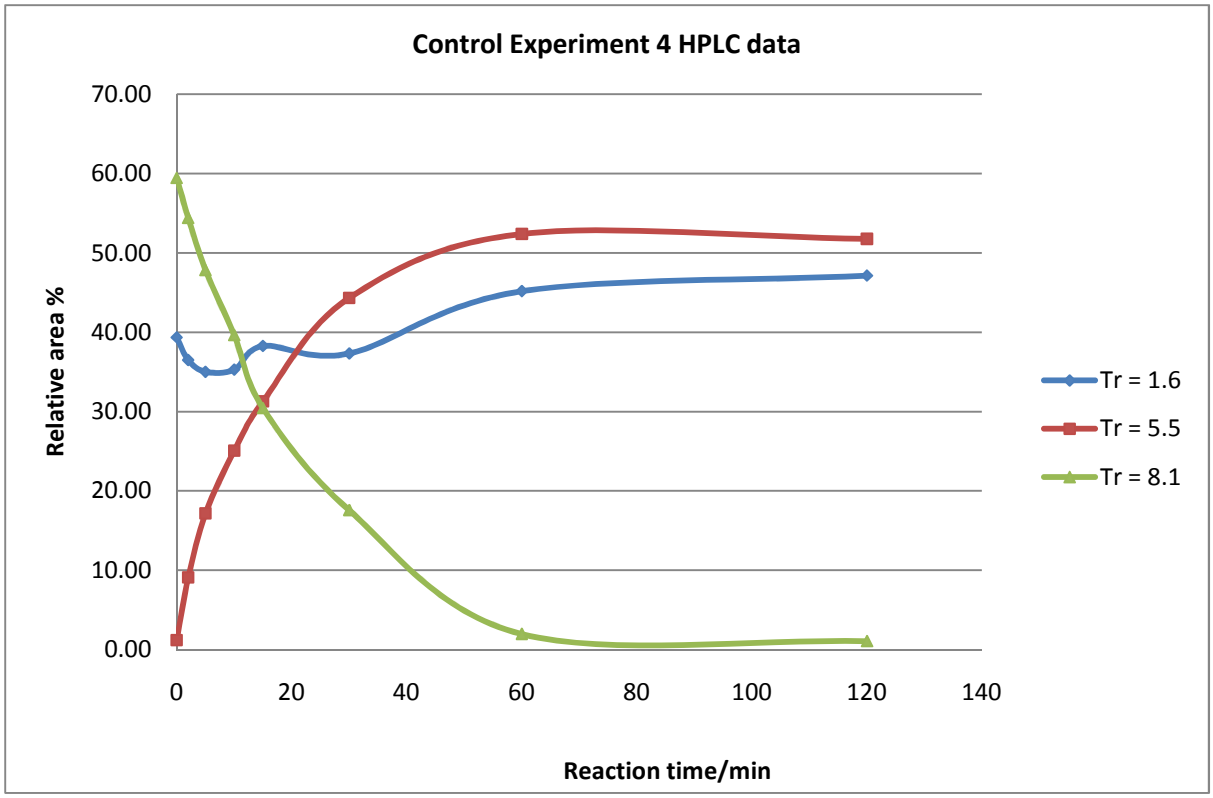


**Figure 3.2.2.4i: Control experiment 4 HPLC dat**

The peak at $t_r$ = 1.6 minutes is initially due to GlcOMe, but as seen in previous experiments, the Gal-GlcOMe disaccharide also resides at this retention time, as evidenced by the dips followed by increases in the blue trace on Figure 3.2.2.4i. Lactose ($t_r$ = 8.1 min) is hydrolysed over the course of one hour and there is an associated increase in free glucose at $t_r$ = 5.5 min.

Using lactose as the glycosyl donor may prove more desirable than GalO*p*NP as it produces fewer by products.

### 3.2.2.5 Evaluating the efficacy of the glycosyl donor

We next chose to evaluate both lactose and *p*-nitrophenyl galactose as glycosyl donors under Thiem's reaction conditions. We would then select the better of the two for use in the next stages of the experiment.

This was done using method ENZ 1 for the transglycosylation reaction. The experiments described below are: **ENZ 4a** using GalO*p*NP as the glycosyl donor and **ENZ 4b** using lactose as the glycosyl donor (Figure 3.2.2.5a).

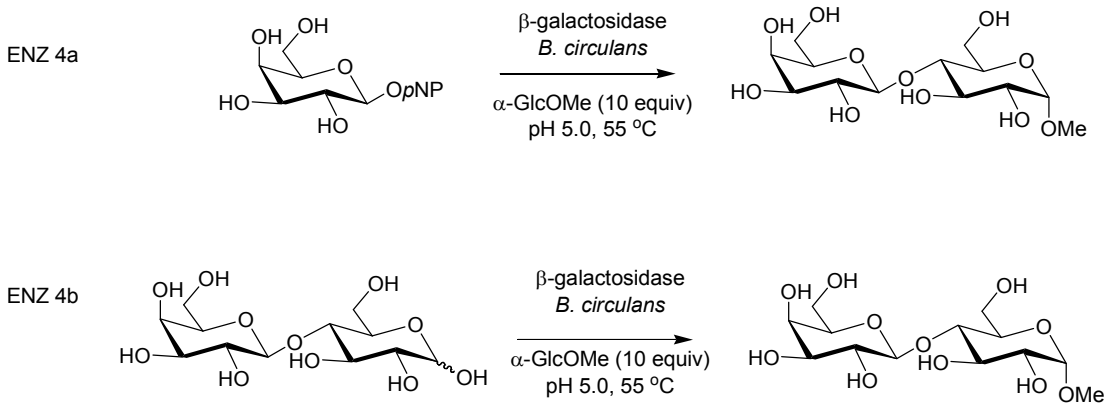


**Figure 3.2.2.5a: Scheme for experiment ENZ 4a and ENZ 4b to evaluate whether GalO*p*NP or lactose are better glycosyl donors**

Aliquots of the reaction mixture were taken at 2, 5, 10, 15, 30, 60 and 120 minutes and analysed by HPLC (Table 3.2.2.5b).

| | ENZ 4a (GalO*p*NP) | | | | ENZ 4b (lactose) | | |
|---|---|---|---|---|---|---|---|
| Reaction time/ min | $T_r$ =1.6 (GlcOMe/ Gal-GlcOMe) | $T_r$ = 5.7 (Gal) | $T_r$ = 6.8 (GalO*p*NP) | $T_r$ = 9.4 (Gal-Gal) | $T_r$ =1.6 (GlcOMe) | $T_r$ = 5.7 (Gal) | $T_r$ = 9.0 (Lac) |
| 0 | 70.85 | 0.00 | 29.15 | 0.00 | 49.61 | 0.00 | 50.39 |
| 2 | 73.45 | 0.00 | 25.36 | 1.19 | 50.24 | 1.11 | 48.65 |
| 5 | 75.07 | 0.69 | 23.07 | 1.17 | 47.95 | 3.23 | 48.82 |
| 10 | 81.71 | 1.02 | 16.37 | 0.91 | 54.87 | 6.15 | 38.98 |
| 15 | 85.38 | 0.93 | 12.48 | 1.20 | 53.67 | 10.81 | 35.52 |
| 30 | 91.41 | 1.20 | 6.68 | 0.72 | 46.29 | 25.16 | 28.55 |
| 60 | 92.96 | 1.31 | 4.63 | 1.11 | 53.03 | 38.21 | 8.76 |
| 120 | 92.70 | 1.25 | 5.18 | 0.88 | 54.44 | 44.45 | 1.11 |

**Table 3.2.2.5b: Tabulated HPLC data from experiments ENZ 4a and ENZ 4b**

Peaks at similar retention times were found in both reactions – as expected. In both cases there was an increase in the relative area of the peak at $t_r$ =1.6 consistent with the evolution of the Gal-GlcOMe disaccharide which has a similar retention time to the starting material GlcOMe. The presence of this Gal-GlcOMe disaccharide target in both reactions was confirmed by mass spectrometry as a peak was detected at m/z = 379 which corresponded to the Gal-GlcOMe disaccharide ($[M + Na]^+$). In **ENZ 4a** there was a decrease in the GalO*p*NP donor, and, as expected, a decrease in lactose in **ENZ 4b** also (see Figures 3.2.2.5c and 3.2.2.5d).

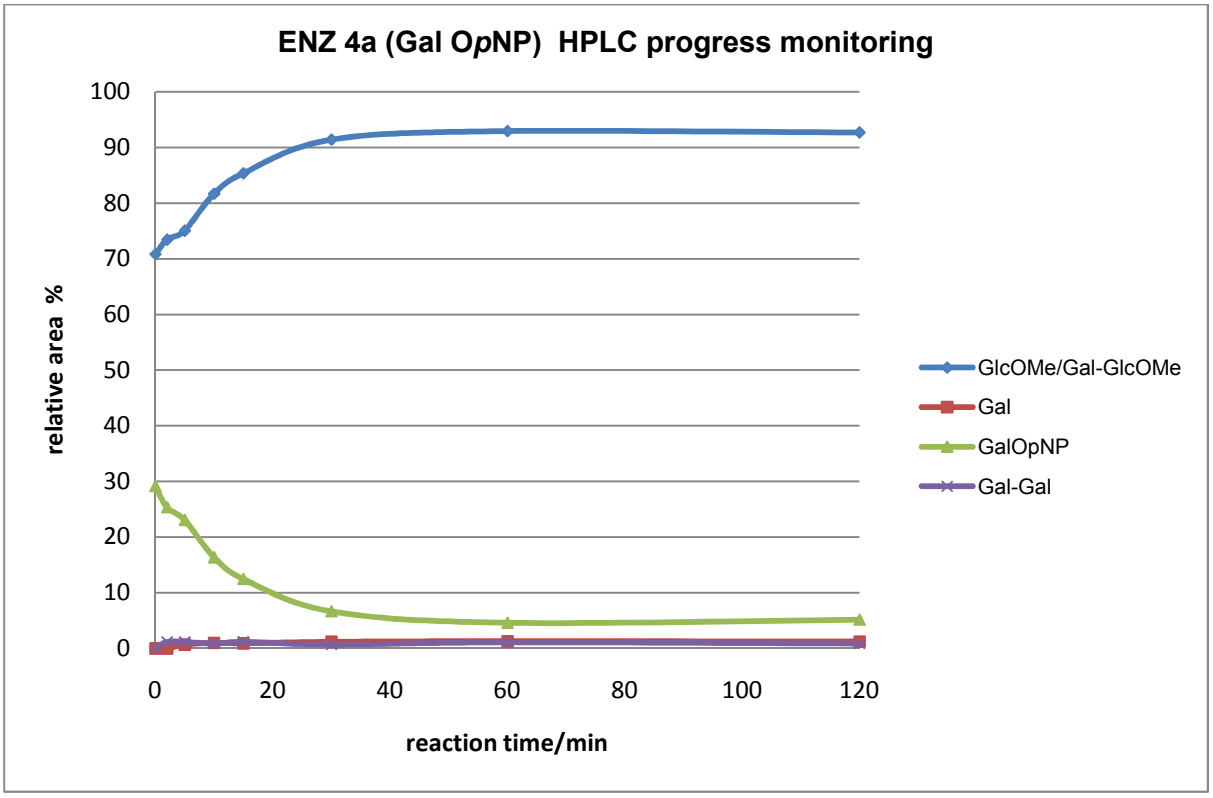


**Figure 3.2.2.5c: ENZ 4a (GalO*p*NP) HPLC progress graph**

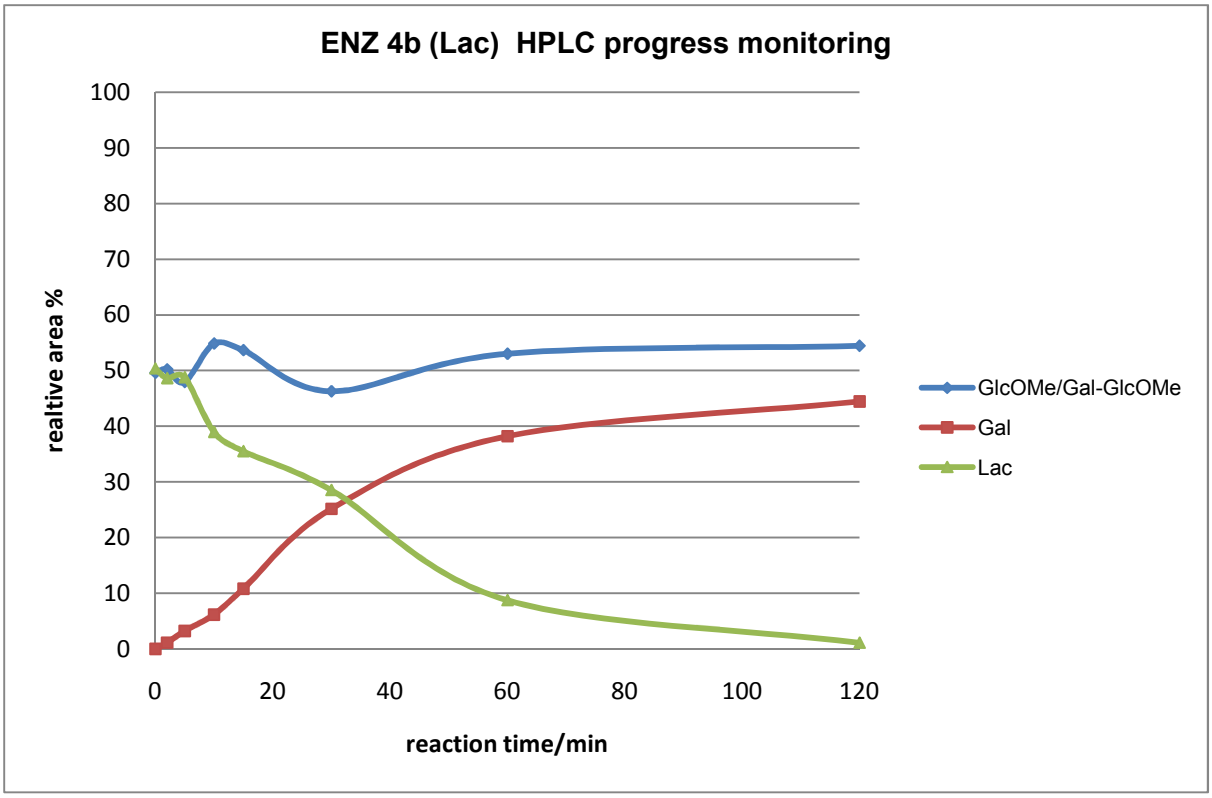


**Figure 3.2.2.5d: ENZ 4b (lactose) HPLC progress graph**

Given all of the data we had collected, it was still not clear which of the two possible glycosyl donors would be the most suitable. Comparing the evolution of the product in HPLC is not conclusive. The best we could say at this point was that the use of GalO*p*NP resulted in a smoother evolution of product when compared to using lactose as the glycosyl donor. We tentatively suggest this because the blue line in the graph shown in Figure 3.2.2.5e (**ENZ 4a**) steadily increases over the first 30 minutes, whereas the red line (**ENZ 4b**) dips and peaks unsteadily over the same timescale.

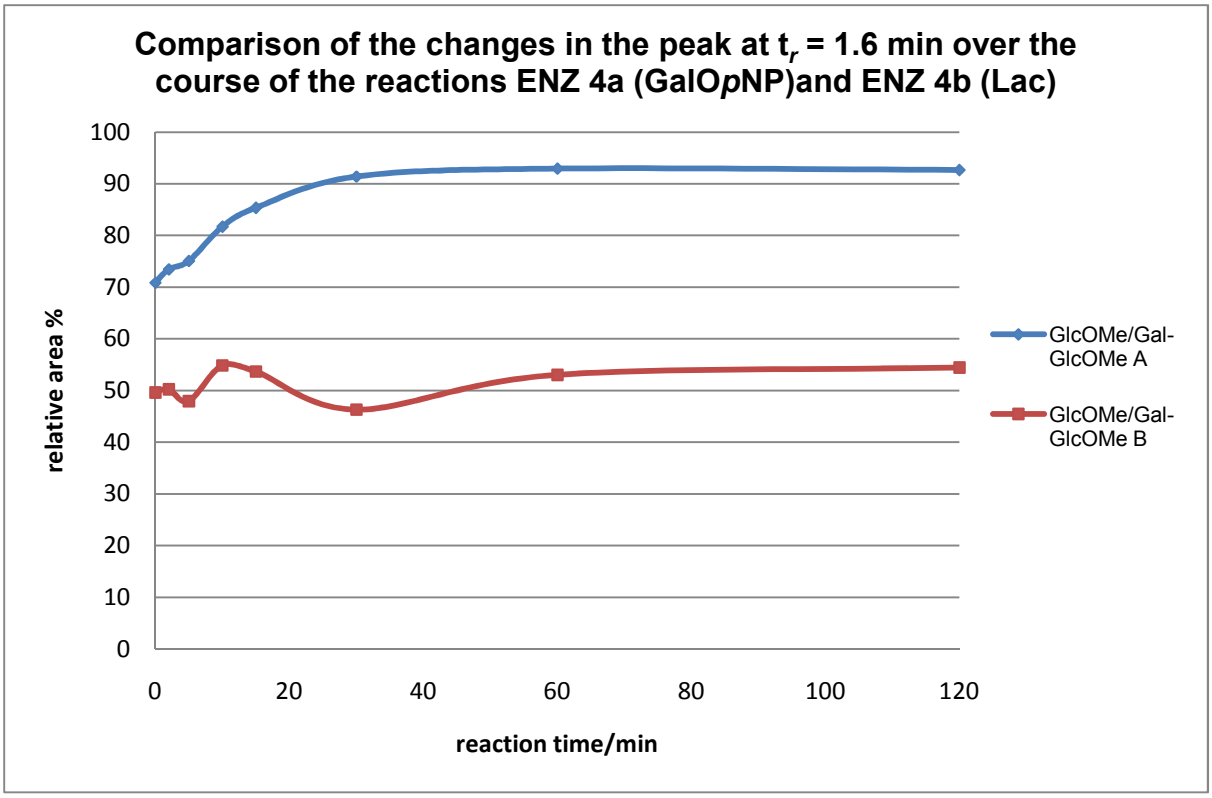


**Figure 3.2.2.5e: Comparison of the peak at $t_r$ = 1.6 minutes in ENZ 4a and ENZ 4b**

At this point, our preliminary studies were complete. We had succeeded in using the enzyme to make disaccharides, had refined the methods of using the enzyme with the sugars and also our reaction monitoring tools. At this stage we had found the optimum conditions for using the enzyme to make disaccharides to be:

| | |
|---|---|
| Ratio of acceptor:donor | 6:1 |
| Units of enzyme | 30 |
| Reaction concentration | 0.2 M |
| Reaction pH | 5.0 |
| Reaction temperature | 30 $^{o}$C |
| Glycosyl donor | GalO*p*NP or lactose |

The next task was to develop a method that worked when using our novel naphthyl-functionalised glucosides as the glycosyl acceptors.

## 3.3 Transglycosylation using Naphthyl-Functionalised Methyl Glucosides

At this point in the project we had successfully determined the activity of the enzyme and had explored two different methods for transglycosylation reactions. We now needed to develop a suitable method (starting from the previous investigations) for performing transglycosylation reactions between the glycosyl donor and our naphthyl-functionalised glucosyl acceptors (Figure 3.3a). The final optimisation of techniques would all be carried out using NpCH2GlcOMe (**32**) as the glycosyl acceptor. Once optimised, the procedure would then be applied to the remaining two glycosyl acceptors EGNpGlcOMe (**33**) and DEGNpGlcOMe (**34**).

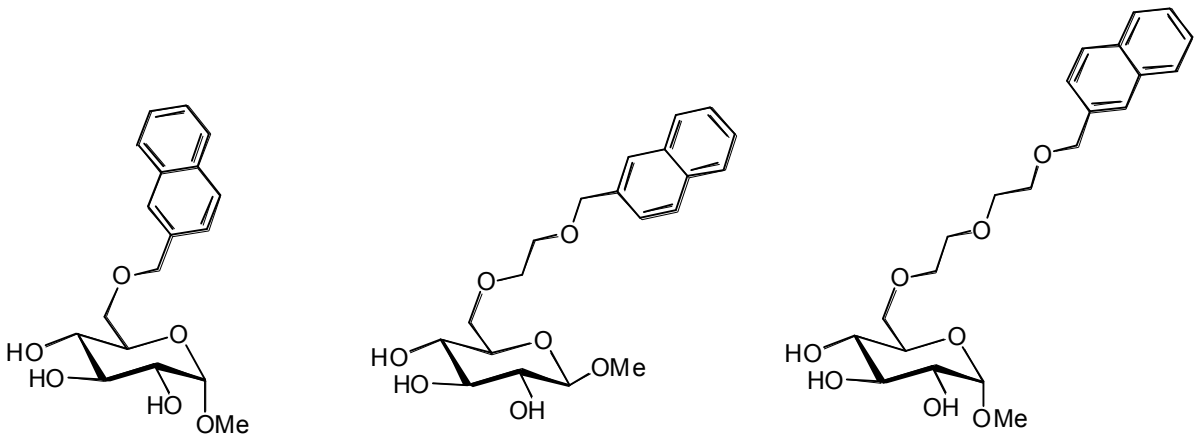


$CH_2$NpGlcOMe
32

EGNpGlcOMe
33

DEGNpGlcOMe
34

**Figure 3.3a: The three naphthyl-functionalised glycosyl acceptor substrates for the transglycosylation studies**

We chose to optimise the reaction by varying the following parameters:

- solvent system;
- pH of buffer;
- temperature;
- amount of enzyme needed.
- reaction concentration

### 3.3.1 Optimising the reaction conditions

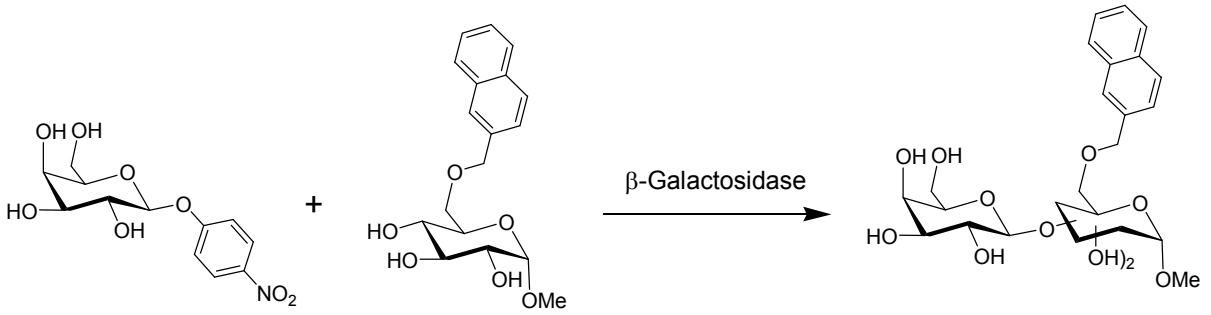


**Figure 3.3.1a: Initial scheme for optimising the reaction conditions using the simplest of the three naphthyl sugar candidates**

In order to carry out a full investigation into the conditions needed for the transglycosylation reaction shown in Figure 3.3.1ab, we would need a relatively large quantity of NpCH2GlcOMe. We would be monitoring the screening reactions by HPLC but it would be extremely difficult at this early stage to quantify and identify any peaks that developed. This is because at this stage we did not know what glycosides would be made in the reaction. Moreover, different reaction conditions could lead to different types of linkages being formed, β(1→4) or β(1→3), for example. We need a quantifiable and easily-repeatable way to measure the ability of the enzyme to work under various conditions.

To investigate the effect of these factors on the transglycosylation we needed to go back to the basic function of the enzyme. We would monitor the hydrolysis of the enzyme's natural substrate: lactose. By finding conditions in which the enzyme works optimally to hydrolyse lactose we can then apply those conditions to the transglycosylation reaction knowing that the enzyme will function as well as it possibly can in these unnatural conditions.

Having established an appropriate set of reaction conditions we would again attempt transglycosylation using GlcOMe as the glycosyl acceptor to evaluate the conditions with

respect to transglycosylation. Once the conditions had been optimised, we would then try the reaction conditions with our novel glycosyl acceptors.

We first chose to investigate the solvent conditions needed for the transglycosylation reaction. None of the glycosyl acceptors are soluble in the aqueous buffer solution so a mixed solvent system would be needed to aid the solubility of the glycosyl acceptors. However, using an organic co-solvent inhibits the action of the enzyme so a full screening experiment would be carried out to find a combination of conditions that enabled the best activity.

#### 3.3.1.1 Optimising solvent and temperature conditions

There is a great deal of precedent for employing a mixed solvent system when using glycosidases to make glycosides. Firstly, in the initial work on the synthesis of glycosides using glycosidases, the reverse hydrolysis technique required a high concentration of organic solvent to water to push the enzyme into transferase activity (see Section 1.3.3.2).[28-30] Various organic solvents are tolerated by the β-galactosidase from *B. circulans* in various concentrations when using the enzyme for transglycosylation.

In general terms the use of organic solvents with β-galactosidases, and indeed other glycosidases, is that the use of organic solvents causes enzyme deactivation. It is accepted that the price for being able to perform your desired transglycosylation under these conditions is a reduction in yield and a longer reaction time. However, by optimising conditions through experimentation it is possible to get acceptable results which allow researchers to take advantage of the desired regio- and stereoselectivity of these enzymes.[27]

A report by Beau[87] records the use of 75% MeCN with the β-galactosidases from *A. oryzae* to perform a number of glycosylations. This procedure uses a relatively high proportion of

MeCN in a reverse-hydrolysis-type synthesis using an excess of the alcohol acceptor coupled with a low water concentration (Figure 3.3.1.1a).

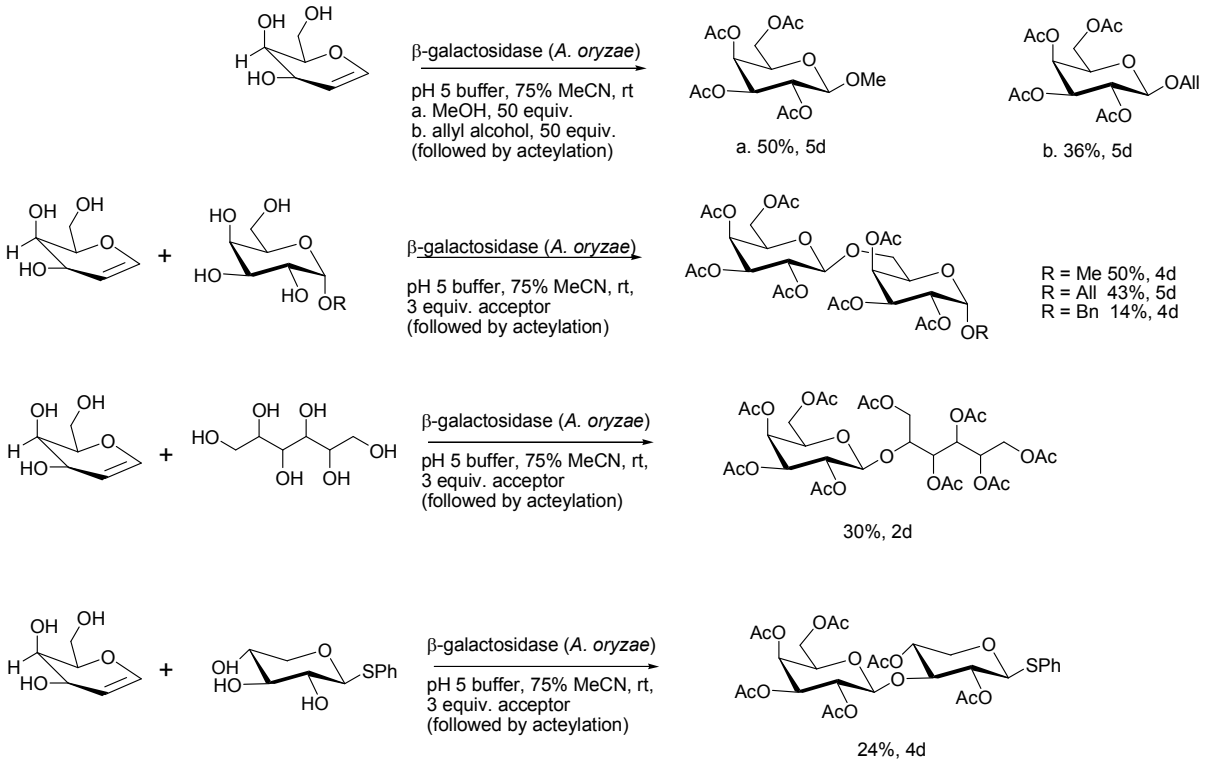


**Figure 3.3.1.1a: An investigation into the effects of s high concentration of MeCN in the reaction solution on the transglycosylation efficacy of the β-galactosidase from *B. circulans***

The yields achieved with the enzyme in the presence of 75% MeCN are relatively high, ranging from 14 – 50%, although over the course of 2-5 days. This shows that although the reaction may take longer, acceptable yields are still achievable when using organic co-solvents.

Thiem has also investigated the use of MeCN in β-galactosidase catalysed synthesis.[88] The scheme below (Figure 3.3.1.1b) shows the use of the enzymes from *A. oryzae* and *E. coli* to make Gal-GalO*o*NP disaccharides from β-*o*-nitrophenyl galactose. The yields here appear modest, but again, for a 30 minute reaction in 50% MeCN, this is a very acceptable result

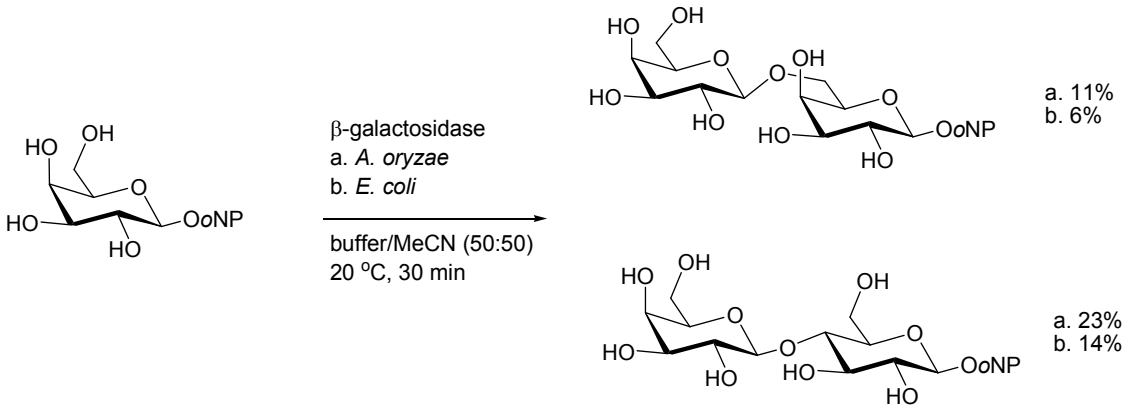


**Figure 3.3.1.1b: Investigation into the effect of using a 50% MeCN reaction solution to perform transglycosylations using the β-galactosidase from *A. oryzae* and *E. coli***

In a report by Finch and Yoon[27] the activities of a number of β-galactosidases in various water-solvent mixtures were investigated. The synthesis shown in Figure 3.3.1.1c below shows the synthesis of two disaccharides using the β-galactosidase from *B. circulans* in the presence of 60% triethyl phosphate. In this case the β(1→6) glycosidic linkage was the major product.

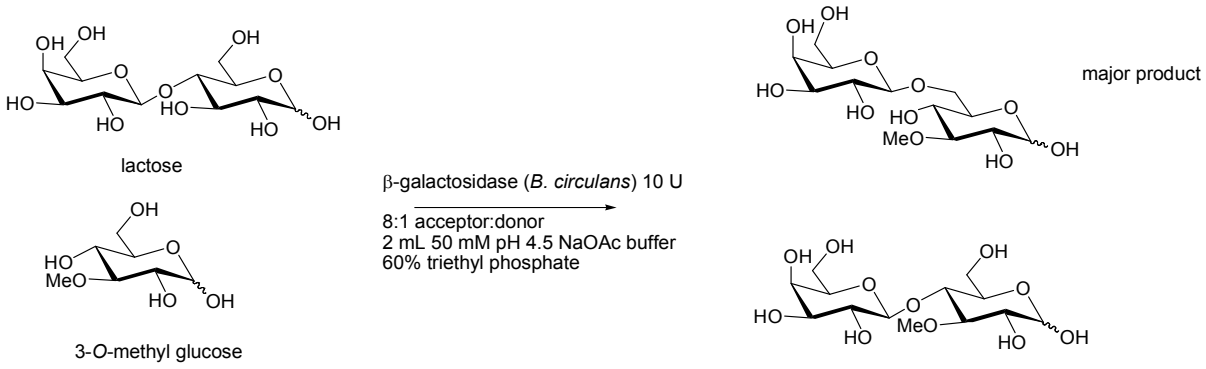


**Figure 3.3.1.1c: A transglycosylation reaction mediated by the β-galactosidase from *B. circulans* in the presence of an organic solvent**

In this report the only organic solvent tried with the β-galactosidase from *B. circulans* was triethyl phosphate. However, given this evidence we might expect it to tolerate other organic solvents as well.

The literature mentioned above suggests that MeCN is a suitable organic solvent to use with β-galactosidases, so we chose to use this in our screening experiment as we will be monitoring the reaction by HPLC and mass spectrometry and MeCN is also a suitable solvent for those applications. Since the pH and temperature of the reaction can also affect the activity of the enzyme we decided to also screen two pH and temperature values that have been reported regularly in the literature for related transglycosylation reactions.[49,86]

In this first screening experiment we followed a modified method (**ENZ 5**), which was based on the procedure developed by Thiem, and varied the pH, temperature and amount of MeCN used. Table 3.3.1.1d shows the combinations of conditions for each separate test reaction.

| | pH 5.0 (NaOAc) | | | | pH 7.0 ($Na_2HPO_4/NaH_2PO_4$) | | | |
|---|---|---|---|---|---|---|---|---|
| % MeCN | 50 | 40 | 30 | 20 | 50 | 40 | 30 | 20 |
| 30 $^oC$ | A | B | C | D | E | F | G | H |
| 55 $^oC$ | I | J | K | L | M | N | O | P |

**Table 3.3.1.1d: Conditions for experiment ENZ 5**

The reactions were carried out by suspending lactose in the mixed solvent system and stirring it at the given temperature with the β-galactosidase from *B. circulans*. Aliquots were taken at regular intervals for HPLC analysis.

The first observation upon beginning the reactions was that lactose was not completely dissolved in some of the reactions. Lactose was completely dissolved only in reactions A and H at 30 $^oC$, but was completely dissolved in all of the reactions at 55 $^oC$.

Following the reactions by HPLC it became apparent that several combinations of conditions were not conducive to the hydrolysis of lactose. Table 3.3.1.1e shows the amount of lactose remaining in each reaction at the end of the 48 hour reaction period. The majority of the

reactions showed very little processing of lactose at all, indicating that the enzyme was inhibited by these reaction conditions. This was not unexpected as the addition of MeCN is known to deactivate the enzyme, as discussed at the beginning of this section.

However, in Table 3.3.1.1e the highlighted reaction letters are those where the most enzyme processing was seen and it is these sets of conditions that will now be discussed.

| | pH 5.0 | | | | pH 7.0 | | | |
|---|---|---|---|---|---|---|---|---|
| % MeCN | 50 | 40 | 30 | 20 | 50 | 40 | 30 | 20 |
| 30 °C | A | B | C | **D** | E | **F** | **G** | **H** |
| % Lac remaining at 48h | 98.16 | 97.66 | 90.60 | **75.65** | 94.38 | **80.89** | **51.06** | **35.06** |
| 55 °C | I | J | K | L | M | N | O | **P** |
| % Lac remaining at 48h | 95.59 | 99.34 | 99.29 | 99.63 | 98.61 | 97.99 | 97.35 | **62.29** |

**Table 3.3.1.1e: Amount of lactose found by HPLC in each reaction at the end of 48 hours**

The graph in Figure 3.3.1.1f gives an idea of the rate of hydrolysis of lactose in these five reactions. We can use this indication of the rate of hydrolysis to rank the five sets of conditions by the amount of hydrolysis that was observed. The set that led to the greatest amount of lactose hydrolysis was H. This can be seen clearly in both Figure 3.3.1.1f and Table 3.3.1.1g. This is then followed by reaction conditions G, P, D and F. These five sets of reaction conditions would be the starting point of the next stage in the screening procedure which was to find out if the enzyme could catalyse transglycosylation reactions under these conditions.

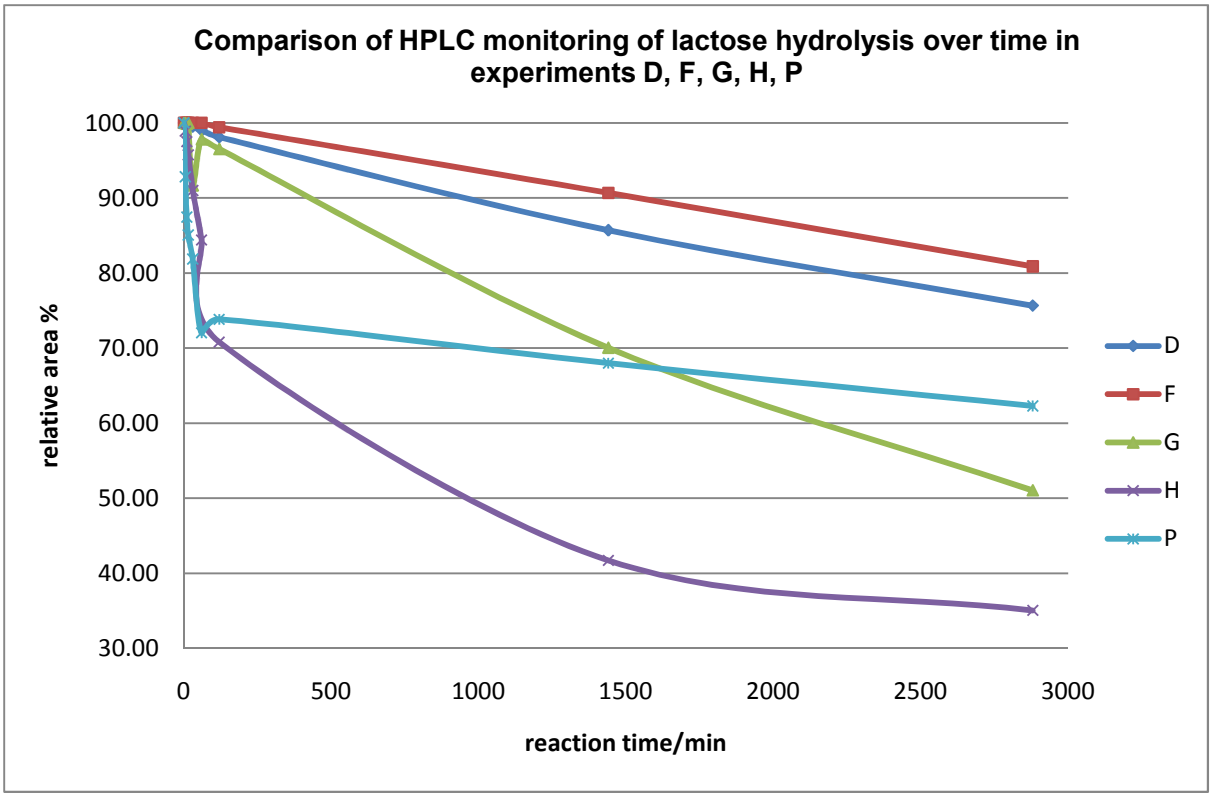


**Figure 3.3.1.1f: Graph to indicate the rate of hydrolysisof lactose in the most promising experiments, ENZ 5 D, F, G, H and P**

| reaction time/min | relative area % lactose in HPLC | | | | |
|---|---|---|---|---|---|
| | D | F | G | H | P |
| 0 | 100.00 | 100.00 | 100.00 | 100.00 | 100.00 |
| 5 | 100.00 | 100.00 | 99.98 | 98.89 | 92.82 |
| 10 | 100.00 | 100.00 | 99.87 | 97.49 | 87.46 |
| 15 | 99.93 | 100.00 | 100.00 | 95.76 | 85.06 |
| 30 | 99.52 | 100.00 | 91.66 | 91.00 | 81.87 |
| 60 | 99.00 | 100.00 | 97.81 | 84.41 | 72.04 |
| 120 | 98.08 | 99.41 | 96.52 | 70.81 | 73.84 |
| 1440 | 85.69 | 90.67 | 70.05 | 41.73 | nr |
| 2880 | **75.65** | **80.89** | **51.06** | **35.06** | **62.29** |

nr – not recorded

**Table 3.3.1.1g: Tabulated HPLC results from the most promising experiments, ENZ 5 D, F, G, H and P**

### 3.3.1.2 Simple transglycosylation reactions under optimised solvent conditions

The next step was therefore to attempt simple transglycosylations with these five sets of conditions. We decided to use both lactose and GalO*p*NP as glycosyl donors. The conditions for these reactions were assessed by measuring the hydrolysis of lactose, so would be optimal for the use of lactose as the glycosyl donor. However, since GalO*p*NP is generally acknowledged to be a very good glycosyl donor we chose to try those successful sets of reaction conditions with GalO*p*NP as well, even though they were not optimised for it. α-Methyl glucose would be used as the glycosyl acceptor (Figure 3.3.1.2a).

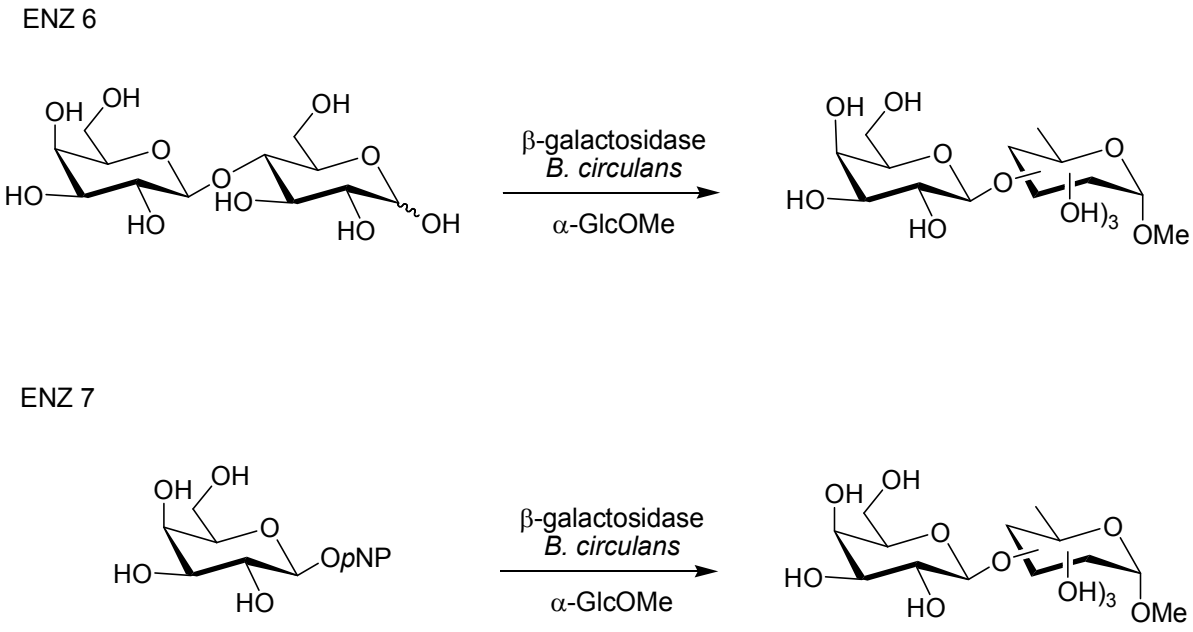


**Figure 3.3.1.2a: Scheme for experiments ENZ 6 and ENZ 7**

| Reaction | pH | % MeCN | Temperature °C |
|---|---|---|---|
| D | 5.0 | 20 | 30 |
| F | 7.0 | 40 | 30 |
| G | 7.0 | 30 | 30 |
| H | 7.0 | 20 | 30 |
| P | 7.0 | 20 | 55 |

**Table 3.3.1.2b: Reaction conditions for experiments ENZ 6 and ENZ 7**

The reactions **ENZ 6** and **ENZ 7** were carried out by suspending the glycosyl donor and GlcOMe in the mixed solvent system, at the given pH and temperature, and stirring with the enzyme. Aliquots were taken at regular intervals and analysed by HPLC and mass spectrometry.

Monitoring of the experiments by HPLC showed the evolution of new peaks in each of the reactions (D, F, G, H, and P). In contrast to the first transglycosylations that we tried in aqueous conditions (Section 3.2), these reactions proceeded very slowly. This was expected however, as the lactose hydrolysis experiments with MeCN were left for 2 days before they were stopped and not much hydrolysis was seen until at least one hour had passed.

The Gal-GlcOMe target again appears around $t_r$ = 1.6 minutes in HPLC which is roughly the same retention time as the glycosyl acceptor, GlcOMe, (see earlier work in Section 3.2.2). At this point monitoring the evolution of the Gal-GlcOMe disaccharide using mass spectrometry became more useful than HPLC because this peak overlap obscured the evolution of the disaccharide. In the HPLCs recorded for these experiments, a shoulder can be seen to appear on the peak for the starting material GlcOMe, which indicates that the disaccharide is forming, but as such its area could not be measured accurately and compared to that of the starting material.

At this point we did not expect to be able to quantify the rate of the reaction or the amount of target disaccharide that was produced. In the mass spectra, the relative peak heights of GlcOMe and the Gal-GlcOMe disaccharide can be compared and from this the effectiveness of the different conditions can be inferred.

In **ENZ 6**, in which lactose was used as the glycosyl donor, the presence of the Gal-GlcOMe disaccharide was detected from 6 hours onwards in the mass spectra of all of the reactions. It is not obvious in the HPLC spectra that the Gal-GlcOMe disaccharide is present for the reasons explained above. In this case the heights of the peaks due to Lac and Gal-GlcOMe

in the mass spectra were compared to give an idea of the extent of enzyme processing of the various sugars.

Examining the data in Table 3.3.1.2c, which shows the peak-height ratio of lactose to the Gal-GlcOMe disaccharide, there is a large difference in the ability of the enzyme to perform the transglycosylation under these different conditions.

| Reaction | Component | 6 h | 24 h | 72 h |
|---|---|---|---|---|
| 6D | Lactose | 1.0 | 1.0 | 1.0 |
| | Gal-GlcOMe | 0.7 | 2.3 | 6.8 |
| 6F | Lactose | 1.0 | 1.0 | 1.0 |
| | Gal-GlcOMe | 0.3 | 1.1 | 2.2 |
| 6G | Lactose | 1.0 | 1.0 | 1.0 |
| | Gal-GlcOMe | 0.4 | 2.2 | 8.5 |
| 6H | Lactose | 1.0 | 1.0 | 1.0 |
| | Gal-GlcOMe | 3.0 | 17.9 | 26.8 |
| 6P | Lactose | 1.0 | 1.0 | 1.0 |
| | Gal-GlcOMe | 0.1 | 0.0 | 0.0 |

**Table 3.3.1.2c: Experiment ENZ 6 – table to show the ratio of lactose to Gal-GlcOMe disaccharide produced in each set of reaction conditions**

Evaluating each set of conditions based on how much of the disaccharide was produced relative to the amount of lactose used, the conditions for reaction **ENZ 6H** clearly produced the best result. When the reactions were stopped at 72 hours **ENZ 6H** had a ratio of 1:27 Lac to Gal-GlcOMe. The results for conditions for **ENZ 6G** and **ENZ 6D** were not as good, **ENZ 6D** being 1:7 and **ENZ 6G** 1:9 Lac to Gal-GlcOMe. Conditions for **ENZ 6F** and **ENZ 6P** showed very little production of the desired disaccharide.

Overall, however, **ENZ 6** was very promising, as we had successfully synthesised our target disaccharide in four of the five reactions.

In **ENZ 7**, in which GalO*p*NP was used as the glycosyl donor, the results were more disappointing: in only two cases, **ENZ 7H** and **ENZ 7P**, was the Gal-GlcOMe disaccharide produced. This was only detected by mass spectrometry and working out the amount relative to the amount of starting material was not possible as GalO*p*NP was not present in the mass spectra.

However, it was possible to conclude that under these reaction conditions, lactose appears to be a better glycosyl donor than GalO*p*NP.

**ENZ8 and ENZ 9 – increased reaction concentration**

At this point we also decided to investigate if increasing the reaction concentration would have any effect on the efficacy of the transglycosylation reaction. We therefore repeated the reactions **ENZ 6** and **ENZ 7** (see table 3.3.1.2b for other conditions), but at three times the concentration. This could decrease the solubility of the reagents in the reaction solution, but we would expect an increase in the amount of the Gal-GlcOMe disaccharide produced should the solubility be adequate.

This reaction was carried out as in the previous two experiments and, as expected, the increased reaction concentration led to more of the reaction components being in suspension.

**ENZ 8**

By comparing the results in Table 3.3.1.2d for **ENZ 8** (lactose, 1.2 M) with those in Table 3.3.1.2c (lactose, 0.4M) it is evident that the production of Gal-GlcOMe was greatly increased by increasing the concentration of the reaction solution.

| Reaction | Component | 6 h | 24 h | 72 h |
|---|---|---|---|---|
| 8D | Lactose | 1.0 | 1.0 | 1.0 |
| | Gal-GlcOMe | 41.7 | 65.0 | 58.0 |
| 8F | Lactose | 1.0 | 1.0 | 1.0 |
| | Gal-GlcOMe | 1.3 | 7.3 | 40.3 |
| 8G | Lactose | 1.0 | 1.0 | 1.0 |
| | Gal-GlcOMe | 1.9 | 13.4 | 53.7 |
| 8H | Lactose | 1.0 | 1.0 | 1.0 |
| | Gal-GlcOMe | 32.2 | 32.2 | 32.2 |
| 8P | Lactose | 1.0 | 1.0 | 1.0 |
| | Gal-GlcOMe | 40.3 | 40.3 | 40.3 |

**Table 3.3.1.2d: Experiment ENZ 8 – table to show the ratio of lactose to Gal-GlcOMe disaccharide produced in each set of reaction conditions**

In **ENZ 9** (GalO*p*NP, 1.2M) the enzyme produced Gal-GlcOMe in each case as it appears in the mass spectra for all five reactions. This is unlike **ENZ 7** (GalO*p*NP, 0.4M) where very little of the disaccharide was made, and only in two sets of reaction conditions, **ENZ 7H** and **ENZ 7P**. Again, due to the lack of GalO*p*NP in the mass spectra and the inability to measure the Gal-GlcOMe peak accurately in the HPLC trace we cannot quantify the extent to which transglycosylation occurred. However, we are able to say that increasing the concentration of the reaction solution markedly increased the transglycosylation reaction when using GalO*p*NP as the glycosyl donor.

Considering the results from these four investigations, it is apparent that increasing the reaction concentration increases the amount of transglycosylation. However, it is also apparent that by adding an organic solvent into the reaction the activity of the enzyme is compromised. It therefore follows that we should determine the activity of the enzyme under these various conditions as this would give us quantifiable results on which to base further studies into transglycosylation.

### 3.3.2 Determining the activity of the enzyme in the presence of MeCN

**ENZ 10**

In this section of the investigation we would determine the activity of the enzyme by monitoring the hydrolysis of GalO*p*NP in the solvent, pH, temperature and concentration conditions used in the previous transglycosylation reactions – experiments **ENZ 6-9** (Figure 3.3.2a).

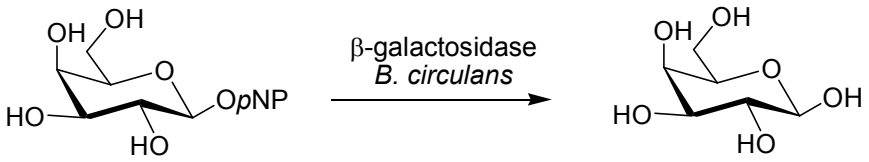


**Figure 3.3.2a: Scheme for the reaction to determine the activity of the enzyme by hydrolysis of GalO*p*NP**

The first investigation would be to determine the activity of the enzyme at the concentration, temperature and pH of the transglycosylation reactions without any MeCN present as control experiments. We would then repeat these experiments with MeCN so that we could compare the difference in the initial rates of the hydrolysis of GalO*p*NP both with and without MeCN.

**Control experiment 1 (ENZ 10C1) – determining the activity of the enzyme in aqueous buffer solution**

The first control experiment was carried out by monitoring the hydrolysis of GalO*p*NP by the β-galactosidase from *B. circulans* over the course of ten minutes. The conditions for each control experiment are given in Table 3.3.2b.

| Reaction number | pH | Concentration/M | Temperature/°C |
|---|---|---|---|
| C1a | 5.0 | 0.170 | 30 |
| C1b | 7.0 | 0.170 | 30 |
| C1c | 5.0 | 0.056 | 30 |
| C1d | 7.0 | 0.056 | 30 |
| C1e | 7.0 | 0.170 | 55 |
| C1f | 7.0 | 0.056 | 55 |

**Table 3.3.2b: Reaction conditions for ENZ 10C1**

An example UV plot showing the hydrolysis of GalO*p*NP is shown in Figure 3.3.2c (the remaining UV plots and the plots for the determination of the molar absorptivity coefficient for *p*-nitrophenolate are in the Appendix Section 3.3.2). The initial rate of hydrolysis of GalO*p*NP has been calculated for each reaction and is shown in Figure 3.3.2d.

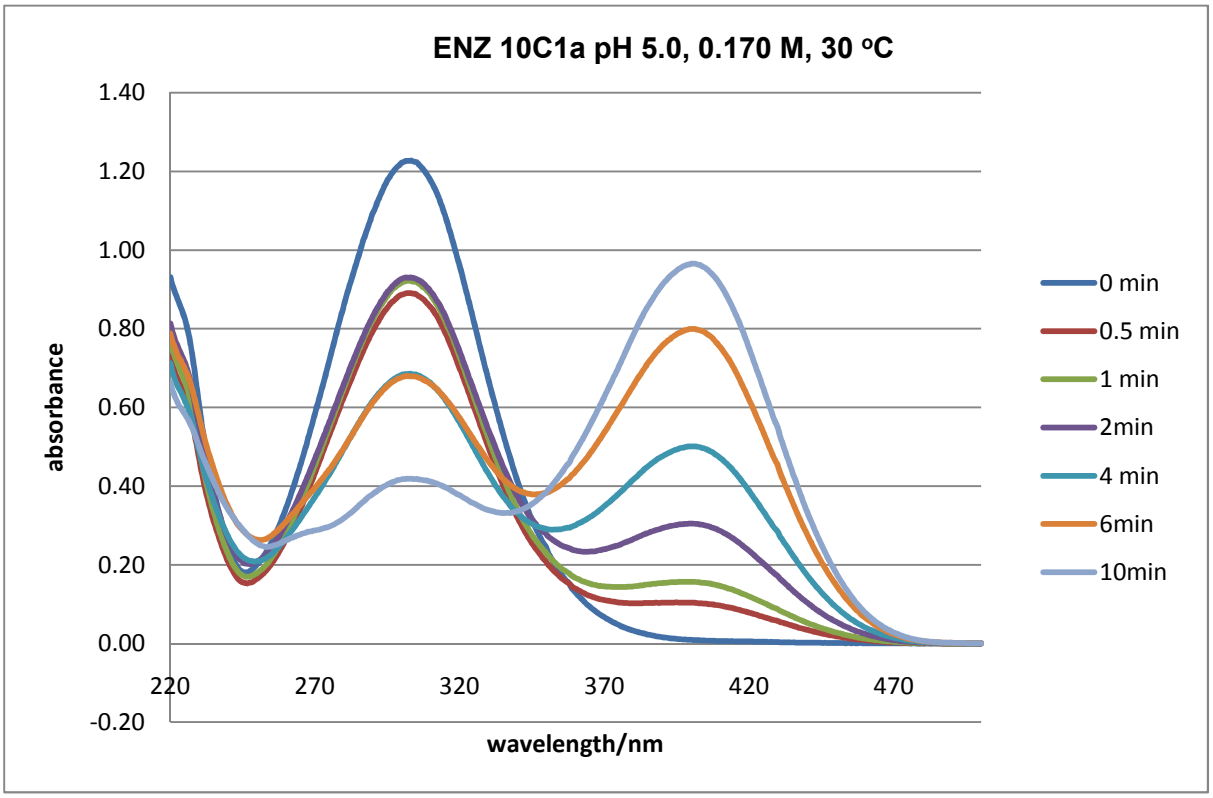


**Figure 3.3.2c: UV plot showing the hydrolysis of GalO*p*NP in reaction conditions ENZ 10C1a**

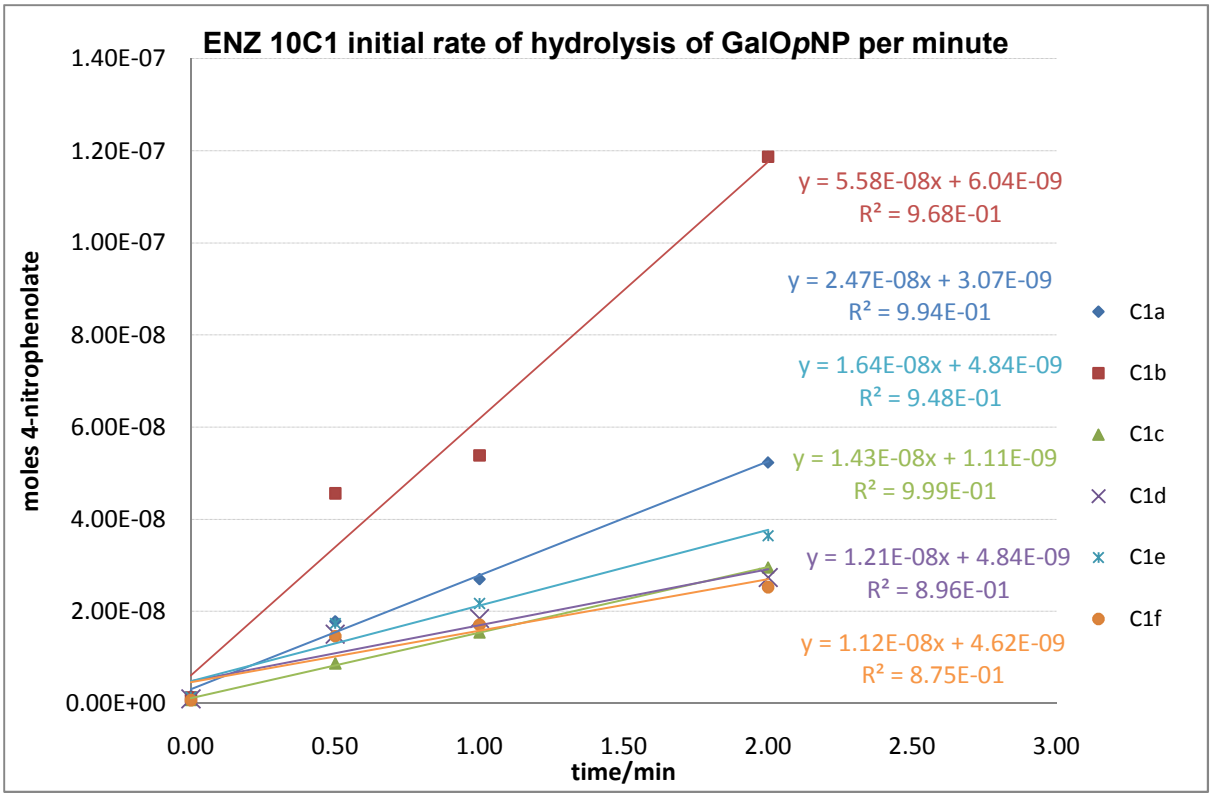


**Figure 3.3.2d: Calculation of the initial rate of hydrolysis of GalO*p*NP in experiment ENZ10 C1**

Examining the initial rate of hydrolysis for each of the six control reactions shown in Figure 3.3.2d and Table 3.3.2e, the conditions used for C2 (pH 7.0, 0.170 M, 30 $^{o}$C) give the fastest rate of hydrolysis at 5.58 x $10^{-8}$ moles of GalO*p*NP hydrolysed per minute.

| Reaction number | pH | Concn/M | Temp/$^{o}$C | Rate of hydrolysis moles GalO*p*NP $min^{-1}$ | Rate of hydrolysis μmoles GalO*p*NP $min^{-1}$ |
|---|---|---|---|---|---|
| C1a | 5.0 | 0.170 | 30 | 2.47 x $10^{-8}$ | 2.47 x $10^{-2}$ |
| C1b | 7.0 | 0.170 | 30 | 5.58 x $10^{-8}$ | 5.58 x $10^{-2}$ |
| C1c | 5.0 | 0.056 | 30 | 1.43 x $10^{-8}$ | 1.43 x $10^{-2}$ |
| C1d | 7.0 | 0.056 | 30 | 1.21 x $10^{-8}$ | 1.21 x $10^{-2}$ |
| C1e | 7.0 | 0.170 | 55 | 1.64 x $10^{-8}$ | 1.64 x $10^{-2}$ |
| C1f | 7.0 | 0.056 | 55 | 1.12 x $10^{-8}$ | 1.12 x $10^{-2}$ |

**Table 3.3.2e: Tabulated data for the initial rate of hydrolysis of GalO*p*NP in experiment ENZ 10 C1**

One unit of activity for a β-galactosidase is defined as "the amount of enzyme needed to release 1 μmol $min^{-1}$ of *p*-nitrophenol from *p*-nitrophenol galactose". Since 7 mg of enzyme hydrolysed 5.58 x $10^{-2}$ μmoles GalO*p*NP $min^{-1}$ in C1b, the activity of the enzyme in these conditions is 1 ÷ 5.58 x $10^{-2}$ x 0.007 = 0.125 g. In our first calculation of enzyme activity (Section 3.2.1) the amount of enzyme needed for this one unit of activity is 0.003 g (pH 6.0 buffer, 2.0 M, 37 $^{o}$C). So, the activity of the enzyme is either not as high under the conditions of the control experiment or has diminished during storage.

Now that we had the control results for comparison, we would now carry out enzyme activity experiments in the presence of MeCN under similar reaction conditions.

**Determining the activity of the enzyme in the presence of MeCN**

**ENZ 11**

In this investigation the activity of the enzyme was determined in ten reactions corresponding to the most successful conditions for the hydrolysis of lactose D, F, G, H and P (see Section 3.3.1.2). Because of the presence of MeCN the rate of hydrolysis would be greatly reduced compared to the previous experiment, so aliquots were taken for monitoring the reaction at greater intervals and over the course of 6 hours.

In order to determine the activity of the enzyme, GalO*p*NP was dissolved in the mixed solvent systems shown in Table 3.2.2f. This was then stirred at the given temperature with the β-galactosidase from *B. circulans* for a total of 6 hours. Aliquots were taken at 30 minute intervals and the amount of *p*-nitrophenol released was determined by monitoring the absorbance of *p*-nitrophenolate by UV-vis spectroscopy in NaOH solution.

| Reaction number | | pH | Concentration/M | % MeCN | Temperature/$^{o}$C |
|---|---|---|---|---|---|
| **ENZ 11 C1** | D | 5.0 | 0.170 | 20 | 30 |
| | F | 7.0 | 0.170 | 40 | 30 |
| | G | 7.0 | 0.170 | 30 | 30 |
| | H | 7.0 | 0.170 | 20 | 30 |
| | P | 7.0 | 0.170 | 20 | 55 |
| **ENZ 11 C2** | D | 5.0 | 0.056 | 20 | 30 |
| | F | 7.0 | 0.056 | 40 | 30 |
| | G | 7.0 | 0.056 | 30 | 30 |
| | H | 7.0 | 0.056 | 20 | 30 |
| | P | 7.0 | 0.056 | 20 | 55 |

**Table 3.3.2f: Reaction conditiond for experiment ENZ 11**

The UV plots showing the hydrolysis of GalO*p*NP are shown in the Appendix Section 3.3.2. In order to highlight the very much reduced activity of the enzyme when MeCN is used as a co-solvent, examples of a typical UV spectrum for these reaction sets C1 and C2 are shown in Figure 3.3.2g.

The initial rate of hydrolysis of GalO*p*NP has been calculated for each reaction and is shown in Figure 3.3.2h. In this case the initial rate has been calculated over the course of 6 hours as the hydrolysis reaction was so slow (which can be seen in the two UV spectra in Figure 3.2.2g).

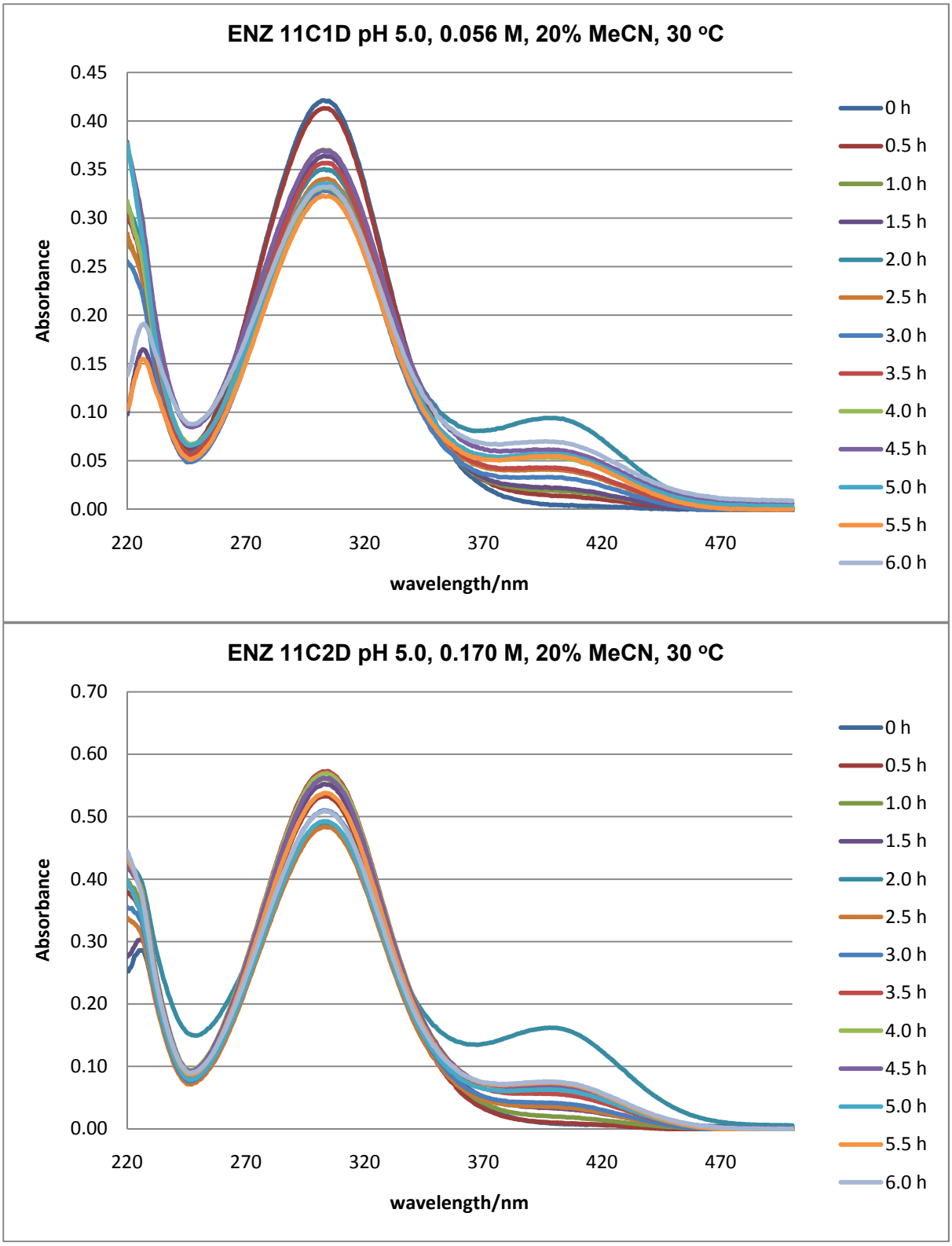


**Figure 3.3.2g: Typical UV spectra for reaction sets ENZ 11C1 and C2**

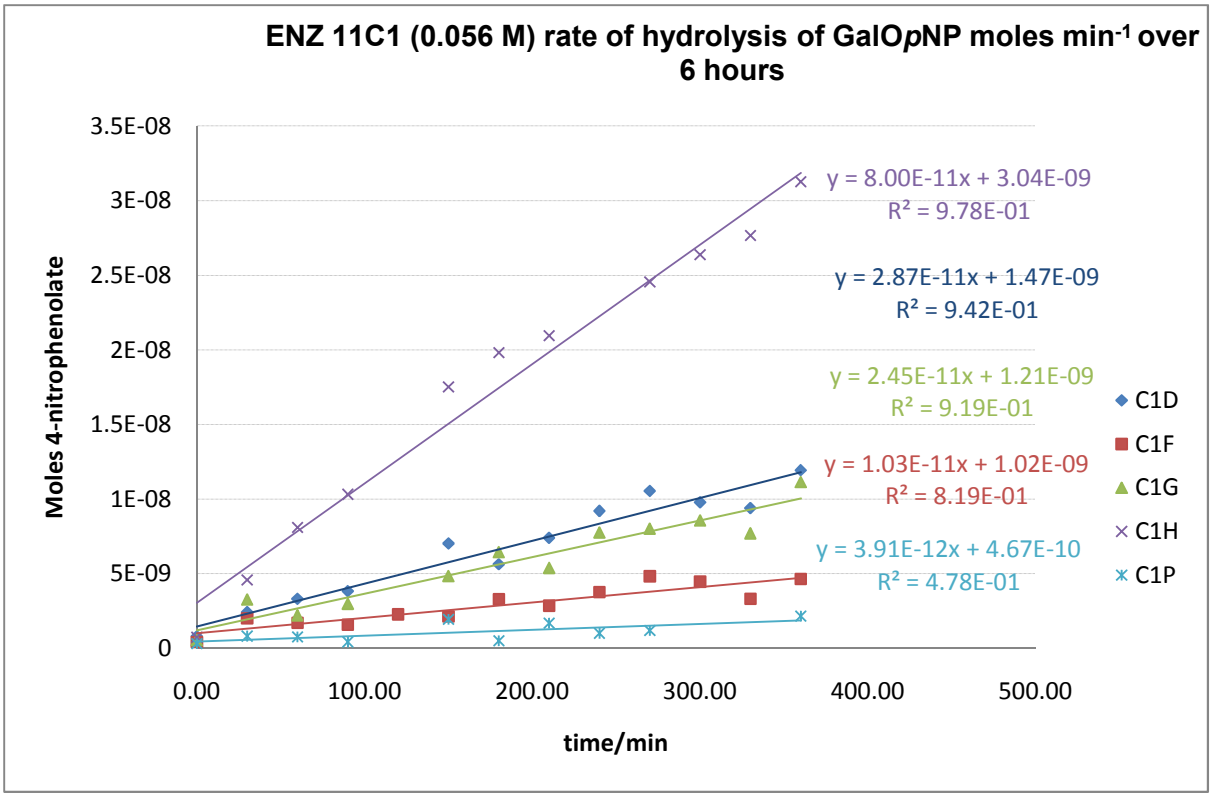


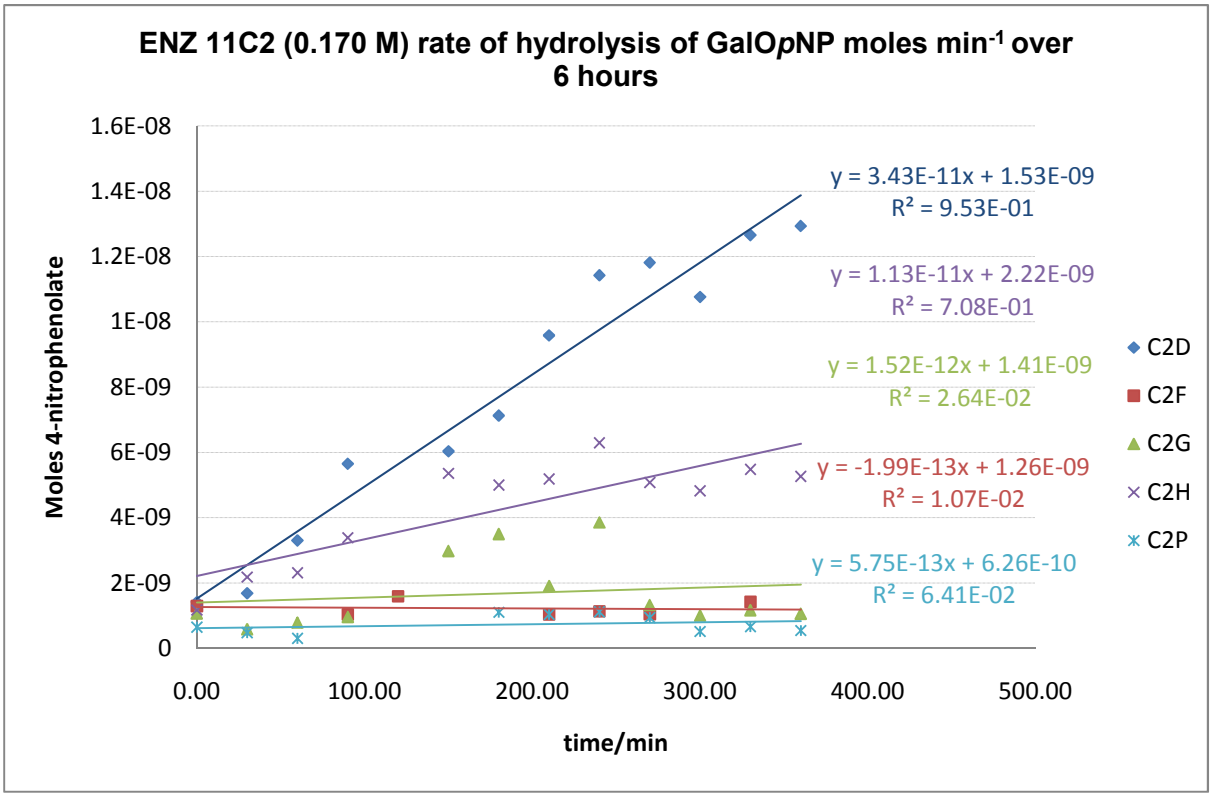


NB – anomalous points due to sampling errors have been removed from the calculation of the rate of hydrolysis in both graphs

**Figure 3.3.2h: Initial rate calculations for experiments ENZ 11C1 and 11C2**

Table 3.3.2i below gives the results for the calculations of the rate of hydrolysis of GalO*p*NP by the β-galactosidase from *B. circulans* in the presence of MeCN co-solvent. There is one set of anomalous results in ENZ 11C2F where a negative rate of hydrolysis is seem. This is most likely due to sampling errors.

| Reaction number | | pH | Conc/M | % MeCN | Temp/$^{o}$C | Rate of hydrolysis moles GalO*p*NP min$^{-1}$ | Rate of hydrolysis μmoles GalO*p*NP min$^{-1}$ |
|---|---|---|---|---|---|---|---|
| | D | 5.0 | 0.170 | 20 | 30 | $2.87 \times 10^{-11}$ | $2.87 \times 10^{-5}$ |
| **ENZ** | F | 7.0 | 0.170 | 40 | 30 | $1.03 \times 10^{-11}$ | $1.03 \times 10^{-5}$ |
| **11** | G | 7.0 | 0.170 | 30 | 30 | $2.45 \times 10^{-11}$ | $2.45 \times 10^{-5}$ |
| **C1** | H | 7.0 | 0.170 | 20 | 30 | $8.00 \times 10^{-11}$ | $8.00 \times 10^{-5}$ |
| | P | 7.0 | 0.170 | 20 | 55 | $3.91 \times 10^{-12}$ | $3.91 \times 10^{-6}$ |
| | D | 5.0 | 0.056 | 20 | 30 | $3.43 \times 10^{-11}$ | $3.43 \times 10^{-5}$ |
| **ENZ** | F | 7.0 | 0.056 | 40 | 30 | $-1.99 \times 10^{-13}$ | $-1.99 \times 10^{-7}$ |
| **11** | G | 7.0 | 0.056 | 30 | 30 | $1.52 \times 10^{-12}$ | $1.52 \times 10^{-6}$ |
| **C2** | H | 7.0 | 0.056 | 20 | 30 | $1.13 \times 10^{-11}$ | $1.13 \times 10^{-5}$ |
| | P | 7.0 | 0.056 | 20 | 55 | $5.75 \times 10^{-13}$ | $5.75 \times 10^{-7}$ |

**Table 3.3.2i: Tabulated data for the initial rate of hydrolysis of GalOpNP in experiment ENZ 11 C1 and C2**

It was clear from these results that the higher reaction concentration (0.170 M), 20% MeCN and a temperature of 30 $^{o}$C worked best, with pH 7.0 (**ENZ 11C2H**) giving a 2.8 fold increase in hydrolysis compared to the pH 5.0 (**ENZ 11C2D**) reaction.

Set of conditions **ENZ 11C2H** gives the fastest rate of hydrolysis at $8.00 \times 10^{-5}$ μmoles GalO*p*NP min$^{-1}$, although this is still three orders of magnitude lower than when the hydrolysis was carried out in the absence of MeCN co-solvent (refer to Table 3.2.2e; fastest rate $5.58 \times 10^{-2}$ μmoles GalO*p*NP min$^{-1}$). Since 7 mg of enzyme hydrolysed $8.00 \times 10^{-5}$

μmoles GalO*p*NP $min^{-1}$ in **ENZ 11C2H**, the activity of the enzyme under these conditions is 1 ÷ 8.00 x $10^{-5}$ x 0.007 = 87.5 g $\mu mol^{-1}$ GalO*p*NP. When compared to the value for the activity of BC04 C1b, which was 0.125 g $\mu mol^{-1}$ GalO*p*NP, this is a staggering difference in activity.

87.5 g of enzyme is just not a sensible amount to put into such a small reaction; it is completely impractical and inefficient. However, the presence of MeCN is having a huge impact on the efficacy of the enzyme, and we needed to find a sensible way to overcome this problem. The solution lies in using more catalyst. So, more enzyme, but a sensible amount of it.

### 3.3.3 Increasing the rate of hydrolysis of GalO*p*NP in the presence of MeCN by increasing the amount of enzyme used

The next step to optimising the conditions for our transglycosylation reactions would be to investigate the effect of increasing the amount of enzyme added, thereby increasing the rate hydrolysis of the glycosyl donor, GalO*p*NP. In the previous Section, Table 3.3.2i shows the rate of hydrolysis by the enzyme under various sets of conditions. We chose the two best sets of conditions (those with the highest rate of hydrolysis) for further investigation.

In the previous experiment, conditions **ENZ 11C2D** and **ENZ 11C2H** gave the highest rates of hydrolysis, so we would begin our investigation using these two sets of conditions. The conditions that worked best were:

- 20% MeCN
- 0.170 M wrt donor (1.2 M wrt acceptor)
- 30 $^{o}$C
- pH 5.0 and pH 7.0

So, aside from the amount of enzyme being added, the only difference between the two reactions is the pH.

Before carrying on with the concentration at 1.2 M with respect to the glycosyl donor, GlcOMe, we felt it prudent to carry out a solubility test under these conditions using $NpCH_2GlcOMe$ (**32**). We attempted to dissolve 50 mg of the naphthyl-functionalised sugar into a 0.4 M, 80:20 mixture of water and MeCN respectively. The solution was opaque, so the sugar had not fully dissolved. Given this result we felt that we needed to press on using a lower concentration as we were certain that using a more concentrated solution would mean that little of the naphthyl-sugar substrate would dissolve in the solution and therefore there would not be much available for the enzyme to process. Although any that does go into solution and is processed would shift the equilibrium to allow more acceptor to go into solution.

We would therefore carry out eight screening reactions using a 2-, 4-, 8- and 16-fold increase in the amount of enzyme added as detailed in Table 3.3.3a below.

**ENZ 12**

In order to determine the activity of the enzyme, GalO*p*NP was dissolved in buffer with 20% MeCN co-solvent. The reaction mixtures were then stirred at 30 $^{o}$C with different amounts of the β-galactosidase from *B. circulans* (see Table 3.3.3a for details) for a total of 6 hours. Aliquots were taken at 30 minute intervals and the amount of *p*-nitrophenol released was determined by monitoring the absorbance of *p*-nitrophenolate by UV-vis spectroscopy in NaOH solution.

| Reaction conditions | | Standard amount of enzyme added/g | Increased amount of enzyme added /g | | | |
|---|---|---|---|---|---|---|
| | | | X2 | X4 | X8 | X16 |
| | | 0.007 | **0.014** | **0.028** | **0.056** | **0.112** |
| D | pH | | | | | |
| | 5.0 | reaction number | 2D | 4D | 8D | 16D |
| H | pH | | | | | |
| | 7.0 | reaction number | 2H | 4H | 8H | 16H |

**Table 3.3.3a: Reaction conditions and numbering for experiment ENZ 12**

The screening experiment was carried out successfully, the UV-vis spectra for each of the eight experiments are in the Appendix.

In all of the reaction solutions there was a proportion of the enzyme that had not dissolved. Experiments **16D** and **16H** were extremely thick with solid compared to experiments **8D** and **8H**. A suspension of the enzyme in the reaction solution is expected, but the extent of the solid in experiments **16D** and b seemed far too great to be of any benefit to the progress of the reaction. From a practical and efficiency perspective, using 16 times the 'normal' amount of enzyme did not seem a sensible path to take.

Compared to the UV-vis spectra recorded for the previous experiment (Section 3.3.2), the curves in this screening experiment showed a much greater processing of GalO*p*NP over the same time period and at a faster rate – as we had predicted.

Using the results from the UV-vis spectra, initial rate plots have been produced. The initial rate period was taken to be the first 90 minutes. Plots of the moles of 4-nitrophenolate released over the six hours of the reaction period all showed the characteristic sigmoidal shape of a rate graph.

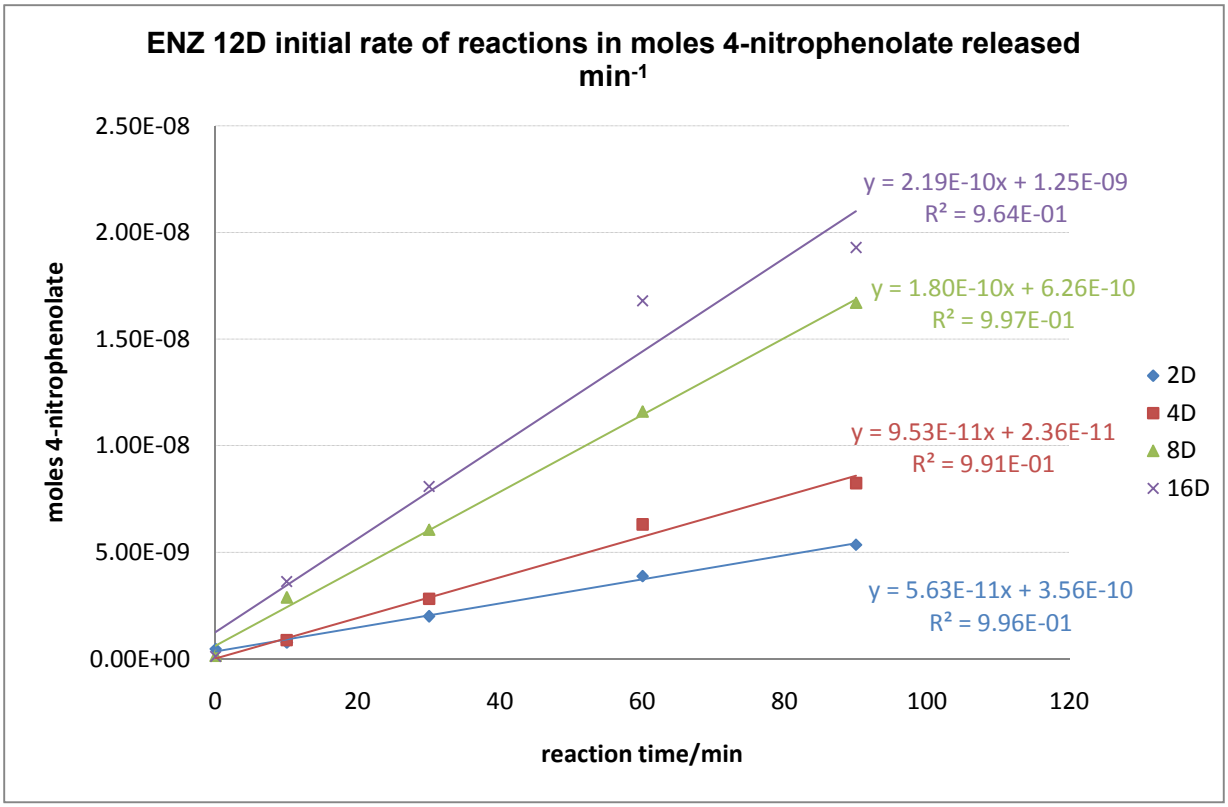


**Figure 3.3.3b: Calculation of initial rate of reaction in ENZ 12D**

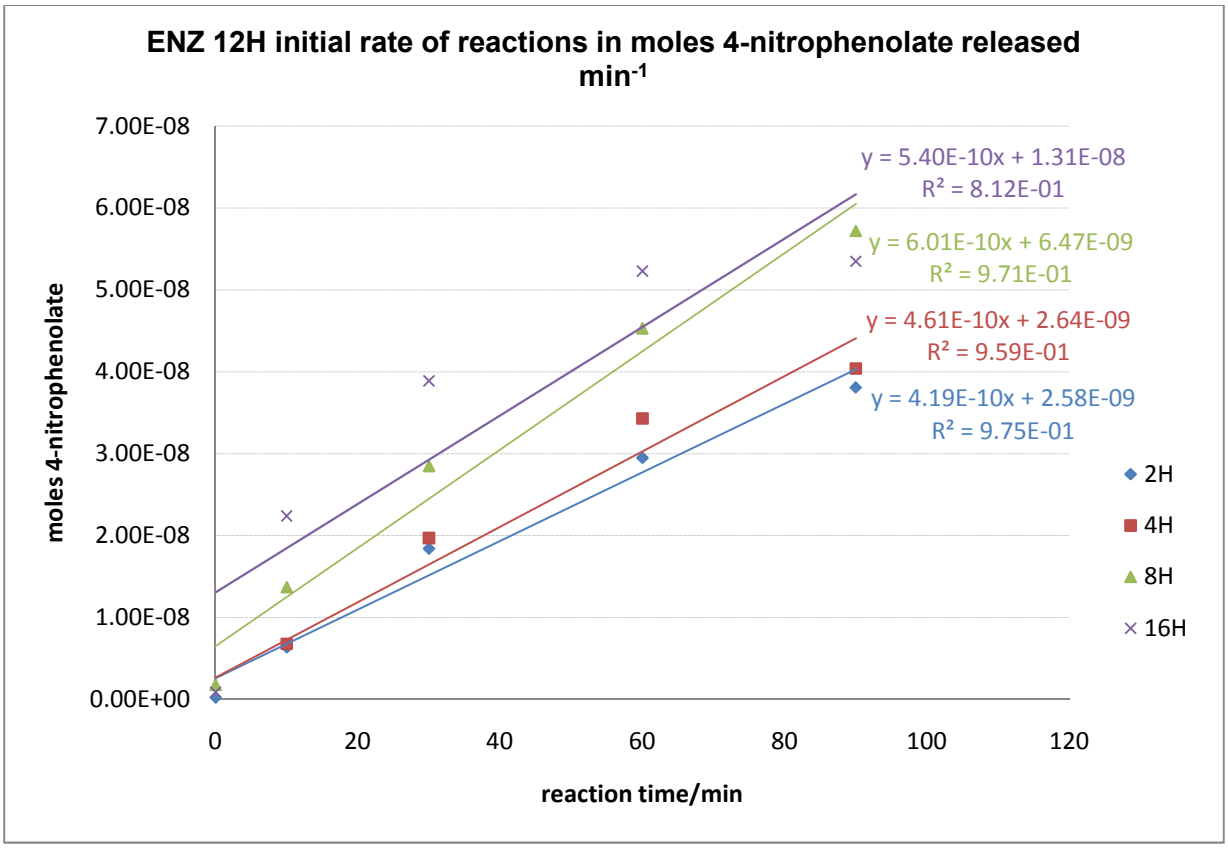


**Figure 3.3.3b: Calculation of initial rate of reaction in ENZ 12H**

| Reaction number | pH | Rate of hydrolysis moles GalO*p*NP $min^{-1}$ | Rate of hydrolysis μmoles GalO*p*NP $min^{-1}$ |
|---|---|---|---|
| 2D | 5.0 | $5.63 \times 10^{-11}$ | $5.63 \times 10^{-5}$ |
| 4D | 5.0 | $9.53 \times 10^{-11}$ | $9.53 \times 10^{-5}$ |
| 8D | 5.0 | $1.80 \times 10^{-10}$ | $1.80 \times 10^{-4}$ |
| 16D | 5.0 | $2.19 \times 10^{-10}$ | $2.19 \times 10^{-4}$ |
| 2H | 7.0 | $4.19 \times 10^{-10}$ | $4.19 \times 10^{-4}$ |
| 4H | 7.0 | $4.61 \times 10^{-10}$ | $4.61 \times 10^{-4}$ |
| 8H | 7.0 | $6.01 \times 10^{-10}$ | $6.01 \times 10^{-4}$ |
| 16H | 7.0 | $5.40 \times 10^{-10}$ | $5.40 \times 10^{-4}$ |

**Table 3.3.3d: Tabulated results of initial rate calculationd for experiment ENZ 12**

Examining the results in Table 3.3.3d, the fastest rate of hydrolysis of GalO*p*NP was with the set of conditions **8H**. A rate of $6.01 \times 10^{-4}$ μmoles GalO*p*NP $min^{-1}$ was achieved at pH 7.0 with 8 times the amount of enzyme used (compared to ENZ 11). In terms of the activity of the enzyme this works out that 1 unit of enzyme is 11.6 g. This is still unmanageable in terms of the experiments we wish to carry out if we were to follow the original procedure. However, we did now have an optimum set of conditions on which to base those experiments and evidence to show that the enzyme can process GalO*p*NP at an acceptable rate even in the presence of MeCN.

As explained previously, although in the case of **16D** using a greater amount of enzyme did increase the initial rate of the reaction, the sheer amount of solid that remains un-dissolved in solution makes this reaction difficult to work with. For these reasons and the results from the rate calculations, we chose to begin the next phase of the enzyme work based upon the following reaction conditions:

- pH 5.0/7.0;
- 8 x 2.45 U enzyme;
- 0.4M reaction concentration wrt the glycosyl acceptor;
- 20% MeCN;
- 30 $^{o}$C;
- minimum 6 hour reaction time.

### 3.3.4 Transglycosylations using the naphthyl-functionalised methyl glucosides

The next stage in the project was to use our optimised reaction conditions to make disaccharides containing our three naphthyl-functionalised methyl glucosides, **32**, **33** and **34**. We began by checking our optimised reaction using **32** first as this is the most easily accessed of the three naphthyl-functionalised glucosides (Figure 3.3.4a)

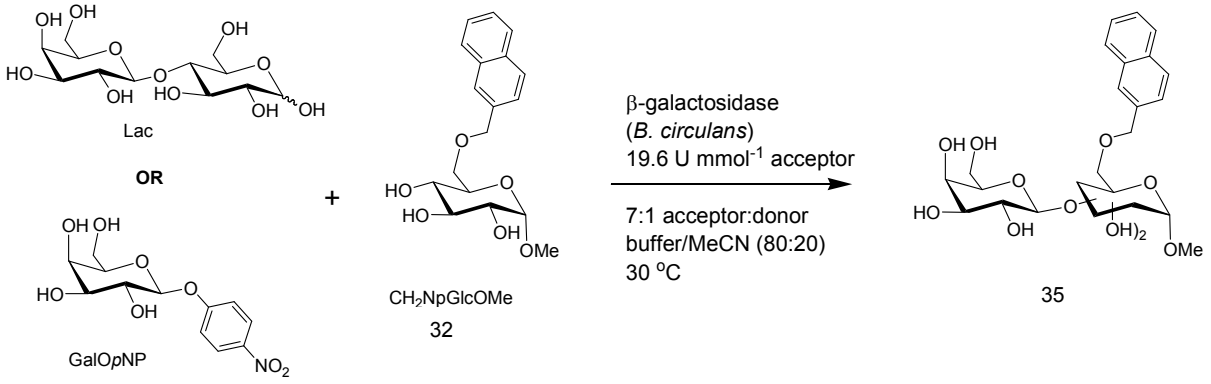


**Figure 3.3.4a: Scheme for the initial investigation into the use of our novel naphthyl-functionalised methyl glucosides as substrates for the β-galactosidase from *B. circulans***

In this first attempt at the transglycosylation we chose to assess which pH (5.0 or 7.0) and which glycosyl donor (Lac or GalO*p*NP) gave the best results.

### 3.3.4.1 Initial syntheses of napthyl-functionalised Gal-NpCH2GlcOMe disaccharide 35

**ENZ 13 & ENZ 14**

In the first instance we carried out four test reactions using naphthyl-functionalised sugar **32** (NpCH2GlcOMe) as the glycosyl acceptor to determine which of these four sets of conditions gave the best result in terms of yield and ability to monitor the reaction. Following the scheme shown in Figure 3.3.4a, the following reaction conditions would be tested (Table 3.3.4.1a):

| Reaction number | pH | Glycosyl donor |
|---|---|---|
| ENZ 13D | 5.0 | Gal*O*pNP |
| ENZ 13H | 7.0 | Gal*O*pNP |
| ENZ 14D | 5.0 | Lac |
| ENZ 14H | 7.0 | Lac |

**Table 3.3.4.1a: Reaction details for experiments ENZ 13 and ENZ 14**

The reactions were carried out by suspending the glycosyl donor (Gal*O*pNP or Lac) and naphthyl-functionalised sugar **32** in the mixed solvent system (pH 5.0 or 7.0 buffer/MeCN 80:20) at 30 $^{o}$C. The β-galactosidase from *B. circulans* was then added and aliquots of the reaction solution were taken at regular intervals for analysis by HPLC and mass spectrometry. After 24 hours the reaction was stopped by denaturing the enzyme by heating. The reaction mixture was then freeze-dried and the carbohydrate residues were acetylated to facilitate the separation (by column chromatography) and characterisation of the products.

HPLC monitoring was done using a UV (224 nm) and an ECD detector simultaneously. As our target disaccharide is UV-active we focused on the appearance of new UV-active peaks in the HPLC.

**ENZ 13: Experiments using GalO*p*NP as the glycosyl donor**

**ENZ 13D (pH 5.0)**

The first new UV-active peak seen in the HPLC monitoring appeared at 30 minutes as a shoulder on the broad peak at $t_r$ = 7.1 min which is the acceptor **32** (Figure 3.3.4.1b).

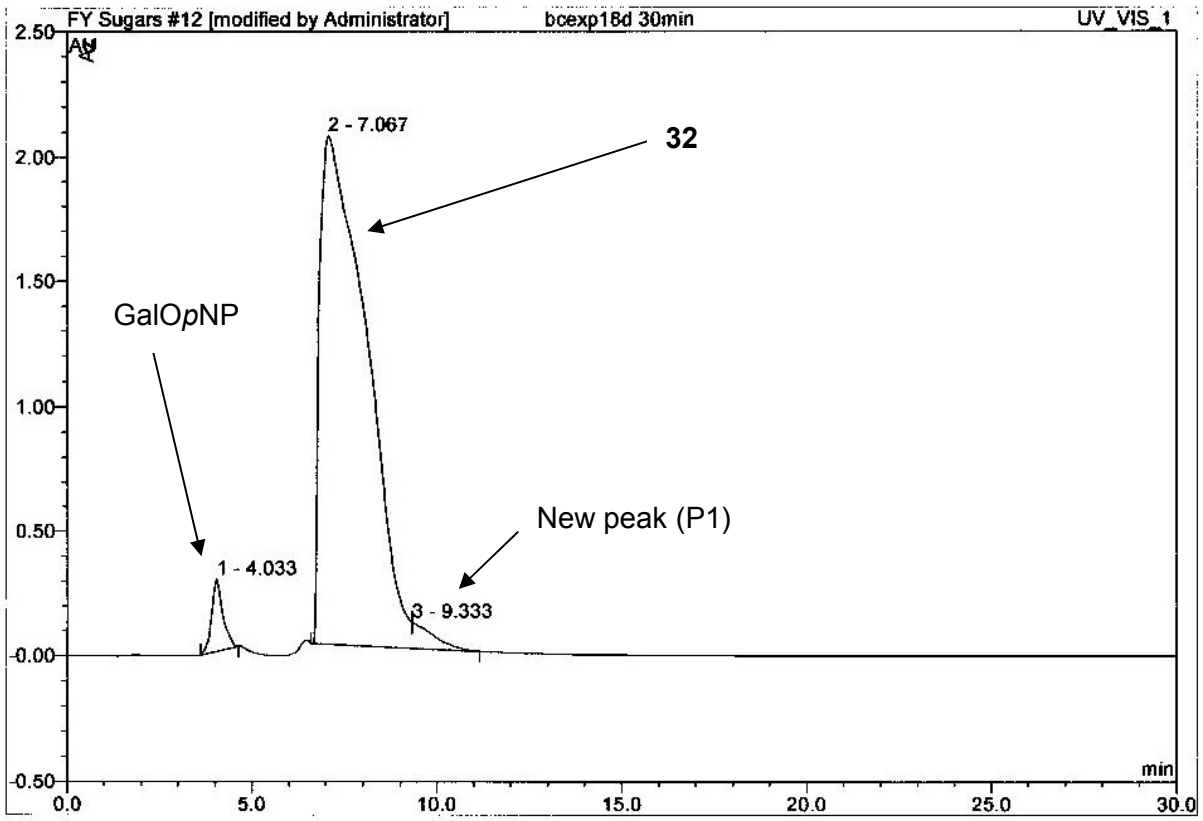


| No. | Ret.Time min | Peak Name | Height AU | Area AU*min | Rel.Area % | Amount | Type |
|---|---|---|---|---|---|---|---|
| 1 | 4.03 | n.a. | 0.289 | 0.101 | 3.25 | n.a. | BMB* |
| 2 | 7.07 | n.a. | 2.037 | 2.941 | 94.64 | n.a. | BM * |
| 3 | 9.33 | n.a. | 0.101 | 0.066 | 2.12 | n.a. | MB* |
| Total: | | | 2.427 | 3.107 | 100.00 | 0.000 | |

**Figure 3.3.4.1b: ENZ 13D HPLC at 30 minutes**

The HPLC trace at 1 hour was very similar to this and the shoulder at $t_r$ = 9.3 minutes (P1) continued to increase until at 24 hours it was large enough to have become a significant part of the peak at $t_r$ = 7.1 minutes corresponding to naphthyl-functionalised sugar **32** (Figure

3.3.4.1c). The peak at $t_r$ =11.5 minutes appeared after 5 hours but was a relatively small amount of the mixture of compounds.

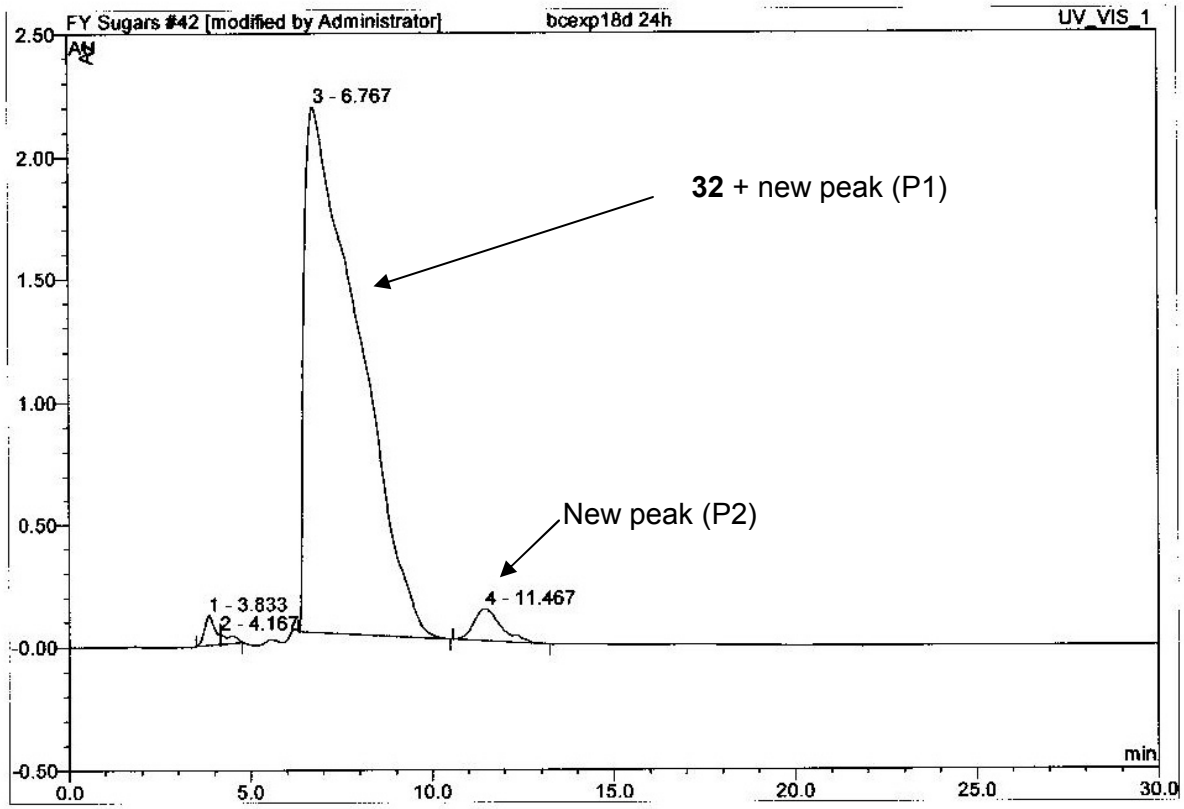


| No. | Ret.Time min | Peak Name | Height AU | Area AU*min | Rel.Area % | Amount | Type |
|---|---|---|---|---|---|---|---|
| 1 | 3.83 | n.a. | 0.119 | 0.039 | 1.03 | n.a. | BM * |
| 2 | 4.17 | n.a. | 0.037 | 0.013 | 0.35 | n.a. | MB* |
| 3 | 6.77 | n.a. | 2.142 | 3.630 | 95.69 | n.a. | BMB |
| 4 | 11.47 | n.a. | 0.129 | 0.111 | 2.93 | n.a. | BMB* |
| **Total:** | | | 2.427 | 3.793 | 100.00 | 0.000 | |

**Figure 3.3.4.1c: ENZ 13D HPLC at 24 hours**

The graph and in Figure 3.3.4.1d show these changes over the whole 24 hour period of the reaction. The amount of naphthyl-functionalised sugar **32** decreases over the course of the reaction, as one would expect, and Gal*O*p*NP shows very slow hydrolysis as there is still a significant amount remaining at 24 hours.

| Reaction time | Relative area % | | | |
|---|---|---|---|---|
| | $t_r$ = 4.0 - 4.7 min (GalO*p*NP + unknown) | $t_r$ = 7.0 min (**32**) | $t_r$ = 9.3 min (P1) | $t_r$ = 11.5 min (P2) |
| 0 min | 4.47 | 95.53 | | |
| 10 min | 3.66 | 96.34 | | |
| 30 min | 3.25 | 94.64 | 2.12 | |
| 1 h | 3.5 | 92.08 | 4.42 | |
| 2 h | 3.42 | 90.24 | 6.35 | |
| 3 h | 2.38 | 90.59 | 7.03 | |
| 4 h | 2.64 | 88.27 | 9.08 | |
| 5 h | 2.63 | 85.41 | 11.55 | 0.41 |
| 6 h | 2.43 | 83.91 | 12.99 | 0.66 |
| 24 h | 1.38 | 95.69 | | 2.93 |

**Tabulated HPLC data from experiment ENZ 13D**

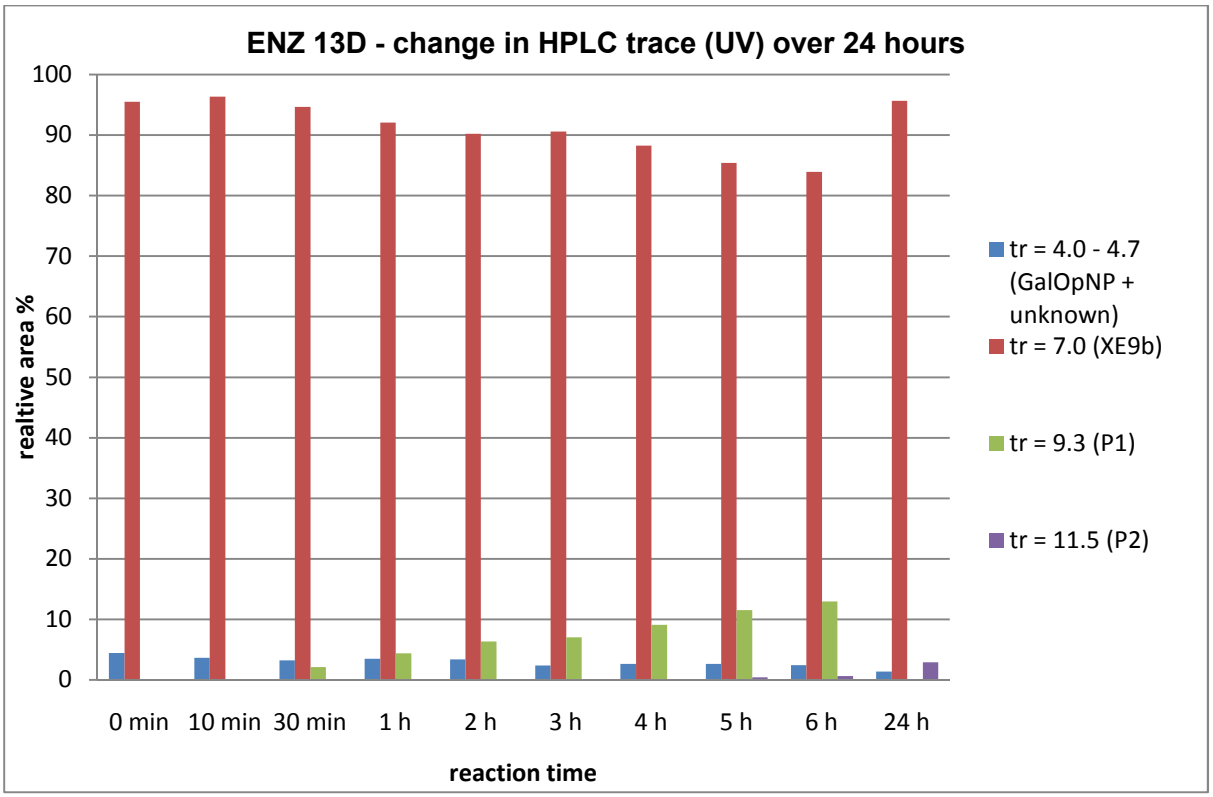


**Figure 3.3.4.1d: Graph to show the overall progress of ENZ 13D over the course of the reaction**

**ENZ 13H (pH 7.0)**

The first new UV-active peak observed in the HPLC monitoring of this reactions appeared after 10 minutes as a shoulder on the broad peak at $t_r$ = 7.1 min which is naphthyl-functionalised sugar **32**. Under these reaction conditions (pH 7.0) the consumption of **32** and the increase in P1 was much faster than in 13D. There are also more distinct peaks in the HPLC trace, suggesting a number of similar compounds. This was different from the HPLC observed in 13D where an indistinct shoulder formed instead. The trace recorded at 24 hours has a broad peak from 7.0 – 9.7 minutes which can be clearly split into four separate peaks (Figure 3.3.4.1e). For ease of comparison I have grouped the peaks due to P1 together in the table and graph shown in Figure 3.3.4.1f.

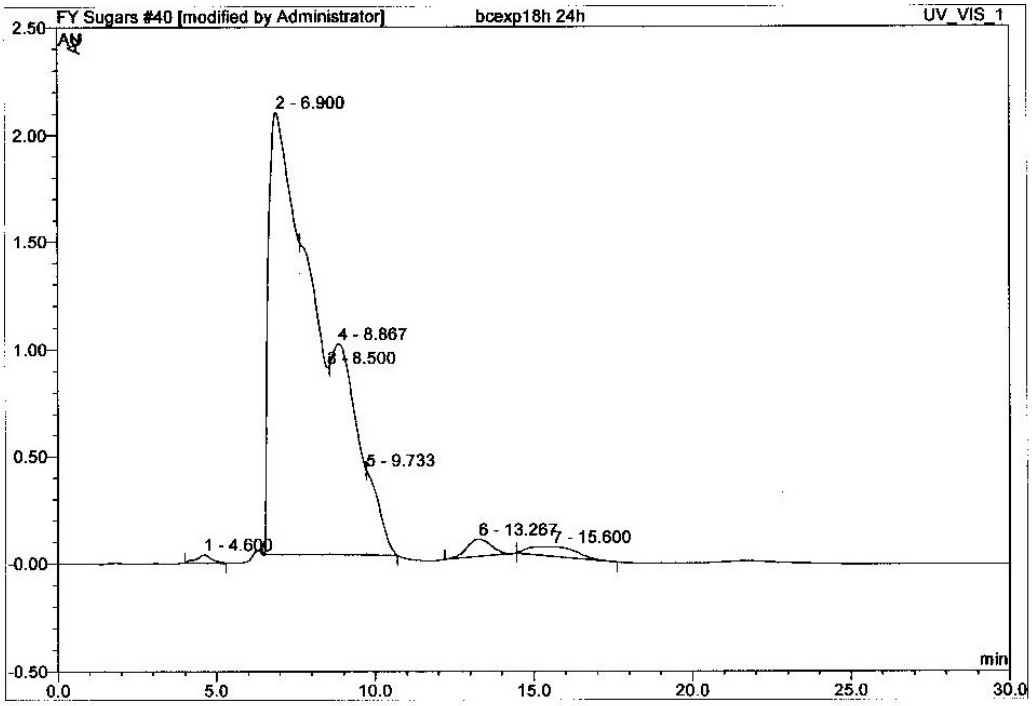


| No. | Ret.Time min | Peak Name | Height AU | Area AU*min | Rel.Area % | Amount | Type |
|---|---|---|---|---|---|---|---|
| 1 | 4.60 | n.a. | 0.036 | 0.019 | 0.47 | n.a. | BMB* |
| 2 | 6.90 | n.a. | 2.058 | 1.829 | 43.94 | n.a. | BM * |
| 3 | 8.50 | n.a. | 0.870 | 1.105 | 26.55 | n.a. | M * |
| 4 | 8.87 | n.a. | 0.983 | 0.897 | 21.54 | n.a. | M * |
| 5 | 9.73 | n.a. | 0.393 | 0.174 | 4.18 | n.a. | MB* |
| 6 | 13.27 | n.a. | 0.078 | 0.067 | 1.62 | n.a. | BMb* |
| 7 | 15.60 | n.a. | 0.042 | 0.071 | 1.70 | n.a. | bMB* |
| Total: | | | 4.461 | 4.162 | 100.00 | 0.000 | |

**Figure 3.3.4.1e: ENZ 13H HPLC at 24 hours**

| Reaction time | Relative area % | | | |
|---|---|---|---|---|
| | $t_r$ = 4.0 - 4.7 min (GalO*p*NP + unknown) | $t_r$ = 7.0 min (**32**) | $t_r$ = 8.5 - 9.7 min (P1) | tr = 13.2-15.6 min (P3) |
| 0 min | 4.73 | 95.27 | | |
| 10 min | 4.05 | 93.24 | 2.7 | |
| 30 min | 2.61 | 91.04 | 6.36 | |
| 1 h | 1.47 | 82.77 | 14.2 | 1.56 |
| 2 h | 1.16 | 75.84 | 19.47 | 3.53 |
| 3 h | 0.78 | 69.86 | 24.77 | 4.59 |
| 4 h | 0.6 | 67.46 | 26.43 | 5.5 |
| 5 h | 0.58 | 66.22 | 28.08 | 5.11 |
| 6 h | 0.5 | 63.46 | 29.74 | 6.3 |
| 24 h | 0.47 | 43.94 | 52.27 | 3.32 |

**Tabulated HPLC data from experiment ENZ 13 H**

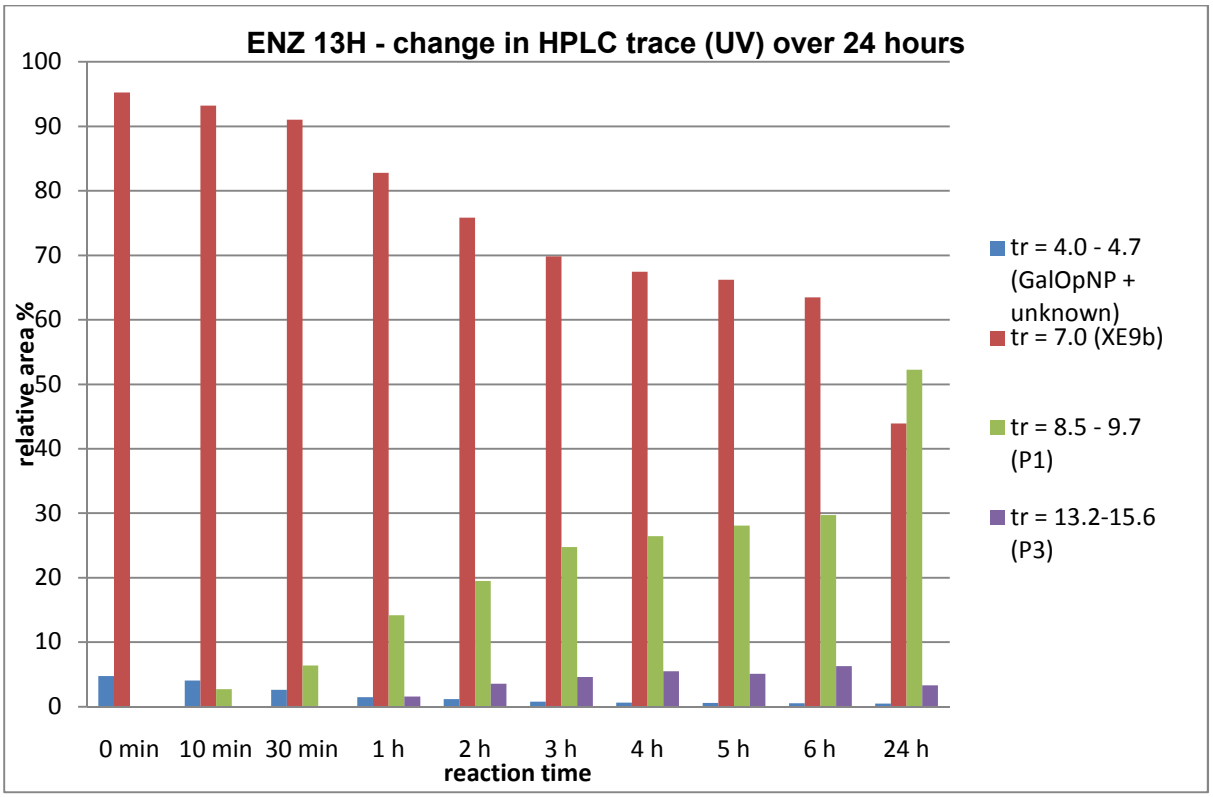


**Figure 3.3.4.1f: Graph to show the overall progress of ENZ 13H over the course of the reaction**

**Comparison of Experiments ENZ 13D and ENZ 13H**

Both reactions **13D** and **13H** showed processing of naphthyl-functionalised sugar **32** in the HPLC spectra. However, in comparing the two experiments it was clear from the graphs in Figures 3.3.4.1d and 3.3.4.1f, that **13H** (pH 7.0) showed the greatest amount of **32** processed and the greatest amount of UV-active products formed.

At the end of the 24 hour reaction time the reactions were acetylated. Mass spectrometric analysis of the crude material from both reactions revealed the presence of our desired disaccharide Gal-NpCH2GlcOMe **36** at *m/z* 771 (Table 3.3.4.1g).

| Reaction | MS Peak *m/z* | RMM | Assignment (acetylated sugars) | comments |
|---|---|---|---|---|
| 13D | 483 $[M + Na]^+$ | 460 | XE9b | Major peak |
| | 701 $[M + Na]^+$ | 678 | Gal-Gal | Apparent upon |
| | **771 $[M + Na]^+$** | **748** | **Gal-NpCH2GlcOMe 36** | expansion of the |
| | 989 $[M + Na]^+$ | 966 | Gal-Gal-Gal | baseline |
| 13H | 483 $[M + Na]^+$ | 460 | XE9b | Major peak |
| | 701 $[M + Na]^+$ | 678 | Gal-Gal | ~1/4 height **XE9b** |
| | **771 $[M + Na]^+$** | **748** | **Gal-NpCH2GlcOMe 36** | ~1/5 height **XE9b** |
| | 989 $[M + Na]^+$ | 966 | Gal-Gal-Gal | baseline |

**Table 3.3.4.1g: ENZ 13D and ENZ 13H tabulated mass spectra results**

TLC analysis of the acetylated material in EtOAc/hexane (1:1) using UV and ammonium molybdate to visualise the components showed a set of intense spots at $R_f$ = 0.45 corresponding to naphthyl-functionalised sugar **32**. The remaining material was seen as UV- and ammonium molybdate-active spots on the baseline of the plate. The column was therefore flushed with 5% MeOH in EtOAc once the other spots had eluted (**32** could be recovered for use in subsequent reactions). Mass spectra of the material in the flush are shown in Figure 3.3.4.1h and the analysis in Table 3.3.4.1i.

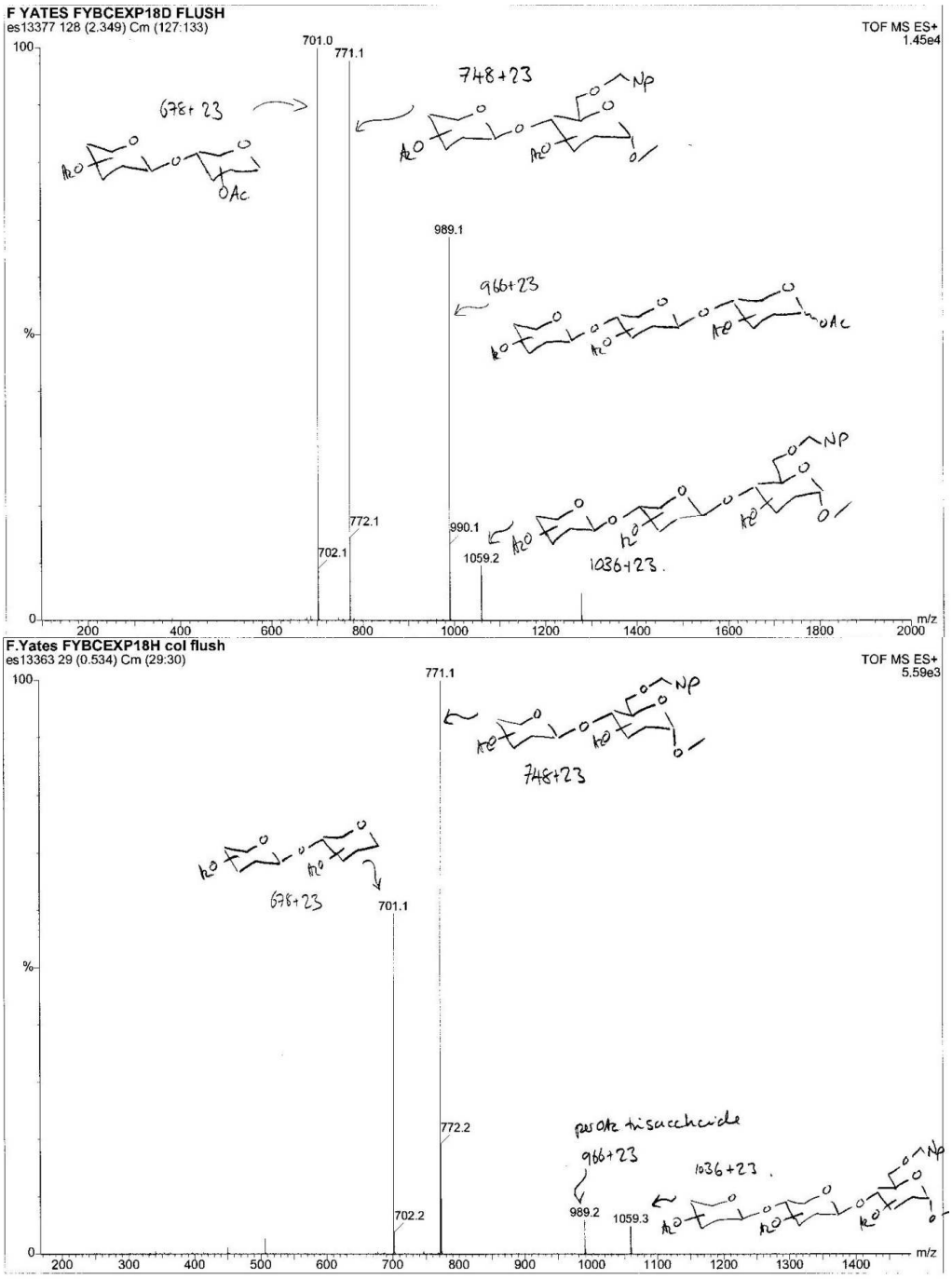


**Figure 3.3.4.1h: mass spectrum form ENZ column flush (top); mass spectrum from ENZ 13H column flush (bottom)**

| Reaction | MS Peak *m/z* | RMM | Assignment (acetylated sugars) | comments |
|---|---|---|---|---|
| 13D | 701 $[M + Na]^+$ | 678 | Gal-Gal | |
| | **771 $[M + Na]^+$** | **748** | **Gal-NpCH2GlcOMe 36** | Major peaks |
| | 989 $[M + Na]^+$ | 966 | Gal-Gal-Gal | |
| | **1059 $[M + Na]^+$** | **1036** | **Gal-Gal-NpCH2GlcOMe** | Minor peak |
| 13H | 701 $[M + Na]^+$ | 678 | Gal-Gal | ~2/3 peak at 771 |
| | **771 $[M + Na]^+$** | **748** | **Gal-NpCH2GlcOMe 36** | Major peak |
| | 989 $[M + Na]^+$ | 966 | Gal-Gal-Gal | Minor peaks |
| | **1059 $[M + Na]^+$** | **1036** | **Gal-Gal-NpCH2GlcOMe** | |

**Table 3.3.4.1i: ENZ 13D and ENZ 13H tabulated mass spectra results for the compounds contained in the column flush**

The major components in the mass spectra of the flushed material were a Gal-Gal disaccharide and our desired acetylated Gal-NpCH2GlcOMe disaccharide **36**. A minor peak in both spectra was a trisaccharide containing NpCH2GlcOMe which can be 'added' to the yield of the disaccharide as it has been doubly processed by the enzyme.

Although the desired sugars were minor components of the reactions as a whole, it was extremely encouraging that the enzyme was able to process the novel sugars and produce disaccharides containing them.

In comparing the two reactions qualitatively based on the HPLC and mass spectrometric data, the reaction carried out at pH 7.0 produced the greatest amount of our desired disaccharide.

**Experiments using Lac as the glycosyl donor**

The results from Experiments **ENZ 14D** and **ENZ 14H** were almost identical to their counterparts in **ENZ 13** in that the pH of the reaction had a much greater impact than the glycosyl donor used. The detailed results from the HPLC and mass spectrometry work from Experiment ENZ 14 are shown in the Appendix Section 3.3.4.1.

**Summary of results from experiments ENZ 13 and ENZ 14**

We carried out four test reactions to evaluate the effect of pH on the transglycosylation reaction between a glycosyl donor (GalO*p*NP and Lac) and the novel glycosyl acceptor naphthyl-functionalised sugar **32**.

From the data collected, it was clear that a reaction pH of 7.0 gives rise to more enzyme activity under these conditions than pH 5.0 as more processing was seen in reactions **ENZ 13H** and **ENZ 14H** than in reactions **ENZ 13D** and **ENZ 14D**. Two graphical representations of this are shown in Figure 3.3.4.1s below. Values for 24 hours are not included as in experiments **13D** and **14D** (pH 5.0) it was not possible to distinguish between the peak for **32** and that of P1 at 24 hours. For the purpose of this comparison the trends over the first 6 hours of the reaction are sufficient.

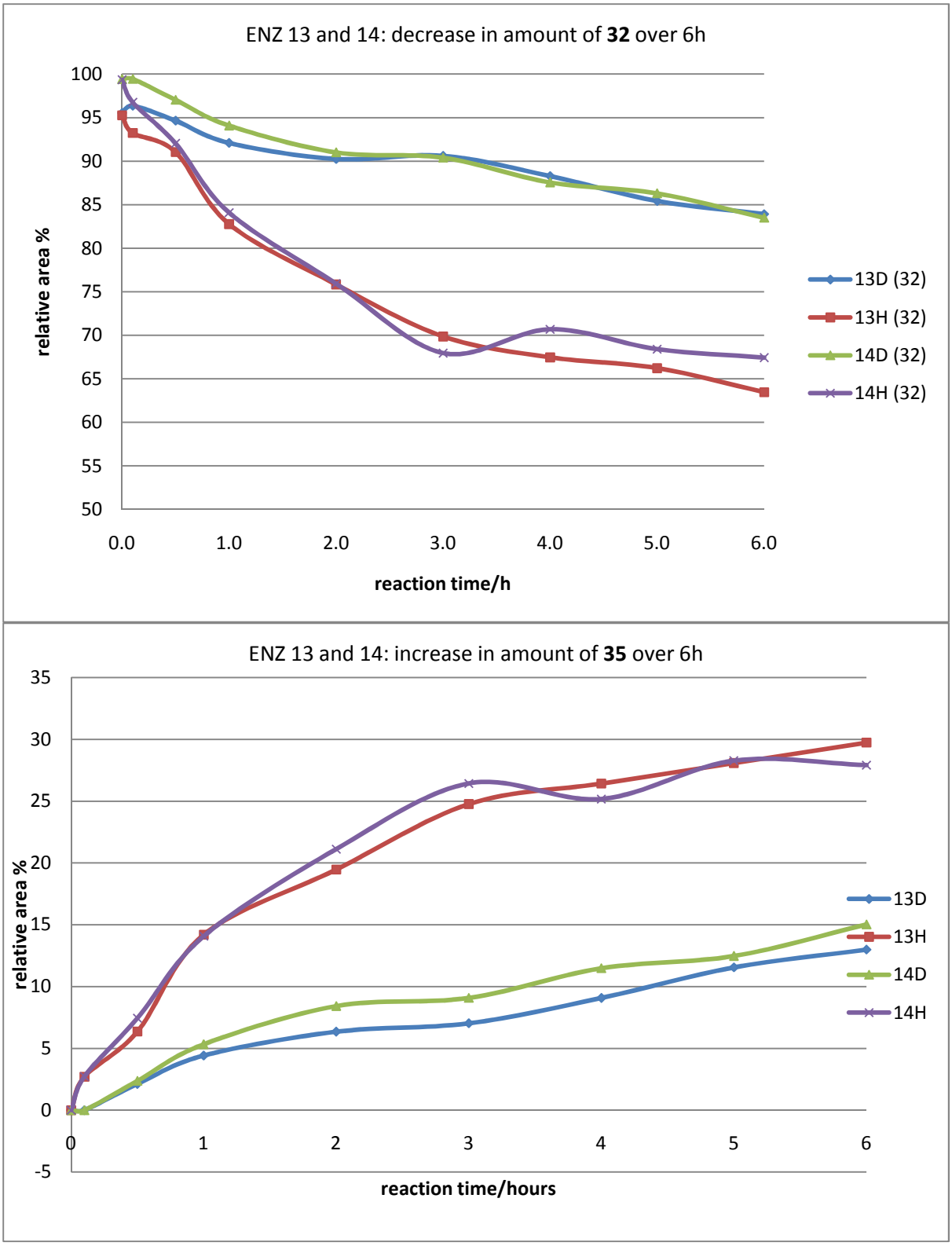


**Figure 3.3.4.1s: Comparison of the results of experiments ENZ 13 and ENZ 14. The graphs give an indication of the extent of glycosyl processing in each reaction**

The top graph in Figure 3.3.4.1s shows the consumption of **32** over the course of the reaction. The linear trendlines show the consumption of **32** is higher in experiments 13H and 14H (pH 7.0). There was a concomitant trend when looking at the increase in the amount of P1 (desired Gal-NpCH2GlcOMe disaccharide **35**), in that the amount of P1 in experiments 13H and 14H was almost double that observed in 14D and 14D.

The choice of glycosyl donor had little or no impact on the transglycosylation reaction under the reaction conditions used in this case. There may be a slight advantage in using GalO*p*NP over lactose as the data showed that experiment 13H (GalOpNP) produced slightly more P1 over the course of the reaction. However, the increase is very small and by far the biggest factor influencing the efficacy of transglycosylation reactions under the conditions used in this experiment is the pH of the buffer solution used. Using a pH of 7.0 greatly increases the amount of processing carried out by the enzyme.

### 3.3.4.2 Larger scale synthesis of Gal-NpCH2GlcOMe using optimised conditions

In the previous Section we have reported the successful application of the β-galactosidase from *B. circulans* in the synthesis of di- and trisaccharides containing the naphthyl functionalised methyl glucoside **32**. The best conditions for this reaction are shown in Figure 3.3.4.2a. There was no marked advantage to using GalO*p*NP over lactose as the glycosyl donor.

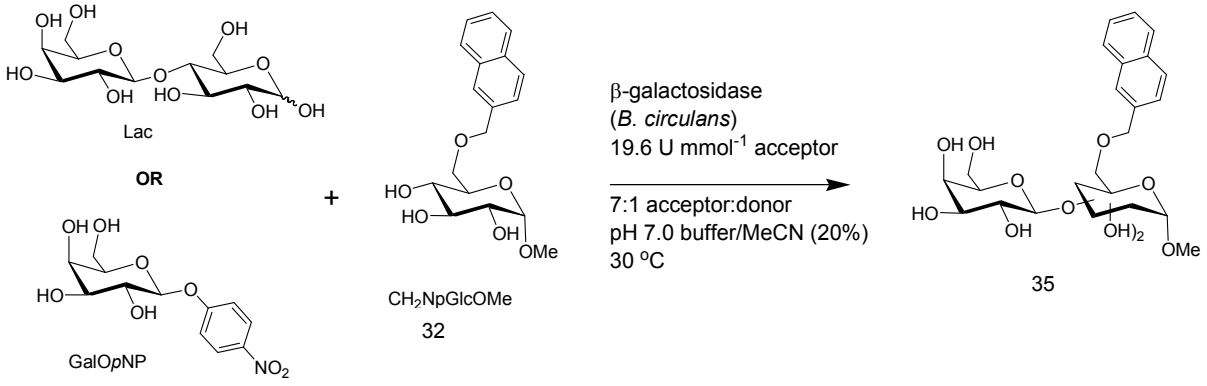


**Figure 3.3.1.2a: optimised conditions for the tranglycosylation reactions using the β-galactosidase from *B. circulans***

In these next syntheses we would prepare the disaccharide Gal-NpCH2GlcOMe **35** in greater quantity so that the regioselectivity of glycosidic bond formation can be determined.

Two identical reactions were performed simultaneously using GalO*p*NP (**ENZ 15**) and Lac (**ENZ 16**) as the glycosyl donors. The reactions were carried out in the same manner as experiments **ENZ 13** and **ENZ 14**. Aliquots of the reaction mixture were taken at 30 minute intervals and reaction progress monitored by HPLC and mass spectrometry.

Both reactions proceeded smoothly; monitoring by HPLC mirrored the results from experiments **ENZ 13H** and **ENZ 14H**. Following the reaction by mass spectrometry it was possible to see the evolution of a baseline peak at *m/z* = 519 corresponding to Gal-NpCH2GlcOMe **35** (RMM 496). The reactions were stopped at six hours by heating at 100 $^{o}$C for five minutes to denature the enzyme. The reaction mixture was then lyophilised and the carbohydrate residues acetylated to facilitate separation and characterisation. Mass spectrometric analysis of the crude acetylated material confirmed the presence of the acetylated Gal-NpCH2GlcOMe disaccharide **36** at *m/z* = 771. The crude reaction mixtures were then partially purified by column chromatography. The starting material **32** was recovered in both cases, 210 mg (84%) in experiment **ENZ 15** and 203 mg (81%) in experiment **ENZ 16**. **32** was in a 7-fold excess so recovering this amount of material is not an indication of the efficacy of the reaction.

The 'flushed' fraction of the columns were then analysed by HPLC so that this mixture of disaccharides could be purified further to yield our desired acetylated disaccharide **36** (Figure 3.3.4.2b).

The HPLC spectra 5.of these crude mixtures were very similar. Both had a broad peak at $t_r$ = 12.2 minutes and a broad set of overlapping and adjacent peaks between $t_r$ = 33.2 and 35.7 minutes. It was within the latter area that we expected to find our target disaccharide.

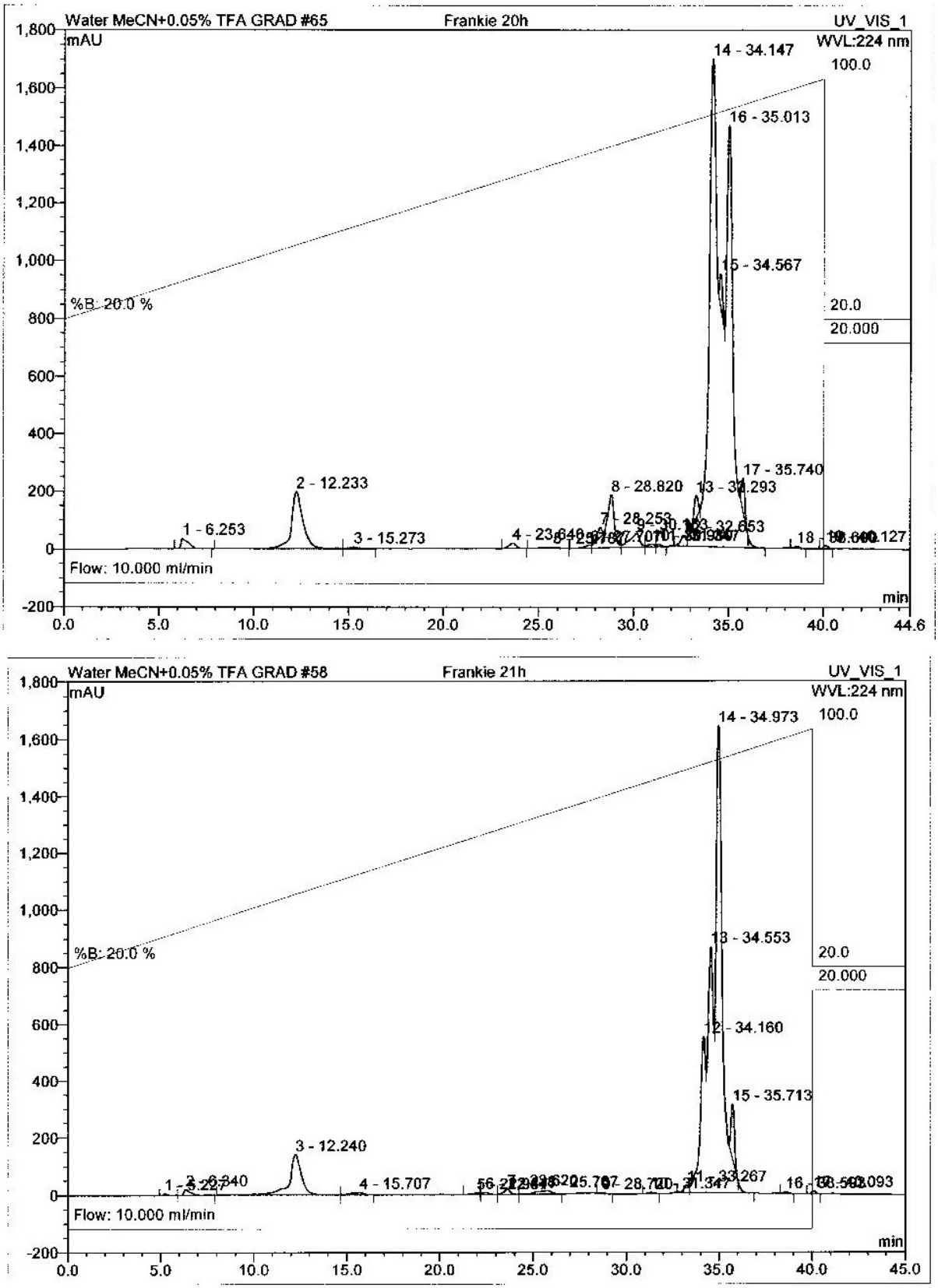


**Figure 3.3.4.2b: HPLC analysis of the crude mixtures from experiments ENZ 15 (top) and ENZ 16 (bottom)**

The peaks were successfully separated using HPLC and the resultant samples submitted for mass spectrometry. The results from this are shown in Table 3.3.4.2c.

| Peak $t_r$/ min | *m/z* | Assignment | Mass recovered/mg | |
|---|---|---|---|---|
| | | | ENZ 15 | ENZ 16 |
| 12.2 | | Insufficient material for analysis | | |
| 34.1 | 483 $[M + Na]^+$ | XE9b | 17 | 7 |
| | 757 $[M + Na]^+$ | Gal-Gal | | |
| **35.0** | **771 $[M + Na]^+$** | **Gal-NpCH2GlcOMe 36** | **15 (12 %)** | **12 (9.5%)** |
| 35.7 | | Insufficient material for analysis | | |

**Table 3.3.4.2c: Results from HPLC separation of the two crude mixtures obtained from experiments ENZ 15 and ENZ 16 and the assignment of peaks from mass spectra**

In both cases the peak at $t_r$ = 35.0 minutes was found to contain a single major peak at *m/z* = 771 ($[M + Na]^+$ Gal-NpCH2GlcOMe **36**, RMM = 748). The mass recovery of this product was 15 mg from **ENZ 15** (12% wrt donor) and 12 mg from **ENZ 16** (9.5% wrt donor). This was an excellent result and the yields were encouraging. Yields from enzymatic transglycosylation reactions do vary widely, but 12 and 9.5% were good results.

A preliminary $^1H$ NMR spectrum of the combined, purified Gal-NpCH2GlcOMe **36** from both of these experiments showed the presence of a single compound. This sample was then submitted for more detailed $^1H$, $^{13}C$ and 2D NMR spectroscopy to determine the regiochemistry of the new glycosidic linkage. The full spectroscopic assignment is in the Experimental Section (5.3)

The disaccharide proved to be a $\beta(1\rightarrow2)$ linked disaccharide (Figure 3.3.4.2d) after a full 2D NMR analysis using HSQC, HMBC and COSY90.

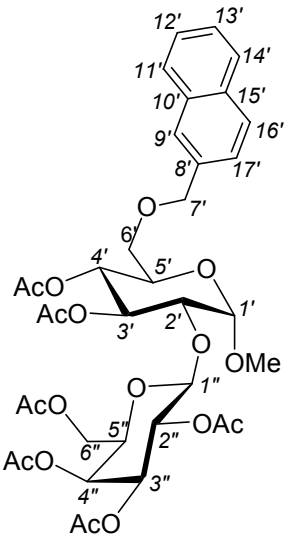


$C_{36}H_{44}O_{17}$
Exact Mass: 748.2578
Mol. Wt.: 748.7244
C, 57.75; H, 5.92; O, 36.33

**Figure 3.3.4.2d: β-D-(-2,3,4,6-tetra-*O*-acetyl)galactopyranoside-(1→2)-α-D-methyl-((2,3,4-tris-*O*-acetyl)-6-*O*-(2-naphthylmethyl))glucopyranoside 36**

### Discussion of structural assignment

The anomeric carbons are clear at 101.9 and 99.0 ppm in the $^{13}C$ NMR spectrum; by examining the HMBC the methoxy group on the glucose ring shows $^{3}J$ coupling to C1' at 99.0 ppm. C1" is therefore at 101.9 ppm, with HSQC to the corresponding anomeric proton H1" at 4.58 ppm; H1' is at 4.88 ppm. The glycosidic linkage is, as expected, *beta*; confirmed by the coupling constant $^{3}J_{H1"-H2"}$ = 8.1 Hz, typical for a β-linked disaccharide. COSY90 allows assignment of the protons within the sugar rings which, in turn, identifies the carbons within the sugar rings by HSQC (Figure 3.3.4.2e).

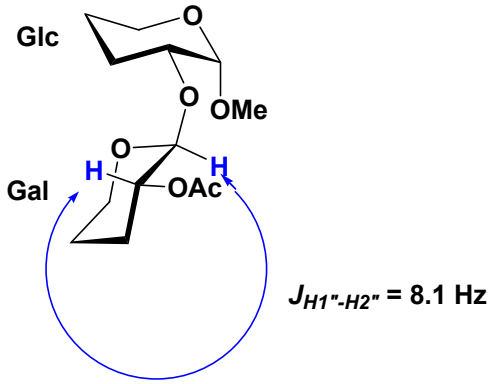


**Figure 3.3.4.2e: confirming the stereoselectivity of the glycosidic bond formation**

In order to determine the position of glycosylation, examination of the HMBC of H1" on the galactose ring shows $^{3}J$ coupling to C2' of the glucose ring; confirming C2' as the point of attachment (Figure 3.3.4.2f).

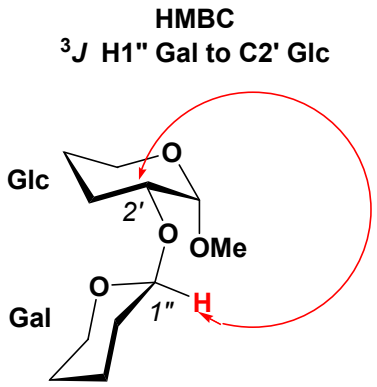


**Figure 3.3.4.2f: determining the regioselectivity of the glycosidic bond formation**

**Summary**

In this part of the project we have successfully developed and used a method for carrying out transglycosylation reactions between a glycosyl donor and a novel methyl glucoside functionalised with a naphthyl group at C6 using the β-galactosidase from *B. circulans*. This is an excellent result, and, the use of the enzyme to make disaccharides containing a bulky organic chromophore at C6 of the glycosyl acceptor has not been done before. It was particularly interesting to note the point of glycosidic linkage: β(1→2). The enzyme we have chosen to use has a marked preference for forming β(1→4) and β(1→6) glycosidic bonds. Obviously in our case C6 was not available for glycosylation as it was blocked by the naphthylmethyl group; however, the formation of a β(1→2) linkage rather than β(1→4) linkage was a surprise. No other naphthyl-functionalised disaccharides were detected in our screening and analytical studies of this set of reactions, so we can say that for this donor/acceptor set, the β-galactosidase from *B. circulans* is β(1→2)-selective.

We would now use the knowledge and experience gained through Experiments 18-21 to make disaccharides using our two other naphthyl-functionalised methyl glucosides, **33** and **34**.

### 3.3.4.3 Synthesis of disaccharides using novel glucosides 33 and 34

Having successfully made our first naphthyl-functionalised disaccharide we would now use the same reaction conditions to attempt the synthesis of two more, shown in Figure 3.3.4.3a.

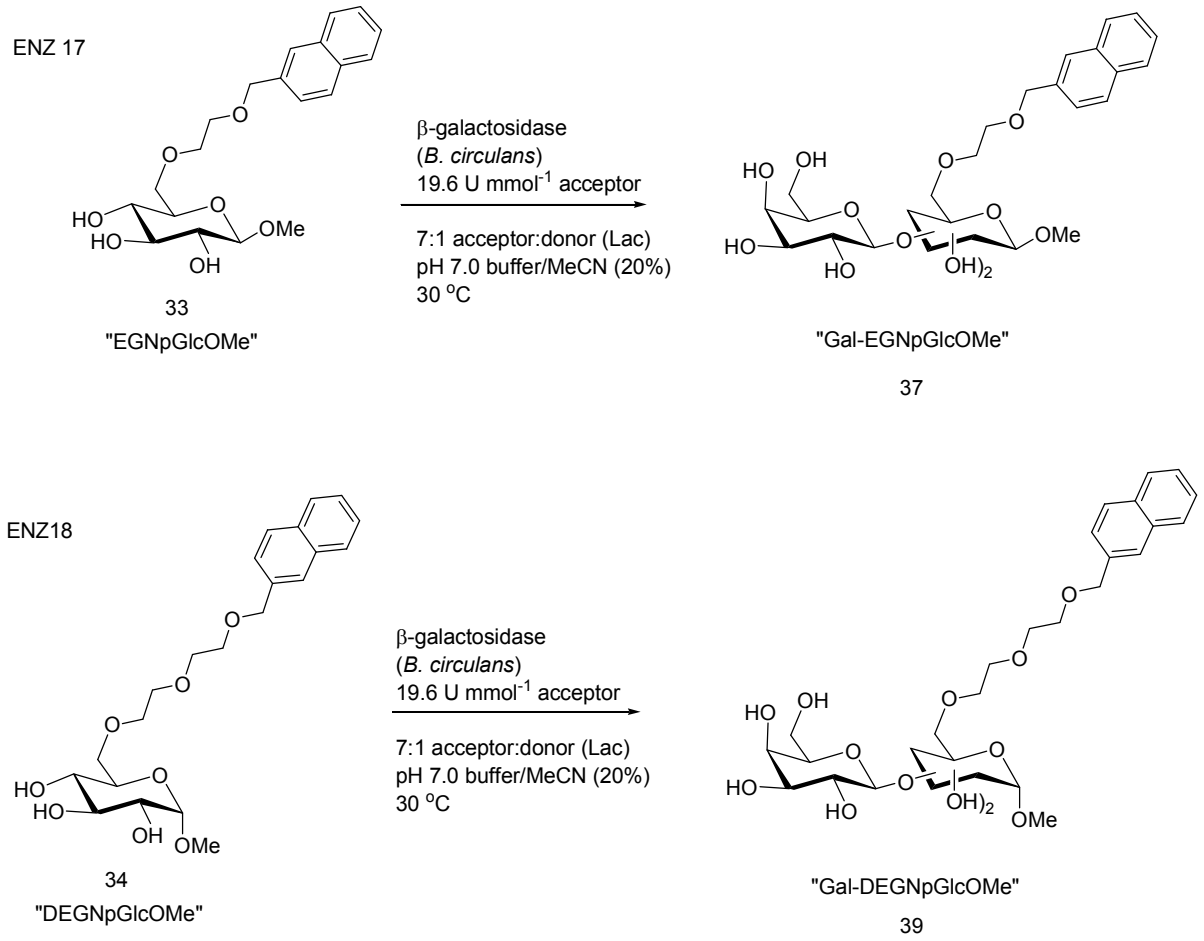


**Figure 3.3.4.3a: Scheme for transglycosylation reactions using the two other novel, naphthalene functionalised methyl glucosides using the β-galactosidase from *B. circulans***

Experiment **ENZ 17** would make the disaccharide using **33** as the glycosyl acceptor, and Experiment **ENZ 18** would make the disaccharide using **34** as the glycosyl acceptor. Lactose would be used as the glycosyl donor as i) it is not UV active and ii) the retention time of GalO*p*NP was very similar to the retention times of **33** and **34** (HPLC traces of this are in the Appendix). So, using lactose as the glycosyl donor makes monitoring the reaction by UV detection in HPLC easier. In light of the results with naphthyl acceptor **32**, It would be interesting to see where the glycosidic bond formed if we succeeded in making both of these disaccharides.

**ENZ 17 Synthesis of disaccharide Gal-EGNpGlcOMe 37**

The transglycosylation reaction between **33** and lactose was carried out as described in method ENZ 17 in the Experimental Section (5.3).

HPLC monitoring of the reaction showed the evolution of a new peak at $t_r$ = 7.4 minutes after 30 minutes. The HPLC results are shown in Table 3.3.4.3b and Figure 3.3.4.3c. However, a peak with *m/z* = 563 corresponding to a disaccharide of **33** was not seen in the mass spectra until 4 hours had passed.

| Reaction time | Relative area % | | |
|---|---|---|---|
| | $t_r$ = 4.5 min (**29b**) | $t_r$ = 7.4 min (P1) | $t_r$ = 15.2 min (P2) |
| 0 min | 100 | | |
| 30 min | 96.78 | 3.22 | |
| 1 h | 95.02 | 4.98 | |
| 2 h | 93.62 | 6.38 | |
| 4 h | 90.8 | 9.2 | |
| 6 h | 89.6 | 9.29 | 1.1 |
| 24 h | 81.89 | 15.25 | 2.86 |

**Table 3.3.4.3b: ENZ 17 tabulated HPLC results**

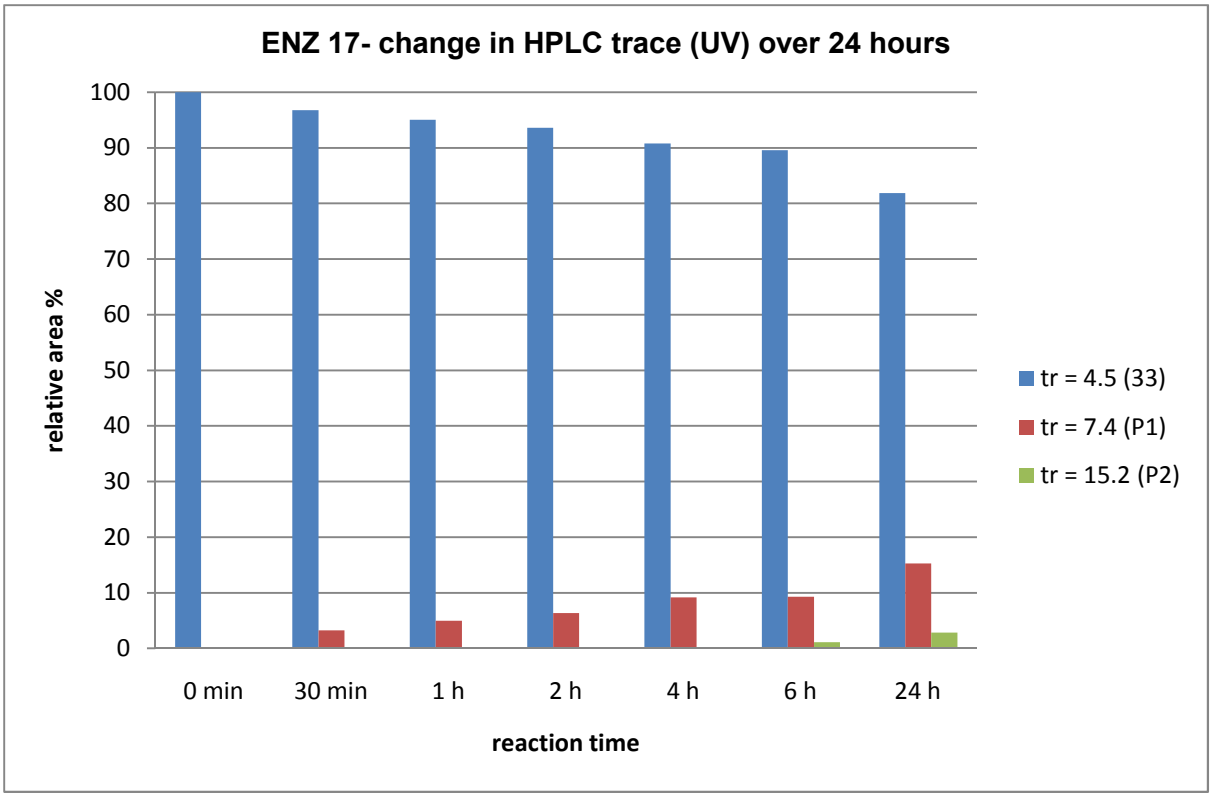


**Figure 3.3.4.3c: ENZ 17 graphical representation of HPLC results**

The graph in figure 3.3.4.3c shows the slow evolution of the peak P1 which we attributed to our desired disaccharide **37** as the simultaneous evolution of a peak with the correct *m/z* was seen in the mass spectra. Peak P2 was present in such small amounts in the HPLC trace (3%), and thus the reaction mixture, that no new other peaks were seen in the mass spectra.

The reaction was terminated after 24 hours, the reaction mixture was freeze-dried and the carbohydrate residues acetylated. Figure 3.3.4.3d shows the expanded baseline region of the mass spectrum of the acetylated reaction mixture.

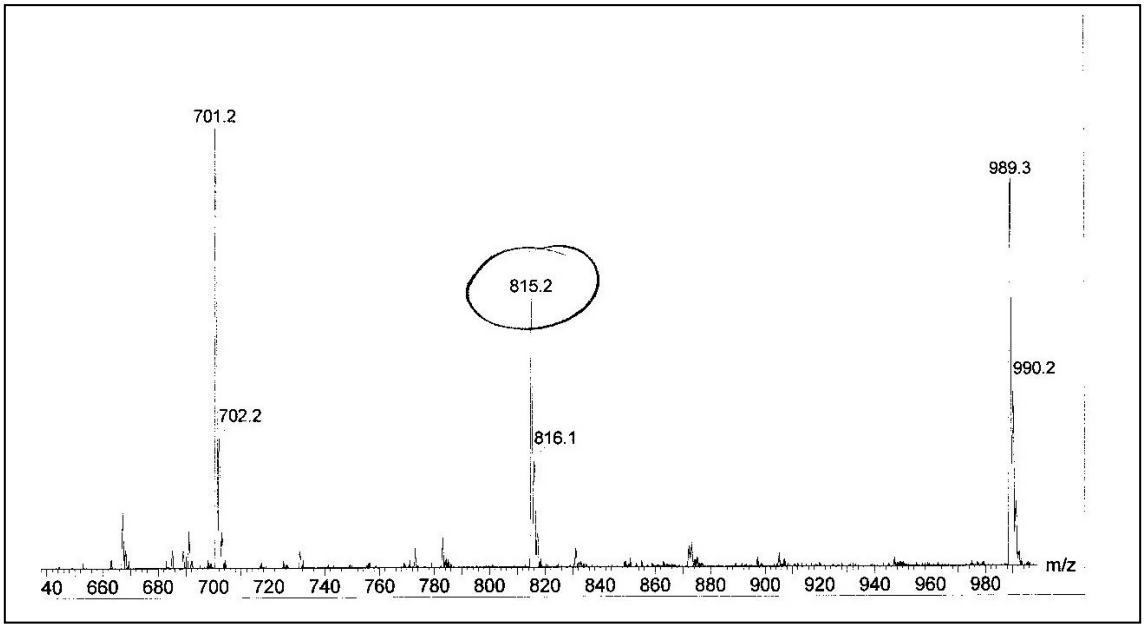


**Figure 3.3.4.3d: Expanded baseline of the mass spectrum for ENZ 17 showing the peak at *m/z* = 815 corresponding to the acetylated Gal-EGNpGlcOMe 38**

Mass spectrometric analysis of the crude acetylated material confirmed the presence of the desired acetylated Gal-EGNpGlcOMe disaccharide **38** at *m/z* = 815. The crude reaction mixture was then partially purified by column chromatography. Most of the starting material **33** was recovered (79 mg, 70%) The mass spectrum of the flushed fractions contained four peaks, detailed in Table 3.3.4.3e.

| MS Peak *m/z* | RMM | Assignment (acetylated sugars) | comments |
|---|---|---|---|
| 527[M + Na]$^+$ | 504 | **33** | Major peak |
| 701 [M + Na]$^+$ | 678 | Gal-Gal | ~3/4 height major peak |
| **815 [M + Na]$^+$** | **792** | **Gal-EGNpGlcOMe 38** | ~1/3 height major peak |
| 989 [M + Na]$^+$ | 966 | Gal-Gal-Gal | ~1/3 height major peak |

**Table 3.3.4.3e: ENZ mass spectrometric analysis of the contents of the 'flush' fractions**

HPLC separation of this mixture was then carried out (Figure 3.3.4.3f). Three peaks were isolated and submitted for mass spectrometric analysis. The second peak at $t_r$ = 33.6 minutes contained the target disaccharide Gal-EGNpGlcOMe **38**.

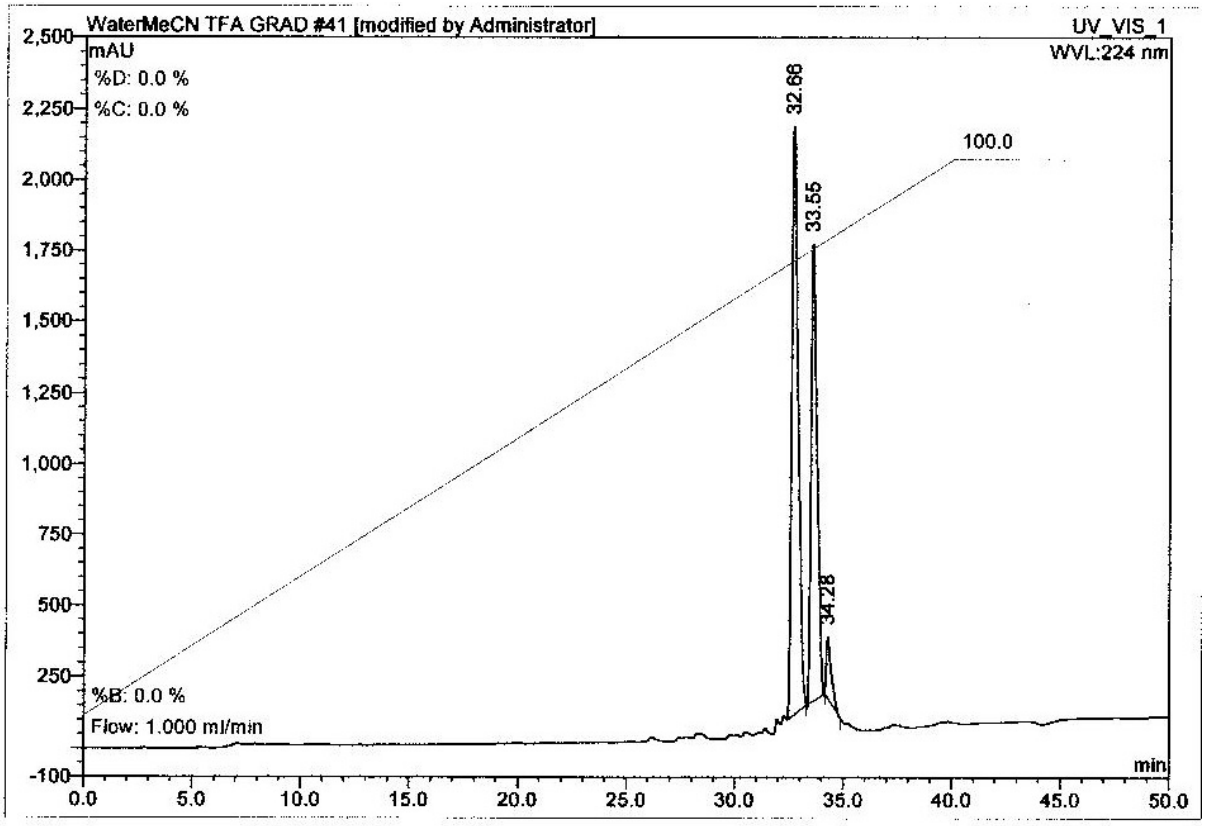


**Figure 3.3.4.3f: HPLC separation of the acetylated material containg the target compound 38**

There was very little material from this reaction, so it was repeated on a larger scale and 14 mg (41% yield wrt lactose) of the desired disaccharide was isolated following the procedure described above. This sample was then submitted for analysis by $^{1}H$, $^{13}C$ and 2D NMR spectroscopy to determine the regiochemistry of the glycosidic linkage. Again, only one regioisomer was found, the full spectroscopic assignment is in the Experimental Section 5.3. In this instance, the disaccharide proved to be a $\beta(1\rightarrow3)$ linked disaccharide (Figure 3.3.4.3g) after a full 2D NMR analysis using HSQC, HMBC and COSY90.

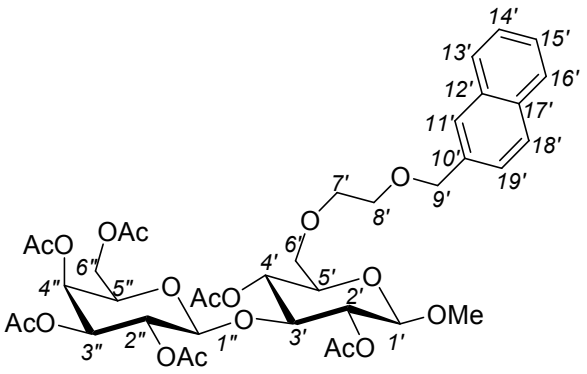


$C_{38}H_{48}O_{18}$
Exact Mass: 792.2841
Mol. Wt.: 792.7769
C, 57.57; H, 6.10; O, 36.33

**Figure 3.3.4.3g: "Gal-EGNpGlcOMe" β-D-(-2,3,4,6-tetra-*O*-acetyl)-galactopyranoside-(1→3)-β-D-methyl-((2,3,4-tris-*O*-acetyl)-6-*O*-[2-(2-naphthylmethoxy)ethyl]glucopyranoside 38**

## Discussion of structural assignment

The anomeric carbons are clear at 101.3 and 101.2 ppm in the $^{13}C$ NMR spectrum, HSQC gives the corresponding protons at 4.28 and 4.54 ppm respectively. H1' (glucose) is located by HMBC $^{2}J$ coupling to O*C*H$_3$ at 4.28 ppm. COSY90 then allows for assignment of protons on each of the sugar rings and subsequent HSQC analysis then determines the corresponding carbon atoms. The disaccharide is beta linked as the coupling constant from H1" to H2" is 8.0 Hz, a typical value for axial-axial coupling in a sugar (Figure 3.3.4.3h).

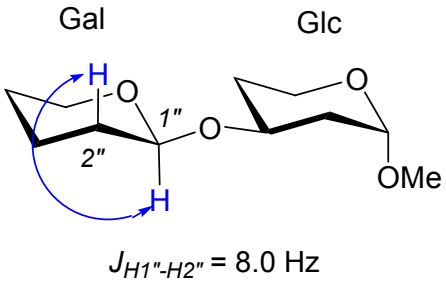


**Figure 3.3.4.3h: confirming the stereochemistry of the glycosidic bond formation**

The point of glycosidic bond linkage is found by examining the HMBC couplings from H1". H1" shows $^{2}J$ coupling to C2" and $^{3}J$ coupling to C3" and C3', thus showing that the disaccharide is 1→3 linked (Figure 3.3.4.3i).

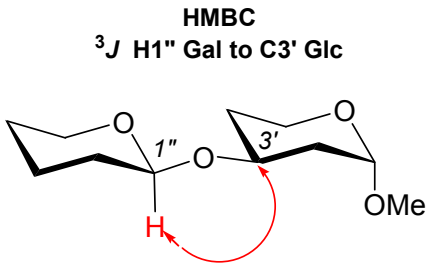


**Figure 3.3.4.3i: determining the regioselectivity of the glycosidic bond formation**

The β(1→3) regioselectivity of glycosidic bond formation observed in this case is different to the disaccharide made with **32,** which possesses a β(1→2) glycosidic bond. The point of glycosidic linkage is determined by the way in which the glycosyl acceptor sits in the active site of the enzyme. Clearly, **32** and **33** sit quite differently within the active site, thus resulting in a different regioselectivity.

**ENZ 18 Synthesis of Gal-DEGNpGlcOMe 39**

The transglycosylation reaction between naphthyl-functionalised glucoside **34** and lactose was carried out as described in method **EN18** in the Experimental Section.

HPLC monitoring of the reaction showed the evolution of a new peak at $t_r$ = 7.5 min after 1 hour. The HPLC results are shown in Table 3.3.4.3j and Figure 3.3.4.3k. A peak with *m/z* = 607 corresponding to a disaccharide of **30b** was observed in the mass spectra from 1 hour into the reaction.

| Reaction time | Relative area % | |
|---|---|---|
| | $t_r$ = 3.1 min (**XE11b**) | $t_r$ = 7.5 min (P1) |
| 0 min | 100 | |
| 30 min | 100 | |
| 1 h | 99.53 | 0.47 |
| 2 h | 98.86 | 1.14 |
| 4 h | 97.22 | 2.78 |
| 6 h | 96.29 | 3.71 |
| 24 h | 94.95 | 5.05 |

**Table 3.3.4.3j: ENZ 18 tabulated HPLC results**

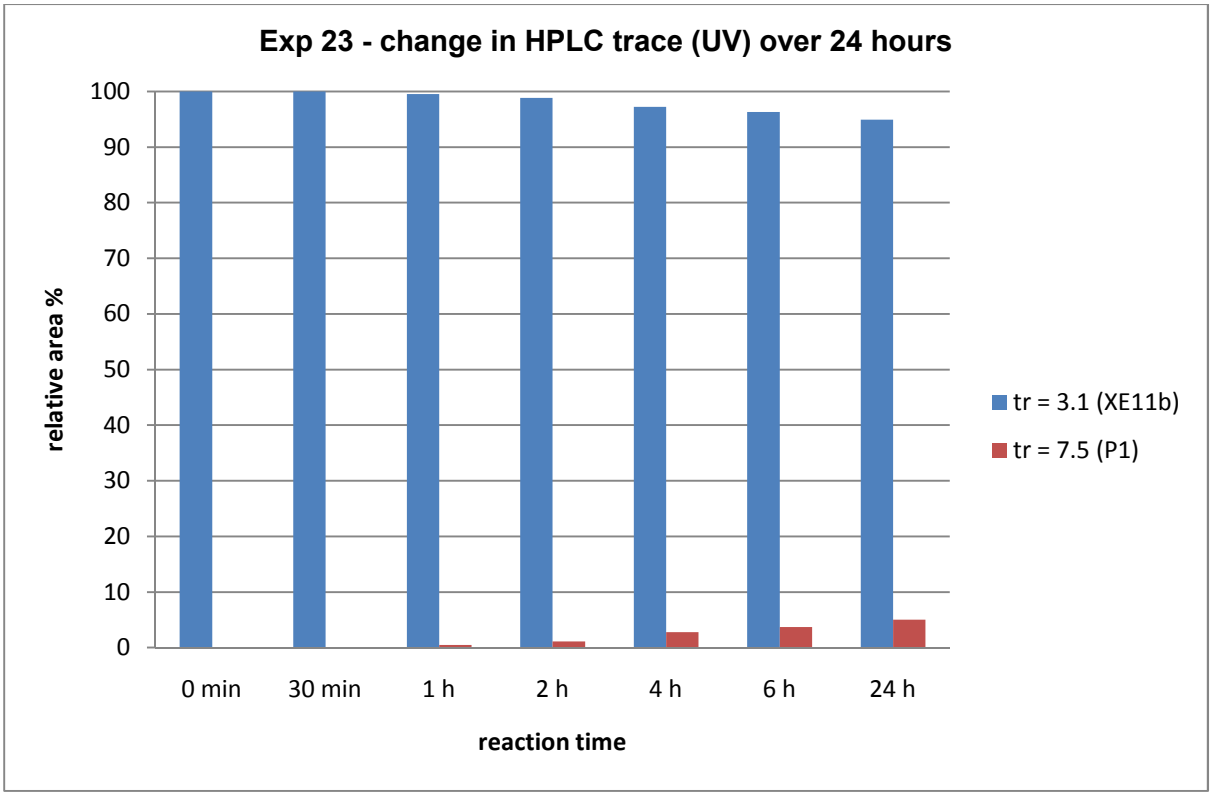


**Figure 3.3.4.3k: ENZ 18 graphical representation of HPLC results**

The reaction mixture was stopped at 24 hours and the carbohydrate residues acetylated. Partial purification was carried out as before, with the disaccharides known to be contained in

the fraction 'flushed' from the silica-gel chromatography column using 5% MeOH in EtOAc after other spots had eluted.

The crude mass spectrum of this fraction contained four major peaks (Table 3.3.4.3l)

| MS Peak *m/z* | RMM | Assignment (acetylated sugars) | comments |
|---|---|---|---|
| 571[M + Na]$^+$ | 548 | **30b** | Major peaks |
| 701 [M + Na]$^+$ | 678 | Gal-Gal | |
| **859 [M + Na]$^+$** | **836** | **Gal-DEGNpGlcOMe 40** | |
| 989 [M + Na]$^+$ | 966 | Gal-Gal-Gal | |

**Table 3.3.4.3l: ENZ 18 mass spectrometric analysis of the contents of the 'flush' fractions**

HPLC separation of this mixture was then carried out (Figure 3.3.4.3m). The three peaks were isolated and submitted for mass spectrometric analysis. The second peak at $t_r$ = 33.2 minutes contained the target disaccharide Gal-DEGNpGlcOMe. 4 mg of disaccharide **40** was isolated and submitted for $^1$H, $^{13}$C and 2D NMR spectroscopy to determine the regiochemistry of the the glycosidic linkage. Only one regioisomer was found, the full spectroscopic assignment is in the Experimental Section (5.3).

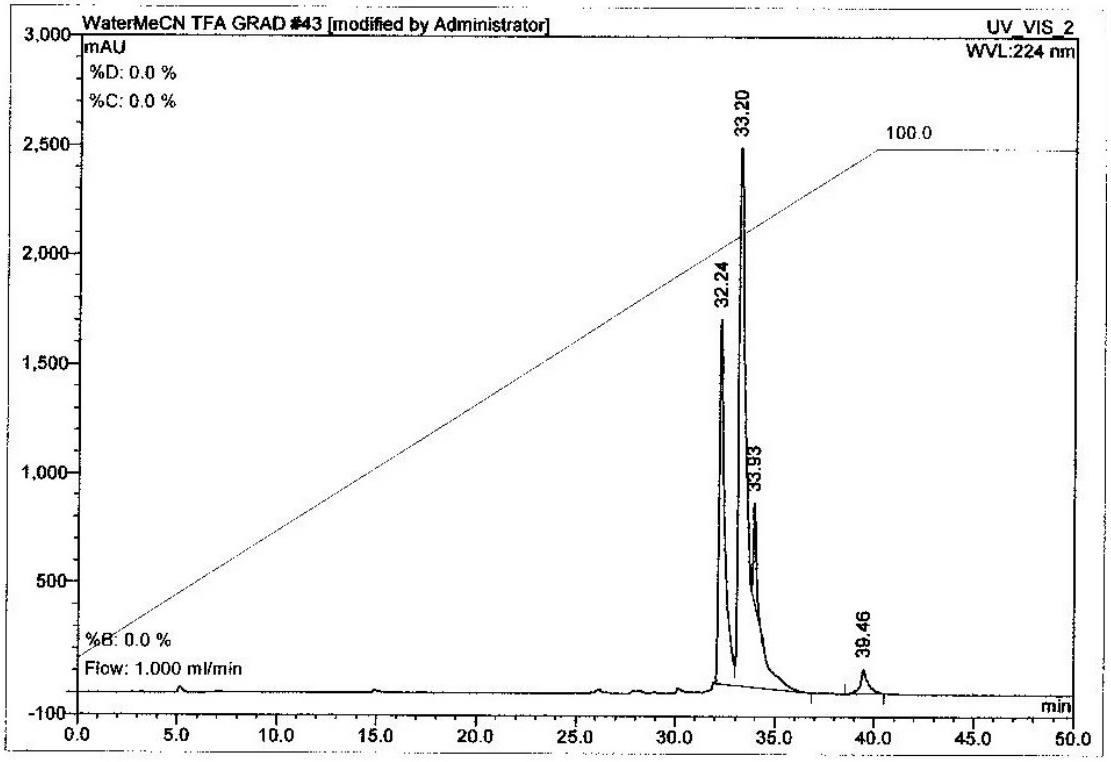


**Figure 3.3.4.3m: HPLC separation of the acetylated material containing the target compound from ENZ 18**

Full 2D NMR analysis using HSQC, HMBC and COSY90 confirmed that the disaccharide possessed a β(1→2) glycosidic linkage (Figure 3.3.4.2n). This is the same regioselectivity observed when NpCH2GlcOMe **32** was employed as the glycosyl acceptor. We would conclude from this that both **32** and DEGNpGlcOMe **34** enter the enzyme active site in a different way to EGNpGlcOMe **33** which results in a different regioselectivity (β(1→3) linked disaccharide).

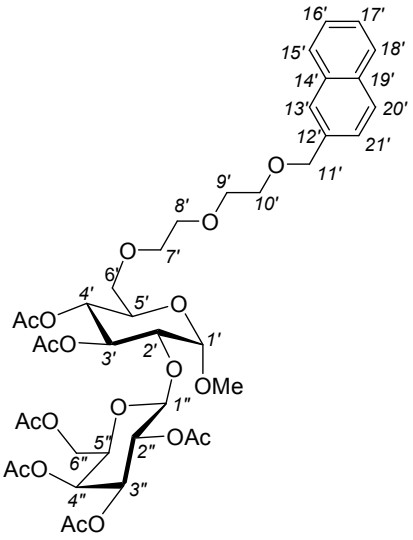


$C_{40}H_{52}O_{19}$
Exact Mass: 836.3103
Mol. Wt.: 836.8295
C, 57.41; H, 6.26; O, 36.33

**Figure 3.3.4.3n: "Gal-DEGNpGlcOMe" β-d-(-2,3,4,6-tetra-O-acetyl)-galactopyranoside-(1→2)-α-d-methyl-((2,3,4-O-acetyl)-6-O-{2-[2-(2-naphthylmethoxy)ethoxy]ethyl}glucopyranoside 40**

### Discussion of structural assignment

The anomeric carbons are clear at 98.9 and 101.9 ppm in the $^{13}C$ NMR spectrum. Examination of the HMBC spectrum reveals $^{3}J$ coupling between the protons of the methoxy group at C1' to this carbon at 98.9 ppm. C1" is thus at 101.9 ppm with HSQC to the corresponding anomeric proton H1" at 4.54 ppm; H1' is at 4.83 ppm. The glycosidic linkage is, as expected, beta; confirmed by the coupling constant $^{3}J_{H1"-H2"}$ = 8.1 Hz, typical for a β-linked disaccharide. COSY90 allows assignment of the protons within the sugar rings which, in turn, identifies the carbons within the sugar rings by HSQC (Figure 3.3.4.3m).

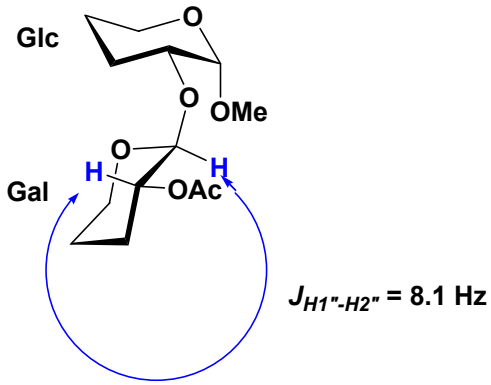


**Figure 3.3.4.3m: confirming the stereoselectivity of the glycosidic bond formation**

Further examination of the HMBC spectrum in order to determine regioselectivity of glycosylation shows $^{3}J$ coupling from H1" on the galactose ring to C2' of the glucose ring. $^{3}J$ coupling between H2' and C1" is also observed, confirming that the glycoside is 1-2 linked (Figure 3.3.4.3n).

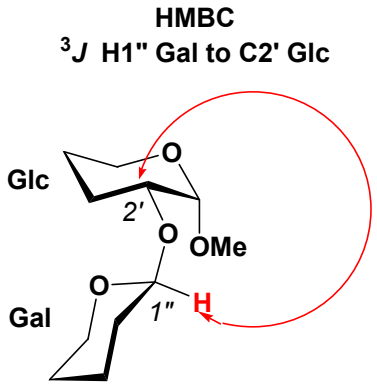


**Figure 3.3.4.3n: determining the regioselectivity fo the glycosidic bond formation**

**Summary**

In this part of the project we have successfully used our developed method for carrying out transglycosylation reactions, using the β-galactosidase from *B. circulans*, between lactose and two further novel methyl glucosides (**33** and **34**) functionalised with a naphthyl group at C6.

The differences in regioselectivity caused by the naphthyl-functionalised glucosides **32**, **33** and **34** are both interesting and seemingly unusual as this enzyme generally favours β(1→4) linkages. Using **32** and **34** as glycosyl acceptors gave a β(1→2) linkage, whereas **33** gave a β(1→3) linkage. This must be to do with how the glycosyl acceptor sits in the active site of the enzyme and is thus presented to the glycosyl donor.

The β(1→3) linked disaccharide was made using a β-methyl glucoside as the glycosyl acceptor, unlike the other two which were made with α-methyl glucosides. Given the

promiscuity of the enzyme active site towards the glycosyl acceptor it is unlikely that the anomeric configuration of the glycosyl acceptor caused this difference in regioselectivity. However, we cannot say with absolute certainty that it did not.

We postulate that it is much more likely that the length of the linker between the methyl glucoside and the naphthyl group caused this change in regioselectivity. The naphthyl group is a relatively large, flat, hydrophobic residue which might interact with similar hydrophobic amino acid residues in or around the enzyme active site. No other regioisomers of any of the disaccharides made were detected in our analysis, leading us to conclude that these transglycosylations are regioselective, and that the selectivity is most likely to be dependent on the linker length in the naphthyl-functionalised glycosyl acceptor.

## 3.4 Conclusions upon Completion of the Transglycosylation Reactions using the β-Galactosidase from *B. circulans*

During the course of this project we have investigated established methods to perform transglycosylation reactions catalysed by the β-galactosidase from *B. circulans*. These methods were used successfully to carry out transglycosylation reactions between GalO*p*NP and GlcOMe, resulting in the formation of numerous different disaccharides.

We then optimised the conditions used for the simple transglycosylation reactions for use with our three novel glycosyl acceptors **32**, **33** and **34**. To do this we successfully overcame the aqueous insolubility of these three novel sugars by developing an optimised method using MeCN as a co-solvent to the buffer solution. We quantitatively determined the activity of the enzyme in these unnatural conditions and from this were able to increase the enzyme function under these conditions by investigating the effect of increasing the amount of enzyme added to the reaction.

After these optimisation studies we then began work on making disaccharides containing our novel sugars. Using naphthyl functionalised glucoside **32** to begin with, we determined that the pH of the reaction solution had a marked effect on enzyme activity; thus, pH 7.0 reaction conditions led to much higher enzyme function than pH 5.0. We found that using GalO*p*NP or lactose as the glycosyl donor had similar effects and thus we could choose the glycosyl donor that was most appropriate/convenient for the transglycosylation we were to perform.

The transglycosylation reaction using naphthyl functionalised glucoside **32** resulted in the production of a single β(1→2) linked disaccharide, the same glycosidic linkage was made when using naphthyl functionalised glucoside **34** as the glycosyl acceptor. In constrast, when naphthyl functionalised glucoside **33** was used, a β(1→3)-linked disaccharide was produced. The length of the linker used to attach the sensitiser to the glycosyl acceptor has a profound effect on the regioselectivity of the glycosidic bond formation. This is most likely due to the way in which the glycosyl acceptor sits in the active site. As previously discussed, other groups they have noted a strong preference of the enzyme from *B. circulans* for forming β(1→4) and β(1→6) linked disaccharide. Because of the position of our sensitiser at C6, our novel glycosyl donors do not sit in the active site in the same way to the glycosyl acceptors in other studies of the enzyme, so the β(1→2) and β(1→3) glycosidic linkages that we have formed are, to our knowledge, particular to the novel glycosyl acceptor that we have synthesised.

The purpose of this study was to determine if the enzyme was able to process our novel glycoside acceptors, and we have succeeded in that. With regard to the development of a probe for β-galactosidases, the enzyme in its natural function hydrolyses lactose. Out of the three novel naphthyl-functionalised disaccharides made, the β(1→3) linked disaccharide is perhaps closest to lactose structurally, as lactose is β(1→4) linked. We can suggest that using a disaccharide with a glycosyl acceptor carrying a sensitiser linked *via* a relatively

short, four atom chain (an ethylene glycol linker in our case) to probe β-galactosidase activity may have the best chance of success.

This method of screening for substrates, whilst effective, is very slow due to the long synthesis of the functionalised monosaccharides and the capricious nature of some of the reactions. We felt that this screening process could be done more efficiently using a combinatorial approach. By creating a library of glycosyl acceptors, and then glycosyl donors, we could screen for suitable substrates for the enzyme more quickly and definitively. Chapter 4 discusses our work on forming a combinatorial library of glycosyl acceptors and the ability of the enzyme to process this library.

# 4. A Dynamic Combinatorial Approach to Efficient Screening of Novel Substrates for the β-Galactosidase from *B. circulans*

Combinatorial synthesis is based on efficient, parallel synthesis so that a large number of compounds can be generated to make a library of substrates without the need to synthesise each component as a separate entity.[89] Using a combinatorial technique to generate such a library can save a lot of time and money in identifying suitable substrates for drug discovery and other research purposes. The scheme in Figure 4a below outlines the basic principle behind the formation of a combinatorial library.

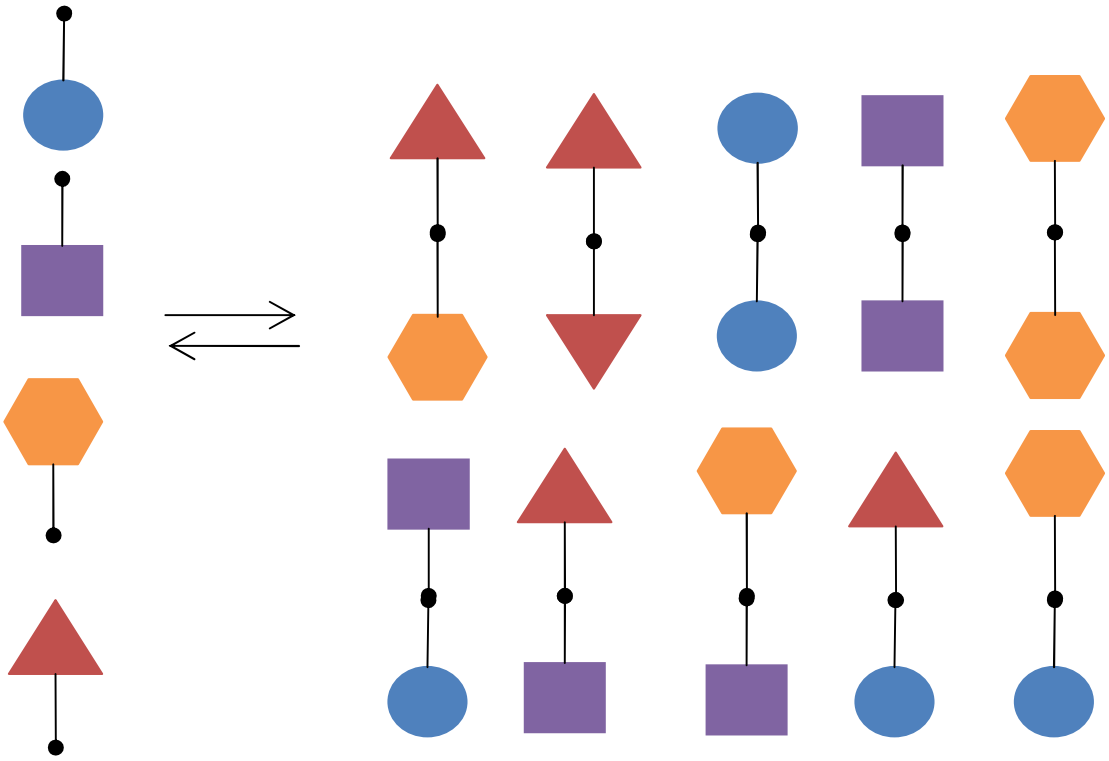

**Figure 4a: Schematic for a dynamic combinatorial library**

The dynamic library is based on reversible connections between a set of building blocks – the components of substrates you wish to test – which exist in an ever changing mixture of the components. This should equilibrate over time to form a statistical mixture of all the

possible combinations of the starting components, allowing for the simple, one step generation of extended libraries.[90] At this point the library can be frozen when the equilibrium is reached, or further screening can be carried out on the library by adding in another component. Because of the dynamic aspect of the library, it allows for self-screening processes that may lead to the preferential expression of active species which shows the strongest binding/interaction with that other component.[91]

In order to improve the efficiency of the screening process to identify suitable substrates to use in our luminescent probe we turned to combinatorial chemistry as a potentially fast method of producing monosaccharides with a naphthyl group introduced at C6. We knew from our earlier work that the β-galactosidase from *B. circulans* can process a methyl glucoside with a naphthyl group at C6 as the glycosyl acceptor, but we do not yet know if it can accept a similarly functionalised galactoside as the glycosyl donor. We proposed to use combinatorial techniques to find out which linker lengths and types are suitable for use in our probe much more easily and efficiently. We would then identify substrates from the library by using the enzyme to 'choose' the best-fitting sugars. Once we have identified the sugars that the enzyme is able to process we would then synthesise these individually (in a non-combinatorial fashion) for use in the probe (Figure 4b).

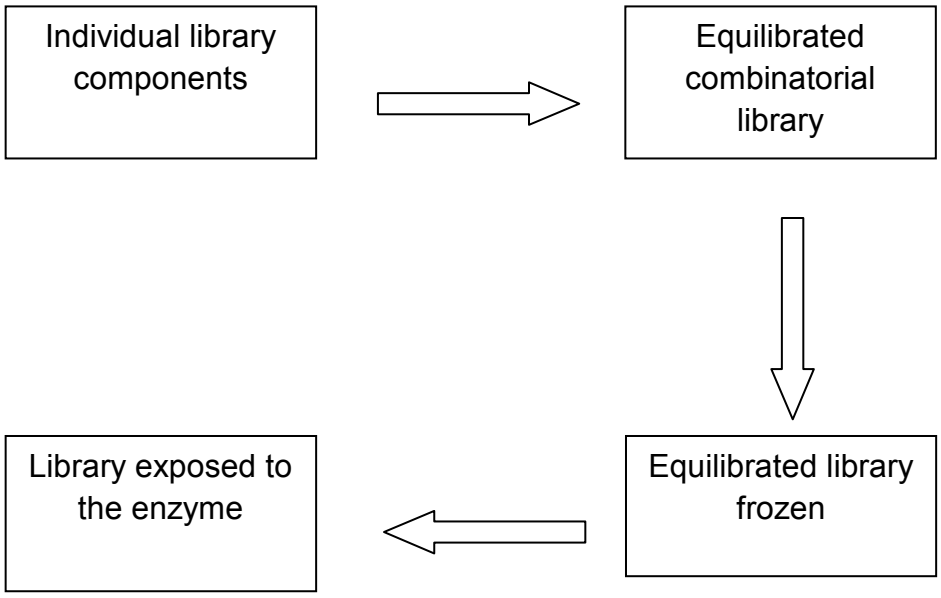


**Figure 4b: The planned process for our combinatorial library investigation**

Our intention is to generate the library, allow it to equilibrate and then stop the reaction. This static combinatorial library is what will be presented to the enzyme.

## 4.1 Choosing the Method for the Generation of the Dynamic Combinatorial Library

Dynamic combinatorial chemistry relies on reversible bond formation and a wide variety of these reactions has been used for dynamic combinatorial applications. There are a number of ways of forming a combinatorial library using reversible covalent bond formation. The early attempts were based on transesterification (Sanders), and then Schiff base exchange (Lehn), but transesterification requires harsh conditions. The hydrazone exchange reaction and reversible C=N bond formation have also been used to form libraries of oximes.

However, our attention was caught by the use of disulfides for forming combinatorial libraries.[92,93] The mechanism of the disulfide exchange reaction had been studied extensively by Whitesides[94] among others[95] and their findings indicate that:

- disulfides form readily from thiols in the presence of oxygen and small amounts of base;
- disulfide exchange takes place efficiently under mild conditions in the presence of a substoichiometric amount of thiol;
- disulfide exchange is neglible under acidic conditions;
- disulfides are stable towards many different functional groups.[96]

A disulfide exchange reaction will fit best with our intended experiments as we do not wish to introduce any moieties that differ too much from the ether linkage we are already using. For

example, an imine exchange reaction would introduce a double bond which would make the linkage much more rigid compared to the the single bonds in the ether linkage. We also need to use a mixture of organic and aqueous solvents in the enzyme reaction; an ester exchange reaction is driven by removal of water from the system which would therefore not be suitable. The need for pH control is crucial to our plan; we know that our enzyme works well at both pH 5 and pH 7 which is ideal for use with the disulfide. This means we can do the disulfide exchange reaction in the pH range 7 – 9 , lower the pH to 5 to stop the reaction and add in the enzyme which will function at pH 5. An imine exchange reaction occurs between pH 8.5 and pH5 so this would not be compatible with our plans.

The disulfide exchange reaction is compatible with biomolecules as long as surface exposed thiol or disulfide groups are not present.[97] We do not know what amino acid residues might be present in the enzyme active site, however, this should not be a problem as the exchange itself will not be done in the presence of the enzyme. We will be doing the experiments with the enzyme at pH 5 which means that disulfide exchange should not be taking place anyway. It is important to remember that this work is a screening experiment to find out quickly and efficiently what lengths of linker the enzyme will process. When it comes to later work and if the disulfide is not suitable, it can be replaced with a similar functionality such as an ether or alkyl linker.

## 4.2 Synthetic Targets for the Formation of the Dynamic Combinatorial Library

To test the viability of using a combinatorial library with the β-galactosidase from *B. circulans* we first investigated conditions for forming the library using the glycosyl acceptor – methyl glucose. Our target substrates would be based on the ether-linked naphthyl sugars that we

had made using stepwise synthesis as we knew from our initial investigation that the enzyme would accept this type of substrate (**32**, **33** and **34**).

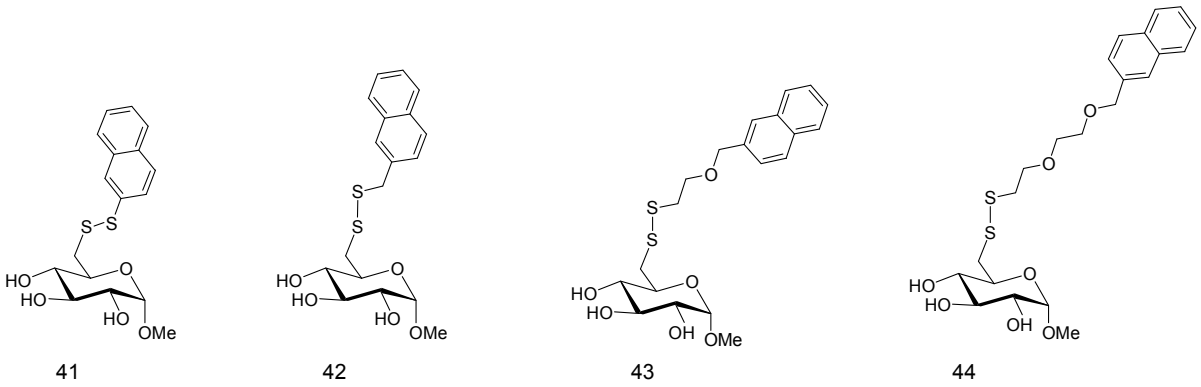


**Figure 4.2a: Glycosyl acceptor targets for the use in the dynamic combinatorial library**

These target substrates would be generated using combinatorial synthesis from a library shown in figure 4.2b. The combinatorial library generated from the components above would also contain dimers of all of the substrates.

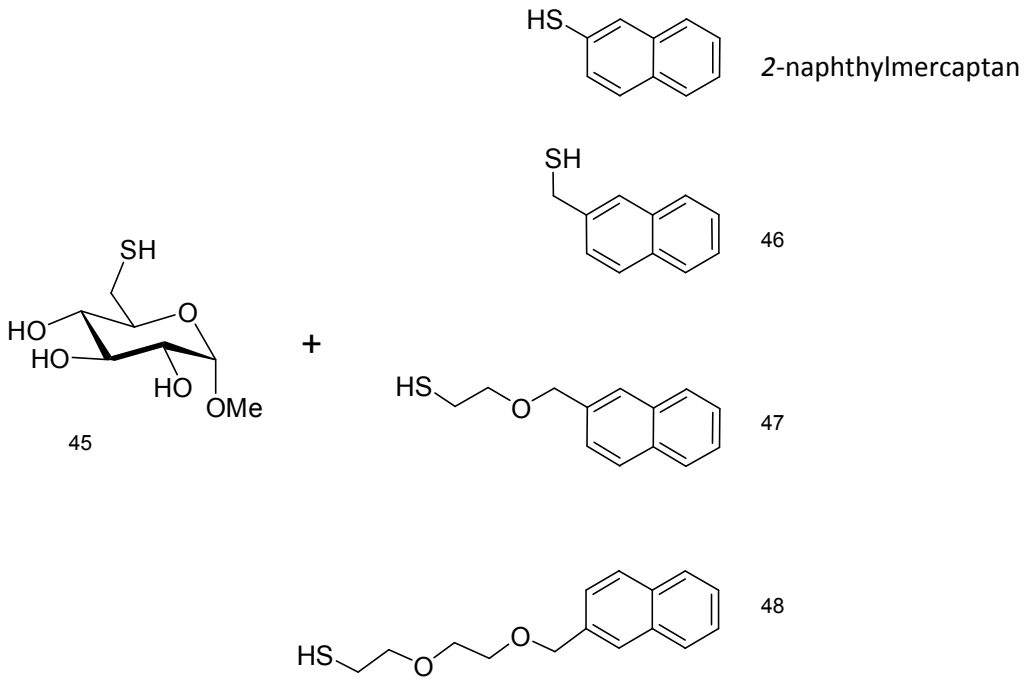


**Figure 4.2b: Library components for the glycosyl acceptor dynamic combinatorial library**

Once the library has been formed, we plan to 'freeze' the library at a stage when all the desired sugar-naphthyl disulfides have been generated so that no disulfide exchange takes place duing the enzyme reaction. It is not our intention to create a dynamic combinatorial library (DCL) for use with the enzyme. In our case, if the enzyme were to make a disaccharide from a DCL of glycosyl acceptors there would be nothing to stop the disulfide bond between the glycosyl acceptor and its partner from exchanging with another thiol in the mixture. This would then give us a false result as we would not be able to say definitively that the sulfide linked to the glycosyl acceptor was present at the time of the glycosyl transfer. This is why we plan to freeze the library at an optimised point at which we have generated a library with the maximum product diversity (Figure 4.2c) and this is what would then be put through the trans glycosylation reaction.

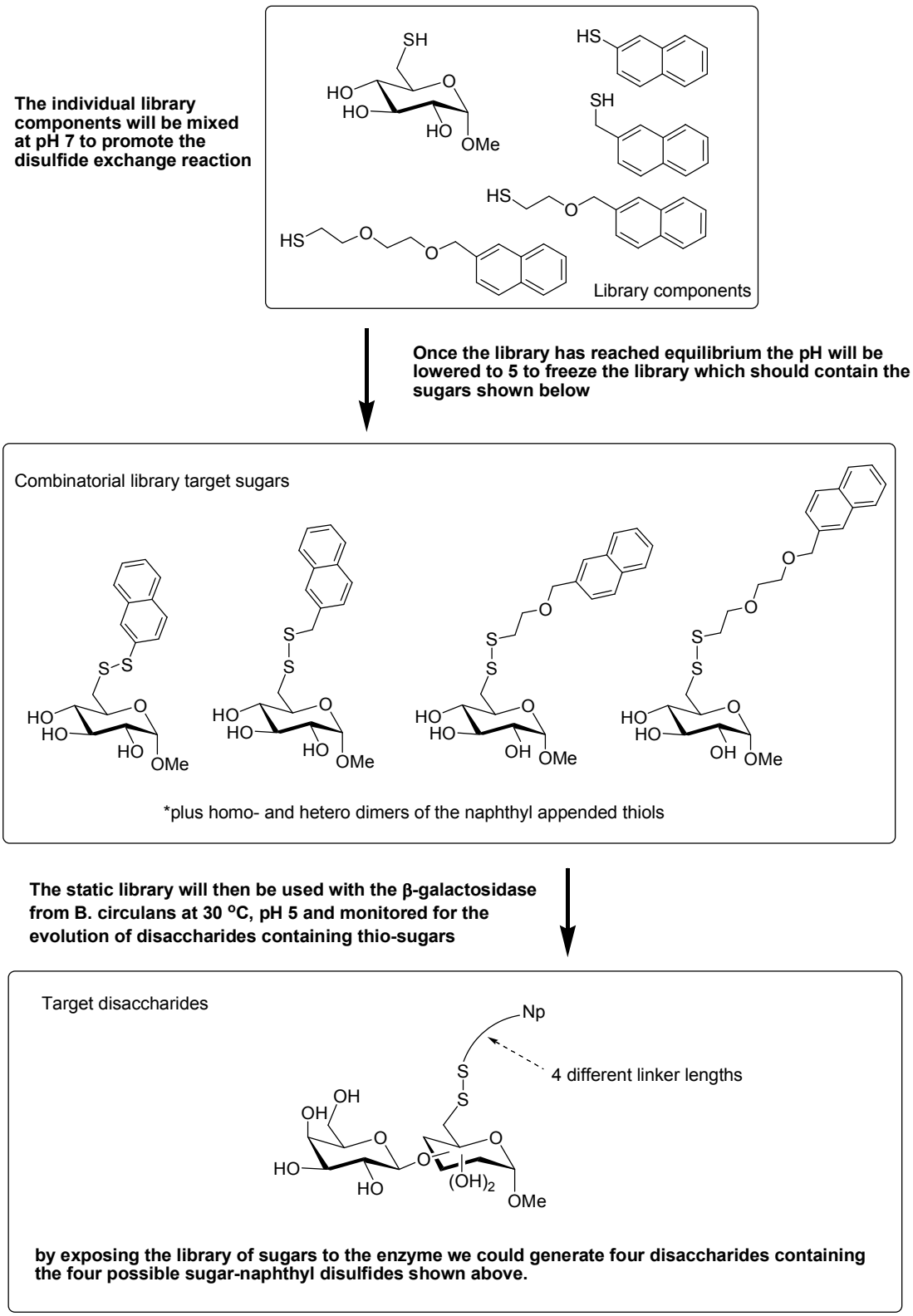


**Figure 4.2c: Proposed scheme of work for the dynamic combinatorial library studies.**

Once the viability of this technique has been proven on the glycosyl acceptor we would then test it using the glycosyl donor, GalO*p*NP. The combinatorial library of glycosyl donors would be formed from the components in Figure 4.2d and would generate the sugars shown in Figure 4.2e (as well as the homo- and hetero-dimers of the naphthyl functionalised thiols).

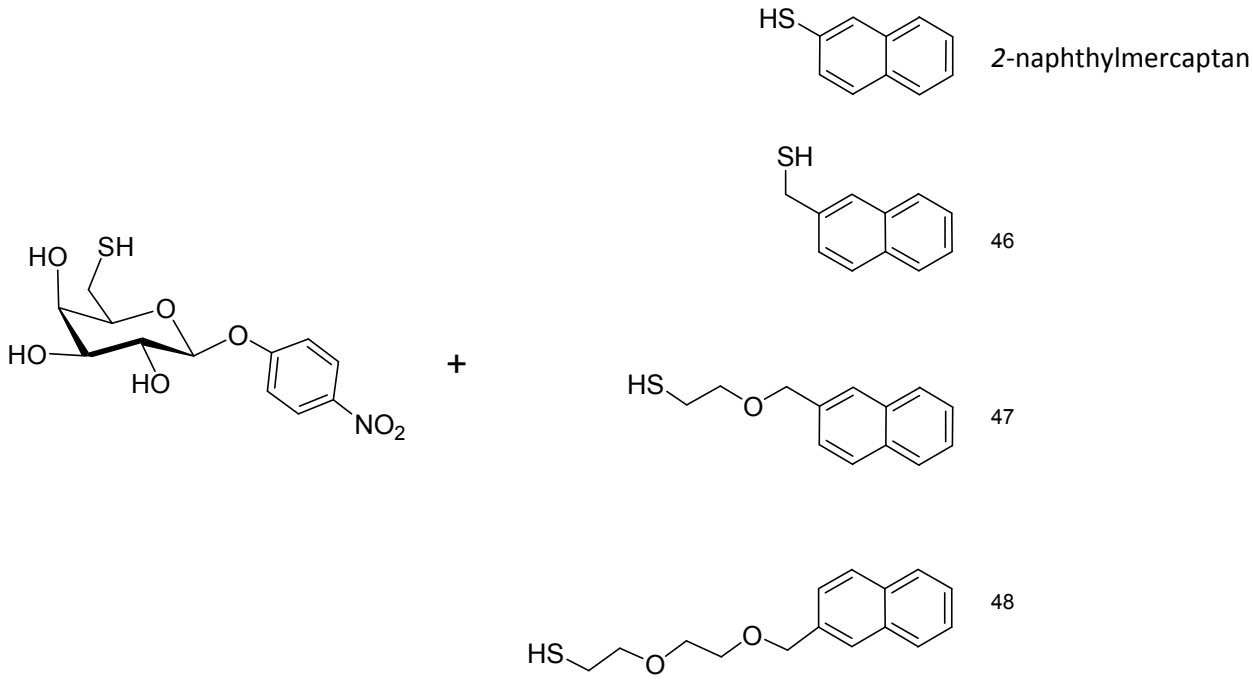


**Figure 4.2d: Library components for the glycosyl donors dynamic combinatorial library**

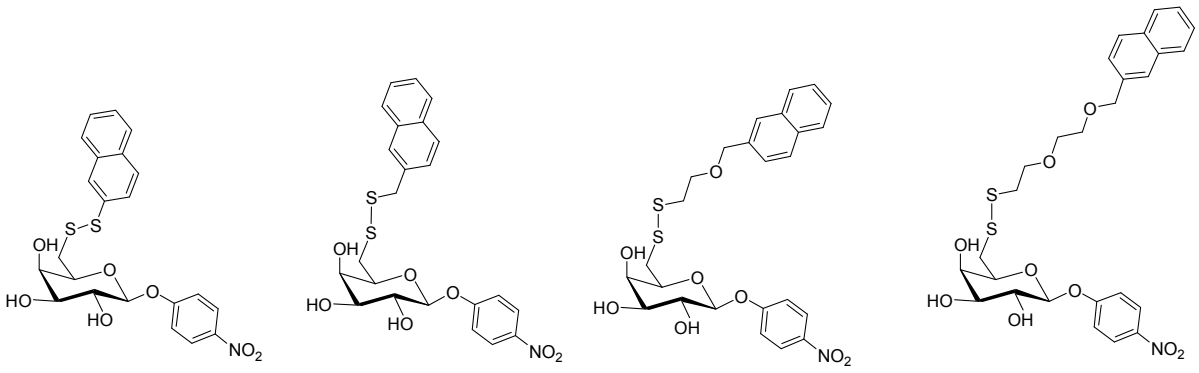


**Figure 4.2e: Glycosyl donor targets for the use in the dynamic combinatorial library**

In total, for this combinatorial study we only have to synthesise six components, all of which are relatively simple to produce as they can be made from compounds that we have already

synthesised or can buy directly. This makes this approach potentially synthetically efficient with a potential fast turnaround on results.

### 4.2.1 Synthesis of the thiol-functionalised naphthyl linkers

There are four naphthyl linker substrates needed for the combinatorial library (Fig 4.2b). The smallest, 2-naphthylmercaptan was purchased directly; the other three needed to be synthesised.

We began our synthesis of the requisite thiols by starting from alcohols and bromides that we had already synthesised.

The first reaction we attempted was to form a thiol from the alcohol **24** by refluxing the alcohol in conc. HCl with thiourea for 9 hours (Figure 4.2.1a).[98]

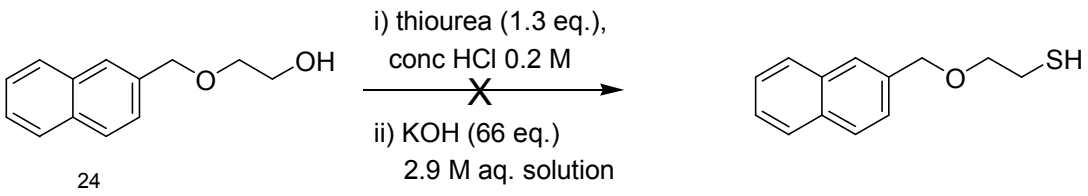


24

**Figure 4.2.1a: First attempt to convert an alchol 24 into a thiol**

Unfortunately this reaction did not work very well. In the first part of the reaction a less polar spot was seen to move to a lower $R_f$ value and there was consumption of starting material. However, the yellow oil which resulted from the basic work up procedure contained only trace amounts of the target thiol which were detected by EI mass spectrometry. There was no evidence to suggest that we had produced the dimer. NMR spectroscopy of the oil showed a very impure substance.

A further attempt of the reaction shown in Figure 4.2.1a was tried without success using the same conditions. We then elected to instead use our previously synthesised bromides as a starting point for the synthesis of the thiols. The bromides were successfully transformed to the thiols by heating under reflux with thiourea in ethanol.[99] This reaction resulted in a crude mixture of both thiols and their disulfide dimers as a dark yellow oil directly from work up. The crude yields from this reaction were in the region of 90%. The crude material obtained from this reaction was directly acetylated for ease of purification and characterisation (Figure 4.2.1c).

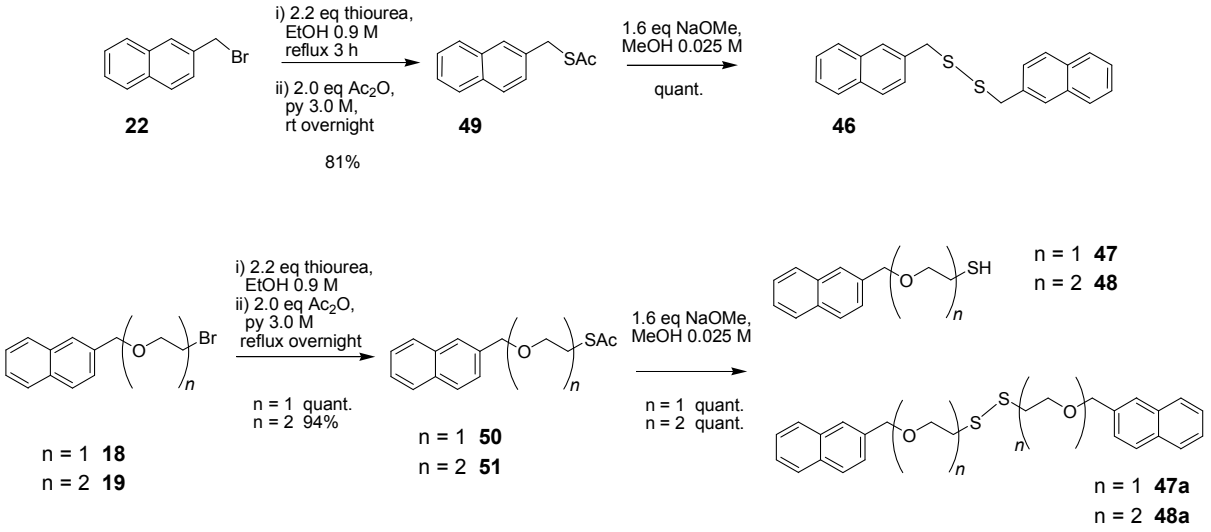


**Figure 4.2.1b: Successful syntheses of the thio-naphthyl linkers**

Purification of the acetylated thiols by column chromatography worked very well and yields of the combined thiol and disulfide products were high, between 84 and 100% over two steps. Deacetylation of the thiols was carried out in the usual manner using NaOMe. This sometimes resulted in a mixture of thiols and disulfides or just the disulfide in the case of **46**. This did not present a problem for forming the library of disulfides as homo-dimers added as starting material will be subject to disulfide exchange in the library-forming reaction. Overall this process worked very well and gave us reliable, easy access to our naphthyl-based library components.

### 4.2.2 Synthesis of thio-sugars

#### 4.2.2.1 Synthesis of Methyl-(6-thio-6-deoxy)-α-D-glucopyranoside

6-Thio sugars can be prepared directly from 6-tosyl sugars and since we had previously synthesised methyl (6-tosyl)-α-D-glucopyranoside we chose to start from this compound (Figure 4.1.2.2a).

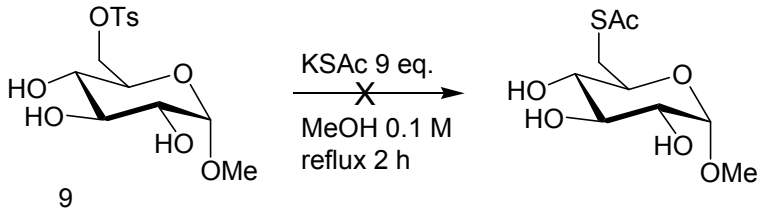


**Figure 4.2.2.1a: Attempted synthesis of 6-deoxy-6-thioacetyl-glucopyranoside**

Following a method by Gigg[100] the 6-tosyl sugar was treated with potassium thioacetate by heating under reflux in methanol. Gigg reported that this afforded the corresponding 6-thio-acetyl sugar from a benzyl protected sugar. We tried it first on the unprotected tosyl sugar as this would have given us a shorter route to our target. Unfortunately, this reaction did not work and only starting material was recovered. This method was also attempted on the acetyl protected tosyl sugar but again only starting material was recovered. We decided not to continue with this method as our next step would be to benzyl protect the secondary alcohols prior to treatment with potassium thioacetate. This would introduce a longer protecting group strategy which we wanted to avoid. The benzyl groups would have to be removed after the thioacetate was installed and replaced with acetates for characterisation. So, we chose a different route as detailed below.

Our next approach was based on the use of thiourea to displace bromine in our synthesis of the naphthyl components of the library (Section 4.2.1). When making 6-thio sugars it is usual to use iodine rather than bromine as iodine will selectively react at the primary alcohol of a

free glycoside. Figure 4.2.2.1b shows the successful synthesis of methyl 2,3,4-tri-*O*-acetyl-(6-acetylthio-6-deoxy)-α-D-glucopyranoside (**53**).

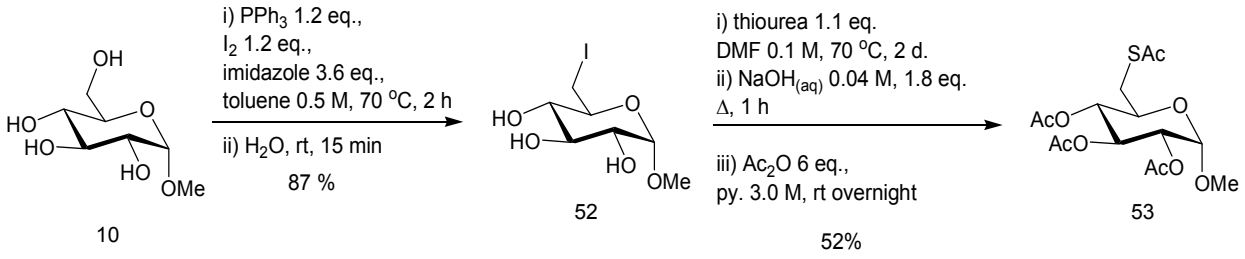


**Figure 4.2.2.1b: Successful synthesis of thio acetate 53 *via* a 6-iodo sugar**

The 6-iodo sugar **52** was prepared directly from methyl-α-D-glucose according to a method by Murphy.[101] The reaction proceeded well and with a good yield of 87%. The following transformation of the 6-iodo group to the 6-thioacetate group[102] also proceeded well, although in a less satisfactory yield of 52% over the two steps. Again, the acetate-protected sugar was made for ease of storage and characterisation. The deactetylation reaction was carried out in the usual manner by addition of NaOMe in MeOH with stirring overnight (see Experimental Section). This furnished **45**, methyl-(6-thio-6-deoxy)-α-D-glucopyranoside (see Figure 4.2b), in 99% yield, ready for use in the combinatorial library.

## 4.3 Forming the Combinatorial Library

Design of the conditions to be used for our combinatorial experiments has to be done sensitively to the needs of the disulfide exchange reaction and later the trans-glycosylation by the β-galactosidase from *B. circulans*. A four-stage process to the investigation began with gathering the individual components, then involved forming the library and allowing it to equilibrate, followed by freezing the equilibrated library and exposing it to the enzyme to determine if it can process any of the sugars in the library.

### 4.3.1 Optimisation of Conditions for the Formation of the Combinatorial Library

In order to determine the conditions under which our combinatorial libraries will form, it was necessary to consider:

- the solvent and reaction concentration;
- pH;
- temperature;
- method of initiating the disulfide exchange reaction;
- stoichiometry of the library components.

Our work to find suitable conditions to promote the formation of the combinatorial library and optimise them is described below.

#### Initial investigation to identify suitable reaction conditions for the disulfide exchange reaction

From our experience in the enzyme experiments, we knew that it would be necessary for some organic solvent to be present in the reaction mixture so that all components of the reaction would be fully dissolved – this is true for both the disulfide exchange and the trans-glycosylation. Our intention was to form the library under solvent conditions that would also be compatible with the enzyme. Having already done a very thorough screening test on the solvent conditions under which the enzyme would function (see Section 3), we needed to investigate if any of those sets of conditions would work for the disulfide exchange. Once we had established the solvent conditions for the disulfide exchange and the enzyme reaction, we would then form the library at pH 7. When it had equilibrated the pH would be lowered to

5 to stop the disulfide exchange after which the enzyme would be added. The enzyme reaction would then be followed by HPLC and MS to establish whether any of our target disulfide linked sugar-naphthalene compounds were generated.

Our initial experiment involved the disulfide exchange on just two of the library components (Figure 4.3.1a).

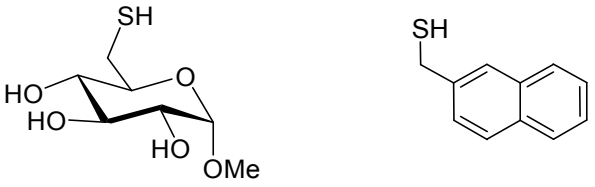


45 46

**Figure 4.3.1a: First test subjects for forming the combinatorial library**

The disulfide exchange reaction is mediated by deprotonated thiol. A reaction pH of 7 – 9 is usually adequate in order to generate enough thiolate anion for the reaction to proceed. There are two ways of starting the exchange reaction: i) using thiols in the presence of air; ii) using substoiciometric amounts of free thiol.[97] Which of these methods to use will depend on the solvent used for the exchange reaction and the susceptibility of the thiol components to be oxidised in the presence of air.

Comparing the two compounds in Figure 4.3.1a, it is apparent that their solubility will be very different. A brief test confirmed that whilst the sugar **45** was partially soluble in a pH 7 buffer solution, (2-naphthyl)methanethiol (**46**) was not. We therefore decided to first establish a method for the disulfide exchange between the two library components in organic solvent. However, this would not be compatible with the conditions needed for the enzyme experiment as the amount and type of organic solvent needed for the disulfide exchange would potentially inhibit the enzyme. To get around this problem we came up with a simple solution: to do the disulfide exchange in organic solvent and once it had equilibrated to remove the solvent under reduced pressure. The resultant combinatorial library residue

would then be taken up in a pH 5.0 buffer with 20% acetonitrile in order to perform the enzyme experiments. We expected the sugar-naphthalene compounds to be soluble in these conditions as the similar compounds we had tested in the preceding enzyme experiments were soluble enough to undergo the enzymatic reaction. Moreover, any mixed naphthalene-naphthalene disulfides should not be soluble in and would therefore not interfere with the enzyme experiment.

We tested solvent conditions for the exchange reaction by adapting a method by Still *et al*.[103] for a non-aqueous disulfide exchange. We used a mixed solvent system due to the different solubilities of **45** and **46**. Two separate 8.6 mM solutions were made up: (A) **45** in MeOH and (B) **46** in $CHCl_3$. 1 mL of B was added to 0.5 mL of A and 2.3 mol% of an activating solution of thiophenol and $Et_3N$ was added (Figure 4.3.1b).

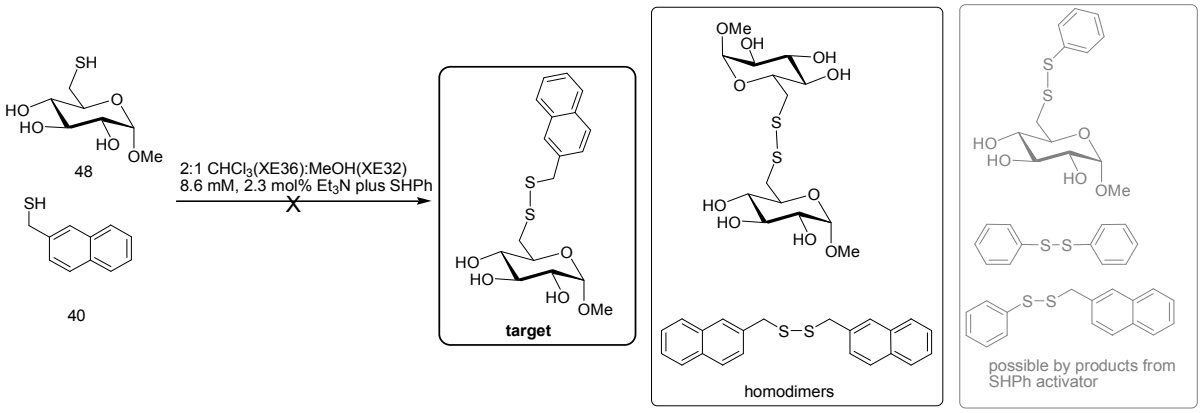


**Figure 4.3.1b: Attempted initial screening reaction for disulfide bond formation**

20 μL aliquots were taken at 10, 30, 60 and 120 minutes and examined by HPLC and MS to check for the formation of any of the mixed disulfides we hoped to generate. Since no mixed disulfides were found (neither the target nor the possible by product), we then resorted to a broader screening experiment in order to find a set of reaction conditions that would work.

### 4.3.1.1 Refinement of reaction conditions for disulfide exchange

We began by addressing each issue that would affect the exchange reaction in order to design an optimal screening experiment.

**Stoichiometry:** It is stated in a paper by Nicolaou *et. al.*[104] that:

*"If two homodimeric disulfides, A-SS-A and B-SS-B are mixed under basic conditions in the presence of a suitable catalyst they will undergo rapid exchange reactions to afford a statistical mixture of 3 disulfides A-SS-A, A-SS-B, B-SS-B in a ratio of 1:2:1 respectively, resulting from the degeneracy of A-SS-B and B-SS-A products."*

This holds true if the homodimeric disulfides in question have similar activities to each other, and this depends upon sterics, $pK_a$ etc. In our case, the starting thiols are similar to each other in terms of sterics (see Figure 4.2b) and the $pK_a$ values can also be approximated from available data (Figure 4.3.1.1a).

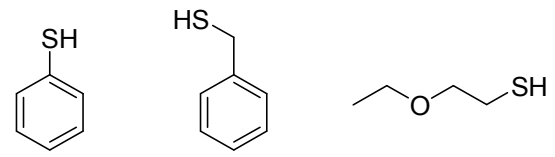


**Figure 4.3.1.1a: $pK_a$s of relevant thiols[105]**

Given this information we decided that the stoichiometry of our reaction components should be 1:1 sugar to naphthyl linker in order to maximise the amount of mixed disulfides produced.

**Activation of the exchange reaction:** The disulfide exchange reaction needs to be activated. For this, the reaction solution should be basic and contain a substoiciometric amount of free thiol. We would use an activating solution of thiophenol and $Et_3N$ since this is a common reagent combination for inducing the disulfide exchange reaction. We would try

adding varying amounts of the activating solution to the reaction and also investigate if adding additional activating solution over the course of the reaction had an effect on the exchange reaction.

Figure 4.3.1a shows the two components we will be using to investigate optimal reaction conditions. We would expect thiols **45** (sugar) and **46** (naphthyl) to have a $pK_a$ of ~9.5 by comparison with the thiols in Figure 4.3.1.1a. Thiophenol is used to activate the disulfide exchange reaction in the presence of base ($Et_3N$) as it has a lower $pK_a$ and is thus more susceptible to deprotonation than **45** and **46**. We must also bear in mind that following deacetylation of the acetate-protected thiols some disulfide homodimers may be present. For this reason it is necessary to add the thiophenol to ensure activation of the disulfide exchange reaction.

**Reaction solution and temperature:** The other two factors to investigate were the reaction concentration itself which tends to be quite low, between 1 and 10 mM, and the temperature of the reaction. The solvents used also need to be miscible, so a standard solution of **46** would be made up in $CHCl_3$ whilst two standard solutions of the thio sugar **45** would be made up in MeOH and acetone.

The first reaction we had tried had a concentration of 8.6 mM, so we planned to investigate reaction concentrations of 5 and 10 mM which seemed a good starting point either side of the literature suggestion.

Heating can increase the rate of disulfide exchange which is desirable as many of these types of reactions can take days to equilibrate at room temperature. Given the boiling points of the solvents we planned to use ($CHCl_3$, MeOH and acetone), a reaction temperature of 40 $^oC$ was chosen.

Having decided on the variables for the screening reaction, we set up an experiment to simultaneously test 12 sets of conditions.

**DCC1 Screening reaction to determine the best conditions for the generation of the combinatorial library**

Using a 12-reaction carousel, 1 mL of each of the equimolar solutions of the thio sugar and the thio-napthyl compound (stoichiometry thus 1:1) were mixed and stirred at 40 $^{o}$C with the activating solution. The concentration of the reaction and the amount of activating solution added is detailed in Table 4.3.1.1b. Aliquots (40 μL) were taken at 0, 24, 48 and 72 h, then diluted in 500 μL of MeOH prior to analysis by MS.

| Reaction number | **46** solvent | **46** conc m/M | **45** (MeOH) conc /mM | **x** equiv. of activating solution | Activating solution added: |
|---|---|---|---|---|---|
| **i** | $CHCl_3$ | 5 | 5 | 0.3 | daily |
| **ii** | $CHCl_3$ | 5 | 5 | 0.6 | daily |
| **iii** | $CHCl_3$ | 10 | 10 | 0.3 | daily |
| **iv** | $CHCl_3$ | 10 | 10 | 0.6 | daily |
| **v** | acetone | 5 | 5 | 0.3 | daily |
| **vi** | acetone | 5 | 5 | 0.6 | daily |
| **vii** | acetone | 10 | 10 | 0.3 | daily |
| **viii** | acetone | 10 | 10 | 0.6 | daily |
| **ix** | $CHCl_3$ | 5 | 5 | 0.6 | once |
| **x** | $CHCl_3$ | 10 | 10 | 0.6 | once |
| **xi** | acetone | 5 | 5 | 0.6 | once |
| **xii** | acetone | 10 | 10 | 0.6 | once |

**Table 4.3.1.1b: Reaction conditions for experiment DCC1**

**Results from mass spectrometry of each sample**

Each sample was analysed using mass spectrometry for the presence of sugar disulfides shown in Figure 4.3.1.1c. Hetero- and homo-dimers of (2-naphthyl)methanethiol and thiophenol were not monitored as the compounds of interest are the sugars.

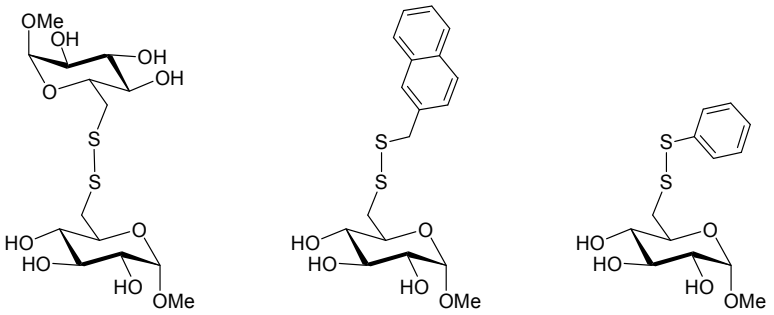


**Figure 4.3.1.1c: Disulfide targets - glucosides**

In order to determine the optimum conditions for the formation of our combinatorial library we compared the ratio of the peak heights of the disulfides above (Fig 4.3.1.1c) in the mass spectra. An example of the mass spectra recorded is below (Fig 4.3.1.1d). By comparing the peak heights due to the three expected sugar disulfides this will give us an indication of the ratio of the components and thus allow us to semi-quantitatively assess when the disulfide exchange reaches equilibrium.

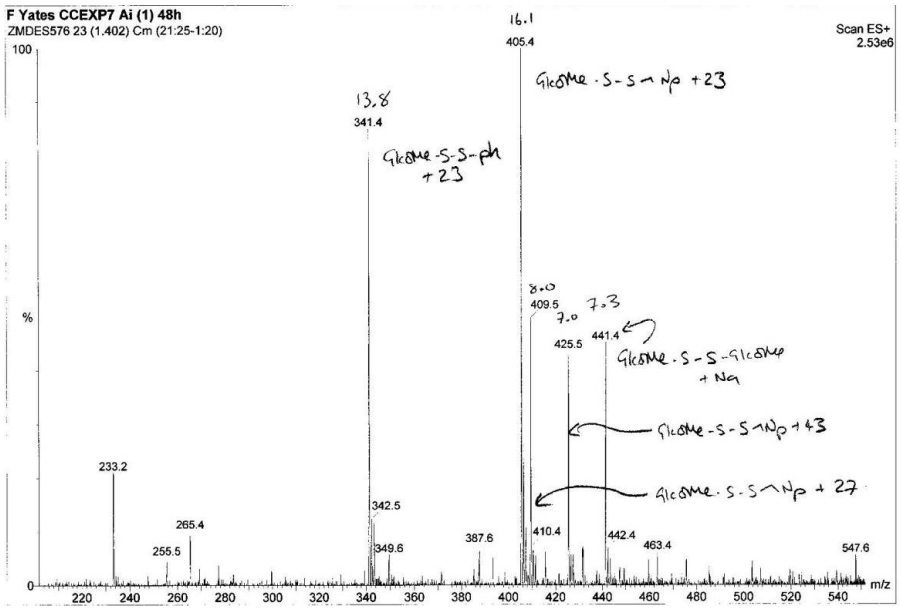


**Figure 4.3.1.1d: Example mass specrum from experiment DCC1,**

The peaks of interest are:

| Disulfide | RMM | M |
|---|---|---|
| GlcOMe-S-S-Ph | 318 | 341 (+ 23) |
| GlcOMe-S-S-$CH_2$Np | 382 | 405 (+ 23) |
| GlcOMe-S-S-GlcOMe | 418 | 441 (+ 23) |

**Table 4.3.1.1e: Target peaks in mass spectra analysis**

We measured the heights of the peaks of interest shown in Table 4.3.1.1e for each sample and assessed the ratio of products in each combinatorial reaction. The peak heights obtained for GlcOMe-S-S-GlcOMe have been doubled in the comparison as the thio sugar starting material was added as a monomer. Again, this investigation will give us an indication of the most suitable reaction conditions in a semi-quantitative fashion.

Within the results we looked for the reactions conditions that matched or bettered our theoretical ratio of 1:2 GlcOMeSH:GlcOMe-S-S-$CH_2$Np, where the latter is our target compound. Table 4.3.1.1f shows the ratios of the peak heights obtained in the twelve experiments (refer to Table 4.3.1.1b for reaction conditions). Selected bar graphs showing the ratio of peak heights follow Table 4.3.1.1f. The most promising sets of results are highlighted.

| reaction | Disulfide** | 0 h | 24 h | 48 h | 72 h |
|---|---|---|---|---|---|
| i | GlcOMeSH | 1.0 | 1.0 | **1.0** | 1.0 |
| | GlcOMe-S-S-$CH_2$Np | 0.0 | 0.9 | **2.1** | 2.1 |
| | GlcOMe-S-S-Ph | 0.0 | 0.3 | **0.9** | 1.5 |
| ii | GlcOMeSH | 1.0 | **1.0** | 1.0 | 1.0 |
| | GlcOMe-S-S-$CH_2$Np | 0.0 | **3.0** | 2.5 | 2.5 |
| | GlcOMe-S-S-Ph | 0.0 | **1.1** | 2.2 | 2.9 |
| iii | GlcOMeSH | 1.0 | 1.0 | 1.0 | 1.0 |
| | GlcOMe-S-S-$CH_2$Np | 0.0 | 0.7 | 1.7 | 1.8 |
| | GlcOMe-S-S-Ph | 0.0 | 0.3 | 0.7 | 1.2 |
| iv | GlcOMeSH | 1.0 | 1.0 | 1.0 | 1.0 |
| | GlcOMe-S-S-$CH_2$Np | 0.0 | 1.2 | 1.7 | 1.8 |
| | GlcOMe-S-S-Ph | 0.0 | 0.8 | 1.4 | 1.9 |
| v | GlcOMeSH | 1.0 | **1.0** | 1.0 | 1.0 |
| | GlcOMe-S-S-$CH_2$Np | 0.0 | **2.0** | 2.1 | 2.0 |
| | GlcOMe-S-S-Ph | 0.0 | **0.4** | 1.1 | 1.4 |
| vi | GlcOMeSH | 1.0 | 1.0 | 1.0 | 1.0 |
| | GlcOMe-S-S-$CH_2$Np | 0.0 | 1.4 | 2.4 | 2.4 |
| | GlcOMe-S-S-Ph | 0.0 | 0.7 | 2.2 | 2.8 |
| vii | GlcOMeSH | 1.0 | 1.0 | 1.0 | 1.0 |
| | GlcOMe-S-S-$CH_2$Np | 0.0 | 0.8 | 1.3 | 1.8 |
| | GlcOMe-S-S-Ph | 0.0 | 0.3 | 0.7 | 1.3 |
| viii | GlcOMeSH | 1.0 | 1.0 | 1.0 | 1.0 |
| | GlcOMe-S-S-$CH_2$Np | 0.0 | 1.3 | 2.2 | 2.5 |
| | GlcOMe-S-S-Ph | 0.0 | 0.8 | 2.0 | 2.1 |
| ix | GlcOMeSH | 1.0 | **1.0** | **1.0** | 1.0 |
| | GlcOMe-S-S-$CH_2$Np | 0.0 | **2.5** | **2.5** | 1.6 |
| | GlcOMe-S-S-Ph | 0.0 | **1.2** | **1.2** | 0.8 |
| x | GlcOMeSH | 1.0 | 1.0 | 1.0 | 1.0 |
| | GlcOMe-S-S-$CH_2$Np | 0.0 | 0.9 | 1.5 | 1.4 |
| | GlcOMe-S-S-Ph | 0.0 | 0.7 | 0.8 | 0.7 |
| xi | GlcOMeSH | 1.0 | 1.0 | 1.0 | 1.0 |
| | GlcOMe-S-S-$CH_2$Np | 0.0 | 1.6 | 1.8 | 1.8 |
| | GlcOMe-S-S-Ph | 0.0 | 0.8 | 1.1 | 1.0 |
| xii | GlcOMeSH | 1.0 | 1.0 | 1.0 | 1.0 |
| | GlcOMe-S-S-$CH_2$Np | 0.0 | 1.2 | 1.5 | 1.6 |
| | GlcOMe-S-S-Ph | 0.0 | 0.9 | 1.0 | 0.9 |

**Table 4.3.1.1f: comparison of peak height ratios found in mass spectra for DCC1**

** GlcOMeSH is shown rather than the dimer as the comparison must be made with the amount of starting material added. GlcOMeSH was added as the thiol but during the exchange reaction it exists solely as the dimer

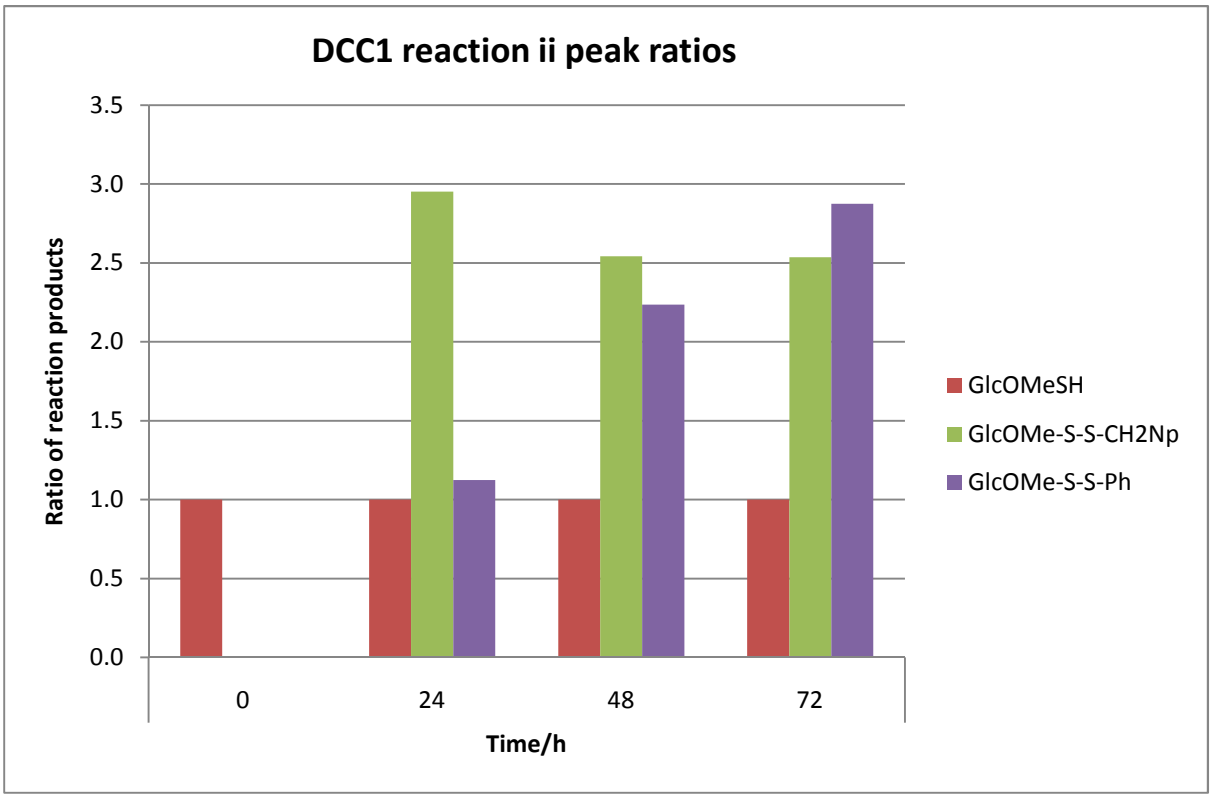


**Figure 4.3.1.1g: peak height ratios from reaction ii ($CHCl_3$, 5 mM, 0.6 eq. daily addition)**

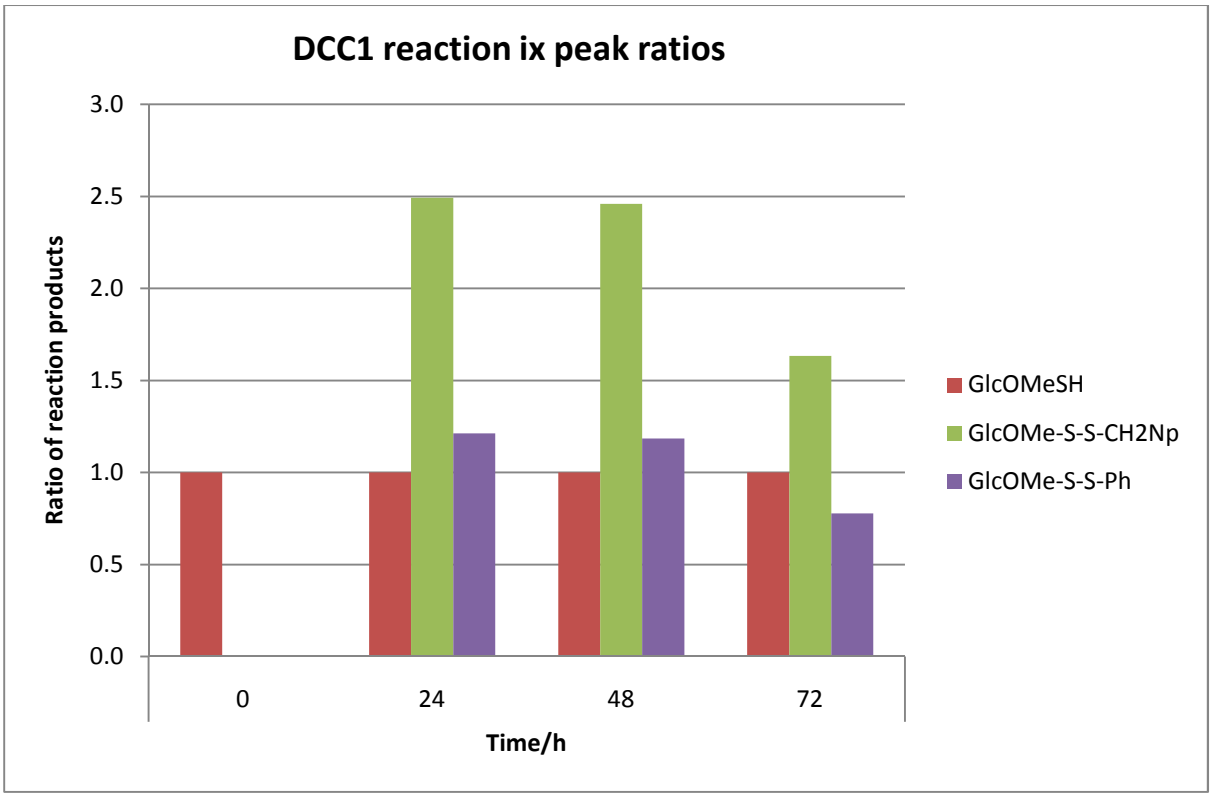


**Figure 4.3.1.1h: peak height ratios from reaction ii ($CHCl_3$, 5 mM, 0.6 eq. single addition)**

The data collected[††] show that our target product, GlcOMe-S-S-$CH_2$Np, was successfully produced in all twelve test reactions. This was a very pleasing result, more so that the majority of reactions produced a good proportion of this target disulfide. Figure 4.3.1.1g shows the results from reaction ii, in this reaction 0.6 equivalents of the activating solution were added each day. At 24 hours the ratio of GlcOMeSH to GlcOMe-S-S-$CH_2$Np to GlcOMe-S-S-Ph is 1:3:1. Due to the daily addition of 0.6 equivalents of activating solution at 72 hours the ratio of GlcOMeSH to GlcOMe-S-S-$CH_2$Np is around 1:2 but the relative amount of GlcOMe-S-S-Ph is greater than the target disulfide. In contrast, Figure 4.3.1.1h shows the results from reaction ix where there was a single addition of 0.6 equivalents of the activating solution, the other reaction conditions are as in reaction ii. This shows a much more promising result as the ratio of GlcOMeSH to GlcOMe-S-S-$CH_2$Np is around 1:2 at 24 and 48 hours and the relative amount of GlcOMe-S-S-Ph is much less than the target disulfide as less thiophenol is added. At 72 hours, the relative amount of GlcOMe-S-S-$CH_2$Np has fallen so the optimum point at which to freeze the library from reaction ix would have been 48 hours. For reaction ii, it would have been 24 hours.

The reactions conditions which produced the target values of 1:2 starting material to target disulfide shared one particular factor: the reaction concentration was 5 mM (See Table 4.3.1.1i).

| Reaction number | **46** solvent | **46** conc m/M | **45** (MeOH) conc /mM | **x** equiv. of activating solution | Activating solution added: |
|---|---|---|---|---|---|
| **i** | $CHCl_3$ | 5 | 5 | 0.3 | daily |
| **ii** | $CHCl_3$ | 5 | 5 | 0.6 | daily |
| **v** | acetone | 5 | 5 | 0.3 | daily |
| **ix** | $CHCl_3$ | 5 | 5 | 0.6 | once |

**Table 4.3.1.1i: Summary of reaction conditions giving the most promising results from DCC1**

[††] The rest of the graphs showing the results from this experiment are in the Appendix, Section 4.3.2.1.

Of the twelve sets of reaction conditions the most promising were those for reaction ix:

- 40 $^{o}$C
- 48 h
- 5 mM reaction concentration
- thio-naphthyl linker in $CHCl_3$
- sugar in MeOH
- 0.6 equiv. of activating solution – single addition at t = 0

A deciding factor in choosing this set of conditions was the single addition of the activating solution. When adding more of the activating solution each day, the amount of GlcOMe-S-S-Ph will increase which is undesirable. The ratio of starting material to desired product using reaction conditions ix was 1.0:2.5, and although a higher ratio of 1.0:3.0 was seen using reaction conditions ii (the same conditions as ix but with daily addition of activating solution) we felt it best to use the conditions requiring less activating solution as this would ultimately lead to less by product.

#### 4.3.1.2 Further analysis of combinatorial library products

To confirm that the desired disulfide GlcOMe-S-S-$CH_2$Np had been produced in the reactions, preparative HPLC was carried out on a pooled mixture from all twelve test reactions.

Analytical HPLC on the pooled samples revealed four UV-active peaks, those corresponding to sugar-naphthyl disulfides were found between 25 – 30 minutes, whilst those at 45 – 50 minutes corresponded to naphthyl-thiol dimers and mixed disulfides. Preparative HPLC was then used to separate the pooled reaction mixture. The UV-active fractions were submitted for analysis by mass spectrometry. The mixed disulfides GlcOMe-S-S-Ph and GlcOMe-S-S-$CH_2$Np were found at $t_r$ = 25.24 and $t_r$ = 28.95 min respectively.

| Disulfide | Mass recovered / mg | Moles | Yield wrt thiosugar |
|---|---|---|---|
| GlcOMe-S-S-Ph | 9 | $2.83 \times 10^{-5}$ | 17% |
| GlcOMe-S-S-$CH_2$Np | 4 | $1.05 \times 10^{-5}$ | 6% |

**Table 4.3.1.2a: Yields of glucosidic hetero disulfides from DCC1 – pooled reaction contents**

It can be seen from the results in Table 4.3.1.3a that the yield of our desired disulfide was very low when taken across all twelve reactions. This was not a concern as this investigation was purely to discover a reliable method of forming a combinatorial library. However, the amount of by-product due to thiophenol is almost three times that of our desired sugar. We expect that our chosen best method, which has a single addition of the activating solution, will limit the amount of thiophenol by-products produced.

These two compounds were then submitted for NMR to confirm their structures. Using $^{1}H$ and $^{13}C$ NMR spectroscopy, the structure of the sugar GlcOMe-S-S-$CH_2$Np was confirmed to be that shown in Figure 4.3.1.1c.

### 4.3.1.3 Repeating the successful reaction conditions

A larger scale reaction using the chosen conditions from the initial screening experiment was then undertaken to follow the progress of the reaction more closely. The intention was also to use the resultant combinatorial reaction mixture in a test reaction with the enzyme.

**DCC2 larger scale reaction conditions ix**

The experiment was carried out in the same way as in the preceding section. Two identical reactions were done on a slightly larger scale – 8 mL rather than 4 mL reaction volume – and under the following conditions:

- 40 $^{o}$C
- 48 h
- 5 mM reaction concentration; thio-naphthyl linker in $CHCl_3$, sugar in MeOH
- 0.6 equiv. of activating solution – single addition

Aliquots were taken at more frequent intervals (0, 1, 2, 4, 6, 8, 24, 30 and 48 h) so that the evolution of the desired products could be inspected more closely by mass spectrometry.

As before, we compared the relative peak heights seen in the mass spectra for the three compounds of interest (shown in Table 4.3.1.3a and Figures 4.3.1.3b and c).

| reaction | disulfide | 0 h | 1 h | 2 h | 4 h | 6 h | 8 h | 24 h | 30 h | 48 h |
|---|---|---|---|---|---|---|---|---|---|---|
| A | GlcOMeSH | 1.0 | 1.0 | 1.0 | 1.0 | 1.0 | 1.0 | 1.0 | 1.0 | 1.0 |
| | GlcOMe-S-S-$CH_2$Np | 0.2 | 0.2 | 0.3 | 0.4 | 0.5 | 0.6 | 1.4 | 1.6 | 1.9 |
| | GlcOMe-S-S-Ph | 0.0 | 0.1 | 0.1 | 0.2 | 0.3 | 0.3 | 0.6 | 0.7 | 0.9 |
| B | GlcOMeSH | 1.0 | 1.0 | 1.0 | 1.0 | 1.0 | 1.0 | 1.0 | 1.0 | 1.0 |
| | GlcOMe-S-S-$CH_2$Np | 0.2 | 0.2 | 0.3 | 0.5 | 0.7 | 0.6 | 1.2 | 1.7 | 2.1 |
| | GlcOMe-S-S-Ph | 0.0 | 0.1 | 0.1 | 0.3 | 0.4 | 0.3 | 0.5 | 0.6 | 0.7 |

**Table 4.3.1.3a: Relative mass spectra peak heights of components in experiment DCC2**

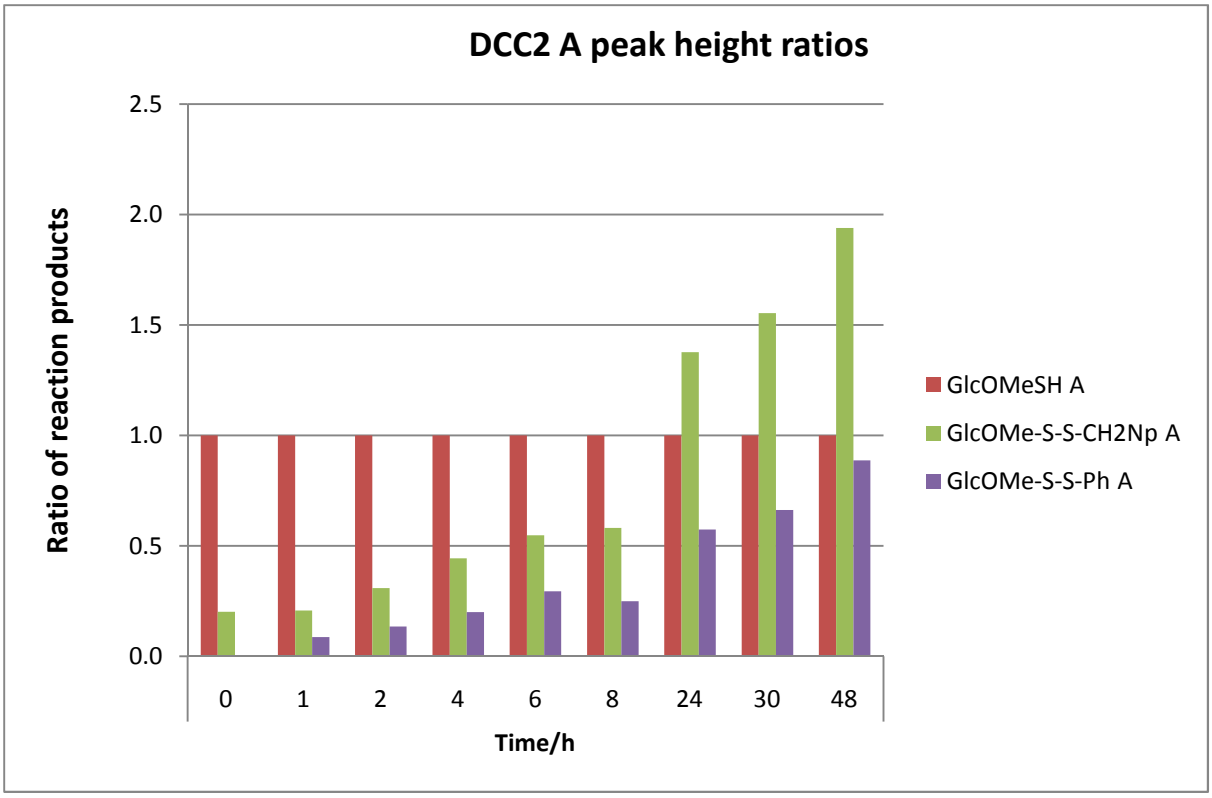


**Figure 4.3.1.3b: DCC2 experiment A results**

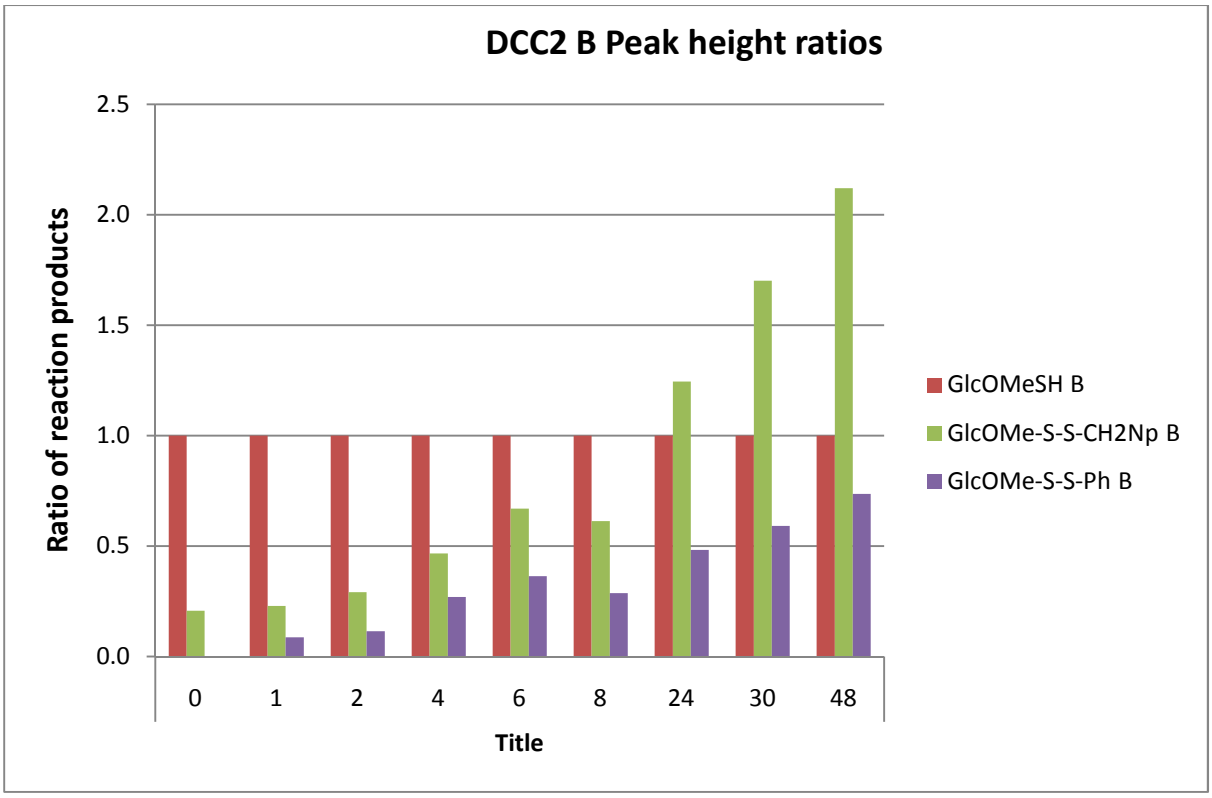


**Figure 4.3.1.3c: DCC2 experiment B results**

The ratio of components GlcOMeSH to GlcOMe-S-S-$CH_2$Np at 48 hours is 1:2, which is consistent with our results from the initial screening reaction (1:2.5, see Table 4.3.1.2f, reaction ix). A small amount of GlcOMe-S-S-$CH_2$Np can be seen at the very start of the reaction, indicating that the disulfide exchange reaction begins immediately upon adding the activating solution. The amount of the target disulfide then increased steadily until the reaction was stopped at 48 hours (the point at which the predicted optimum ratios of components had been reached in the screening reaction). No further characterisation was carried out on these two libraries.

The results from this larger scale combinatorial library confirmed that we had designed and selected suitable reaction conditions for the generation of our combinatorial library. However, before we investigated the formation of the larger library featuring all of the thio-naphthyl linkers we performed a test reaction of the small test library with the enzyme. At this stage we needed to test our plan to remove the organic solvent from the library, take up the residue in a pH 5 solution and then add the enzyme.

### 4.3.2 Investigation into the use of the β-galactosidase from *B. circulans* with a test combinatorial library

Using the pooled combinatorial libraries from experiments DCC1 and DCC2 we attempted a trans-glycosylation reaction using the β-galactosidase from *B. circulans* (Figure 4.3.2a).

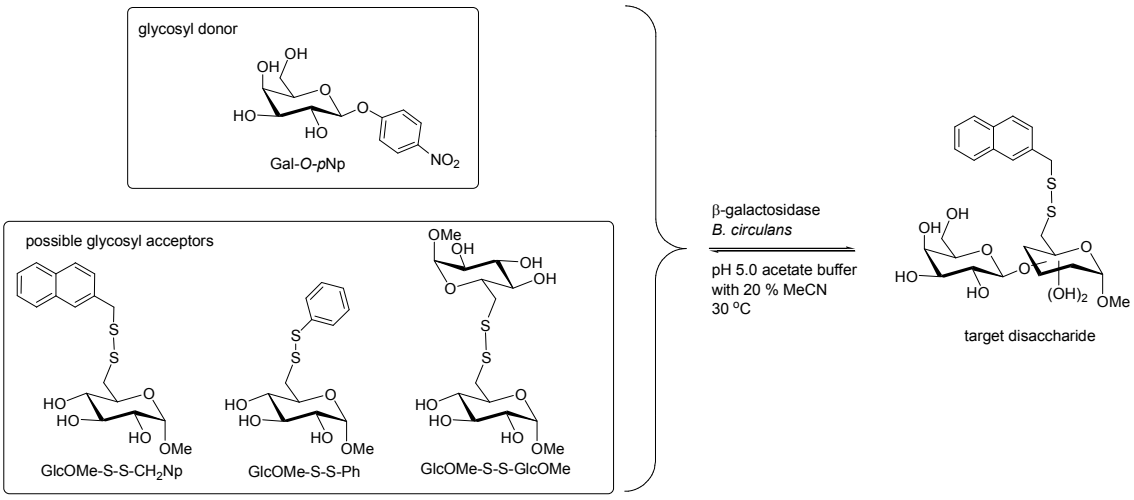


**Figure 4.3.2a: Scheme for the test reaction using the glycosyl acceptor disulfide library with the β-galactosidase from *B. circulans***

The free thiol-sugar **45** (initially present in the combinatorial library synthesis) may function as a glycosyl acceptor. However, the combinatorial libraries had been examined by mass spectrometry and no peaks corresponding to the thio-sugar **45** had been found. Any disulfides of the (2-naphthyl)methanethiol and thiophenol are not soluble in aqueous solution, and would not be expected to take any part in the enzyme reaction.

**DCC3**

The set of reaction conditions we had developed for the enzyme experiments (see Chapter 3) would now be applied to this test reaction, with a few slight differences, as shown in Table 4.3.2b.

| Conditions: | **enzyme experiments** | **enzyme/combinatorial library** |
|---|---|---|
| **reaction conc. (wrt acceptor)** | 0.4 M (20% MeCN) | 0.2 M (20% MeCN) |
| **acceptor:donor** | 7:1 | 7:1 |
| **pH** | pH 7 phosphate buffer | pH 5 acetate buffer |
| **temperature** | 30 °C | 30 °C |
| **units of enzyme** | 19.6/mmol acceptor | 19.6/mmol acceptor |

**Table 4.3.2b: Differences between the original enzyme experiment conditions and those we would use for the combinatorial library**

We would halve the concentration for this enzyme reaction to aid the solubility of the library components. In the previous enzyme experiment a reaction concentration of 0.4 M was found to be optimal although the naphthyl-functionalised sugars were only partially soluble at that concentration. We found that that the disulfide sugars had a lower solubility in the buffer solution, hence decreasing the concentration to 0.2 M. This concentration has been shown to still allow the β-galactosidase mediated trans-glycosylation to occur (Chapter 3).

As previously discussed, the enzyme reaction will done at pH 5 rather than pH 7. This is so that no disulfide exchange can take place during the enzyme reaction.

The rest of the reaction conditions would be the same as used previously for the enzyme experiments.

#### 4.3.2.1 Examination of the results from mass spectrometry

Owing to the very small aliquot volume taken from the reaction solution (5 μL in this case compared to 40 and 24 μL in the two previous experiments respectively) it is not reasonable to attempt to quantify any peak height ratios seen in the mass spectra. In this instance we simply look for the presence of peaks that correspond to any possible reaction constituents.

Table 4.3.2.1a shows the peaks found in the mass spectra at various points in the experiment, Figure 4.3.2.1b shows the structures of the compounds found in the mass spectra.

| Reaction time/h | Peaks m/z | Components | RMM |
|---|---|---|---|
| 0 | Error with sample – no peaks recorded | | |
| 1 | 341 | GlcOMe-S-S-Ph | 318 |
| | 405<br>409 | GlcOMe-S-S-$CH_2$Np | 382 |
| | 441 | GlcOMe-S-S-GlcOMe | 418 |
| | 486 | Gal-Gal-*O*-*p*Np | 463 |
| 2 | 405<br>409 | GlcOMe-S-S-$CH_2$Np | 382 |
| | 441 | GlcOMe-S-S-GlcOMe | 418 |
| | 486 | Gal-Gal-*O*-*p*Np | 463 |
| | **567** | **Gal-GlcOMe-S-S-$CH_2$Np** | **526** |
| 3 | 341 | GlcOMe-S-S-Ph | 318 |
| | 405<br>409 | GlcOMe-S-S-$CH_2$Np | 382 |
| | 441 | GlcOMe-S-S-GlcOMe | 418 |
| | 486 | Gal-Gal-*O*-*p*Np | 463 |
| | **567** | **Gal-GlcOMe-S-S-$CH_2$Np** | **526** |
| 4 | 341 | GlcOMe-S-S-Ph | 318 |
| | 405<br>409 | GlcOMe-S-S-$CH_2$Np | 382 |
| | 441 | GlcOMe-S-S-GlcOMe | 418 |
| | 486 | Gal-Gal-*O*-*p*Np | 463 |
| | 503 | Gal-GlcOMe-S-S-Ph | 462 |
| | **567** | **Gal-GlcOMe-S-S-$CH_2$Np** | **526** |
| 5 | 441 | GlcOMe-S-S-GlcOMe | 418 |
| | 486 | Gal-Gal-*O*-*p*Np | 463 |
| | **567** | **Gal-GlcOMe-S-S-$CH_2$Np** | **526** |

| | | | |
|---|---|---|---|
| 6 | 405<br>409 | GlcOMe-S-S-$CH_2$Np | 382 |
| | 441 | GlcOMe-S-S-GlcOMe | 418 |
| | 486 | Gal-Gal-*O*-*p*Np | 463 |
| | 503 | Gal-GlcOMe-S-S-Ph | 462 |
| | **567** | **Gal-GlcOMe-S-S-$CH_2$Np** | **526** |
| 24 | 405<br>409 | GlcOMe-S-S-$CH_2$Np | 382 |
| | 441 | GlcOMe-S-S-GlcOMe | 418 |
| | 486 | Gal-Gal-*O*-*p*Np | 463 |
| | 503 | Gal-GlcOMe-S-S-Ph | 462 |
| | **567** | **Gal-GlcOMe-S-S-$CH_2$Np** | **526** |

**Table 4.3.2.1a: peaks found in the mass spectra during the enzyme experiment DCC3**

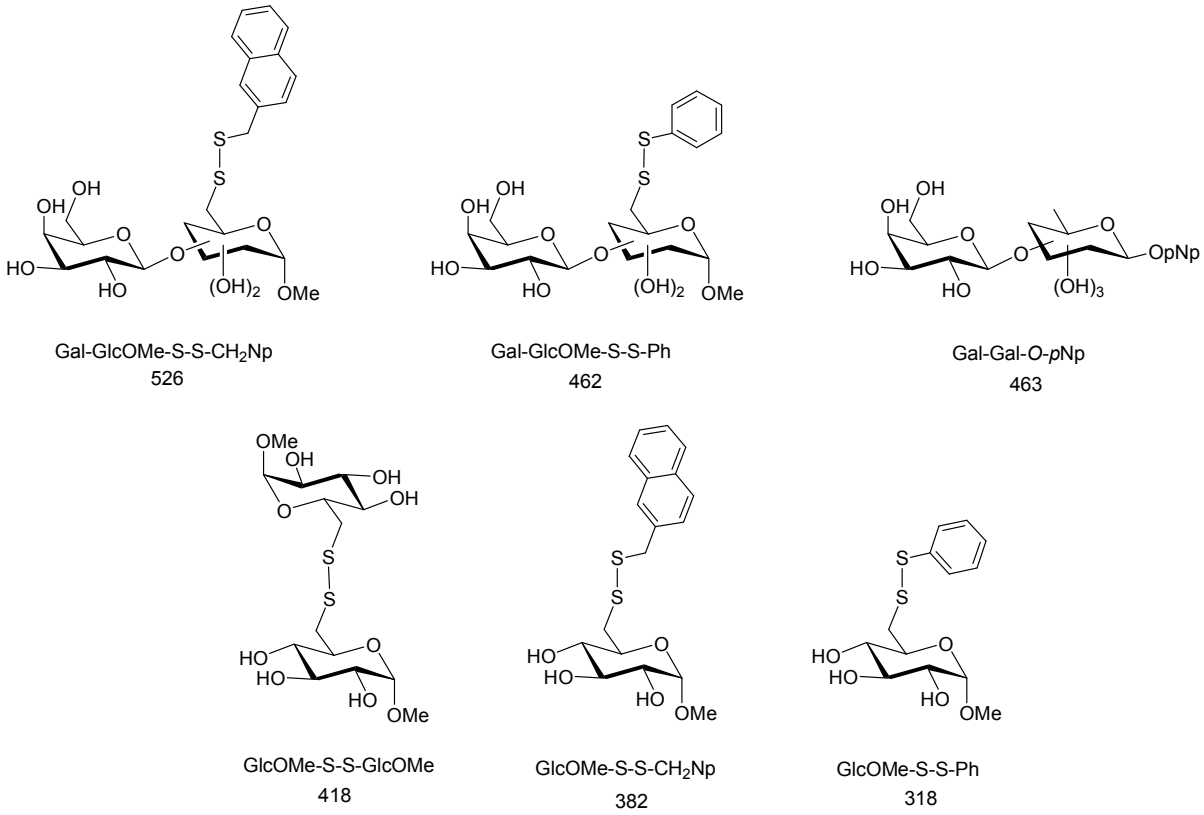


**Figure 4.3.2.1b: structures and RMM of the compounds found in the mass spectra for DCC3.**

We were extremely pleased to see the appearance of a peak corresponding to a disaccharide of galactose and GlcOMe-S-S-$CH_2$Np. At 2 hours, the peak at 567 m/z corresponded to Gal-GlcOMe-S-S-$CH_2$Np (526 + 41); this same peak was then seen in each aliquot after 2 hours. At 4 hours, a peak at 503 m/z corresponding to Gal-GlcOMe-S-S-Ph (462 + 41) was also observed.

#### 4.3.2.2 Examination of the results from HPLC

Each of the aliquots submitted for mass spectrometry was also submitted for HPLC. From the initial aliquot at 0 hours, new peaks are seen as the reaction progresses.

In order to identify which peaks correspond to which reaction product it was necessary to submit the entire reaction mixture for preparative HPLC. Mass spectrometry was then performed on each of the peaks obtained from this separation, the results from this are summarised in Table 4.3.2.1c below:

| Retention time/min | m/z | Component |
|---|---|---|
| 14.0 | 603 | Gas-phase dimer Gal-*O*-*p*Np + 1 |
| 15.2 | 441 | GlcOMe-S-S-GlcOMe +23 (Na) |
| 16.4 | 486 | Gal-Gal-*O*-*p*Np +23 (Na) |
| **16.9** | **485** | **Gal-GlcOMe-S-S-Ph +23 (Na)** |
| **21.0-23.0** | **503** | **Gal-GlcOMe-S-S-Ph +41 (MeCN)** |
| | **665** | **Gal-Gal-GlcOMe-S-S-Ph +41 (MeCN)** |
| **23.8 – 25.** | **567** | **Gal-GlcOMe-S-S-$CH_2$Np +41 (MeCN)** |
| 28.7 | 405 | GlcOMe-S-S-$CH_2$Np +23 (Na) |

**Table 4.3.2.1c: Results from the HPLC analysis and separation of the products from experiment DCC3 – the desired disaccharides containing a naphthyl- (or phenyl-) functionalised sugar are highlighted.**

The highlighted section of the table shows the results of interest. The disaccharide Gal-GlcOMe-S-S-$CH_2$Np can be clearly seen between 23.8 and 25.0 minutes retention time. Interestingly, and unsurprisingly, the disaccharide of GlcOMe-S-S-Ph (Gal-GlcOMe-S-S-Ph) can also be seen, though it has a shorter retention time. A trisaccharide is also observed between 21-23 minutes Gal-Gal-GlcOMe-S-S-Ph.

#### 4.3.2.3 Summary from the first enzyme reaction using a test combinatorial library

We were extremely pleased that during the experiment we detected the presence of di- and tri-saccharides of the disulfide sugars from the combinatorial library. It is clear from our results that our treatment of the combinatorial library and the conditions used for the enzyme study that our method is suitable for determining if the β-galactosidase from *B. circulans* can process our disulfide sugars.

### 4.3.3 Formation of a combinatorial library of mixed glucose and naphthyl disulfides

Up to this point we had established a set of reaction conditions for the formation of the combinatorial library and had also successfully used the test library with the enzyme. The next task was to form the whole combinatorial library using the components shown in Figure 4.2b (also shown in Figure 4.3.3a below).

In terms of stoichiometry, all of the library components should be in employed in equimolar amounts in order to generate the maximum amount possible of sugar-naphthyl disulfides. This means that there must be a 1:1 ratio of the thio sugar to each of the thio naphthyl linkers giving an overall 4:1:1:1:1 stoichiometry (Figure 4.3.2a).

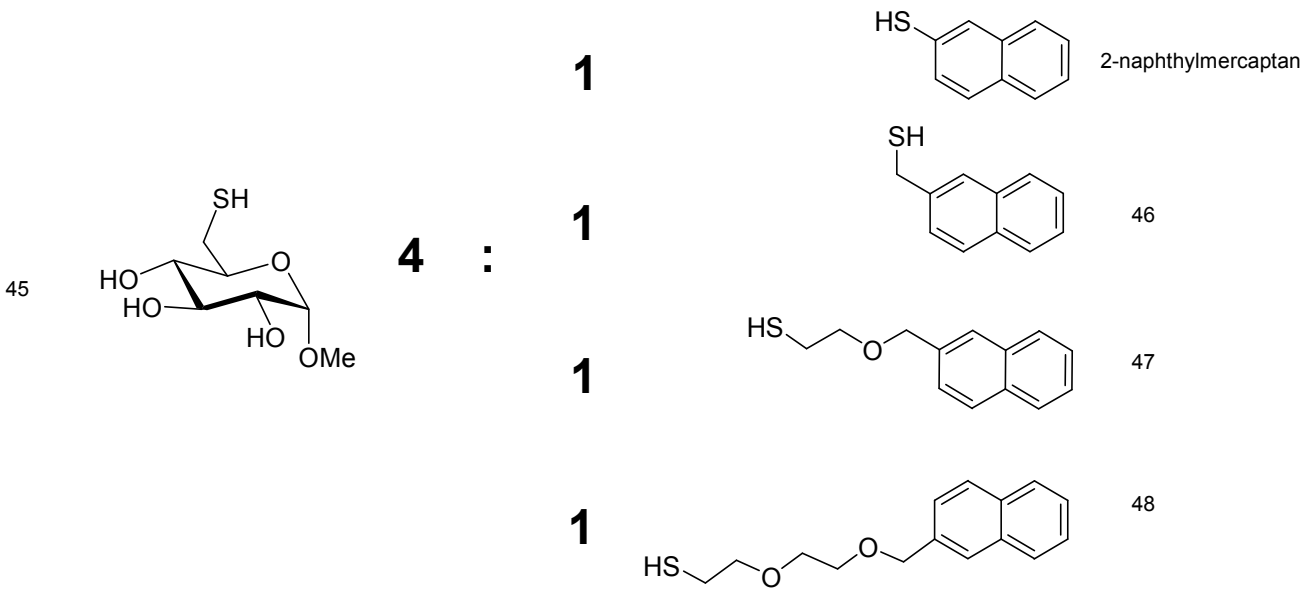


**Figure 4.3.3a Library components and ratios for the glycosyl acceptor dynamic combinatorial library**

We would expect the experiment to result in the formation of nineteen disulfides (16 mixed, 5 dimers) from the library components, all of the possible desired mixed disulfides (sugar-naphthyl disulfides) we would expect from this experiment are shown in Figure 4.3.3b.

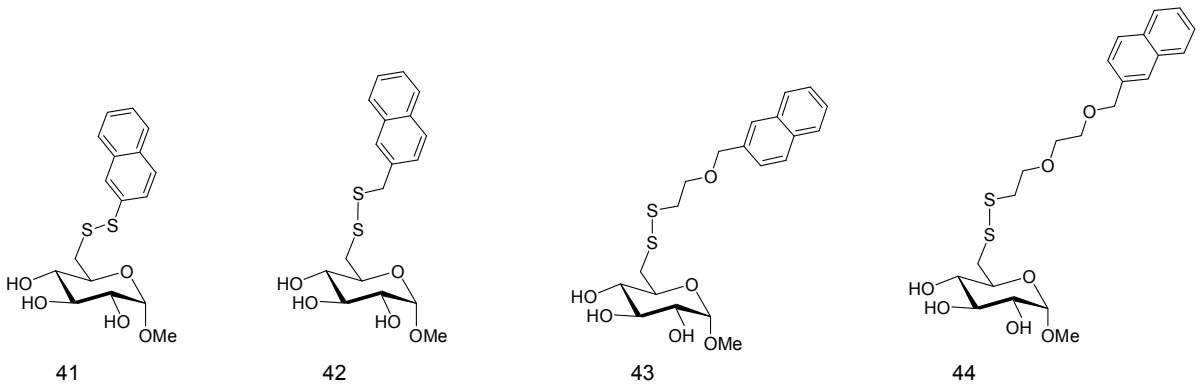


**Figure 4.3.3b: Glycosyl acceptor targets for the use in the dynamic combinatorial library**

In order to form the library we used the successful conditions from DCC1. Using a 12-reaction carousel 12 identical reactions were set up in order to test the reproducibility of the method. 5 mM standard solutions were made up of all five components of the library. One condition we did change was the omission of thiophenol as part of the activating solution. Since we were using 2-naphthalene thiol as a library component, we would expect this to have a similar $pK_a$ to thiophenol and thus initiate the disulfide exchange reaction in the same way. 500 μL aliquots were taken at 0, 2, 4, 6, 24, 48, 72, 96 hours. There was no discernible change in the mass spectra of the libraries from 72 to 96 hours, but to be sure that equilibrium had been reached a final set of aliquots was taken at 11 days. The mass spectra from these final aliquots showed no discernible change from those taken at 96 hours so the reaction was then stopped. Acetic acid was added to each reaction solution to freeze the libraries in that equilibrated state.

#### 4.3.3.2 Analysis of the data from the formation of the combinatorial library of mixed glucose and naphthyl disulfides

Table 4.3.3.1a lists the peaks found by mass spectrometry across all twelve library forming reactions. Mixed disulfides and dimers due to naphthyl thiols are not noted here unless they are also possible candidates for peaks. At this stage we are only interested in evidence of the formation of the sugar-naphthyl disulfides. Mass spectrometry was done on all of the separate components of the library and peaks found in those spectra were useful when considering how to assign peaks in the mass spectra recorded for the formation of the library.

| Reaction time/h | Peaks m/z | Components | RMM |
|---|---|---|---|
| 0 | 441 | GlcOMe-S-S-GlcOMe + Na | 418 |
| 1 | 441 | GlcOMe-S-S-GlcOMe + Na | 418 |
| 2 | 405 | **GlcOMe-S-S-$CH_2$Np + Na** | 382 |
| | 441 | GlcOMe-S-S-GlcOMe + Na | 418 |
| 4 | 405 | **GlcOMe-S-S-$CH_2$Np + Na** | 382 |
| | 441 | GlcOMe-S-S-GlcOMe + Na | 418 |
| 6 | 405 | **GlcOMe-S-S-$CH_2$Np + Na** | 382 |
| | 441 | GlcOMe-S-S-GlcOMe + Na | 418 |
| 24 | 405 | **GlcOMe-S-S-$CH_2$Np + Na** | 382 |
| | 441 | GlcOMe-S-S-GlcOMe + Na | 418 |
| | 457 | Np$CH_2$EG-S-S-EG$CH_2$Np + Na | 434 |
| | | Np$CH_2$-S-S-DEG$CH_2$Np + Na | 434 |
| | 493 | **GlcOMe-S-S-DEG$CH_2$Np + Na** | 470 |
| | 501 | Np$CH_2$EG-S-S-DEG$CH_2$Np + Na | 478 |
| 48 | 405 | **GlcOMe-S-S-$CH_2$Np + Na** | 382 |
| | 441 | GlcOMe-S-S-GlcOMe + Na | 418 |
| | 449 | **GlcOMe-S-S-EG$CH_2$Np + Na** | 426 |
| | 457 | Np$CH_2$EG-S-S-EG$CH_2$Np + Na | 434 |
| | | Np$CH_2$-S-S-DEG$CH_2$Np + Na | 434 |
| | 493 | **GlcOMe-S-S-DEG$CH_2$Np + Na** | 470 |
| | 501 | Np$CH_2$EG-S-S-DEG$CH_2$Np +Na | 478 |
| 72 | 405 | **GlcOMe-S-S-$CH_2$Np + Na** | 382 |
| | 441 | GlcOMe-S-S-GlcOMe + Na | 418 |
| | 449 | **GlcOMe-S-S-EG$CH_2$Np + Na** | 426 |
| | 457 | Np$CH_2$EG-S-S-EG$CH_2$Np + Na | 434 |
| | | Np$CH_2$-S-S-DEG$CH_2$Np + Na | 434 |
| | 493 | **GlcOMe-S-S-DEG$CH_2$Np + Na** | 470 |

| | | | |
|---|---|---|---|
| | 501 | $NpCH_2EG$-S-S-$DEGCH_2Np$ +Na | 478 |
| 96 | 405 | **GlcOMe-S-S-$CH_2Np$ + Na** | 382 |
| | 441 | GlcOMe-S-S-GlcOMe + Na | 418 |
| | 449 | **GlcOMe-S-S-$EGCH_2Np$ + Na** | 426 |
| | 457 | $NpCH_2EG$-S-S-$EGCH_2Np$ + Na | 434 |
| | | $NpCH_2$-S-S-$DEGCH_2Np$ + Na | 434 |
| | 493 | **GlcOMe-S-S-$DEGCH_2Np$ + Na** | 470 |
| | 501 | $NpCH_2EG$-S-S-$DEGCH_2Np$ +Na | 478 |
| 11 days | 405 | **GlcOMe-S-S-$CH_2Np$ + Na** | 382 |
| | 441 | GlcOMe-S-S-GlcOMe + Na | 418 |
| | 449 | **GlcOMe-S-S-$EGCH_2Np$ + Na** | 426 |
| | 457 | $NpCH_2EG$-S-S-$EGCH_2Np$ + Na | 434 |
| | | $NpCH_2$-S-S-$DEGCH_2Np$ + Na | 434 |
| | 493 | **GlcOMe-S-S-$DEGCH_2Np$ + Na** | 470 |
| | 501 | $NpCH_2EG$-S-S-$DEGCH_2Np$ +Na | 478 |

**Table 4.3.3.1a: results from analysis of the mass spectra carried out on all sample taken from experiment DCC4**

By examining the peaks found in the mass spectra of all twelve reactions over the whole time of the experiment we can say that we have formed a number of mixed sugar-naphthyl disulfides. There are points to consider when evaluating these results however. It was only at 24 hours that we began to see peaks at 493 m/z (corresponding to GlcOMe-S-S-$DEGCH_2Np$ + Na) without having to examine the peaks near to the baseline of the spectrum. The new peaks emerging as time progressed were all initially identified by expansion of the baseline of the spectra. Also, the peak at 405 m/z is present in the mass spectrum of **48** as an impurity (MS of this compound alone prior to use in the library contained this peak). It is therefore unlikely that any material at this m/z prior to 24 hours – when other sugar-naphthyl disulfides began to show – is due to GlcOMe-S-S-$CH_2Np$ + Na.

Another point to note is that the results from the mass spectra indicate that we appear to have made just three of our target four sugar-naphthyl disulfides. There is no evidence that the disulfide from thio-sugar **45** and 2-naphthylmercaptan was formed, since we expected this to react in a similar way to the thiophenol activator we had used in previous experiments we were surprised at the absence of this disulfide. In our first two successful combinatorial library syntheses the peaks due to the sugar-naphthyl and sugar-phenyl disulfides were very prominent, eventually becoming much higher than the peaks due to the starting sugar (see Section 4.3.1.1). In this larger library the peaks in the mass spectra due to our target sugars are relatively small in comparison to that due to the thio-sugar starting material.

This means that we cannot say anything about the quantity of target disulfides produced or estimate a ratio. In order to confirm that we had produced the three target sugars found in the mass spectrometry results we pooled the reaction solutions and submitted them for HPLC analysis. Using the same HPLC conditions as in CCEXP7X we targeted the section at 25 – 30 minutes retention time which had been shown to correspond only to UV active sugar-naphthyl disulfides (see Section 4.3.1.3). The peaks in this region were isolated as a group and then the sample submitted for mass spectrometry. To our delight the mass spectrum showed three peaks, corresponding to the three peaks in the HPLC trace (see Figures 4.3.3.1b, c, d) at 405, 449 and 493 m/z.

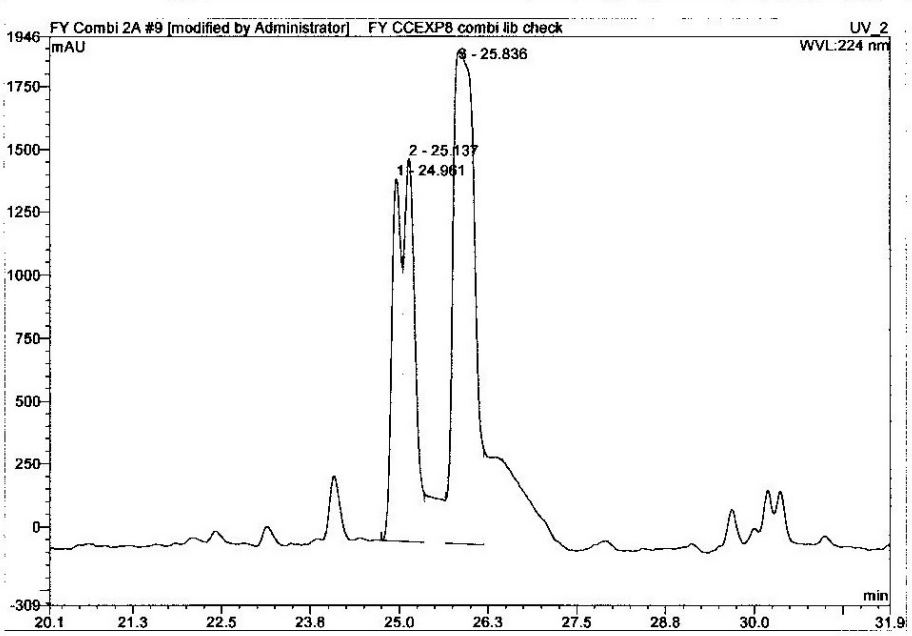


| No. | Ret.Time min | Peak Name | Height mAU | Area mAU*min | Rel.Area % | Amount | Type |
|---|---|---|---|---|---|---|---|
| 1 | 24.96 | n.a. | 1437.643 | 229.281 | 19.49 | n.a. | BM * |
| 2 | 25.14 | n.a. | 1520.075 | 266.907 | 22.69 | n.a. | M * |
| 3 | 25.84 | n.a. | 1954.457 | 679.922 | 57.81 | n.a. | M * |
| Total: | | | 4912.175 | 1176.110 | 100.00 | 0.000 | |

**Figure 4.3.3.1b entire HPLC run of partially purified combinatorial library 25-30 minutes**

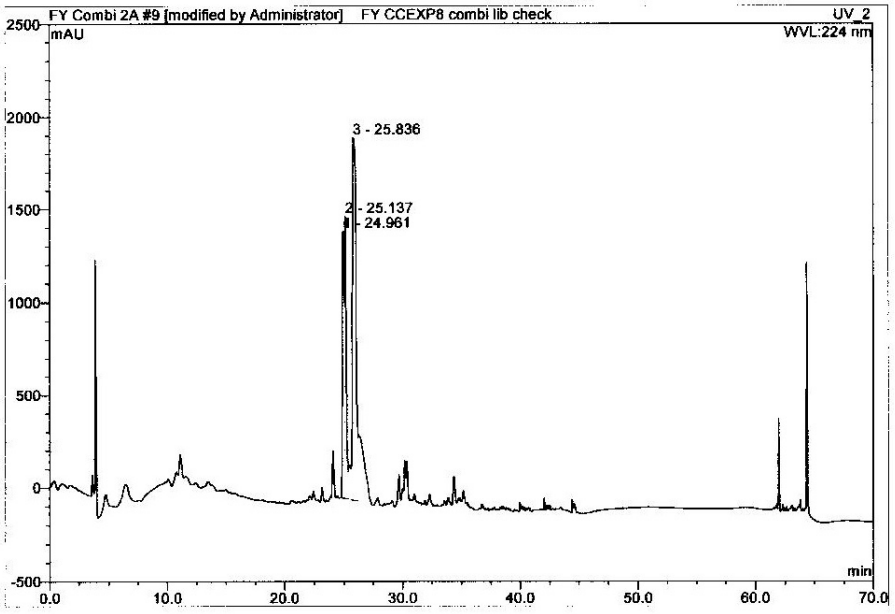


| No. | Ret.Time min | Peak Name | Height mAU | Area mAU*min | Rel.Area % | Amount | Type |
|---|---|---|---|---|---|---|---|
| 1 | 24.96 | n.a. | 1437.643 | 229.281 | 19.49 | n.a. | BM * |
| 2 | 25.14 | n.a. | 1520.075 | 266.907 | 22.69 | n.a. | M * |
| 3 | 25.84 | n.a. | 1954.457 | 679.922 | 57.81 | n.a. | M * |
| Total: | | | 4912.175 | 1176.110 | 100.00 | 0.000 | |

**Figure 4.3.3.1c: HPLC expansion of area of interest – there are three distinct peaks at $t_r$ = 24.96, 25.14 and 25.84 minutes**

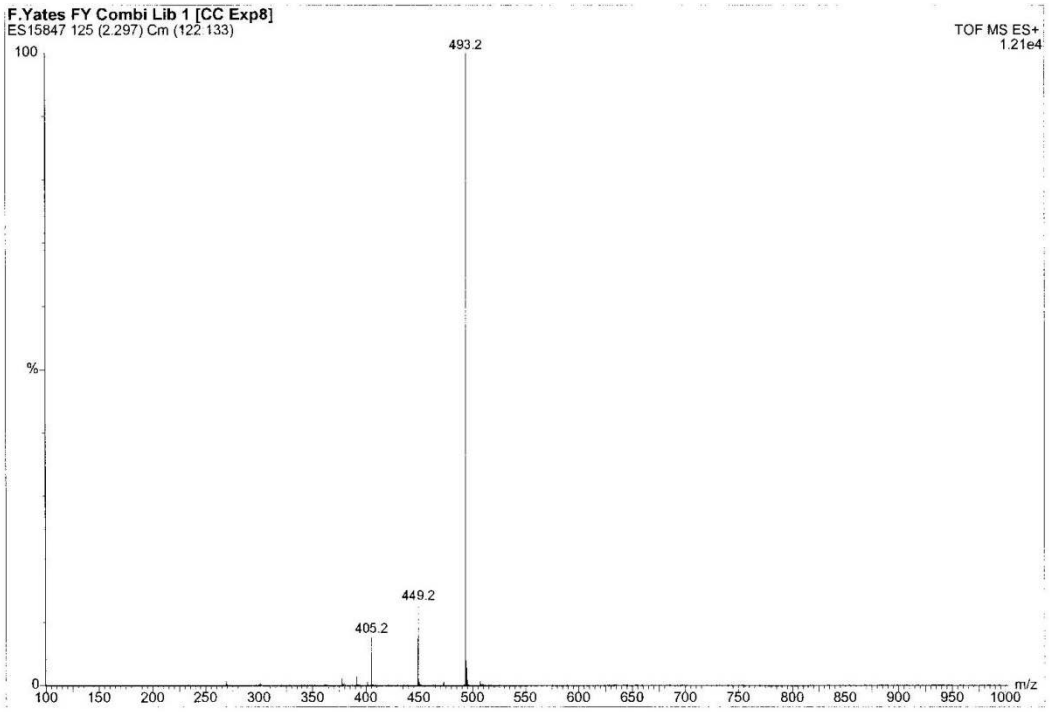


**Figure 4.3.3.1d: Mass spectrum of the HPLC run in Figure 4.3.3.1b; the three peaks shown correspond to the three desired naphthyl disulfides 42, 43 and 44**

In this first attempt at making a larger, mixed sugar-naphthyl disulfide library the following disulfides were generated: GlcOMe-S-S-$CH_2$Np (**42**), GlcOMe-S-S-EG$CH_2$Np (**43**) and GlcOMe-S-S-DEG$CH_2$Np (**44**) (Figure 4.3.3.1e).

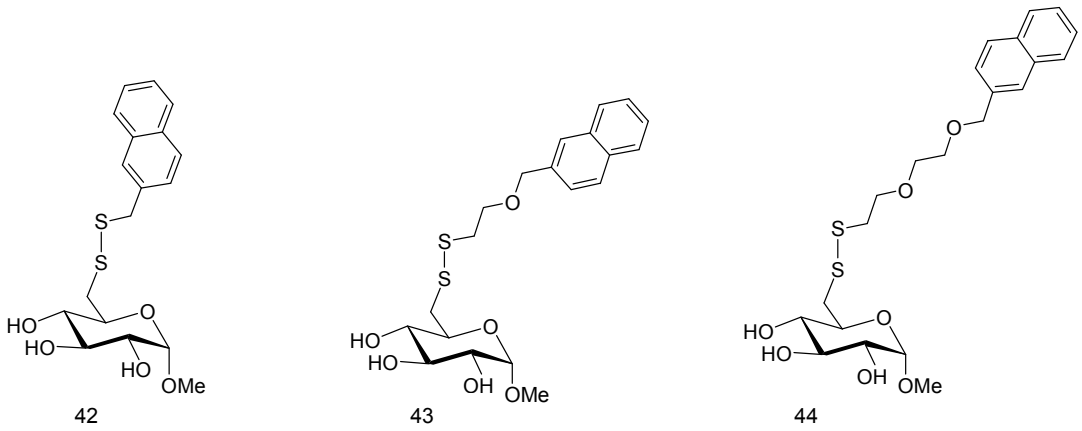


**Figure 4.3.3.1e: methyl glucoside-naphthyl disulfides formed**

The results from our first attempt to form a larger combinatorial library indicate that we have had a degree of success in forming a library of sugar-naphthyl disulfides. However, much

more development is needed into the method to form this library, and those planned using a galactoside rather than a glucoside,

### 4.3.4 Summary of work on combinatorial synthesis of a library of substrates for enzyme testing

We have investigated the possibility of using combinatorial synthesis to generate suitable substrates for our work to develop a new type of sensor for monitoring β-galactosidase action.

We have successfully synthesised methyl-(6-thio-6-deoxy)-α-D-glucopyranoside **(45)** and three thiol-functionalised naphthyl-linker molecules **46**, **47** and **48**. **45** and **46** were used to develop a suitable method for forming a novel DCL for use with the β-galactosidase from *B. circulans*. The resultant DCL was then used in a β-galactosidase-catalysed transglycosylation reaction which resulted in the successful synthesis of disaccharides containing naphthyl- and phenyl moieties linked via a disulfide bond at C6 of methyl-α-D-glucose. This confirmed to us that our idea of using combinatorial synthesis to synthesise substrates suitable for use with the β-galactosidase from *B. circulans* was a viable method for this purpose.

Following the success of the enzyme reaction, we then began work on forming the larger DCL that would be used in a β-galactosidase-catalysed trans-glycosylation reaction with thio-sugar **45**. We succeeded in forming a DCL with the components in Figure 4.2.3a but work remained to optimise the formation of the larger DCL before using this with the enzyme.

### 4.3.5 Further Work

The first step in the completion of this work would be to develop a reliable method for forming a large DCL of substrates to test with the enzyme.

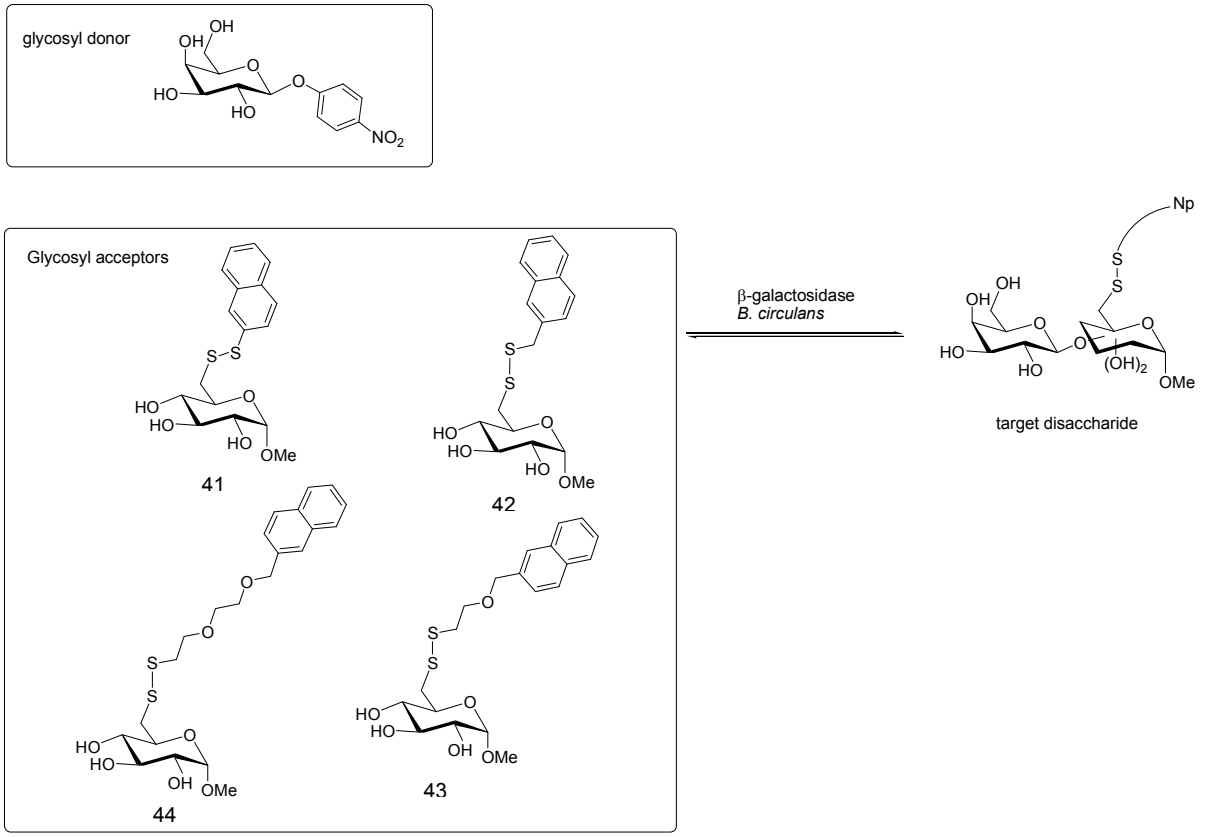


**Figure 4.3.5a: DCC enzyme experiment featuring the four sugar-naphthyl disulfide targets with GalO*p*NP as the glycosyl donor**

Initially the formation of the desired DCL shown in Figure 4.3.5a would need to be optimised and reproducible. Once this library had been successfully developed, work would then move on to forming a DCL based on galactose. As stated at the beginning of this chapter, we have already shown that the glycosyl acceptor (methyl α-D-glucose) when functionalised with a naphthyl group at C6 can be processed by the β-galactosidase from *B. circulans*. Our next objective would be to investigate whether the glycosyl donor (*p*-nitrophenyl galactose) would be processed by the enzyme when similarly functionalised.

Future work for this chapter of the project is therefore to synthesise *p*-nitrophenyl (6-thio-6-deoxy)-β-D-galactopyranoside and use this in the formation of the DCL shown in Figure 4.3.5b below.

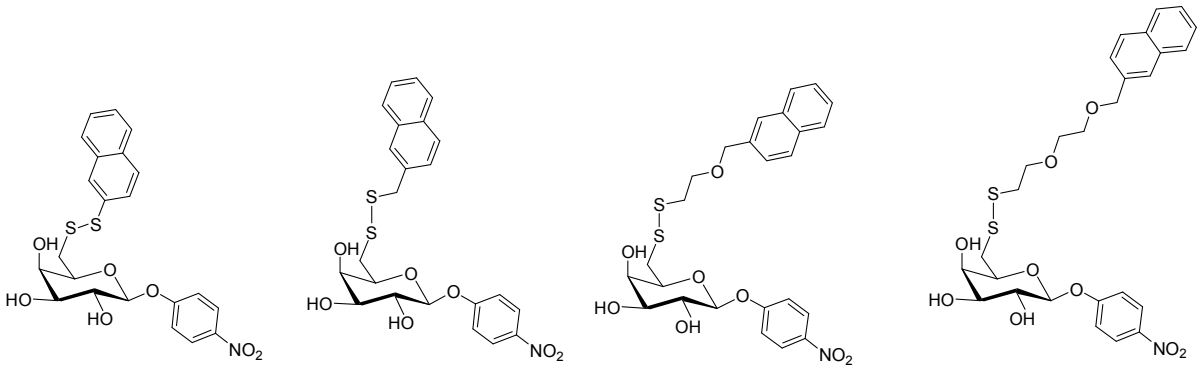

**Figure 4.3.5b: Planned glycosyl donor disulfides**

Once this DCL has been successfully generated, our work would conclude with the investigation into the use of this DCL of glycosyl donors in a β-galactosidase-catalysed trans-glycosylation reaction (Figure 4.3.5c).

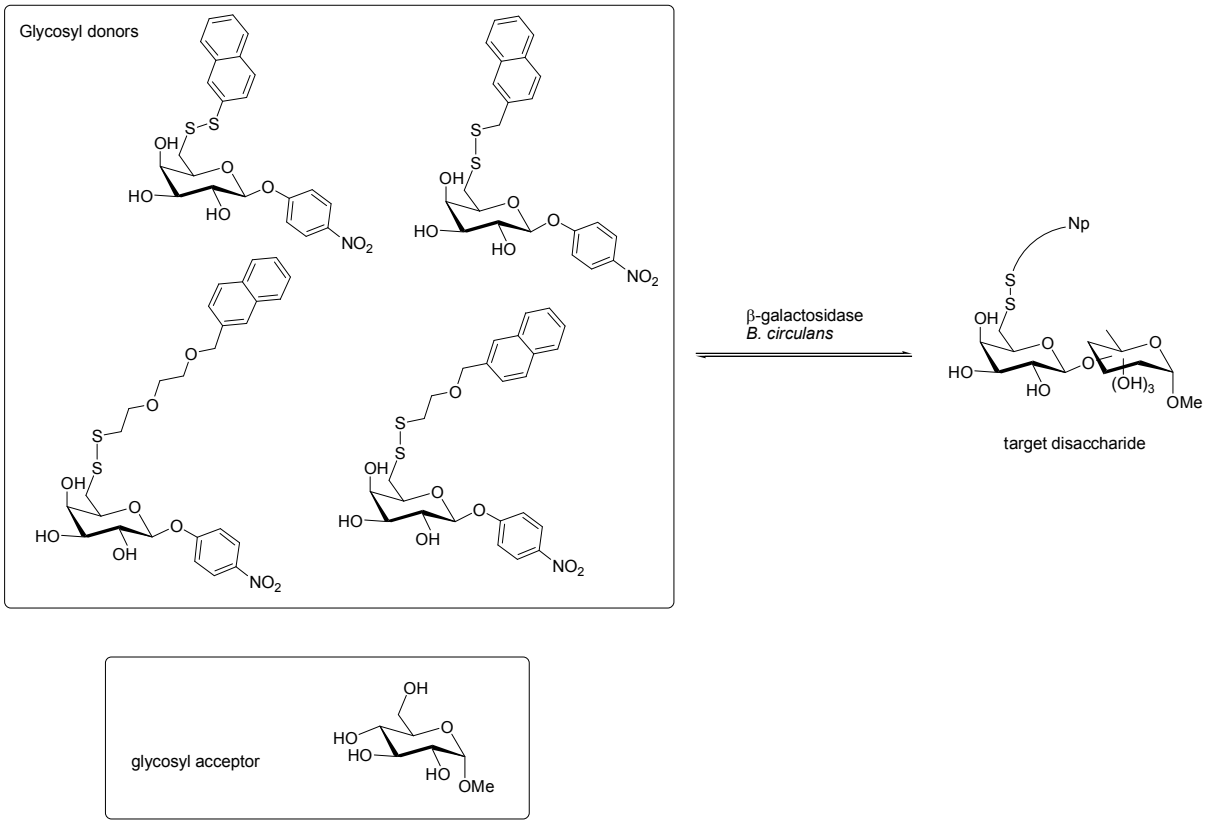


**Figure 4.3.5c: Planned enzyme experiment using the library of glycosyl donor disulfides with GlcOMe as the glycosyl acceptor**

### 4.3.5.1 Planned synthesis of *p*-nitrophenol (6-thio-6-deoxy)-β-D-galactopyranoside

The planned synthesis of *p*-nitrophenyl (6-thio-6-deoxy)-β-D-galactopyranoside is broadly the same as that for the corresponding methyl glucoside. The retrosynthesis is shown in Figure 4.3.5.1a.

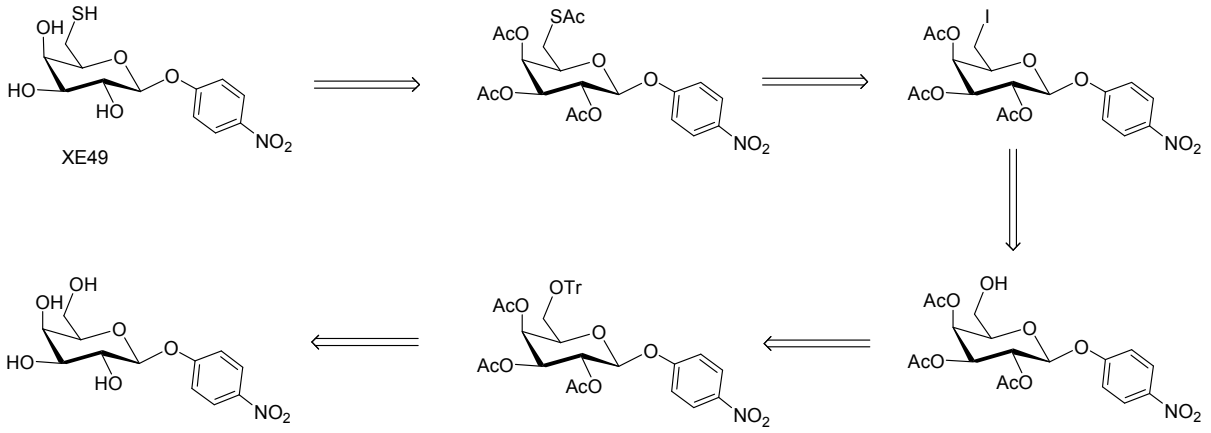


**Figure 4.3.5.1a: retrosynthesis for *p*-nitrophenyl (6-thio-6-deoxy)-β-D-galactopyranoside**

The first step would be to protect the alcohol at C6 with a trityl group and then to acetylate the remaining alcohols. When we used trityl protection previously the orthogonal protecting group was PMB, but this would not be suitable in this case as a paper by Williams discussed the installation of iodide at the primary alcohol of methyl 2,3,4-tri-*O*-benzyl-β-D-galactoside. In a competing reaction the 3,6-anhydro sugar was also prepared as shown in Figure 4.3.5.1b.[106]

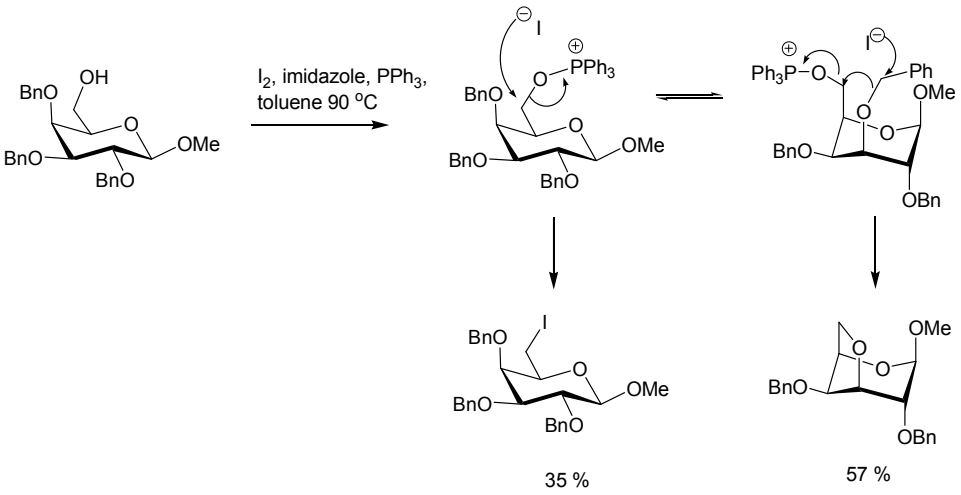


**Figure 4.3.5.1b: The formation of a 3,6-anhydro sugar when attempting an iodination on a benzyl-protected 6-hydroxy galactoside**

Given this information we chose to avoid the use of any sort of benzylic protecting group. We planned to use acetates instead as the trityl group can be selectively removed using TMSI in the presence of acetates.[107]

After the iodide has been installed we would then proceed as in the synthesis of **45** by using thiourea to displace the iodide and form the thiol to be used in the combinatorial experiments.

# 5. Experimental Section

## Instrumentation

Elemental analyses were recorded on a Carlo Erba EA1110 simultaneous CHNS analyser. Infrared spectra were recorded as thin films, or as a Nujol mull between sodium chloride discs, on a Perkin Elmer 1600 FTIR spectrometer. The intensity of each band is described as s (strong), m (medium) or w (weak), and with the prefix v (very) and suffix br (broad) where appropriate. $^{1}$H- and $^{13}$C-NMR spectra were recorded on a Bruker AC300 (at 300.13 MHz and 75.47 MHz respectively), a Bruker AV300 (at 300.13 MHz and 75.48 MHz respectively), a Bruker AMX400 (at 400.08 MHz and 100.61 MHz) or a Bruker DRX500 (at 500.13 MHz and 125.77 MHz). All 75 MHz $^{13}$C spectra were recorded using the PENDANT pulse sequence. Chemical shifts are reported as $\delta$ values (ppm). Individual spectra were referenced relative to residual solvent peaks according to the values quoted by Gottlieb and Nudelman.[108] The multiplicity of signals in $^{1}$H NMR spectra is expressed as follows: s = singlet, br s = broad singlet, d = doublet, t = triplet, q = quartet, m = multiplet *etc*... Coupling constants *J* are reported in Hz. The term "stack" is used to describe a region where resonances arising from non-equivalent nuclei are coincident, and multiplet, m, is used to describe a resonances arising from a single nucleus (or equivalent nuclei) where coupling constants cannot be readily assigned. In analysing AB systems, where the resonance pattern forms two well separated groups, each of two lines, these are separately reported as "A of AB" or "B of AB", along with $J_{A\text{-}B}$. Connectivities were deduced from COSY90, HSQC and HMBC experiments. Mass spectra were recorded on a Micromass LCT spectrometer utilising electrospray ionisation (and a MeOH mobile phase). HRMS were recorded on a Micromass LCT spectrometer using a lock mass incorporated in the mobile phase. EI mass spectra were recorded on either a VG ProSpec or VG Zabspec instrument at 70 eV. High resolution EI spectra were measured using perfluorokerosene (PFK) as an internal calibrant. Mass spectrometric monitoring of enzyme and combinatorial reactions was carried out on a

Waters/Micromass ZMD electrospray mass spectrometer. All mass spectral data are reported as (*m/z* (%)). Optical rotations were measured in $H_2O$, $CHCl_3$ or MeOH solution using an Optical Activity PolAAr2001 automatic polarimeter. Unless otherwise stated, the cell path length used was 0.5 dm and concentrations used are expressed in grammes of solute per 100 mL. Optical rotation calculated using: $[\alpha]_D = 100\alpha/(l \times c)$ where $\alpha$ is the measured rotation, l is the path length in decimetres and c is the concentration in g/100 mL. $[\alpha]_D$ Values are reported in units of $10^{-1}$ deg $cm^2$ $g^{-1}$. UV absorption spectra were recorded on a Perkin-Elmer Lambda 17 UV-vis spectrometer, using 1 cm path length cuvettes using HPLC grade solvents. Data fitting was carried out using Microsoft Excel 2007. Melting points were determined in open glass capillaries using a Stuart Scientific SMP1 apparatus and are uncorrected.

HPLC was performed on Dionex Summit HPLC systems using helium degassed HPLC grade solvents. Data were collected, recorded and processed using the Dionex Chromeleon 6.11 software package.

*Analytical HPLC:*

Pump: Summit P580 Quaternary Low Pressure Gradient Pump with built in vacuum degasser.

Detector: Summit UVD 170s UV/Vis Multi-Channel Detector with analytical flow cell.

Column: Phenomenex Luna 10μ C18 (250 mm x 4.6 mm).

*Preparative HPLC:*

Pump: Summit P580P High Pressure Binary Gradient Pump with built in vacuum degasser.

Detector: Summit UVD 170s UV/Vis Multi-Channel Detector with preparative flow cell.

Column: Phenomenex Luna 10μ C18 (250 mm x 21.2 mm) with Phenomenex Luna 10μ C18 (60 mm x 21.1 mm) guard.

*Analytical carbohydrate and combinatorial HPLC was carried out on a Dionex DX500 HPLC system with an AS3500 Autosampler:*

Pump: GP40 Gradient Pump with GM4 Gradient Mixer with built in vacuum degasser.

Detector: AD20 Absorbance Detector and ED40 Electrochemical Detector

Column: Analytical Phenomenex Luna 10u C18(2) 100A (250 x 4.6mm)

Liquid phase: 16 mM NaOH solution at 1 mL/min

**Chemicals and Reagents**

Tetrahydrofuran (THF) were distilled from sodium benzophenone ketyl. $CH_2Cl_2$ was distilled from $CaH_2$. MeOH was distilled under $N_2$ from Mg turnings/$I_2$ and stored over activated 4 Å molecular sieves. Anhydrous pyridine and 'Extra Dry' DMF were purchased from Acros Organics (Fisher Scientific). Other chemicals were used as purchased, unless otherwise stated. All aqueous solutions are saturated, unless otherwise stated.

The buffer solutions used in the enzymatic reactions were 50 mM pH 5.0 sodium acetate buffer and 50 mM pH 7.0 sodium phosphate buffers.

Analytical thin layer chromatography (TLC) was performed on Merck 60 Å $F_{254}$ pre-coated glass-backed plates and visualised by UV (254 nm) and using ammonium molybdate solution. Flash column chromatography was carried out using FluoroChem 60 (40-60 μm mesh) silica gel.

'Biolacta' (β-galactosidase from *B. circulans*) was a gift from Daiwa Kasei K.K. (Japan) through Amano Enzyme Europe. http://www.amano-enzyme.co.jp/aee/index.html

## Reactions

All synthetic reactions were carried out under a $N_2$ atmosphere in flame-dried glassware, and at rt, unless otherwise stated. Volumes under 1 mL were measured and dispensed with Hamilton gastight syringes. Evaporation and concentration under reduced pressure was performed at 50-500 mbar. Residual solvent was removed under high vacuum (1 mbar). For UV-vis experiments, and enzymatic and combinatorial reactions, all volumes were measured using Brand Transferpette® S Single Channel Pipettes (100 μL and 1000 μL). Enzymatic reactions were carried out in 2 mL and 10 mL reaction vessels as appropriate. Larger enzymatic reactions and combinatorial work were carried out using a 'Radleys Carousel 12 Classic' parallel reaction system.

Convention for Carbohydrate numbering

In this Experimental Section, all characterisation of monosaccharides will be described using the following numbering convention unless otherwise stated.

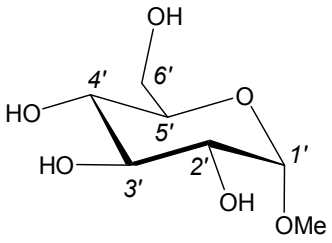

## 5.1 General Experimental Procedures

**General procedure A: acetylation of alcohols and thiols[53]**

$Ac_2O$ (2 equiv. per hydroxyl/thiol group) was added to a stirred solution of the alcohol or thiol in pyridine (3.0 M reaction concentration). Full conversion was usually complete within 12 h. The reaction mixture was then concentrated under reduced pressure and the residue purified by column chromatography.

**General procedure B: deacetylation of acetates and thioacetates[53]**

NaOMe (1.6 equiv. per ester group) was added to a solution of the ester (1.0 equiv.) in MeOH (0.025 M reaction concentration). The reaction mixture was stirred overnight at rt and then acidified to pH 2 with Amberlite IR120 H+ resin. The resin was removed by filtration, and the filtrate concentrated under reduced pressure to yield the deprotected product, which required no further purification.

**General procedure C: bromination of alcohols[83]**

$CBr_4$ (1.5 equiv.) was added to a stirred solution of the alcohol (1.0 equiv.) in THF (0.1 M reaction concentration) at rt. After 15 min, $PPh_3$ (1.5 equiv.) was added and the reaction mixture was stirred until consumption of starting alcohol was evidenced by TLC. The reaction was then quenched with $H_2O$ (1 x volume of organic phase) and extracted with $CH_2Cl_2$ (2 x volume of organic phase). The combined organic fractions were washed with brine (1 x volume of organic phase), dried ($MgSO_4$) and concentrated under reduced pressure to provide a residue, which was purified by column chromatography.

**General procedure D: etherification of methyl (2,3,4-tris-*O*-*p*-methoxybenzyl)-6-hydroxy-D-glucopyranoside**

NaH (1.1 equiv. per OH group, 60 wt% dispersion in mineral oil) was added portionwise over 2 min to a stirred solution of methyl (2,3,4-tris-*O*-*p*-methoxylbenzyl)-D-glucopyranoside (1.0 equiv.) in DMF (0.5 M reaction concentration) at 0 °C. After 30 min, the bromide (3.0 equiv.) was added at 0 °C and the reaction mixture allowed to warm to rt over the course of 1 h. The reaction mixture was stirred at rt until no further progress was evidenced by TLC and then diluted with $CH_2Cl_2$ (20 x reaction volume). The reaction mixture was washed with $H_2O$ (twice with 15 x reaction volume) and brine (15 x reaction volume) and then dried ($MgSO_4$). Removal of the solvent under reduced pressure and purification of the residue by column chromatography provided the desired ether.

**General procedure E: deprotection of PMB ethers[74]**

CAN (1.9 equiv.) was added to a solution of the glycoside (1.0 equiv.) in acetone/$H_2O$ (9:1, 0.1 M reaction concentration) at 0 °C. Once the initial exotherm had ceased, more CAN (6.0 equiv.) in acetone/$H_2O$ (9:1, 0.05 M solution concentration) was added dropwise over 10 min. After stirring at rt overnight, the reaction mixture was poured into $NaHCO_3$ solution (4 x total reaction volume) and the mixture was extracted with EtOAc (10 x reaction volume). The combined organic phases were dried ($MgSO_4$) and concentrated under reduced pressure to provide the product, which was purified by column chromatography.

**General procedure F: conversion of bromides to thiols**

Thiourea (2.2 equiv.) was added to a solution of the bromide in EtOH (0.9 M reaction concentration). The reaction mixture was heated under reflux overnight and then cooled to rt. 40% aq. KOH solution (0.5 equiv.) was added and the mixture heated under gentle reflux. After 1 h, this solution was cooled, acidified to pH 1 with 10% aq. hydrochloric acid and then extracted 3 times with $Et_2O$ (2 x reaction volume). The organic extracts were dried over $MgSO_4$ and then concentrated under reduced pressure.

## 5.2 Synthesis

**Methyl D-glucopyranoside 10**

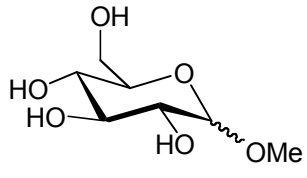


$C_7H_{14}O_6$
Exact Mass: 194.079
Mol. Wt.: 194.1825
C, 43.30; H, 7.27; O, 49.44

D-Glucose (5.00 g, 28.0 mmol) was added to a suspension of DOWEX 50WX8-400 resin (10.00 g) in MeOH (100 mL). The reaction mixture was stirred at 65 ºC for 24 h and then cooled to rt. The resin was removed by filtration and the filtrate concentrated under reduced pressure to yield methyl glucoside **10** as a white, crystalline solid, which was used in the next step without further purification (5.42 g, 99%, $\alpha$:$\beta$ 1.0:0.8). Data on the mixture: mp 101 ºC - 120 ºC; (Found: C, 43.18; H, 7.13. $C_7H_{14}O_6$ requires C, 43.30; H, 7.27%); $\nu_{max}$(Nujol mull)/cm$^{-1}$ 3242 br, m (O-H), 1593w, 1401w, 1304w, 1224w, 1187m, 1100m, 1030s, 992m, 898w, 843w, 722w; $\delta_H$(300 MHz, $D_2O$)* 3.21 – 3.91 (9H, stack, including 2 x OC*H*$_3$ from both anomers), 4.33 (0.4H, d, *J* 8.0, *H*1' ($\beta$-anomer)), 4.76 (0.6H, d, *J* 3.7, *H*1' ($\alpha$-anomer)); $\delta_C$(75 MHz, $D_2O$) [53.4, 55.5 ($CH_3$, O*C*H$_3$)], [58.9, 59.1 ($CH_2$, *C*6')], [67.9, 68.0, 69.6, 69.9, 71.4, 74.1, 74.2 (CH) - some resonance overlap], 97.6 (CH, *C*1' ($\alpha$ anomer)), 101.6 (CH, *C*1' ($\beta$ anomer)); *m/z* (TOF ES$^+$) 217.0 (100%, [M+Na]$^+$). [HRMS *m/z* (TOF ES$^+$) Found: [M+Na]$^+$ 217.0684. $C_7H_{14}O_6Na$ requires 217.0688].

* Note: since ratio of $\alpha$:$\beta$ is 1.0:0.8; then total number of protons should be 14 + (14 x 0.8) = 25.2

**Methyl 6-*O*-tosyl-D-glucopyranoside 9**

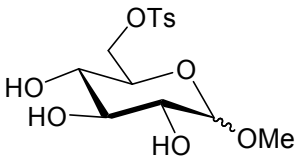


$C_{14}H_{20}O_8S$
Exact Mass: 348.0879
Mol. Wt.: 348.3688
C, 48.27; H, 5.79; O, 36.74; S, 9.20

TsCl (4.90 g, 26.0 mmol) was slowly added to a stirring solution of methyl D-glucopyranoside **10** (5.44 g, 28.0 mmol) and DMAP (0.34 g, 2.8 mmol) in pyridine (90 mL) at 0 $^{o}$C. The reaction solution was stirred overnight. The solvent was then removed under reduced pressure and the residue purified by column chromatography (1% MeOH in EtOAc; $R_f$ = 0.09) to yield the tosylate **9** as white, crystalline solid (2.56 g, 30%, $\alpha$:$\beta$ 1.0:0.8 mixture of anomers). Data on the mixture: mp 26 ºC - 34 ºC; (Found: C, 48.27; H, 5.79. $C_{14}H_{20}O_8S$ requires C, 48.02; H, 5.97%); $\nu_{max}(CH_2Cl_2)/cm^{-1}$ 3396 br, m (O-H), 3056m, 2843w, 1732w, 1361s, 1266 s; $\delta_H$(300 MHz, $CDCl_3$) 2.42 (3H, s, ArC*H*$_3$), 3.32 (3H, s, OC*H*$_3$), 3.40 – 3.50 (2.5H, stack),,3.68 – 3.74 (1.5H, stack), 4.16 – 4.32 (2.5H, stack), 4.66 (0.5H, d, *J* 3.2, *H*1' ($\alpha$-anomer)), 7.32 (2H, d, *J* 8.2, Ar*H*), 7.78 (2H, d, *J* 8.2, Ar*H*); $\delta_C$(75 MHz, $CD_3OD$) 21.6 ($CH_3$, Ar*C*H$_3$), [55.3, 57.0 ($CH_3$, O*C*H$_3$)], [69.2 ($CH_2$, *C*H$_2$OTs) resonance overlap], [69.4, 69.6, 70.9, 71.0, 71.7, 73.1, 73.3, 74.0, (CH)], 99.4 (CH, *C*1' ($\alpha$ anomer)), 103.2 (CH, *C*1' ($\beta$ anomer)), [128.0, 129.0 (CH, Ar)], 132.7 (quat. C, Ar), 144.9 (quat. C, Ar); *m/z* (TOF ES$^+$) 371.1 (100%, $[M+Na]^+$). [HRMS *m/z* (TOF ES$^+$) Found: $[M+Na]^+$ 371.0779. $C_{14}H_{20}O_8SNa$ requires 371.0777].

**Methyl 6-azido-6-deoxy-2,3,4-tri-*O*-acetyl-D-glucopyranoside[109] 8**

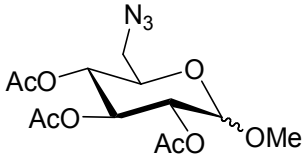


$C_{13}H_{19}N_3O_8$
Exact Mass: 345.1172
Mol. Wt.: 345.3053
C, 45.22; H, 5.55; N, 12.17; O, 37.07

Tosylate **9** (0.50 g, 1.4 mmol) was dissolved in DMF (4.8 mL) and the solution was heated to 60 $^{o}$C. $NaN_3$ (1.03 g, 16.0 mmol) was then added portionwise over 10 min and the reaction mixture heated at 60 $^{o}$C overnight. The solution was then cooled to rt and the white precipitate removed by filtration. The reaction solvent was removed under reduced pressure and the resultant azide residue was then acetylated according to general procedure A using $Ac_2O$ (0.88 mL, 8.6 mmol) and pyridine (0.1.76 mL). The reaction solution was stirred overnight at rt and then the solvent removed under reduced pressure. The acetylated sugar residue was purified by column chromatography (4:6 $Et_2O$/hexane; $R_f$ = 0.36) to yield the acetylated azido-sugar **8** as a mixture of anomers and as a white, crystalline solid (0.35 g, 70%, $\alpha$:$\beta$ 1.0:0.8); Data on the mixture: (Found: C, 45.44; H, 5.49; N 12.01. $C_{14}H_{19}O_8N_3$ requires C, 45.22; H, 5.55; N 12.17%); $\delta_H$(300 MHz, $CDCl_3$) 1.86 – 1.93 (9H, stack, 3 x C(O)C$H_3$), 3.06 – 3.38 (5H, stack, including (3.31 (1.5H, s, OC$H_3$), 3.38 (1.5H, s, OC$H_3$)), 3.60-3.64 (0.5H, m), 3.81-3.86 (0.5H, m), 4.36 (0.5H, d, *J* 8.0, *H*1' ($\beta$-anomer)), 4.72 – 4.89 (2.5H, stack), 5.08 (0.5H, app. t, *J* 9.5), 5.31 (0.5H, app. t, *J* 9.8); $\delta_C$(75 MHz, $CDCl_3$) 20.2 ($CH_3$, C(O)$CH_3$ (resonance overlap)), [50.6, 50.8 ($CH_2$, $CH_2N_3$,)], [55.1, 56.5 ($CH_3$, O$CH_3$) resonance overlap], [68.2, 69.4, 69.5, 70.4, 70.9, 72.3, 73.3 (CH) resonance overlap], 96.3 (CH, *C*1' ($\alpha$ anomer)), 101.0 (CH, *C*1' ($\beta$ anomer)), [168.9, 169.9, 169.2, 169.6, 169.6, 169.7 (quat. C, *C*=O)]*; m/z* (TOF $ES^+$) 368.0 (100%, $[M+Na]^+$). [HRMS *m/z* (TOF $ES^+$) Found: $[M+Na]^+$ 368.1054. $C_{13}H_{19}O_8N_3Na$ requires 368.1070].

**Methyl 6-amino-6-deoxy-2,3,4-tri-*O*-acetyl-D-glucopyranoside 7**

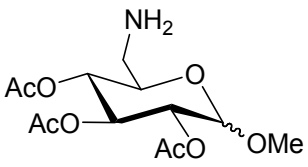


$C_{13}H_{21}NO_8$
Exact Mass: 319.1267
Mol. Wt.: 319.3077
C, 48.90; H, 6.63; N, 4.39; O, 40.09

Azide **8** (0.35 g, 1.0 mmol) was dissolved in degassed EtOAc (5.8 mL). Pd/C (0.34 g) was added to the reaction solution which was then stirred under a $H_2$ atmosphere for 2 d. The

reaction mixture was filtered through Celite and the solvent in the filtrate removed under reduced pressure to yield the acetyl-protected amino sugar **7** as a pale yellow solid without the need for further purification (0.31 mg, 97%, α:β 1.0:0.8 mixture of anomers); $\nu_{max}(CH_2Cl_2)/cm^{-1}$ 3374 br, m ($NH_2$), 3062m, 2942m, 1749s (C=O), 1653s ($NH_2$), 1551m, 1374s, 1165m, 1054s; $\delta_H$(300 MHz, $CDCl_3$) 2.03 (3H, s, COC*H*$_3$), 2.05 (3H, s, COC*H*$_3$), 2.06 (3H, s, COC*H*$_3$), 3.07-3.21 (1.5H, stack), 3.27-3.36 (3.5H, stack), 3.48 (1.5H, s, OC*H*$_3$), 3.63-3.71 (0.5H, m), 3.97-4.10 (1H, stack), 4.38 (0.5H, d, *J* 8.0, *H*1' (β-anomer)), 4.75 (0.5H, dd, *J* 10.2, 3.7), 4.81-4.87 (1H, stack), 5.08-5.15 (0.5H, m), 5.38 (0.5H, app t, *J* 9.9), 6.07-6.15 (1H, stack); $\delta_C$(75 MHz, $CDCl_3$) [20.7 ($CH_3$, C(O)*C*H$_3$), 20.8 ($CH_3$, C(O)*C*H$_3$), 23.0 ($CH_3$, C(O)*C*H$_3$) for both anomers], [38.7, 38.8 ($CH_2$, *C*6')], [55.2, 57.3 ($CH_3$, O*C*H$_3$)], 68.2 (CH, (α anomer)), [69.0, 70.5, 70.9, 71.3 (CH, (β anomer))], [71.7, 73.5, 75.0 (CH (α anomer))], 97.0 (CH, *C*1' (α anomer)), 103.4 (CH, *C*1' (β anomer)), [169.7, 170.5, 172.4, 172.7 (quat. C, *C*=O) resonance overlap]; *m/z* (TOF $ES^+$) 342.1 (100%, $[M+Na]^+$). [HRMS *m/z* (TOF $ES^+$) Found: $[M+Na]^+$ 342.1171. $C_{13}H_{21}NO_8Na$ requires 342.1165].

**_N_-(methyl-2,3,4-tris-_O_-acetyl-D-glucopyranose-6-succinamic acid 6**

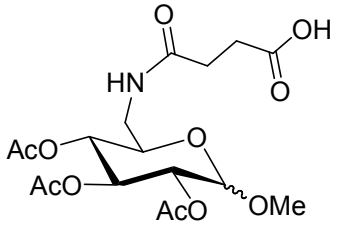


$C_{17}H_{25}NO_{11}$
Exact Mass: 419.1428
Mol. Wt.: 419.3805
C, 48.69; H, 6.01; N, 3.34; O, 41.97

Amino sugar **7** (2.10 g, 6.6 mmol) and succinic anhydride (0.73 g, 7.2 mmol) were suspended in $CH_2Cl_2$ (16.5 mL), and DIPEA (2.3 mL, 13.2 mmol) was added. The reaction mixture was allowed to stir at rt for 1 d. More succinic anhydride (0.73 g, 7.2 mmol) was then added and the reaction mixture was stirred at rt for a further 1 d. The reaction mixture was diluted with $CH_2Cl_2$ (50 mL) and washed with hydrochloric acid (1.0 M solution, 2 x 30 mL). The organic layer was dried over $MgSO_4$ and then the solvent removed under reduced

pressure to yield amide **6** as a pale yellow syrup without the need for further purification (2.52 g, 91%, $\alpha$:$\beta$ 1.0:0.8 mixture of anomers); $\nu_{max}$(thin film)/cm$^{-1}$ 3056m, 2987m, 1788s (C=O), 1754s (C=O), 1653s ($NH_2$), 1535w, 1371m, 1265s, 1243br, s, 1047s;

**Chloro-*N*-(2-methyl-4-quinolyl)ethanamide 14a[38] and**

**bromo-*N*-(2-methyl-4-quinolyl)ethanamide 14b**

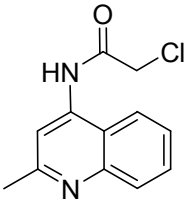


**14a**

$C_{12}H_{11}ClN_2O$
Exact Mass: 234.056
Mol. Wt.: 234.6815
C, 61.41; H, 4.72; Cl, 15.11; N, 11.94; O, 6.82

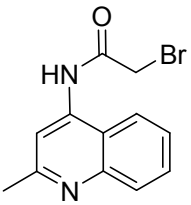


**14b**

$C_{12}H_{11}BrN_2O$
Exact Mass: 278.0055
Mol. Wt.: 279.1325
C, 51.63; H, 3.97; Br, 28.63; N, 10.04; O, 5.73

4-Aminoquinaldine (2.00 g, 12.6 mmol) and $Et_3N$ (2.6 mL, 18.5 mmol) were dissolved in THF (42mL) and the mixture cooled to $-10$ $^oC$. Subsequently a solution of the appropriate acyl halides, chloroacetyl chloride or bromoacetyl bromide, (1.5 equiv.) in THF (1.0 M) was added over the course of 20 min to the solution containing 4-amino quinaldine. The resulting suspension was then stirred at $-10$ $^oC$ for 1 h and then at room temperature for 4 h. The precipitate was removed by filtration and the filtrate washed once with hydrochloric acid (1 M, 15 mL). The acidic solution was then washed with $CH_2Cl_2$ (20 mL) and basified using $NaHCO_3$ solution. The basic solution was extracted with $CH_2Cl_2$ (3 x 20 mL) and the organic solution dried over $MgSO_4$. The solvent was removed under reduced pressure and the resultant residue purified by column chromatography (both **14a** and **14b** – 1:1 EtOAc/hexane; $R_f$ = 0.50) to yield chloride **14a** as a yellow oil (1.23 g, 42%), and bromide **14b** as yellow oil (0.70 g, 20%). **Data for the chloride 14a**: $\delta_H$(300 MHz, $CDCl_3$) 2.74 (3H, s, $CH_3$), 4.34 (2H, s, $CH_2$), 7.52 – 7.57 (1H, m, Ar*H*), 7.68 – 7.74 (1H, m, Ar*H*), 7.78 (1H, app d, *J* 8.35), 8.05 (1H, app d, *J* 8.35, Ar*H*), 8.17 (1H, s, Ar*H*), 9.16 (1H, br s, N*H*); $\delta_C$(75 MHz,

$CDCl_3$) 26.8 ($CH_3$), 44.5 ($CH_2$), 112.5 (CH, Ar), 119.5 (quat. C, Ar), [119.7, 127.1, 130.6, 130.8 (CH, Ar)], 140.1 (quat. C, Ar), 149.5 (quat. C, Ar), 161.1 (quat. C, Ar), 166.0 (quat. C=O); *m/z* (TOF $ES^+$) 235.1 (100%, $[M+H]^+$ $^{35}Cl$), 237.1 (20%, $[M+H]^+$ $^{37}Cl$). [HRMS *m/z* (TOF $ES^+$) Found: $[M+H]^+$ 235.0632. $C_{12}H_{12}N_2O_1{}^{35}ClNa$ requires 23.0633].

Data were in agreement with those reported in the literature[38]

Selected data for **14b**: $\delta_H$(300 MHz, $CDCl_3$) 2.75 (3H, s, $CH_3$), 4.20 (2H, s, $CH_2$), 7.54 – 7.59 (1H, m, Ar*H*), 7.708 – 7.76 (1H, m, Ar*H*), 7.78 (1H, app d, *J* 8.38), 8.07 (1H, app d, *J* 8.38, Ar*H*), 8.16 (1H, s, Ar*H*), 9.12 (1H, br s, N*H*); *m/z* (TOF $EI^+$) 280.0 (35%, $[M]^+$ $^{81}Br$), 199.0 (28%, $[M - {}^{81}Br]^+$), 158.0 (100, $[M–COCH_2{}^{81}Br]^+$).

**Methyl 6-*O*-(*t*-butyldiphenylsilyl)-D-glucopyranoside[59] 13**

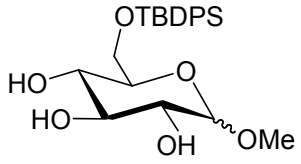


$C_{23}H_{32}O_6Si$
Exact Mass: 432.1968
Mol. Wt.: 432.5821
C, 63.86; H, 7.46; O, 22.19; Si, 6.49

Imidazole (0.39 g, 5.7 mmol) and TBDPSCl (0.74 mL, 2.8 mmol) were added sequentially to a stirring solution of **10** (0.50 g, 2.6 mmol) in DMF (2.60 mL). The reaction mixture was stirred at rt for 24 h, after which time it was diluted with $Et_2O$ (10 mL) and washed with $H_2O$ (5 mL) and $NH_4Cl$ solution (2 x 5 mL). The organic phase was dried over $MgSO_4$ and purified by column chromatography (8:2 hexane/EtOAc; $R_f$ anomer 1 = 0.51, $R_f$ anomer 2 = 0.59). The silylated sugar **13** was isolated as a mixture of anomers as a white, crystalline solid (0.68 g, 86%); Data on the mixture: mp 40 ºC – 56 ºC; (Found: C, 63.75; H, 7.50. $C_{23}H_{32}O_6Si$ requires C, 63.86; H, 7.46%); $\nu_{max}(CH_2Cl_2)/cm^{-1}$ 3338br, w (O-H), 2931s, 2858s, 1428s, 1050br, s, 702s; $\delta_H$(300 MHz, $CDCl_3$) 1.08 (9H, stack, C($CH_3$)$_3$), 3.36 – 4.23 (10.5H, stack), 4.2 (0.5H, d, *J* 7.6, *H*1' (β-anomer)), 7.37 – 7.40 (7H, stack, Ar*H*), 7.76 – 7.74 (5H, stack, Ar*H*); $\delta_C$(125 MHz, $CDCl_3$) 19.0 (quat. C, *C*($CH_3$)$_3$), 26.5 ($CH_3$, C(*C*$H_3$)$_3$), [54.6 ($CH_3$, O*C*$H_3$ (β-anomer)), 56.4 ($CH_3$, O*C*$H_3$ (α-anomer))], [63.8 ($CH_2$, *C*6' (β-anomer)), 64.0 ($CH_2$,

*C*6' (α-anomer))], [70.8 (CH) resonance overlap], [71.4, 71.8 (CH, β-anomer)], 73.1 (CH, α-anomer), 74.1 (CH, β-anomer), [75.4, 76.3 (CH, α-anomer)], [98.9 (CH, *C*1' (β-anomer)), 103.0 (CH, *C*1' (α-anomer))], [127.4, 129.4, (CH, Ph) resonance overlap], [133.0, 133.1 (quat. C, Ph)], [135.4 (CH, Ar) resonance overlap]; *m/z* (TOF ES$^+$) 455.2 (100%, [M+Na]$^+$). [HRMS *m/z* (TOF ES$^+$) Found: [M+Na]$^+$ 455.1872. $C_{23}H_{32}O_6Si$ Na requires 455.1866].

**Methyl 2,3,4-tri-*O*-benzyl-6-*O*-(*t*-butyldiphenylsilyl)-D-glucopyranoside 12**

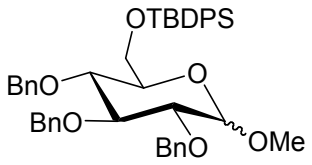


$C_{44}H_{50}O_6Si$
Exact Mass: 702.3377
Mol. Wt.: 702.9497
C, 75.18; H, 7.17; O, 13.66; Si, 4.00

NaH (0.18 g, 60 wt% dispersion in mineral oil, 4.4 mmol) was added to a solution of **13** (0.32 g, 0.7 mmol) in DMF (3.0 mL) at 0 $^oC$. After 30 min, BnBr (0.53 mL, 4.4 mmol) was added over the course of 5 min. The reaction mixture was then allowed to warm to rt and then stirred overnight. The reaction solution was slowly quenched with $H_2O$ (5 mL) at 0 $^oC$. The solution was diluted with $Et_2O$ (10 mL) and washed with $NH_4Cl$ solution (2 x 10 mL), the organic solution was dried over $MgSO_4$ and purified by column chromatography (9:1 hexane/$Et_2O$; $R_f$ both anomers = 0.23) to yield the benzylated silyl sugar **12** as a pale yellow syrup (0.37 g, 71%, mixture of anomers). Selected data for the mixture of anomers **12**: *m/z* (TOF ES$^+$) 725.3 (100%, [M+Na]$^+$). [HRMS *m/z* (TOF ES$^+$) Found: [M+Na]$^+$ 725.3247. $C_{44}H_{50}O_6NaSi$ requires 725.3247]. Very careful separation by column chromatography allowed separation of the two anomers for characterisation (9.5:0.5 hexane/$Et_2O$; Rf **12b** (β-anomer) = 0.18, $R_f$ **12a** (α-anomer) = 0.17) in order of elution: **Data on the β anomer 12b:**[59] pale yellow syrup; $[\alpha]_D^{20}$ -3.6° (*c* 1.0 in $CHCl_3$); (Found: C, 74.96; H, 7.08. $C_{44}H_{50}O_6Si$ requires C, 75.18; H, 7.17%); $\nu_{max}$(thin film)/cm$^{-1}$ 3068w, 3031w, 2975s, 2930s, 2857s, 1958w, 1888w, 1816w, 1736m, 1454s, 1428s, 1113br, s, 1070br, s, 738s, 701s; $\delta_H$(300 MHz, $CDCl_3$) 1.08 (9H, stack, C(C*H*$_3$)$_3$), 3.36 (1H, app dt, *J* 9.5, 2.8), 3.49 (1H, dd, *J* 9.0, 7.8), 3.62 (3H, s, OC*H*$_3$), 3.69 (1H, t, *J* 9.1), 3.80 (1H, t, *J* 9.3), 4.00 (2H, app d, *J* 2.8), 4.35 (1H, d, *J*

7.7, *H*1'), 4.74 (2H, app t, *J* 11.2, *C*$H_2$Ar), 4.82 – 5.00 (4H, stack, *C*$H_2$Ar), 7.20 – 7.47 (21H, stack, Ar*H*) 7.71 – 7.74 (2H, m, SiAr*C)* 7.77 – 7.80 (2H, m, SiAr*C*); $\delta_C$(75 MHz, $CDCl_3$) 21.1 (quat. C, *C*$(CH_3)_3$), 28.4 ($CH_3$, C(*C*$H_3)_3$), 58.4 ($CH_3$, O*C*$H_3$), (64.3 ($CH_2$, *C*6'), [76.5, 76.8 ($CH_2$, Ar*C*$H_2$)], 77.3 (CH), 77.6 ($CH_2$, Ar*C*$H_2$), [79.3, 84.3, 86.4 (CH)], 106.2 (CH, *C*1'), [129.23, 129.29, 129.4, 129.6, 130.06, 130.10 (CH, SiPh) resonance overlap], [131.3 (CH, Ph), [134.8, 135.2 (quat. C, SiAr*C*)], [137.3, 137.6 (CH, Ph)], [140.1, 141.2 (quat. C, $CH_2$Ar*C*)]; *m/z* (TOF $ES^+$) 725.3 (100%, $[M+Na]^+$). [HRMS *m/z* (TOF $ES^+$) Found: $[M+Na]^+$ 725.3298. $C_{44}H_{50}O_6SiNa$ requires 725.3274].

Data were in agreement with those reported in the literature.[59]

**Data on the α anomer 12a:** white crystalline solid; mp 109 ºC – 111 ºC, $[\alpha]_D^{20}$ +10.0° (*c* 1.0 in $CHCl_3$); (Found: C, 75.04; H, 7.21. $C_{44}H_{50}O_6Si$ requires C, 75.18; H, 7.17%); $\nu_{max}$(thin film)/$cm^{-1}$ 3584w, 3032w, 2923br, s, 2855s, 1588w, 1464s, 1428m, 1160s, 1106s, 1075s, 10.74s, 1035s, 743m, 700s; $\delta_H$(300 MHz, $CDCl_3$) 1.05 (9H, stack, C(C*H*$_3)_3$), 3.38 (3H, s, OC*H*$_3$), 3.54 – 3.65 (2H, stack), 3.70 (1H, app dt, *J* 10.6, 3.0), 3.87 (2H, app d, *J* 3.0), 4.03 (app t, *J* 8.9), 4.60 (1H, A of AB, $J_{AB}$ 10.8, C*H*$_a$H$_b$Ar), 4.67 (1H, d, *J* 3.6, *H*1'), 4.71 (1H, A of AB, $J_{AB}$ 12.1, C*H*$_a$H$_b$Ar), 4.81 – 4.90 (3H, stack, C*H*$_2$Ar), 4.99 (1H, B of AB, $J_{BA}$ 10.8, CH$_a$*H*$_b$Ar), 7.13 – 7.16 (2H, stack, Ar*H*) 7.24 – 7.45 (19H, stack, Ar*H)* 7.66 – 7.71 (4H, m, SiAr*C*); $\delta_C$(75 MHz, $CDCl_3$) 20.9 ($CH_3$, *C*$(CH_3)_3$), 28.7 ($CH_3$, C(*C*$H_3)_3$), 56.8 ($CH_3$, O*C*$H_3$), (64.9 ($CH_2$, *C*6'),73.4 (CH), [75.3, 77.0, 77.9 ($CH_2$, Ar*C*$H_2$)], [79.7, 82.2, 84.2 (CH)], 99.8 (CH, *C*1'), [129.5, 129.6, 129.8, 130.0, 130.1, 130.3, 130.4, 131.50 (CH, SiPh) resonance overlap], 131.52 (CH, Ph), [134.9, 134.2 (quat. C, SiAr*C*)], [137.6, 137.7 (CH, Ph)], [139.0, 139.4 (quat. C, $CH_2$Ar*C*)]; *m/z* (TOF $ES^+$) 725.3 (100%, $[M+Na]^+$). [HRMS *m/z* (TOF $ES^+$) Found: $[M+Na]^+$ 725.3247. $C_{44}H_{50}O_6SiNa$ requires 725.3274].

**Methyl 2,3,4-tri-*O*-benzyl-D-glucopyranoside 11**

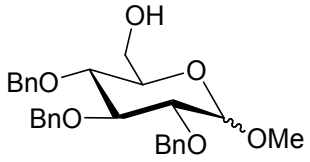


$C_{28}H_{32}O_6$
Exact Mass: 464.2199
Mol. Wt.: 464.5501
C, 72.39; H, 6.94; O, 20.66

TBAF (1.04 mL of a 1 M solution in THF, 1.0 mmol) was added to a solution of **12** (0.37 g, 0.5 mmol) in THF (2.6 mL) at rt. The reaction mixture was stirred overnight and then quenched with $H_2O$ (10 mL), diluted with $CH_2Cl_2$ (15 mL) and washed with brine (2 x 10 mL). The organic layers were dried over $MgSO_4$ and purified by column chromatography (7:3 hexane/EtOAc; $R_f$ both anomers = 0.11) to yield the benzylated 6-hydroxy sugar **11** as a pale yellow syrup (0.22 g, 90%, mixture of anomers); Very careful separation by column chromatography allowed separation of the two anomers for characterisation (7:3 hexane/$Et_2O$; Rf **11b** ($\beta$-anomer) = 0.11, $R_f$ **11a** ($\alpha$-anomer) = 0.10) in order of elution: **Selected data on the β anomer 11b:** pale yellow syrup; $\nu_{max}$(thin film)/$cm^{-1}$ 3583w, 3470br, m (O-H), 3031m, 2922s, 1736m, 1496m, 1454s, 1360s, 1159s, 1071br, s,1028s, 738s, 698s; $\delta_H$(300 MHz, $CDCl_3$) 3.40 – 3.51 (2H, stack), 3.63 (3H, s, OC*H*$_3$), 3.65 – 3.82 (3H, stack), 3.94 (1H, app dd, *J* 12.0, 2.6), 4.42 (1H, d, *J* 7.8, *H*1'), 4.71 (1H, A of AB, $J_{AB}$ 10.9), 4.78 (1H, A of AB, $J_{AB}$ 11.0), 4.88 (1H, A of AB, $J_{AB}$ 10.9), 4.91 – 5.02 (3H, stack, including 5.00, (B of AB, $J_{BA}$ 10.9)), 7.31 – 7.42 (15H, stack, Ar*H); $\delta_C$*(75 MHz, $CDCl_3$) 57.5 ($CH_3$, O*C*$H_3$), 62.1 ($CH_2$, *C*6'), [75.1, 75.3 ($CH_2$, Ar*C*$H_2$)], 75.4 (CH), [77.8, 82.6, 84.7 (CH)], 105.1 (CH, *C*1'), [127.8, 127.9, 128.3, 128.6, 128.7 (CH, Ar*C*H) resonance overlap], [138.3, 138.76, 138.84 (quat. C, Ar*C*)]; *m/z* (TOF $ES^+$) 487.2 (100%, $[M+Na]^+$). **Data on the α anomer 11a:** pale yellow syrup; $\delta_H$(300 MHz, $CDCl_3$) 3.40 (3H, s, OC*H*$_3$), 3.54 – 3.62 (2H, stack), 3.69 – 3.84 (3H,stack), 4.07 (app t, *J* 9.2), 4.62 (1H, d, *J* 3.5), 4.68 (1H, d *J* 2.6), 4.72 (1H, d, *J* 3.8), 4.82 – 4.96 (3H, stack), 5.05 (1H, B of AB, $J_{BA}$ 10.9, $CH_aH_bAr$), 7.33 – 7.43 (15H, stack, Ar*H);* $\delta_C$(75 MHz, $CDCl_3$) 55.1 ($CH_3$, O*C*$H_3$), 61.7 ($CH_2$, *C*6'), 70.8 (CH), [73.3, 75.0, 75.7 ($CH_2$, Ar*C*$H_2$)], [77.4, 78.0, 81.9 (CH)], 98.1 (CH, *C*1'), [127.6, 127.8, 127.9, 128.0, 128.3, 128.4 (CH, Ar*C*H) resonance overlap], [138.1, 138.2, 138.7 (quat. C, Ar*C*)]; *m/z* (TOF $ES^+$) 487.2

(100%, $[M+Na]^+$). [HRMS *m/z* (TOF $ES^+$) Found: $[M+Na]^+$ 487.2086. $C_{28}H_{32}O_6Na$ requires 487.2097].

**Methyl 2,3,4-tri-*O*-benzyl-6-*O*-(*N*-(2-methyl-4-quinolyl)ethanamide)-β-D-glucopyranoside 15**

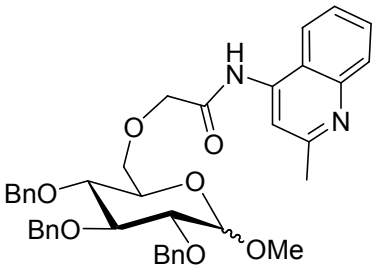


$C_{40}H_{42}N_2O_7$
Exact Mass: 662.2992
Mol. Wt.: 662.7707
C, 72.49; H, 6.39; N, 4.23; O, 16.90

NaH (0.04 g, 60 wt% dispersion in mineral oil, 1.00 mmol) was added to a solution of **11a** (0.15 g, 0.03 mmol) in DMF (0.7 mL) at 0 °C. After 30 min, bromide **14b** (0.53 mL, 4.44 mmol) was added over the course of 5 min. The reaction mixture was allowed to warm to rt and then stirred overnight. The reaction solution was slowly quenched with $H_2O$ (1 mL) at 0 °C. The solution was diluted with $CH_2Cl_2$ (5 mL) and washed with $NH_4Cl$ solution (2 x 5 mL). The organic solution was dried over $MgSO_4$, concentrated under reduced pressure, and purified by column chromatography (1:1 hexane/EtOAc; $R_f$ = 0.26) to yield the quinaldine functionalised sugar **15** as a white crystalline solid (0.12 g, 57%). $[\alpha]_D^{20}$ +18.4° (*c* 1.0 in $CHCl_3$); $\delta_H$(300 MHz, $CDCl_3$) 2.76 (3H, s, C*H*$_3$), 3.42 (3H, s, OC*H*$_3$), 3.49 – 3.54 (2H, stack), 3.69 – 3.84 (3H, stack), 3.90 (1H, app dd, *J* 10.3, 3.8), 4.12 (2H, s, COC*H*$_2$), 4.39 (1H, d, *J* 7.8, *H*1'), 4.66 (1H, A of AB, $J_{AB}$ 11.2), 4.76(1H, A of AB, $J_{AB}$ 11.0), 4.85 (1H, A of AB, $J_{AB}$ 10.9), 4.90 – 5.02 (3H, stack), 7.26 – 7.40 (15H, stack, Ph*H)*, 7.47 – 7.52 (1H, m, Ar*H*), 7.67 – 7.72 (1H, m, Ar*H*), 7.90 (1H, d, *J* 8.4, Ar*H*), 8.05 (1H, d, *J* 8.4, Ar*H*), 8.30 (1H, s, Ar*H*), 9.41 (1H, s, N*H*); $\delta_C$(75 MHz, $CDCl_3$) 25.8 ($CH_3$, C*C*$H_3$) 57.5 ($CH_3$, O*C*$H_3$), [70.1, 70.8 ($CH_2$)], 73.9 (CH), [74.8, 75.0, 75.6 ($CH_2$, Ar*C*$H_2$)], [76.9, 82.3, 84.5 (CH)], 104.9 (CH, *C*1'), 110.7 (CH), 118.3 (quat. C), 125.8 (CH), [127.6, 127.7, 127.8, 128.1, 128.3, 128.5, (CH, Ph*C*H) resonance overlap], [129.3, 129.5 (CH)] [137.8, 138.2, 138.3 (quat. C, Ar*C*)], 139.6 (quat. C,

*C*O); *m/z* (TOF ES$^+$) 663.4 (100%, [M+H]$^+$). [HRMS *m/z* (TOF ES$^+$) Found: [M+H]$^+$ 663.3084. $C_{40}H_{43}N_2O_7$ requires 663.3084].

**Methyl 6-*O*-trityl-D-glucopyranoside 20**

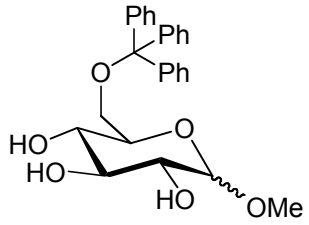


$C_{26}H_{28}O_6$
Exact Mass: 436.1886
Mol. Wt.: 436.4969
C, 71.54; H, 6.47; O, 21.99

TrCl (10.87 g, 39.0 mmol) and DMAP (0.16 g, 1.3 mmol) were added to a solution of methyl D-glucopyranoside **10** (5.00 g, 26.0 mmol) in pyridine (80 mL). The reaction mixture was heated at 80 ºC for 5 h, cooled, and the solvent removed under reduced pressure. The resulting syrup was dissolved in $CH_2Cl_2$ (150 mL) and washed with $NH_4Cl$ solution (2 x 100 mL). The organic layer was dried over $MgSO_4$ and the solvent removed under reduced pressure. The crude solid was purified by column chromatography (gradient: 5% hexane in EtOAc to EtOAc; $R_f$ = 0.22 in EtOAc) to yield the trityl ether **20** as a white, crystalline solid (9.78 g, 86%, 1.0:0.8 mixture of $\alpha$:$\beta$ anomers). Data on the mixture: mp 73 ºC – 90 ºC; (Found: C, 71.29; H, 6.25. $C_{26}H_{28}O_6$ requires C, 71.54; H, 6.47%); $\nu_{max}$(film)/cm$^{-1}$ 3338br,w (O-H), 1595w, 1489w, 1264w, 1213w, 1048br,s, 889w, 701m; $\delta_H$(300 MHz, $CD_3OD$) data for $\alpha$-anomer: 3.14 – 3.25 (2H, stack), 3.33 – 3.40 (2H, stack), 3.44 (3H, s, OC*H*$_3$), 3.52 – 3.58 (1H, m), 3.68 – 3.73 (1H, m), 4.69 (1H, d, *J* 3.6, *H*1'), 7.11 – 7.23 (9H, stack, Ar-*H*), 7.40 – 7.42 (6H stack, Ar-*H*); selected data for $\beta$-anomer: 4.18 (1H, d, *J* 7.5, *H*1'); $\delta_C$(75 MHz, $CDCl_3$) data for $\alpha$-anomer: 55.5 ($CH_3$, O*C*H$_3$), 65.0 ($CH_2$, *C*6'), [72.3, 72.5, 73.6 (CH)], 75.4 (CH), 87.7 (quat. C, O*C*Ph$_3$), 101.1 (CH, *C*1'), [128.0, 128.7, 130.0 (CH, Ph)], [145.6 (quat. C, Ph); selected data for $\beta$-anomer: 57.1 ($CH_3$, O*C*H$_3$), 72.0 (CH), 75.1 (CH), 76.9 (CH), 78.3 (CH), 105.3 (CH, *C*1'); *m/z* (TOF ES$^+$) 459.2 (100%, [M+Na]$^+$).

**Methyl (2,3,4-*O*-*p*-methoxylbenzyl)-6-*O*-trityl-α-D-glucopyranoside 21a**

**Methyl (2,3,4-*O*-*p*-methoxylbenzyl)-6-*O*-trityl-α-D-glucopyranoside 21b**

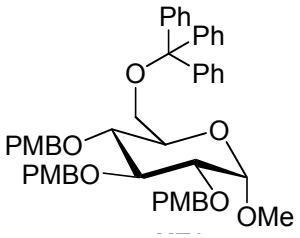


21a

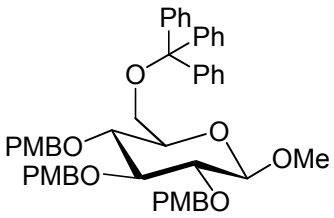


21b

$C_{50}H_{52}O_9$
Exact Mass: 796.3611
Mol. Wt.: 796.9425
C, 75.35; H, 6.58; O, 18.07

NaH (1.16 g 60 wt% dispersion in mineral oil, 29.0 mmol) was added portionwise over 10 min to a solution of triol **20** (3.84 g, 8.80 mmol) in DMF (20 mL) at 0 °C. After 30 min, PMBCl (3.93 mL, 29.0 mmol) was added dropwise over 5 min and the reaction temperature maintained at 0 °C for 1 h before allowing the solution to warm to rt over the course of 1 h. After stirring overnight, the reaction mixture was quenched with MeOH (10 mL) and then diluted with $CH_2Cl_2$ (200 mL) and extracted with $H_2O$ (2 x 60mL) and brine (60 mL). The organic layer was dried over $MgSO_4$, concentrated under reduced pressure and subjected to column chromatography (8:2 hexane/EtOAc) to yield the PMB ethers as a white, crystalline solid, (5.16 g, 74%, 1.0:0.8 mixture of α:β anomers). This mixture was usually used directly in the next step; however, careful purification by column chromatography ($R_f$ (α anomer) = 0.13, $R_f$ (β anomer) = 0.20, in 8:2 hexane/EtOAc) enabled separation of the two anomers for full characterisation.

**Data on the α anomer 21a:** white, crystalline solid; mp 41 ºC – 46 ºC; $[\alpha]_D^{25}$ +12.8° (*c* 1.0 in $CHCl_3$); (Found: C, 75.33; H, 6.53. $C_{50}H_{52}O_9$ requires C, 75.35; H, 6.58%); $\nu_{max}$(Nujol mull)/$cm^{-1}$ 1610m, 1511m, 1301w, 1246m, 1171w, 1032br,m; $\delta_H$(300 MHz; $CDCl_3$) 3.20 (1H, A of ABX, $J_{AB}$ 10.0, $J_{AX}$ 4.8, C6'$H_aH_b$), 3.45 (3H, s, OC$H_3$), 3.52 (1H, B of ABX, $J_{BA}$ 10.0, $J_{BX}$ 1.5, C6'$H_aH_b$), 3.60 – 3.64 (2H, stack), 3.81 – 3.84 (10H, stack including: 3.81 (3H, s ArOC$H_3$), 3.83 (3H, s, ArOC$H_3$), 3.85 (3H, s, ArOC$H_3$)), 3.97 (1H, t, *J* 9.3), 4.26 (1H, A of AB,

$J_{AB}$ 10.2, C$H_a$H$_b$Ar), 4.65 – 4.85 (5H, stack including 4.72 (1H, d, *J* 3.7, *H*1'), 2 x AB C$H_a$$H_b$Ar,), 4.91 (1H, B of AB, $J_{BA}$ 10.2 CH$_a$H$_b$Ar), 6.73 – 6.83 (4H, stack, Ar*H*), 6.90 – 6.95 (4H, stack, Ar*H*), 7.23 – 7.39 (13H, stack, Ar*H*), 7.49 – 7.52 (6H, stack, Ar-*H*); $\delta_c$(75 MHz; $CDCl_3$) [54.8, 55.2 ($CH_3$, O*C*H$_3$) resonance overlap], 62.6 ($CH_2$, C6'), 70.2 (CH), [72.9, 74.5, 75.5 ($CH_2$, *C*H$_2$Ar)], [77.8, 79.9, 82.0 (CH)], 86.2 (quat. C, O*C*Ph$_3$), 97.9 (CH, *C*1'), [113.5, 113.8, 126.8, 127.7, 128.8, (CH, Ar) ,resonance overlap], [129.5, 129.6, 129.7 (CH, Ar), resonance overlap], [130.2, 130.4, 131.0 (quat. C, PMB)], [143.9 (quat. C, Tr)], [159.0, 159.2, 159.3 (quat. C, PMB)]; *m/z* (TOF ES$^+$) 819.5 (100%, [M+Na]$^+$). [HRMS *m/z* (TOF ES$^+$) Found: [M+Na]$^+$ 819.3515. $C_{50}H_{52}O_9Na$ requires 819.3509].

**Data on the β anomer 21b:** white, crystalline solid: mp 105 ºC – 109 ºC, $[\alpha]_D^{20}$ +10.4° (*c* 1.0 in $CHCl_3$); (Found: C, 75.31; H, 6.75. $C_{50}H_{52}O_9$ requires C, 75.35; H, 6.58%); $\nu_{max}(CH_2Cl_2)/cm^{-1}$ 1613m, 1514s, 1449w, 1302w, 1248s, 1173w, 1069s, 1036s; $\delta_H$(300 MHz; $CDCl_3$) 3.26 (1H, dd, *J* 10.0, 3.7, *H*4'), 3.41 (1H, app dd, *J* 9.3, 1.7, *H*5'), 3.50 – 3.63 (4H, stack, C6'$H_a$,$H_b$, *H*2', *H*3'), 3.70 (3H, s, C1'OC$H_3$), 3.79 (3H, s ArOC$H_3$), 3.82 (3H, s ArOC$H_3$), 3.83 (3H, s ArOC$H_3$), 4.32 (1H, A of AB, $J_{AB}$ 9.9), 4.37 (1H, d, *J* 7.2, *H1'*), 4.65 (1H, B of AB, $J_{BA}$ 9.9), 4.73 (1H, A of AB, $J_{AB}$ 10.6), 4.76 (1H, A of AB, $J_{AB}$ 9.8)), 4.86 (1H, B of AB, $J_{BA}$ 9.8), 4.93 (1H, B of AB, $J_{BA}$ 10.6), 6.72 – 6.81 (4H, stack, Ar*H*), 6.88 – 6.92 (4H, stack, Ar*H*), 7.26 – 7.37 (13H, stack, Ar*H*), 7.54 – 7.57 (6H, stack, Ar*H*); $\delta_c$(75 MHz; $CDCl_3$) [55.2 ($CH_3$, ArO*C*H$_3$), resonance overlap], 56.6 ($CH_3$, C1'O*C*H$_3$), 62.3 ($CH_2$, *C*6'), [74.5, 74.6, 75.5 ($CH_2$, *C*H$_2$Ar), resonance overlap], 76.1 (CH, *C*4'), 77.8 (CH, *C*5'), 82.3 (CH, *C*2'), 84.4 (CH, *C*3'), 86.3 (quat. C, O*C*Ph$_3$), 104.6 (CH, *C*1'), [113.6, 113.8, 126.8, 127.7, 128.8 (CH, Ar), resonance overlap], [129.6, 129.7, 129.8 (CH, Ar), resonance overlap], [130.1, 130.9 (quat. C, Ar), resonance overlap], [143.9, 159.2 (quat. C, Ar), resonance overlap]; *m/z* (TOF ES$^+$) 819.5 (100%, [M+Na]$^+$). [HRMS *m/z* (TOF ES$^+$) Found: [M+Na]$^+$ 819.3525. $C_{50}H_{52}O_9Na$ requires 819.3509].

**Methyl (2,3,4-*O*-*p*-methoxylbenzyl)-α-D-glucopyranoside 17a**

**Methyl (2,3,4-*O*-*p*-methoxylbenzyl)-β-D-glucopyranoside 17b**

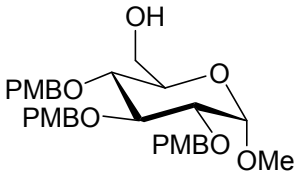


17a

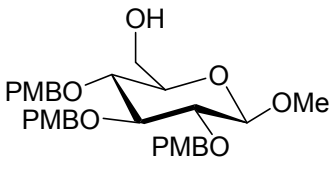


17b

$C_{31}H_{38}O_9$
Exact Mass: 554.2516
Mol. Wt.: 554.628
C, 67.13; H, 6.91; O, 25.96

A solution of trityl ethers **21a** and **21b** (5.16 g, 6.5 mmol, 1.0:0.8 mixture of anomers) in AcOH/EtOH (1:1; 28 mL) was heated at 80 °C overnight. After cooling to rt, the solvent was removed under reduced pressure to yield a pale residue, which was purified by column chromatography to yield the two anomers (3.33 g, 92%) in order of elution: the **β** anomer **17b** as a white, crystalline solid; ($R_f$ (β anomer) = 0.32 in 1:1 hexane/EtOAc): mp 56 ºC – 58 ºC; $[\alpha]_D^{20}$ +10.4° (*c* 1.0 in $CHCl_3$); (Found: C, 66.94; H, 6.71. $C_{31}H_{38}O_9$ requires C, 67.13; H, 6.91%); $\nu_{max}$(Nujol mull)/$cm^{-1}$ 3282br,w (O-H), 2924s (C-H), 2854s (C-H), 1613m, 1514s, 1302w, 1250s, 1068m, 1034m, 820m; $\delta_H$(300 MHz, $CDCl_3$) 1.92 (1H, s, O*H*), 3.31 – 3.40 (2H, stack, including 3.37 (1H, dd, *J* 9.0, 7.8)), 3.53 (1H, app t, *J* 9.2), 3.59 (3H, s, C1'OC$H_3$), 3.63 (1H, app t, *J* 9.0), 3.70 (1H, dd, *J* 11.9, 4.6), 3.79 (3H, s, ArOC$H_3$), 3.80 (3H, s, ArOC$H_3$), 3.81 (3H, s, ArOC$H_3$), 3.86 (1H, dd, *J* 11.9, 2.7), 4.34 (1H, d, *J* 7.8, *H*1'), 4.57 (1H, A of AB, $J_{AB}$ 10.6), 4.66 (1H, A of AB, $J_{AB}$ 10.6), 4.75 (1H, A of AB, $J_{AB}$ 10.6), 4.80 (1H, B of AB, $J_{BA}$ 10.6), 4.84 (1H, B of AB, $J_{BA}$ 10.6), 4.87 (1H, B of AB, $J_{BA}$ 10.6), 6.85 – 6.89 (6H, stack, Ar*H*), 7.20 – 7.32 (6H, stack, Ar*H*); $\delta_C$(75 MHz, $CDCl_3$) [55.2, 57.2 ($CH_3$, O$CH_3$), resonance overlap], 62.0 ($CH_2$), 74.4 ($CH_2$), 74.7 ($CH_2$), 74.9 (CH), 75.3 ($CH_2$), 77.2 (CH), 82.0 (CH), 98.0 (CH), 104.8 (CH, *C*1'), [113.7, 113.8, 129.4, 129.7 (CH, Ar), resonance overlap], [130.1, 130.5, 130.7 (quat. C, Ar)], [159.1, 159.2, 159.3 (quat. C, Ar-*C*OCH$_3$)]; *m/z* (TOF $ES^+$) 577.3 (100%, [M+Na]). [HRMS *m/z* (TOF $ES^+$) Found: $[M+Na]^+$ 577.2402. $C_{31}H_{38}O_9Na$ requires 577.2414]; and then the α anomer **17a** as a white, crystalline solid: ($R_f$

($\alpha$ anomer) = 0.17 in 1:1 hexane/EtOAc); mp 74 °C – 76 ºC; $[\alpha]_D^{20}$ +3.2 ° (*c* 1.0 in $CHCl_3$); $\nu_{max}$(film)/$cm^{-1}$ 3252br,w (O-H), 1615m, 1515s, 1301w, 1254s, 1098m, 1081m, 1057m, 1032m, 819m; $\delta_H$(300 MHz; $CDCl_3$) 1.94 (1H, s, O*H*), 3.38 (3H, s, OC$H_3$), 3.48 – 3.53 (2H, stack, *H*2', *H*3'), 3.63 – 3.71 (2H, stack, H5', $H_aH_b$6'), 3.74 (1H, B of ABX, $J_{BA}$ 11.5, $J_{BX}$ 2.6, $H_aH_b$6'), 3.80 (3H, s, ArOC$H_3$), 3.81 (6H, s, 2 x ArOC$H_3$), 3.95 (1H, app t, *J* 9.2, H4'), 4.47 (1H, d, *J* 3.5, *H*1'), 4.60 (1H, A of AB, $J_{AB}$ 10.5), 4.63 (1H, A of AB, $J_{AB}$ 11.5), 4.77 (1H, B of AB, $J_{BA}$ 11.5), 4.80 (1H, A of AB, $J_{AB}$ 10.6), 4.84 (1H, B of AB, $J_{BA}$ 10.5), 4.94 (1H, B of AB, $J_{BA}$ 10.6), 6.88 – 6.91 (6H, stack, Ar*H*), 7.24 – 7.26 (2H, stack, Ar*H*), 7.31 – 7.34 (4H, stack, Ar*H*); $\delta_c$(75 MHz; $CDCl_3$) [54.9, 55.0 ($CH_3$, OC$H_3$), resonance overlap], 61.5 ($CH_2$, *C*6'), 70.6 (CH, *C*5'), [72.7, 74.4, 75.1 ($CH_2$)], 77.0 (CH, *C*3'), 79.5 (CH, *C*2'), 81.5 (CH, *C*4'), 98.0 (CH, *C*1'), [113.7, 129.4, 129.4 (CH, Ar), resonance overlap], [130.1, 130.2, 130.8 (quat. C, Ar)], [158.9, 159.1, 159.2 (quat. C, Ar)]; *m/z* (TOF $ES^+$) 577.3 (100, $[M+Na]^+$). [HRMS *m/z* (TOF $ES^+$) Found: $[M+Na]^+$ 577.2420. $C_{31}H_{38}O_9Na$ requires 577.2414].

**2-bromomethylnaphthalene 22** [110,111]

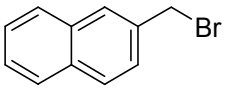


$C_{11}H_9Br$
Exact Mass: 219.9888
Mol. Wt.: 221.0932
C, 59.76; H, 4.10; Br, 36.14

NBS (6.35 g, 36.0 mmol) and then AIBN (0.58 g, 3.5 mmol) were added to a solution of 2-methyl naphthalene (5.00 g, 35.0 mmol) in $CH_2Cl_2$ (293 mL) at rt. The reaction mixture was then heated under reflux overnight. The reaction mixture was cooled to rt and then refrigerated overnight to facilitate the precipitation of succinamide. The resultant white solid was removed by vacuum filtration and the filtrate washed with NaOH solution (0.1 M, 100 mL) and $H_2O$ (100 mL). The organic layers were then dried over $MgSO_4$ and the solvent removed under reduced pressure to yield a brown solid, which was purified by recrystallisation from hexane to yield the naphthylmethyl bromide as a pale yellow crystalline solid (7.00 g, 91%). Selected data for **22**: $\delta_H$(300 MHz, $CDCl_3$) 4.64 (2H, s, C$H_2$Br), 7.46 –

7.52 (3H, stack, Ar*H*), 7.78 – 7.81 (4H, stack, Ar*H*); $\delta_C$(75 MHz, $CDCl_3$) 35.6 ($CH_2$, *C*$H_2$Br), [128.0, 128.1, 128.3, 129.2, 129.4, 129.5, 130.3 (CH, Ar)], [134.6, 134.7, 136.6 (quat. C, Ar)].

Data were in agreement with those reported in the literature[110,111]

**2-[(2-Hydroxyethoxy)methyl]naphthalene 24**

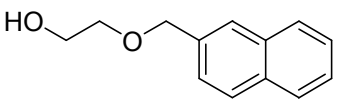


$C_{13}H_{14}O_2$
Exact Mass: 202.0994
Mol. Wt.: 202.2491
C, 77.20; H, 6.98; O, 15.82

$Ag_2O$ (1.40 g, 6.0 mmol) was added to a solution of ethylene glycol (0.25 g, 4.0 mmol) in $CH_2Cl_2$ (27 mL) and the reaction vessel was wrapped in foil. After 30 min, 2-bromomethylnaphthalene (0.97 g, 4.4 mmol) was added, and the reaction mixture was stirred for 2 d at rt. The reaction mixture was then filtered through Celite, washing with $CH_2Cl_2$ (50 mL), and the solution concentrated under reduced pressure. Purification of the residue by column chromatography (6:4 hexane/EtOAc, $R_f$ = 0.23 in 1:1 hexane/EtOAc) yielded the naphthyl ether **24** as a pale, waxy solid (0.56 g, 71%): mp 27 ºC – 29 ºC; $\nu_{max}$(Nujol mull)/$cm^{-1}$ 3340br,m (O-H), 1597w, 1506w, 1276w, 1170w, 1122m, 1106s, 1078m, 1065m, 1038m, 896m, 824m, 748m; $\delta_H$(300 MHz, $CDCl_3$) 2.52 (1H, s, O*H*), 3.61 – 3.64 (2H, br m, OC$H_2$C$H_2$O), 3.77 – 3.80 (2H, br m, -OC$H_2$C$H_2$O-), 4.71 (2H, s, ArC$H_2$), 7.47 – 7.53 (3H, stack, Ar*H*), 7.79 (1H, s, Ar*H*), 7.83 – 7.86 (3H, stack, Ar*H*); $\delta_C$(75 MHz, $CDCl_3$) [61.7, 71.4, 73.2 ($CH_2$)], [125.6, 125.8, 126.0, 126.4, 127.6, 127.7, 128.1 (CH, Ar)], [132.9, 133.1, 135.3 (quat. C, Ar)]; *m/z* (TOF $ES^+$) 225.0 (100%, [M+Na]). [HRMS *m/z* (TOF $ES^+$) Found: $[M+Na]^+$ 225.0888. $C_{13}H_{14}O_2Na$ requires 225.0891].

**2-[(2-Bromoethoxy)methyl]naphthalene 18**

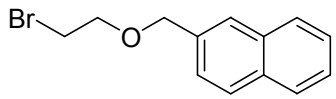


$C_{13}H_{13}BrO$
Exact Mass: 264.015
Mol. Wt.: 265.1457
C, 58.89; H, 4.94; Br, 30.14; O, 6.03

$CBr_4$ (2.56 g, 7.8 mmol) was added to a solution of alcohol **24** (1.05 g, 5.2 mmol) in THF (52 mL) at rt, followed by $PPh_3$ (2.05 g, 7.1 mmol) after 15 min, according to the general procedure C. After 3 h, work up and purification by column chromatography (9:1 hexane/EtOAc, $R_f$ = 0.44 in 8:2 hexane/EtOAc) furnished bromide **18** as a pale yellow, waxy solid (1.37 g, 99%): mp 28 ºC – 30 ºC; (Found: C, 58.92; H, 4.95. $C_{13}H_{13}BrO$ requires C, 58.89; H, 4.94%); $\nu_{max}$(Nujol mull)/$cm^{-1}$ 3048m, 1600w, 1509w, 1421w, 1274s, 1225w, 1180w, 1123m, 1109s, 1040m, 1008m, 813s, 749s; $\delta_H$(300 MHz, $CDCl_3$) 3.52 (2H, br t, *J* 6.2, C*H*$_2$CH$_2$), 3.83 (2H, br t, *J* 6.2, CH$_2$C*H*$_2$), 4.76 (2H, s, ArC*H*$_2$), 7.47 – 7.52 (3H, stack, Ar*H*), 7.80 (1H, s, Ar*H*), 7.83 – 7.87 (3H, stack, Ar*H*); $\delta_C$(75 MHz, $CDCl_3$) 30.5 ($CH_2$, BrC*H*$_2$), [69.9, 73.2 ($CH_2$, 2 x O*C*H$_2$)], [125.6, 125.9, 126.1, 126.5, 127.7, 127.8, 128.3 (CH, Ar)], [133.0, 133.2, 135.1 (quat. C, Ar)]; *m/z* ($EI^+$) 264.0 ([$M^{79}Br$]$^+$, 52%) 266.0 ([$M^{81}Br$]$^+$, 50%) 141.0 (100, [$NpCH_2$]$^+$). [HRMS *m/z* ($EI^+$) Found: [M]$^+$ 264.0149. $C_{13}H_{13}{}^{79}BrO$ requires 264.0150].

**2-[2-[2-hydroxyethoxy]ethoxymethyl]naphthalene 25**

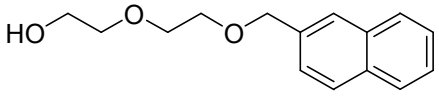


$C_{15}H_{18}O_3$
Exact Mass: 246.1256
Mol. Wt.: 246.3016
C, 73.15; H, 7.37; O, 19.49

$Ag_2O$ (1.40 g, 6.0 mmol) was added to a solution of diethylene glycol (0.43 g, 4.0 mmol) in $CH_2Cl_2$ (40 mL) and the reaction vessel was wrapped in foil. After 30 min, 2-bromomethyl naphthalene (0.97 g, 4.4 mmol) was added. The reaction mixture was stirred for 2 d at rt, and then filtered through Celite, washing with $CH_2Cl_2$ (80 mL). Concentration of the solution under reduced pressure and purification of the residue by column chromatography ($R_f$ = 0.14

in 1:1 hexane/EtOAc) yielded alcohol **25** as a colourless oil (0.98 g, 98%); (Found: C, 73.24; H, 7.49. $C_{15}H_{18}O_3$ requires C, 73.15; H, 7.37%); $\nu_{max}$(film)/cm$^{-1}$ 3429br,m (O-H), 3053w, 2868s (C-H), 1602w, 1508w, 1457w, 1351m, 1270w, 1097br,s, 893w, 819m, 750m; $\delta_H$(300 MHz, $CDCl_3$) 2.94 (1H, s, O*H*), 3.58 – 3.61 (2H, br m, OC$H_2$C$H_2$O), 3.64 – 3.70 (4H, stack, internal OC$H_2$C$H_2$O), 3.71 – 3.75 (2H, br m, OC$H_2$C$H_2$O), 4.73 (2H, s, ArC$H_2$), 7.44 – 7.52 (3H, stack, Ar*H*), 7.79 (1H, s, Ar*H*), 7.82 – 7.85 (3H, stack, Ar*H*); $\delta_C$(75 MHz, $CDCl_3$) [61.6, 69.3, 70.3, 72.4, 73.2 ($CH_2$)], [125.6, 125.8, 126.0, 126.4, 127.5, 127.7, 128.1 (CH, Ar)], [132.8, 133.1, 135.3 (quat. C, Ar)]; *m/z* (TOF ES$^+$) 269.0 (100%, [M+Na]). [HRMS *m/z* (TOF ES$^+$) Found: [M+Na]$^+$ 269.1157. $C_{15}H_{18}O_3Na$ requires 269.1154].

**2-[2-[2-bromoethoxy]ethoxymethyl]naphthalene 19**

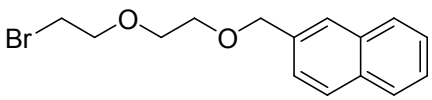


$C_{15}H_{17}BrO_2$
Exact Mass: 308.0412
Mol. Wt.: 309.1983
C, 58.27; H, 5.54; Br, 25.84; O, 10.35

$CBr_4$ (0.84 g, 2.5 mmol) was added to a solution of alcohol **25** (0.42 g, 1.7 mmol) in THF (17 mL) at rt. After 15 min, $PPh_3$ (0.66 g, 2.5 mmol) was added and the reaction mixture was stirred for a further 3 h according to the general procedure C. After work up, column chromatography of the residue (9:1 hexane/EtOAc, $R_f$ = 0.33 in 8:2 hexane/EtOAc) furnished bromide **19** as a pale brown semi-solid (0.50 g, 92%): (Found: C, 58.39; H, 5.53. $C_{15}H_{17}BrO_2$ requires C, 58.27; H, 5.54%); $\nu_{max}$($CH_2Cl_2$)/cm$^{-1}$ 2868s (C-H), 1602w, 1509w, 1461w, 1354m, 1275m, 1101s, 895w, 818m, 750m; $\delta_H$(300 MHz, $CDCl_3$) 3.50 (2H, br t, *J* 6.3, C$H_2$$CH_2$), 3.67 – 3.75 (4H, stack, internal OC$H_2$C$H_2$O), 3.84 (2H, br t, *J* 6.3, $CH_2$C$H_2$), 4.75 (2H, s, ArC$H_2$), 7.44 – 7.52 (3H, stack, Ar*H*), 7.80 (1H, s, Ar*H*), 7.82 – 7.85 (3H, stack, Ar*H*); $\delta_C$(75 MHz, $CDCl_3$) 30.3 ($CH_2$, BrC$H_2$), [69.4, 70.6, 71.2, 73.4 ($CH_2$)], [125.7, 125.8, 126.1, 126.5, 127.7, 127.8, 128.2 (CH, Ar)], [133.0, 133.2, 135.6 (quat. C, Ar)]; *m/z* (TOF ES$^+$) 333.0 ([M$^{81}$Br +

Na]$^+$, 89%), 331.0 ([M$^{79}$Br + Na]$^+$, 100%), 333.0 ([M$^{81}$Br + Na]$^+$, 99%). [HRMS *m/z* (TOF ES$^+$) Found: [M$^{79}$Br +Na]$^+$ 331.0314. $C_{15}H_{17}{}^{79}BrO_2Na$ requires 331.0310].

**Methyl (2,3,4-tris-*O*-*p*-methoxylbenzyl)-6-*O*-(2-naphthylmethyl)-α-D-glucopyranoside 26**

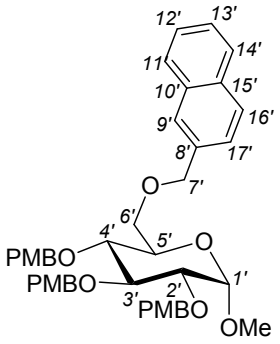


$C_{42}H_{46}O_9$
Exact Mass: 694.3142
Mol. Wt.: 694.8092
C, 72.60; H, 6.67; O, 20.72

NaH (0.05 g, 60 wt% dispersion in mineral oil, 1.4 mmol) was added to a solution of alcohol **17a** (0.50 g, 0.9 mmol) in DMF (1.8 mL) at 0 °C, followed by 2-bromomethylnaphthalene (0.30 g, 1.4 mmol) according to the general procedure D. After stirring overnight and work up, the resultant yellow residue was purified by column chromatography (gradient: 8:2 to 6:4 hexane/EtOAc, $R_f$ = 0.52 in 1:1 hexane/EtOAc) to yield the naphthyl glucoside **26** as a pale yellow syrup (0.58 g, 92%): $[\alpha]_D^{20}$ −13.2 ° (*c* 1.0 in $CHCl_3$); $\nu_{max}$(film)/cm$^{-1}$ 2999s (C-H), 2910br,s (C-H), 2836s, 1613s, 1586s, 1513s, 1463s, 1359s, 1301s, 1244br,s, 1037br,s, 906s, 819s, 732s; $\delta_H$(300 MHz; $CDCl_3$) 3.38 (3H, s, C1'OC*H*$_3$), 3.55 (1H, A of ABX, $J_{AB}$ 9.6, $J_{AX}$ 3.5, $H_aH_b$6'), 3.60 – 3.75 (7H, stack including 3.72 (3H, s, ArOC*H*$_3$), *H*2', *H*3', *H*5', $H_aH_b$6'), 3.81 (6H, s, 2 x ArOC*H*$_3$), 3.95 (1H, app t, *J* 9.2, *H*4'), 4.34 (1H, A of AB, $J_{AB}$ 10.6), 4.58 – 4.65 (3H, stack including 4.58 (1H, d, *J* 3.6, *H*1')), 4.73 – 4.82 (4H, stack including 4.78 (1H, A of AB, $J_{AB}$ 10.5), 4.77 (1H, B of AB, $J_{BA}$10.6)), 4.91 (1H, B of AB, $J_{BA}$ 10.5), 6.63 (2H, d, *J* 8.6, Ar*H*), 6.87 – 6.93 (6H, stack, Ar-*H*), 7.30 (4H, d, *J* 8.5, Ar*H*), 7.50 – 7.46 (3H, stack, Ar*H*), 7.84 – 7.78 (4H, stack, Ar*H*); $\delta_c$(75 MHz; $CDCl_3$) [55.1, 55.2 , 55.3 (O*C*H$_3$), resonance overlap], 68.3 ($CH_2$, *C*6'), 70.0 (CH, *C*5'), [73.0, 73.5, 74.6, 75.7 ($CH_2$)], 77.3 (CH, *C*3'), 79.4 (CH, *C*2'), 81.8 (CH, *C*4'), 98.2 (CH, *C*1'), [113.6, 113.7, 125.8, 125.9, 126.0,

126.7, 127.6, 127.8, 128.2, 129.3, 129.6, 129.7 (CH, Ar), resonance overlap], [130.2, 131.0, 133.0, 133.1, 135.3 (quat. C, Ar), resonance overlap], [159.0, 159.1, 159.3 (quat. C, Ar)]; *m/z* (TOF ES$^+$) 717.3 (100%, [M+Na]$^+$). [HRMS *m/z* (TOF ES$^+$) Found: [M+Na]$^+$ 717.3045. $C_{42}H_{46}O_9Na$ requires 717.3040].

**Methyl (2,3,4-tris-*O*-acetyl)-6-*O*-(2-naphthylmethyl)-α-D-glucopyranoside 29**

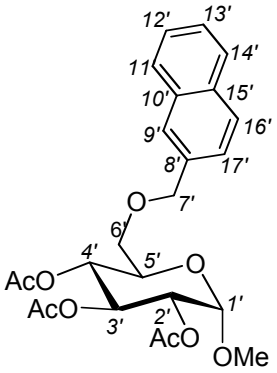


$C_{24}H_{28}O_9$
Exact Mass: 460.1733
Mol. Wt.: 460.4737
C, 62.60; H, 6.13; O, 31.27

According to general procedure E; CAN (0.86 g, 1.6 mmol) was added to a solution of **26** (0.58 g, 0.8 mmol) in acetone/$H_2O$ (9:1, 8.3 mL) at 0 °C. Further CAN (2.72 g, 5.0 mmol) in acetone/$H_2O$ (9:1, 10 mL) was added dropwise over 10 min after the initial exotherm had ceased. After stirring overnight, work up yielded a yellow oil which was directly acetylated following general procedure A. Work up and purification by column chromatography (8:2 hexane/EtOAc, $R_f$ = 0.28 in 1:1 hexane/EtOAc) furnished the triacetate **29** as a pale yellow syrup (0.26 g, 64%): $[\alpha]_D^{20}$ +112.0 ° (*c* 1.0 in $CHCl_3$); (Found: C, 62.52; H, 6.11. $C_{24}H_{28}O_9$ requires C, 62.60; H, 6.13%); $\nu_{max}$(film)/cm$^{-1}$ 2937br,w (C-H), 1749s (C=O), 1435w, 1370s, 1225s, 1045br,s; $\delta_H$(400 MHz, $CDCl_3$) 1.77 (3H, s, *C*OC*H*$_3$), 1.94 (3H, s, *C*OC*H*$_3$), 1.99 (3H, s, *C*OC*H*$_3$), 3.43 (3H, s, OC*H*$_3$), 3.48 – 3.56 (2H, stack, C6'*H*$_2$), 3.90 (1H, app td, *J* 10.2, 3.6, *H*5'), 4.57 (1H, A of AB, $J_{AB}$ 12.2, *H*$_a$H$_b$7'), 4.69 (1H, B of AB, $J_{BA}$ 12.2, H$_a$*H*$_b$7'), 4.88 (1H, dd, *J* 10.0, 3.7, *H*2'), 4.93 (1H, d, *J* 3.7, *H*1'), 5.13 (1H, app t, *J* 9.8, *H*4'), 5.43 (1H, app t, *J* 10.0, *H*3'), 7.36 – 7.42 (3H, stack, Ar*H*), 7.69 (1H, s, *H*9'), 7.38 – 7.77 (3H, stack, Ar*H*); $\delta_C$(125 MHz, $CDCl_3$) [20.6, 20.7 ($CH_3$, CO*C*H$_3$), resonance overlap], 55.3 ($CH_3$, C1'O*C*H$_3$), 68.1

($CH_2$, *C*6'), 58.2 (CH, *C*5'), 69.1 (CH, *C*4'), 70.3 (CH, *C*3'), 70.9 (CH, *C*2'), 73.6 ($CH_2$, *C*7'), 96.7 (CH, *C*1'), [125.8, 125.9, 126.1 (CH, Ar)], 126.6 (CH, *C*9'), [127.6, 127.8, 128.1 (CH, Ar)], [133.0, 133.1, 135.1 (quat. C, Ar)], [169.6, 170.1, 170.2 (quat. C, *C*=O)]; *m/z* (TOF $ES^+$) 499.2 ($[M+K]^+$, 5%) 483.1 (100, $[M+Na]^+$). [HRMS *m/z* (TOF $ES^+$) Found: $[M+Na]^+$ 483.1617. $C_{24}H_{28}O_9Na$ requires 483.1631].

**Methyl 6-*O*-(2-naphthylmethyl)-α-D-glucopyranoside 32**

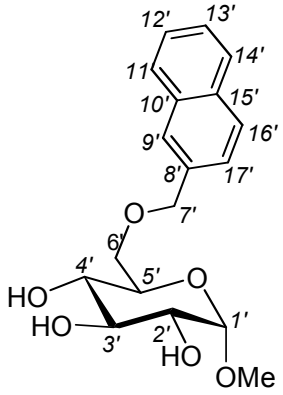


$C_{18}H_{22}O_6$
Exact Mass: 334.1416
Mol. Wt.: 334.3637
C, 64.66; H, 6.63; O, 28.71

NaOMe (0.27 g, 4.9 mmol) was added to a solution of triacetate **29** (0.63 g, 1.4 mmol) in MeOH (55 mL) according to general procedure B. After stirring overnight, work up afforded a pale syrup which was then taken up in $H_2O$ (approx. 5 mL) and lyophilised to yield the triol **32** as a white solid (0.45 g, quant.): mp 70 °C – 73 °C; $\delta_H$(300 MHz, $CD_3OD$) 3.22 – 3.38 (5H, stack), 3.54 – 3.74 (4H, stack), 4.62 (1H, d, *J* 3.7, *H*1'), 4.64 (2H, s, C7'$H_2$), 7.35 – 7.42 (3H, stack, Ar*H*), 7.72 – 7.75 (4H, stack, Ar*H*); $\delta_C$(75 MHz, $CD_3OD$) 55.7 ($CH_3$, O*C*$H_3$), 70.9 ($CH_2$), [71.9, 72.5, 73.5 (CH)], 74.6 ($CH_2$), 75.2 (CH), 101.3 (CH, *C*1'), [126.8, 126.9, 127.1, 127.4, 128.7, 128.9, 129.1 (CH, Ar)], [134.4, 134.9, 137.2 (quat. C, Ar)]; *m/z* (TOF $ES^+$) 357.1 (100, $[M+Na]^+$). [HRMS *m/z* (TOF $ES^+$) Found: $[M+Na]^+$ 357.1308, $C_{18}H_{22}O_6Na$ requires 357.1314]. UV spectrum in Section 2 of the Appendix.

**Methyl (2,3,4-tris-*O*-*p*-methoxybenzyl)-6-*O*-[2-(2-naphthylmethoxy)ethyl]-β-D-glucopyranoside 27**

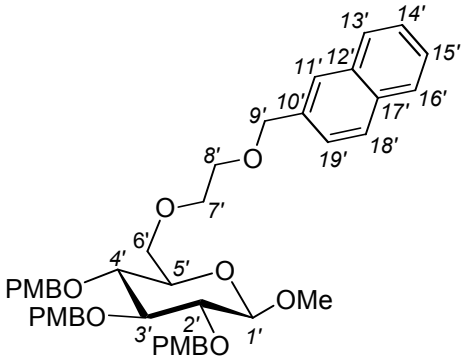


$C_{44}H_{50}O_{10}$
Exact Mass: 738.3404
Mol. Wt.: 738.8618
C, 71.52; H, 6.82; O, 21.65

NaH (0.05 g, 60 wt% dispersion in mineral oil, 1.1 mmol) was added to a solution of alcohol **17b** (0.55 g, 1.0 mmol) in DMF (2.0 mL) at 0 °C, followed by bromide **18** (0.79 g, 3.0 mmol) after 30 min, as detailed in general procedure D. After 4 d, work up furnished a yellow residue which was purified by column chromatography (6:4 hexane/EtOAc, $R_f$ = 0.45 in 1:1 hexane/EtOAc) to yield ether **27** as a pale yellow syrup (0.38 g, 52%): $[\alpha]_D^{20}$ −1.3 ° (*c* 1.00 in $CHCl_3$); (Found: C, 71.42; H, 6.70. $C_{44}H_{50}O_{10}$ requires C, 71.52; H, 6.82%); $\nu_{max}$(film)/cm$^{-1}$ 3052w, 3001w, 2926br,s (C-H), 1612s, 1513s, 1461m, 1355s, 1248s, 1174m, 1070br,s; $\delta_H$(300 MHz, $CDCl_3$) 3.42 – 3.50 (2H, stack), 3.61 (3H, s, OC$H_3$), 3.63 – 3.66 (2H, stack), 3.72 – 3.83 (15H, stack including 3.79 (3H, s, ArOC$H_3$), 3.82 (3H, s, ArOC$H_3$), 3.83 (3H, s, ArOC$H_3$)), 4.33 (1H, d, *J* 7.8, *H*1'), 4.65 (1H, A of AB, $J_{AB}$ 10.5), 4.70 (1H, A of AB, $J_{AB}$ 10.6), 4.76 (2H, s, $H_2$9'), 4.79 (1H, A of AB, $J_{AB}$ 10.6), 4.82 (1H, B of AB, $J_{BA}$ 10.5)), 4.89 (1H, B of AB, $J_{BA}$ 10.6), 4.91 (1H, B of AB, $J_{BA}$ 10.6), 6.84 – 6.92 (6H, stack, Ar*H*), 7.22 – 7.35 (6H, stack, Ar*H*), 7.47 – 7.52 (3H, stack, Ar*H*), 7.81 – 7.86 (4H, stack, Ar*H*); $\delta_C$(75 MHz, $CDCl_3$) [55.1, 57.0 ($CH_3$, O*C*$H_3$), resonance overlap], [69.5, 70.0, 71.1, 73.1, 74.3, 74.5 ($CH_2$)], 74.8 (CH), 75.2 ($CH_2$), [77.5, 81.9, 84.2 (CH)], 104.6 (CH, *C*1'), [113.6, 125.6, 125.9, 126.2, 127.5, 127.7, 128.0, 129.3, 129.5, 129.6 (CH, Ar), resonance overlap], [130.3, 130.6, 130.8, 132.8, 133.1, 135.7 (quat. C, Ar)], [159.0, 159.1 (quat. C, Ar), resonance overlap]; *m/z* (TOF ES$^+$) 761.5 (100%, [M+Na]$^+$). [HRMS *m/z* (TOF ES$^+$) Found: [M+Na]$^+$ 761.3309. $C_{44}H_{50}O_{10}$Na requires 761.3302].

**Methyl (2,3,4-tris-*O*-acetyl)-6-*O*-[2-(2-naphthylmethoxy)ethyl]-β-D-glucopyranoside 30**

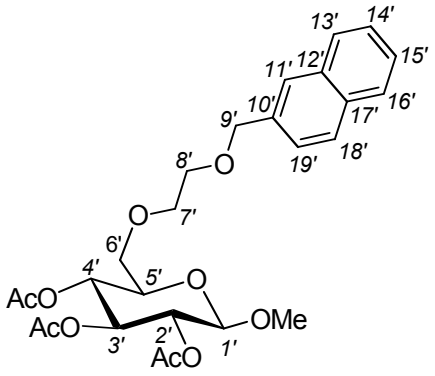


$C_{26}H_{32}O_{10}$
Exact Mass: 504.1995
Mol. Wt.: 504.5263
C, 61.90; H, 6.39; O, 31.71

CAN (0.77 g, 1.4 mmol) was added to ether **27** (0.54 g, 0.74 mmol) in acetone/$H_2O$ (9:1, 7.4 mL) at 0 °C as described in general procedure E. Further CAN (2.43 g, 4.4 mmol) in acetone/$H_2O$ (9:1, 9.0 mL) was added after the initial exotherm had ceased. After stirring at rt overnight, and subsequent work up, the resultant yellow oil was directly acetylated following general procedure A. Purification of the crude acetylated material by column chromatography (8:2 hexane/EtOAc, $R_f$ = 0.5, in 1:1 hexane/EtOAc) furnished the triacetate **30** as a pale yellow syrup (0.22 g, 59%): $[\alpha]_D^{20}$ +1.7 ° (*c* 1.0 in $CHCl_3$); (Found: C, 61.63; H, 6.24. $C_{26}H_{32}O_{10}$ requires C, 61.90; H, 6.39%); $\nu_{max}$(film)/$cm^{-1}$ 3486w , 3056w, 2941 br,s (C-H), 2871br,s (C-H), 1756br,s (C=O), 1603w, 1510m, 1447m, 1373s, 1220br,s, 1039br,s, 906m , 820m, 754m; $\delta_H$(400 MHz, $CDCl_3$) 1.88 (3H, s, COC*H*$_3$), 1.90 (3H, s, COC*H*$_3$), 1.95 (3H, s, COC*H*$_3$), 3.37 (3H, s, OC*H*$_3$), 3.49 – 3.59 (7H, stack, *H*5', *H*6', *H*7', *H*8'), 4.30 (1H, d, *J* 8.0, *H*1'), 4.60 (2H, s, *H*9'), 4.90 (1H, dd, *J* 9.6, 8.0, *H*2'), 4.97 (1H, app t, *J* 9.4, *H*4'), 5.14 (1H, app t, *J* 9.5, *H*3'), 7.34 – 7.39 (3H, stack, 3 x Ar*H*), 7.69 (1H, s, *H*11'), 7.72 – 7.74 (3H, stack, 3 x Ar*H*); $\delta_C$(125 MHz, $CDCl_3$) [20.4, 20.5 ($CH_3$, CO*C*$H_3$), resonance overlap], 56.7 ($CH_3$, OC*H*$_3$), 69.2 (CH), [69.3, 70.2, 71.1 ($CH_2$) ], [71.2, 72.8 (CH)], 73.1 ($CH_2$), 73.2 (CH), 101.2 (CH, *C*1'), [125.5, 125.6, 125.9, 126.2, 127.5, 127.6, 127.9 (CH, Ar)], 132.7, 133.0, 135.5 (quat. C, Ar)], [169.2, 169.4, 170.1 (quat. C, *C*=O)]; *m/z* (TOF $ES^+$) 527.2 (100%, $[M+Na]^+$). [HRMS *m/z* (TOF $ES^+$) Found: $[M+Na]^+$ 527.1902. $C_{26}H_{32}O_{10}Na$ requires 527.1893].

**β-Methyl 6-*O*-[2-(2-naphthylmethoxy)ethyl]-D-glucopyranoside 33**

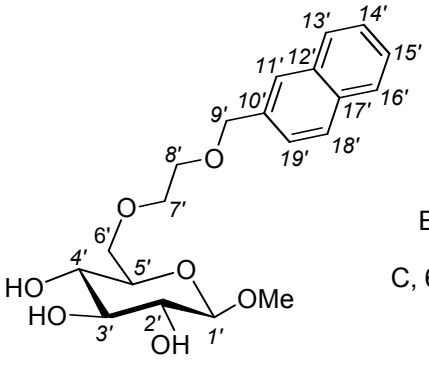


$C_{20}H_{26}O_7$
Exact Mass: 378.1679
Mol. Wt.: 378.4162
C, 63.48; H, 6.93; O, 29.60

NaOMe (0.17 g, 3.1 mmol) was added to a solution of triacetate **30** (0.43 g, 0.85 mmol) in MeOH (34 mL). The reaction was carried out according to general procedure B. After stirring overnight, work up afforded triol **33** as a pale yellow syrup (0.22 g, 75%); Selected data for XE10b: *m/z* (TOF ES$^+$) 401.1 (100%, [M+Na]$^+$). [HRMS *m/z* (TOF ES$^+$) Found: [M+Na]$^+$ 401.1584. $C_{20}H_{26}O_7Na$ requires 401.1576]. Structure inferred from previous compound **30**. UV spectrum in Section 2 of the Appendix.

**Methyl (2,3,4-tris-*O*-*p*-methoxybenzyl)-6-*O*-{2-[2-(2-naphthylmethoxy)ethoxy]ethyl}-α-D-glucopyranoside 28**

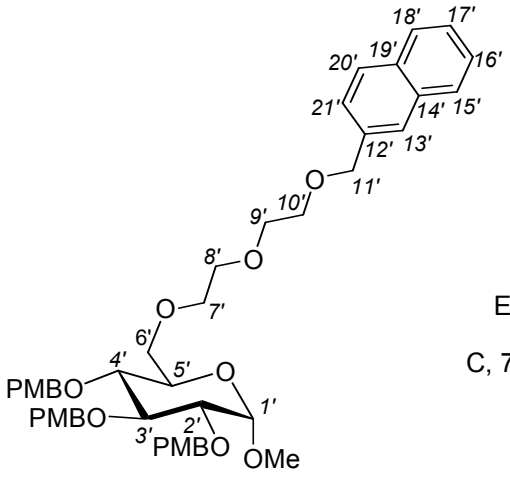


$C_{46}H_{54}O_{11}$
Exact Mass: 782.3666
Mol. Wt.: 782.9144
C, 70.57; H, 6.95; O, 22.48

NaH (0.03 g, 60 wt% dispersion in mineral oil, 0.66 mmol) was added to a solution of alcohol **17a** (0.33 g, 0.60 mmol) in DMF (1.0 mL) at 0 °C. After 30 min, a solution of bromide **19**(0.55 g, 1.8 mmol) in DMF (5 mL) was added and the reaction carried out according to general

procedure D. After 4 d, work up afforded a yellow residue which was purified by column chromatography ($R_f$ = 0.30 in 6:4 hexane/EtOAc) to yield ether **28** as a pale yellow syrup (0.26 g, 56%): $[\alpha]_D^{20}$ −12.7 ° (*c* 1.0 in $CHCl_3$); (Found: C, 70.39; H, 7.10. $C_{46}H_{54}O_{11}$ requires C, 70.57; H, 6.95%); $\nu_{max}$(film)/$cm^{-1}$ 3000m, 2907s (C-H), 2836s (C-H), 1613s, 1586m, 1514s, 1464m, 1357s, 1302s, 1249s, 1173s, 1077br,s, 820s; $\delta_H$(300 MHz, $CDCl_3$) 3.34 (3H, s, OC$H_3$), 3.49 (1H, A of ABX, $J_{AB}$ 9.6, $J_{AX}$ 3.6, $H_aH_b$6'), 3.54 – 3.71 (12H, stack), 3.75 (3H, s, ArOC$H_3$), 3.78 (3H, s, ArOC$H_3$), 3.76 (3H, s, ArOC$H_3$), 3.93 (1H, t, *J* 9.2), 4.52 (1H, d, *J* 3.5, *H*1'), 4.58 (1H, A of AB, $J_{AB}$ 11.8), 4.59 (1H, A of AB, $J_{AB}$ 10.7), 4.65 (2H, s, $H_2$11'), 4.73 (1H, A of AB, $J_{AB}$ 11.8), 4.77 (1 H, A of AB, $J_{AB}$ 10.5), 4.81 (1H, B of AB, $J_{BA}$ 10.7)), 4.89 (1H, B of AB, $J_{BA}$ 10.5), 6.83 – 6.88 (6H, stack, Ar*H*), 7.22 – 7.31 (6H, stack, Ar*H*), 7.41 – 7.48 (4H, stack, Ar*H*), 7.73 (1H, s, Ar*H*), 7.73 – 7.81 (2H, stack, Ar*H*); $\delta_C$(75 MHz, $CDCl_3$) [55.0, 55.1 ($CH_3$, O*C*$H_3$), resonance overlap], [69.4, 69.7 ($CH_2$)], 69.9 (CH), [70.4, 70.6, 70.8, 72.9, 73.2, 74.6, 75.3 ($CH_2$)], [77.3, 79.4, 81.7 (CH)], 98.14 (CH, *C*1'), [113.7, 125.7, 125.9, 126.3, 127.5, 127.7, 128.0, 129.4, 129.5, 129.6 (CH, Ar), resonance overlap], [130.2, 130.6, 131.0, 132.8, 133.1, 135.6 (quat. C, Ar)], [159.0, 159.1, 159.2 (quat. C, Ar)]; *m/z* (TOF $ES^+$) 805.5 (100%, $[M+Na]^+$). [HRMS *m/z* (TOF $ES^+$) Found: $[M+Na]^+$ 805.3577. $C_{46}H_{54}O_{11}Na$ requires 805.3564].

**Methyl (2,3,4-tris-*O*-acetyl)-6-*O*-{2-[2-(2-naphthylmethoxy)ethoxy]ethyl}-α-D-glucopyranoside 31**

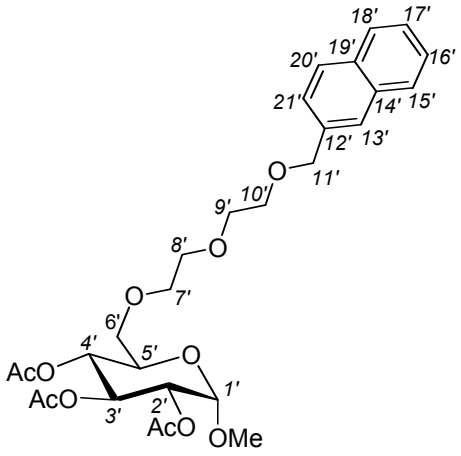


$C_{28}H_{36}O_{11}$
Exact Mass: 548.2258
Mol. Wt.: 548.5788
C, 61.30; H, 6.61; O, 32.08

CAN (0.83 g, 1.5 mmol) was added to a solution of ether **28** (0.63 g, 0.80 mmol) in acetone/$H_2O$ (9:1, 8.0 mL) at rt as detailed in general procedure E. Further CAN (2.63 g, 4.8 mmol) in acetone/$H_2O$ (9:1, 12.0 mL) was added after the initial exotherm had ceased. After stirring at rt overnight, work up yielded a dark oil which was directly acetylated following general procedure A. Purification of the crude product by column chromatography ($R_f$ =0.17 in 6:4 hexane/EtOAc) afforded the triacetate **31** as a pale yellow syrup (0.22 g, 51%): $[\alpha]_D^{20}$ +85.5 ° (*c* 1.0 in $CHCl_3$); $\nu_{max}$(film)/$cm^{-1}$ 3056w, 2911br, m (C-H), 1748s (C=O), 1441w, 1369s, 1226br,s, 1126 m, 1048br,s, 931m, 820m, 733m, (Ar-H); $\delta_H$(400 MHz, $CDCl_3$) 1.95 (3H, s, COC*H*$_3$), 1.96 (3H, s, COC*H*$_3$), 2.01 (3H, s, COC*H*$_3$), 3.33 (3H, s, OC*H*$_3$), 3.53 (1H, A of ABX, $J_{AB}$ 11.1, $J_{AX}$ 5.1, C6'*H*$_a$H$_b$), 3.56 – 3.65 (9H, stack, C6'H$_a$*H*$_b$, 2 x *H*7', 2 x *H*8', 2 x *H*9', 2 x *H*10'), 3.88 (1H, app ddd, *J* 9.9, 4.8, 2.9, *H*5'), 4.67 (2H, s, 2 x *H*11'), 4.81 (1 H, dd, *J* 9.9, 3.6, *H*2'), 4.89 (1H, d, *J* 3.6, *H*1'), 5.02 (1H, app t, *J* 9.9, *H*4'), 5.44 (1H, app t, *J* 9.9, *H*3'), 7.39 – 7.44 (3H, stack, 3 x Ar*H*), 7.72 (1H, s, *C*13'), 7.76 – 7.78 (3H, stack, 3 x Ar*H*); $\delta_C$(125 MHz, $CDCl_3$) [20.5 ($CH_3$, CO*C*H$_3$), resonance overlap], 55.1 ($CH_3$, O*C*H$_3$), 68.2 (CH, *C*5'), 69.0 (CH, *C*4'), [69.2, 69.7 ($CH_2$)], 70.0 (CH, *C*3'), [70.4 (2 x $CH_2$), resonance overlap], 70.7 ($CH_2$), 71.0 (CH, *C*2'), 73.0 ($CH_2$, *C*11'), 96.3 (CH, *C*1'), [125.5, 125.6, 125.8, 126.2, 127.4, 127.6, 127.9 (CH, Ar)], [132.7, 133.0, 135.5 (quat. C, Ar)], [169.4, 169.8 (quat. C, *C*=O),

resonance overlap]; *m/z* (TOF ES$^+$) 571.1 (100%, [M+Na]$^+$). [HRMS *m/z* (TOF ES$^+$) Found: [M+Na]$^+$ 571.2131. $C_{28}H_{36}O_{11}Na$ requires 571.2155].

**Methyl 6-*O*-{2-[2-(2-naphthylmethoxy)ethoxy]ethyl}-α-D-glucopyranoside 34**

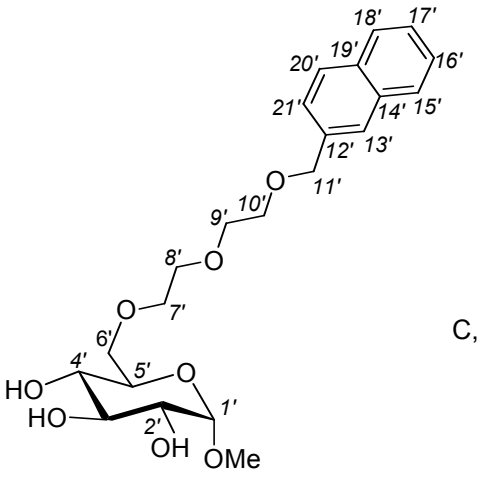


$C_{22}H_{30}O_8$
Exact Mass: 422.1941
Mol. Wt.: 422.4688
C, 62.55; H, 7.16; O, 30.30

NaOMe (0.03 g, 0.7 mmol) was added to a solution of triacetate **31** (0.10 g, 0.18 mmol) in MeOH (7.0 mL) as directed in general procedure B. After stirring overnight, work up yielded triol **34** as a pale brown syrup (0.08 g, quant.): $[\alpha]_D^{20}$ +7.9 ° (*c* 1.0 in $H_2O$); $\delta_H$(300 MHz, $CD_3OD$) 3.24 – 3.36 (5H, stack including 3.25 (3H, s, C1'OC*H*$_3$)), 3.53 – 3.70 (12H, stack), 4.57 (1H, d, *J* 3.7, *H*1'), 4.60 (2H, s, *H*11'), 7.37 – 7.41 (3H, stack, Ar*H*), 7.72 – 7.67 (4H, stack, Ar*H*); $\delta_C$(75 MHz, $CD_3OD$) 55.6 ($CH_3$, O*C*H$_3$), [70.6, 71.5, 71.6, 71.7 ($CH_2$)], 71.8 (CH), 72.0 ($CH_2$), [72.4, 73.5 (CH)], 74.1 ($CH_2$), 75.0 (CH), 101.2 (CH, *C*1'), [126.9, 127.0, 127.5, 128.7, 128.9, 129.1 (CH, Ar), resonance overlap], [134.4, 134.7, 137.1 (quat. C, Ar)]; *m/z* (TOF ES$^+$) 445.1 (100%, [M+Na]$^+$). [HRMS *m/z* (TOF ES$^+$) Found: [M+Na]$^+$ 445.1848. $C_{22}H_{30}O_8Na$ requires 445.1838]. UV spectrum in Section 2 of the Appendix.

**Methyl (6-iodo-6-deoxy)-α-D-glucopyranoside 52**

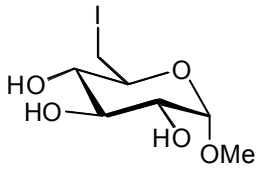


$C_7H_{13}IO_5$
Exact Mass: 303.9808
Mol. Wt.: 304.0796
C, 27.65; H, 4.31; I, 41.73; O, 26.31

$Ph_3P$ (1.62 g, 6.2 mmol), $I_2$ (1.57 g, 6.2 mmol) and imidazole (1.26 g, 18.5 mmol) were added to a solution of methyl α-D-glucose **10** (1.00 g, 5.2 mmol) in toluene (10.3 mL) at 70 °C. The reaction vessel was then covered in foil and heated at 70 °C for 3.5 h, after which time, the reaction mixture was allowed to cool to rt. $H_2O$ (20 mL) was added and the reaction mixture was stirred vigorously for 15 min. The aqueous phase was retained and the organic phase extracted with $H_2O$ (1 x 20 mL). The combined aqueous extracts were concentrated under reduced pressure and purified by column chromatography through a short silica plug. The combined fractions were then concentrated under reduced pressure to yield the iodo sugar **52** as a white, crystalline solid (1.36 g, 87%, $R_f$ = 0.29; 3:4 MeOH/EtOAc); $[\alpha]_D^{20}$ +97.9 ° (*c* 1.0 in $CHCl_3$); (Found: C 27.48; H 4.50. $C_7H_{13}O_5I$ requires C 27.65; H 4.31%); $\nu_{max}$(Nujol mull)/$cm^{-1}$ 3438s, br (OH), 2521m, br, 1329w, 1252w, 1185m, 113m, 1041s, 1020s, br; $\delta_H$(300 MHz, $D_2O$) 3.23 – 3.44 (6H, s, including OC*H*$_3$), 3.54 – 3.70 (3H, stack), 4.76 (1H, d, *J* 3.7, *H*1'); $\delta_C$(75 MHz, $D_2O$) 8.9 ($CH_2$, *C*$H_2$I), 57.4 ($CH_3$, O*C*$H_3$), [75.5, 74.5, 73.2, 72.2 (CH)], 101.4 (CH, *C*1'); *m/z* (TOF ES+) 329.6 ([M + Na]$^+$ 100%); [HRMS Found: 326.9709. $C_7H_{13}O_5INa$ requires 326.9705].

**Methyl 2,3,4-tri-*O*-acetyl-(6-acetylthio-6-deoxy)-α-D-glucopyranoside 53**

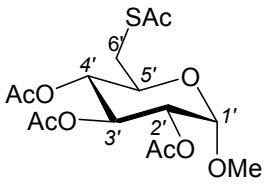


$C_{15}H_{22}O_9S$
Exact Mass: 378.0985
Mol. Wt.: 378.3948
C, 47.61; H, 5.86; O, 38.05; S, 8.47

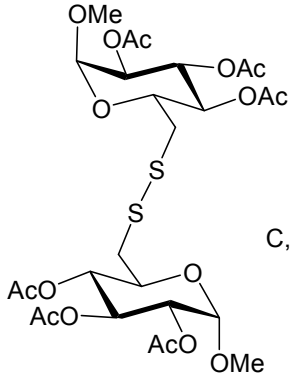


$C_{26}H_{38}O_{16}S_2$
Exact Mass: 670.1601
Mol. Wt.: 670.7003
C, 46.56; H, 5.71; O, 38.17; S, 9.56

Thiourea (0.33 g, 4.4 mmol) was added to a solution of **XE30** (1.20 g, 3.95 mmol) in DMF (40 mL). The reaction mixture was then covered in foil and heated to 70 °C for 2 d after which time the reaction mixture was allowed to cool to rt and the DMF was removed under reduced pressure. The residue was dissolved in $H_2O$ (100 mL) and NaOH (0.30 g, 7.1 mmol) was added before heating the resulting solution under reflux for 1 h. The reaction mixture was cooled to rt and acidified with hydrochloric acid (0.1 M) to ~ pH 4 and then concentrated to ~ 30 mL under reduced pressure. The concentrated mixture was extracted with EtOAc (3 x 20 mL), the aqueous phase was retained and concentrated under reduced pressure. The residue was acetylated according to general procedure A: $Ac_2O$ (3.01 mL, 31.6 mmol) in pyridine (6.00 mL) overnight. The resultant reaction mixture was concentrated under reduced pressure and the crude residue was purified by column chromatography (1:1 hexane/EtOAc; $R_f$ = 0.34) to yield the thioacetate **47a**, along with disulfide **47b**, as a colourless oil (0.72 g, 52%). Careful separation by column chromatography (7:3, hexane/EtOAc , $R_f$(monomer) = 0.22, $R_f$(dimer) = 0.23) allowed separation of the two compounds for characterisation. Data for the thioacetate:[112] $[\alpha]_D^{20}$ +98.5 ° (*c* 1.0 in $CHCl_3$); $\nu_{max}$(Nujol mull)/$cm^{-1}$ 3478w, 3375w, 2941s, br (C-H), 2844m (C-H), 1748s, br (C=O), 1694s, br (C=O), 1433m, br, 1372s, 1224s, br, 1167s, 1129s, 1046s, br, 929s, 734s; $\delta_H$(300 MHz, $CDCl_3$) 1.94 (3H, s, C(O)C$H_3$), 2.01 (3H, s, C(O)C$H_3$), 2.02 (3H, s, C(O)C$H_3$), 2.29 (3H, s, SC(O)C$H_3$), 2.98 - 3.05 (1H, dd, *J* 14.2, 6.8), 3.12 – 3.17 (1H, dd, *J* 14.2, 3.1), 3.34 (3H, s,

OC$H_3$), 3.86 (1H, app. ddd, *J* 10.0, 6.9, 3.0), 4.77 – 4.92 (3H, stack), 5.37 (1H, app. t, *J* 9.6); $\delta_C$(75 MHz, $CDCl_3$) 20.6 ($CH_3$, C(O)*C*$H_3$), 29.9 ($CH_2$, *C*$H_2$SC(O)$CH_3$), 30.2 ($CH_3$, SC(O)*C*$H_3$), 55.2 ($CH_3$, O*C*$H_3$), [68.1, 69.9, 70.8, 70.8 (CH)], 96.5 (CH, *C*1'), 170.0 (quat C, O*C*O$CH_3$ resonance overlap), 194.4 (quat. C, -S*C*O$CH_3$); *m/z* (TOF ES+) 401.4 ([M + Na]$^+$ 100%); *m/z* 401.0890 ([M + Na]$^+$ $C_{15}H_{22}O_9NaS$ requires 401.0882). Data for the disulfide: $[\alpha]_D^{20}$ +197.2 ° (*c* 1.0 in $H_2O$); $\nu_{max}$(Nujol mull)/cm$^{-1}$ 3479w, 2922s, br (C-H), 2852s, br (C-H), 1745s, br (C=O), 1376s, 1217s, br, 1165m, 1125m, 1033s, br, 929m; $\delta_H$(300 MHz, $CDCl_3$) 1.91 (6H, s, C(O)C*H*$_3$), 1.97 (6H, s, C(O)C*H*$_3$), 1.98 (6H, s, C(O)C*H*$_3$), 2.63-2.86 (4H, stack), 3.35 (6H, s, OC*H*$_3$), 3.81-3.97 (2H, m), 4.75-4.89 (4H, stack), 5.30-3.39 (2H, m); $\delta_C$(75 MHz, $CDCl_3$) [20.5 ($CH_3$, 3 x C(O)*C*$H_3$), resonance overlap], 34.3 ($CH_2$, *C*$H_2$S), 55.4 ($CH_3$, O*C*$H_3$), [67.3, 69.7, 70.7, 71.6 (CH)], 96.3 (CH, *C*1'), [169.6, 169.7, 169.8 (quat. C, *C*=O)]; *m/z* (TOF ES+) 693.4 ([M + Na]$^+$ 100%); *m/z* 693.1488 ([M + Na]$^+$ $C_{26}H_{38}O_{16}NaS_2$ requires 693.1499).

**Methyl (6-thio-6-deoxy)-α-D-glucopyranoside 45**

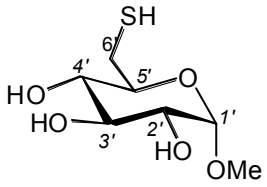


$C_7H_{14}O_5S$
Exact Mass: 210.0562
Mol. Wt.: 210.2481
C, 39.99; H, 6.71; O, 38.05; S, 15.25

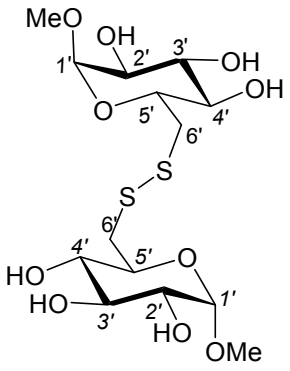


$C_{14}H_{26}O_{10}S_2$
Exact Mass: 418.0967
Mol. Wt.: 418.4802
C, 40.18; H, 6.26; O, 38.23; S, 15.32

Following general procedure B: NaOMe (1.28 g, 4.9 mmol) was added to a solution of thioacetate 53 (1.86 g, 2.9 mmol) in MeOH (200 mL) and stirred overnight. After work up, the solution was concentrated under reduced pressure to furnish the deprotected thiol as a mixture of the thiol and disulfide as a pale yellow, crystalline solid (1.02g, 99 %): selected

data: mp 78 °C - 91 °C; $[\alpha]_D^{20}$ +33.5 ° (*c* 1.0 in $H_2O$); $\delta_C$(75 MHz, $CD_3OD$) 32.9 ($CH_2$, *C*$H_2$SC(O)$CH_3$), 39.8 ($CH_2$, *C*$H_2$S-S), [52.5, 52.6 ($CH_3$, O*C*$H_3$) for thiol and disulfide], [68.2, 70.5, 71.6, 71.7, 72.0 (CH) resonance overlap], [97.9 (CH, *C*1') resonance overlap]; *m/z* (TOF ES+) 441.2 ([M + Na]$^+$ 100%); *m/z* 441.0857 ([M + Na]$^+$ $C_{14}H_{26}O_{10}NaS_2$ requires 441.0865).

**2-(acetylthio) methylnaphthalene 49**

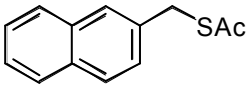


$C_{13}H_{12}OS$
Exact Mass: 216.0609
Mol. Wt.: 216.2988
C, 72.19; H, 5.59; O, 7.40; S, 14.82

Following general procedure F, thiourea (0.52 g, 6.8 mmol) was added to a solution of 2-bromomethylnaphthalene **22** (1.00 g, 4.5 mmol) in EtOH (5 mL) and the reaction mixture was heated under reflux for 3 h. The solution was cooled to rt. 40% aq. KOH solution (5 mL) was added and the mixture heated under gentle reflux for 1 h. This solution was cooled to rt, acidified to pH 1 with 10% aq. hydrochloric acid and then extracted with $Et_2O$ (3 x 15 mL). The organic extracts were dried over $MgSO_4$ and concentrated under reduced pressure. The residue was acetylated according to general procedure A: $Ac_2O$ (1.00 mL, 4.5 mmol) in pyridine (2.00 mL). The reaction mixture was then concentrated under reduced pressure and purified by column chromatography to furnish the thioacetate **49** as a pale yellow oil (0.80 g, 81%; 9:1 hexane/EtOAc; $R_f$ = 0.33); $\nu_{max}$(Nujol mull)/cm$^{-1}$ 3054w, 1637s (C=O), 1132s, br, 827m, 748s; $\delta_H$(300 MHz, $CDCl_3$) 2.39 (3H, s, C*H*$_3$), 4.31 (2H, s, C*H*$_2$S), 7.34 – 7.52 (3H, stack, Ar*H*), 7.78 – 7.84 (4H, stack, Ar*H*); $\delta_C$(75 MHz, $CDCl_3$) 30.3 ($CH_3$, SC(O)*C*$H_3$), 33.7 ($CH_2$, *C*$H_2$SAc), [125.9, 126.2, 126.8, 127.4, 127.6, 127.7, 128.4 (CH, Ar)], [132.5, 133.3, 134.9 (quat. C, Ar)]; *m/z* (TOF ES+) 239.0 ([M + Na]$^+$ 100%); *m/z* 239.0501 ([M + Na]$^+$ $C_{13}H_{12}ONaS$ requires 239.0507).

**2-Naphthylmethyl disulfide[113] 46**

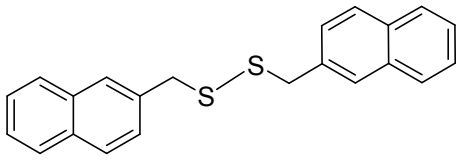

$C_{22}H_{18}S_2$
Exact Mass: 346.085
Mol. Wt.: 346.5083
C, 76.26; H, 5.24; S, 18.51

Following general procedure B, NaOMe (0.185 g, 3.4 mmol) was added to a solution of thioacetate **49** (0.616 g, 2.85 mmol) in MeOH (114 mL). After stirring overnight at rt, $CH_2Cl_2$ (20 mL) was added to aid dissolution before continuing the work up as per general procedure B. The resultant solution was concentrated under reduced pressure to furnish the deprotected disulfide as a pale yellow, crystalline solid (0.014 g, quant.): mp 43°C - 48 °C $\nu_{max}$(Nujol mull)/cm$^{-1}$ 3054w, 1598w, 1377m, 842s, 744s; $\delta_H$(300 MHz, $CDCl_3$) 3.73 (4H, s, $CH_2SH$), 7.35 (2H, dd, *J* 8.4, 1.7, ArH), 7.46 – 7.55 (6H, stack, Ar*H*), 7.77 – 7.85 (6H, stack, Ar*H*); $\delta_C$(75 MHz, $CDCl_3$) 43.6 ($CH_2$, *C*$H_2$SH), [125.9, 126.2, 127.2, 127.7, 128.2, 128.3 (CH, Ar), resonance overlap], [132.6, 133.2, 134.5 (quat. C, Ar)]; *m/z* (TOF ES+) 346.1 ([M + Na]$^+$ 100%).

Data were in agreement with those reported in the literature[113]

**2-(2Acetylthioethoxy)ethoxy methylnaphthalene 50**

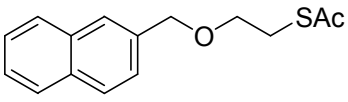

$C_{15}H_{16}O_2S$
Exact Mass: 260.0871
Mol. Wt.: 260.3513
C, 69.20; H, 6.19; O, 12.29; S, 12.32

Following general procedure F, thiourea (0.64 g, 8.3 mmol) was added to a solution of bromide **18** (1.00 g, 3.8 mmol) in EtOH (4.2 mL). The reaction mixture was heated under reflux overnight. The solution was then cooled to rt and aq. KOH solution (40% w/v, 2.5 mL) was added and the resulting mixture heated under gentle reflux for 1 h. This solution was then cooled to rt, acidified to pH 1 with 10% aq. hydrochloric acid and then extracted with

$Et_2O$ (3 x 10 mL). The organic extracts were concentrated under reduced pressure and then acetylated using general method A: $Ac_2O$ (0.80 mL, 3.8 mmol) in pyridine (1.60 mL). The resultant residue was purified by column chromatography (9:1 hexane/EtOAc; $R_f$ = 0.30) to yield the thioacetate **50** as a colourless oil (0.82 g, quant.); (Found: C, 68.91; H, 6.07. $C_{15}H_{16}O_2S$ requires C, 69.20; H, 6.19%); $\nu_{max}$(film)/cm$^{-1}$ 3055m, 2932 (C-H), 2858 (C-H), 1691s (C=O), 1602w, 1509m, 1366m, 1353m, 1124s, 1101s, br, 817m; $\delta_H$(300 MHz, $CDCl_3$) 2.35 (3H, s, SC(O)C*H*$_3$), 3.19 (2H, t, *J* 6.3, OC*H*$_2$CH$_2$SAc), 3.66 (2H, t, *J* 6.3, OCH$_2$C*H*$_2$SAc), 4.70 (2H, s, NpC*H*$_2$O), 7.49 - 7.52 (3H, stack, Ar*H*), 7.80 (1H, s, Ar*H*), 7.85-7.88 (3H, stack, Ar*H*); $\delta_C$(75 MHz, $CDCl_3$) 28.9 ($CH_2$, AcS*C*H$_2$), 30.3 ($CH_3$, SC(O)*C*H$_3$), 68.5 ($CH_2$), 72.8 ($CH_2$), [125.5, 125.7, 125.9, 126.2, 127.5, 127.7, 128.0 (CH, Ar)], [132.8, 133. , 135.3 (quat. C, Ar)], 195.1 (quat. C, *C*=O); *m/z* (TOF ES+) 283.1 ([M + Na]$^+$ 100%); *m/z* 283.0771 ([M + Na]$^+$ $C_{15}H_{16}O_2NaS$ requires 283.0769).

**2-(2-mercaptoethoxy) methylnaphthalene 47 and 47a**

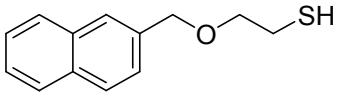


$C_{13}H_{14}OS$
Exact Mass: 218.0765
Mol. Wt.: 218.3147
C, 71.52; H, 6.46; O, 7.33; S, 14.69

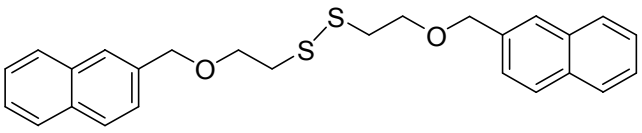


$C_{26}H_{26}O_2S_2$
Exact Mass: 434.1374
Mol. Wt.: 434.6134
C, 71.85; H, 6.03; O, 7.36; S, 14.76

Following general procedure B: NaOMe (0.20 g, 3.7 mmol) was added to a solution of thioacetate **50** (0.80 g, 3.1 mmol) in MeOH (124 mL). After work up, the solution was concentrated under reduced pressure to furnish the thiol and disulfide **47** and **47a** (ratio 4.4:1.0), as a pale brown oil (0.014 g, quant.); Data on the mixture: $\nu_{max}$(film)/cm$^{-1}$ 3053w, 2931m, 2855m, 1601w, 1508m, 1366m, 1124s, 1100s, br; $\delta_H$(300 MHz, $CDCl_3$) 1.74 (1H, t, *J* 8.2, S*H*), 2.80 (2H, app. q, *J* 6.4, OCH$_2$C*H*$_2$SH), 3.02 (4H, t, *J* 6.4, OCH$_2$C*H*$_2$S-S), 3.67 (2H, t,

*J* 6.4, C*H*$_2$CH$_2$SH), 3.82 (4H, t, *J* 6.4, OC*H*$_2$CH$_2$S-S), 4.72 (2H, s, NpC*H*$_2$O for both thiol and disulfide), 7.56 – 7.59 (3H, stack, Ar*H* for both thiol and disulfide), 7.87 (1H, s, Ar*H* for both thiol and disulfide), 7.92 – 7.94 (3H, stack, Ar*H* for both thiol and disulfide); $\delta_C$(75 MHz, $CDCl_3$) 24.1 ($CH_2$, OCH$_2$*C*H$_2$SH), 38.5 ($CH_2$, OCH$_2$*C*H$_2$S-S), 68.1 ($CH_2$, 1 x *C*H$_2$O for disulfide), [71.5, 72.6 ($CH_2$, 2 x *C*H$_2$O in thiol with resonance overlap with 1 x *C*H$_2$O disulfide], [125.3, 125.6, 125.8, 126.0, 127.4, 127.5, 127.9 (CH, Ar, for thiol and disulfide)], [132.6, 132.9, 135.3 (quat. C, Ar, resonance overlap for both thiol and disulfide]; *m/z* (TOF ES+) 241.1 ([M + Na]$^+$ 100%); *m/z* 241.0666 ([M + Na]$^+$ $C_{13}H_{14}ONaS$ requires 241.0663).

**2-[2-(2-Acetylthioethyl)ethoxy] methylnaphthalene 51**

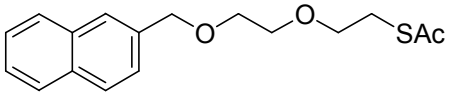


$C_{17}H_{20}O_3S$
Exact Mass: 304.1133
Mol. Wt.: 304.4039
C, 67.08; H, 6.62; O, 15.77; S, 10.53

Following general procedure F, thiourea (0.54 g, 7.1 mmol) was added to a solution of **XE8** (1.00 g, 3.2 mmol) in EtOH (3.6 mL) and the reaction mixture was heated under reflux overnight. The solution was cooled to rt, 40% aq. KOH solution (2.0 mL) was added and the mixture heated under gentle reflux for 1 h. This solution was cooled, acidified to pH 1 with 10% aq. hydrochloric acid and then extracted with $Et_2O$ (3 x 10 mL). The organic extracts were concentrated under reduced pressure and then subjected to acetylation overnight following general method A: $Ac_2O$ (1.36 mL, 6.4 mmol) in pyridine (2.72 mL). After this time, the reaction mixture was concentrated under reduced pressure and the residue purified by column chromatography (gradient: 9:1 hexane/EtOAc to 1:1 hexane/EtOAc, $R_f$ = 0.16) to yield the thioacetate **44** as a colourless oil (0.80 g, 94%); (Found: C, 67.16; H, 6.21. $C_{17}H_{20}O_3S$ requires C, 67.08; H, 6.62%); $\nu_{max}$(film)/cm$^{-1}$ 3054m, 2863 (C-H), 1690s (C=O), 1602w, 1509m, 1354m, 1124s, 1100s, br, 818m; $\delta_H$(300 MHz, $CDCl_3$) 2.31 (3H, s, SC(O)C*H*$_3$), 3.13 (2H, t, *J* 6.4, OC*H*$_2$CH$_2$SAc), 3.61 – 3.65 (6H stack, (including 3.61 (2H, t, *J*

6.4, C$H_2$SAc), 2 x OC$H_2$, C$H_2$SAc), 4.72 (2H, s, NpC$H_2$O), 7.44 – 7.50 (3H, stack, Ar*H*), 7.80 – 7.85 (4H, stack, Ar*H*); $\delta_C$(75 MHz, $CDCl_3$) 28.6 ($CH_2$, AcS*C*$H_2$), 30.2 ($CH_3$, SC(O)*C*$H_3$), [69.1, 69.5, 70.1, 73.0 ($CH_2$)], [125.46, 125.53, 125.8, 126.1, 127.4, 127.6, 127.8 (CH, Ar)], [132.7, 133.0, 135.5 (quat. C, Ar)], 195.0 (*C*=O); *m/z* (TOF ES+) 327.2 ([M + Na]$^+$, 100%); *m/z* 327.1039 ([M + Na]$^+$ $C_{17}H_{20}O_3NaS$ requires 327.1031).

**2-[2-(2-mercaptoethyl)ethoxy]naphthalene 48 and 48a**

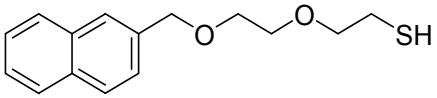


$C_{15}H_{18}O_2S$
Exact Mass: 262.1028
Mol. Wt.: 262.3672
C, 68.67; H, 6.92; O, 12.20; S, 12.22

Following general procedure B: NaOMe (0.20 g, 3.7 mmol) was added to a solution of thioacetate **51** (0.80 g, 3.1 mmol) in MeOH (124 mL). After work up, the solution was concentrated under reduced pressure to furnish the thiol and disulfide **48** and **48a** (ratio 4.4:1.0), as a pale brown oil (0.014 g, quant.); selected data on the mixture: $\delta_H$(300 MHz, $CDCl_3$) 1.74 (1H, t, *J* 8.2, S*H*), 2.71 (2H, t, *J* 6.4, $OCH_2CH_2SH$), 3.02 (2H, t, *J* 6.4, $OCH_2CH_2$S-S), 3.62 – 3.66 (4H, stack), 3.68 (4H, s s, NpC$H_2$O for disulfide), 4.72 (2H, s, NpC$H_2$O for thiol), 7.44 – 7.51 (6H, stack, Ar*H* for both thiol and disulfide), 7.80 – 7.85 (8H, stack, Ar*H* for both thiol and disulfide); $\delta_C$(75 MHz, $CDCl_3$) 24.3 ($CH_2$, $OCH_2CH_2SH$), (31.8 ($CH_2$, $OCH_2CH_2$S-S), 38.5 ($CH_2$, $OCH_2CH_2$S-S), [68.3, 69.6, 70.3, 70.4, 72.9, 73.3 ($CH_2$, OCH2 for thiol and disulfide) resonance overlap], [125.5, 125.8, 126.1, 126.4, 127.6, 127.8, 128.1 (CH, Ar, for thiol and disulfide)], [132.9, 133.2, 135.6 (quat. C, Ar, resonance overlap for both thiol and

disulfide]; *m/z* (TOF EI+) 262.0 ([M]$^+$, 12%); *m/z* 262.1016 ([M]$^+$ $C_{15}H_{18}O_2S$ requires 262.1028).

**D-Galactose-penta-*O*-acetate[114] 54**

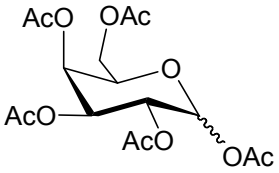


$C_{16}H_{22}O_{11}$
Exact Mass: 390.1162
Mol. Wt.: 390.3393
C, 49.23; H, 5.68; O, 45.09

D-Galactose (5.0 g, 28.0 mmol) was added portion-wise over 10 minutes to a solution of $I_2$ (0.5 g, 4.0 mmol) in $Ac_2O$ (56.0 mL). The reaction mixture was stirred for 2 h at rt, after which time the reaction solution was diluted with $CH_2Cl_2$ (175 mL) and poured onto a mixture of saturated $Na_2SO_3$ solution (75 mL) and ice (50 mL). Once the ice had melted the organic phase was retained and washed with further saturated $Na_2SO_3$ solution (75 mL) and saturdated $NaHCO_3$ solution (4 x 75 mL). The organic layers were dried over MgSO4 and then the solvent removed under reduced pressure to yield the per-acetylated galactoside **54** without the need for further purification as a white, crystalline solid (10.9 g, quant.); $\delta_H$(300 MHz, $CDCl_3$) 1.92 (3H, s, C(O)C*H*$_3$), 1.94 (3H, s, C(O)C*H*$_3$), 1.95 (3H, s, C(O)C*H*$_3$), 2.07 (3H, s, C(O)C*H*$_3$), 2.08 (3H, s, C(O)C*H*$_3$), 3.95 – 4.07 (2H, stack), 4.27 (1H, app. t, *J* 6.7, C*H*), 5.23 – 5.24 (2H, stack), 5.41 (1H, app. s, C*H*), 6.28 (1H, d, *J* 2.2, *H*1'); $\delta_C$(75 MHz, $CDCl_3$) [20.3, 20.4, 20.6 ($CH_3$, C(O)*C*H$_3$ (resonance overlap))], 61.0 ($CH_2$), [66.2, 67.1, 67.2, 68.5 (CH)], 89.5 (CH, *C*1'), [168.7, 169.6, 169.8, 169.9, 170.0 (quat. C, *C*=O)].

**Bromo (2,3,4,6-tetra-O-acetyl)-α-D-galactoside[115] 55**

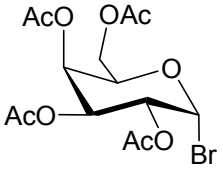


$C_{14}H_{19}BrO_9$
Exact Mass: 410.0212
Mol. Wt.: 411.1993
C, 40.89; H, 4.66; Br, 19.43; O, 35.02

AcBr (11.1 g, 90.0 mmol) and MeOH (1.46 mL, 36.0 mmol) were added sequentially to a solution of **54** (10.9 g, 28.0 mmol) in AcOH (93 mL). The reaction mixture was stirred at rt for 4 h, after which time the solvent was removed under reduced pressure to yield the galactosyl bromide **55** as a pale yellow syrup without the need for further purification (11.5 g, quant.); $[\alpha]_D^{20}$ +150.4 ° (*c* 1.0 in $CHCl_3$); $\nu_{max}$(film)/$cm^{-1}$ 2967br, s (C-H), 1749br, s (C=O), 1431m, 1372s, 1221br, s, 1079br, s; $\delta_H$(300 MHz, $CDCl_3$) 1.93 (3H, s, C(O)C$H_3$), 1.97 (3H, s, C(O)C$H_3$), 2.03 (3H, s, C(O)C$H_3$), 2.07 (3H, s, C(O)C$H_3$), 3.99 – 4.14 (2H, stack), 4.41 (1H, app. t, *J* 6.5, C*H*), 4.95 (1H, dd, *J* 10.7, 3.9), 5.31 (1H, dd, *J* 10.7, 3.3), 5.43 (1H, app. dd, J 3.3, 1.2), 6.28 (1H, d, *J* 2.2, *H*1'); $\delta_C$(75 MHz, $CDCl_3$) [19.6, 20.3, 20.5 ($CH_3$, C(O)*C*$H_3$ (resonance overlap))], 60.6 ($CH_2$), [66.8, 67.6, 67.8, 70.9 (CH)], 88.0 (CH, *C*1'), [169.4, 169.6, 169.7, 170.0 (quat. C, *C*=O)].

**_p_-Nitrophenyl (2,3,4,6-tetra-O-acetyl)-β-D-galactoside[116] 56**

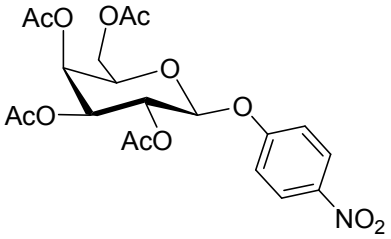


$C_{20}H_{23}NO_{12}$
Exact Mass: 469.122
Mol. Wt.: 469.3961
C, 51.18; H, 4.94; N, 2.98; O, 40.90

*p*-Nitrophenol (7.6 g, 0.20 mol) and then $Et_3N$ (24 mL, 0.18 mol) were added sequentially to a solution of □ (4.0 g, 9.7 mmol) in MeCN (200 mL). The reaction mixture was stirred at rt for 4 d after which time the reaction solution was diluted with $CH_2Cl_2$ (100 mL) and washed with 0.1M NaOH solution (4 x 200 mL) and then $H_2O$ (2 x 200 mL). The organic phases were dried over MgSO4 and then the solvent removed under reduced pressure. The resultant residue was purified by column chromatography to yield the *p*NP-functionalised acetyl sugar as a white crystalline

solid[¤] (1.84 g, 42%; $R_f$ = 0.50, 6:4 hexane/EtOAc): mp 138 °C – 140 °C; $[\alpha]_D^{20}$ -14.4° (*c* 1.0 in $CHCl_3$); (Found: C, 51.27; H, 4.70; N, 2.68. $C_{20}H_{23}NO_{12}$ requires C, 51.18; H, 4.94; N, 2.98%); $\nu_{max}$(film)/$cm^{-1}$ 3057m, 2986m, 2306w, 1753br,s (C=O), 1594m, 1522m, 1370m, 1346s, 1266s, 1233br, s, 1078s, 738s; $\delta_H$(300 MHz, $CDCl_3$) 2.00 (3H, s, C(O)C*H*$_3$), 2.05 (6H, s, 2 x C(O)C*H*$_3$), 2.17 (3H, s, C(O)C*H*$_3$), 2.07 (3H, s, C(O)C*H*$_3$), 4.11 – 4.24 (3H, stack), 5.12 (1H, dd, *J* 10.4, 3.4, C*H*), 5.18 (1H, d, *J* 7.9), 5.46 – 5.53 (2H, stack), 7.04 – 7.10 (2H, m, Ar*H*), 8.16 – 8.21 (2H, m, Ar*H*); $\delta_C$(75 MHz, $CDCl_3$) [20.5, 20.6 ($CH_3$, C(O)*C*H$_3$ (resonance overlap))], 61.3 ($CH_2$), [66.7, 68.2, 70.5, 71.4(CH)], 98.5 (CH, *C*1'), [116.5, 125.7 (CH, Ar*H*)],143.1 (quat. C, Ar*C*$NO_2$), 143.13 (quat. C, Ar*C*O), [169.1, 169.9, 170.0, 170.2 (quat. C, *C*=O)]; *m/z* (TOF ES+) 492.1 ([M + Na]$^+$, 100%); *m/z* 492.1111 ([M + Na]$^+$ $C_{20}H_{23}NO_{12}Na$ requires 492.1118).

**_p_-Nitrophenyl β-D-galactoside 57**

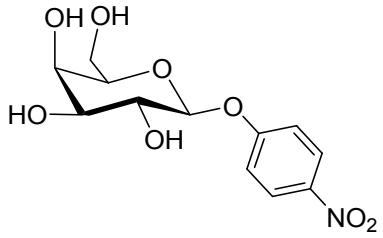


$C_{12}H_{15}NO_8$
Exact Mass: 301.0798
Mol. Wt.: 301.2494
C, 47.84; H, 5.02; N, 4.65; O, 42.49

NaOMe (1.33 g, 24.3 mmol) was added to a solution of **GalO*p*NPOAc** (1.84 g, 3.9 mmol).) in MeOH (156 mL). The reaction mixture was stirred overnight at rt and then acidified to pH 2 with Amberlite IR120 H+ resin. The resin was removed by filtration, and the filtrate concentrated under reduced pressure to yield the *p*-NP-functionlised galactoside as a white solid which required no further purification (1.16 g, quant.); mp 171 °C – 174 °C; $[\alpha]_D^{20}$ -147.2° (*c* 1.0 in $H_2O$); (Found: C, 47.77; H, 5.27; N, 4.35. $C_{12}H_{15}NO_8$ requires C, 47.84; H,

[¤] On large scale the compound was isolated as a pale yellow syrup, but when lyophilised gave a white crystalline solid.

5.02; N, 4.65%); $\nu_{max}$(nujol mull)/$cm^{-1}$ 3339br, s (O-H), 1495m, 1376m, 1346s, 1256m, 1086s, 1031m; $\delta_H$(300 MHz, $CDCl_3$) 3.62 (1H, dd, *J* 9.7, 3.4) 3.73 – 3.88 (4H, stack), 3.92 (1H, d, *J* 3.36), 5.02 (1H, d, *J* 7.7, *H*1'), 7.22- 7.28 (2H, m, Ar*H*), 8.19 – 8.24 (2H, m, Ar*H*); $\delta_C$(75 MHz, $CD_3OD$) 62.5 ($CH_2$), [70.2, 72.0, 74.8, 77.3 CH)], 102.3 (CH, *C*1'), [117.8, 126.6 (CH, Ar*H*)],143.9 (quat. C, Ar*C*), 164.0 (quat. C, Ar*C*); *m/z* (TOF ES+) 324.1 ($[M + Na]^+$, 100%).

## 5.3 Enzymatic Reactions

**Method for the determination of the activity of the enzyme**

**Method ENZ 1**

Methyl α-D-glucose (1.0 mmol, 0.194 g [glycosyl acceptor]) and *p*-nitrophenyl galactose (0.1 mmol, 0.030 g [glycosyl donor]) suspended in aq. NaOAc buffer (0.5 mL, 50 mM, pH 5.0) were stirred at 55 °C with β-galactosidase from *B. circulans* (1.2 U/mmol acceptor). 20 mL aliquots were taken at 5, 10, 20, 40, 80 and 120 min and were heated for 5 min at 100 °C to terminate the reaction prior to analysis by HPLC.

**Method ENZ 2**

Methyl α-D-glucose (0.6 mmol, 0.116 g) and *p*-nitrophenyl galactose (0.1 mmol, 0.030 g) dissolved in aq. NaOAc buffer (3.0 mL, 50 mM, pH 5.0) were stirred at 30 °C with β-galactosidase from *B. circulans* (30.0 U/mmol acceptor). 20 mL aliquots were taken at 2, 4, 6, 8, 10, 15, 20, 30, 45, 60, 90, 120, 180 and 240 min and were heated for 5 min at 100 °C to terminate the reaction prior to analysis by HPLC.

**ENZ 3a and ENZ 3b**

These experiments were carried out according to the method for ENZ1 but omitting the glycosyl acceptor GlcOMe. ENZ 3a was carried out at 55 $^{o}$C and ENZ 3b at 30 $^{o}$C.

**Control Experiments**

These experiments were carried out according to the method for ENZ1 in the following conditions:

C1: no glycosyl donor added

C2: D-galactose added as the glycosyl donor, *p*-nitrophenol added as the glycosyl donor.

C3: only GalO*p*NP added as glycosyl donor

C4: Lactose as the glycosyl donor, Methyl $\alpha$-D-glucose as the glycosyl acceptor.

**ENZ 4a and ENZ 4b**

These experiments were carried out according to the method for ENZ1 but ENZ 4a using GalOpNP as the glycosyl donor and ENZ 4b using Lac as the glycosyl donor.

**Method for experiment ENZ 5**

Lactose (0.30 mmol, 0.100 g) was suspended in a mixed solvent system (0.73 $\mu$L, 0.4 M, see Table 3.3.1a for permutations) and was stirred at a given temperature (see Table 3.3.1.1d) with the $\beta$-galactosidase from *B. circulans* (0.7 U, 0.002 mg). 10 $\mu$L aliquots were taken at 5, 10, 15, 30, 60 and 120 min then at 24 h and 48 h. Aliquots heated for 5 min at 100 $^{o}$C to terminate the reaction and diluted in $H_2O$ (600 $\mu$L) prior to analysis by HPLC.

**ENZ 6 & 7**

Variables:

| Reaction | pH | % MeCN | Temperature $^{o}$C |
|---|---|---|---|
| D | 5.0 | 20 | 30 |
| F | 7.0 | 40 | 30 |
| G | 7.0 | 30 | 30 |
| H | 7.0 | 20 | 30 |
| P | 7.0 | 20 | 55 |

Table 3.3.1.2b

**Method for experiment ENZ 6**

Lactose (0.14 mmol, 0.048 g) and α-methyl glucose (1.00 mmol, 0.194 g) were suspended in a mixed solvent system (2.50 mL, 0.4 M wrt acceptor, see Table 3.3.1.2b for details) and was stirred at a given temperature (see Table 3.3.1.1f) with the β-galactosidase from *B. circulans* (2.45 U/mmol acceptor, 0.008 mg). 10 μL aliquots were taken at 10, 30, 60, 120, 240 and 360 min and then at 24, 48 and 72 h. Aliquots were heated for 5 min at 100 $^{o}$C to terminate the reaction and diluted in $H_2O$ (600 μL) prior to analysis by HPLC and mass spectrometry.

**Method for experiment ENZ 7**

Gal*O*p*NP* (0.14 mmol, 0.042 g) and α-methyl glucose (1.00 mmol, 0.194 g) were suspended in a mixed solvent system (2.50 mL, 0.4 M wrt acceptor, see Table 3.3.1.1f for details) which was stirred at a given temperature (see Table 3.3.1.1f) with the β-galactosidase from *B. circulans* (2.45 U/mmol acceptor, 0.008 mg). 10 μL aliquots were taken at 10, 30, 60, 120, 240 and 360 min and then at 24 h and 48 h. Aliquots were heated for 5 min at 100 $^{o}$C to terminate the reaction and diluted in $H_2O$ (600 μL) prior to analysis by HPLC and mass spectrometry.

**ENZ 8 & ENZ 9**

Variables:

| Reaction | pH | % MeCN | Temperature $^{o}$C |
|---|---|---|---|
| D | 5.0 | 20 | 30 |
| F | 7.0 | 40 | 30 |
| G | 7.0 | 30 | 30 |
| H | 7.0 | 20 | 30 |
| P | 7.0 | 20 | 55 |

Table 3.3.1.2b

**Method for experiment ENZ 8**

Lactose (0.14 mmol, 0.048 g) and α-methyl glucose (1.00 mmol, 0.194 g) were suspended in a mixed solvent system (2.50 mL, 1.2 M wrt acceptor, see Table 3.3.1.1f for details), which was stirred at a given temperature (see Table 3.3.1.1f) with the β-galactosidase from *B. circulans* (2.45 U/mmol acceptor, 0.008 mg). 10 μL aliquots were taken at 10, 30, 60, 120, 240 and 360 min and then at 24, 48 and 72 h. Aliquots were heated for 5 min at 100 $^{o}$C to terminate the reaction and diluted in $H_2O$ (600 μL) prior to analysis by HPLC and mass spectrometry.

**Method for experiment ENZ 9**

Gal*O*p*NP* (0.14 mmol, 0.042 g) and α-methyl glucose (1.00 mmol, 0.194 g) were suspended in a mixed solvent system (2.50 mL, 1.2 M wrt acceptor, see Table 3.3.1.1f for details), which was stirred at a given temperature (see Table 3.3.1.1f) with the β-galactosidase from *B. circulans* (2.45 U/mmol acceptor, 0.008 mg). 10 μL aliquots were taken at 10, 30, 60, 120, 240 and 360 min and then at 24 h and 48 h. Aliquots were heated for 5 min at 100 $^{o}$C to terminate the reaction and diluted in $H_2O$ (600 μL) prior to analysis by HPLC and mass spectrometry.

**ENZ10**

**Method for experiment ENZ 10C1**

GalO*p*NP (0.14 mmol, 0.042 g) was dissolved in aqueous buffer solution (2.50 mL, 0.056 M or 0.17030 M; see Table 3.3.2b for details) and was stirred at a given temperature (see Table 3.3.2b) with the β-galactosidase from *B. circulans* (1.2 U, 0.007 mg). 10 μL aliquots were taken at 0, 0.5, 1, 2, 4, 6 and 10 min. Aliquots were heated for 5 min at 100 °C to terminate the reaction and diluted in aqueous NaOH solution (0.1 M) prior to analysis by UV-vis spectroscopy. UV-vis spectroscopy was carried out on 2.8 mL of the solution at a concentration of 1 x $10^{-5}$ M in a 1cm path length cuvette.

**Method for experiment ENZ 11**

Variables:

| Reaction number | | pH | Concentration/M | % MeCN | Temperature/°C |
|---|---|---|---|---|---|
| **ENZ 11 C1** | D | 5.0 | 0.170 | 20 | 30 |
| | F | 7.0 | 0.170 | 40 | 30 |
| | G | 7.0 | 0.170 | 30 | 30 |
| | H | 7.0 | 0.170 | 20 | 30 |
| | P | 7.0 | 0.170 | 20 | 55 |
| **ENZ 11 C2** | D | 5.0 | 0.056 | 20 | 30 |
| | F | 7.0 | 0.056 | 40 | 30 |
| | G | 7.0 | 0.056 | 30 | 30 |
| | H | 7.0 | 0.056 | 20 | 30 |
| | P | 7.0 | 0.056 | 20 | 55 |

Table 3.3.2f

GalO*p*NP (0.14 mmol, 0.042 g) was dissolved in a mixed solvent system (2.50 mL, 0.056 M or 0.170 M; see Table 3.3.2f for details) and stirred at a given temperature (see Table 3.3.2f) with the β-galactosidase from *B. circulans* (1.2 U, 0.007 mg). 10 μL aliquots were taken at 0, 30, 60, 90, 120, 180, 210, 240, 270, 300, 330 and 360 min. Aliquots were heated for 5 min at 100 °C to terminate the reaction and diluted in aqueous NaOH solution (0.1 M) prior to

analysis by UV-vis spectroscopy. UV-vis spectroscopy was carried out on 2.8 mL of the solution at a concentration of 1 x $10^{-5}$ M in a 1cm path-length cuvette.

**ENZ 12**

Variables:

| Reaction conditions | | Standard amount of enzyme added/g | Increased amount of enzyme added/g | | | |
|---|---|---|---|---|---|---|
| | | | X2 | X4 | X8 | X16 |
| | | 0.007 | **0.014** | **0.028** | **0.056** | **0.112** |
| D | pH | | | | | |
| | 5.0 | reaction number | 2D | 4D | 8D | 16D |
| H | pH | | | | | |
| | 7.0 | reaction number | 2H | 4H | 8H | 16H |

Table 3.3.3a

**Method for experiment ENZ 12**

GalO*p*NP (0.14 mmol, 0.042 g) was dissolved in a mixed solvent system (2.50 mL, 0.056 M; 20 % MeCN, see Table 3.3.3a for pH) and was stirred at a 30 $^{o}$C with the β-galactosidase from *B. circulans* (see Table 3.3.3a for details). 10 μL aliquots were taken at 0, 10, 30, 60, 90, 120, 180, 210, 240, 270, 300, 330 and 360 min. Aliquots were heated for 5 min at 100 $^{o}$C to terminate the reaction and diluted in aqueous NaOH solution (0.1 M) prior to analysis by UV-vis spectroscopy. UV-vis spectroscopy was carried out on 2.8 mL of the solution at a concentration of 1 x $10^{-5}$ M in a 1 cm path-length cuvette.

**ENZ 13 & ENZ 14**

Variables:

| Reaction number | pH | Glycosyl donor |
|---|---|---|
| ENZ 13D | 5.0 | GalO*p*NP |
| ENZ 13H | 7.0 | GalO*p*NP |
| ENZ 14D | 5.0 | Lac |
| ENZ 14H | 7.0 | Lac |

Table 3.3.41.a

**Method for experiments ENZ 13 and ENZ 14**

The reactions were carried out by suspending the glycosyl donor (0.05 mmol [GalO*p*NP or Lac]) and naphthyl-functionalised methyl glucoside **32** ( 0.4 mmol, 0.128 g) in the mixed solvent system (pH 5.0 [ENZ13] or 7.0 [ENZ 14] buffer/MeCN 80:20, 1 mL) at 30 $^{o}$C. The β-galactosidase from *B. circulans* (7.84 U, 0.024 g [19.6 U mmol$^{-1}$ acceptor]) was then added and aliquots of the reaction solution were taken at 0, 15, 30, 45, 60, 90, 120, 150, 180, 210, 240, 270, 300, 330 and 360 min, and 24h for analysis by HPLC and mass spectrometry. HPLC monitoring was done using a UV (224 nm) and an ECD detector simultaneously. After 24 hours the reaction was stopped by denaturing the enzyme by heating. The reaction mixture was then freeze-dried and the carbohydrate residues were acetylated to facilitate separation (by column chromatography, 6:4 hexane/EtOAc) of starting material from the products which were recovered by flushing the column with 5% MeOH in EtOAc. This flushed fraction was further analysed and separated using analytical HPLC ($H_2O$/MeCN (+ 0.05 % TFA) gradient 20% to 100 % over 40 minutes, 10 mL min$^{-1}$) and then mass spectrometry was performed on the components.

**ENZ 15 and ENZ 16**

The reactions were carried out by suspending the glycosyl donor (0.16 mmol [GalO*p*NP or Lac]) and naphthyl-functionalised methyl glucoside **32** ( 0.75 mmol, 0.250 g) in the mixed solvent system pH 7.0 buffer/MeCN 80:20 (1.87 mL) at 30 $^{o}$C. The β-galactosidase from *B. circulans* (14.7 U, 0.044 g [19.6 U mmol$^{-1}$ acceptor]) was then added and aliquots of the

reaction solution were taken at 0, 15, 30, 45, 60, 90, 120, 150, 180, 210, 240, 270, 300, 330 and 360 min, and 24h for analysis by HPLC and mass spectrometry. HPLC monitoring was done using a UV (224 nm) and an ECD detector simultaneously. After 24 hours the reaction was stopped by denaturing the enzyme by heating. The reaction mixture was then freeze-dried and the carbohydrate residues were acetylated to facilitate separation (by column chromatography, 6:4 hexane/EtOAc) of starting material from the products which were recovered by flushing the column with 5% MeOH in EtOAc. This flushed fraction was further analysed and separated using analytical HPLC ($H_2O$/MeCN (+ 0.05 % TFA) gradient 20% to 100 % over 40 minutes, 10 mL $min^{-1}$) and then mass spectrometry was performed on the components. Acetylated disaccharide **36** was recovered in 12% yield from ENZ 15 and 9.5% yield from ENZ 16.

**β-D-(-2,3,4,6-tetra-*O*-acetyl)-galactopyranoside-(1→2)-α-D-methyl-((2,3,4-tris-*O*-acetyl)-6-*O*-(2-naphthylmethyl))-glucopyranoside 36**

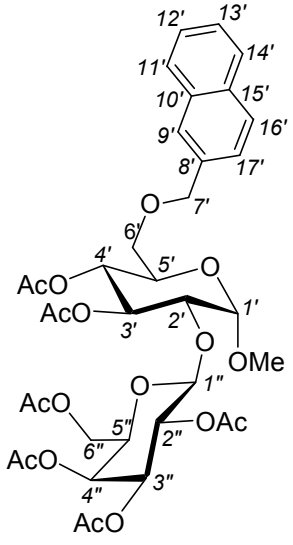


$C_{36}H_{44}O_{17}$
Exact Mass: 748.2578
Mol. Wt.: 748.7244
C, 57.75; H, 5.92; O, 36.33

Appearance: white powder; $[\alpha]_D^{20}$ +66.0 ° (*c* 1.0 in $CHCl_3$); $\nu_{max}$(film)/$cm^{-1}$ 3022w, 2935br, m (C-H), 1747s (C=O), 1433w, 1368s, 1227br,s, 1044br,s, 753m; $\delta_H$(500 MHz, $CDCl_3$) 1.80 (3H, s, C4'COC*H*$_3$), 1.96 (3H, s, C3"COC*H*$_3$), 2.00 (3H, s, C2"COC*H*$_3$), 2.05 (3H, s, C3'COC*H*$_3$), 2.06 (3H, s, C6"COC*H*$_3$), 2.15 (3H, s, C4"COC*H*$_3$), 3.52 (3H, s, OC*H*$_3$), 3.51

(1H, A of ABX, $J_{AB}$ 10.8, $J_{AX}$ 4.0, C6'$H_aH_b$), 3.58 (1H, B of ABX, $J_{BA}$ 10.8, $J_{BX}$ 2.5, C6'$H_aH_b$), 3.81 (1H, dd, *J* 10.0, 3.5, *H*2'), 3.88 (1H, app t, *J* 6.5, *H*5"), 3.91 (1H, app dt, *J* 10.1, 3.1, *H*5'), 4.09 (1H, A of ABX, $J_{AB}$ 11.3, $J_{AX}$ 6.5, C6"$H_aH_b$), 4.15 (1H, B of ABX, $J_{BA}$ 11.3, $J_{BX}$ 6.5, C6"$H_aH_b$), 4.58 (1H, d, *J* 8.1, *H*1"), 4.62 (1H, A of AB, $J_{AB}$ 12.2, C7'$H_aH_b$), 4.78 (1H, B of AB, $J_{BA}$ 12.2, C7'$H_aH_b$), 4.88 (1H, d, *J* 3.5, *H*1'), 4.95 (1H, dd, *J* 10.4, 3.4, *H*3"), 5.14 (1H, app t, *J* 9.7, *H*4'), 5.19 (1H, dd, *J* 10.4, 8.1, *H*2"), 5.36 (1H, br d, *J* 2.8, *H*4"), 5.42 (1H, app t, *J* 9.7, *H*3'), 7.44 (1H, dd, *J* 8.5, 1.4, *H*17'), 7.46 – 7.49 (2H, stack, 2 x Ar*H*), 7.75 (1H, s, *H*9'), 7.81 – 7.84 (3H, stack, 3 x Ar*H*); $\delta_C$(125 MHz, $CDCl_3$) 20.5 ($CH_3$, C2"CO*C*$H_3$), 20.6 (2 x $CH_3$, C3"CO*C*$H_3$, C4'CO*C*$H_3$), 20.6 ($CH_3$, C4"CO*C*$H_3$), 20.7 ($CH_3$, CO*C*$H_3$), 20.9 ($CH_3$, CO*C*$H_3$), 55.5 ($CH_3$, O*C*$H_3$), 61.4 ($CH_2$, *C*6"), 67.1 (CH, *C*4"), 67.8 ($CH_2$, *C*6'), 68.1 (CH, *C*5'), 68.6 (CH, *C*2"), 69.2 (CH, *C*4'), 71.0 (2 x CH, *C*3", *C*5"), 72.1 (CH, *C*3'), 73.7 ($CH_2$, *C*7'), 76.9 (CH, *C*2'), 99.0 (CH, *C*1'), 101.9 (CH, *C*1"), 125.9 (CH, *C*17'), 126.0 (*C*H, Ar), 126.1 (*C*H, Ar), 126.8 (CH, *C*9'), 127.7 (*C*H, Ar), 127.9 (CH, *C*11'), 128.2 (*C*H, Ar), 133.0 (quat. C, *C*15'), 133.2 (quat. C, *C*10'), 135.1 (quat. C, *C*8'), 169.8 (quat. C, C2"*C*O$CH_3$), 169.8 (quat. C, C4'*C*O$CH_3$), 169.9 (quat. C, C3'*C*O$CH_3$), 170.1 (quat. C, C3"*C*O$CH_3$), 170.2 (quat. C, C4"*C*O$CH_3$), 170.4 (quat. C, C6"*C*O$CH_3$); *m/z* (TOF $ES^+$) 771.2 (100%, $[M+Na]^+$). [HRMS *m/z* (TOF $ES^+$) Found: $[M+Na]^+$ 771.2466. $C_{36}H_{44}O_{17}Na$ requires 771.2476].

**ENZ 17**

Lactose (0.015 g, 0.043 mmol) and **33** (0.113 g, 0.30 mmol) were suspended in the mixed solvent system pH 7.0 buffer/MeCN 80:20 (0.75 mL) at 30 °C. The β-galactosidase from *B. circulans* (5.9 U, 17.6 mg, 19.6 U $mmol^{-1}$ acceptor) was then added and aliquots of the reaction solution were taken at regular intervals for analysis by HPLC and mass spectrometry. After 24 hours the reaction was stopped by denaturing the enzyme by heating. The reaction mixture was then freeze-dried and the carbohydrate residues were acetylated to facilitate the separation (by column chromatography, 6:4 hexane/EtOAc) of starting material from the products which were recovered by flushing the column with 5%

MeOH in EtOAc. This flushed fraction was further analysed and separated using analytical HPLC ($H_2O$/MeCN gradient 00% to 100 % over 50 minutes, 1 mL $min^{-1}$) and then mass spectrometry was performed on the components. Acetylated disaccharide **38** was recovered in 41% yield (14 mg).

**β-D-(-2,3,4,6-tetra-*O*-acetyl)-galactopyranoside-(1→2)-β-D-methyl-((2,3,4-tris-*O*-acetyl)-6-*O*-[2-(2-naphthylmethoxy)ethyl]glucopyranoside 38**

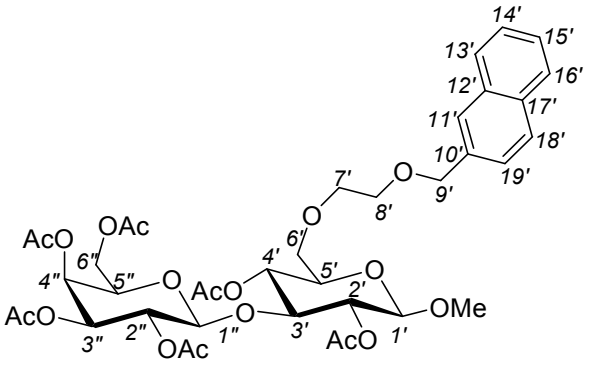


$C_{38}H_{48}O_{18}$
Exact Mass: 792.2841
Mol. Wt.: 792.7769
C, 57.57; H, 6.10; O, 36.33

Appearance: white powder; $\delta_H$(500 MHz, $CDCl_3$) 1.96 (3H, s, C3"COC*H*$_3$), 2.00 (3H, s, C4'COC*H*$_3$), 2.02 (3H, s, C2"COC*H*$_3$), 2.06 (3H, s, C6"COC*H*$_3$), 2.11 (3H, s, C2'COC*H*$_3$), 2.14 (3H, s, C4"COC*H*$_3$), 3.44 (3H, s, OC*H*$_3$), 3.58 (1H, A of ABX, $J_{AB}$ 11.6, $J_{AX}$ 6.9, C6'$H_aH_b$), 3.63 – 3.71 (6H, stack, including: B of ABX, C6'$H_aH_b$, 2 x *H*7', 2 x *H*8', *H*5'), 3.86 – 3.90 (2H, stack, *H*5", *H*3'), 4.17 (1H, A of ABX, $J_{AB}$ 11.1, $J_{AX}$ 6.2, C6"$H_aH_b$), 4.05 (1H, B of ABX, $J_{BA}$ 11.1, $J_{BX}$ 7.3, C6"$H_aH_b$), 4.28 (1H, d, *J* 8.0, *H*1'), 4.54 (1H, d, *J* 8.0, *H*1"), 4.72 (2H, s, 2 x *H*9'), 4.84 (1H, app t, *J* 9.4, *H*4'), 4.92 – 4.97 (2H, stack, *H*3", *H*2'), 5.07 (1H, dd, *J* 10.4, 8.0, *H*2"), 5.35 (1H, app d, *J* 2.8, *H*4"), 7.44 – 7.49 (3H, stack, *H*14', *H*15', *H*19'), 7.78 (1H, s, *H*11'), 7.81 – 7.83 (3H, stack, *H*13', *H*16', *H*18'); $\delta_C$(125 MHz, $CDCl_3$) 20.4 ($CH_3$, C2"CO*C*H$_3$), 20.5 ($CH_3$, C3"CO*C*H$_3$), 20.7($CH_3$, C6"CO*C*H$_3$, C4"CO*C*H$_3$), 20.8 ($CH_3$, C4'CO*C*H$_3$), 21.0 ($CH_3$, C2'CO*C*H$_3$), 56.6 ($CH_3$, O*C*H$_3$), 61.0 ($CH_2$, *C*6"), 66.8 (CH, *C*4"), 68.6 (CH, *C*2"), 69.5

(2 x CH, *C*8', *C*4'), 70.4 (CH, *C*5"), 70.8 ($CH_2$, *C*6'), 71.1 (CH, *C*3"), 71.3 ($CH_2$, *C*7'), 72.7 (CH, *C*2'), 73.3 ($CH_2$, *C*9'), 73.8 (CH, *C*5'), 78.6 (CH, *C*3'), 101.2 (CH, *C*1"), 101.3 (CH, *C*1'), 125.7 (CH, Ar), 125.8 (CH, Ar), 126.1 (CH, Ar), 126.4 (CH, *C*11'), 127.7 (CH, *C*18'), 127.8 (CH, *C*13'), 128.1 (CH, *C*16'), 133.0 (quat. C, *C*12'), 133.3 (quat. C, *C*17'), 135.7 (quat. C, *C*10'), 168.9 (quat. C, C2'*C*$OCH_3$), 169.3 (quat. C, C2"*C*$OCH_3$), 169.4 (quat. C, C4'*C*$OCH_3$), 170.2 (quat. C, C4"*C*$OCH_3$), 170.2 (quat. C, C3"*C*$OCH_3$), 170.4 (quat. C, C6"*C*$OCH_3$); *m/z* (TOF $ES^+$) 815.2 (100%, $[M+Na]^+$). [HRMS *m/z* (TOF $ES^+$) Found: $[M+Na]^+$ 815.2761. $C_{38}H_{48}O_{18}Na$ requires 815.2738].

**ENZ 18**

Lactose (0.011 g, 0.032 mmol) and **34** (0.096 g, 0.23 mmol) were suspended in the mixed solvent system pH 7.0 buffer/MeCN 80:20 (0.58 mL) at 30 $^oC$. The β-galactosidase from *B. circulans* (4.5 U, 13.5 mg, 19.6 U $mmol^{-1}$ acceptor) was then added and aliquots of the reaction solution were taken at regular intervals for analysis by HPLC and mass spectrometry. After 24 hours the reaction was stopped by denaturing the enzyme by heating. The reaction mixture was then freeze-dried and the carbohydrate residues were acetylated to facilitate the separation (by column chromatography, 6:4 hexane/EtOAc) of starting material from the products which were recovered by flushing the column with 5% MeOH in EtOAc. This flushed fraction was further analysed and separated using analytical HPLC ($H_2O$/MeCN (+ 0.05 % TFA) gradient 20% to 100 % over 40 minutes, 1 mL $min^{-1}$) and then mass spectrometry was performed on the components. Acetylated disaccharide **40** was recovered in <1% yield (4 mg).

**β-D-(-2,3,4,6-tetra-*O*-acetyl)-galactopyranoside-(1→2)-α-D-methyl-((2,3,4-tris-*O*-acetyl)-6-*O*-{2-[2-(2-naphthylmethoxy)ethoxy]ethyl}glucopyranoside 40**

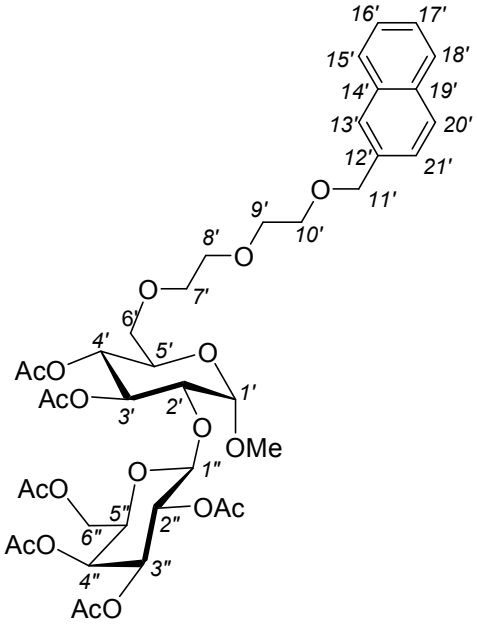


$C_{40}H_{52}O_{19}$
Exact Mass: 836.3103
Mol. Wt.: 836.8295
C, 57.41; H, 6.26; O, 36.33

Appearance: white powder; $\delta_H$(500 MHz, $CDCl_3$) 1.96 (3H, s, COC*H*$_3$), 1.99 (3H, s, COC*H*$_3$), 2.00 (3H, s, COC*H*$_3$), 2.04 (3H, s, COC*H*$_3$), 2.05 (3H, s, COC*H*$_3$), 2.15 (3H, s, COC*H*$_3$), 3.37 (3H, s, OC*H*$_3$), 3.54 (1H, A of ABX, $J_{AB}$ 11.1, $J_{AX}$ 4.6, C6'*H*$_a$H$_b$ ), 3.58 – 3.67 (9H, stack, C6'H$_a$*H*$_b$, C7'*H*$_2$, C8'*H*$_2$, C9'*H*$_2$, C10'*H*$_2$), 3.74 (1H, dd, *J* 10.1, 3.5, *H*2'), 3.83 (1H, app t, *J* 6.6, *H*5"), 3.85 – 3.89 (1H, m, *H*5'), 4.08 (1H, A of ABX, $J_{AB}$ 11.3, $J_{AX}$ 6.5, C6"*H*$_a$H$_b$), 4.13 (1H, B of ABX, $J_{BA}$ 11.3, $J_{BX}$ 6.5, C6"H$_a$*H*$_b$), 4.54 (1H, d, *J* 8.1, *H*1"), 4.71 (2H, s, C11'*H*$_2$), 4.83 (1H, d, *J* 3.5, *H*1'), 4.93 (1H, dd, *J* 10.4, 3.4, *H*3"), 5.02 (1H, app t, *J* 9.7, *H*4'), 5.18 (1H, dd, *J* 10.4, 8.1, *H*2"), 5.35 (1H, br d, *J* 2.7, H4"), 5.42 (1H, app t, *J* 9.7, *H*3'), 7.47 – 7.48 (3H, stack), 7.78 (1H, s), 7.82 – 7.84 (3H, stack); $\delta_C$(125 MHz, $CDCl_3$) 20.5 (CO*C*H$_3$), 20.6 (CO*C*H$_3$), 20.7 (CO*C*H$_3$), 20.9 (CO*C*H$_3$), 55.4 (CH$_3$, O*C*H$_3$), 61.4 (CH$_2$, *C*6"), 67.0 (CH, *C*4"), 68.2 (CH, *C*5'), 68.6 (CH, *C*2"), 69.4 (CH, *C*4'), 69.5 (CH$_2$), 69.8 (CH$_2$, *C*6'), 70.7 (CH$_2$), 70.8 (CH$_2$), 71.0 (CH, *C*5"), 71.1 (CH, *C*3"), 71.2 (CH$_2$, *C*7'), 72.0 (CH, *C*3'), 73.3 (CH$_2$, *C*11'), 77.1 (CH, *C*2'), 98.8 (CH, *C*1'), 101.9 (CH, *C*1"), 125.8 (CH, Ar), 125.9 (CH, Ar), 126.1 (CH, Ar), 126.4 (CH, Ar), 127.7 (CH, Ar), 127.8 (CH, Ar), 128.1 (CH, Ar), 133.0 (quat. C, Ar), 133.3 (quat. C, Ar), 135.8 (quat. C, Ar), 169.0 (quat. C, *C*=O), 169.8 (quat. C, *C*=O), 169.9 (quat. C, *C*=O), 170.1 (quat. C, *C*=O), 170.2 (quat. C, *C*=O), 170.3 (quat. C, *C*=O); *m/z* (TOF ES$^+$)

859.3 (100%, $[M+Na]^+$). [HRMS *m/z* (TOF $ES^+$) Found: $[M+Na]^+$ 859.3015. $C_{40}H_{52}O_{19}Na$ requires 859.3000].

## 5.4 Combinatorial Reactions

**DCC1**

Using a 12-position reaction carousel, a solution of **46** (1 mL, concentration and solvent shown in table below) was added to a solution of the thio-sugar **45** in MeOH (1 mL, concentration shown in table 4.3.1.1b below). To this was added x equiv. of a 1 M activating solution of 1:1 $Et_3N$ and thiophenol. The reaction mixtures were heated to 40 $^oC$ and stirred for 72 h. In the case of reactions i – viii, additional activating solution was added at 24 and 48 h. 40 μL aliquots were taken from each reaction at 0, 24, 48 and 72 h. These aliquots were diluted in MeOH (500 μL) and refrigerated prior to analysis by MS.

Variables:

| Reaction number | **46** solvent | **46** conc m/M | **45** (MeOH) conc /mM | **x** equiv. of activating solution | Activating solution added: |
|---|---|---|---|---|---|
| **i** | $CHCl_3$ | 5 | 5 | 0.3 | daily |
| **ii** | $CHCl_3$ | 5 | 5 | 0.6 | daily |
| **iii** | $CHCl_3$ | 10 | 10 | 0.3 | daily |
| **iv** | $CHCl_3$ | 10 | 10 | 0.6 | daily |
| **v** | acetone | 5 | 5 | 0.3 | daily |
| **vi** | acetone | 5 | 5 | 0.6 | daily |
| **vii** | acetone | 10 | 10 | 0.3 | daily |
| **viii** | acetone | 10 | 10 | 0.6 | daily |
| **ix** | $CHCl_3$ | 5 | 5 | 0.6 | once |
| **x** | $CHCl_3$ | 10 | 10 | 0.6 | once |

| | | | | | |
|---|---|---|---|---|---|
| **xi** | acetone | 5 | 5 | 0.6 | once |
| **xii** | acetone | 10 | 10 | 0.6 | once |

Table 4.3.1.1b

**DCC2 larger scale reaction conditions ix**

Two identical reaction mixtures (A and B) were prepared by adding of a solution of **46** in $CHCl_3$ (4 mL, 5 mM) to a solution of the thio-sugar **45** in MeOH (4 mL, 5 mM). 0.6 equiv. of the activating solution of 1:1 $Et_3N$ and thiophenol (24 μL, 1 M) was then added. The reaction mixtures were heated to 40 °C and stirred for 48 h. 40 μL aliquots were taken from each reaction at 0, 1, 2, 4, 6, 8, 24, 30 and 48 h. These aliquots were diluted in 1000 μL of MeOH and refrigerated prior to analysis by MS. At 48 h the two reaction mixtures were cooled and refrigerated to freeze the disulfide exchange reaction.

**DCC3**

The solvent in the pooled combinatorial libraries from DCC1 and DCC2 was removed under reduced pressure. The resultant residue was then taken up in a mixture of buffer and MeCN (300 μL, pH 5.0 NaOAc buffer with 20% MeCN). Gal-*O*-*p*Np (3.0 mg, 0.017 mmol) was added to the reaction solution which was then heated at 30 °C. A control aliquot (5 μL) was taken prior to adding 2.4 U of the β-galactosidase from *B. circulans* (3.0 mg, 19.6 U/mmol acceptor). 5 μL aliquots were taken at 0, 1, 2, 3, 4, 6 and 24 h at which point the reaction was stopped by heating to 90 °C for 5 min. Each aliquot was diluted in 62.5 μL of MeCN and submitted for mass spectrometry and HPLC [analytical HPLC, $H_2O$/MeCN (+0.05% TFA) gradient 20% to 100% over 50 minutes]. Separation of the components generated from the enzyme reaction was done by preparative HPLC under the same conditions.

**DCC4**

12 identical reaction mixtures were prepared by adding of a solution of **46**in MeOH (16 mL, 5 mM) to a reaction vessel containing the following solutions in $CHCl_3$: 2-naphthyl mercaptan (4 mL, 5 mM), **46** (4 mL, 5 mM), **47** (4 mL, 5 mM), **48** (4 mL, 5 mM). 0.6 equiv of a solution of $Et_3N$ in $CHCl_3$ (96 μL,. 1 M) was then added. The reaction mixtures were heated to 40 $^oC$ and stirred for 11 d. 500 μL aliquots were taken from each reaction at 0, 1, 2, 4, 6, 24, 48, 72, 96 h and finally at 11 days. These aliquots were diluted in 1000 μL of MeOH and refrigerated prior to analysis by MS.

## References


(1) Dwek, R. A. *Chem. Rev.* **1996**, *96*, 683-720.
(2) Thobhani, S.; Ember, B.; Siriwardena, A.; Boons, G.-J. *J. Am. Chem. Soc.* **2003**, *125*, 7154-7155.
(3) Varki, A. *Glycobiology* **1993**, *3*, 97 - 130.
(4) Ambrosi, M.; Cameron, N. R.; Davis, B. G. *Org. Biomol. Chem.* **2005**, *3*, 1593-1608.
(5) Ramström, O.; Lehn, J.-M. *ChemBioChem* **2000**, *1*, 41-48.
(6) Wong, C.-H.; Whitesides, G. M. *Enzymes in Synthetic Organic Chemistry*; Academic Press, 1994, 392.
(7) Cantarel, B.; Coutinho, P.; Rancurel, C.; Bernard, T.; Lombard, V.; Henrissat, B. *Nucleic. Acids. Res.* **2009**, D233-238.
(8) Wong, C. H.; Haynie, S. L.; Whitesides, G. M. *J. Org. Chem.* **1982**, *47*, 5416-5418.
(9) MartÃ-n, R. n.; Murruzzu, C.; PericÃ s, M. A.; Riera, A. *The Journal of Organic Chemistry* **2005**, *70*, 2325-2328.
(10) Pi-Hui, L.; Wei-Chieh, C.; Yi-Ling, L.; Han-Pang, Y.; Ying-Ta, W.; Yi-Ling, L.; Chi-Huey, W. *ChemBioChem* **2006**, *7*, 165-173.
(11) Kumar, N. S.; Pinto, B. M. *Carb. Res.* **2006**, *341*, 1685-1691.
(12) Sinnott, M. L. *Chem. Rev.* **1990**, *90*, 1171-1202.
(13) Galjaard, H.; Hoogeveen, A.; Keijzer, W.; De Wit-Verbeek, H. A.; Reuser, A. J. J.; Wan Ho, M. A. E.; Robinson, D. *Nature* **1975**, *257*, 60-62.
(14) Lee, W. C.; Tsoi, Y. K.; Troendle, F. J.; DeLucia, M. W.; Ahmed, Z.; Dicky, C. A.; Dickson, D. W.; Eckman, C. B. *The FASEB Journal* **2007**, *21*, 2520-2527.
(15) Swagerty, D. J.; Walling, A.; Klein, R. *Am. Fam. Physician* **2002**, *65*, 1845-1850.
(16) Andrew, P. B.; Charles, G. H., Jr.; Clyde, H. A. *Biotechnol. Bioeng.* **1992**, *39*, 408-417.
(17) Kren, V.; Thiem, J. *Chem. Soc. Rev.* **1997**, *26*, 463 - 473.
(18) Oberthur, M.; Leimkuhler, C.; Kruger, R. G.; Lu, W.; Walsh, C. T.; Kahne, D. *J. Am. Chem. Soc.* **2005**, *127*, 10747-10752.
(19) Fialová, P.; Carmona, A. T.; Robina, I.; Ettrich, R.; Sedmera, P.; Prikrylová, V.; Petrásková-Husáková, L.; Kren, V. *Tetrahedron Lett.* **2005**, *46*, 8715-8718.
(20) Satoh, T.; Takeichi, H.; Mitsuo, N. *Chem. Pharm. Bull.* **1984**, *32*, 1183 - 1187.
(21) Murata, T.; Kosugi, M.; Nakamura, T.; Urashima, T.; Usui, T. *Biosci. Biotechnol. Biochem.* **2001**, *65*, 2456-2464.
(22) Scigelova, M.; Singh, S.; Crout, D. H. G. *J. Mol. Catal. B: Enzym.* **1999**, *6*, 483-494.
(23) Crout, D. H. G.; Vic, G. *Curr. Opin. Chem. Biol.* **1998**, *2*, 98-111.
(24) Augé, C.; Crout, D. H. G. *Carb. Res.* **1997**, *305*, 307-312.
(25) Withers, S. G. *Pure Appl. Chem.* **1995**, *67*, 1673 - 1682.
(26) Vic, G.; Thomas, D. *Tetrahedron Lett.* **1992**, *33*, 4567-4570.
(27) Finch, P.; Yoon, J. H. *Carb. Res.* **1997**, *303*, 339-345.
(28) Hopkinson, S. M.; Pridham, J. B. *Biochem. J.* **1967**, *105*, 655-662.
(29) Pan, S. C. *Biochemistry* **1970**, *9*, 1833-1838.
(30) Vic, G.; Crout, D. H. G. *Tetrahedron: Asymmetry* **1994**, *5*, 2513-2516.
(31) Itano, K.; Yamasaki, K.; Kihara, C.; Tanaka, O. *Carb. Res.* **1980**, *87*, 27-34.
(32) Weingarten, S.; Thiem, J. *Org. Biomol. Chem.* **2004**, *2*, 961-962.
(33) Teiji, K.; Shuichi, T.; Hongmei, H.; Chi-Huey, W. *Angew. Chem. Int. Ed.* **1996**, *35*, 2348-2350.
(34) Kaltsoyannis, N.; Scott, P. *The f-elements*; Oxford University Press, 1999, 85.
(35) Sardar, P. S.; Samanta, S.; Roy, M. B.; Ghosh, S. *Mol. Phys.* **2008**, *106*, 827-840.
(36) Zucchi, G.; Scopelliti, R.; Bunzli, J.-C. G. *J. Chem. Soc., Dalton Trans.* **2001**, 1975-1985.
(37) Bunzli, J.-C. G.; Piguet, C. *Chem. Soc. Rev.* **2005**, *34*, 1048-1077.
(38) Gunnlaugsson, T.; Mac Donaill, D. A.; Parker, D. *J. Am. Chem. Soc.* **2001**, *123*, 12866-12876.
(39) Maffeo, D.; Williams, J. A. G. *Inorg. Chim. Acta* **2003**, *355*, 127-136.

(40) Bunzli, J.-C. G. *Chem. Rev.* **2010**, *110*, 2729-2755.
(41) Glover, P. B.; Ashton, P. R.; Childs, L. J.; Rodger, A.; Kercher, M.; Williams, R. M.; De Cola, L.; Pikramenou, Z. *J. Am. Chem. Soc.* **2003**, *125*, 9918-9919.
(42) Corinna, M. S.; Christian, S.; Michael, S. *Ann. N.Y. Acad. Sci.* **2008**, *1130*, 138-148.
(43) Michael, S.; Otto , S. W. *Chem. Eur. J.* **2007**, *13*, 4342-4349.
(44) Douglas, H. J.; Raymond, H. J.; Dale, W.; Xue-Jun, Z.; Reuben, E. H.; Dale, E. T.; Brian, W. M. *Protein Sci.* **2000**, *9*, 1685-1699.
(45) Richard, J. P.; Westerfeld, J. G.; Lin, S. *Biochemistry* **1995**, *34*, 11703-11712.
(46) Takayama, S.; Shimazaki, M.; Qiao, L.; Wong, C.-H. *Bioorg. Med. Chem. Lett.* **1996**, *6*, 1123-1126.
(47) Farkas, E.; Schmidt, U.; Thiem, J.; Kowalczyk, J.; Kunz, M.; Vogel, M. *Synthesis* **2003**, *2003*, 0699-0706.
(48) Vic, G.; Hao Tran, C.; Scigelova, M.; H. G. Crout, D. *Chem. Commun.* **1997**, *0*, 169-170.
(49) Singh, S.; Scigelova, M.; Vic, G.; Crout, D. H. G. *J. Chem. Soc., Perkin Trans. 1* **1996**, 1921-1926.
(50) Cadotte, J. E.; Smith, F.; Spriestersbach, D. *J. Am. Chem. Soc.* **1952**, *74*, 1501-1504.
(51) Wang, P.; Shen, G. J.; Wang, Y. F.; Ichikawa, Y.; Wong, C. H. *J. Org. Chem.* **1993**, *58*, 3985-3990.
(52) Wu, X.; Tang, X.; Xian, M.; Brauschweiger, P. G.; Wang, P. G. *Bioorg. Med. Chem.* **2002**, *10*, 2303-2307.
(53) Beignet, J. PhD Thesis, University of Birmingham, 2004.
(54) Murphy, P. V.; Bradley, H.; Tosin, M.; Pitt, N.; Fitzpatrick, G. M.; Glass, W. K. *J. Org. Chem.* **2003**, *68*, 5692-5704.
(55) Domagala, J. M.; Heifetz, C. L.; Hutt, M. P.; Mich, T. F.; Nichols, J. B.; Solomon, M.; Worth, D. F. *J. Med. Chem.* **1988**, *31*, 991-1001.
(56) Hans, P. M.; Yvo, C.; Rainer, E.; Anna, K.; Henri, R.; Karl, B.; Murray, G.; Kenneth, L. M. *Helv. Chim. Acta* **1988**, *71*, 320-336.
(57) Foroughifar, N.; Leffek, K. T.; Lee, Y. G. *Can. J. Chem.* **1993**, *71*, 164-166.
(58) Barbara, C.; Valerie, D. H.; Sergey, A. N.; Françisco, M. R.; Neil, S.; Stoddart, J. F. *Chem. Eur. J.* **1998**, *4*, 1244-1254.
(59) Roen, A.; Padron, J. I.; Vazquez, J. T. *J. Org. Chem.* **2003**, *68*, 4615-4630.
(60) Hanessian, S.; Lavallee, P. *Can. J. Chem.* **1975**, *53*, 2975-2977.
(61) Corey, E. J.; Venkateswarlu, A. *J. Am. Chem. Soc.* **1972**, *94*, 6190-6191.
(62) Davis, B. G.; Nash, R. J.; Watson, A. A.; Smith, C.; Fleet, G. W. J. *Tetrahedron* **1999**, *55*, 4501-4520.
(63) Smith, G. V.; Notheisz, F. In *Heterogeneous Catalysis in Organic Chemistry*; Academic Press: San Diego, 1999.
(64) Horita, K.; Yoshioka, T.; Tanaka, T.; Oikawa, Y.; Yonemitsu, O. *Tetrahedron* **1986**, *42*, 3021-3028.
(65) Maji, S.; Viswanathan, K. S. *J. Lumin.* **2008**, *128*, 1255-1261.
(66) Quici, S.; Cavazzini, M.; Raffo, M. C.; Botta, M.; Giovenzana, G. B.; Ventura, B.; Accorsi, G.; Barigelletti, F. *Inorg. Chim. Acta* **2007**, *360*, 2549-2557.
(67) Conover, C. D.; Zhao, H.; Longley, C. B.; Shum, K. L.; Greenwald, R. B. *Bioconjugate Chem.* **2003**, *14*, 661-666.
(68) Ross, P. C.; Hui, S. W. *Biochim. Biophys. Acta, Biomembr.* **1999**, *1421*, 273-283.
(69) Park, I. K.; Kim, T. H.; Park, Y. H.; Shin, B. A.; Choi, E. S.; Chowdhury, E. H.; Akaike, T.; Cho, C. S. *J. Controlled Release* **2001**, *76*, 349-362.
(70) Wittmann, V.; Takayama, S.; Gong, K. W.; Weitz-Schmidt, G.; Wong, C. H. *J. Org. Chem.* **1998**, *63*, 5137-5143.
(71) Visintin, C.; Aliev, A. E.; Riddall, D.; Baker, D.; Okuyama, M.; Hoi, P. M.; Hiley, R.; Selwood, D. L. *Org. Lett.* **2005**, *7*, 1699-1702.
(72) Laville, I.; Pigaglio, S.; Blais, J. C.; Doz, F.; Loock, B.; Maillard, P.; Grierson, D. S.; Blais, J. *J. Med. Chem.* **2006**, *49*, 2558-2567.
(73) Takaya, K.; Nagahori, N.; Kurogochi, M.; Furuike, T.; Miura, N.; Monde, K.; Lee, Y. C.; Nishimura, S. I. *J. Med. Chem.* **2005**, *48*, 6054-6065.
(74) Wright, J. A.; Yu, J.; Spencer, J. B. *Tetrahedron Lett.* **2001**, *42*, 4033-4036.

(75) Corey, F. A.; Sundberg, R. J. *Advanced Organic Chemistry part B: Reactions and Synthesis*; 5th ed.; Springer-Verlag, 2007, 1322.
(76) Chaudhary, S. K.; Hernandez, O. *Tetrahedron Lett.* **1979**, *20*, 95-98.
(77) Robertson, G. J. *J. Chem.Soc* **1933**, 737-739.
(78) Kocienski, P. J. *Protecting Groups*; 3rd ed.; Thieme, 2005, 679.
(79) Tennant-Eyles, R. J.; Davis, B. G.; Fairbanks, A. J. *Tetrahedron: Asymmetry* **2000**, *11*, 231-243.
(80) Kang, S. U.; Worthy, K. M.; Bindu, L. K.; Zhang, M.; Yang, D.; Fisher, R. J.; Burke, T. R. *J. Med. Chem.* **2005**, *48*, 5369-5372.
(81) Bullpitt, M.; Kitching, W.; Doddrell, D.; Adcock, W. *J. Org. Chem.* **1976**, *41*, 760-766.
(82) Bouzide, A.; Sauvé, G. *Tetrahedron Lett.* **1997**, *38*, 5945-5948.
(83) Simpkins, S. M. E.; Kariuki, B. M.; Cox, L. R. *J. Organomet. Chem.* **2006**, *691*, 5517-5523.
(84) Reeve, W.; McCaffery, E. L.; Kaiser, T. E. *J. Am. Chem. Soc.* **1954**, *76*, 2280-2281.
(85) Hernaiz, M. J.; Crout, D. H. G. *Enzyme Microb. Technol.* **2000**, *27*, 26-32.
(86) Erzsébet, F.; Joachim, T. *Eur. J. Org. Chem.* **1999**, *1999*, 3073-3077.
(87) Petit, J.-M.; Paquet, F.; Beau, J.-M. *Tetrahedron Lett.* **1991**, *32*, 6125-6128.
(88) Sauerbrei, B.; Thiem, J. *Tetrahedron Lett.* **1992**, *33*, 201-204.
(89) Lehn, J.-M.; Eliseev, A. V. *Science* **2001**, *291*, 2331-2332.
(90) Huc, I.; Nguyen, R. *Combinatorial Chemistry & High Throughput Screening* **2001**, *4*, 53-74.
(91) Ramström, O.; Lohmann, S.; Bunyapaiboonsri, T.; Lehn, J.-M. *Chem. Eur. J.* **2004**, *10*, 1711-1715.
(92) West, K. R.; Ludlow, R. F.; Corbett, P. T.; Besenius, P.; Mansfeld, F. M.; Cormack, P. A. G.; Sherrington, D. C.; Goodman, J. M.; Stuart, M. C. A.; Otto, S. *J. Am. Chem. Soc.* **2008**, *130*, 10834-10835.
(93) Otto, S.; Furlan, R. L. E.; Sanders, J. K. M. *Science* **2002**, *297*, 590-593.
(94) Lees, W. J.; Whitesides, G. M. *J. Org. Chem.* **1993**, *58*, 642-647.
(95) Bach, R. D.; Dmitrenko, O.; Thorpe, C. *J. Org. Chem.* **2007**, *73*, 12-21.
(96) Otto, S.; Furlan, R. L. E.; Sanders, J. K. M. *J. Am. Chem. Soc.* **2000**, *122*, 12063-12064.
(97) Corbett, P. T.; Leclaire, J.; Vial, L.; West, K. R.; Wietor, J.-L.; Sanders, J. K. M.; Otto, S. *Chem. Rev.* **2006**, *106*, 3652-3711.
(98) Guyon, V.; Guy, A.; Foos, J.; Lemaire, M.; Draye, M. *Tetrahedron* **1995**, *51*, 4065-4074.
(99) Nasyrov, D. V.; Bobyleva, A. A.; Abramov, A. A.; Anfilogova, S. N.; Vasil'kov, M. A.; Anisimov, A. V. *Chem. Heterocycl. Compd.* **2002**, *38*, 456-465.
(100) Gigg, R.; Penglis, A. A. E.; Conant, R. *J. Chem. Soc., Perkin Trans. 1* **1980**, 2490-2493.
(101) Enright, P. M.; O'Boyle, K. M.; Murphy, P. V. *Org. Lett.* **2000**, *2*, 3929-3932.
(102) Rojas, M. T.; Koeniger, R.; Stoddart, J. F.; Kaifer, A. E. *J. Am. Chem. Soc.* **1995**, *117*, 336-343.
(103) Hioki, H.; Still, W. C. *J. Org. Chem.* **1998**, *63*, 904-905.
(104) Nicolaou, K. C.; Robert, H.; Jeffrey, A. P.; Sofia, B.; Roecker, A. J. *Chem. Eur. J.* **2001**, *7*, 4280-4295.
(105) Kreevoy, M. M.; Harper, E. T.; Duvall, R. E.; Wilgus, H. S.; Ditsch, L. T. *J. Am. Chem. Soc.* **1960**, *82*, 4899-4902.
(106) Dinev, Z.; Gannon, C. T.; Egan, C.; Watt, J. A.; McConville, M. J.; Williams, S. J. *Org. Biomol. Chem.* **2007**, *5*, 952-959.
(107) Aspinall, G. O.; Carpenter, R. C.; Khondo, L. *Carb. Res.* **1987**, *165*, 281-298.
(108) Gottlieb, H. E.; Kotlyar, V.; Nudelman, A. *J. Org. Chem.* **1997**, *62*, 7512-7515.
(109) Card, P. J.; Reddy, G. S. *J. Org. Chem.* **1983**, *48*, 4734-4743.
(110) Waykole, L.; Prashad, M.; Palermo, S.; Repic, O.; Blacklock, T. J. *Synth. Commun.* **1997**, *27*, 2159-2163.
(111) Demirci-Gültekin, D.; Günbas, D. D.; Taskesenligil, Y.; Balci, M. *Tetrahedron* **2007**, *63*, 8151-8156.
(112) Valérie, P.; Astrid , A. V.; Erick , M. C. *Chem. Eur. J.* **2008**, *14*, 2465-2481.

(113) Newcomb, L. F.; Haque, T. S.; Gellman, S. H. *J. Am. Chem. Soc.* **1995**, *117*, 6509-6519.
(114) Kartha, K. P. R.; Field, R. A. *Tetrahedron* **1997**, *53*, 11753-11766.
(115) Hunsen, M.; Long, D. A.; D'Ardenne, C. R.; Smith, A. L. *Carb. Res.* **2005**, *340*, 2670-2674.
(116) Roy, R.; Tropper, F. D.; Morrison, T.; Boratynski, J. *J. Chem. Soc., Chem. Commun.* **1991**, 536-538.

# APPENDIX

## Additional data for chapter 2

**Experimental data, UV plots for:**

**Methyl-6-*O*-(2-naphthylmethyl)-α-D-glucopyranoside 32**

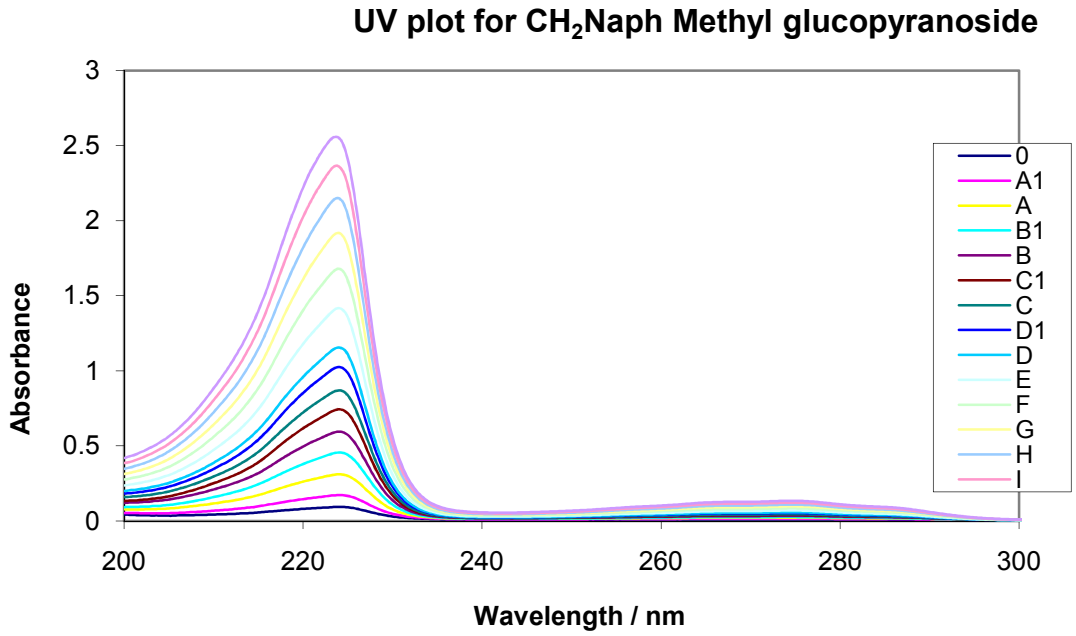


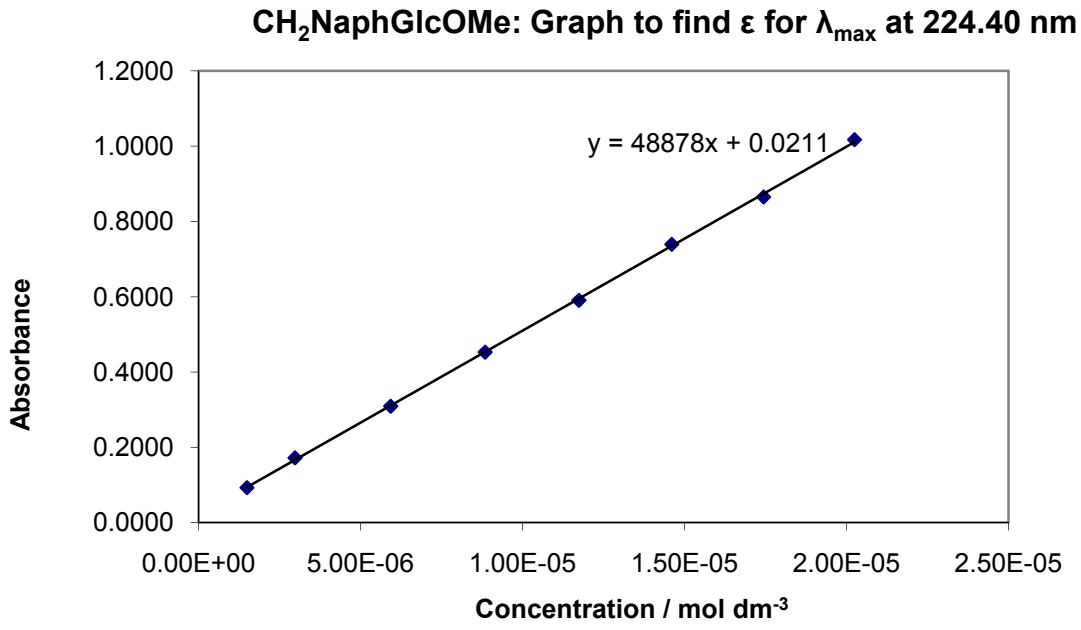

**β-Methyl-6-*O*-(ethoxy-2-naphthylmethyl)-D-glucopyranoside 33**

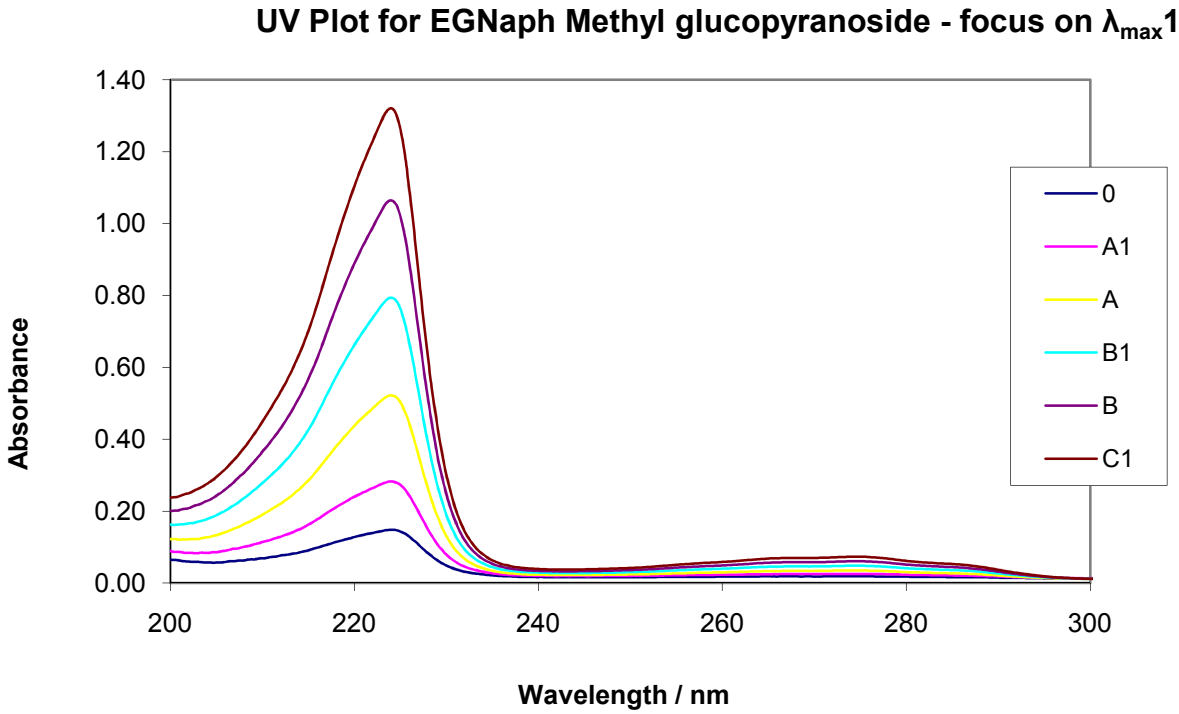


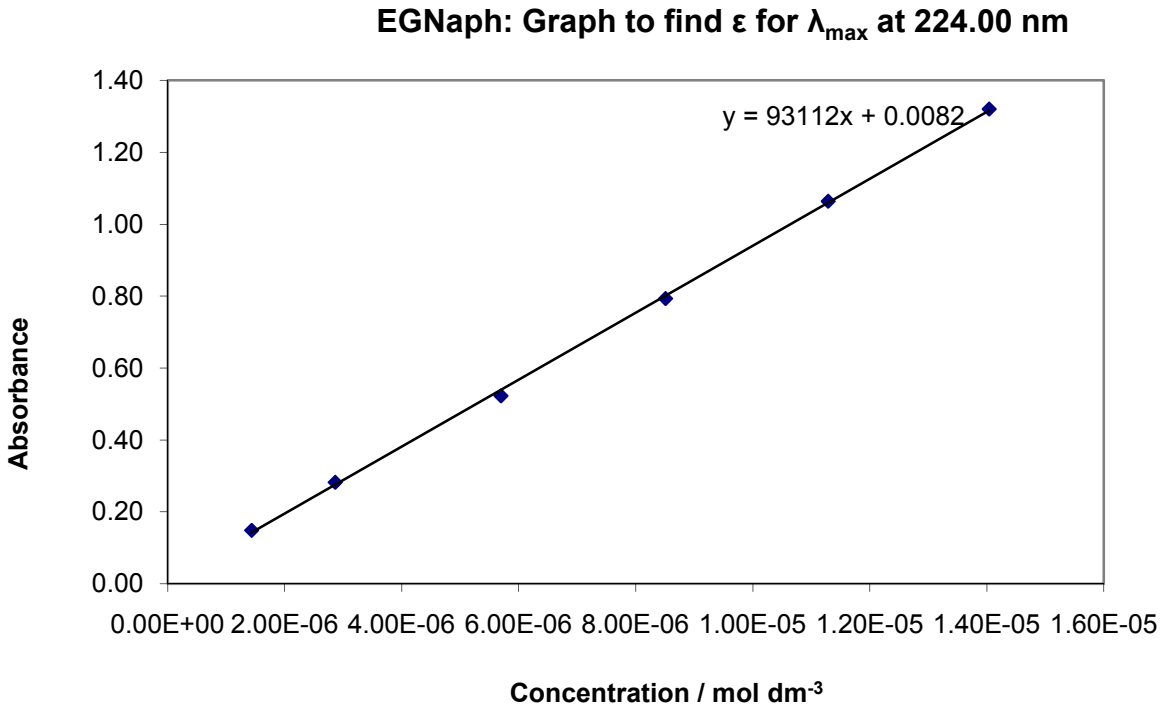

**Methyl-6-*O*-(7'-ethoxy-9'[ethoxy-2-naphthylmethyl])-α--D-glucopyranoside 34**

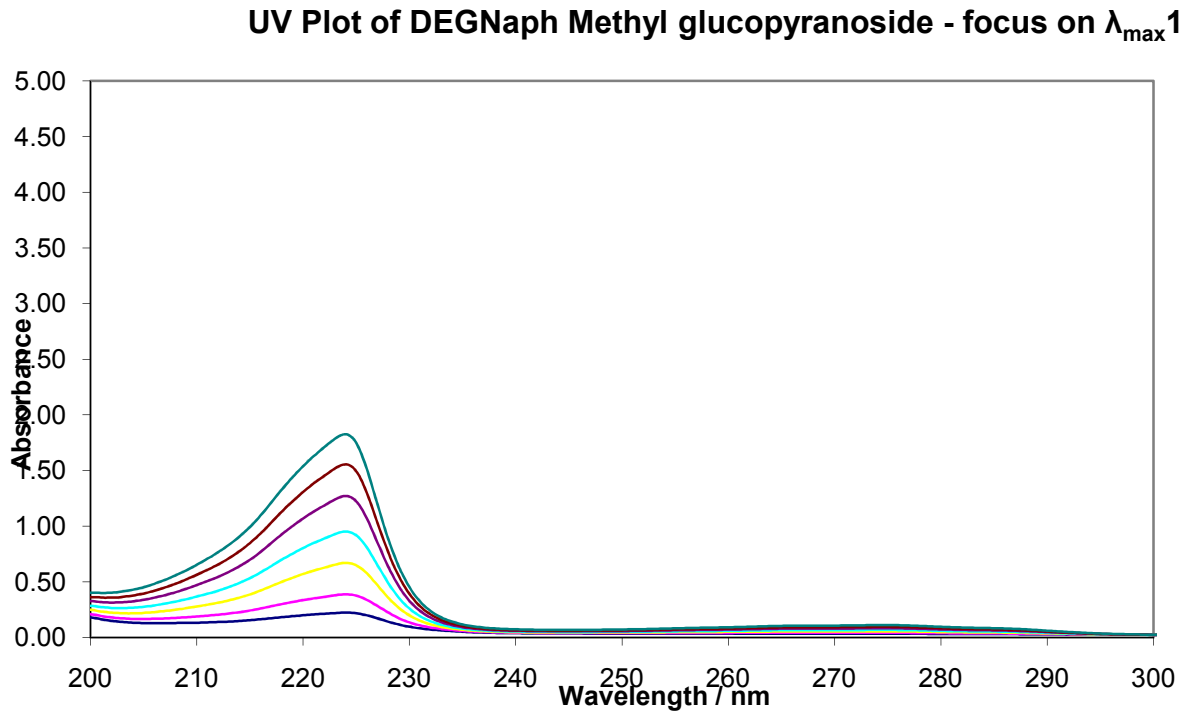


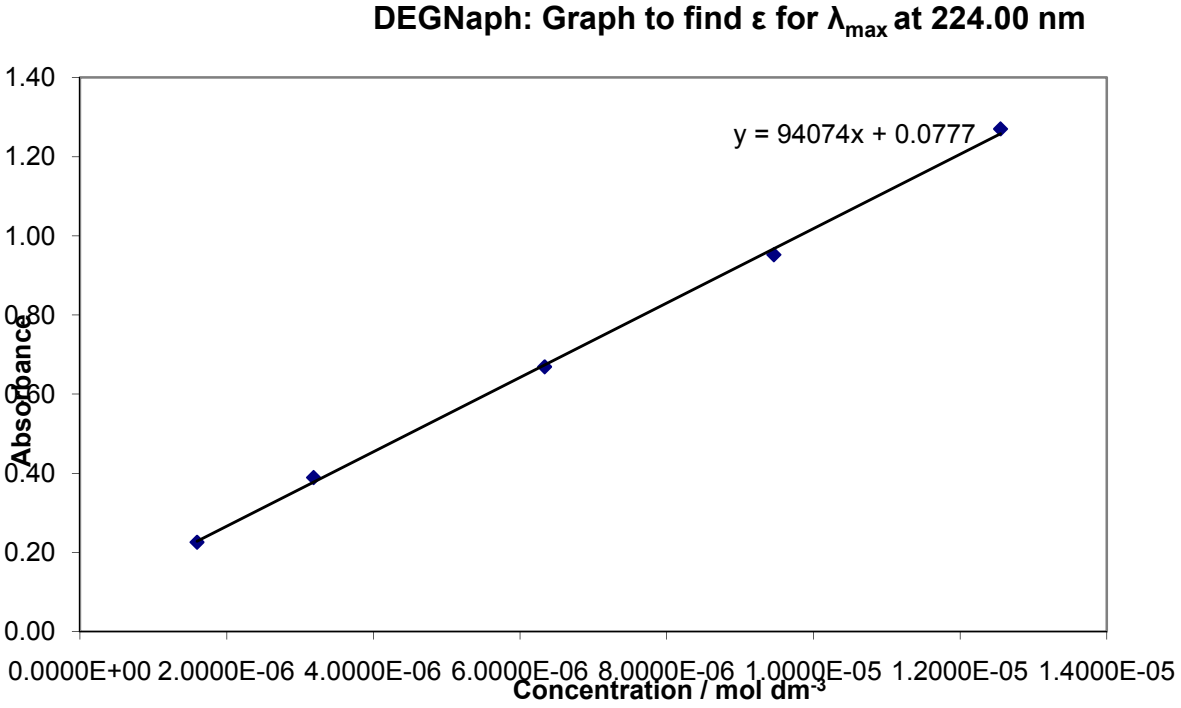

# Additional data for chapter 3

## 3.3.2

UV plot for p-nitrophenolate to determine the Molar Extinction Coeffient

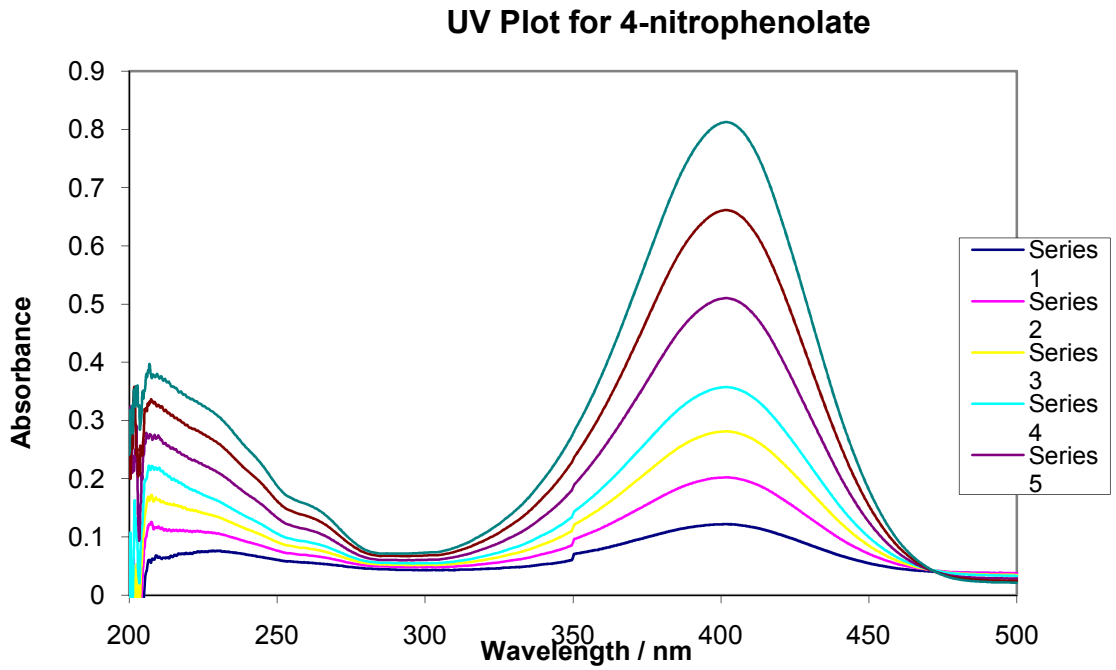


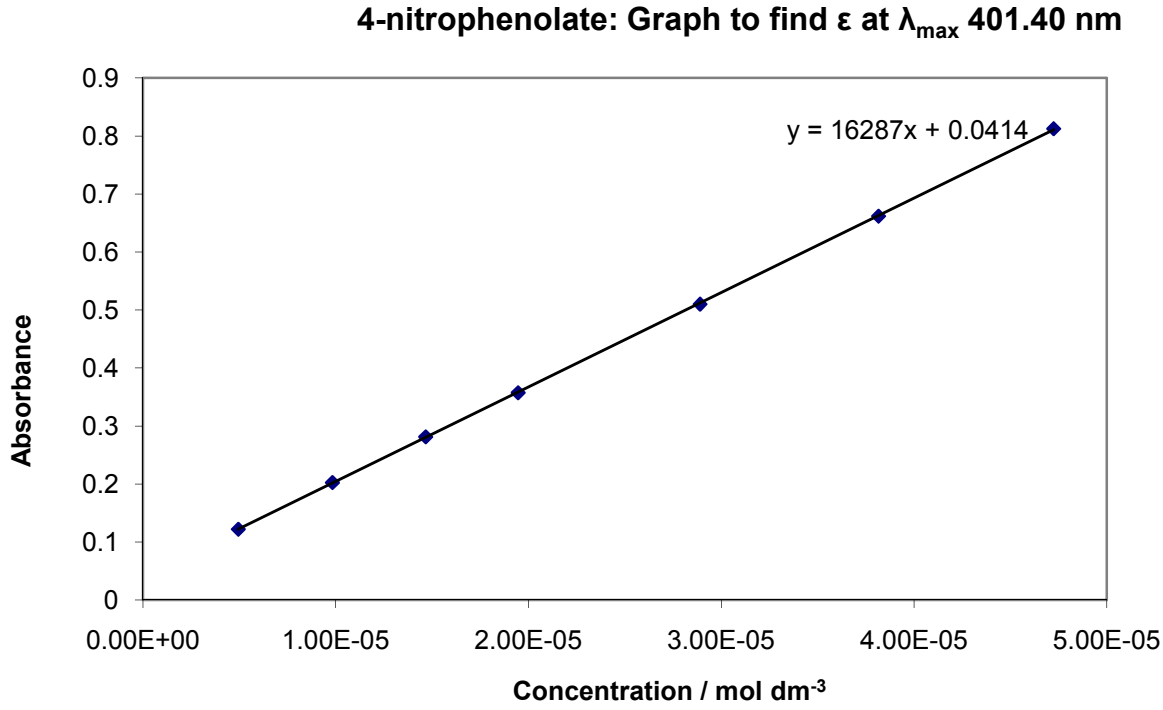

**ENZ 10 (P115)**

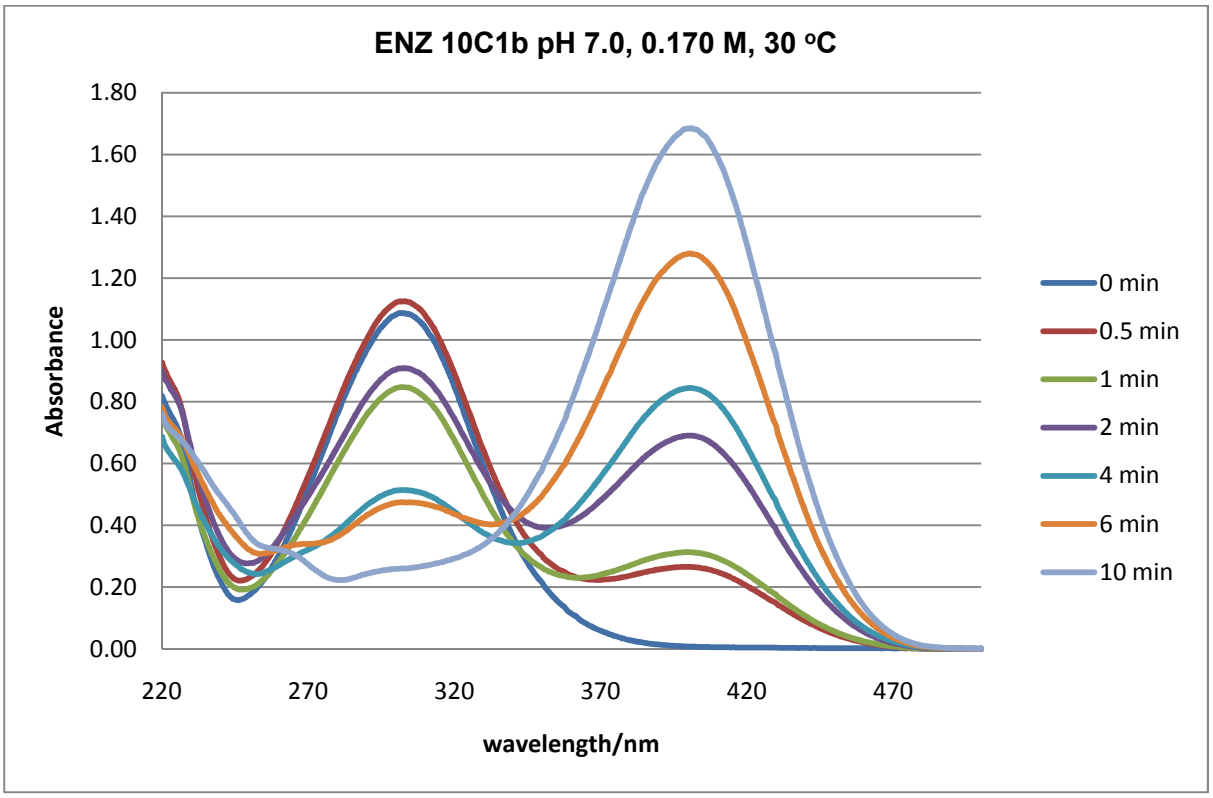
ENZ 10C1b pH 7.0, 0.170 M, 30 °C
Absorbance
1.80
1.60
1.40
1.20
1.00
0.80
0.60
0.40
0.20
0.00
220
270
320
370
420
470
wavelength/nm
0 min
0.5 min
1 min
2 min
4 min
6 min
10 min

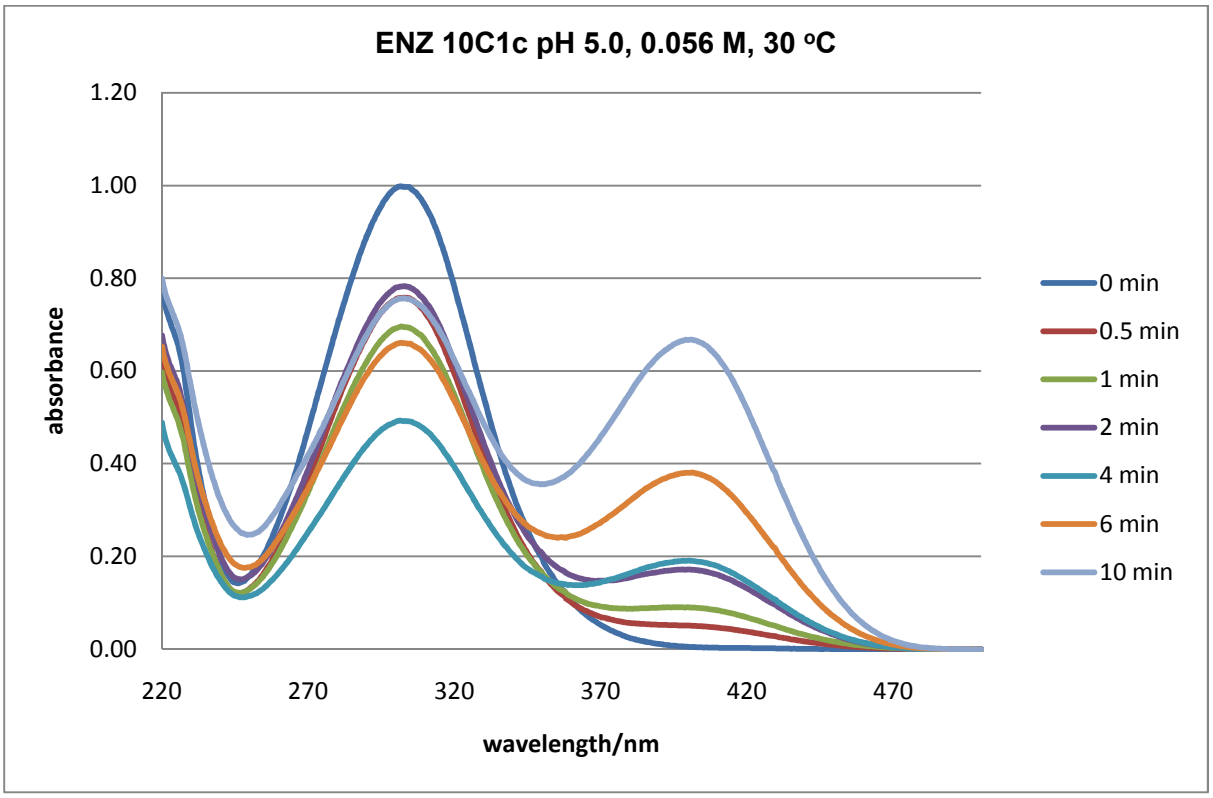
ENZ 10C1c pH 5.0, 0.056 M, 30 °C
absorbance
1.20
1.00
0.80
0.60
0.40
0.20
0.00
220
270
320
370
420
470
wavelength/nm
0 min
0.5 min
1 min
2 min
4 min
6 min
10 min

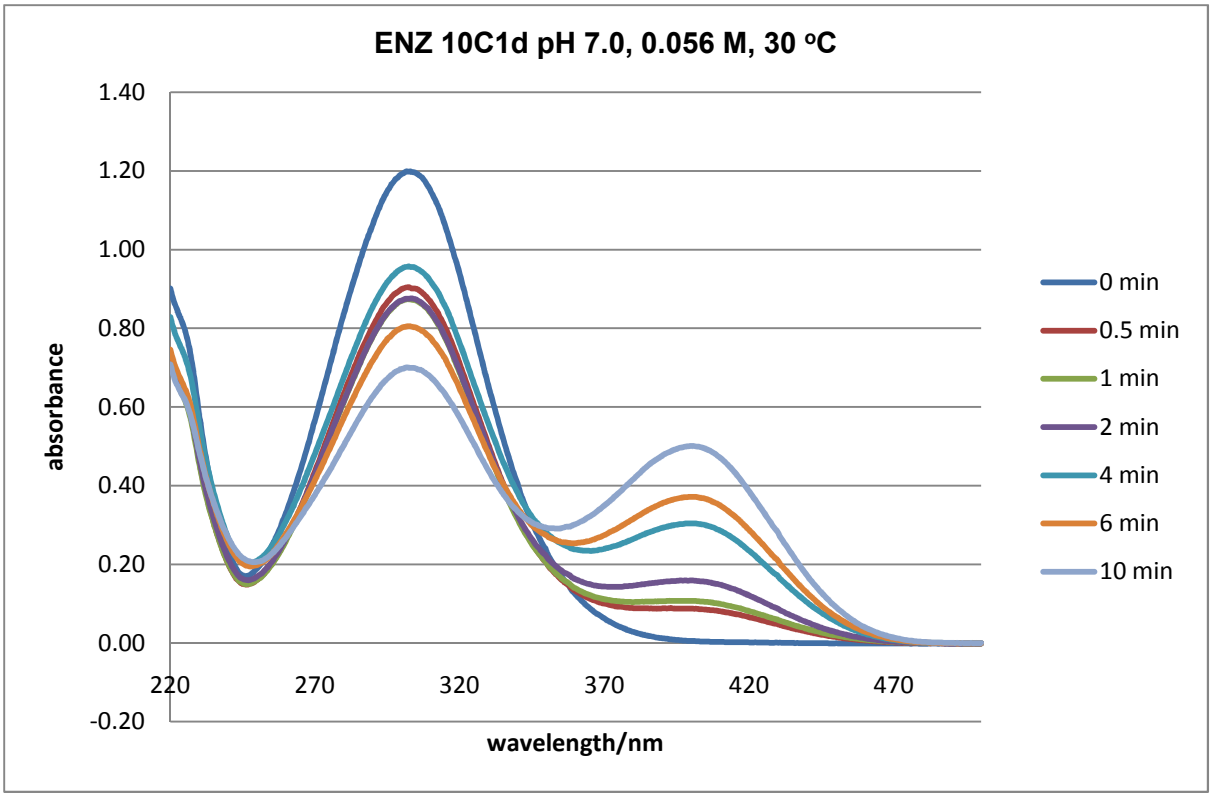
ENZ 10C1d pH 7.0, 0.056 M, 30 °C
absorbance
1.40
1.20
1.00
0.80
0.60
0.40
0.20
0.00
-0.20
220
270
320
370
420
470
wavelength/nm
0 min
0.5 min
1 min
2 min
4 min
6 min
10 min

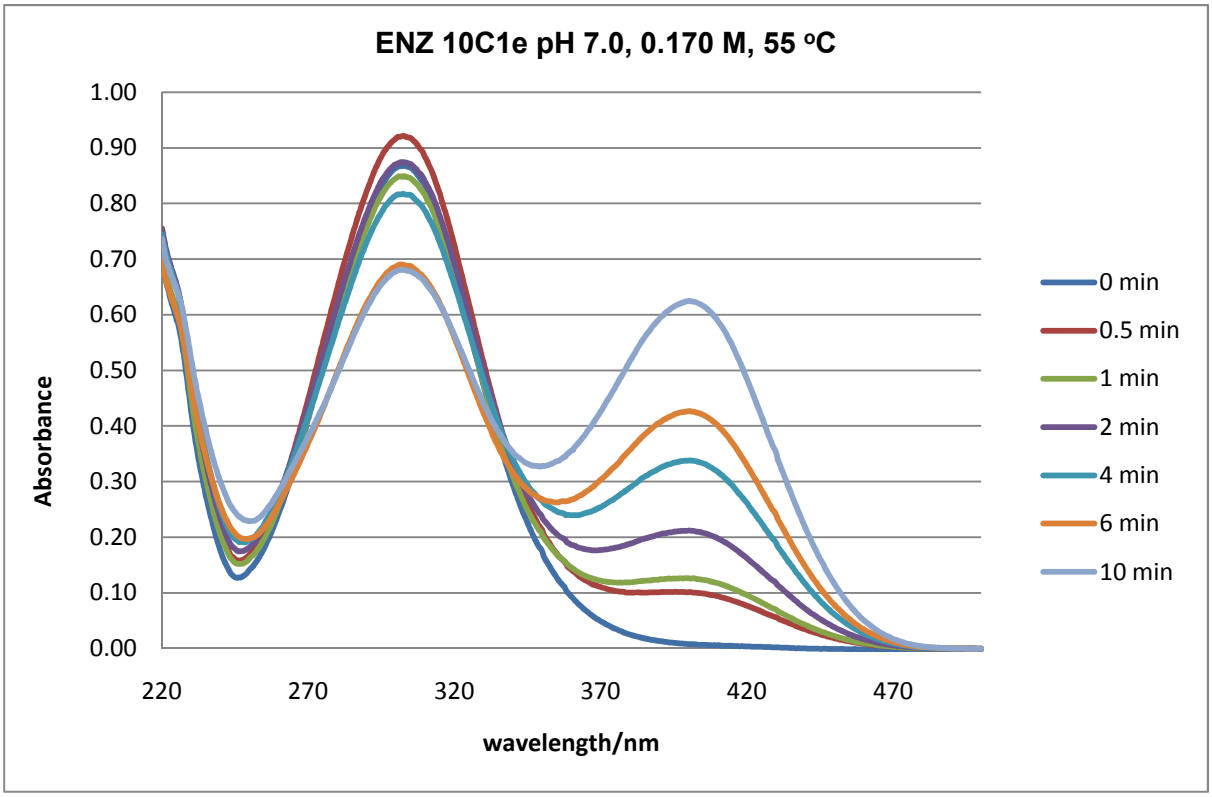
ENZ 10C1e pH 7.0, 0.170 M, 55 °C
Absorbance
1.00
0.90
0.80
0.70
0.60
0.50
0.40
0.30
0.20
0.10
0.00
220
270
320
370
420
470
wavelength/nm
0 min
0.5 min
1 min
2 min
4 min
6 min
10 min

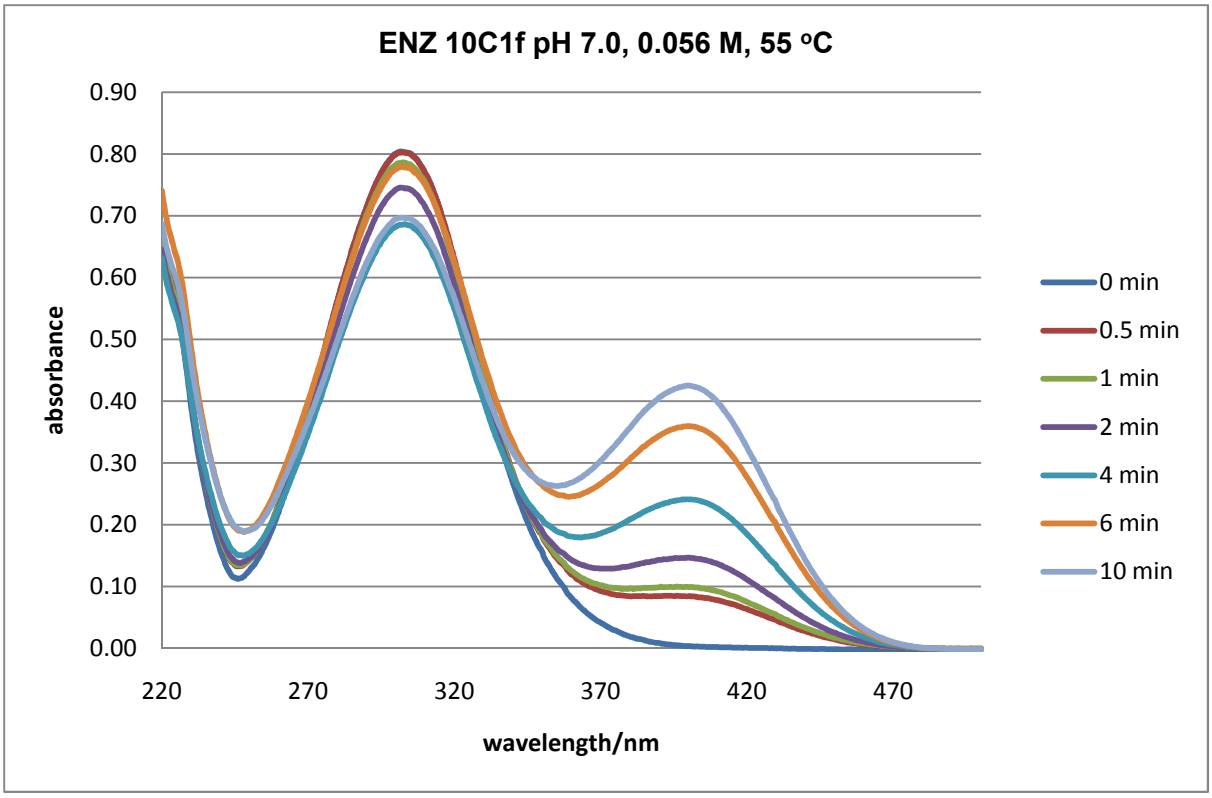


## ENZ 11 (P122)

### MeCN UV plots

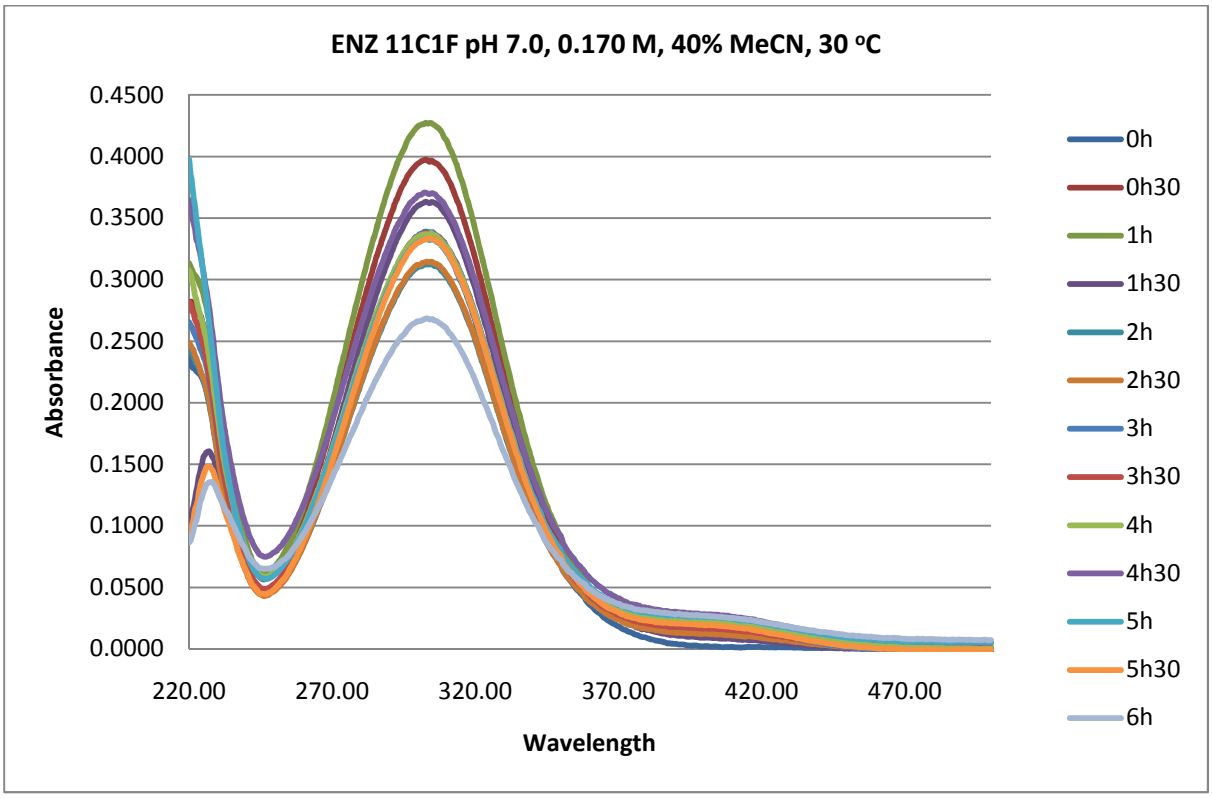

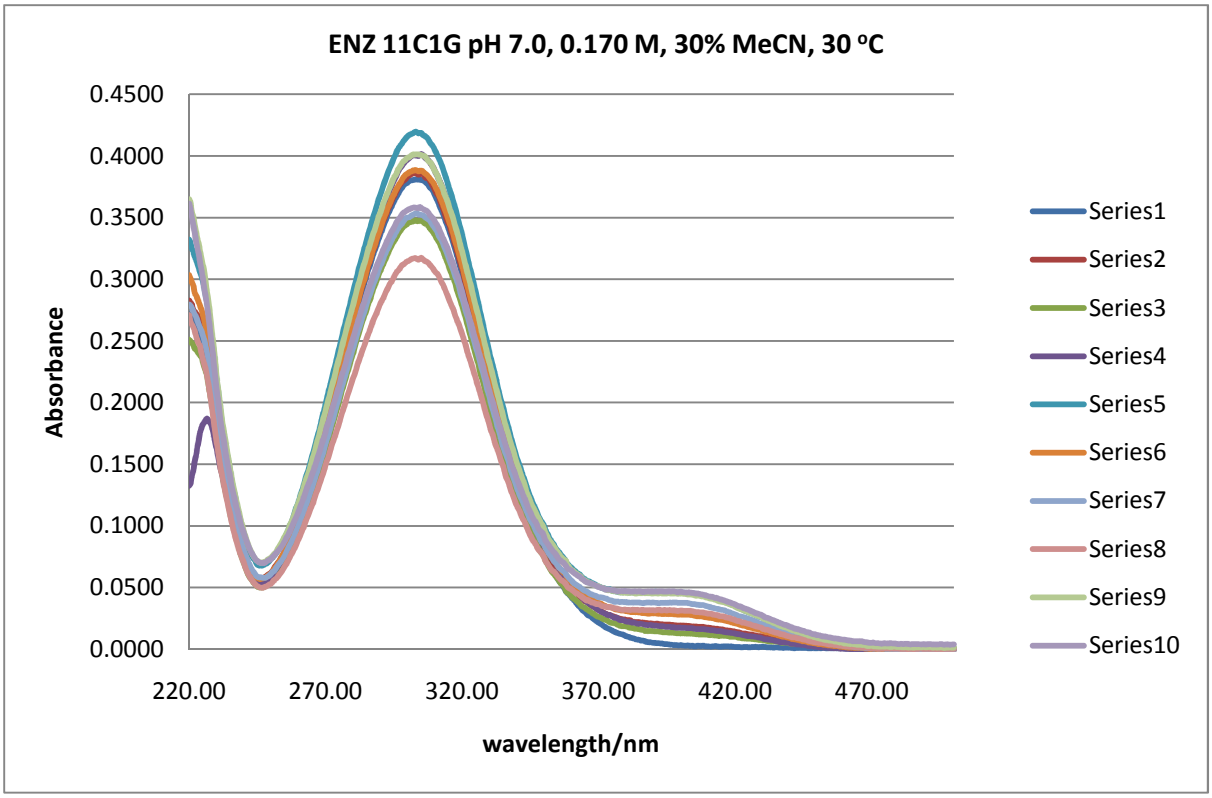
ENZ 11C1G pH 7.0, 0.170 M, 30% MeCN, 30 °C
Absorbance
0.4500
0.4000
0.3500
0.3000
0.2500
0.2000
0.1500
0.1000
0.0500
0.0000
220.00
270.00
320.00
370.00
420.00
470.00
wavelength/nm
Series1
Series2
Series3
Series4
Series5
Series6
Series7
Series8
Series9
Series10

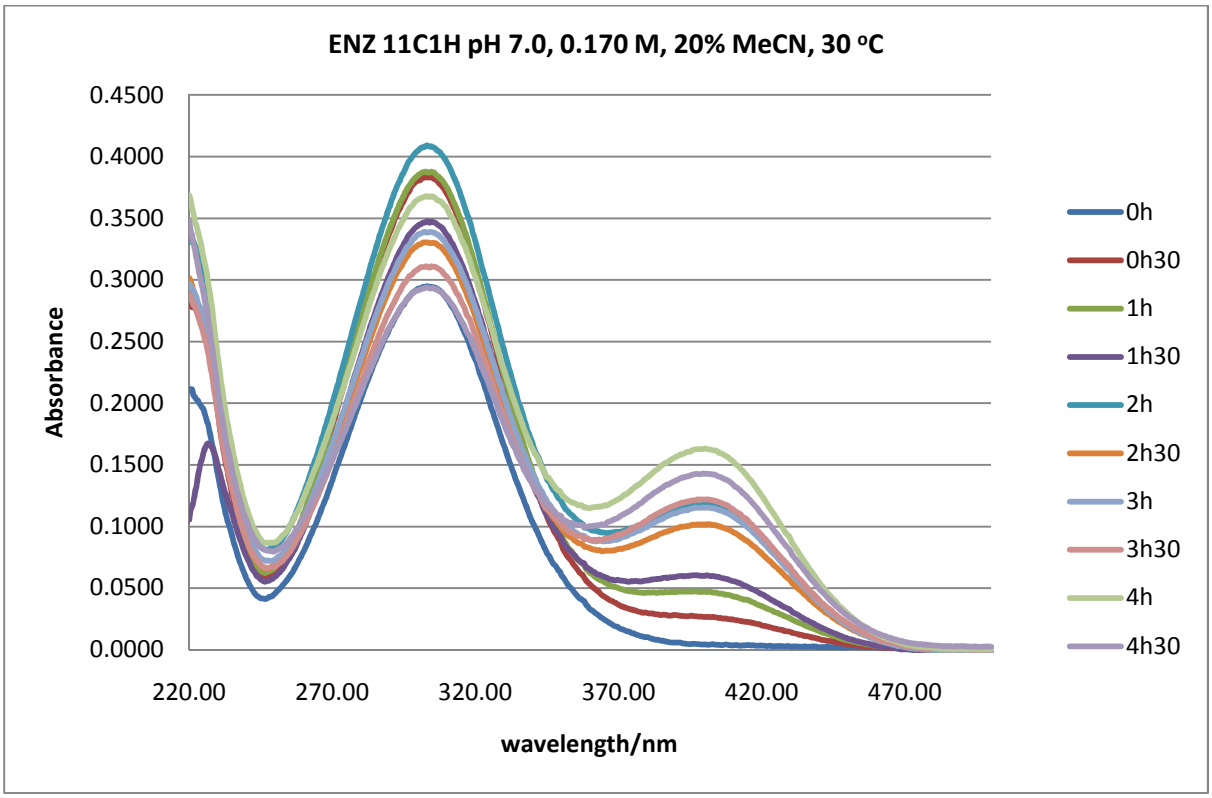
ENZ 11C1H pH 7.0, 0.170 M, 20% MeCN, 30 °C
Absorbance
0.4500
0.4000
0.3500
0.3000
0.2500
0.2000
0.1500
0.1000
0.0500
0.0000
220.00
270.00
320.00
370.00
420.00
470.00
wavelength/nm
0h
0h30
1h
1h30
2h
2h30
3h
3h30
4h
4h30

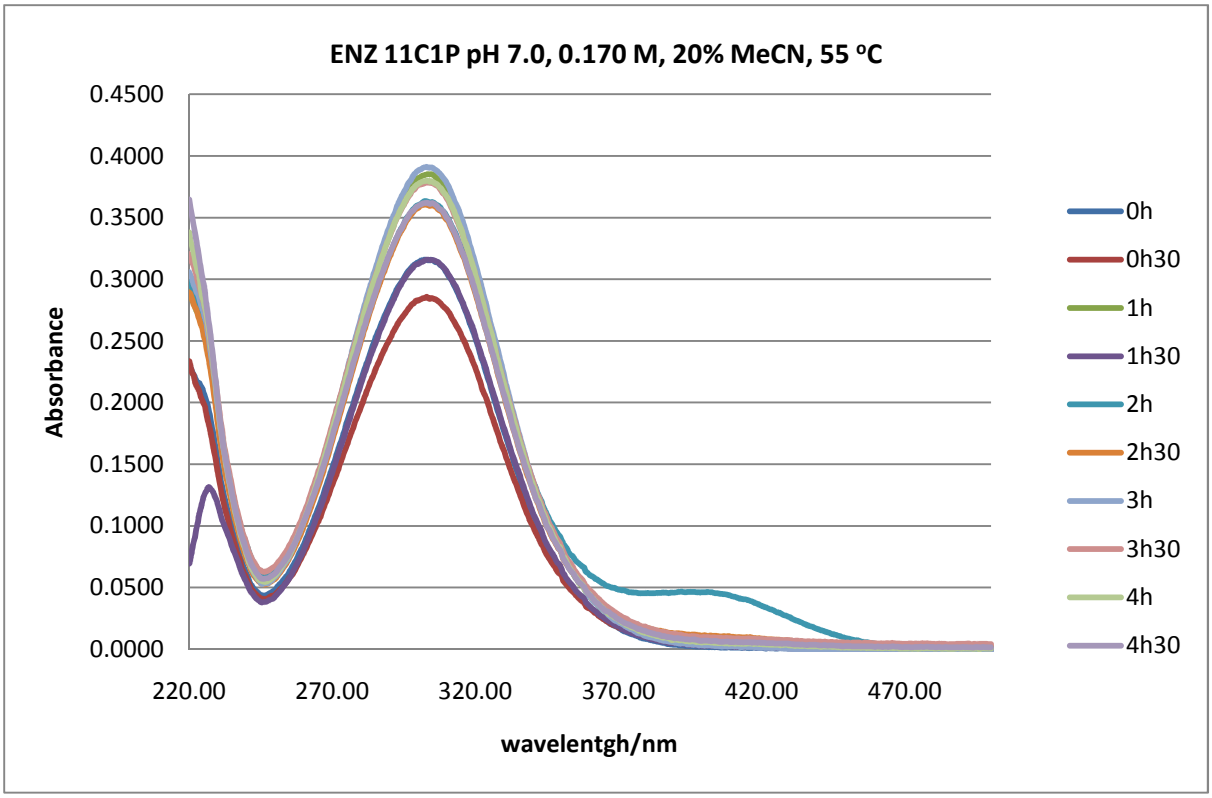
ENZ 11C1P pH 7.0, 0.170 M, 20% MeCN, 55 ºC
Absorbance
0.4500
0.4000
0.3500
0.3000
0.2500
0.2000
0.1500
0.1000
0.0500
0.0000
220.00
270.00
320.00
370.00
420.00
470.00
wavelentgh/nm
0h
0h30
1h
1h30
2h
2h30
3h
3h30
4h
4h30

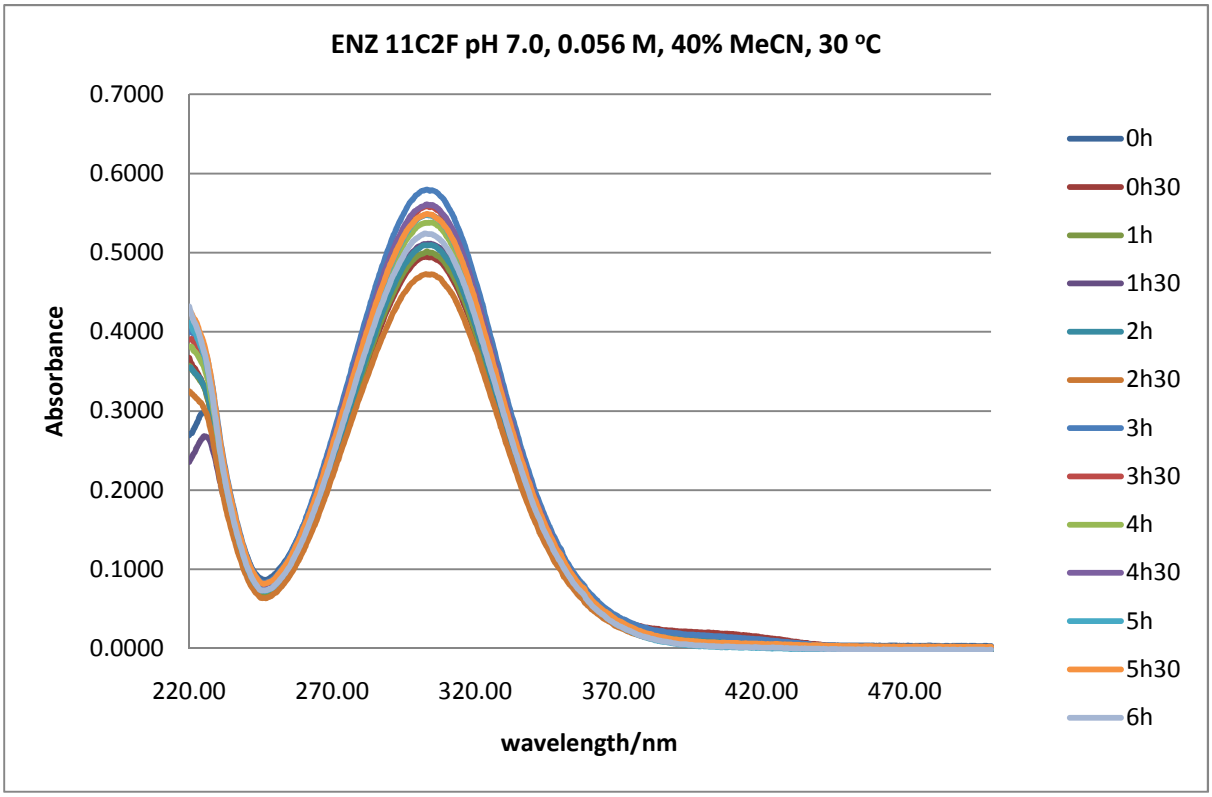
ENZ 11C2F pH 7.0, 0.056 M, 40% MeCN, 30 ºC
Absorbance
0.7000
0.6000
0.5000
0.4000
0.3000
0.2000
0.1000
0.0000
220.00
270.00
320.00
370.00
420.00
470.00
wavelength/nm
0h
0h30
1h
1h30
2h
2h30
3h
3h30
4h
4h30
5h
5h30
6h

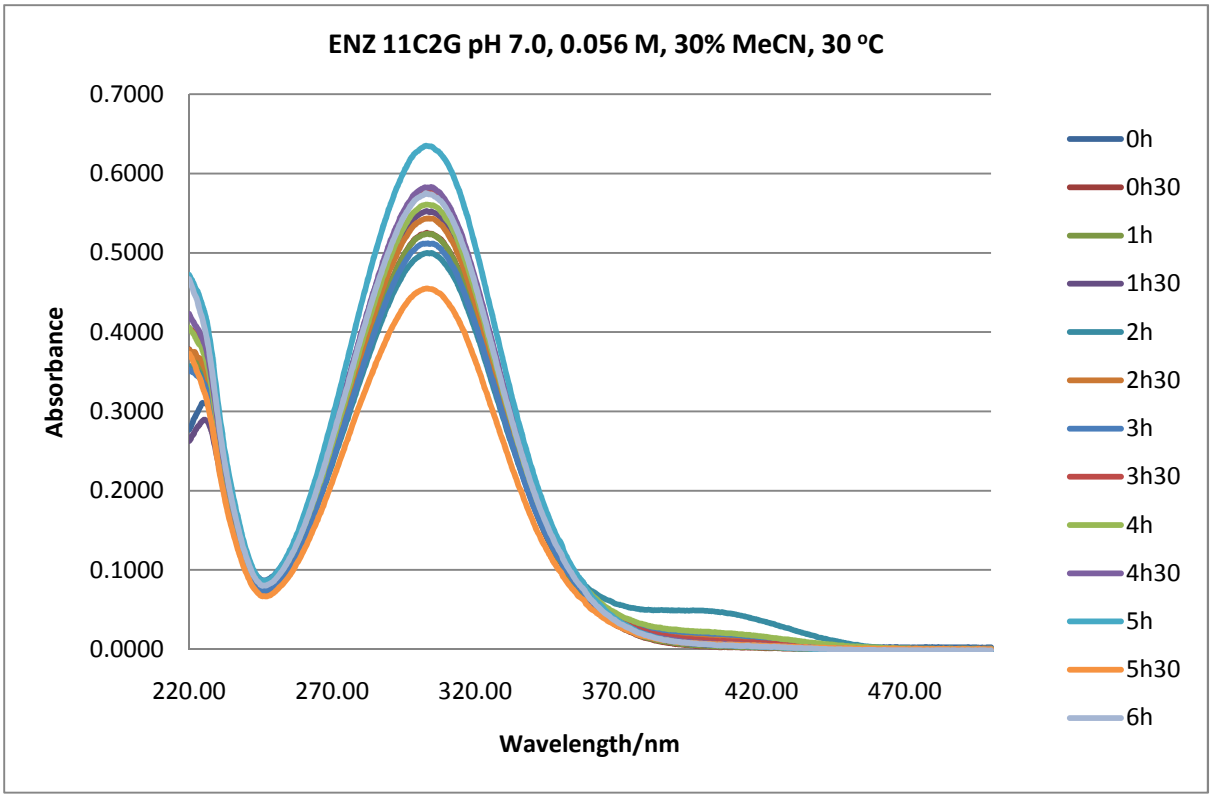
ENZ 11C2G pH 7.0, 0.056 M, 30% MeCN, 30 °C
Absorbance
0.7000
0.6000
0.5000
0.4000
0.3000
0.2000
0.1000
0.0000
220.00
270.00
320.00
370.00
420.00
470.00
Wavelength/nm
0h
0h30
1h
1h30
2h
2h30
3h
3h30
4h
4h30
5h
5h30
6h

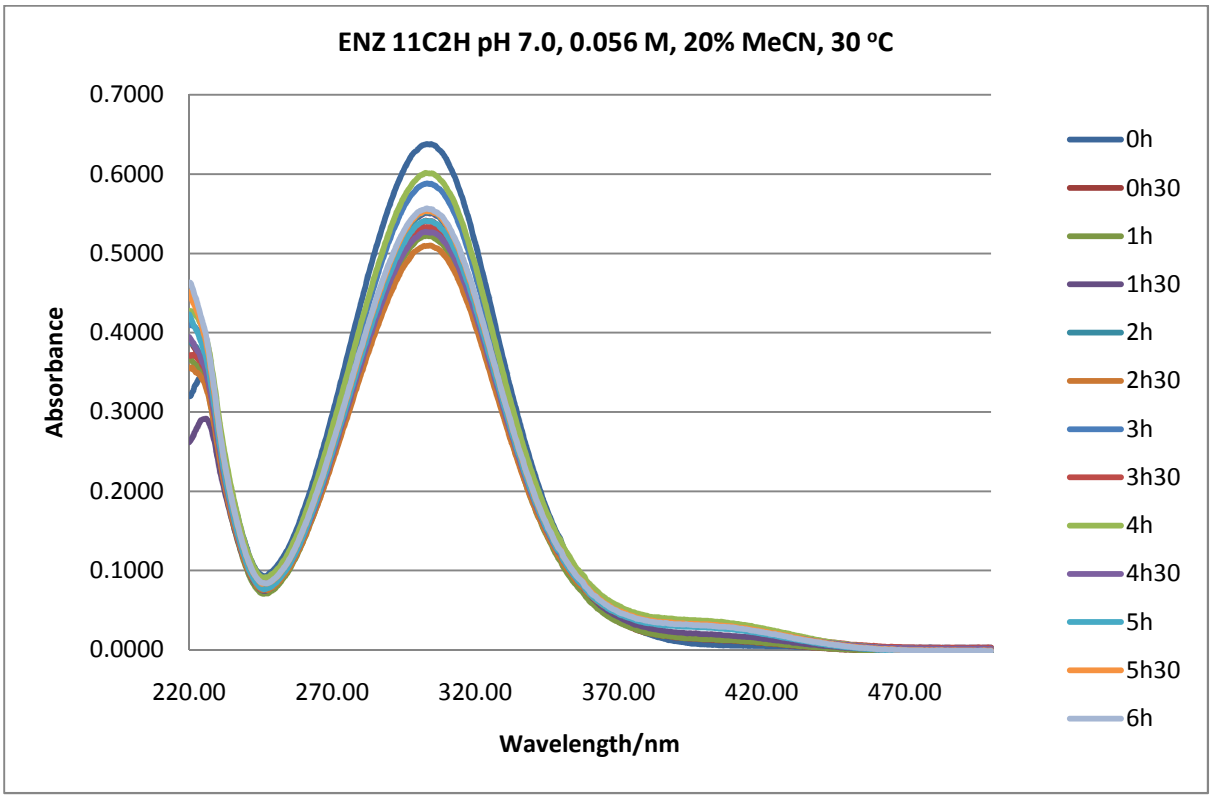
ENZ 11C2H pH 7.0, 0.056 M, 20% MeCN, 30 °C
Absorbance
0.7000
0.6000
0.5000
0.4000
0.3000
0.2000
0.1000
0.0000
220.00
270.00
320.00
370.00
420.00
470.00
Wavelength/nm
0h
0h30
1h
1h30
2h
2h30
3h
3h30
4h
4h30
5h
5h30
6h

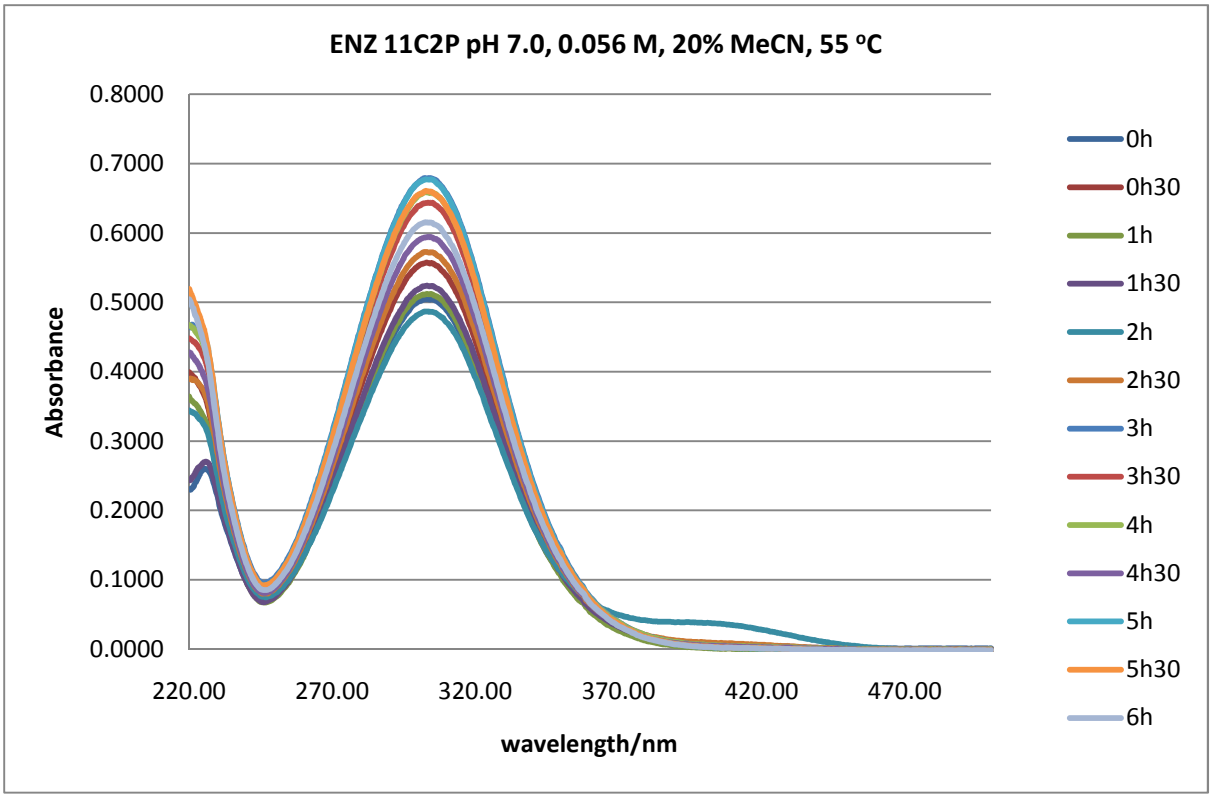


## ENZ12 (P127)

### Increased enzyme UV plots

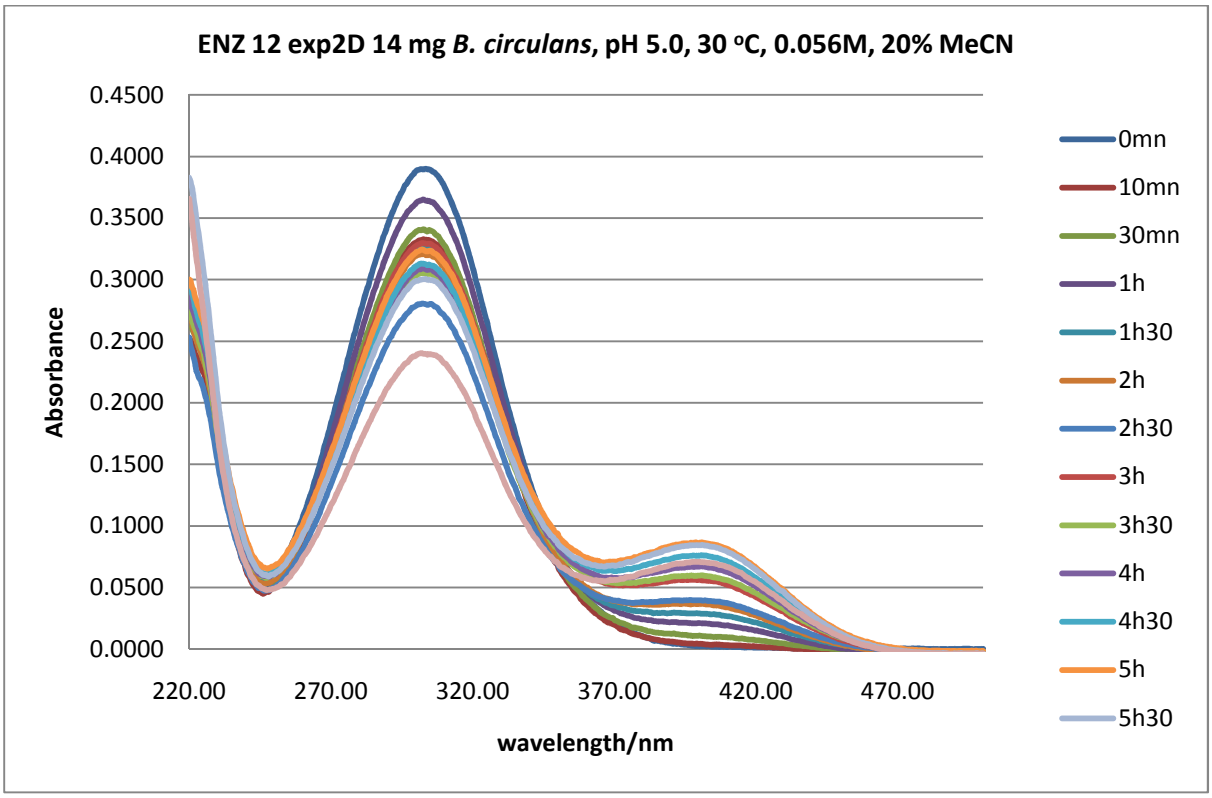

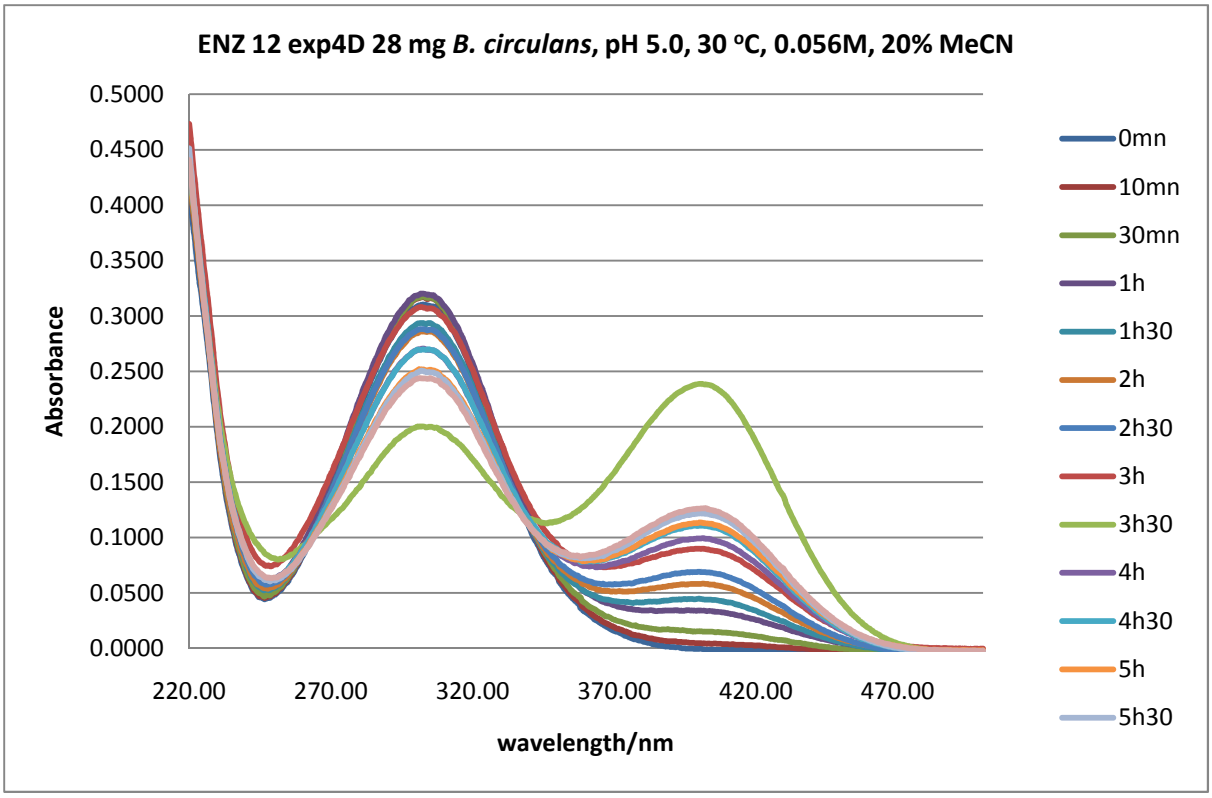
ENZ 12 exp4D 28 mg B. circulans, pH 5.0, 30 °C, 0.056M, 20% MeCN
Absorbance
0.5000
0.4500
0.4000
0.3500
0.3000
0.2500
0.2000
0.1500
0.1000
0.0500
0.0000
220.00
270.00
320.00
370.00
420.00
470.00
wavelength/nm
0mn
10mn
30mn
1h
1h30
2h
2h30
3h
3h30
4h
4h30
5h
5h30

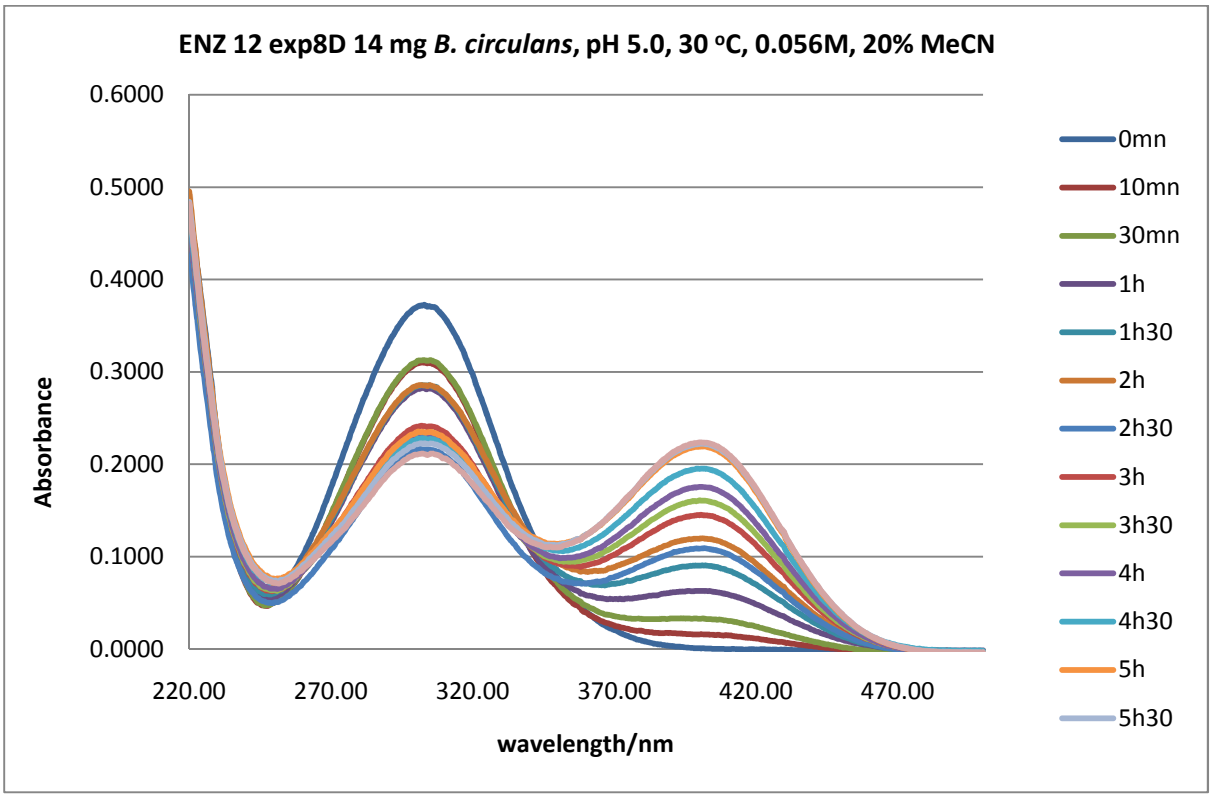
ENZ 12 exp8D 14 mg B. circulans, pH 5.0, 30 °C, 0.056M, 20% MeCN
Absorbance
0.6000
0.5000
0.4000
0.3000
0.2000
0.1000
0.0000
220.00
270.00
320.00
370.00
420.00
470.00
wavelength/nm
0mn
10mn
30mn
1h
1h30
2h
2h30
3h
3h30
4h
4h30
5h
5h30

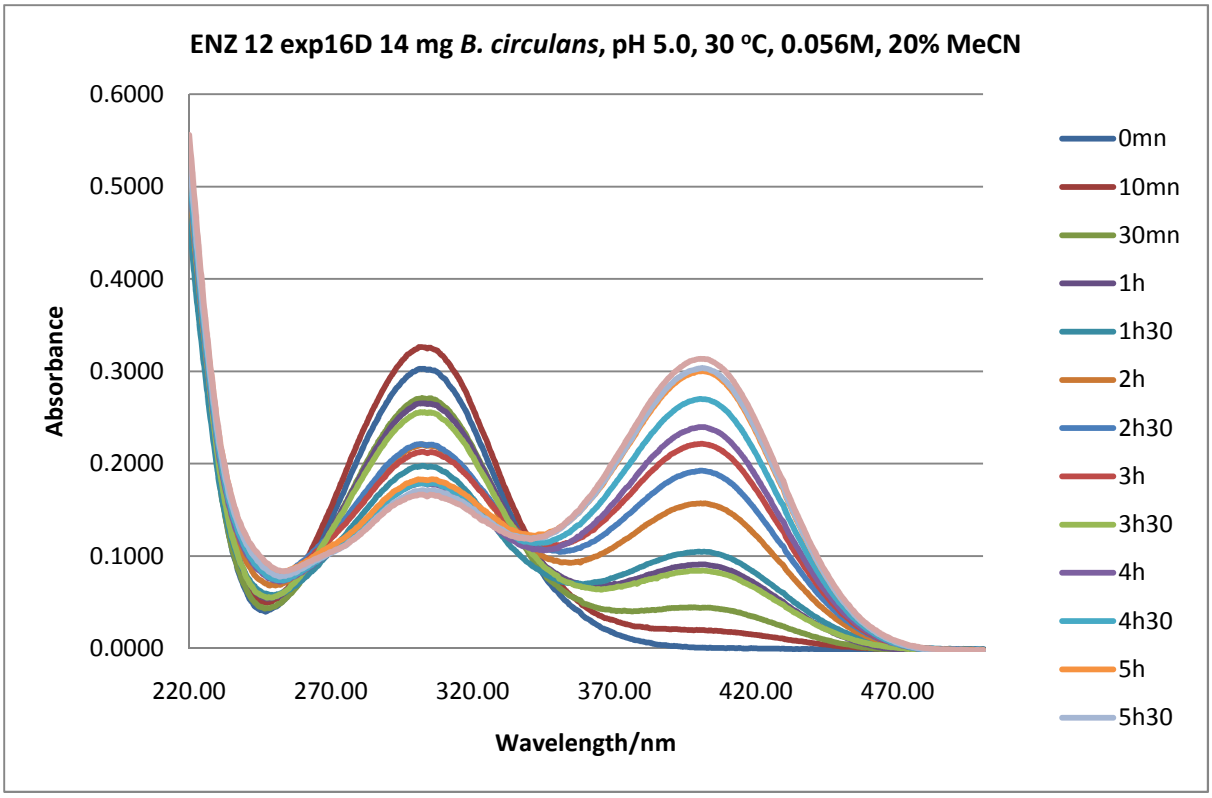
ENZ 12 exp16D 14 mg B. circulans, pH 5.0, 30 °C, 0.056M, 20% MeCN
Absorbance
0.6000
0.5000
0.4000
0.3000
0.2000
0.1000
0.0000
220.00
270.00
320.00
370.00
420.00
470.00
Wavelength/nm
0mn
10mn
30mn
1h
1h30
2h
2h30
3h
3h30
4h
4h30
5h
5h30

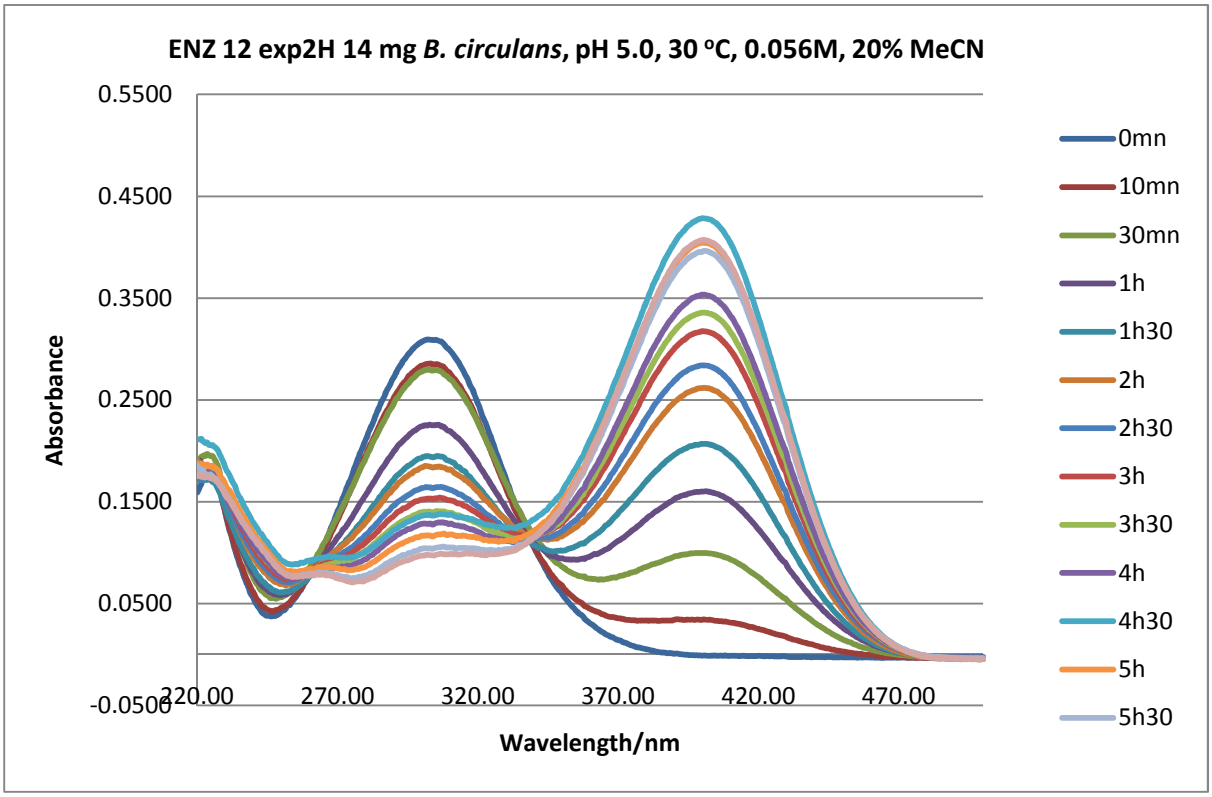
ENZ 12 exp2H 14 mg B. circulans, pH 5.0, 30 °C, 0.056M, 20% MeCN
Absorbance
0.5500
0.4500
0.3500
0.2500
0.1500
0.0500
-0.0500
220.00
270.00
320.00
370.00
420.00
470.00
Wavelength/nm
0mn
10mn
30mn
1h
1h30
2h
2h30
3h
3h30
4h
4h30
5h
5h30

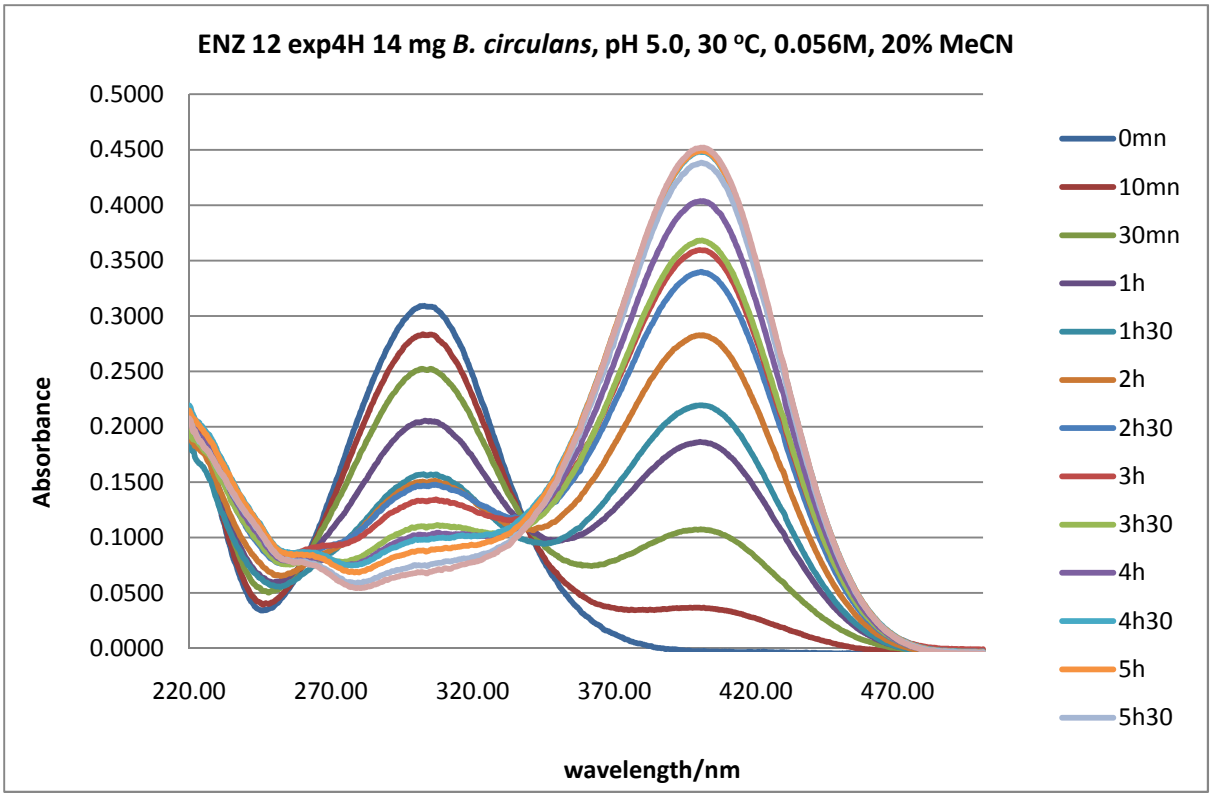
ENZ 12 exp4H 14 mg B. circulans, pH 5.0, 30 °C, 0.056M, 20% MeCN
Absorbance
0.5000
0.4500
0.4000
0.3500
0.3000
0.2500
0.2000
0.1500
0.1000
0.0500
0.0000
220.00
270.00
320.00
370.00
420.00
470.00
wavelength/nm
0mn
10mn
30mn
1h
1h30
2h
2h30
3h
3h30
4h
4h30
5h
5h30

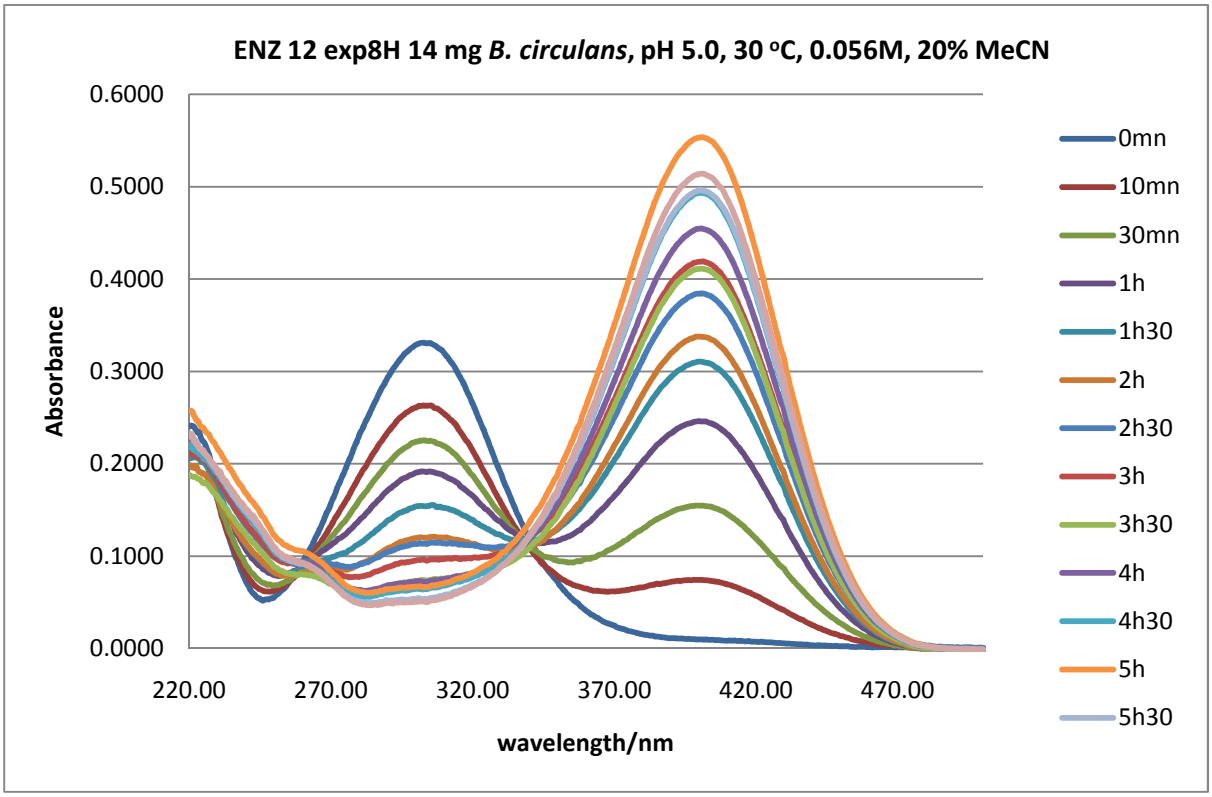
ENZ 12 exp8H 14 mg B. circulans, pH 5.0, 30 °C, 0.056M, 20% MeCN
Absorbance
0.6000
0.5000
0.4000
0.3000
0.2000
0.1000
0.0000
220.00
270.00
320.00
370.00
420.00
470.00
wavelength/nm
0mn
10mn
30mn
1h
1h30
2h
2h30
3h
3h30
4h
4h30
5h
5h30

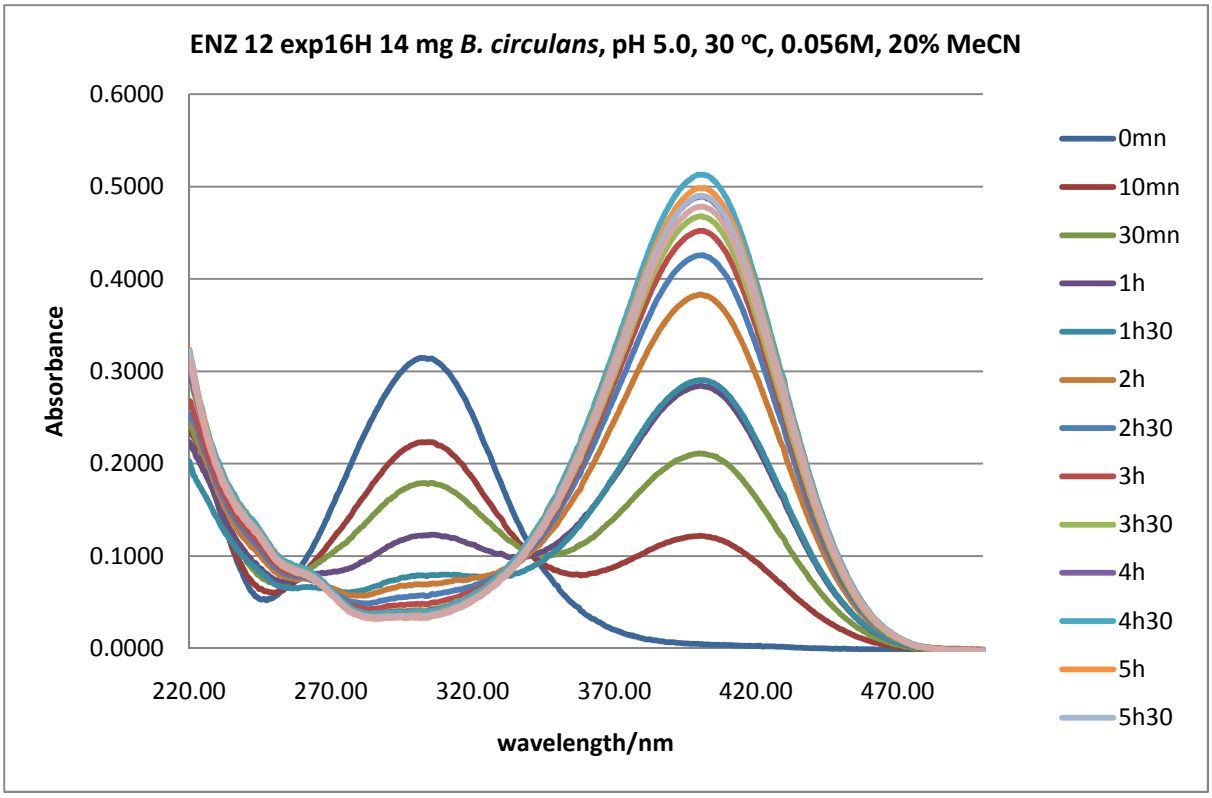


## 3.3.4.1

**ENZ 14D and 14H (P142)**

**ENZ 14D (pH 5.0)**

The first new UV-active peak observed in the HPLC monitoring of this reaction was at 30 minutes as a shoulder on the broad peak at $t_r$ = 7.1 min which corresponds to **32** (Figure 3.3.4.1j).

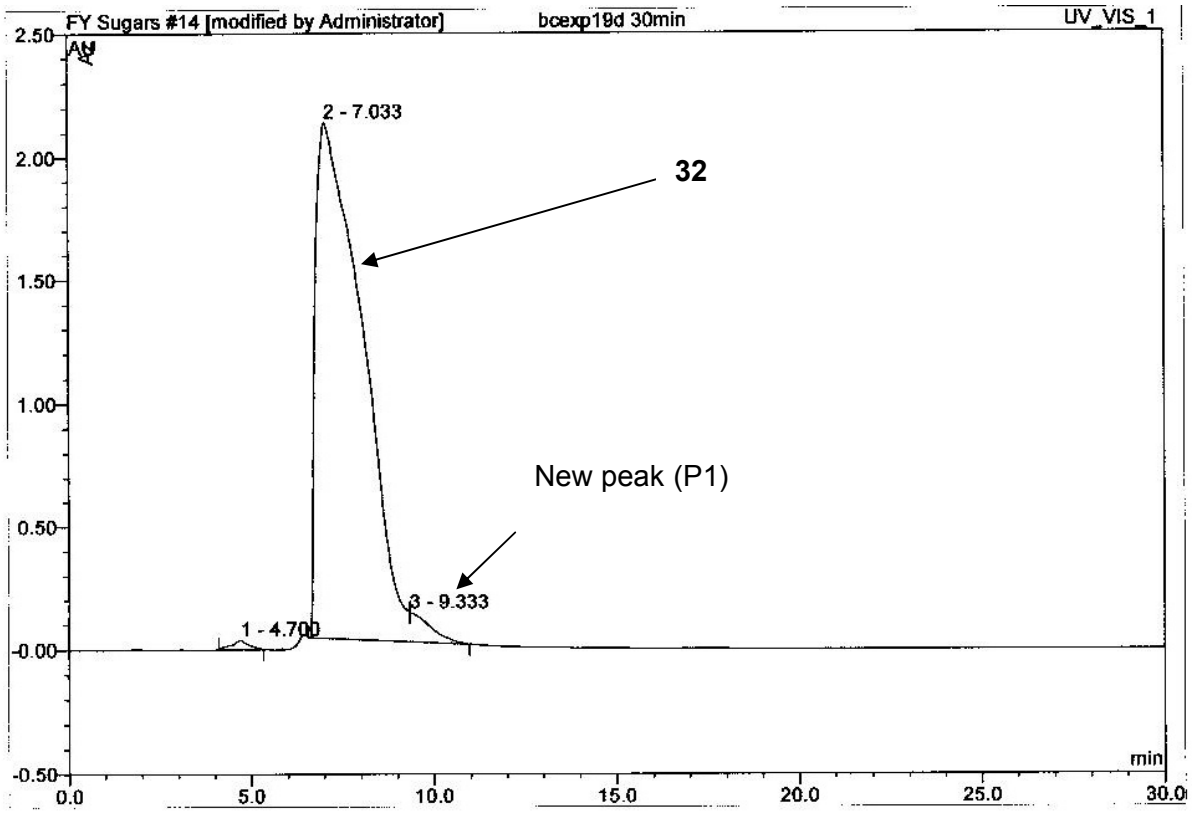


| No. | Ret.Time min | Peak Name | Height AU | Area AU*min | Rel.Area % | Amount | Type |
|---|---|---|---|---|---|---|---|
| 1 | 4.70 | n.a. | 0.035 | 0.019 | 0.59 | n.a. | BMB* |
| 2 | 7.03 | n.a. | 2.092 | 3.059 | 97.05 | n.a. | BM * |
| 3 | 9.33 | n.a. | 0.116 | 0.075 | 2.37 | n.a. | MB* |
| **Total:** | | | 2.243 | 3.152 | 100.00 | 0.000 | |

**Figure 3.3.4.1j**

The reaction progressed in much the same way as reaction 18D (pH 5.0, GalO*p*NP), so much so that the results are almost identical. The HPLC trace at 24 hours again showed the new peak (P1) to have become a significant part of the peak at $t_r$ = 7.1 minutes corresponding to **32** (Figure 3.3.4.1k).

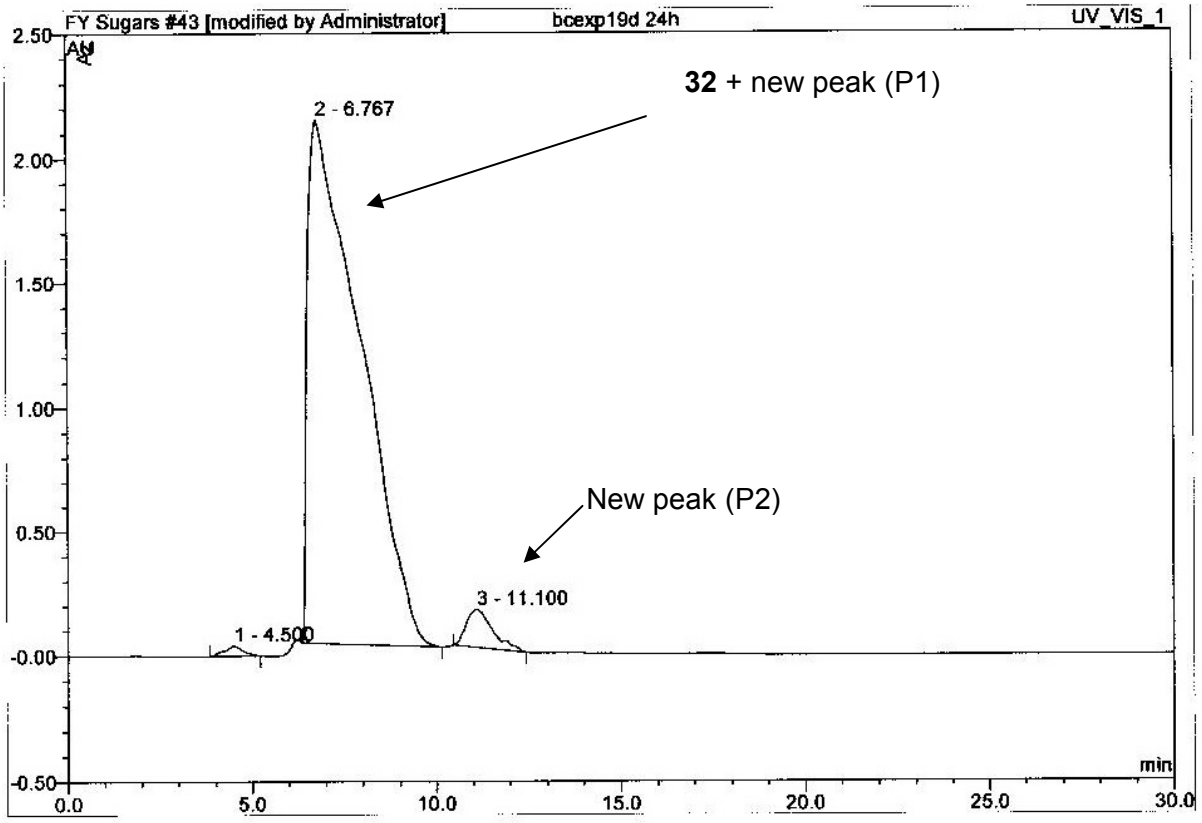


| No. | Ret.Time min | Peak Name | Height AU | Area AU*min | Rel.Area % | Amount | Type |
|---|---|---|---|---|---|---|---|
| 1 | 4.50 | n.a. | 0.039 | 0.023 | 0.63 | n.a. | BMB* |
| 2 | 6.77 | n.a. | 2.103 | 3.470 | 95.96 | n.a. | BMB |
| 3 | 11.10 | n.a. | 0.150 | 0.123 | 3.41 | n.a. | BMB* |
| Total: | | | 2.292 | 3.616 | 100.00 | 0.000 | |

**Figure 3.3.4.1k**

The graph and table in Figure 3.3.4.1l show these changes over the whole 24 hour period of the reaction. The amount of **32** decreased over the course of the reaction, as one would expect, although the UV detector does not show the processing of lactose, examination of the HPLC spectra using ECD shows very slow hydrolysis of lactose ($t_r$ = 3.0 min) as there is still a significant amount remaining at 24 hours.

| Reaction time | Relative area % | | | |
|---|---|---|---|---|
| | $t_r$ = 4.7 min (impurity) | $t_r$ = 7.0 min (**32**) | $t_r$ = 9.3min (P1) | tr = 12.0 - 14.7 min (P2) |
| 0 min | 0.57 | 99.43 | | |
| 10 min | 0.55 | 99.45 | | |
| 30 min | 0.59 | 97.05 | 2.37 | |
| 1 h | 0.58 | 94.09 | 5.33 | |
| 2 h | 0.57 | 91.01 | 8.42 | |
| 3 h | 0.52 | 90.4 | 9.08 | |
| 4 h | 0.47 | 87.56 | 11.48 | 0.48 |
| 5 h | 0.39 | 86.30 | 12.47 | 0.84 |
| 6 h | 0.58 | 83.50 | 15.02 | 0.91 |
| 24 h | 0.63 | 95.96 | | |

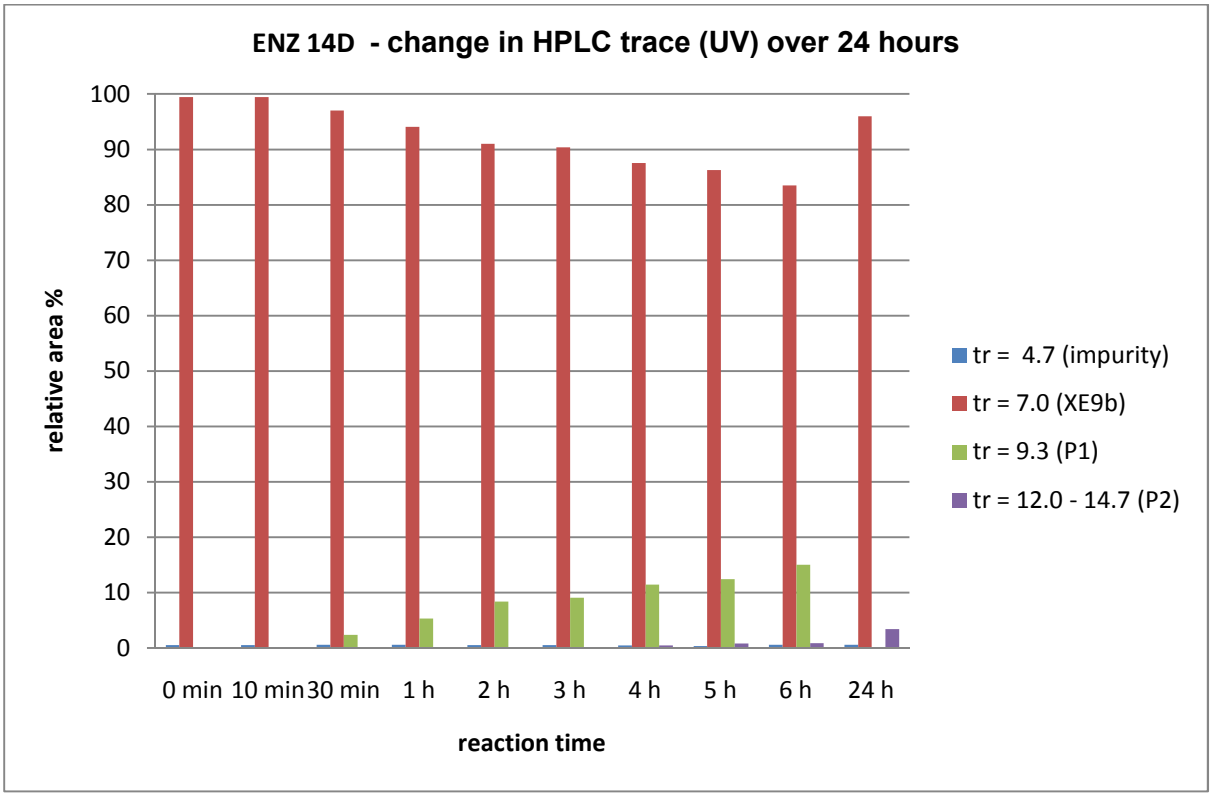


**Figure 3.3.4.1l**

Looking back to experiment 18D (the HPLC results of which are shown in Figure 3.3.4.1d), the two reactions were virtually indistinguishable from each other even though a different glycosyl donor was used. Experiment **ENZ 13H** was very different to **ENZ 13D**, so we might expect the results from experiment **ENZ 14H** to be different to **ENZ 14D**. Thus far it seems that pH has a bigger impact on the reaction results than the choice of glycosyl donor.

**ENZ 14H (pH 7.0)**

The first new UV-active peak appeared in the HPLC monitoring of this reaction at 10 minutes as a shoulder on the broad peak at $t_r$ = 7.1 min which is **32**. Under these reaction conditions (pH 7.0) the consumption of **32** and the increase in P1 was much faster than in 19D. There were also more distinct peaks in the HPLC trace, similarly to 18H. The trace recorded at 24 hours had a broad peak from 7.0 – 9.7 minutes which can be split into 4 separate peaks (Figure 3.3.4.1m). Again, for ease of comparison the peaks due to P1 are grouped together in the table and graph shown in Figure 3.3.4.1n. These results are very similar to those in experiment 18H (pH 7.0, GalO*p*NP as glycosyl donor).

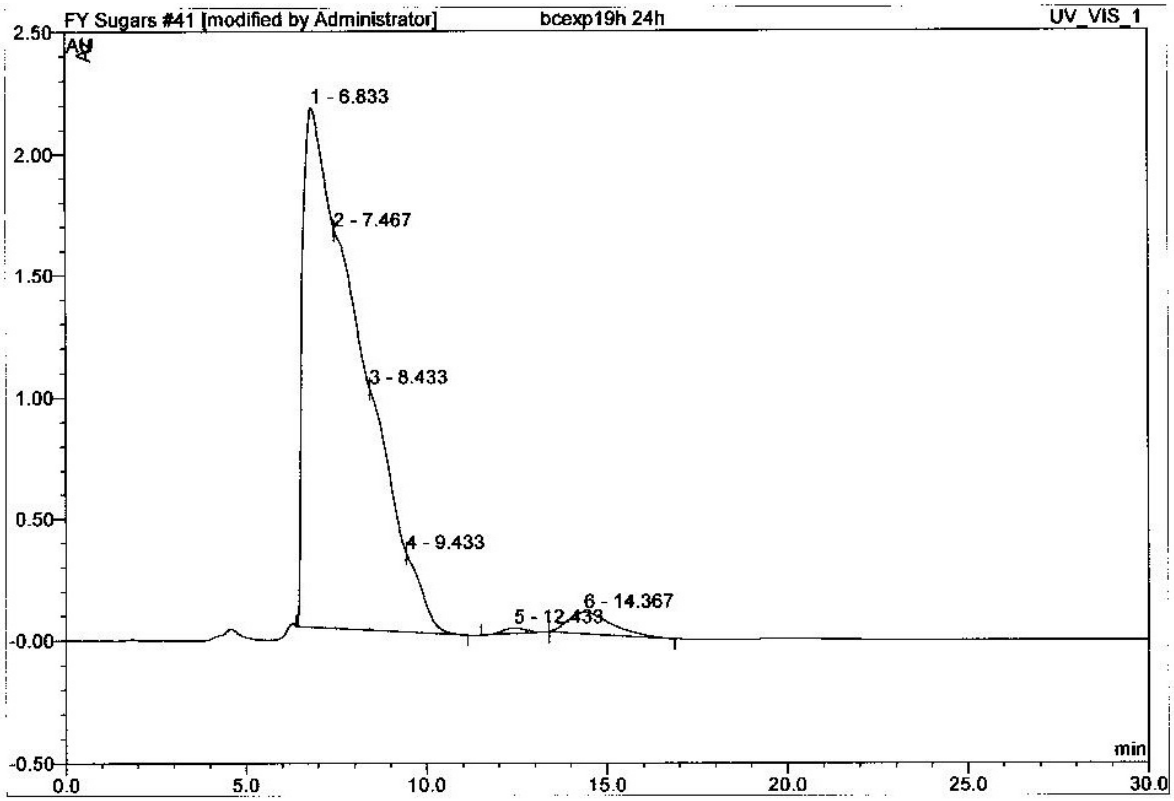


| No. | Ret.Time min | Peak Name | Height AU | Area AU*min | Rel.Area % | Amount | Type |
|---|---|---|---|---|---|---|---|
| 1 | 6.83 | n.a. | 2.134 | 1.778 | 44.06 | n.a. | BM * |
| 2 | 7.47 | n.a. | 1.633 | 1.297 | 32.14 | n.a. | M * |
| 3 | 8.43 | n.a. | 0.994 | 0.672 | 16.65 | n.a. | M * |
| 4 | 9.43 | n.a. | 0.323 | 0.154 | 3.83 | n.a. | MB* |
| 5 | 12.43 | n.a. | 0.021 | 0.014 | 0.36 | n.a. | BMb* |
| 6 | 14.37 | n.a. | 0.086 | 0.120 | 2.96 | n.a. | bMB* |
| **Total:** | | | 5.190 | 4.035 | 100.00 | 0.000 | |

**Figure 3.3.4.1m**

| Reaction time | Relative area % | | | |
|---|---|---|---|---|
| | $t_r$ = 4.0 - 4.7 min (GalO*p*NP + unknown) | $t_r$ = 7.0 min (**32**) | $t_r$ = 8.5 - 9.7 min (P1) | tr = 13.2-15.6 min (P3) |
| 0 min | 0.65 | 99.35 | | |
| 10 min | 0.52 | 96.76 | 2.72 | |
| 30 min | 0.51 | 92.05 | 7.44 | |
| 1 h | 0.52 | 84.09 | 14.07 | 1.32 |
| 2 h | 0.36 | 75.94 | 21.12 | 2.57 |
| 3 h | 0.73 | 67.95 | 26.43 | 4.89 |
| 4 h | 0.44 | 70.68 | 25.17 | 3.18 |
| 5 h | 0.39 | 68.4 | 28.27 | 2.93 |
| 6 h | 0.5 | 67.43 | 27.91 | 4.16 |
| 24 h | 0 | 44.06 | 52.62 | 3.32 |

**19H HPLC UV results**

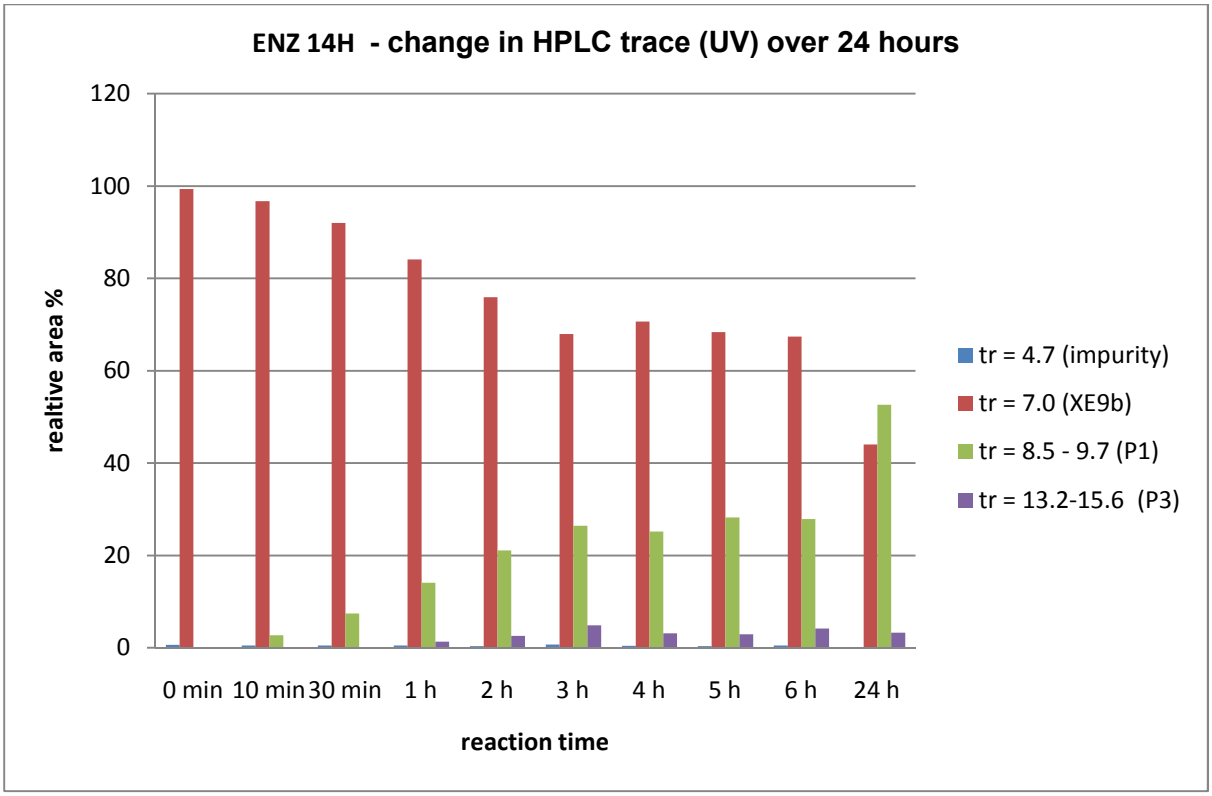


**Figure 3.3.4.1n**

**Comparison of Experiments ENZ 14D** & **ENZ 14H**

Both reactions 1**4D** and **14H** showed processing of **32** in the HPLC spectra. However, in comparing the two experiments it was clear from the graphs in Figures 3.3.4.1l and 3.3.4.1n that 19H (pH 7.0) showed the the greatest amount of **32** processed and the greatest amount of UV-active products formed.

At the end of the 24 hour reaction time the reactions were acetylated for ease of characterisation and separation. Mass spectrometric analysis of the crude material from both reactions revealed the presence of our desired disaccharide Gal-$CH_2$NpGlcOMe **36** at *m/z* 771 (Table 3.3.4.1p).

| Reaction | MS Peak *m/z* | RMM | Assignment (acetylated sugars) | comments |
|---|---|---|---|---|
| 19D | 483 $[M + Na]^+$ | 460 | XE9b | Major peak |
| | 701 $[M + Na]^+$ | 678 | Gal-Gal | ~1/3 height XE9b |
| | **771 $[M + Na]^+$** | **748** | **Gal-$CH_2$NpGlcOMe 36** | Minor peak |
| | 989 $[M + Na]^+$ | 966 | Gal-Gal-Gal | Minor peak |
| 19H | 483 $[M + Na]^+$ | 460 | XE9b | Major peak |
| | 701 $[M + Na]^+$ | 678 | Gal-Gal | ~1/2 height **XE9b** |
| | **771 $[M + Na]^+$** | **748** | **Gal-$CH_2$NpGlcOMe 36** | Minor peak |
| | 989 $[M + Na]^+$ | 966 | Gal-Gal-Gal | baseline |

**Table 3.3.4.1p**

TLC analysis of the acetylated material in EtOAc/Hexane (1:1) using UV and ammonium molybdate to visualise the components showed a set of intense spots at $R_f$ = 0.45 corresponding to **32**. The remaining material was seen as UV- and ammonium molybdate-active spots on the baseline of the plate. The column was flushed with 5% MeOH in EtOAc once the other spots had eluted (**32** could be recovered for use in subsequent reactions).

Mass spectra of the material in the flush are shown in Figure 3.3.4.1q and the analysis in Table 3.3.4.1r.

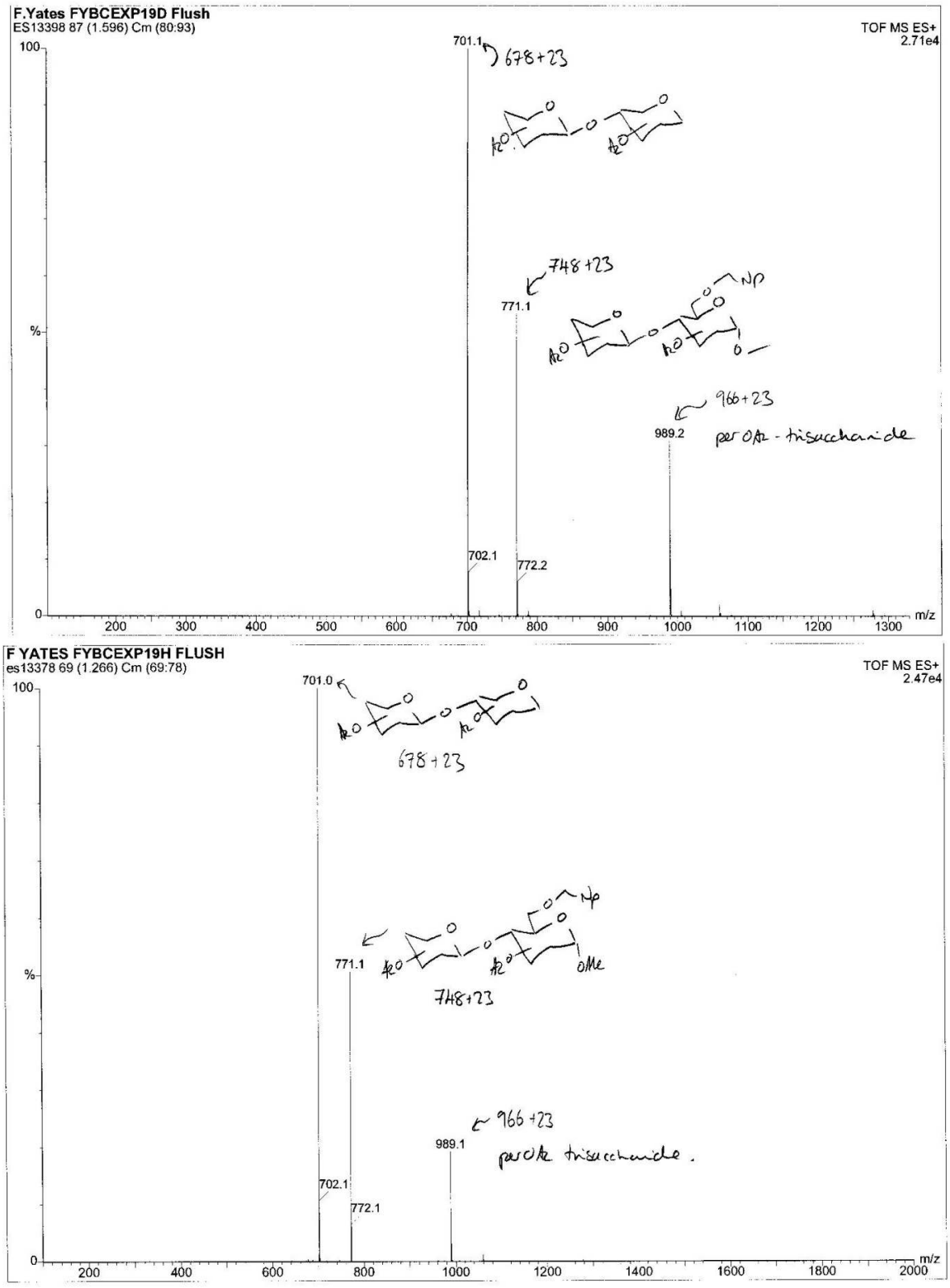


**Figure 3.3.4.1q**

| Reaction | MS Peak *m/z* | RMM | Assignment (acetylated sugars) | comments |
|---|---|---|---|---|
| 19D | 701 $[M + Na]^+$ | 678 | Gal-Gal | Major peak |
| | **771 $[M + Na]^+$** | **748** | **Gal-$CH_2$NpGlcOMe** | ~1/2 peak at 701 |
| | 989 $[M + Na]^+$ | 966 | Gal-Gal-Gal | ~1/3 peak at 701 |
| | **1059 $[M + Na]^+$** | **1036** | **Gal-Gal-$CH_2$NpGlcOMe** | baseline |
| 19H | 701 $[M + Na]^+$ | 678 | Gal-Gal | Major peak |
| | **771 $[M + Na]^+$** | **748** | **Gal-$CH_2$NpGlcOMe** | ~1/2 peak at 701 |
| | 989 $[M + Na]^+$ | 966 | Gal-Gal-Gal | ~1/4 peak at 701 |
| | **1059 $[M + Na]^+$** | **1036** | **Gal-Gal-$CH_2$NpGlcOMe** | baseline |

**Table 3.3.4.1r**

The major components in the mass spectra of the flushed material were Gal-Gal disaccharide and our desired Gal-CH2NpGlcOMe disaccharide. A baseline peak in both spectra was a trisaccharide containing CH2NpGlcOMe.

## 3.3.4.3 (P153)

**HPLC traces (UV) of the 4 sugars of interest**

GalO*p*NP

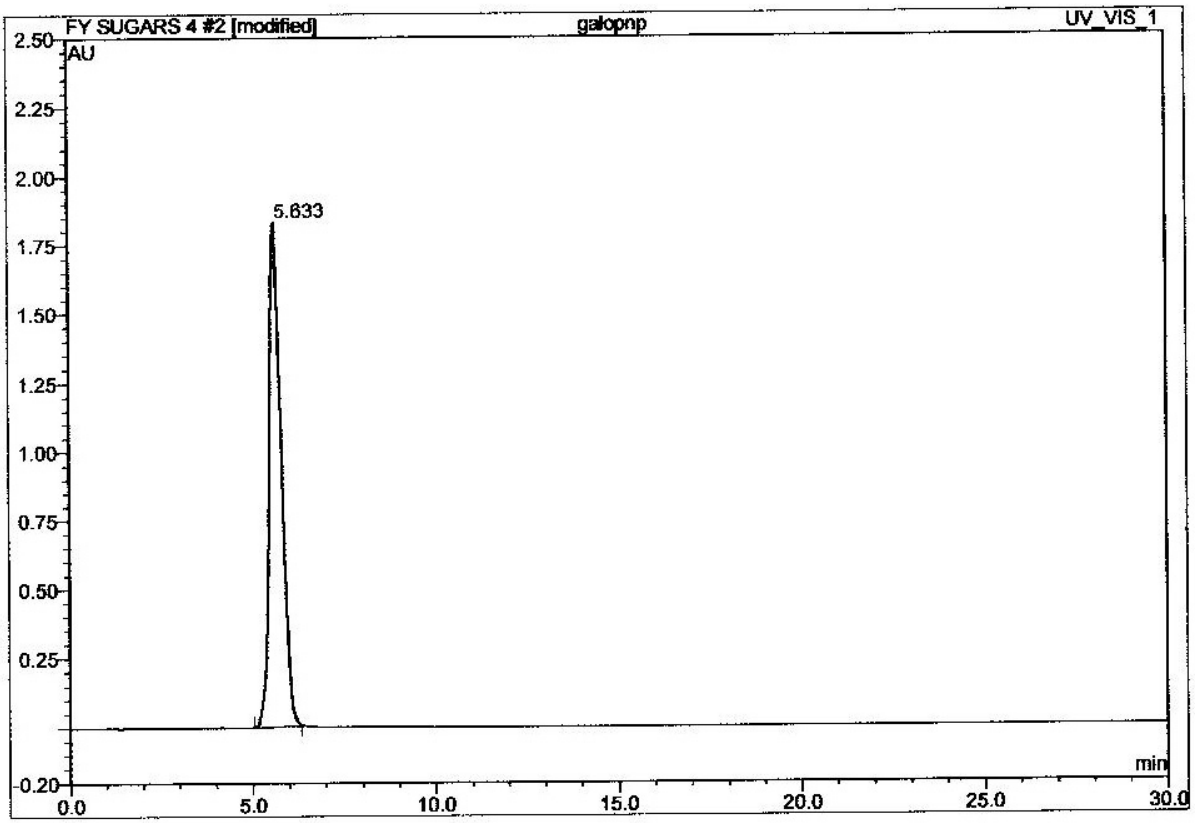


| No. | Ret.Time min | Peak Name | Height AU | Area AU*min | Rel.Area % | Amount | Type |
|---|---|---|---|---|---|---|---|
| 1 | 5.63 | n.a. | 1.829 | 0.705 | 100.00 | n.a. | BMB* |
| Total: | | | 1.829 | 0.705 | 100.00 | 0.000 | |

$CH_2$NpGlcOMe

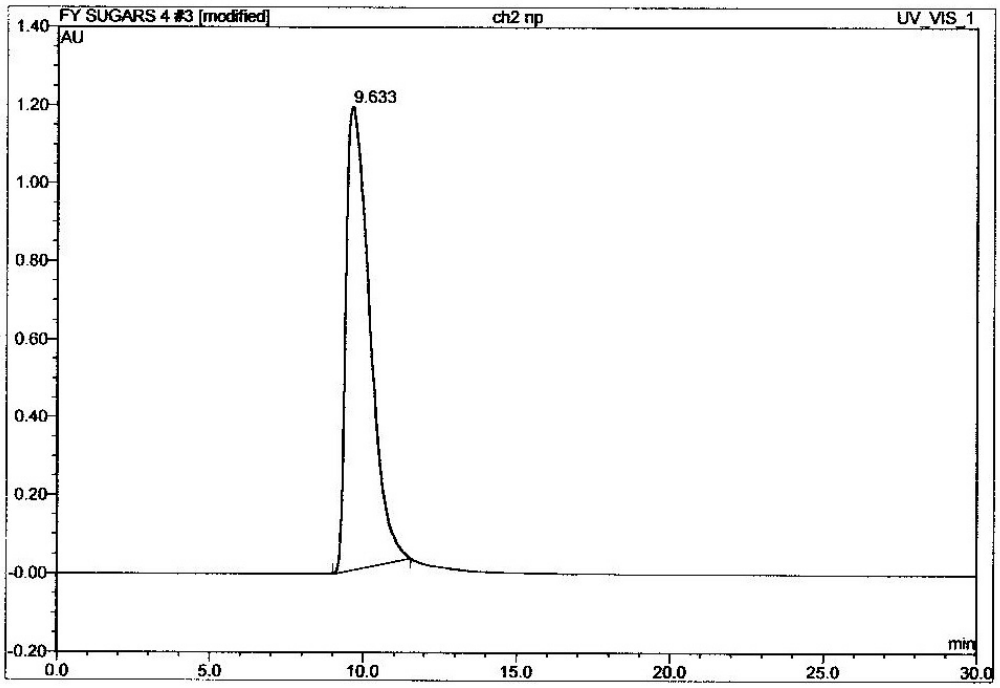


| No. | Ret.Time min | Peak Name | Height AU | Area AU*min | Rel.Area % | Amount | Type |
|---|---|---|---|---|---|---|---|
| 1 | 9.63 | n.a. | 1.189 | 1.069 | 100.00 | n.a. | BMB* |
| Total: | | | 1.189 | 1.069 | 100.00 | 0.000 | |

EGNpGlcOMe

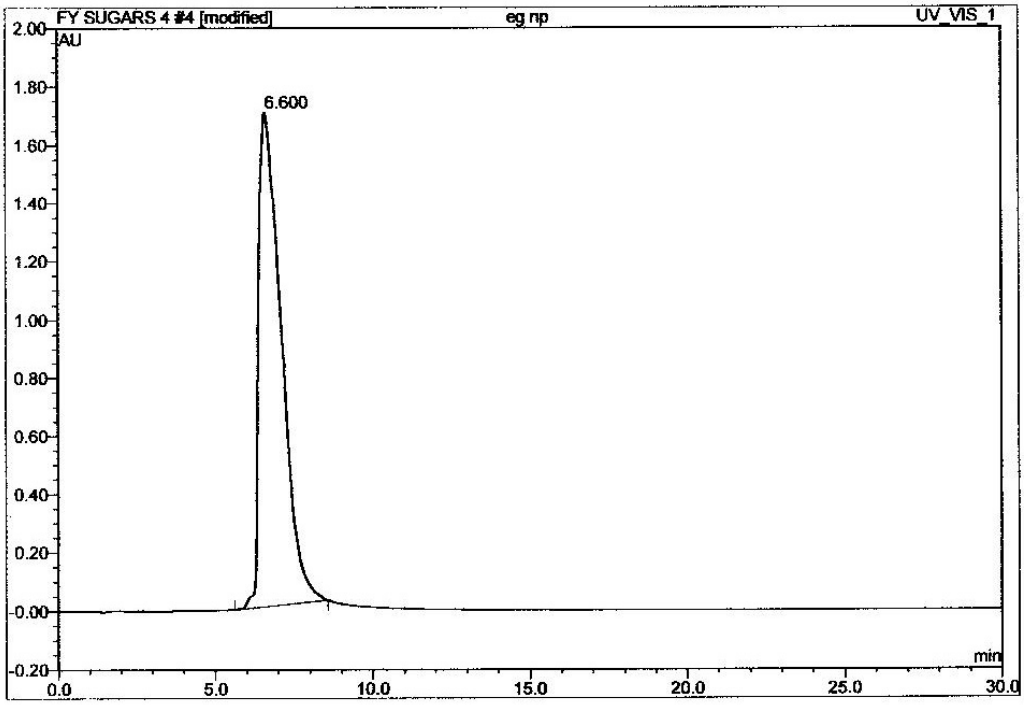


| No. | Ret.Time min | Peak Name | Height AU | Area AU*min | Rel.Area % | Amount | Type |
|---|---|---|---|---|---|---|---|
| 1 | 6.60 | n.a. | 1.698 | 1.408 | 100.00 | n.a. | BMB* |
| Total: | | | 1.698 | 1.408 | 100.00 | 0.000 | |

DEGNpGlcOMe

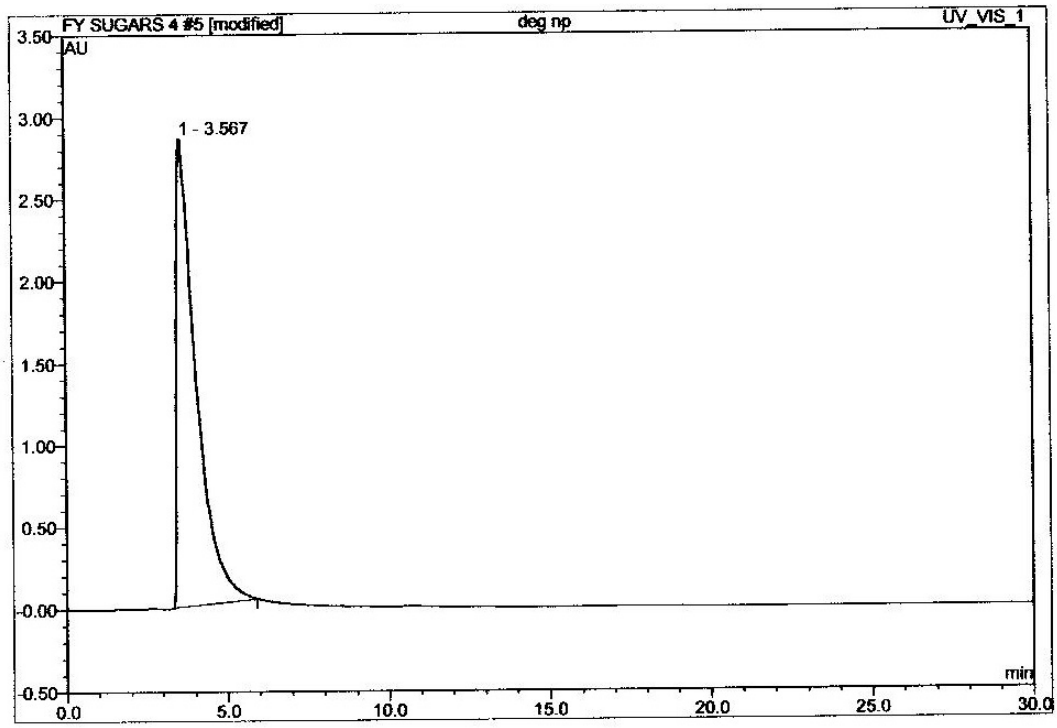


| No. | Ret.Time min | Peak Name | Height AU | Area AU*min | Rel.Area % | Amount | Type |
|---|---|---|---|---|---|---|---|
| 1 | 3.57 | n.a. | 2.857 | 1.996 | 100.00 | n.a. | BMB* |
| Total: | | | 2.857 | 1.996 | 100.00 | 0.000 | |

Combined plot of all naphthyl functionalised sugars

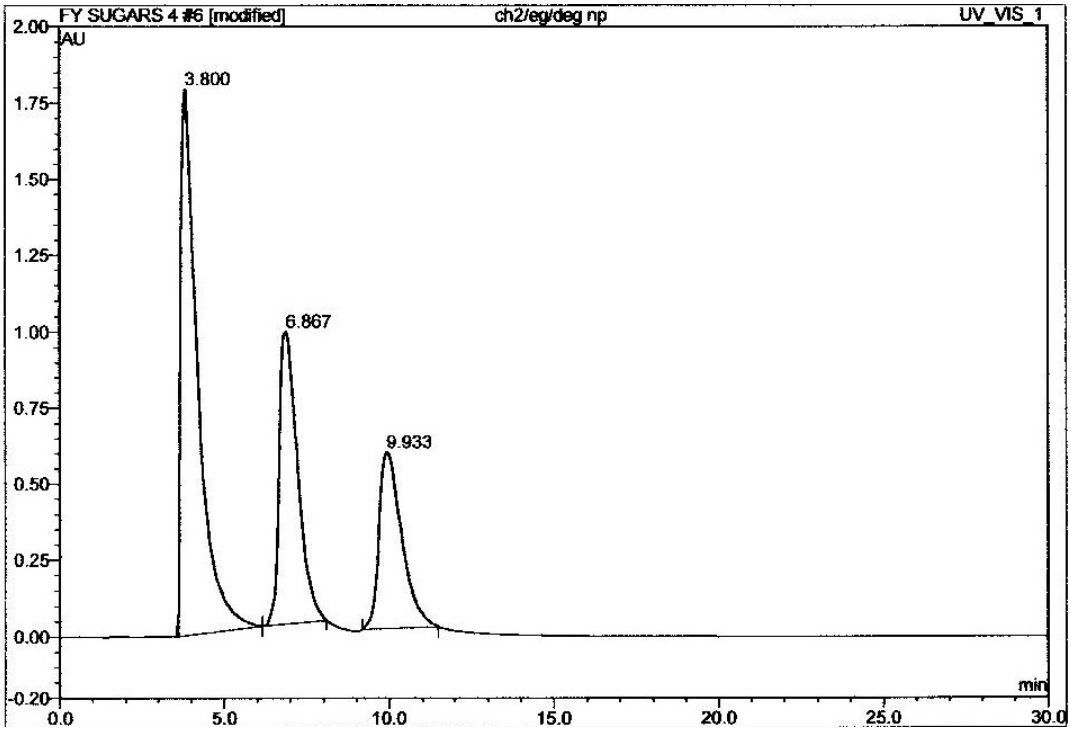

# Additional Data for Chapter 4

## Section 4.3.1.2

**DCC1**

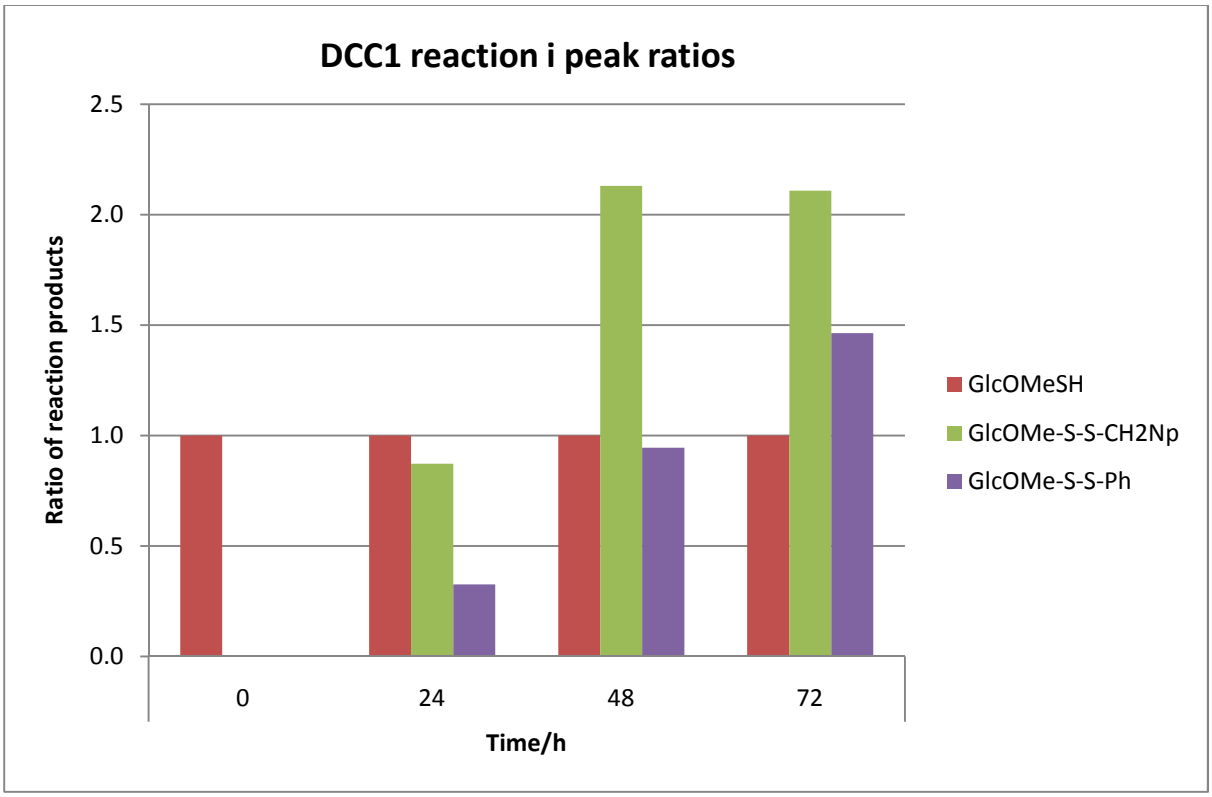


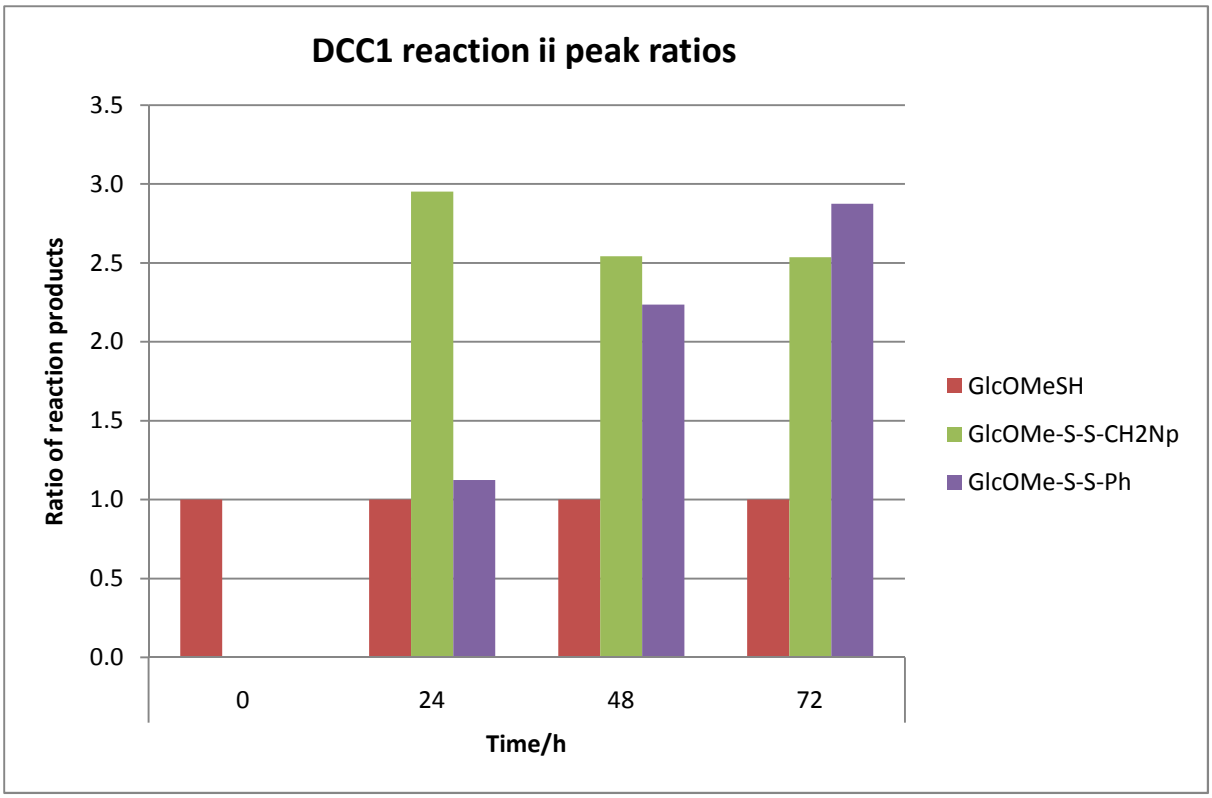

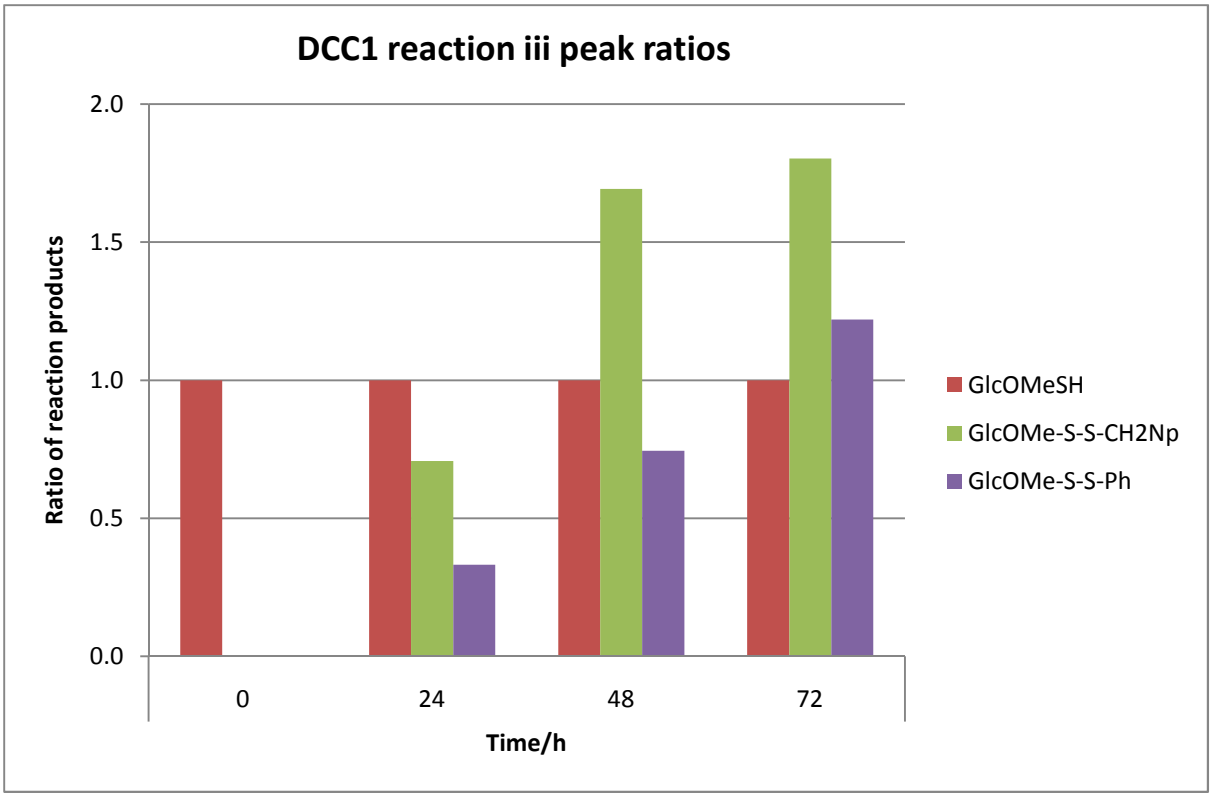
DCC1 reaction iii peak ratios
Ratio of reaction products
2.0
1.5
1.0
0.5
0.0
0
24
48
72
Time/h
GlcOMeSH
GlcOMe-S-S-CH2Np
GlcOMe-S-S-Ph

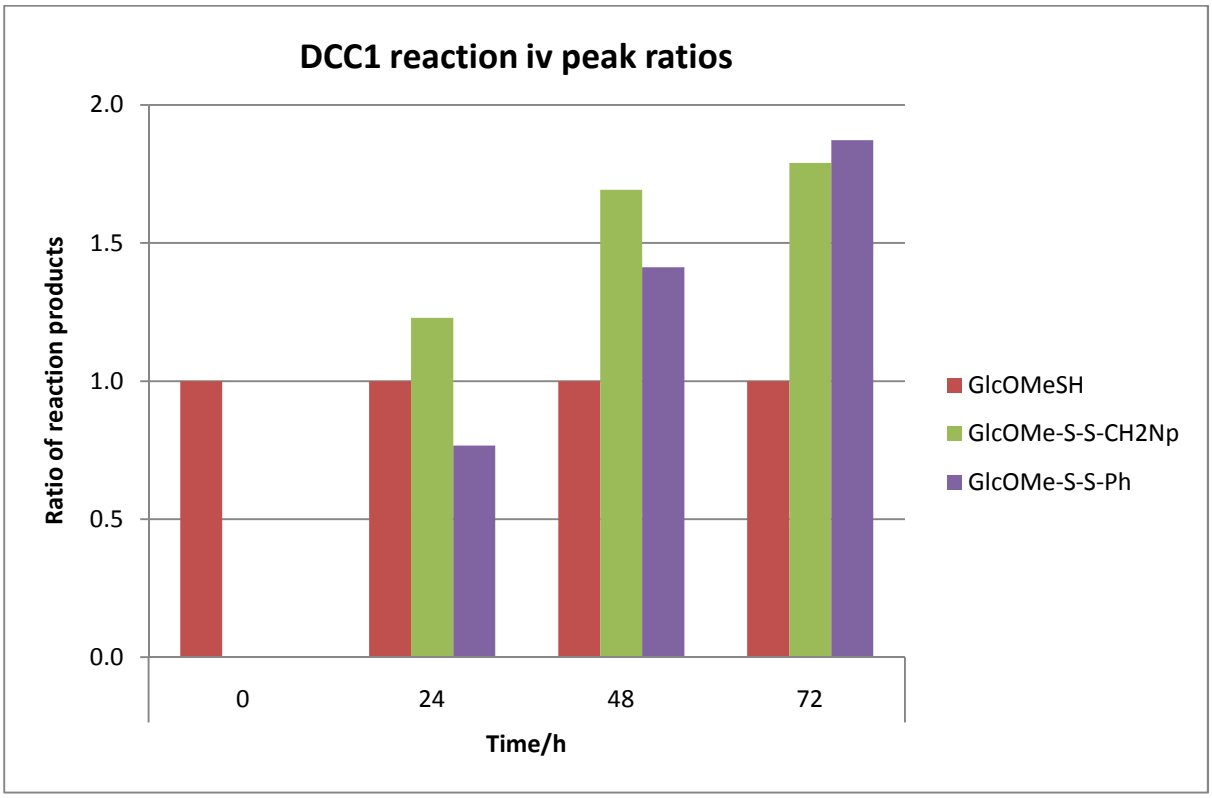
DCC1 reaction iv peak ratios
Ratio of reaction products
2.0
1.5
1.0
0.5
0.0
0
24
48
72
Time/h
GlcOMeSH
GlcOMe-S-S-CH2Np
GlcOMe-S-S-Ph

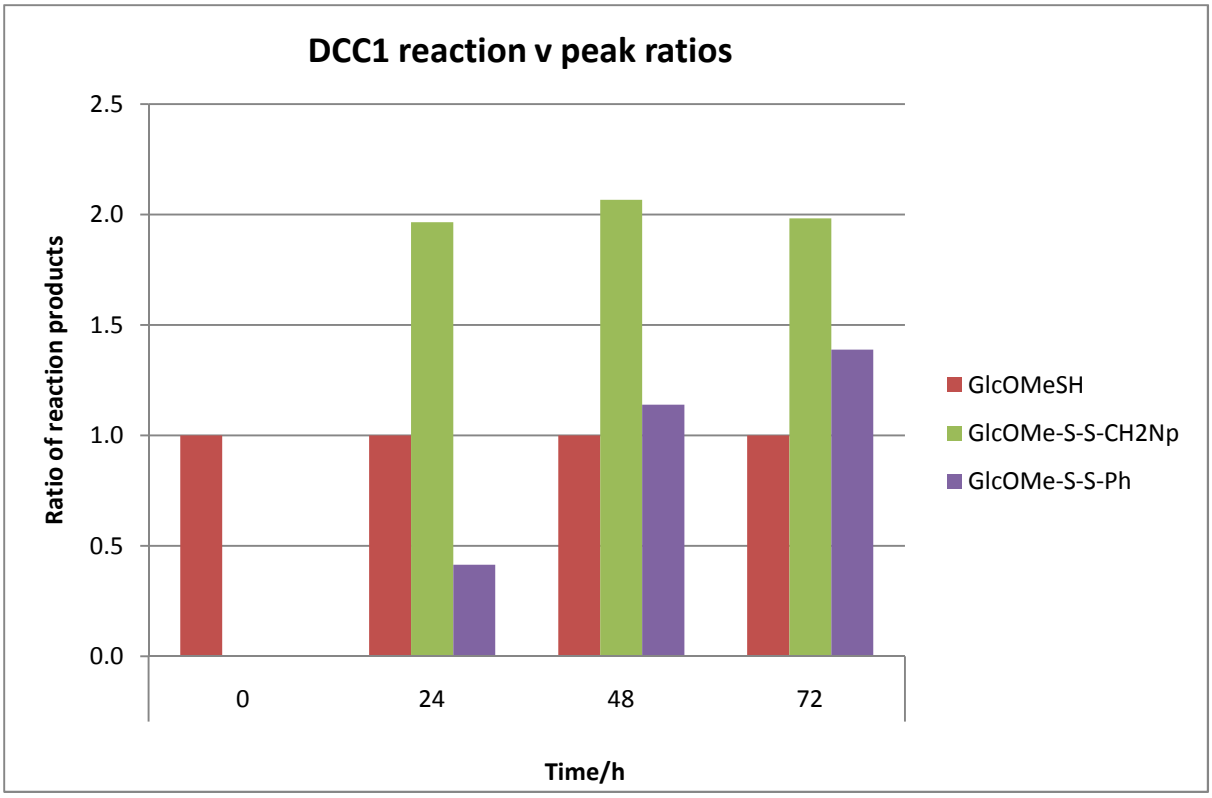
DCC1 reaction v peak ratios
Ratio of reaction products
2.5
2.0
1.5
1.0
0.5
0.0
0
24
48
72
Time/h
GlcOMeSH
GlcOMe-S-S-CH2Np
GlcOMe-S-S-Ph

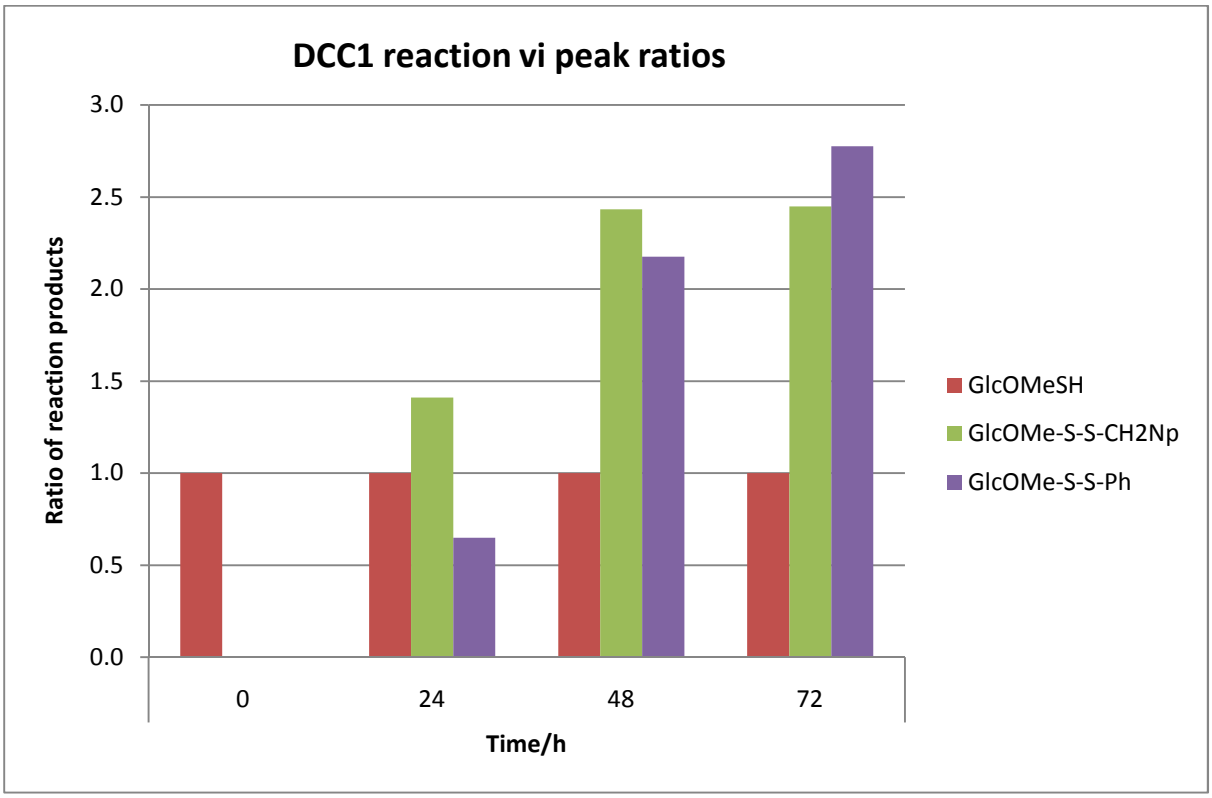
DCC1 reaction vi peak ratios
Ratio of reaction products
3.0
2.5
2.0
1.5
1.0
0.5
0.0
0
24
48
72
Time/h
GlcOMeSH
GlcOMe-S-S-CH2Np
GlcOMe-S-S-Ph

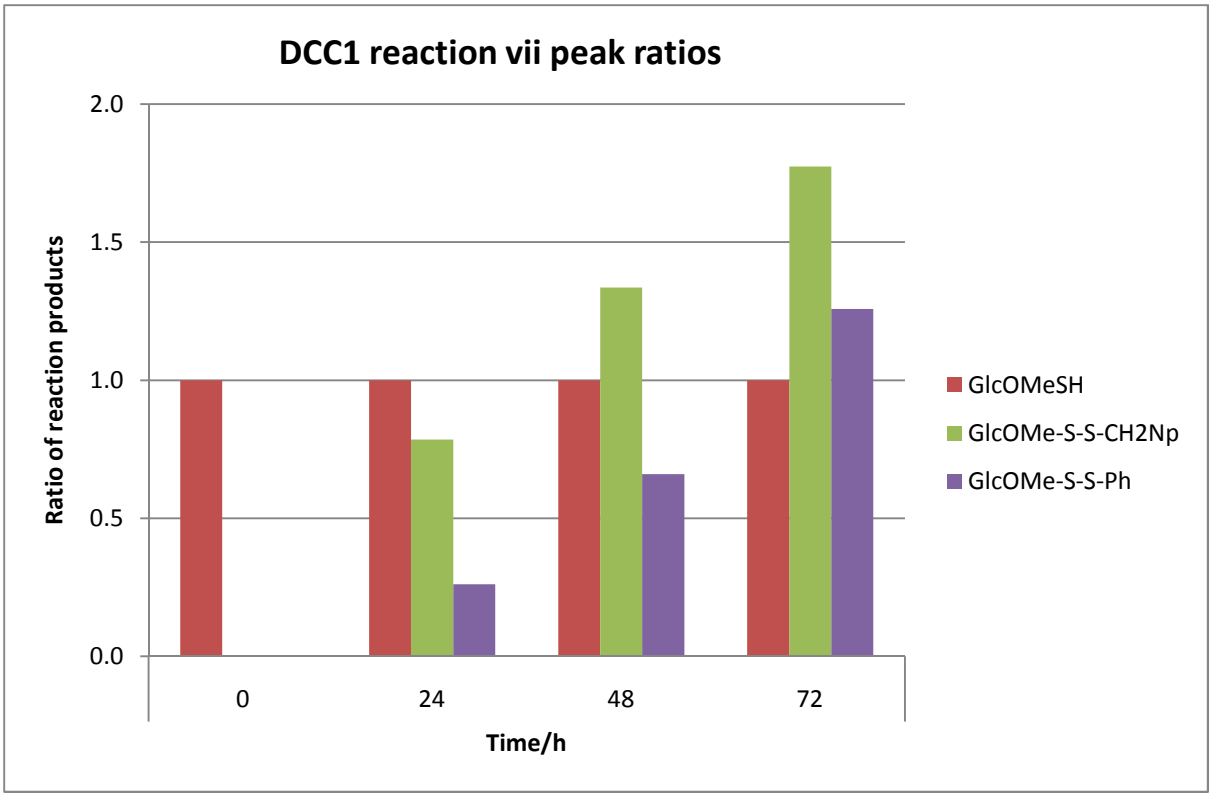
DCC1 reaction vii peak ratios
Ratio of reaction products
2.0
1.5
1.0
0.5
0.0
0
24
48
72
Time/h
GlcOMeSH
GlcOMe-S-S-CH2Np
GlcOMe-S-S-Ph

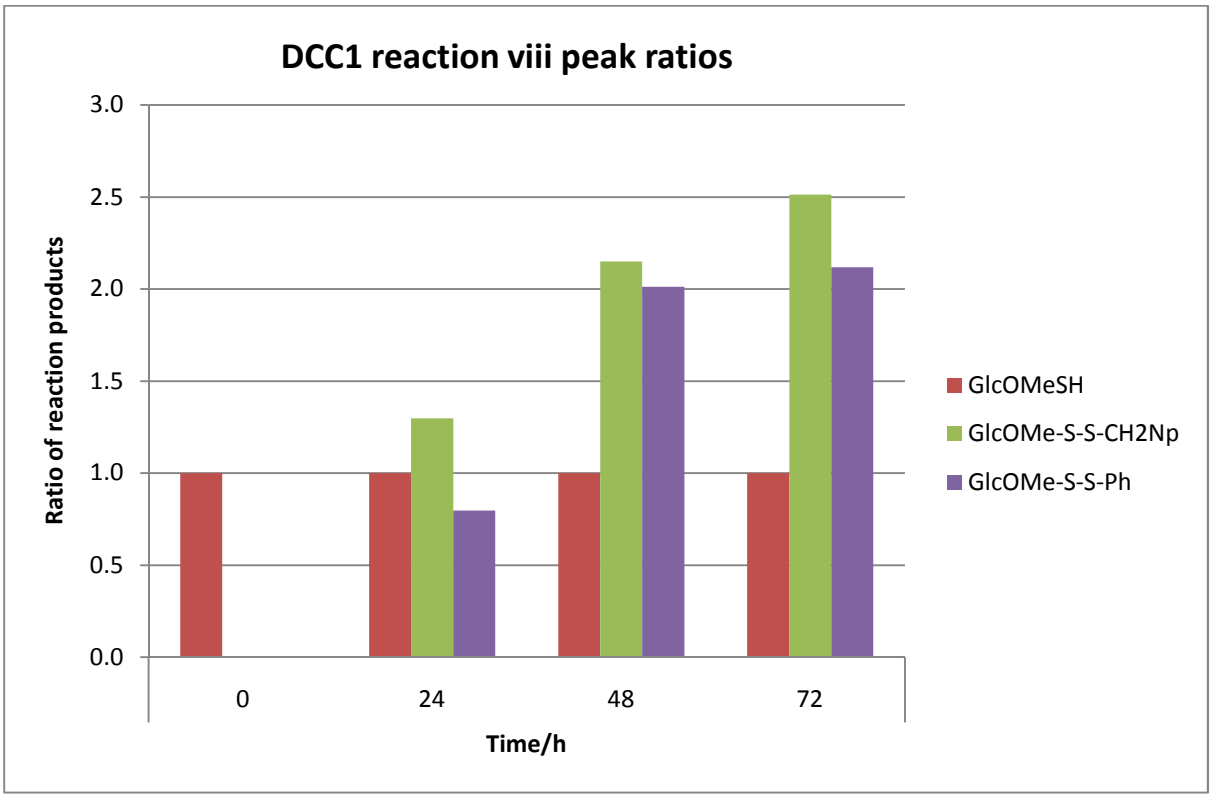
DCC1 reaction viii peak ratios
Ratio of reaction products
3.0
2.5
2.0
1.5
1.0
0.5
0.0
0
24
48
72
Time/h
GlcOMeSH
GlcOMe-S-S-CH2Np
GlcOMe-S-S-Ph

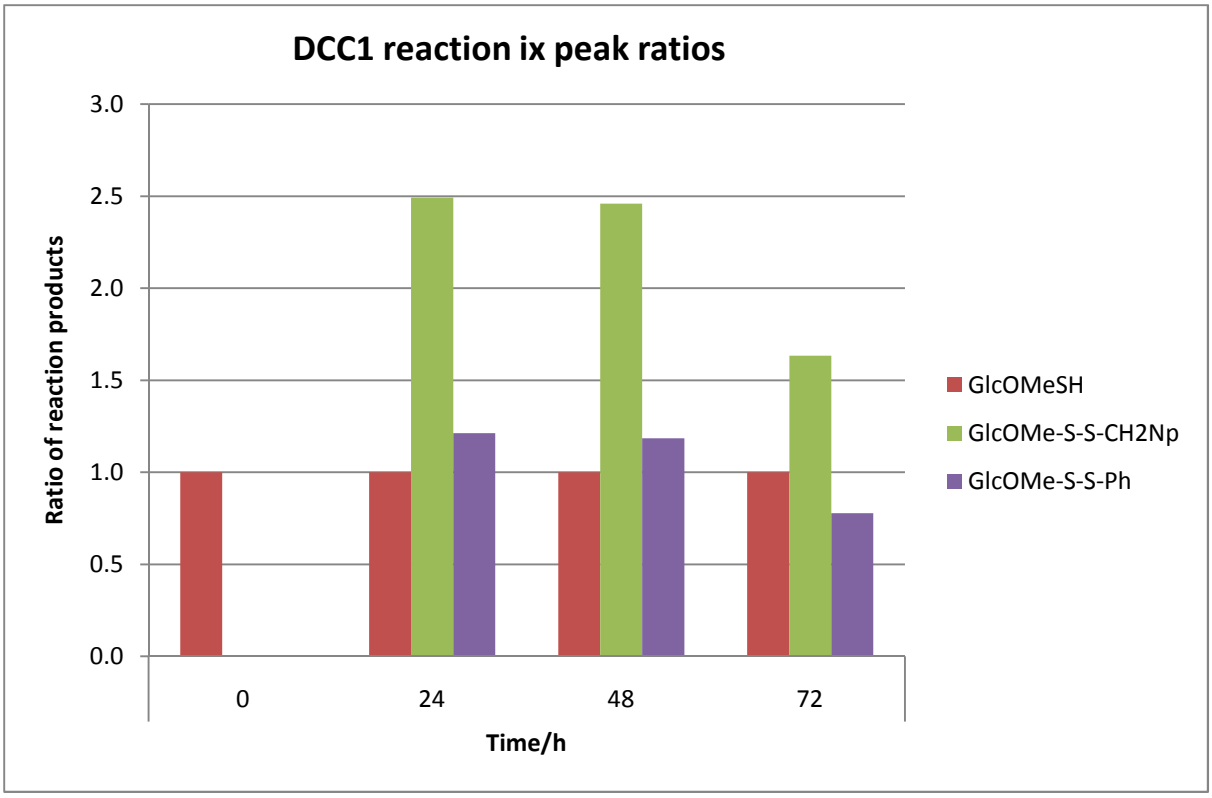
DCC1 reaction ix peak ratios
Ratio of reaction products
3.0
2.5
2.0
1.5
1.0
0.5
0.0
0
24
48
72
Time/h
GlcOMeSH
GlcOMe-S-S-CH2Np
GlcOMe-S-S-Ph

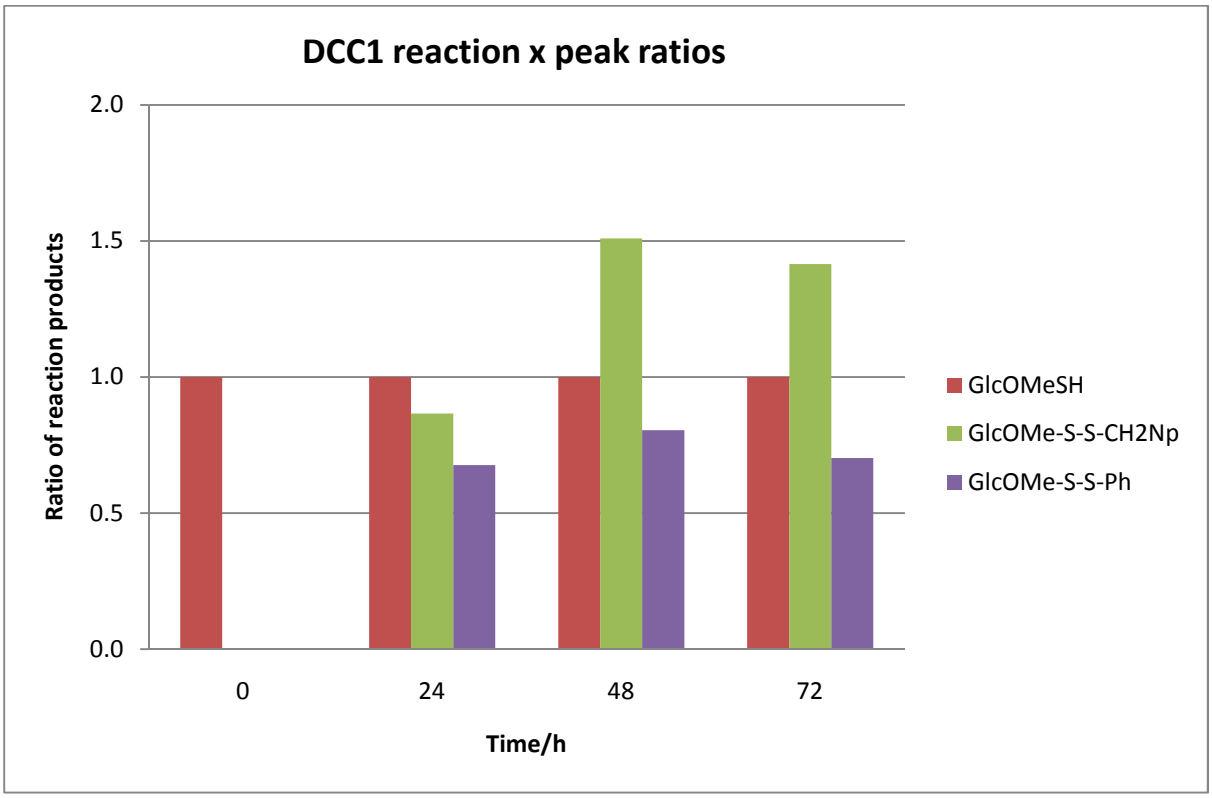
DCC1 reaction x peak ratios
Ratio of reaction products
2.0
1.5
1.0
0.5
0.0
0
24
48
72
Time/h
GlcOMeSH
GlcOMe-S-S-CH2Np
GlcOMe-S-S-Ph

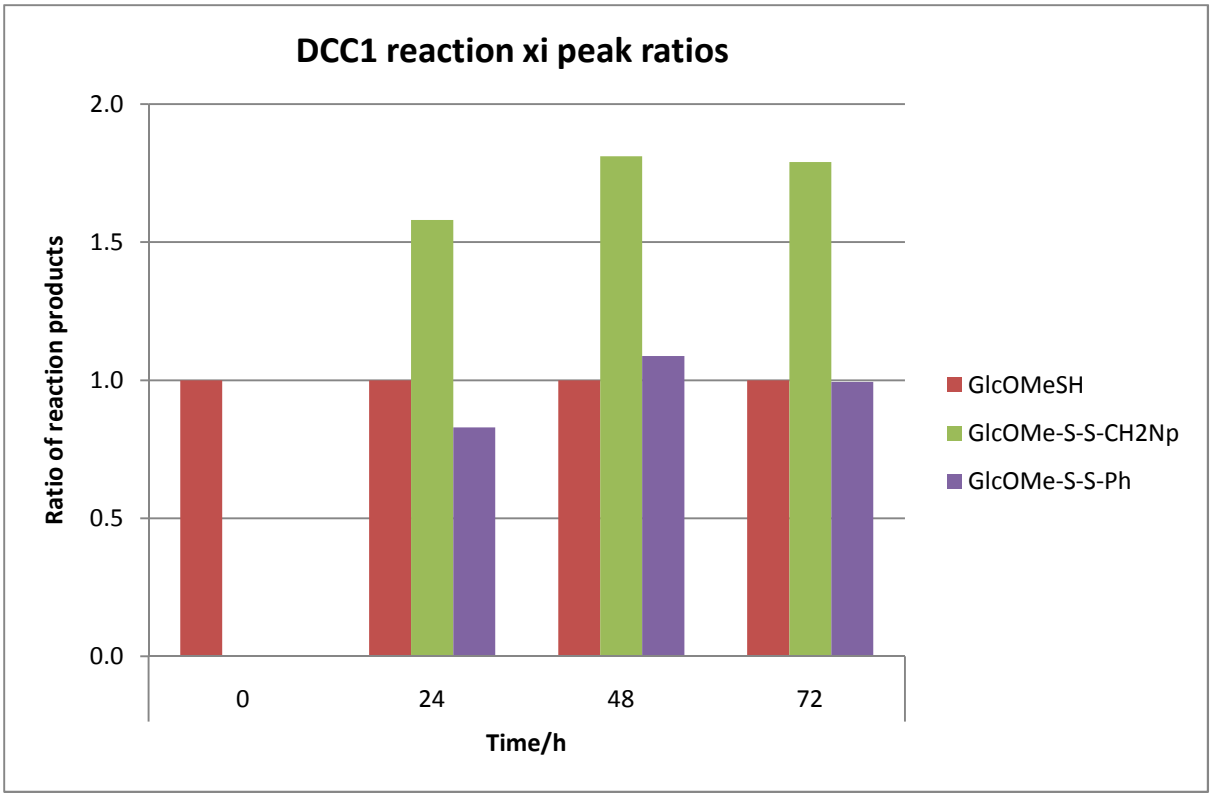
DCC1 reaction xi peak ratios
Ratio of reaction products
2.0
1.5
1.0
0.5
0.0
0
24
48
72
Time/h
GlcOMeSH
GlcOMe-S-S-CH2Np
GlcOMe-S-S-Ph

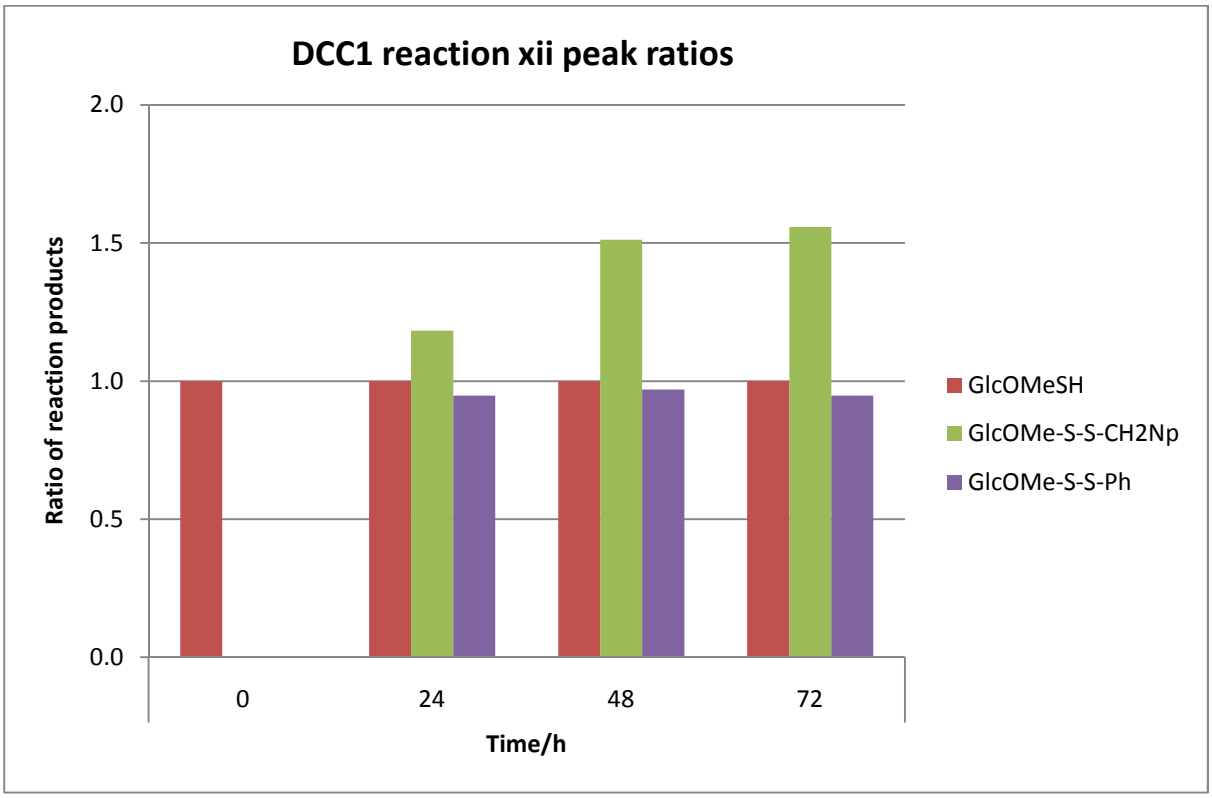
DCC1 reaction xii peak ratios
Ratio of reaction products
2.0
1.5
1.0
0.5
0.0
0
24
48
72
Time/h
GlcOMeSH
GlcOMe-S-S-CH2Np
GlcOMe-S-S-Ph